Preface

These proceedings of the Driving Simulation Conference Europe 2012 are the second issue in the edition of Les collections de l'INRETS. The DSC Europe conference held this year again at the Arts et Métiers ParisTech, is a gathering event between two communities: scientific researchers interested in driver's behavior and perception and developers of technologies for the rendering of the behavior and environment of vehicles.

This year, as the number of submitted papers has increased significantly, parallel sessions were organized and a larger poster session was added with an independent Exhibition area. These proceedings contain the full paper versions of the oral presentation given at the conference and short summaries of the posters presented at the conference.

Authors of the best papers were asked to submit an extended version to the Journal of Computing and Information Science in Engineering (JCISE), Special Issue in Driving Simulation. In addition an electronic version of the conference papers are available on line on the DSC Europe website, two years after the conference, thus in September 2012 the electronic versions of the papers presented in September 2010.

Thus, these DSC Europe 2012 proceedings bring a panorama of recent developments in simulation rendering techniques and virtual prototyping applications as well as of perception and human factors studies in the field of driving simulation.

The DSC Europe Organization Committee

Introduction

Andras Kemeny
Technical Center for Simulation, Renault
Institut Image, Arts et Métiers ParisTech
Andras.kemeny@renault.com

I have the privilege to contribute to the research and advance engineering in the field of flight and driving simulation since the mid 80ths. First at Thales Training and Simulation, followed by Renault, but also at the CNRS, College de France and more recently at Arts et Métiers ParisTech. I also had the privilege to organize the Driving Simulation Conferences since 1995 and thus see the evolution of both simulation techniques and applications through these years. The new domain of automotive driving simulation was born in the 70ths and went through a dramatic mutation which today is entering in a new era: high performance real time motion and image rendering as well as the effective industrial use of driving simulation for automotive vehicle design.

The different sections of this book witness this evolution. As you can see, the main human factors session is providing data on the use of dynamic simulators, especially on the effect of motion on driving behavior, both for lateral and longitudinal accelerations. A more technical oriented session on Motion rendering, together with a Simulation design and architecture section give insight of the necessary rendering techniques to provide the necessary motion and environmental cues for correct driver perception.

Different types of applications in driving simulation, including economical and VE driving and fuel efficiency, subjects becoming of social importance these days, are sections in this book are Perception and human factors, Virtual prototyping and applications, this latter including a specific the application areas, Automotive Driver Aid Systems (ADAS), Motion rendering and Simulation design and architecture, completed with a Short summaries. All of these sections deal with the subjects of the paper and poster sessions of the last, 11th edition of the Driving Simulation Europe conferences, held on September 6 and 7 in Paris.

Virtual prototyping becomes a key area in vehicle engineering design, contributing to the zero physical prototype vehicle development. ADAS are the newest and progressively most visible part of this trend, as cars nowadays are proposing sophisticated driver aid systems. These are costly to develop and difficult to validate in realistic driving conditions with more and more sophisticated man machine interfaces which have to stay understandable and easy to use. These systems necessitate the use of high performance driving simulators as the behavior of the vehicle needs to be of high fidelity.

As the question of simulation validity is thus crucial, a particularly large Perception and presented in a well furnished Virtual prototyping and training session of full papers. An additional section of Short summary papers allow to learn more about high performance simulators, such as that of Renault, University of Stuttgart or University of Tongji, as well as other experiments and developments in driving simulation. These sections all together present the view of authors from the academic world and the simulation industry from more than 10 countries worldwide, including Europe, Israel, the USA, Japan and China.

I would like to thank my colleague, Frédéric Mérienne, from Arts et Métiers ParisTech, for his help in the organization of the DSC Europe 2012 conference, this year with a specific Exhibition area. I would also like to thank Stéphane Espié, from IFSTTAR, for his help in the publication of the conference proceedings under the form of this text book. I hope strongly that this book will help the readers to learn more about the latest technological and scientific advances in the domain of driving simulation and gain insight on the use driving simulators.

Constrained Linear Quadratic Optimal Controller for Motion Control of ATMOS Driving Simulator

Imad Al Qaisi [1], Ansgar Traechtler [1]

(1) Heinz Nixdorf Institute, University of Paderborn, Pohlweg 98, 33098 Paderborn, Germany
Email:{alqaisi, Ansgar.Traechtler}@hni.uni-paderborn.de
Tel : +49(0) 5251 605580 Fax : +49(0) 5251 605579

Abstract - *In this paper, a new model based motion cueing approach based on a constrained finite horizon linear quadratic optimal controller for ATMOS driving simulator is presented. In addition, a new approach is used to represent the sustained acceleration for the tilt coordination. The basic idea of the new approach is based on minimizing the difference between the perceived motions of the vehicle and the simulator. Compared to the conventional motion cueing algorithms, the proposed approach provides a more realistic impression, the workspace of the simulator is better exploited and all the constraints of the driving simulator are respected. Models of the human perception system in combination with simulator dynamic model are used to design the constrained linear quadratic optimal controller. The proposed controller has a feedback from the measured accelerations of the simulator and has a feedforward part from the reference trajectory.*

Keywords: *Driving simulators, Motion Cueing, Optimal control, Perception model, Online optimization.*

Introduction

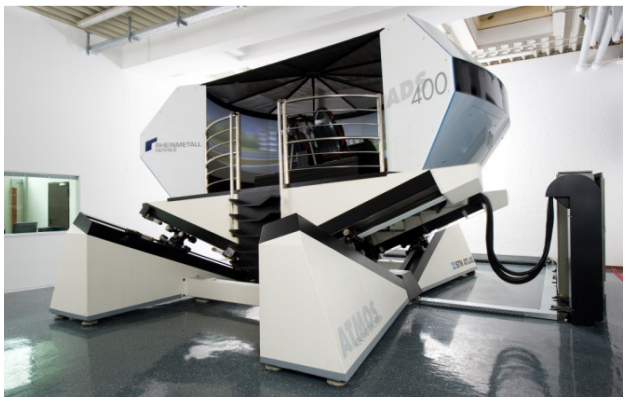

Figure 1: ATMOS Driving Simulator

Driving simulators are used in many different areas. They can be used for research purposes to study the behavior of the driver or develop and evaluate the new subsystems of the vehicle, or they can be used for training of drivers or for entertainment as in video games.

The general goal of any simulator is to give a realistic impression of the vehicle motion to the driver. Due to the limitations of workspace and the technological constraints of the motion systems, the vehicle translational accelerations and angular velocities generated by the vehicle dynamic model cannot be provided directly to the motion systems. Therefore, vehicle signals should be reproduced in a specific manner in order to produce admissible motion commands that could provide the simulator's driver in virtual reality environment the same feeling as in reality. The method that is used to reproduce the vehicle accelerations and velocities is commonly known as motion cueing algorithm.

One of the most widely used motion control strategies used for motion cueing is called classical motion cueing algorithm (figure 2). It was initially developed for the flight simulators [Sch21, Gra10]. This strategy is a combination of different linear filters used to render the vehicle signals by extracting a specific bandwidth from the vehicle signals. In this algorithm, the high pass filters are used to extract the transient part from the vehicle signals. Then, the extracted signals are single or double integrated to find the desired positions or angles. Since the workspace of the motion system is limited, the representation of the sustained component of the longitudinal and lateral vehicle accelerations is executed by tilting the moving platform. This mechanism is known as tilt coordination. The last stage of the classical motion cueing is the washout process which is required to bring the simulator back to its neutral position. The washout and the tilt coordination should be carried out under the perception thresholds of the driver [Rey20].

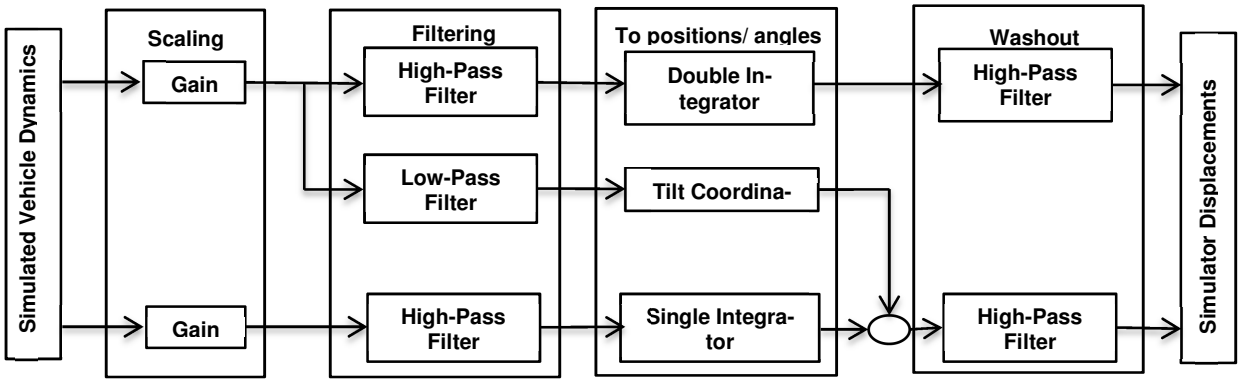

Figure 2: Classical Motion Cueing

Different algorithms based on the classical motion cueing algorithm have been developed to render the vehicle signals such as adaptive motion cueing where the parameters of the filters are changeable and computed at each time step of simulation [Rei18, Rei19, and Par17], and the optimal algorithm which uses high order filters chosen through an optimization method consisting of the human perception model in order to reduce the perception error between the driver at the vehicle and the driver at the simulator [Rei18, Rei19, Tel26, and Siv24].

The majority of developed approaches are based on extracting the transient and the sustained cues from the vehicle accelerations using linear high- and low-pass filters respectively [Neh15, Neh16]. The parameters of these filters (cutoff frequency, damping, and gain) are adjusted according to the worst case and tuned traditionally by trial and error heuristic procedures, therefore the constraints of the simulator are not always maintained and the workspace is not exploited very well. In addition, few model-based approaches have been developed for motion control of the driving simulators but they have some limitations [Dag6 and Aug1].

In this work, a completely different motion cueing approach based on the constrained linear quadratic optimal controller will be presented. The design of the linear quadratic optimal controller has been extensively discussed in the literature, see for example [Bri4, Chm5, and Sco22] and the idea of integrating the constraints in the controller has also been discussed in [Goo9].

Constrained linear Quadratic Optimal Controller

A. Driving Simulator Dynamics and Controller

The ATMOS driving simulator (figure 1) which is used at the Heinz Nixdorf Institute in University of Paderborn for research purposes has a projection system with 270° to view the details of the environments during the experiments and it is constructed from two dynamical parts with 5 degrees of freedom (DOFs). These two parts are independent of each other and the system is fully actuated. Therefore, each degree of freedom can be controlled independently. The first dynamical part is the moving platform (figure 3). It has 2 DOFs and is used to simulate the lateral and longitudinal accelerations of the vehicle. It can move in the lateral plane and at the same time it has the ability to tilt around lateral axis with a maximum angle of 13.5° and around the longitudinal axis with a maximum angle of 10°. Four linear actuators are used to control the movements in both directions. However, the control of each two actuators in each direction is done independently but synchronously. The second dynamical part is the shaker system (figure 4) which has 3 DOFs to simulate the roll and pitch angular velocities and the vertical acceleration of the vehicle. It is driven by three drive crank mechanism (three actuators).

Figure 3: Moving platform with cockpit

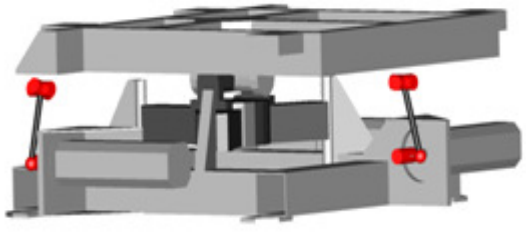

Figure 4: Shaker system

The two dynamical parts of the simulator are modeled independently and the principle of Newton-Euler is used to model the accelerations of the two dynamical parts in minimal coordinates. The dynamics of the moving platform and the shaker mechanical system can be written as:

$$M_q(q)\ddot{q} + h_q(q,\dot{q}) = Q_q(t) \quad (1)$$

where $\ddot{q},\dot{q},q$ represent the accelerations, velocities and positions(angles) respectively. $M_q(q)$ is the inertial matrix, $h_q(q,\dot{q})$ represents the gravitational and centrifugal forces and $Q_q(t)$ is the external forces and torques acting on the simulator during its motion.

To synthesize a controller for actuators of motion system, a controller based on the inverse dynamic technique which is known as computed torque method, is used to handle the high nonlinearities of the dynamics of the simulator. The computed torque controller generates the input command:

$$Q_q(t) = M_q(q)v + h_q(q,\dot{q}) \quad (2)$$

where v is the new control input to be designed. The typical choice of v is:

$$v = \ddot{q}_d + k_v(\dot{q}_d - \dot{q}) + k_p(q_d - q) \quad (3)$$

where q_d is the desired position. k_v and k_p are the gain matrices. It follows that the resulting linear error dynamics are:

$$\ddot{e}_q + k_v\dot{e}_q + k_p e_q = 0 \quad (4)$$

The error dynamics are exponentially stable by a suitable choice of the gain matrices.

It is important to note that this kind of control method converts the complicated nonlinear controller design into a simple design problem for linear system [Sic23]. By using this principle, the whole dynamic system can be assumed to be a linear and decoupled system. The following linear system represents the dynamics of the motion system for one degree of freedom

$$\begin{aligned} \dot{x}_m(t) &= A_m x_m(t) + B_m u_m(t) \\ y_m(t) &= C_m x_m(t) + D_m u_m(t) \end{aligned} \quad (5)$$

where $u_m(t)$ represents the acceleration control inputs of the motion system, $x_m(t)$ is the current state vector, $y_m(t)$ is the acceleration of the motion system, and A_m, B_m, C_m, D_m are matrices of proper dimensions.

B. Motion Perception System Dynamic Modeling

Human beings can detect the movements by the vestibular system which is located in the inner ear and it plays the main role to provide the perceptual system of the human beings with information about linear and angular inertial movements of the body. The vestibular system consists of two sensory parts, the semicircular canals that detect the angular motion and the otoliths organs that are sensitive to the translational motion and gravity i.e. specific force.

The biological phenomena which reflects the response of the vestibular system has been deeply studied [Fer7, Man13] and several dynamical models for the vestibular system based on empirical tests as well as describing it's working principle are available in the literature.

Young and Meiry [Mei14] modified the second order low pass filter otoliths model proposed by Meiry [You28] in order to model the response of the sustained acceleration. The resulting otoliths dynamical model has the following transfer function:

$$\frac{\hat{a}}{a} = 0.4\frac{0.06s+1}{(1+5.33s)(1+0.66s)} \quad (6)$$

where $\hat{a}$ is the perceived acceleration and a is the acceleration of the driver's head.

Young and Oman [You29] modified the semicircular canals dynamical model that was proposed by Steinhausen [Ste25], by integrating additional time constant to include the adaptation effect of the sustained angular acceleration. The proposed model that reflects the response of the perception organs to the rotation movements has the following transfer function:

$$\frac{\hat{\omega}}{\omega} = 5.41\frac{30s^2}{(1+5.3s)(1+0.1s)(1+30s)} \quad (7)$$

where $\hat{\omega}$ is the perceived angular velocity and ω is the angular velocity of the driver's head.

Therefore, state space differential equations corresponding to the Eq.6 and Eq.7 can be written as:

$$\begin{aligned} \dot{x}_{oto}(t) &= A_{oto}x_{oto}(t) + B_{oto}u_{oto}(t) \\ y_{oto}(t) &= C_{oto}x_{oto}(t) + D_{oto}u_{oto}(t) \\ \dot{x}_{sc}(t) &= A_{sc}x_{sc}(t) + B_{sc}u_{sc}(t) \\ y_{sc}(t) &= C_{sc}x_{sc}(t) + D_{sc}u_{sc}(t) \end{aligned} \quad (8)$$

where A_{oto}, B_{oto}, C_{oto}, D_{oto}, A_{sc}, B_{sc}, C_{sc} *and* D_{sc} are matrices modeling the vestibular system (filter).

The vestibular system of the humans can only detect the movements if they are above the perception thresholds. Many studies in series of experiments reported that the human detection threshold of the rotational movements is between 0.1°/s and 3.0°/s and the detection threshold of the linear motions is between 0.014 m/s^2 and 0.25 m/s^2. These detection threshold values depend on the duration of motion stimuli as well as the rates of the acceleration and they vary from person to person [Ste25, Ben2, Ben3, Gue11, Gun12, and Zac30].

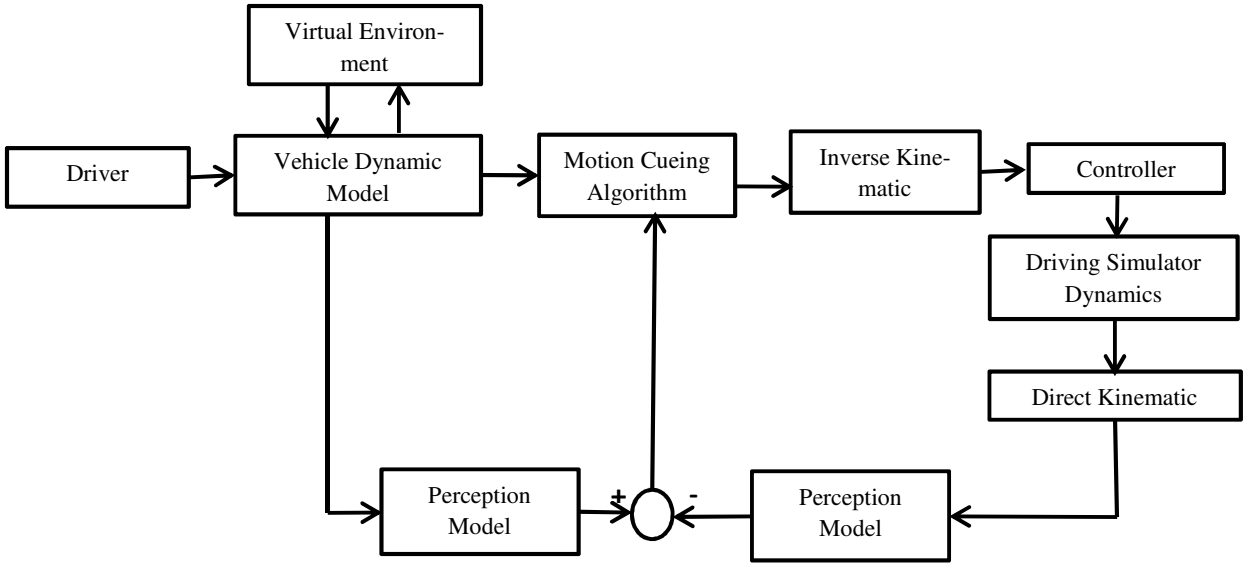

Figure 5: Motion Control Strategy

C. Constrained Linear Quadratic Optimal Controller

Figure (5) provides an overview of the block diagram of the proposed control strategy of the ATMOS driving simulator. The dynamic virtual reality model which consists of the vehicle dynamic model and the virtual environment generates according to the driver inputs, the movement trajectories which should be rendered by the motion cueing algorithm into restricted movements achievable by the simulator and at the same time gives the driver a realistic impression of the simulated vehicle motion.

The input signals of the driving simulators are the linear positions in longitudinal, lateral and vertical directions; the tilting angles resulting from the sustained longitudinal and lateral accelerations as well as the roll and pitch angles. The inverse kinematic modeling is used to determine the actuators angles by the given simulator middle point and the direct kinematic modeling is used to determine the middle point of the simulator by the given actuators angles.

In order to extract the acceleration that is used to calculate the tilt angle of the body of the driver around the x-axis and y-axis, the linear movement perception filter is used. By using this approach, many sensation dynamics missed by using the classical approaches are presented here and the rotation speed is done under the threshold of the perception model. In addition, the limitations on the extracted tilt coordination acceleration are guaranteed by using the proposed constrained linear quadratic controller.

The tilt angles can be calculated by [Rey20]:

$$\theta_{pitch} = sin^{-1}\left(\frac{a_{tilt-long.}}{g}\right), \theta_{roll} = sin^{-1}\left(\frac{a_{tilt-lateral}}{g}\right) \qquad (9)$$

where θ_{pitch} and θ_{roll} are the tilt angles around y-axis and x-axis respectively, $a_{tilt-long.}$ and $a_{tilt-lateral}$ are the extracted accelerations form the vehicle signals that are used to generate the tilt angles, and g is the acceleration of the gravity. The tilt rotation speed $\frac{d\theta_{roll}}{dt}$ and $\frac{d\theta_{pitch}}{dt}$ should be limited to the perception threshold of the semicircular canals.

In this proposed motion control approach, the comparison is carried out between the perceived signals at the vehicle and that at the simulator. Therefore, $a_{tilt-long.}$ and $a_{tilt-lateral}$ are added to the extracted transient accelerations that are used for linear movements of the simulator in longitudinal direction (a_x) and in lateral direction (a_y). Therefore,

$$\begin{aligned} a_{s/x} &\cong a_x + a_{tilt-long.} \\ a_{s/y} &\cong a_y + a_{tilt-lateral} \end{aligned} \qquad (10)$$

In order to simplify the notation, the matrices of the discrete state space model are denoted as in the continuous time models. The augmented discrete-time states $x_s = [x_m \quad x_{oto/sc} \quad x_{oto}]$ are the states of dynamic model of the simulator (x_m), the semicircular canals or otoliths dynamical model ($x_{oto/sc}$) and the states of the otoliths dynamical model (x_{oto}). Therefore, the augmented discrete-time state space differential equations can be defined as:

$$\begin{aligned} x_s(k+1) &= A_s x_s(k) + B_s u_s(k) \\ y_s(k) &= C_s x_s(k) + D_s u_s(k) \end{aligned} \qquad (11)$$

where

$$A_s = \begin{bmatrix} A_m & 0 & 0 \\ B_{oto/sc}C_m & A_{oto/sc} & 0 \\ 0 & 0 & A_{oto} \end{bmatrix}, \; B_s = \begin{bmatrix} B_m & 0 \\ B_{oto/sc}D_m & 0 \\ 0 & B_{oto} \end{bmatrix}$$

$$C_s = \begin{bmatrix} D_{oto/sc}C_m & C_{oto/sc} & C_{oto} & 0 \\ 0 & 0 & 0 & C_m \end{bmatrix}, \; D_s = \begin{bmatrix} D_{oto/sc}D_m & 0 \\ D_m & D_{oto} \end{bmatrix}$$

where u_s are the control inputs of the simulator and y_s are the perceived signal at the simulator, the velocity

and the position or angle of the simulator. A_s, B_s, C_s and D_s are matrices with appropriate dimensions.

In this strategy, an optimization problem is solved online over a finite time horizon (*N*). The objective of this optimization problem is to generate a control sequence that minimizes the difference between the perceived signals at the vehicle and the perceived signals at the simulator and keeps the simulator within its physical constraints and capabilities. The objective function that has to be minimized has the following form

$$J = \sum_{i=0}^{N-1} \left\| \left(\hat{a}_s(k+i|k) - \hat{r}(k+i|k)\right) \right\|_Q^2 + \left\| \Delta u_s(k+i|k) \right\|_R^2 \qquad (12)$$

subject to simulator constraints:

$$\begin{aligned} & x_s(k+1+i|k) = A_s x_s(k+i|k) + B_s u_s(k+i|k), \quad i = 0 \cdots N-1 \\ & y_s(k+i|k) = C_s x_s(k+i|k) + D_s u_s(k+i|k), \quad i = 0 \cdots N-1 \\ & x_{min} \le x_s(k+1+i|k) \le x_{max}, \quad i = 0 \cdots N-1 \\ & u_{min} \le u_s(k+i|k) \le u_{max}, \quad i = 0 \cdots N-1 \\ & y_{min} \le y_s(k+i|k) \le y_{max}, \quad i = 0 \cdots N-1 \end{aligned} \qquad (13)$$

where *J* is the cost function, $\hat{a}_s$ are the perceived reference signal at the simulator, the velocity and the position of the middle point, $\hat{r}$ is the perceived signal at the vehicle where $r(k) = \cdots = r(k+N-1)$, *R* and *Q* are positive definite weighting matrices, *k* is the computational step, and Δu_s are the input increments. Here the input increments are used instead of the input signals since in case of steady state, the input is not zero for offset free tracking but Δu_s is zero, therefore, by using Δu_s the cost function *J* is guaranteed to be consistent with zero tracking errors. Δu_s is defined as:

$$\Delta u_s(k) = u_s(k) - u_s(k-1) \qquad (14)$$

In order to bring the simulator back to its neutral position, additional reference signals are added to the perceived reference signals. The neutral position is added as a reference position for the actual position of the simulator and a velocity with a value less than the perception threshold of the linear motion, is set as a reference signal for the simulator actual velocity. By this additional reference signals, the simulator washout can be ensured which allows more freedom of movements for the next movements and avoids actuators saturation.

Now the fixed horizon optimal control problem (Eq.12 and Eq.13) for linear systems with quadratic cost function and linear inequality and equality constraints can be set up as a quadratic program. In the following part, the state, output and control sequences will be reformulated for the finite time horizon *N* for each computational step *k*.

The recursive state and output sequences from 0 to *N-1* can be written as:

$$\begin{aligned} & X(k) = \Psi_x x_s(k) + \Gamma_x u_s(k-1) + \Theta_x \Delta U(k) \\ & Y = \Psi x_s(k) + \Gamma u_s(k-1) + \Theta \Delta U(k) \end{aligned} \qquad (15)$$

where *X, Y* and $\Delta U(k)$ are the state, output and input increment sequences respectively, $\Psi_x, \Gamma_x, \Theta_x, \Psi, \Gamma$ and Θ are the recursive matrices of the state space model matrices A_s, B_s, C_s, and D_s. At steady state, where $\Delta u_s = 0$ and the free tracking error $E(k) = 0$, $R_{ref} = Y$. Therefore, the reference signal can be assumed as:

$$R_{ref} = \Psi x_s(k) + \Gamma u_s(k-1) + E(k) \qquad (16)$$

where *E(k)* is the tracking error.

Then, the unconstrained optimal solution of the cost function is:

$$\Delta U_{opt}^{uc} = \frac{1}{2} (\Theta^T \tilde{Q} \Theta + \tilde{R})^{-1} \Theta^T \tilde{Q} E(k) \qquad (17)$$

where $\tilde{Q}$ =blockdiag{*Q*,...,*Q*}, $\tilde{R}$ =blockdiag{*R*,…,*R*}.

Since $(\Theta^T \tilde{Q} \Theta + \tilde{R})^{-1}$ does not depend on the computational step *k*, it can be calculated offline.

From the last calculations, the equality constraints in the Eq.13 are eliminated by integrating them in the cost function. In order to handle the linear inequality constraints of the motion system, the inequality constraints can be represented as:

$$L \Delta u_s \le W \qquad (18)$$

where *L* is a matrix which consists of identity matrices and a combination of the state space matrices of the dynamical model (Eq.11) and *W* is a vector of all constrains of the motion system define in Eq.13. In *W* vector, the constraints on the output and the states are defined in terms of the last input control signal, the current estimation of the state vector and the limits of the motion system, therefore *W* vector should be calculated at each computational step, whereas *L* can be calculated offline.

Using the above formulation, the optimal solution $\Delta U(k)_{opt}$ of minimizing Eq.12 subject to the inequality constraints in Eq.13 can be expressed as a quadratic problem:

$$\begin{aligned} \Delta U(k)_{opt} = \underset{L\Delta u \le W}{\arg} \min_{\Delta U} & \Delta U(k)^T (\Theta^T \tilde{Q} \Theta + \tilde{R}) \Delta U(k) \\ & - 2 \Delta U(k)^T \Theta^T \tilde{Q} E(k) + E(k)^T \tilde{Q} E(k) \end{aligned} \qquad (19)$$

The matrix $(\Theta^T \tilde{Q} \Theta + \tilde{R})$ is called the Hessian of the quadratic problem. Since $\tilde{Q}$, $\tilde{R}$ and the Hessian matrix are positive definite, the quadratic programming problem is convex.

Many standard numerical quadratic programming algorithms are available to solve the above optimization problem such as the active set method [Goo9, Fle8] or interior point methods [Fle8, Wri27].

Since the controller is supposed to run continuously, a common way to apply the linear quadratic optimal

controller is by using only the first m rows of the calculated optimal controller, therefore

$$\Delta u_s(k)_{opt} = \lfloor I_m \quad 0_m \quad \dots \quad 0_m \rfloor \Delta U(k)_{opt} \qquad (20)$$

The designed controller here has a feedback from the measured accelerations of the simulator and has a feedforward part from the reference trajectory.

Simulation Results

Since the ATMOS driving simulator is fully actuated, the control of each degree of freedom will be carried out independently but synchronously. ATMOS driving simulator features a unique moving platform structure. Basically, this moving platform features unique motion capabilities in terms of combined motion i.e. when the simulator moves in longitudinal or lateral direction, it has the ability to rotate (tilt) around the y-axis or x-axis respectively with tilting angular velocity under the perception threshold of the semicircular canals. Therefore, a major part of the sustained acceleration will be rendered directly through the movements of the moving platform and the other part will be rendered through tilting the shaker system i.e. adding the resulting tilt angle to the corresponding angle generated by rendering the roll and pitch velocities of the vehicle.

In this section, simulation results show the performance comparison between the classical motion cueing algorithm and the proposed motion control method. The Automotive simulation model(ASM-dSPACE) is used to generate the accelerations of the vehicle. A scenario of normal driving situation consisting of an assortment of accelerations, decelerations and braking maneuvers is carried out. The generated translational accelerations and angular velocities by ASM are used as reference inputs for the motion control strategies. The simulations are executed by using Matlab/Simulink. In this part, simulation results only show the rendering of the longitudinal acceleration and the pitch velocity and the remaining degree of freedoms are rendered in a similar manner. The parameters of the classical motion algorithm are adjusted to keep the simulator within its constraints and the positive-definite weighting matrices R and Q are chosen by trial and error to guarantee the best tracking of the perceived signals at the vehicle. Table 1 shows the capabilities of ATMOS driving simulator and figures 6 and 7 show the workspace of the shaker and moving platform respectively.

Table (1) ATMOS driving simulator capabilities

	Displ.\Rotation	Velocity	Acceleration
Longitudinal	±733 (mm)/ ±13.5°	±1.3 m/s	±3 (m/s^2)
Lateral	±522 (mm)/ ±10°	±1 m/s	±2.2 (m/s^2)
Vertical	±72.5 (mm)	±0.6 m/s	±4 (m/s^2)
Pitch	±7 (°)	±50 (°/s)	±360 (°/s^2)
Roll	±7 (°)	±50 (°/s)	±360 (°/s^2)

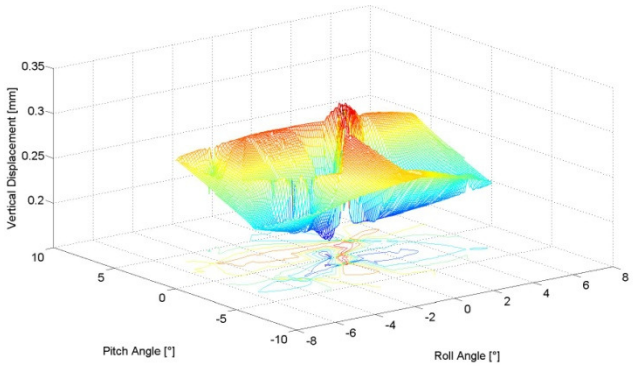

Figure 6: Shaker workspace

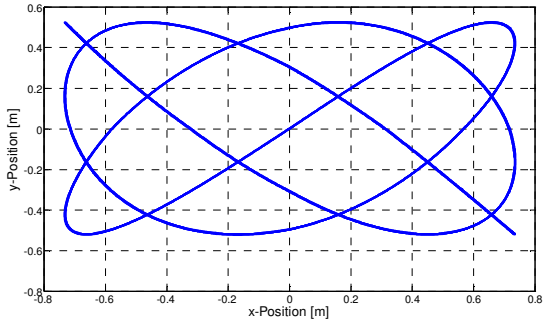

Figure 7: Moving platform workspace

In order to validate the modeling of ATMOS driving simulator such as in longitudinal direction, a sinus signal with different amplitude is applied to the two linear actuators of the simulator. Figure 8 shows a good matching between the measured and modeled longitudinal acceleration.

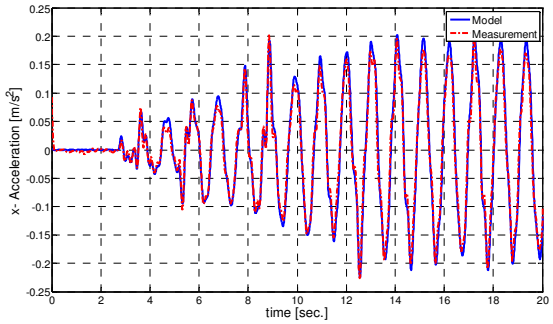

Figure 8: Acceleration in x- direction

Figure 9 shows a comparison between the transient acceleration of the platform and the vehicle longitudinal acceleration. However, Figures 10 and 11 show a comparison between the perceived signals at the simulator generated by the classical motion cueing algorithm and by the new approach as well as the perceived signal at the vehicle. The results show a very good matching between the two perceived signals at the driving simulator generated by the new approach and at the vehicle.

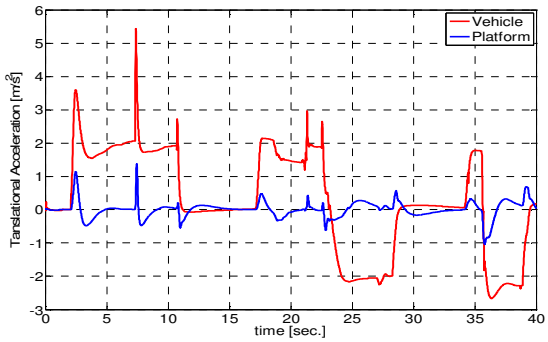

Figure 9: Vehicle and platform translational acceleration

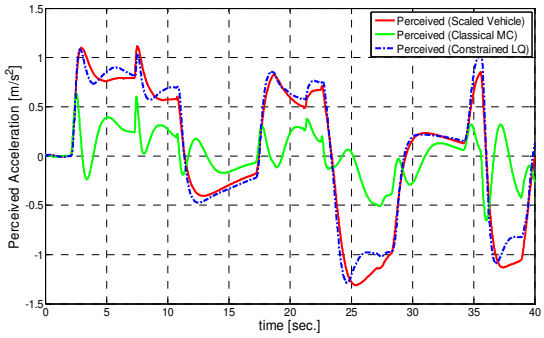

Figure 10: Perceived longitudinal acceleration

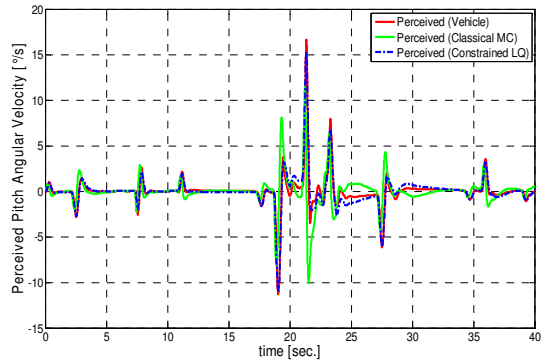

Figure 11: Perceived pitch angular velocity

Figure 12 shows the tilting angular rate generated by the new approach. It is clear that the tilting velocity is guaranteed to be under the detectable thresholds of the perception system of the driver.

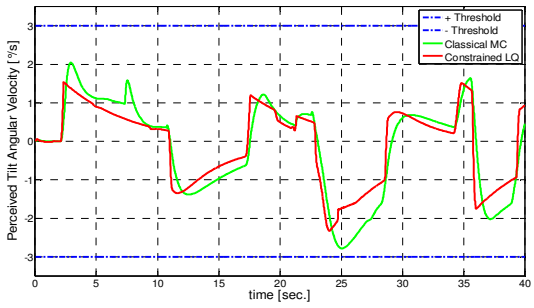

Figure 12: Tilting angular rate

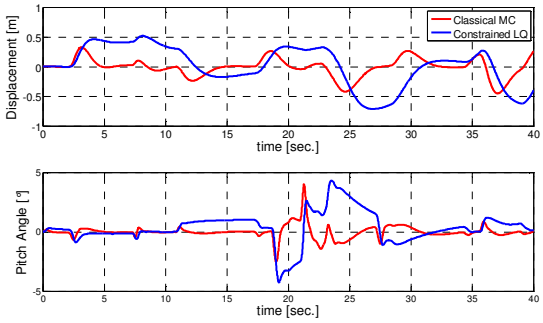

Figure 13: Longitudinal displacement and pitch angle

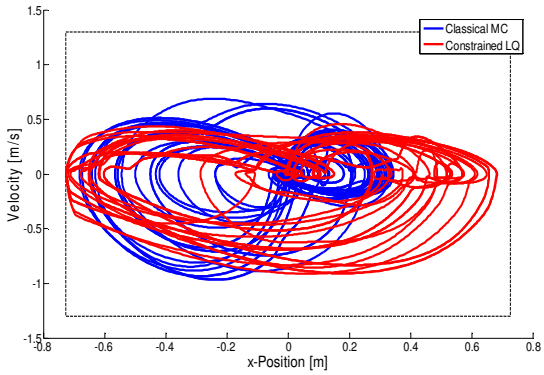

Figure 14: Exploited workspace during 5 minutes of simulated driving session

Conclusion

The purpose of the motion cueing algorithms is to render the physical movements of the vehicle so that the driver of the simulator perceives the motion in virtual environment similar to reality. The new motion control strategy based on the constrained linear quadratic optimal controller was developed with a focus on reducing the perception difference between the perceived signal at the simulator and the perceived signal at the vehicle. Therefore, the proposed optimal controller provides the simulator with sequences of control signals that minimize the difference between the perceived acceleration at the vehicle and the perceived acceleration at the simulator and take into account the simulator constraints and capabilities.

A case study was conducted by two trajectories to compare the performance of the proposed model-based approach with the classical motion cueing algorithm. From the simulation results, it can be stated that the proposed approach provides more realistic impression than the conventional classical motion cueing and the exploited workspace is much better. In addition, the constraints of the simulator are always respected.

In future, the new constrained linear quadratic optimal controller will be implemented on the ATMOS

driving simulator and a subjective quality criterion will be carried out to compare this new approach with the conventional well know approaches.

Acknowledgment

The authors would like to thank the International Graduate School of Dynamic Intelligent System at the University of Paderborn for the financial support of this research.

References

[Aug1] Augusto, B.; Loureiro, R.:Motion Cueing in the Chalmers Driving Simulator: A Model Predictive Control Approach. Master thesis, Chalmers University of Technology, Goeteborg, 2009.

[Ben2] Benson, A.: Thresholds for the perception of whole body angular movement about a vertical axis. Aviat., Space Environ.Med., vol. 60, pp. 205-213, 1989.

[Ben3] Benson, A.J.: Sensory functions and limitations of the vestibular systems, in: Perception and Control of Self Motion, R.Warren and A.H. Wertheim, eds, Laurence Erlbaum Associates, Hinsdale, New Jersey, pp. 145–170, 1990.

[Bri4] Brian D. O. Anderson and John B. Moore. Optimal Control. Linear Quadratic Methods. Prentice Hall, Englewood Cliffs, NJ, 1990.

[Chm5] Chmielewski, D. and Manousiouthakis, V.: On Constrained Infinite-Time Linear Quadratic Optimal Control. Systems and Control Letters, vol. 29, pp. 121-129, 1996.

[Dag6] Dagdelen, M.; Reymond, G.; Kemeny, K.; Bordier, M.; and Maýzi, N.: Model-based predictive motion cueing strategy for vehicle driving simulators. Control Engineering Practice, 2009.

[Fer7] Fernandez, C. and Goldberg, J. M.: Physiology of Peripheral Neurons Innervating Otolith Organs of the Squirrel Monkey, I: Response to Static Tilts and to Long Duration Centrifugal Force. Journal of Neurophysiology, vol. 39, no. 5, pp. 970-983, 1976.

[Fle8] Fletcher, R.: Practical Methods of Optimization. John Wily \& Sons Ltd., 1987.

[Goo9] Goodwin, G.; Seron, M.; and Doná, J.: Constrained Control and Estimation: An Optimization Approach, Springer, Berlin, 2010.

[Gra10] Grant, P. R. and Reid, L. D.: Motion washout filter tuning: Rules and requirements, Journal of Aircraft, vol. 34, pp. 145-151, March-April, 1997.

[Gue11] Guedry F.E.: Psychophysics of vestibular sensation. In: Handbook of Sensory Physiology (Kornhuber H.H. (Ed.)), vol. V1/2, pp.3-154. Springer Verlag: Berlin, Heidelberg, New York, 1974.

[Gun12] Gundry, A. J. Thresholds of perception for periodic linear motion. Aviation, Space, and Environ. Med.,vol. 49, pp. 679-686, 1978.

[Man13] Mann, C.W. and Ray, J.: Absolute thresholds of perception of direction of angular acceleration. Joint Proj. Report No.41. Naval School of Aviation Medicine, Pensacola, FL, 1956.

[Mei14] Meiry, J. L.: The vestibular system and human dynamic space orientation. Ph.D. thesis, MIT, Cambridge, 1965.

[Neh15] Nehaoua, L.; Arioui, H.; Espie, S.; and Mohellebi, H.: Motion cueing algorithms for small driving simulator. IEEE International Conference on Robotics and Automation. Orlando, Florida, May 2006.

[Neh16] Nehaoua, L.; Mohellebi, H.; Amouri, A.; Arioui, H.; Espié, S.; and Kheddar, A.: Design and control of a small-clearance driving simulator. IEEE Transactions on Vehicular Technology, vol. 57, no. 2, pp. 736-746, March 2008.

[Par17] Parrish, R. V.; Dieudonne, J. E.; Bowles, R. L. and Martin, D. J.: Coordinated Adaptive Washout for Motion Simulators. Journal of Aircraft, vol. 12, pp. 44-50, July 1975.

[Rei18] Reid, L. D. and Nahon, M. A.: Flight Simulation Motion-base Drive Algorithms: Part 1 - Developing and Testing the Equations, UTIAS Report No. 296, University Of Toronto, 1985.

[Rei19] Reid, L. D. and Nahon, M. A.: Flight Simulation Motion-base Drive Algorithms: Part 2 - Selecting the System Parameters, UTIAS Report No. 307, University Of Toronto, 1986.

[Rey20] Reymond, G. and Kemeny, A.: Motion Cueing in the Renault Driving Simulator. Vehicle System Dynamics, vol. 34, no. 4, pp. 249-259, 2000.

[Sch21] Schmidt, S.F. and Conrad, B.: Motion drive signals for piloted flight simulators. Technical Report CR-1601,NASA, 1970.

[Sco22] Scokaert, P. O. M. and Rawlings, J. B.: Constrained Linear Quadratic Regulation. IEEE Trans. Automat. Contr., vol. 43, pp. 1163-1169, 1998.

[Sic23] Siciliano, B. and Khatib, O.: Springer Handbook of Robotics. ISBN 978-3-540-23957-4, Springer, 2008.

[Siv24] Sivan, R.; Ish-shalom, J.; and Huang, J.: An optimal control approach to the design of moving flight simulators. IEEE Transactions on Systems, Man and Cybernetic, vol. 12, pp. 818-827, July-Aug. 1982.

[Ste25] Steinhausen,W.: Ueber den Nachweis der Bewegung der Cupula in der intakten Bogengangsampulle des Labyrinthes bei der natuerlichen rotatorischen und calorischen Reizung. Pflueg. Arch. Ges. Physiol, vol. 228, no. 1, pp. 322-328, 1931.

[Tel26] Telban, R. J. and Cardullo, F. M.: Motion Cueing Algorithm Development: Human-Centered Linear and Nonlinear Algorithms, NASA CR-2005-213747, NASA Langley Research Center, Hampton, VA, 2005.

[Wri27] Wright, S.: Primal-Dual Interior-Point Methods. Philadelphia, PA: SIAM. ISBN 0-89871-382-X, 1997.

[You28] Young, L. R.; Meiry, J. L.; and Li, Y. T.: Control engineering approaches to human dynamic spatial orientation. In Second symposium on the role of the vestibular organs in space exploration, pp. 227-229, Ames Research Center, 1968.

[You29] Young, L. R. and Oman,C.M.: A model for vestibular adaptation to horizontal rotaion. Aerospace Medicine, vol. 40, no.10, pp.1076-1080, 1969.

[Zac30] Zacharias, G.L.: Motion cue models for Pilot Vehicle Analysis. Technical Report, AMRL-TR-78-2. Cambridge, 1978.

Exploring Travelers' Behavior in Response to Variable Message Signs Using a Driving Simulator

Anam Ardeshiri [1], Mansoureh Jeihani [2], Shiva Narooienezhad [3]
(1) Doctorate Candidate, Department of Transportation and Urban Infrastructure Studies, Morgan State University, 1700 E. Cold Spring Lane, Baltimore, MD 21251, E-mail: anard1@morgan.edu
(2) Associate Professor, Department of Transportation and Urban Infrastructure Studies, Morgan State University, 1700 E. Cold Spring Lane, Baltimore, MD 21251, E-mail: mansoureh.jeihani@morgan.edu
(3) Graduate Research Assistant, Department of Transportation and Urban Infrastructure Studies, Morgan State University, 1700 E. Cold Spring Lane, Baltimore, MD 21251, E-mail: shnar1@morgan.edu

Paper Summary

Variable Message Signs (VMS) have been increasingly utilized in the United States. Transportation agencies strive to ensure that posted messages are consistently informative – especially regarding incidents – so that drivers can make the appropriate decision regarding the recommended or desired route to take without significantly reducing their speed in order to read the message displayed. However, drivers respond to VMS messages differently and their reaction to the displayed messages will affect the usefulness of these signs [Pee3]. With this in mind, a study to identify the human factors involved (driver perception, reaction time, etc.) when displaying travel and safety related messages will help transportation agencies to assess the effectiveness of existing VMS message formats, make changes where necessary, and promote driver education and awareness.

Driving simulator can be a useful tool to make identical controlled traffic and environmental scenarios for each driver and observes their behavior. There are very few studies to use driving simulator to identify the drivers' behavior in response to VMS [Dut1]. However, most of the existing simulators allow the drivers to drive on a route of a pre-determined scenario and have limited number of choices over an imaginary network [Kou2]. This study employs a driving simulator which is capable of supporting a realistic route selection environment.

The authors built a midsize (20*20-km) real road network, in Baltimore, Maryland. The network was constructed using the driving simulator software, UC-Win Road, which is accurate and realistic with respect to road geometry, interchanges, intersections, and traffic signals, in addition to roadside objects (signs, buildings, trees, sidewalks, and VMSs) to represent the real world environment. Different scenarios of traffic regimes, time of day, weather conditions, and various VMS messages was provided. The driver received travel time information for two major alternative routes toward a predefined destination from the first VMS, and decided to take one of them or a third route that is mainly local roads and VMS does not show its travel time information. Drivers were subject to the second VMS with supplementary traffic information. All the test subjects were given a fixed pair of origin-destination and were free to decide their routes. The subjects were from different ages, gender, network familiarity, and socio-economic backgrounds to have a fairly unbiased sample. Fig. 1 shows the VMS on the driving simulator while a subject is driving.

Fig. 1. VMS simulation with the driving simulator.

The drivers' choices and performance measures (speed, actual travel times, and reaction time) were recorded. After driving each scenario, the participants' perceived travel time was asked in order to develop a learning process in response to the contents of VMS. Three questionnaires were also given to the participants. The first one captured participants' age, gender, socio-economic information, their usage of navigation systems and ATIS, and their general attitudes about VMS. The second one was a stated preference questionnaire asking participants which route they would take in each hypothetical scenario with different VMS information before they actually drive the simulator. This stated preference data was then compared to their revealed preferences. The third questionnaire was given to the subjects after the driving task. It mostly addressed their perceived travel time, experience with the VMS and the accuracy of the information given to them, if their idea toward the reliability of applying ATIS has been changed, and what they learned about each route after driving on the network several times. The results of the questionnaires were used to compare the drivers' intention and perceptions with reality.

The collected data from the simulator as well as the questionnaires were processed and a data-base was made to present drivers' responses and choices as well as their attitudes and perceptions along with their socio-economic information. This study conducts statistical analysis and discrete choice models to find the effectiveness of VMS and analyze drivers' diversion decisions. Assuming shortest path as a base choice, driver's route diversion in response to different travel time information on the VMS is formulated with respect to various factors as Eq. 1. The effect of real travel time on the diversion probability demonstrates the effectiveness of VMS content. According to survey questionnaires and preliminary analysis of drivers' choice, road familiarity, aesthetic, and road safety along with driver demographic explain the route diversion significantly.

$$\textit{Diversion rate} = F(\Delta T, PT, PC, f, A) \qquad (1)$$

Where:

ΔT = real travel time difference

PT = perceived travel time of the current route

PC = past route choice

f = familiarity

A = route aesthetic

Recent studies argued that travel time is not the only factor affecting traveler's route choice and many novel determinants are perceived to be significant. Environmental components and human characteristics, along with real time information influence driver's route choice with different trip purposes. In addition, it is shown that cognitive route knowledge explains route choice behavior better than perceived route attributes, which itself is a better explainer of route choice than observed attributes [Zha4]. The result of this study demonstrates that slight differences in travel time (e.g. 5 min in a 30 min trip), may not cause drivers, in particular commuters, to divert to a new route. This may happen basically because of the consequence of past experiences compared to the reliability of VMSs. There is however an uncertainty with different drivers' perception of travel time, which varies likely by drivers' value of time, familiarity, and trip purpose.

References

[Dut1] Dutta, A., Fisher, D. L., and Noyce, D. A. "Use of a Driving Simulator to Evaluate and Optimize Factors Affecting Understandability of variable Message Signs". *Transportation research Part F*, 2004, 7(4-5), pp. 209-227.

[Kou2] Koutsopoulos, H. N., Lotan, T., and Yang Q. "A driving simulator and its application for modeling route choice in the presence of information". *Transportation Research Part C*, 1994, 2 (2), pp. 91–107.

[Pee3] Peeta, S., Romas, L. J., and Pasupathy, R. "Content of Variable Message Signs and On-line Driver Behavior". *79th TRB Annual Meeting*, 2000, Washington, D.C.

[Zha4] Zhang, L., Levinson, D. "Determinants of Route Choice and Value of Traveler Information". *Transportation Research Record*: Journal of the Transportation Research Board, 2008, 2086, pp. 81-92.

Motion Analysis of a Wheeled Mobile Driving Simulator for Urban Traffic Situations

Alexander Betz[1], Hermann Winner[2], Marc Ancochea[3], Maren Graupner[4]
(1) Technische Universität Darmstadt, Institute of Automotive Engineering, Petersenstraße 30, 64287 Darmstadt, E-mail : betz@fzd.tu-darmstadt.de
(2) Technische Universität Darmstadt, Institute of Automotive Engineering, Petersenstraße 30, 64287 Darmstadt, E-mail : winner@fzd.tu-darmstadt.de
(3) Technische Universität Darmstadt, Institute of Automotive Engineering, Petersenstraße 30, 64287 Darmstadt, E-mail : marc.ancochea_vilaplana@stud.tu-darmstadt.de
(4) Technische Universität Darmstadt, Institute of Automotive Engineering, Petersenstraße 30, 64287 Darmstadt, E-mail : graupner@stud.tu-darmstadt.de

Abstract *– The simulation of urban traffic has higher system requirements than that of motorway traffic for driving simulators. The motion information characteristic of urban traffic easily exceeds the motion envelope available for state of the art driving simulators. Augmenting translational motion by rail systems results in increasing moving mass and insufficient system dynamics. The presented wheeled mobile driving simulator (WMDS) moves on powered and active steerable wheels and solves the announced core problems. A feasibility analysis is conducted concerning energy, power and friction demand for a real world test drive on an urban traffic circuit. The presented results prove that a friction limited propulsion system, like the WMDS concept is suitable for performing driving simulation. Energy and power demand are also feasible with regard to state of the art battery technology. The promising new approach allows the combination of a large motion envelope with high system dynamics into a high fidelity driving simulator (DS).*

Key words: *"ideal" motion cueing, wheeled mobile driving simulator, urban traffic simulation.*

Introduction

Driving simulators (DS) are an established development tool in the automotive industry. The versatile areas of application all profit from a high degree of reproducibility and safety. One area of application is the development and evaluation of Advanced Driver Assistance Systems (ADAS). For the analysis of safety critical situations concerning driver behavior and human machine interaction, DS constitute the only adequate tools. For the last decade, the development of ADAS was mainly focused on assistance systems for motorway traffic. ADAS such as, Adaptive Cruise Control or Lane Departure Warning and Lane Keeping Support were developed. Advancements in technology combined with gained knowledge of the development of ADAS led to an increase in effort with focus on urban traffic situations. The main reasons for urban traffic accidents are human errors in common traffic situations such as, turning, U-turning, drive-away and reversing [DES1], [DES2], [DES3]. The upcoming demands for ADAS, with respect to urban traffic situations, result in increasing DS requirements, concerning motion envelope and system dynamics. The increasing requirements arise from the decreased velocity level in urban traffic situations, resulting in higher traction forces. Hence, the average magnitude of the horizontal acceleration vector is higher for urban traffic than for motorway traffic. In addition to the addressed increase of dynamic behavior, urban traffic is characterized by more complex interaction between the driver and his surroundings, including pedestrians, crossing vehicles, traffic signs/lights and lighting conditions. This fact requires further tasks for urban traffic simulation which are not addressed in this paper. DS are usually based on hexapod systems that provide 6 degrees of freedom (DOF). Real world vehicle motion also consists of 6 DOF, however surge (X-direction), sway (Y-direction) and yaw (rotation about Z-axis, ψ) have unlimited stroke, whereas pitch (rotation about Y-axis), roll (rotation about X-axis) and heave (Z-direction) show high frequent behavior with strongly limited stroke. The motion simulation of the unlimited vehicle surge, sway and yaw easily exceeds the physical limits of hexapod systems, imposed by the workspace. On the contrary, the limited pitch, roll and heave motion are adequately simulatable by hexapod systems. In order to fulfill the increasing requirements caused by urban traffic simulation, supplementary actuated subsystems have to be added to the

hexapod — additional DOF are the consequence. Modern-day DS show up to 10 DOF and have reached remarkable quality in simulating real world driving experiences. These improvements incur great costs to system complexity and increasing moving mass of about 80 t [Cla1]. Along with the redundant DOF, the main reason for high moving mass results from the rail systems used to connect the tilt system to the ground. This connection is necessary to resolve the strongly limited translational motion envelope of hexapods. As a result, a linkage between moving mass and motion envelope is caused, thus, limiting motion envelope and system dynamics.

Alternative Concept

General Idea

Wheeled Mobile Driving Simulators (WMDS) solve the core problem of the linkage between moving mass and motion envelope. The main idea is based on the assumption that a system, whose propulsion is limited by friction forces, must be capable of simulating the dynamics of vehicles that are also limited by tire friction forces. The idea of a WMDS is addressed by a patent held by BMW AG [Don1] and a reference by Slob [Slo1]. The references do not deal with feasibility of WMDS. The most important questions are not yet answered and the basic assumption must still be analyzed. In order to analyze the basic assumption, the expected mass reduction and the electric power supply, the following system assembly is considered (Fig. 1).

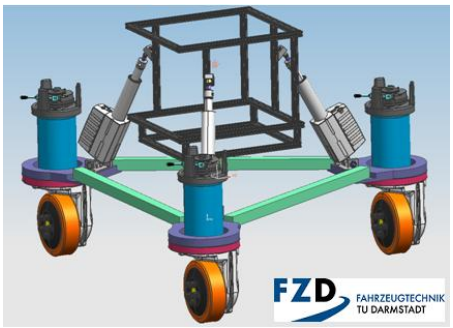

Fig. 1. New approach - WMDS assembly

The presented work is based on a specific assembly of a WMDS showing two subsystems – a wheeled mobile platform and a tilt system (Fig. 1). Each subsystem provides 3 DOF. The wheeled mobile platform includes three powered and active steerable wheels, allowing simulation in 3 unlimited DOF of vehicle motion: surge (X), sway (Y) and yaw (ψ). On top of the platform a tripod system is mounted providing cabin tilt and heave. Tilting the driver is necessary for two reasons. First, translational acceleration can be simulated by cabin tilt due to false perception of gravity. Second, the limited vehicle motion has to be performed – pitch, roll and heave. The required tilt motions show different characteristics. The tilt motion for acceleration simulation is of low frequent and high stroke, whereas the aforementioned vehicle motions are of high frequent and little stroke. Therefore, a decoupling is intended to reduce the overall moving mass by optimizing the properties of the separate tilt systems. The depicted tilt system in Fig. 1 is optimized to tilt about the driver's head position and is used for rotating the whole cabin in order to simulate translational acceleration only. The vehicle pitch, roll and heave motion is not considered further at the current level of research. It is planned to perform these motions by a separate system that only tilts the driver and his vehicle mockup about a point below the driver seat. The additional system has to be installed between the driver seat and cabin structure and also must be optimized for the high frequent motion showing little stroke.

The design shows system immanent stroke, matching real world vehicle motion. Hence, the system is meant to be a lightweight concept. It seems to be promising for next generation of high fidelity DS that allow simulation of a wide range of traffic situations and high system dynamics.

Wheeled Mobile Driving Simulator Characteristics

The dimensions of the cabin tilt system that are necessary for calculating dynamic actuator load are listed in Table 1 and named accordingly to Fig. 2.

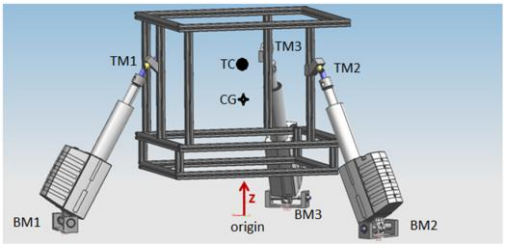

Fig. 2. Design of cabin tilt system

Table 1. Specifications of cabin tilt system

Description	Symbol	Cylindrical coordinates		
		r /m	φ /rad	Z /m
Tilt center for initial condition	TC	0	0	2,15
Center of gravity of cabin for initial condition	CG	0	0	1,65
Top-mount of linear actuator for initial position	TM1	1,43	0	2,15
	TM2	1,52	2,09	2,15
	TM3	1,52	4,19	2,15
Bottom-mount of linear actuator for initial position	BM1	2,6	0	0
	BM2	2,6	2,09	0
	BM3	2,6	4,19	0

The estimation of the WMDS mass properties is based on the PSA Peugeot-Citroën DS [Cha1]. The cell weight repartition of the PSA DS is adapted to the WMDS. A worst and best case estimation is

assumed. The worst case results mainly from a conservative point of view which utilizes state of the art visual systems. The best case results on an outlook of what could be reached in the near future when using enhanced head mounted displays and virtual reality. The honeycomb structure is the heaviest component of the cabin and has to provide sufficient stiffness for moving its first natural frequency above the operating frequency bandwidth. Hence, its mass decreases with reduced cabin mass and dimensions. Fewer fixation devices and bushings are required due to the tripod system concept. The body shell and vehicle standard equipment is reduced to its minimum. The technological progress in the field of visual systems is expected to compensate leaking impression due to the reduction of the vehicle mockup. Further components listed in Table 2 are transferred unchanged. In total the cabin shows an expected mass of about 310 to 550 kg, depending on the degree of virtualization.

Table 2. Mass repartition of cabin

Major components of cabin	PSA [Cha1] /kg	WMDS /kg	
		worst case	best case
Visual system (projectors etc.) including retro vision	30	30	10
Composite honeycomb structure	250	210	150
Fixation device, bushings	40	30	30
Vehicle cab (body shell)	160	100	0
Vehicle standard equipment (dashboards, seats, etc.)	150	100	40
Acoustic reduction material	30	30	30
Passive force feedback system	30	30	30
Steering wheel feedback system	20	20	20
Cabin Mass	**710**	**550**	**310**

A tripod system, comprising three linear actuators, is used for performing cabin tilt. In order to establish a non-ambiguous relation between actuator stroke and cabin tilt, the top-mounts are designed as cardan joints (2 DOF) while the bottom-mounts show one rotational DOF only. The design leads to a 3 DOF motion system, where translational and rotational motion of the tilt center is coupled by the joint constrains. The unsolicited translational motion for the presented system design shows acceleration values that are about one dimension below human perception thresholds. As a result, the coupled motion does not have to be considered further. The actuators are mounted between the base frame and the cabin structure. The components of the tilt system are supposed to amount to a mass of about 400 kg. The wheeled platform carries the tilt system, a base frame, energy supply and three drive units, each consisting of a tire, a steering motor, a gearbox and a drive motor. The used gearbox descends from forklift trucks and allows both motors to be mounted to the base frame [ZF1]. For this reason, necessary connections (cable, cooling, etc.) are possible without additional effort. In total, the first draft of the wheeled platform is expected to show a mass of about 1250 kg, as shown in Table 3.

Table 3. Mass repartition of wheeled platform

Major components of the wheeled platform	Component mass /kg
Tripod tilt system	400
Base frame	200
Energy supply (electric vehicle battery: 16 kWh) [Kna1]	250
Drive units ($M_{0,Drive}$ 90 Nm; $M_{0,Steering}$ 6,5 Nm)	300
Cooling, power electronics, etc.	100
Wheeled platform mass	**1250**

The total system mass of the WMDS, consisting of the cabin, the wheeled platform and a $Q_{.95}$ male person (100 kg) [DIN1], is expected to be in a range between 1660 and 1900 kg, depending on the degree of virtualization.

Methodology

The stated questions concerning feasibility of a WMDS for urban traffic require property identification of urban traffic. Therefore, a representative urban traffic circuit is identified and used for test drives to measure representative motion information (Chapter: *Test Drive*). To answer the feasibility question, detailed information about the WMDS motion is necessary. Hence, the measured target acceleration profiles, from the test drives, have to be transformed into a target trajectory of the WMDS. A trajectory generation is therefore required. Due to the solved linkage between moving mass and motion envelope, an “ideal” motion cueing algorithm (MCA) is used that doesn’t consider translational workspace limitations (Chapter: *Motion cueing Algorithm*).

Based on the moving mass estimation and the generated trajectories, physical relations are applied to determine friction, power and energy demand for high fidelity urban traffic simulation (Chapter: *Calculation of Power, Energy and Friction Demand*).

Implementation

Motion Cueing Algorithm

The “ideal” MCA (Fig. 3) calculates the target DS states that are necessary to perform the target motion information input. The basic idea is to allow as much acceleration simulation from tilt as possible, while considering human perception thresholds for cabin tilt. Therefore, a 2nd order low-pass filter (LPF) is used to determine the change of translational acceleration performed by cabin tilt. The parameterization of the used LPF has to fit human perception thresholds and is tuned for the target acceleration profiles of the discussed test drives on the urban traffic circuit. References show thresholds in a range of 0,05 to 0,2 rad/s for rotational rate and

rotational acceleration from 0,03 to 0,1 rad/s² [Dur1], [McC1], [Dob1], [Dag1], [Cla1]. The used thresholds for rotational rate are 0,1 rad/s and 0,1 rad/s² for rotational acceleration. Furthermore, a rate limiter is implemented that limits the LPF output rate if human perception thresholds are harmed.

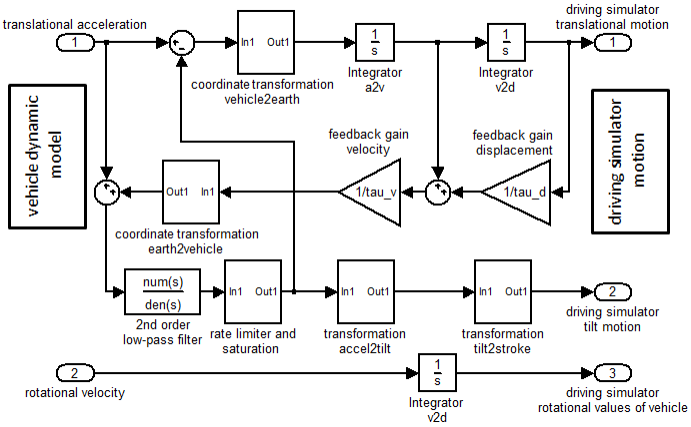

Fig. 3. "Ideal" motion cueing algorithm

The acceleration realized by cabin tilt is subtracted from the target acceleration and leads to the part of acceleration that has to be performed by translational motion. With the described method, an "ideal" motion simulation is reached, considering the usual adverse effects due to tilt. To determine the simulator trajectory, the translational part of acceleration is transformed from vehicle fixed to earth fixed coordinates and then integrated twice. The washout is implemented as a feedback gain of DS velocity ($1/\tau_v$) and displacement from origin ($1/\tau_d$). The stability analysis refers to the loop gain, derived from Eq. 1 and gives a lower boundary for the product of the two feedback gains. The parameter *c* is used to tune the stability margin in view of the Nyquist criterion. According to the analytical limit, the gains are tuned iteratively in order to reduce the required motion envelope for the introduced urban traffic circuit. The physical limitation of cabin tilt is recognized by a saturation block that avoids simulating more than 0,4 *g* translational acceleration by tilt.

$$T = \left(\frac{1 + j\omega\tau_d}{(j\omega)^2 \tau_d \tau_v} \right) \cdot \mathrm{LPF} \qquad (1)$$

$$T = \left(\frac{1 + j\omega\tau_d}{(j\omega)^2 \tau_d \tau_v} \right) \frac{1}{1 + aj\omega + b(j\omega)^2} = -c, c \le 1, \tau_v \ge 0, \tau_d \ge 0$$

Test Drive

The urban traffic circuit is based on an analysis of 130 randomly chosen traffic situations situated in Darmstadt, Germany. The analysis determines the relative frequency of traffic situation categories: crossroads, T-crossroads, bends, lane splitting and merge. The characteristic properties of these categories are analyzed: lane width, number of lanes, speed limit, curvature, distance of road splitting/merging and priority signs. The most representative ones are assembled to make up the Darmstadt urban traffic circuit, considering the relative frequency. In total, 25 representative traffic situations are selected and fitted into a road map. The connection of the relevant situations is determined by *Google Maps* and is slightly adapted in order to improve practicability. The urban traffic circuit is 21 km long and takes about one hour per turn. In total, four urban test drives are analyzed.

The 229 km long motorway traffic circuit used refers to Filzek [Fil1] and represents German motorways. It takes about two hours per turn. Because of its length, it is split into three parts and evaluated separately. Motorway exits and ramps are not part of the circuit. In total, six parts of the motorway test drives are conducted and evaluated.

The test drives are performed in a VW Golf VI R (equipped car with 2 passengers has 1780 kg mass; 199 kW; all wheel drive) which is equipped with a *GeneSys ADMA G* [Gen1] measurement unit, logging data at a rate of 100 Hz.

All test drives are made during the day but off-hour. Each test drive is driven by a different driver. The driver base is not representative of the general public. All drivers are familiar with the urban traffic circuit, resulting in more dynamic driving behaviour and leading to higher requirements for the conducted feasibility analysis, than a normal driver would cause.

Calculation of Power, Energy and Friction Demand

Energy and Power Demand

At the current level of research, aspects like visual systems and data transfer are not executed. The estimation of energy and power demand is focused on motion of the WMDS only. The considered motions consist of translation, yaw and cabin tilt.

For the translational part, the acceleration and velocity profile of the wheeled platform is required. The necessary information is generated by the introduced MCA. For the best case scenario we assume a maximum recuperation power of 29 kW, as it is used for quick charging batteries of electric vehicles [Kna1] and an efficiency coefficient of 0,8 for battery power to wheel hub torque and vice versa. For the worst case scenario a maximum recuperation power of 4 kW is assumed [Kna1]. The calculations are performed in accordance with Eq. 2 and 3.

$$P_{trans} = a_{trans} \cdot v_{trans} \cdot m_{total} \qquad (2)$$

$$E_{trans} = \int P_{in} dt;$$

$$P_{in} = \begin{cases} P_{trans} \cdot \frac{1}{\eta}, P_{trans} > 0; \quad \eta = 0{,}8 \\ P_{trans} \cdot \eta, \; P_{trans,min} \le P_{trans} \le 0 \\ P_{trans,min}; \; P_{trans} \le P_{trans,min} = \begin{cases} -4\mathrm{kW}, \text{worst case} \\ -29\mathrm{kW}, \text{best case} \end{cases} \end{cases} \qquad (3)$$

The yaw rotation causes rotational power and energy demand. Therefore the moment of inertia (about the vertical z-axis) is required and is assumed to be a homogeneous cylinder, with the estimated system mass from chapter *Wheeled Mobile Driving Simulator Characteristics* (Eq. 4). The rotational acceleration profile is derived from the logged rotational velocity of the test drives. The measured velocity profile is filtered by a 1st order LPF with a frequency limit of 5 Hz in order to focus on typical vehicle dynamics and eliminating noise. The energy demand is calculated according to Eq. 3 by substituting P_{trans} with P_{yaw} from Eq. 5.

$$\Theta_z = \tfrac{1}{2} \cdot m_{total} \cdot r_{drive}{}^2, r_{drive} = 2{,}83\text{m} \qquad (4)$$

$$P_{yaw} = \ddot{\psi} \cdot \dot{\psi} \cdot \Theta_z \qquad (5)$$

The power demand for cabin tilt is calculated by the stroke velocity profile and the dynamic axial force of each linear actuator. The energy demand is calculated accordingly to Eq. 3 by substituting P_{trans} with P_{tilt} from Eq. 6. The profiles of the stroke velocities are derived by the used MCA. The part of acceleration simulation that is performed by cabin tilt corresponds to a cabin orientation profile, which is transformed into stroke profiles of each linear actuator. The calculation of dynamic actuator forces is based on the equilibrium of momentum and forces. The degree of concretization does not reach precise actuator level. The power demand for carrying the cabin mass is expected to be about 100 W and is negligible [Moo1]. The method presented does not consider energy required to hold load.

$$P_{tilt_i} = v_{stroke_i} \cdot F_{axial_i} \qquad (6)$$

Friction Demand

Friction demand for a WMDS consists of three parts – target translational acceleration, centripetal acceleration due to cornering and target yaw acceleration. The target translational acceleration is calculated by the MCA.

$$\mu_{trans} = \frac{|a_{trans}|}{g} \qquad (7)$$

The centripetal acceleration is also based on the MCA output but has to be extracted separately from the velocity vector of the WMDS. Therefore, the course angle rate is substituted by yaw and side slip angle rate according to Eq. 8.

$$\mu_{centripetal} = \frac{\left|v \cdot \left(\dot{\psi} + \dot{\beta}\right)\right|}{g} = \frac{|v| \cdot |\dot{v}|}{g} \qquad (8)$$

The friction demand for target yaw acceleration is estimated using Eq. 9 with regard to the estimated moment of inertia from Eq. 4.

$$\mu_{yaw} = \frac{1}{m_{total} \cdot g} \frac{|\ddot{\psi}| \cdot \Theta_z}{r_{drive}}; r_{drive} = 2{,}83\text{m} \qquad (9)$$

The superposition of friction demand at each tire is not determined yet, but a comparison of the different parts is conducted in the following chapter. Furthermore, a worst case analysis is made by superposing all three parts, based on their magnitudes without considering the direction of each.

Results

Urban Traffic vs. Motorway Traffic

The plots of the cumulative distribution function (CDF) in Fig. 5 show translational acceleration, velocity and displacement demand of the two drive cycles discussed in chapter *Test Drive*. The workspace difference is demonstrated by a XY-plot (Fig. 4) of the trajectories determined by the used MCA for exemplary representatives of the drive cycles.

The CDF-plots prove that urban traffic shows higher characteristic motion properties than motorway traffic and verify the assumption made in the introduction, also proving an increase in energy demand. Because of the large workspace demand, an analysis of energy demand is not conducted at this point and will be treated in the following chapter (*MCA Parameterization*). It must be emphasized that even the unscaled motion simulation shows a translational acceleration demand of less than 8 m/s^2, underlining the basic assumption of the feasibility of a WMDS with friction limited transmission of traction forces. A closer look onto friction demand is also conducted in the following chapter.

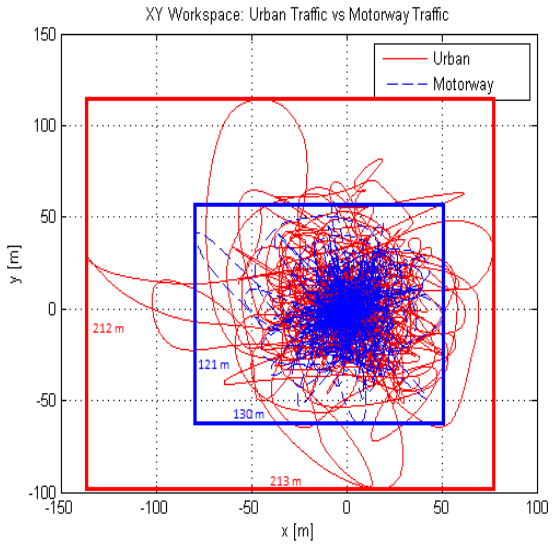

Fig. 4. Comparison of motorway and urban traffic concerning workspace demand

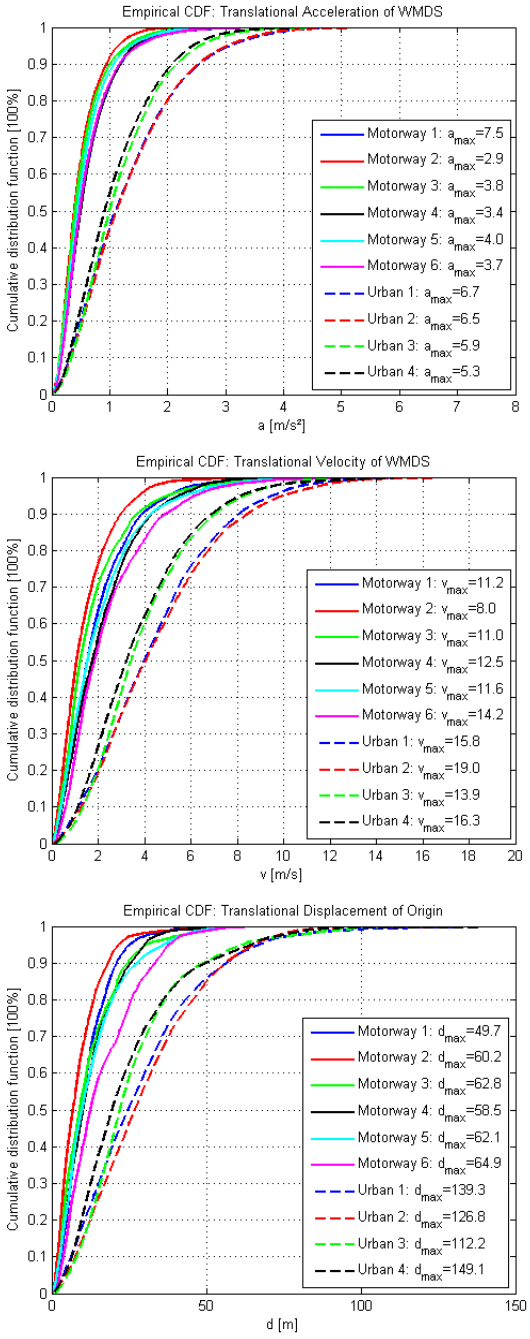

Fig. 5. Comparison of motorway and urban traffic concerning acceleration, velocity and displacement demand (scale factor=1)

MCA Parameterization for Urban Traffic Simulation

Because of the large workspace demand for unscaled driving simulation of sustained acceleration, as it is in urban traffic situations, scale factors that reduce the target horizontal acceleration have to be considered. This approach is common in the field of motion simulation [Gre1], [Cha1]. It must be emphasized that maintaining an unscaled simulation is still possible for specially developed maneuvers fitting DS properties. The influence of scaling horizontal acceleration is shown for three MCA parameterizations listed in Table 4. The parameterization is tuned iteratively for the test drives considering human perception thresholds.

Table 4. MCA parameterization for scale factors

Scale factor	LPF cut-off frequency (ω_{LPF} /s^{-1})	LPF damping ratio (ς_{LPF} /s^{-1})	Feedback gain (τ_v/s)	Feedback gain (τ_d/s)
1	0,559	1,59	4,49	19,77
0,7	0,709	1,202		
0,5	0,834	0,751		

Table 5 shows the influence of the scale factors on power, acceleration, displacement and velocity of the WMDS. The results represent the arithmetical average ($Ø_{urban}$) of the 50 %, 90 % and 100 % quantile for the four urban test drives conducted. The workspace demand strongly depends on the scale factors. For the conducted simulation it is recommendable to reduce target values but now the degree of reduction is only limited by the room and not by moving mass or required system dynamics anymore.

Table 5. Simulation results – acceleration, velocity, displacement and power demand for urban traffic

Scale factor		$Ø_{urban}$ |P| /kW		$Ø_{urban}$ |a| /m/s²	$Ø_{urban}$ |d| /m	$Ø_{urban}$ |v| /m/s
		best case	worst case			
1	$Q_{.5}$	3,5	4,0	1,0	23,2	3,7
	$Q_{.9}$	14,9	17,0	2,3	52,9	7,6
	$Q_{1.0}$	101,1	115,7	6,1	131,8	16,2
0,7	$Q_{.5}$	1,0	1,1	0,6	10,0	1,7
	$Q_{.9}$	4,9	5,6	1,5	23,8	3,7
	$Q_{1.0}$	31,6	36,2	4,0	52,8	8,3
0,5	$Q_{.5}$	0,27	0,31	0,36	4,5	0,88
	$Q_{.9}$	1,72	1,97	1,05	11,0	1.92
	$Q_{1.0}$	12,21	13,97	2,75	26,5	4.56

Regarding WMDS motion, Table 6 contains the average power demand (P_{mean}) for three MCA parameterizations with respect to the urban test drives. The scale factors are only applied to horizontal accelerations, therefore energy demand for yaw motion is independent from scale factors. The distinction of best and worst case scenario is only applied to translational motion because of the energy demand drop of about one dimension for yaw and tilt motion. Specifically the best case scenario shows promising values for energy demand. The order of magnitude is feasible by modern electric vehicle battery systems. The influence of moving mass and the requirement of high recuperation power is highlighted by the comparison of the two cases.

Table 6. Simulation results – energy demand for urban traffic

Scale factor	$\varnothing_{urban}$ $P_{mean_{trans}}$ / kW		$\varnothing_{urban}$ $P_{mean_{yaw}}$ / kW	$\varnothing_{urban}$ $P_{mean_{tilt}}$ / kW	$\varnothing_{urban}$ $\sum P_{mean_i}$ / kW	
	best case	worst case	worst case	worst case	best case	worst case
1	1,4	3,02	0,01	0,032	1,44	3,06
0,7	0,43	0,66		0,029	0,47	0,7
0,5	0,14	0,17		0,028	0,18	0,21

The components of friction demand for performing the urban test drives by the WMDS are shown in Table 7. While translational and centripetal components show similar magnitude, the yaw component is of minor importance. The final superposition of all components, considering magnitude and direction, cannot be performed yet, but even the worst case analysis, superposing only magnitude of all friction components at each time step, shows that a maximum friction coefficient of μ_{max}=1,19 is required to perform an „ideal“ urban driving simulation that can be recognized by suitable tire-ground pairing. For scaled simulation, the maximum value drops to about μ_{max}=0,7 proving the basic assumption that friction limited DS are capable to perform typical driving simulation for normal driver. The worst case analysis also shows that the $Q_{1.0}$ values of the different friction components do not occur simultaneously.

Table 7. Simulation results – friction demand for urban traffic

Scale factor			$\varnothing_{urban}$ $\lvert\mu_{trans}\rvert$	$\varnothing_{urban}$ $\lvert\mu_{centripetal}\rvert$	$\varnothing_{urban}$ $\lvert\mu_{yaw}\rvert$	$\varnothing_{urban}$ $\sum \lvert\mu_i\rvert$
Scale factor	**1**	$Q_{.5}$	0,11	0,05	0,002	0,17
		$Q_{.9}$	0,24	0,17	0,018	0,4
		$Q_{1.0}$	0,62	0,59	0,176	1,19
	0,7	$Q_{.5}$	0,06	0,03	0,002	0,1
		$Q_{.9}$	0,16	0,11	0,018	0,26
		$Q_{1.0}$	0,41	0,34	0,176	0,72
	0,5	$Q_{.5}$	0,04	0,02	0,002	0,06
		$Q_{.9}$	0,11	0,07	0,018	0,18
		$Q_{1.0}$	0,28	0,27	0,176	0,56

Conclusion

The results of the paper show the advantage of the WMDS approach compared to state of the art DS. Even the worst case assumption shows that friction demand, power supply and mass reduction are feasible by WMDS. WMDS are capable to perform a wide range of traffic situations while maintaining system dynamics. It has to be stressed that the field of application of the new WMDS embraces state of the art practice and augments to untapped fields, like high fidelity urban traffic situations. The developed “ideal” motion cueing algorithm shows the necessary workspace in relation to the algorithm parameterization that affects the quality of real world driving experience simulation and the deducible system requirements such as DS velocity and acceleration. The parameterization of the low-pass filter and the adjusted feedback gains have a major effect on the workspace requirement. Further research will show the potential for improvement. The calculated energy and friction demand proves the introduced basic assumption of friction limited DS feasibility. Scaling target motion information is advisable for most simulations but only owes to the room and not to moving mass and required system dynamics anymore.

The presented results allow the aggregation of a large motion envelope with high system dynamics into a high fidelity DS that combines properties of high dynamic simulators, like the one by Daimler AG [Zee1], with the workspace of the Toyota [Mur1] and NADS systems [Cla1].

Concerning the best case assumption, the presented WMDS concept shows promising advantages concerning further improvements that are valuable for system development and validation processes in automotive industry.

Further WMDS behaviour has to be analyzed. Additional DS components like the visual system, data transfer, air conditioning of the cabin and the introduced additional motion system for performing vehicle pitch, roll and heave motion have to be considered. Also a suitable safety concept has to be developed that allows a safe usage of the autonomously moving motion base, even for system failures. Furthermore conventional vehicle dynamic behaviour is inherited causing known problems such as, wheel load change, resulting in increase of control effort to establish smooth DS motion. Greater WMDS analysis has to be conducted to answer advanced open questions.

References

[Cha1] Chapron, T.; Colinot, J.-P.: “The new PSA Peugeot-Citroën Advanced Driving Simulator Overall design and motion cue algorithm”. Driving Simulation Conference, Iowa, 2007.

[Cla1] Clark, A.J.; Sparks, H.V.; Carmein, J.A.: “Unique Features and Capabilities of the NADS Motion System”. 2001.

[Dag1] Dagdelen, M.; Reymond, G.; Kemeny, A.; Bordier, M.; Maïzi, N.**:** “Mpc based Motion Cueing Algorithm: Development and Application to the ULTIMATE Driving Simulator”. DSC Europe Conference, S. 221-233., Paris, September 2004.

[DES1] Deutsches Statistisches Bundesamt: “Unfallgeschehen im Straßenverkehr 2007“. Wiesbaden, 2008.

[DES2] Deutsches Statistisches Bundesamt: "Unfallgeschehen auf deutschen Straßen 2008". Wiesbaden, 2009.

[DES3] Deutsches Statistisches Bundesamt: "Verkehrsunfälle – Unfallentwicklung im Straßenverkehr 2009". Wiesbaden, 2010.

[DIN1] DIN 33402-2:2005-12: "Ergonomics – Human body dimensions – Part 2: Values". December 2005.

[Dob1] Dobbeck, R.: "Darstellung von Beschleunigungen in Fahrsimulatoren bis in den Grenzbereich". Dissertation, TU Berlin, 1974.

[Don1] Donges, E.: "Fahrsimulator". Patent application DE 101 06 150 A 1, BMW AG, 2002.

[Dur1] Durth, W.: „Ein Beitrag zur Erweiterung des Modells für Fahrer, Fahrzeug und Straße in der Straßenplanung". in: Straßenbau und Straßenverkehrstechnik, Heft 163, 1974.

[Fil1] Filzek, B.: "Abstandsverhalten auf Autobahnen – Fahrer und ACC im Vergleich". Fortschritt-Berichte VDI Reihe 12 Nr. 536, Düsseldorf, ISBN 3-18-353612-9, 2003.

[Gen1] GeneSys GmbH: "Technical Data – Automotive Dynamic Motion Analyzer with DGPS". http://www.genesys-adma.de/adma_technik.php?lang=2&ID=6935, 11.03.2011.

[Gre1] Greenberg, J.; Artz, B.; Cathey, L.: "The Effect of Lateral Motion Cues During Simulated Driving". DSC North American Proceedings, Michigan, USA, October 8-10, 2003.

[Kna1] Knauer, M.: "Ampera soll Entwicklungskosten einfahren". Automobilwoche, 06.07.2011, 2011.

[**McC1]** McConnel, W.A.: "Motion Sensitivity as a Guide to Road Design". SAE-Paper No 770, 1957.

[Moo1] Moog, Inc.: "Electric Linear Servoactuators – Standard, Flexible and Servoactuation Packages", Electric Linear Servoactuator TJW/CDL 26400/Rev. A 0709, 2009 http://www.moog.com/literature/ICD/electriclinearservoactuators_-_stard,_flexible,_servoactuation_packages.pdf, 15.03.2012

[Mur1] Murano, T.; Yonekawa, T.; Aga, M.; Nagiri, S.: "Development of High-Performance Driving Simulator". SAE International of Passenger Cars – Mechanical Systems, 2009.

[Slo1] Slob, J.J.; Kuijpers, M.R.L.; Rosielle, P.C.J.N.; Steinbuch, M.: "A New Approach to Linear Motion Technology: the Wall is the Limit". Eindhoven University of Technology, 2009.

[Zee1] Zeeb, E.: "Daimler's New Full-Scale, High-dynamic Driving Simulator – A Technical Overview". Driving Simulation Conference, Paris, 2010.

[ZF1] ZF Friedrichshafen AG: "ZF-Antriebssysteme für Stapler". http://www.zf.com/corporate/de/products/product_range/further_product_ranges/lift_trucks/optimum_productivity/optimum_productivity.html, 11.03.2012.

Formula Symbols

Symbol	Unit	Description
a	m/s²	acceleration
β	rad	Side slip angle
c	1	Parameter to tune stability margin of loop gain
$\varnothing_{urban}$	1	Arithmetical average of the urban test drive results
d	m	Displacement
E	J	Energy
η	1	Efficiency factor
M_0	Nm	Holding torque
m_{Cabin}	kg	Mass of Cabin
m_{total}	kg	Mass of total system
ν	rad	Course angle
μ	1	Friction coefficient
P	kW	Power
ψ	rad	Yaw angle; rotation about vertical z-axis
Q	1	Quantile
r_{drive}	m	Distance from center of base frame to drive unit center; distance from z-axis to wheel contact point
Θ_z	kgm²	Moment of inertia of whole system about vertical z-axis
τ_d	1	Feedback gain for WMDS displacement of origin
τ_v	1	Feedback gain for WMDS velocity
v	m/s	Velocity
ω_{LPF}	Hz	Cut-off frequency
ζ_{LPF}	1	Damping ratio

Driving simulations for commercial vehicles- A technical overview of a robot based approach

Michael Kleer [1,2], Oliver Hermanns [1], Klaus Dreßler [1], Steffen Müller [2]
(1) Fraunhofer Institute for Industrial Mathematics ITWM, Fraunhofer Platz 1, 67663 Kaiserslautern, Germany, :
{Michael.Kleer, Oliver.Hermanns, Klaus.Dressler}@itwm.fraunhofer.de
(2) TU Kaiserslautern, Gottlieb-Daimler-Straße, 67663 Kaiserslautern, Germany
{Michael.Kleer, Steffen.Mueller}@mv.uni-kl.de

Abstract *– This paper gives a technical overview of the world's first motion simulator for interactive driving simulation, based on an anthropomorphic robot with up to 1000 kg payload, installed at Fraunhofer ITWM. First the applications and vehicle specific issues are discussed and presented. Some requirements of simulating commercial vehicle manoeuvres and off-road drives will be derived from measurements and simulations. This paper also describes the system architecture of the simulator and the interaction of the most important subsystems. This work delivers a deeper insight into the design of the moving platform, its control, the cabin concept and the safety features coordinated with the responsible Employer's Liability Insurance Association.*

Key words: *Driving Simulation, Industrial Robot, Commercial Vehicles, Human in the Loop, Environment Interaction*

Introduction and motivation

The design and development of commercial vehicles has to achieve the highest requirements regarding cost, efficiency, safety and durability. The extreme usage variability and versatility of commercial machinery in construction and agricultural applications leads to many restrictions and demands for such mechatronical systems. Human influence is one of the major parameters for a complex mechatronical system like an excavator or tractor etc., depending on many boundary conditions and on the driver's behaviour itself. To simulate the dynamic behaviour, durability and reliability of mechanical and mechatronical systems, it is necessary to provide the model with correct and realistic input data. The way a machine is operated and driven has a significant impact on its service life and durability and hence on the design and development process. A lot of very complex and detailed vehicle models to simulate durability, energy consumption, and dynamic behaviour for a widespread variety of commercial vehicles do exist. But the human influence, which is a very sensitive factor for the validity of simulations, is often covered poorly. To generate realistic stress profiles depending on human influences to a mechatronical system basically several possible approaches can be applied. If the system complexity allows the implementation of a driver model, then it is often possible to extract a limited set of data with this approach.

Another way to derive load cases is to use an invariant excitations method. The problem is that the derived load data depends on the complex interactions between the specific machine, the measured tasks and its operators.

Prototypes as an alternative way are very expensive. Especially for commercial vehicles the usage of prototypes, if existing at all, is extremely expensive.

If driver models are reaching their limits for certain simulations e.g. the task complexity is too high, the human influence has to be included into the simulation by an alternative way.

Therefore the solution is the use of an interactive simulator to support the development process of commercial vehicles. The human operator will be included into the simulation, such that the virtual product model, e.g. a commercial vehicle like an excavator, can be experienced at a high level of immersion.

Another aim is the implementation and test of driver / operator models. The interactive simulator can be useful in both directions. For the extraction of the operators behaviour on the one hand and for the multi-sensory representation of operator models on the other hand. The effects of assistant and safety systems can be examined without any risk for machine and operator in a realistic working scenario and much better than only on a scope or plot.

Applications

The ITWM simulator is designed for development purposes in the context of commercial vehicles. The system has to cover the requirements and expectations of experienced and expert operators of construction, forestry and agricultural machines and trucks. One of the major goals and long-term objectives is the generation of a special load case catalogue for various commercial vehicles. This catalogue is important to handle the extremely high variability and versatility of use of commercial machinery in construction and agricultural applications.

The user data which are the input for both, the interactive simulation and the subsequent detail simulations will be monitored online and stored. Another aim is to derive and validate driver models together with expert operators in the simulator. These models are useful for complex and non real-time simulations like tool-soil interaction or complex tires etc.

The analysis of possible applications and the derivation and definition of requirements for the motion platform is one important preliminary work. Most system parameters only can be defined after the mentioned tasks are analyzed.

Giving a universally valid dimensioning method would go beyond the scope of this work. Nevertheless the mentioned manoeuvres have some similarities, which can be used in the design process. Especially agricultural and construction vehicles mostly drive off road during a standard working scenario and large tilt angles of the cabins are possible. Depending on the vehicle parameters, its velocity and the test track the resulting accelerations varying in amplitude and bandwidth. One example shown in this work is a cross country drive of a SUV vehicle. These all terrain vehicles are lighter than most agricultural or construction vehicles so they usually allow higher movability and stronger excitations in a wide field of use.

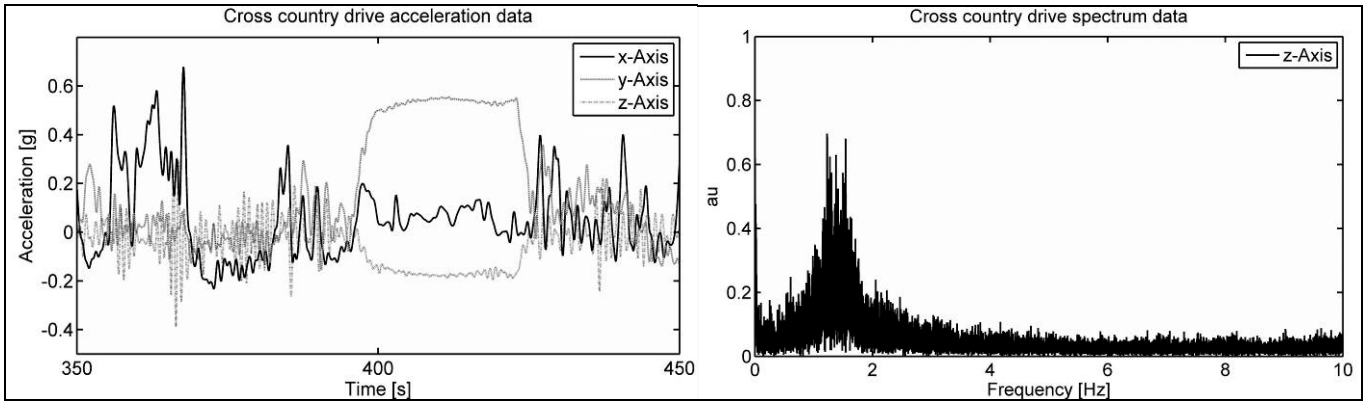

Fig. 1: Time domain (left) and frequency domain (right) of a cross country drive with an all terrain vehicle

Trucks have to be analyzed separately because the demands on the motion system are a bit different for this load case. Looking especially to the accelerations, a heavy duty distribution vehicle has more similarities to a passenger car than to a construction machine.

Detailed researches are done by Evers [Eve1] for a DAF XF 95 which is analyzed as an example (see Fig. 2).

Other manoeuvres e.g. obstacle passing require significant smaller translational displacements. On the other hand the sustained driving situations like breaking or accelerating over a long time or constant cornering could not be presented without a scale or tilt coordination.

With the analysis of different manoeuvres in combination with the vehicle specific motions like the turn of the upper-carriage of an excavator one can derive the major requirements as follows:

- Maximum translational travel: +-1.5m
- Tilt angles up to 180° for yaw and roll
- Translational acceleration min. 5 m/s²
- Min. payload 1000kg
- Interactive simulation with less than 15 ms latency
- Modular simulator setup
- Electrical actuators

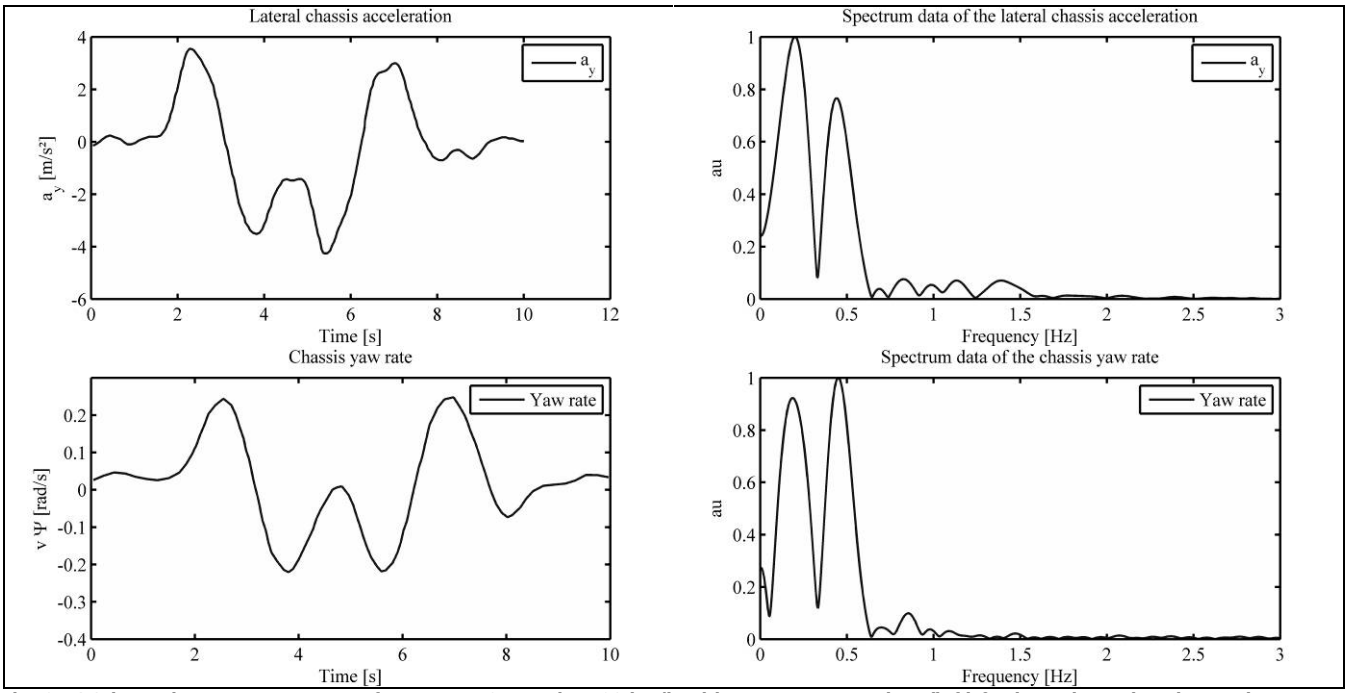

Fig. 2: ISO lane change manoeuvre of a DAF XF 95 truck at 60 km/h with measurement data (left) for lateral acceleration and yaw rate. The calculated frequency response for the manoeuvre (right) (see [Eve1]).

System architecture

Motion Base

One of the most important and challenging parts of the simulation system is the motion base. The motion system has to support the simulation by representing the filtered vehicle accelerations to an experienced operator, which is driving a virtual machine. Critical features are motion clearance, payload, the maximum of the reachable accelerations and their duration and the reachable orientation angles and angular velocities. Other restrictions like maintenance intervals, acquisition and working costs, modularity and the allocated space in the laboratory have to be considered too. A motion platform based on an anthropomorphic industrial robot covers all these features well. It combines large motion envelopes to present relative long lasting cues with relative low costs compared with parallel kinematics systems of the same size. Since the Robocoaster ® has been turned into an interactive motion simulator by several research groups see e.g. [Gio1, Gio2, Kec1, Bel1, Nel1] the system has shown its capacities.

One of the main drawbacks for simulating commercial vehicles with off-the-shelf cabins is the payload of the Robocoaster ® (only 500kg see [Kuk1]). Other restrictions are the fixed end stop limits which only allow a relative small translational workspace.

To solve both problems an industrial robot with larger payload was modified for simulation purposes. After a market analysis the most suitable system was selected as the motion platform. The maximum payload of this structure is about 1300 kg depending on the inertia; the translational workspace volume reaches up to nearly 80m³ (see [Kuk2]).

The off the shelf cabin is connected to the robot with a modular flange. The design of the flange has to handle two opposite demands. It should be a light weight construction to increase the maximum usable payload. On the other hand its stiffness has to be as high as possible to cover the safety demands and to minimize the negative influence of oscillations. The resonant frequencies of the flange have to be significant higher than the robots structure to prevent excitations which will lead e.g. to motion illness. For the first approach, a total weight of the flange below 100kg and an eigenfrequency higher than 20 Hz (fully-equipped with driver) was measured. The mounting position of the cabin was chosen similar to an inverse palletizing robot to increase the lateral workspace. This mounting position is suitable for ground vehicles where vertical displacements are below 0.5 m for the most application cases. To use a large workspace for simulating vehicle accelerations, the end stops for each axis are calculated online with fail safe hardware. This feature allows an orientation dependent deceleration or emergency stop function if a defined clearance is too small. For more details concerning the design process see [Kle1].

In figure 3 the principal setup for the different sensory feedback channels is presented:

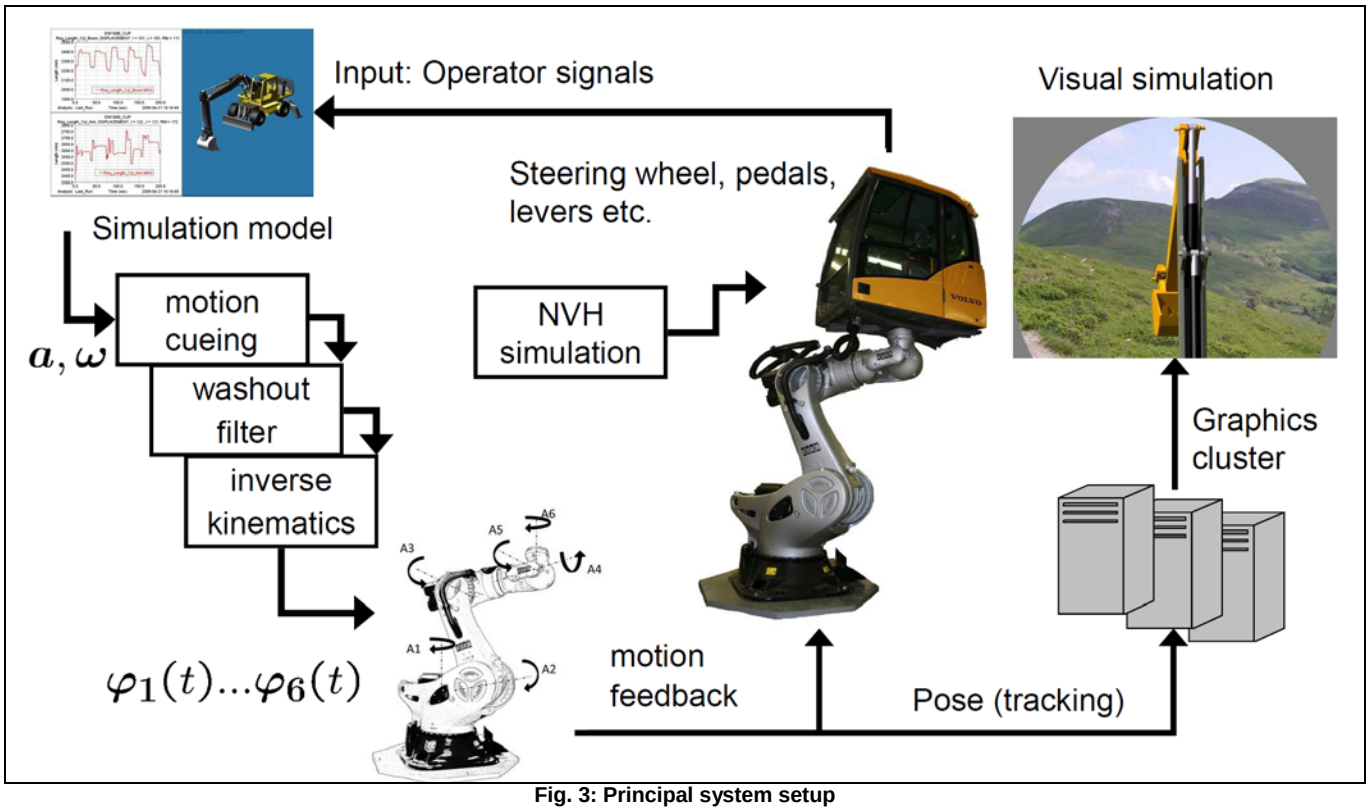

Fig. 3: Principal system setup

Motion simulation and vehicle models

The test person in the simulator cabin solves an interactive working task e.g. driving a passenger car or digging a trench with an excavator. The resulting lever positions, steering angles etc. are the actions of the test operator and will be digitized and transferred to the real-time computer via CAN communication.

Realisation of realistic motion is one of the most important challenges for any simulator. The robot obtains the motion inputs every 12 ms by an interface program executed on a real-time computer. These values, 6 angular velocities and 6 angles, are the output of the motion cueing algorithm (MCA), the washout filter and the inverse kinematics will be transferred to the robot controller hardware via network communication.

Most of the user interfaces in commercial vehicles are electronic devices but in case of conventional hydraulics, the lever or pedal motions have to be digitized. The control actions of the operator are the input data for the vehicle model.

Due to the modular setup it is possible to design the vehicle model with different software systems. Currently the code export is executed with Matlab / Simulink ® to generate a real-time executable model but different sources are possible. Simulink ® is used as a middleware to integrate the different signal sources and models and to manage the signals of the user interfaces. Once deployed, the real-time model generates a set of vehicle accelerations and orientations every time step. The model complexity can vary and it will be possible to scale the real-time calculation system. Currently a simplified vehicle model with a simple tire model (see [Pac1]) runs on one real-time computer.

The resulting accelerations, orientations and rotations of the vehicle model are the input values for the motion cueing algorithm. One of the implemented algorithms is a well known classical washout which dates back to Nahon & Reid [Rei1]. Another MCA is similar to the spherical washout algorithm, running at the MPI Motion Simulator at the Max Planck Institute for Biological Cybernetics in Tübingen (see [Gio1, Gio2]). In contrast, the presented system solves the inverse kinematics of the robot structure analytically. For a special set of manoeuvres the motion cueing algorithm can be adapted to minimize the sensation errors.

Figure 4 shows the setup of the MCA. The low frequency motion is represented directly by the robot's motion. The spectrum from 5 Hz to 200 Hz of the motion signal is reproduced by two electro-dynamic shakers attached to the cabins floor structure. The high frequency band above 200 Hz is generated by an 8-channel audio system, where 4 speakers are inside and 4 outside the cabin.

The development of more suitable MCAs especially for robot-based simulators is one of the important future works.

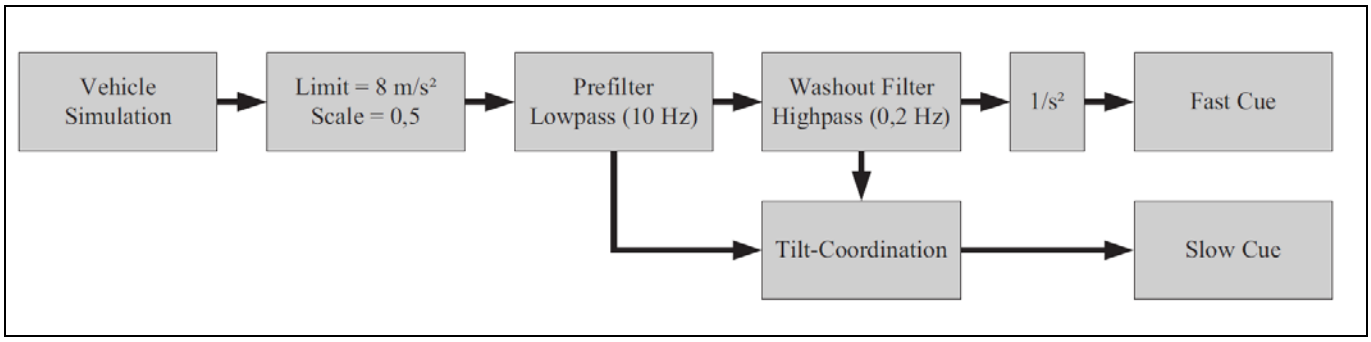

Fig. 4 Principal structure of the motion cueing algorithm

Visualization

The visualization system, designed for the simulator, is a fixed screen system with a spherical dome. The demand of a high resolution combined with a seamless field of view comparable to commercial vehicle cabins is a big challenge. Various possible solutions have been considered against the background of weight, acceptance and modularity of the setup. The planned concept covers the needs and restrictions, especially the limited payload of the robot, very well. The set up uses a modified drywall installation with deformable plasterboards and a steel skeleton with a spherical shape. The finishing of the visible surface has to fulfil the highest demands especially to prevent negative grazing light effects. The visible part of the screen is designed without any joint of dilatation to prevent disturbances during the simulation. The top of the projection dome can be removed for cabin change or maintenance. A displacement of the robot system is necessary to shift the drivers head into the centre of the sphere (see figure 5 right). The field of view (FOV) will be about 110° for the vertical and 300° for the horizontal direction. This corresponds to the FOV in the excavator cabin extended by the tilt, pitch and yaw angles of a motion cueing and tilt coordination algorithm to present a realistic scene for every relevant robot configuration. The distance to the screen in this setup allows that the driver's accommodation is similar to the reality. To allow all feasible robot motions without collisions, a diameter of the spherical projection dome of at least 10 m is necessary. Other side conditions are the shadowing effects, if the cabin structure intersects the optical path of a projector.

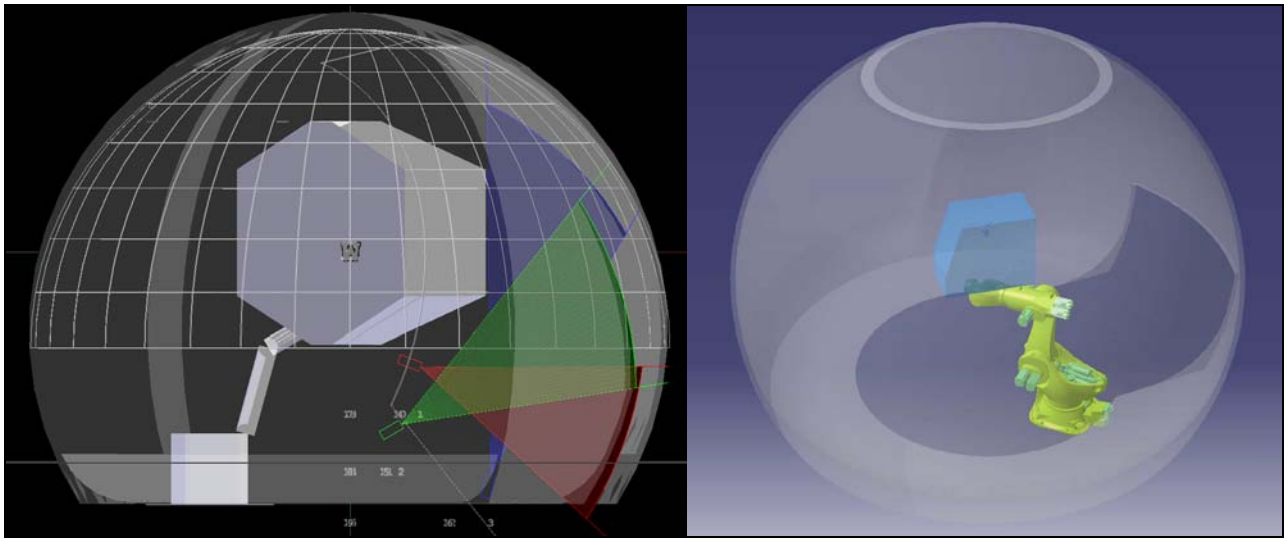

Fig. 5: Visualization setup with one of the 6 projector arrays (left) and the CAD model of the motion system and the projection screen.

The primary concern is the resolution of the presented image and the distance to the screen. The projectors will be arranged in 6 groups with 3 projectors for each group; one of these groups is shown in figure 5. The blue projector is located below the screen and outside the driver's field of view. The red and the green projectors are located below the simulator system. The octagon area in the centre of the picture is the representation of the workspace where no shadows occur. Due to the fact that the screen is fixed in the lab the driver's position has to be tracked. This tracking calculates the position and orientation of the cabin relative to the dome centre by using the encoder values of the robot's axis. After the forward kinematics calculation, the position and orientation of the driver's head is known, which is supposed to be fixed inside the cabin. By removing tilt coordination effects, the tracking of the

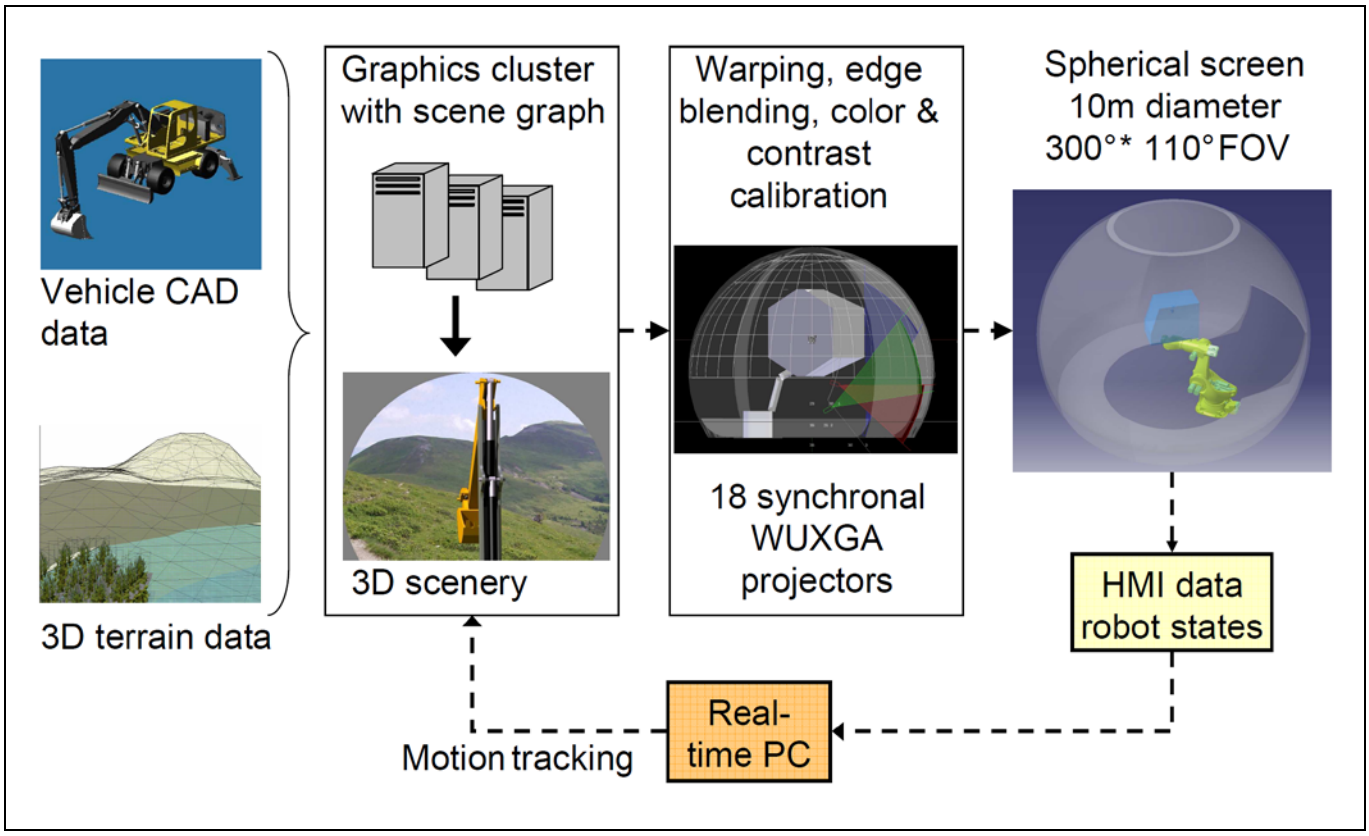

Fig. 6: Setup of the graphical simulation and digital content creation.

driver's head will be calculated. So the viewpoint inside the sphere is updated every frame and the subsequent warping, soft edge blending and colour calibration can be done.

The projector configuration planning and preliminary projector tests and measurements to determine the latencies, delays, colour space, contrast and depth of sharpness was done by Fraunhofer FIRST in Berlin.

Figure 6 shows the setup of the visual system. Starting with a CAD model of the vehicle and a model of the work area, a 3-dimensional scene is created. During the development process different engines have been compared in terms of threading model and clustering capabilities. Currently, the open SG graphics engine, developed by Fraunhofer IGD in Darmstadt [OSG1] renders the images.

The scene graph is rendered on the nodes of a computing cluster, equipped with high end graphic cards to render the different viewports. A master node distributes the content to the render nodes. The synchronous output of every frame is very important and a critical objective. Therefore the scene graph render loop is synchronized on the different nodes. Additionally, the video signals of the graphic cards on the different render nodes are synchronized by means of an add-on card per node. To limit the length of video signal cables and to avoid the use of range extenders, the render nodes are placed next to the projectors.

Safety concept

In comparison to the widespread Steward Gough platforms serial kinematics does not always have a secure final condition in case of errors. Parallel kinematics systems move to their lower end stops and dangerous situations usually do not lead to extensive damages.

The security system of the well known Robocoaster ® is designed conform to the DIN EN 13814 "Fliegende Bauten" (see [DIN1] for details) to allow human interaction, but the industrial version of a robot has no approval to move a person. So a detailed risk analysis and extensive modifications are necessary. The following multistage concept is implemented:

- Offline control of all possible robot motions in a preliminary step:
  The possible accelerations of a vehicle model are known. Together with the filter settings of the washout and motion cueing algorithms and the axis limits, a maximum travel range can be defined.
- Implementation of software limits:
  As closer one of the robot axes reaches their limit the higher priority function will slow down the robot

motion. If the remaining travel is large enough and no dangerous situation is detected then the working point of the washout algorithm will be modified without affecting the simulation. If the motion exceeds the first security distance level a penalty factor will slow down the simulator motion for this direction. In this case the safety concept leads to a motion error but the simulation is still active. By overshooting a maximum travel range a PLC will trigger the emergency stops. This function terminates the simulation and a manual reset is necessary. The software limits use data from the encoders installed in the robot links – not the data extracted from the controller.

- Implementation of proximity switches:
  For the very last possible clearance e.g. the critical areas at axis 3, where the cabin flange could touch the structure, proximity switches trigger a hard stop. In this case the break system will decelerate as fast as possible. This also terminates the simulation.
- Usage of a safety cage for the test subject:
  If a collision between the cabin and the robot structure or the ground is unpreventable e.g. in case of a gear box failure, a safety cage will protect the operator from serious injury.
- Organizationally arrangements and provisions:
  This means, that a procedure for safety checks, inspections and supervisions for both the operator and the test driver are done frequently. Another procedure is the monitoring of all cabin motions for durability calculations of the support structure.

All these safety features were developed in coordination with the responsible Employer's Liability Insurance Association.

Operational modal analysis

The first important experiments are the determination of the robots mechanical eigenfrequencies to ensure that the systems bandwidth is larger than the bandwidth of the vehicles handling dynamics. For this analysis, different robot motions in various configurations are recorded with an inertial measurement unit (IMU) sensor. The measurement results are used to set the bandwidth boundaries for vehicle model dynamics. The test setup is the following:

The robot eigenfrequencies are measured first without any payload and later with the fully-equipped simulator cabin and a driver to determine the maximum possible and typical limit frequencies. Starting with a motion for axis 1 and blocking all other axes, a full stop breaking manoeuvre leads to a characteristic oscillation which is measured by the IMU attached to the robot flange. The same measurements are done for other axes consecutively. The normalized power spectrum plots are shown figure 7.

The corresponding eigenfrequencies for a typical operation point are 8.65 Hz for the robot without a cabin and 4.8 Hz for the configuration with the flange (100 kg), the cabin with force feedback devices (700 kg) and a operator (90 kg). As shown in the figure 7 the above-mentioned eigenfrequencies appear to be dominant compared to others.

A likely reason for this behaviour could be due to the compliance in the joint of axis 1. The stiffness of the bearings in joint 1 leads to a characteristic oscillation for excitation of any robot axis.

Carried out tests suggest that the bandwidth of the fully-equipped robot has enough room to accommodate typical vehicle dynamics as shown in figure 1 and 2 (about 1.5 Hz) while the higher frequency parts have to be excited by the electro-dynamic shakers which are installed at the cabin floor.

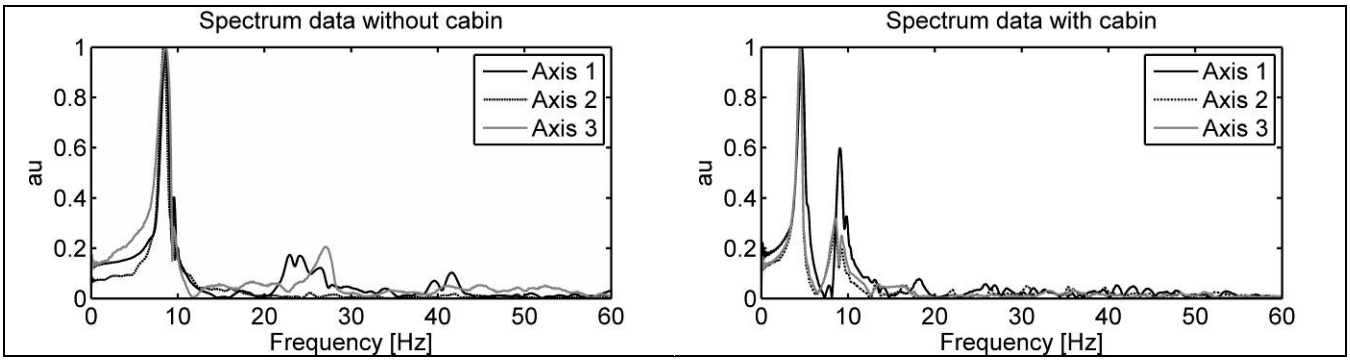

Fig. 7: Normalized frequency spectrum data of the Simulator without (left) and with the fully-equipped cabin (right).

Conclusions and future work

For complex tasks and machines in combination with a versatile user interaction, the interactive driving simulation is a suitable tool to analyse human-machine interaction. The real-time calculation of a vehicle model, in combination with the possibility to present realistic accelerations and tilt angles to a test person, solving a virtual task in an off-the-shelf simulator cabin allows a detailed analysis of typical working scenarios. These results allow predictions of handling, operability and the analysis of the effects of safety and assistant systems. Ad hoc design variations are possible without modifying a hardware system.

On the other hand an improved development of driver models is possible. For example, an expert operator can evaluate the realism and quality of an operator model driving the simulator while being a passive observer in the cabin.

The next task is the evaluation of the simulator system by experienced and expert drivers. This allows a tuning of system features by including the needs and demands of experts to improve the immersion for this user group.

More complex simulations like energy consumption, durability, service time, e.g. of a commercial vehicle usually cannot be executed in real-time. Also the computationally complex simulation, e.g. the tool-soil interaction, is done with the realistic user input data in a subsequent calculation step. The interactive simulation is computed with the help of a simplified model.

One of the future works is the implementation of sophisticated real-time soil interaction models, which are currently part of research projects in our department. These models will be calculated at interactive speed on a computing cluster. The improved results of the tool-soil and tire-soil interaction will increase the simulators level of immersion.

Reference

[Bel1] Bellmann T., Heindl J., Hellerer M., Kuchar R., Sharma K. and Hirzinger G. “The DLR Robot Motion Simulator Part I: Design and Setup”, IEEE International Conference on Robotics and Automation, 2011, pp. 4694-4701

[Din1] DIN EN ISO 13814 „Fliegende Bauten und Anlagen für Veranstaltungsplätze und Vergnügungsparks – Sicherheit“; 2005

[Eve1] Evers W.J.E. “Improving driver comfort in commercial vehicles”, PhD-Thesis University Eindhoven, 2010

[Gio1] Robuffo Giordano P., Masone C., Tesch J., Breidt M., Pollini L. and Bülthoff H. H. “A Novel Framework for Closed-Loop Robotic Motion Simulation: Part I Inverse Kinematics Design”, IEEE International Conference on Robotics and Automation, 2010, pp. 3876-3883

[Gio2] Robuffo Giordano P., Masone C., Tesch J., Breidt M., Pollini L. and Bülthoff H. H. “A Novel Framework for Closed-Loop Robotic Motion Simulation: Part II Motion Cueing Design and Experimental Validation”, IEEE International Conference on Robotics and Automation, 2010, pp. 3896-3903

[Kec1] Kecskemethy A., Masic I., Tändl M. “Workspace fitting and control for a serial-robot motion simulator”, Proceedings of EUCOMES, 2008, pp. 183-190

[Kle1] Kleer M., Hermanns O., Müller S. Konzeption eines Fahrsimulators für die Nutzfahrzeugindustrie auf Basis eines Industrieroboters, CVT Symposium, Kaiserslautern, 2012, pp. 49-58

[Kuk1] ”Specification Robocoaster”, Kuka Roboter GmbH, 2004

[Kuk2] ”Specification KR1000 Titan”, Kuka Roboter GmbH, 2010

[Nel1] Nelson K., Black T., Creighton D., Nahavandi S. “A simulation-based control interface layer for a high-fidelity anthropomorphic training simulator”, I/ITSEC, 2010

[Ope1] Open SG, Homepage: www.opensg.org, 2012

[Pac1] Pacejka H.B. “Tyre and vehicle dynamics”, Butterworth Heinemann, 2005

[Rei1] Reid L.D and Nahon M.A. “Flight Simulation Motion-Base Drive Algorithms: Part 1 - Developing and Testing the Equations”, UTIAS Report, No. 296, Institute for Aerospace Studies, University of Toronto, 1985

Effects of Motion Cueing on Curve Driving

Herman J. Damveld [1,2], Mark Wentink [3], Peter M. van Leeuwen [2], Riender Happee [2]
(1) Delft University of Technology, Faculty of Aerospace Engineering, E-mail: H.J.Damveld@tudelft.nl
(2) Delft University of Technology, Faculty of Mechanical, Maritime and Materials Engineering, E-mail: P.M.vanLeeuwen@tudelft.nl, R.Happee@tudelft.nl
(3) Desdemona B.V., E-mail: Mark.Wentink@desdemona.eu

Abstract *– A curve negotiation task at a prescribed and constant velocity was performed in the presence of external disturbances. The driver's goal was to simultaneously minimize the heading error and lateral position error. The present paper investigates the separate contributions of the road tracking and the disturbance to the heading and position errors, and more important, the effect of motion on these contributions. Four different motion cueing conditions were tested: 1) rumble only, 2) one-to-one yaw, 3) centrifuge with onset yaw, and 4) lateral track with onset yaw. It was concluded that none of the motion cueing conditions had a significant or large effect on the performance or control activity.*

Key words: *curve driving, motion cueing, target tracking, disturbance rejection*

Introduction

In the DRIVOBS project we are developing methods to obtain objective measures representing many aspects of the driver's behavior. Besides using physiological measures, such as heart rate variability or gaze tracking, the driver's behavior can be objectively quantified using system identification and parameter estimation (SIPE) to obtain driver models, both in real cars and in driving simulators. The objectively obtained driver behaviour observations enable industry to gain insight into the effect of several car driving aspects, such as proposed changes to the vehicle dynamics and steering systems. Furthermore such observations can objectively quantify effects of driving simulator configurations, such as the motion cueing system.

System identification methods have been used extensively to identify pilot models while controlling aircraft dynamics [Dam1, Poo1]. The current state of the art allows us to simultaneously identify the separate contributions of the pilot's visual system, the vestibular system and the neuromuscular system [Dam2, Dam3]. System identification was also used successfully to observe changes in the estimated pilot model parameters due to changes in the motion cueing algorithm [Zaa1].

Contrary to the displays used in aircraft control, the visual view in car driving has a rich optical flow, which provides the driver with a good perception of motion [Gib1]. In addition, aircraft displays usually only show an error between a commanded and a tracking symbol, allowing the pilot only to respond to the error, while the typical outside visual in car driving allows the driver to anticipate the future road geometry due to the presence of preview information.

Due to the strong visual cues and the possibility to anticipate it should be questioned whether the addition of motion cues in driving simulators will affect the drivers' control behaviour and performance. This was studied previously by others. For instance in [Val1], significant effects of the cueing algorithm were found in a city drive task using subjective rating scales, but objective measures did not reveal significant effects.

Obviously the effects of motion strongly depend on the task at hand. In a common curve negotiation task, a driver has to perform a combined target following and disturbance rejection task. The target consists of the road geometry, which simultaneously prescribes the car's heading and lateral position. The disturbance can stem from wind or road irregularities, which normally cannot be anticipated.

The goal of the present study is to objectively investigate the effects of several different motion cueing solutions on the human steering behaviour during curve driving in the presence of disturbances. We used the Desdemona simulator to test four different motion cueing algorithms. The experiment was designed to enable system identification and parameter estimation of the driver model. The used design also allows to differentiate between the target following and disturbance rejection effects. The present paper will only focus on those results.

Background

Driver models

A car driver perceives and processes information through a number of systems, including the visual system, the vestibular system and the neuromuscular system. Driver models in path following have traditionally focused on the use of visual information. Several published models realistically capture driving behavior but many models are unsuitable for system identification [Ste1]. The present study is based on the visual driver model derived by Allen and McRuer [All1, McR1]. A slightly adapted model structure is shown in Figure 1. This model is based on the assumption that the human driver is capable of perceiving three signals, the commanded heading ψ_c, the heading angle error ψ, and the lateral position error y (with respect to the center of the lane). The output of the driver is the steering wheel angle δ_s, which is based on a linear, time-invariant function of the inputs, and the remnant n. This remnant represents possible time-varying and non-linear effects. The remnant is usually small compared to the linear contribution and is usually neglected.

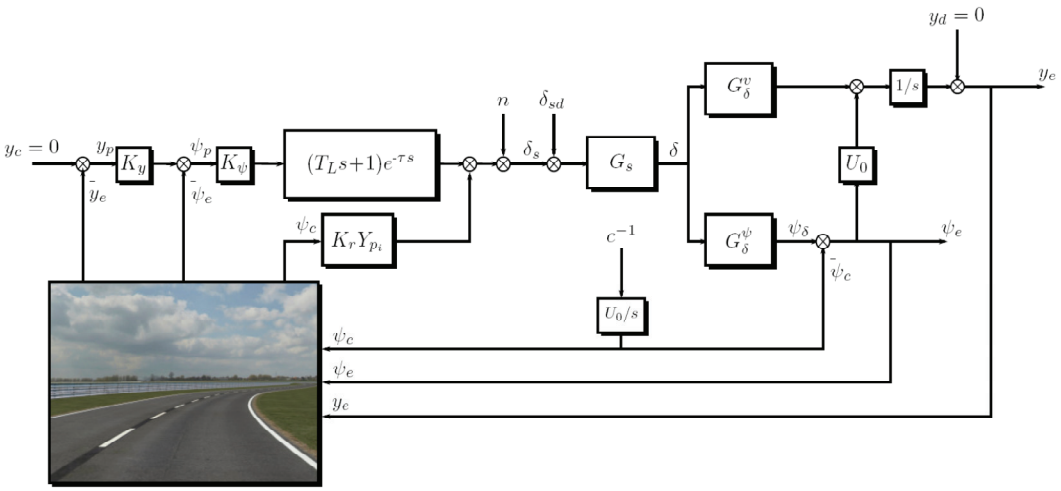

Figure 1. Driver vehicle model for control of road curvature and random disturbances.

Table 1. Description of signals and parameters in the driver-vehicle model.

Signals:

ψ_c	commanded heading
ψ_e	visible heading error
ψ_p	internal heading error incl. lateral error contribution
ψ_δ	car heading
y_c	commanded lateral deviation (= 0)
y_e	visible lateral position error
y_p	internal lateral position error
y_d	lateral position disturbance
n	remnant
δ_s	steering wheel angle
δ_{sd}	steering wheel disturbance
δ	front wheel angle
c	commanded curvature

Driver model parameters:

K_y	lateral position feedback gain
K_r	feedforward gain
K_ψ	heading feedback gain
T_L	lead time constant
τ	time delay
Y_{p_i}	feedforward control dynamics

Car model transfer functions:

G_s	steering wheel to front wheel ratio
G_δ^v	lateral velocity due to front wheel angle
G_δ^ψ	heading due to front wheel angle
U_0	car velocity (constant)

Target Following and Disturbance Rejection

In the curve negotiation task studied, a driver has to perform a combined target following and disturbance rejection task, and his goal is to simultaneously minimize the heading error and lateral position error of the vehicle by turning the steering wheel.

The target is provided as the commanded heading ψ_c, while the wind or road disturbance is simulated by a steering wheel disturbance δ_{sd} which is added to the driver's steering wheel angle before entering the vehicle model. The disturbance does not result in physical steering wheel forces or rotations.

Both target and disturbance signals will result in heading and lateral position errors. The present paper will investigate the separate contributions of the target and the disturbance to the heading and position errors, and more important, the effect of motion on these contributions.

In a situation *without motion*, the driver uses two visual feedback paths (operating on y_e and ψ_e) and one visual feedforward path (operating on ψ_c, see Figure 1). The heading and lateral position feedback paths allow the driver to respond to errors due to the commanded road heading and due to disturbances.

The visual feedforward path allows the driver to respond directly to the commanded heading. The driver can adapt his control behaviour to invert the vehicle dynamics, and as a result the heading and lateral position errors will become very small [Was1]. The visual feedforward path will have no effect on the mitigation of disturbances. These and residual target tracking errors will have to be minimized by the visual feedback paths.

When *motion is added*, the human driver will perceive vestibular information as well, which provides information about the change of the heading ($\dot{\psi}$) and position ($\ddot{y}$) of the vehicle. This allows the driver to respond to both disturbance and target signals. There is one important difference between the motion cues due to the target and disturbance signals: the motion cues due to the target following task are only the result of the drivers own steering actions, while the cues due to the disturbance rejection task are caused by the driver's own steering actions and the steering wheel disturbance. For this reason, the expected main effect of the addition of motion is an increase of the disturbance rejection performance. This was indeed demonstrated by [Zaa2] in an aircraft pitch control task without a preview display.

Method

Two uncorrelated forcing functions were designed in order to be able to distinguish between the effects of motion on the performance contributions of the target tracking task and the disturbance rejection task. Each of the forcing functions was composed of N sinusoids:

$$i(a) = \sum_{j=1}^{N} A_j \sin\left(\omega_j a + \varphi_j\right) \tag{1}$$

With:

i forcing function,

a along track distance,

A_j amplitude of sinusoid j,

ω_j frequency of sinusoid j, and

φ_j phase of sinusoid j.

Both forcing functions were designed as a function of the along track distance, which is the distance measured along the centreline of the lane. Consequently, the frequencies ω_j are spatial frequencies, meaning that both forcing functions are periodic across position in space instead of time.

The frequencies in the target forcing function ψ_c and the disturbance forcing function δ_{sd} are mutually exclusive, which allows us to separate their contributions in the frequency domain. The amplitudes and phases of the forcing functions were selected to result in quasi-random road curves and disturbances [Dam4].

A number of drivers performed the combined tracking and disturbance task several times, during which the heading error $\psi(t)$, the lateral position error $y(t)$ and the steering wheel angle $\delta_s(t)$ were recorded as a function of time. Using cubic interpolation, these recording were transformed from the time domain to the spatial domain as a function of the along track distance a. For example, the transformation for the steering wheel angle is:

$$\delta_s(t) \rightarrow \delta_s(a) \tag{2}$$

The spatial domain data were then transformed to the spatial frequency domain using a Fourier transformation. The Fourier transformed steering wheel angle is:

$$\Delta_s(\omega) = \int_{-\infty}^{\infty} \delta_s(a)\, e^{-j\omega a} da \tag{3}$$

The Fourier transformed data can now be averaged over the repetitions per subject and per condition to reduce the remnant.

The total variance, usually called *power*, of the steering wheel angle is a measure of the control activity, and can be calculated from the Fourier transformed data:

$$\sigma_{\delta_s}^2 = \frac{1}{\pi} \int_0^{\infty} \Phi_{\delta_s \delta_s}(\omega) d\omega \tag{4}$$

in which ω is the spatial frequency, and $\Phi_{\delta_s\delta_s}$ is the (auto) power spectral density of δ_s, here approximated by the periodogram:

$$\Phi_{\delta_s\delta_s}(\omega) = \frac{da}{N_s}\,\overline{\Delta_s(\omega)}\,\Delta_s(\omega) \tag{5}$$

With:

da the sampling interval in meters,

N_s the number of samples in δ_s, and

Δ_s the Fourier transform of δ_s.

Since the target and disturbance forcing functions contain power at distinct frequencies, the amount of power in the steering wheel angle signal caused by each forcing function can be calculated separately by integrating only over the frequencies in each forcing function. For instance, the power in the steering wheel angle signal due to the commanded heading forcing function is:

$$\sigma^2_{\delta_{s\psi_c}} = \frac{1}{\pi}\int_{\omega_{\psi_c}} \Phi_{\delta_s\delta_s}(\omega)d\omega \tag{6}$$

And the power due to the disturbance forcing function can be calculated similarly. The power in the remnant can be approximated by integrating over all frequencies that are not in either forcing function.

In a similar way the variance of the heading error and the lateral position error can be calculated and broken down into components due to the commanded heading, the steering wheel disturbance, and the remnant.

Experiment

We performed an experiment to determine the control activity and tracking performance during a curve negotiation task in the presence of disturbances as shown in Figure 1. The effects of motion were tested using four different motion cueing algorithms, including a condition without task-related motion (rumble only). Five subjects in the age of 20 to 54 performed five repetitions per motion cueing condition. The last three repetitions per condition were averaged to calculate the dependent measures, which are the control activity, and the heading and lateral position tracking performance. These are broken down into the separate contributions of the target forcing function, disturbance forcing function and remnant.

Apparatus

The effects of motion were studied using the high-end motion-based Desdemona simulator [Wen1]. The Desdemona motion platform has six serial degrees-of-freedom, starting with a central yaw axis (centrifuge), a horizontal axis (8m), and a vertical axis (2m), then the cabin itself can rotate freely in roll, yaw and pitch (>360º). All axes can move independently of each other. The exterior is shown in Figure 2a.

The simulator cabin was equipped with a five beamer projection system. The three front beamers produced high resolution images at 1400x1050px, while the side projection had a resolution of 1024x768px. The steering wheel was positioned in the center of the cabin, and was configured to behave as a mass-spring-damper system.

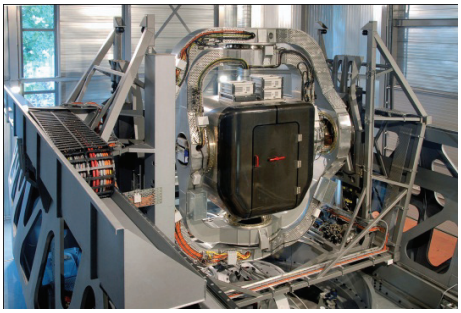

a. exterior

b. Interior

Figure 2. Desdemona motion system and cabin.

Forcing Functions

Both the commanded heading and steering wheel disturbance forcing function were composed of 10 sinusoids. To prevent subjects from learning the forcing functions by heart, we used different phase sets for both forcing functions in each repetition. The road length amounted to 1589.58m, of which 200m were used as lead-in distance, and 1389.58m were used for the actual calculations. The properties of one realization of the commanded heading

and the steering wheel disturbance are listed in Table 2, and the spatial domain signals are show in Figure 3. An impression of the road's characteristics is given in Figure 2b.

Table 2. Forcing function properties, one realization.

Commanded heading ψ_c			
Frequency (rad/m)	Frequency (rad/s)	Amplitude (rad)	Phase (rad)
0.0090	0.1256	0.5310	2.2365
0.0136	0.1884	0.3540	2.3982
0.0317	0.4396	0.1517	2.6802
0.0362	0.5024	0.1328	2.4867
0.0859	1.1932	0.0535	4.0601
0.0904	1.2560	0.0508	0.4553
0.2125	2.9516	0.0181	2.1519
0.2170	3.0144	0.0177	4.1765
0.4476	6.2172	0.0029	-0.0297
0.4522	6.2800	0.0029	-1.3858

Steering wheel disturbance δ_{sd}			
Frequency (rad/m)	Frequency (rad/s)	Amplitude (rad)	Phase (rad)
0.0181	0.2512	0.0361	0.3196
0.0226	0.3140	0.0361	1.5997
0.0407	0.5652	0.0361	-1.2249
0.0452	0.6280	0.0361	1.2446
0.0950	1.3188	0.0361	3.6996
0.0995	1.3816	0.0361	-0.8979
0.2216	3.0772	0.0361	-0.9907
0.2261	3.1400	0.0361	0.8396
0.4567	6.3428	0.0180	2.1313
0.4612	6.4045	0.0180	4.0572

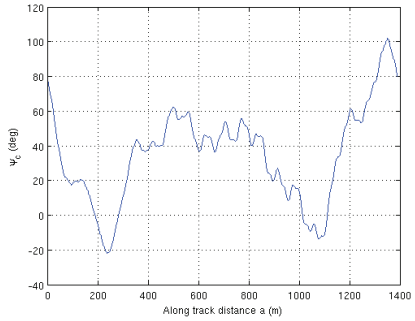

a. Commanded heading.

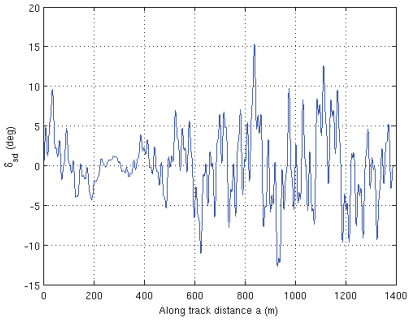

b. Steering wheel disturbance.

Figure 3. One realization of the forcing functions.

Car Model

A two degree-of-freedom car model was used [Rie1], which only describes the horizontal in-plane behaviour. The model uses the front wheel angle δ as an input and its outputs are the vehicle heading angle ψ_c and lateral velocity v. The car's position can be derived from the lateral velocity and heading angle. The vehicle's velocity was kept constant at 50 km/h.

Independent Variables

Four motion conditions were tested. Figure 4 depicts the motion cueing algorithms:

1. *Rumble only*: Only the vertical axis and cabin roll were used to simulate "road feel" contact between tyres and the road. The motion consisted of small amplitude white noise filtered by a low-pass filter, with a cut-off frequency and gain determined by the velocity of the car. Road rumble was also simulated in all other conditions.
2. *One-to-one yaw*: The cabin was positioned on-center, in the middle of the linear rail. The central yaw axis and the cabin yaw axis are then co-linear. High- and low-frequency yaw of the simulated car are divided over the central yaw and gimbal yaw axis, respectively, resulting in a one-to-one simulation of car yaw. In this solution, the accompanying lateral acceleration is not simulated.
3. *Centrifuge and onset yaw*: The cabin is positioned at the end of the linear track (R=4.0m). The central yaw spins the cabin around with 90º/s to produce a centrifugal force of 1g at R=4.0m. The resulting G-force felt by the subject is 1.4g. In addition, the subject is facing out from the center of centrifugation and is pitched 45º on his back, so that the resulting G-force is in the vertical direction again. In this position, the gimbal yaw axis is turned to tilt the centrifugal acceleration vector sideways to produce sustained lateral specific force. Due to the pitched position of the subject, part of this tilt-rotation is felt by the subject as yaw 'into the corner', coherent with the rotation of the simulated car driving through the corner. The part of the tilt-rotation that is felt as roll generates a false cue. The central yaw is used to generate sustained g-forces. The cabin yaw is used to align the centrifugal force with the lateral acceleration in the car. The heave and roll axis provide road rumble cues.

4. *Lateral track and onset yaw*: The horizontal track (R) is used to simulate lateral acceleration onsets (high-pass filtered car acceleration). The solution used about 6m of the horizontal track. Part of the sustained lateral specific force in corners is simulated applying moderate roll tilt (low-pass filtered, no rate limit applied). High-frequency yaw onsets are simulated by turning the yaw gimbal. In order to prevent misalignment of the simulated lateral acceleration the amplitude of the yaw gimbal movement is kept small.

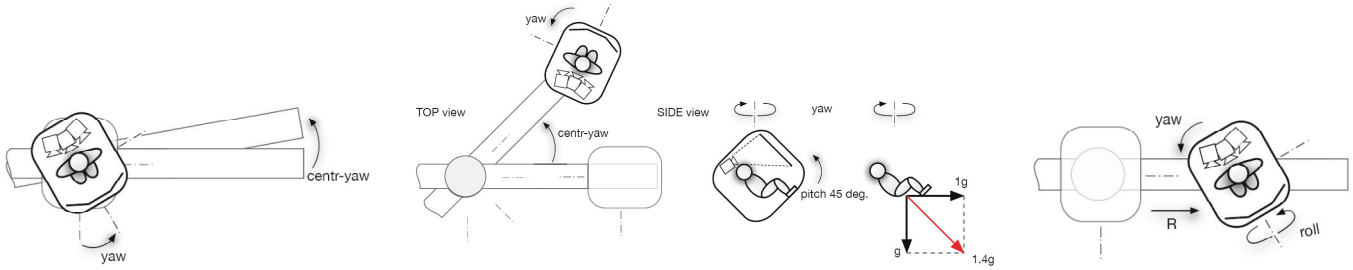

a. One-to-one yaw. **b. Centrifuge and onset yaw.** **c. Lateral track and onset yaw.**

Figure 4. Motion cueing conditions.

Dependent Measures

As discussed in the previous section, the dependent measures of interest are

1. the control activity, expressed by the variance of the steering wheel angle,
2. the heading tracking performance, expressed by the variance of the heading error, and
3. the lateral position tracking performance, expressed by the variance of the lateral position tracking error.

As explained in the Method section, the contributions of the target and disturbance forcing functions to the variances can be determined separately.

Results

Control Activity

Figure 5 shows the variance of the steering wheel angle, which is a measure for the driver's control activity. The gray bars indicate the subject means, averaged over three repetitions. The average over the subject means, which is the condition mean, is indicated by the closed circles. The error bars represent the 1-sigma standard deviation, corrected for between-subject effects.

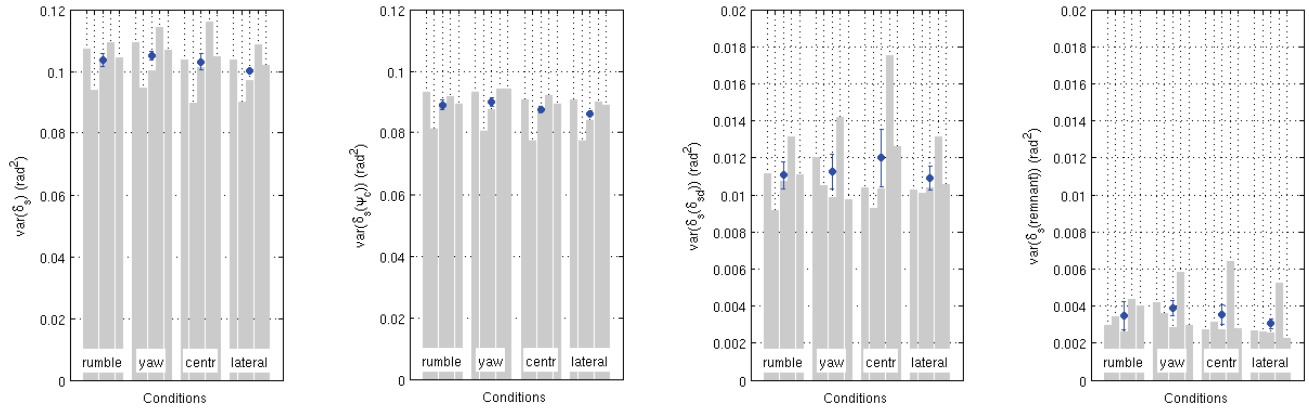

a. Total variance. **b. Variance due to target tracking.** **c. Variance due to disturbance rejection.** **d. Variance due to remnant.**

Figure 5. Control Activity.

The total variance shows little difference between the four conditions. Nevertheless, a repeated measures analysis of variance (ANOVA) indicates a significant effect of the motion condition on the control activity. Planned simple contrasts, comparing each condition to the rumble only condition, only revealed a significant difference between the rumble and lateral conditions.

An ANOVA of the variance contribution due to the commanded heading forcing function (Figure 5b) also indicated a significant, but small, effect of the motion condition. Planned contrasts showed that the control activity was significantly lower during the lateral condition compared to the rumble only condition. Figure 5c and d did not contain any significant differences.

Heading Tracking Performance

The main performance metric is the variance of the heading error, shown in Figure 6.

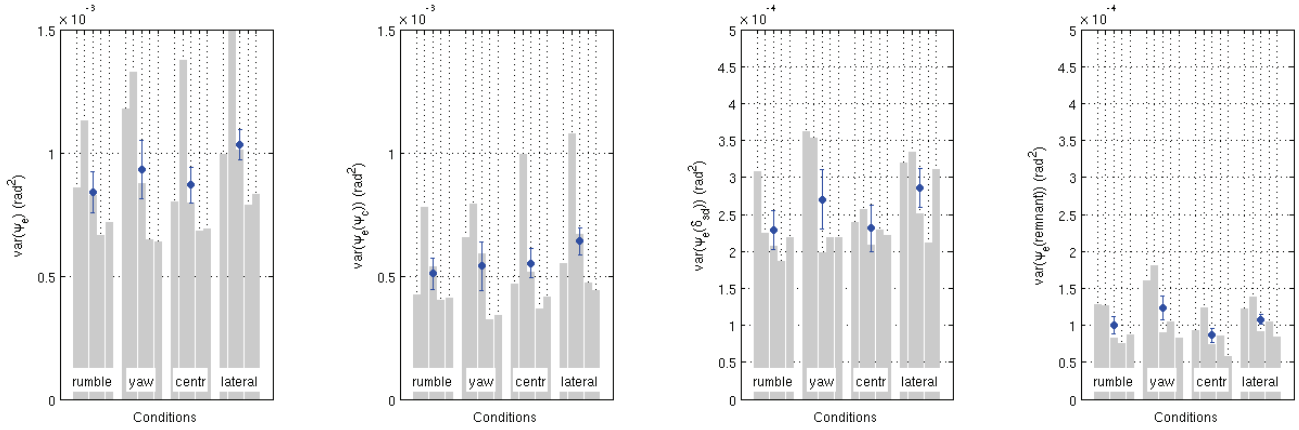

a. Total variance. **b. Variance due to target tracking.** **c. Variance due to disturbance rejection.** **d. Variance due to remnant.**

Figure 6. Heading tracking Performance.

The total variance does not show any improvements for the yaw, centrifuge or lateral conditions compared to the rumble only condition, and the performance in the yaw and lateral conditions seems even to have deteriorated by about 10-20%. An ANOVA confirms a significant effect of motion on the heading tracking performance, and planned contrasts reveal a significant performance deterioration, but only between the rumble and lateral conditions. It appears that this significant effect is caused by the combination of the contributions in Figure 6b, c and d, since the separate contributions are not significant.

Lateral Position Tracking Performance

The variance of the lateral position error is a metric for the positional tracking performance. The lateral position error is partly the result of the integrated heading error, hence similar results are expected.

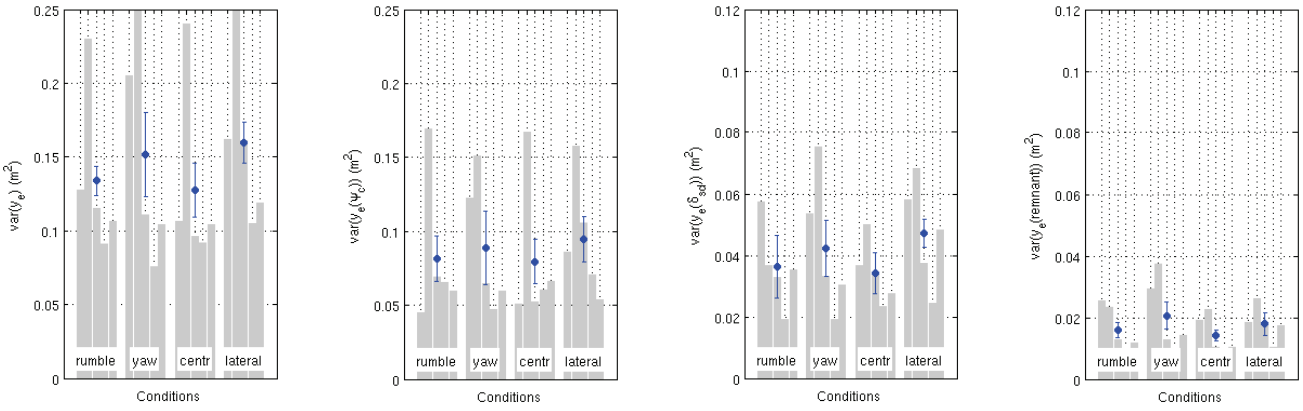

a. Total variance. **b. Variance due to target tracking.** **c. Variance due to disturbance rejection.** **d. Variance due to remnant.**

Figure 7. Lateral position tracking performance.

Although the lateral position performance appears to have decreased by about 13-19% in the yaw and lateral conditions, an ANOVA does not reveal any significant effect of motion. This is also the case for the separate contributions in Figure 7b, c and d.

Discussion

Based on previous work on motion cueing in aircraft pitch tracking tasks [Zaa1] it was expected to see an increase in the control activity when motion was added, both for the target tracking and disturbance rejection task. In the present study, a small decrease in control activity was seen, and only in the lateral motion condition for the target tracking task.

In addition, a heading tracking performance increase was expected, predominantly for the disturbance rejection task. In contrast we only found a very small performance decrease for the target tracking task in the lateral motion condition. The yaw only and centrifuge cueing conditions did not reveal any significant difference compared to the rumble only condition.

A number of explanations for the lack of the expected effects of motion in the present experiment exist. Additional tests indicate that the applied steering wheel disturbance had a fairly low frequency and low amplitude content from a motion perception threshold point of view, although subjects already indicated that the resulting displacements were large. A second explanation could be the information-rich preview display in the current experiment, which already provided excellent visual cues, especially in yaw direction. And, finally, differences in task instructions might have affected the results, since the subjects in [Zaa1] had to track a reference signal as aggressively as possible, while the present study required the subjects to drive as they would normally do, permitting them to ignore to the disturbances as long as they would remain between the lane markers. Further research will have to be performed to provide more insight.

From the data we can only conclude that the addition of motion did not improve performance. It is not possible to draw conclusions about the motion fidelity, or realism of the simulation, since we cannot compare the control activity and performance to data measured in a real car with unfiltered motion cues.

For this reason, we also had our subjects fill out a subjective rating scale during the experiment. All subjects indicated that it was difficult to assess the realism due to the presence of the steering wheel disturbance, which was much more present than in every-day driving. For that reason the fidelity of the ratings is low. Nevertheless the ratings indicated that the centrifuge and lateral track conditions were considered most realistic (average 5.9 and 5.8 out of 10), and the one-to-one yaw and rumble only conditions were less realistic (average 3.8 and 3.2 out of 10).

Based on the objective results, it is argued that the addition of motion during curve driving tasks in the presence of disturbances does not aid the driver in terms of lateral performance or control activity, and it appears only to influence the subjective realism.

Conclusions

A curve negotiation task at a prescribed and constant velocity was performed in the presence of external disturbances to investigate the effects of four different motion cueing algorithms on the control activity and performance.

Under the present experiment conditions, it can be concluded that none of the motion cueing conditions had a significant or large effect on the performance or control activity, neither in the target tracking task, as was expected, nor in the disturbance rejection task, which was unexpected.

The addition of motion only appeared to affect the subjective realism.

References

[All1] R. W. Allen, D. T. McRuer, J. R. Hogge, R. W. Humes, A. C. Stein, J. F. O'hanlon, R. T. Hennessy, G. R. Kelley, and G. V. Bailey, "Drivers' Visibility Requirements For Roadway Delineation, Volume I: Effects of Contrast and Configuration on Driver Performance and Behavior," Systems Technology, Inc., Tech. Rep. FHWA-RD-77-165, Nov. 1977.

[Dam1] H. J. Damveld, "A Cybernetic Approach to Assess the Longitudinal Handling Qualities of Aeroelastic Aircraft," Ph.D. dissertation, Delft University of Technology, Faculty of Aerospace Engineering, May 2009.

[Dam2] H. J. Damveld, D. A. Abbink, M. Mulder, M. Mulder, M. M. van Paassen, F. C. T. van der Helm, and R. J. A. W. Hosman, "Measuring the Contribution of the Neuromuscular System During a Pitch Control Task," in *Proceedings of the AIAA Modeling and Simulation Technologies Conference, Chicago, Illinois, Aug. 10-13, 2009*, no. AIAA-2009-5824. American Institute of Aeronautics and Astronautics, Aug. 2009.

[Dam3] H. J. Damveld, D. A. Abbink, M. Mulder, M. Mulder, M. M. van Paassen, F. C. T. van der Helm, and R. J. A. W. Hosman, "Identification of the Feedback Component of the Neuromuscular System in a Pitch Control Task," in *Proceedings of the AIAA Guidance, Navigation, and Control Conference 2 - 5 August 2010, Toronto, Ontario Canada*, M. Silvestro, Ed., no. AIAA 2010-7915, American Institute of Aeronautics and Astronautics. American Institute of Aeronautics and Astronautics, Aug. 2010, pp. 1–22.

[Dam4] H. J. Damveld, G. C. Beerens, M. M. van Paassen, and M. Mulder, "Design of Forcing Functions for the Identification of Human Control Behavior," Journal of Guidance, Control, and Dynamics, vol. 33, iss. 4, pp. 1064–1081, 2010.

[Gib1] J. J. Gibson, "What gives rise to the perception of motion?" Psychological Review, vol. 75, iss. 3, pp. 335–346, 1968.

[McR1] D. T. McRuer, R. W. Allen, D. H. Weir, and R. H. Klein, “New Results in Driver Steering Control Models,” *Human Factors: The Journal of the Human Factors and Ergonomics Society*, vol. 19, no. 4, pp. 381–397, Aug. 1977.

[Poo1] D. M. Pool, P. M. T. Zaal, H. J. Damveld, M. M. van Paassen, and M. Mulder, “Pilot Equalization in Manual Control of Aircraft Dynamics,” in *Proceedings of the 2009 IEEE International Conference on Systems, Man, and Cybernetics San Antonio, TX, USA - October 2009*, Institute of Electrical and Electronics Engineers. Institute of Electrical and Electronics Engineers, Oct. 2009, pp. 2480–2485.

[Rie1] P. Riekert and T. E. Schunck, "Zur Fahrmechanik des gummibereiften Kraftfahrzeugs," Archive of Applied Mechanics, vol. 11, iss. 3, pp. 210–224, 1940.

[Ste1] J. Steen, H. J. Damveld, R. Happee, M. M. van Paassen, and M. Mulder, “A Review of Visual Driver Models for System Identification Purposes,” in *Proceedings of the 2011 IEEE International Conference on Systems, Man, and Cybernetics Anchorage, AK, USA*, Oct. 2011.

[Val1] A. R. Valente Pais, M. Wentink, M. M. van Paassen, and M. Mulder, "Comparison of Three Motion Cueing Algorithms for Curve Driving in an Urban Environment," Presence: Teleoperators & Virtual Environments, vol. 18, iss. 3, pp. 200–221, 2009.

[Was1] R. J. Wasicko, D. T. McRuer, and R. E. Magdaleno, "Human Pilot Dynamic Response in Single-loop Systems with Compensatory and Pursuit Displays," Air Force Flight Dynamics Laboratory, AFFDL-TR-66-137, 1966.

[Wen1] M. Wentink, Valente Pais, R., Mayrhofer, M., Feenstra, P., Bles, W. (2008). First curve driving experiments in the Desdemona simulator. Proceedings of the Driving Simulation Conference Europe, Monaco, 183–192.

[Zaa1] P. M. T. Zaal, D. M. Pool, M. M. van Paassen, and M. Mulder, "Comparing Multimodal Pilot Pitch Control Behavior Between Simulated and Real Flight," in Proceedings of the AIAA Modeling and Simulation Technologies Conference, Portland, Oregon, Aug. 8-11, 2011

[Zaa2] P. M. T. Zaal, D. M. Pool, J. de Bruin, M. Mulder, and M. M. van Paassen, "Use of Pitch and Heave Motion Cues in a Pitch Control Task," Journal of Guidance, Control, and Dynamics, vol. 32, iss. 2, pp. 366–377, 2009.

A Model-based Motion Cueing strategy for compact driving simulation platforms

Alessandro Beghi [1], Mattia Bruschetta [1], Fabio Maran [1], Diego Minen [2]
(1) University of Padova, Department of Information Engineering Via Gradenigo 6/b, 35131, Padova, Italy, E-mail : {alessandro.beghi, mattia.bruschetta, fabio.maran}@dei.unipd.it
(2) VI-Grade Italy, Via l'Aquila 1c 33010, Tavagnacco, Udine, Italy, E-mail : diego.minen@vi-grade.com

Abstract *– Driving simulators are widely used in different applications: driver training, vehicle development, and medical studies. To fully exploit the potential of such devices, it is crucial to develop motion control strategies that generate realistic driving feelings. This has to be achieved while keeping the platform within its limited operation space. Such strategies are called motion cueing algorithms. In this paper a particular implementation of a motion cueing algorithm is described, based on Model Predictive Control technique. A distinctive feature of such approach is that it exploits a detailed model of the human vestibular system, and consequently differs from standard motion cueing strategies based on washout filters. The algorithm has been evaluated experimentally on a small-size, innovative platform, by performing tests with professional drivers. Results show that the MPC-based motion cueing algorithm allows to effectively handle the platform working area and to devise simple and intuitive tuning procedures.*

Key words: *Motion Cueing, Model Predictive Control, Vestibular System, Dynamic Platform, Optimization.*

Introduction

In recent years, there has been a growing interest in the development of *dynamic* driving simulators with applications in different fields such as racing (e.g., professional driver training, virtual vehicle development and set-up), security control systems (e.g., accident avoidance), medical rehabilitation, and virtual prototyping (providing safe and realistic virtual environment for Hardware-In-the-Loop (HIL) tools). In particular, given the growing number of possible applications, focus has been given to the design of small-size, low-cost platforms.

In a dynamic simulator, it is crucial to faithfully reproduce the driving feelings, so that the driver can fully exploit the virtual experience for the given specific goal. To this aim, the *motion cueing* (MC) strategy, i.e. the algorithm used to transform vehicle accelerations into admissible motion commands to the platform, has a key role. One of the main difficulties in the design of effective motion cueing algorithms is given by the complex nature of the human perception systems, since from a physiological point of view the role and priorities of stimuli of different nature to the overall perception of accelerations is not yet well known.

In most dynamic simulators, motion cueing algorithms are based on the so called "classical" approach **[Nah1]** that basically consists of a sequence of filters (figure 2) combined in order to:

- remove low frequency components of accelerations and velocities obtained from the vehicle dynamic model;
- transfer part of the low frequency translational accelerations to the angular dynamic using a low pass filter (*tilt coordination*);
- limit the platform motions with a further high pass filter to keep the platform in a neutral position. This is commonly called *washout action*.

This simple strategy has seen a wide range of implementations over the years. However, it has some shortcomings:

- being a filtering based approach, it is not possible to guarantee stimuli consistency between the dynamic simulation environment and the real platform movements;
- it cannot explicitly handle hard constraints on the platform movements and accelerations;
- it is not possible to exploit any available information on the driver's behavior in the future;
- the tuning of the algorithm is in general difficult, since it is not easy to give physical interpretation to most of the parameters.

In this paper the experimental application of a MC algorithm based on the Model Predictive Control (MPC) technique for a small size dynamic simulator is described. MPC is a model-based control methodology that allows to effectively handle limits on the working space and to exploit information on future reference signal. The idea of using MPC for MC has been recently proposed in **[Dag1]**, **[Aug1]**, where the motion cueing strategy integrates a model of the human perception systems and takes advantage of predictions of the future trajectory to fully exploit the platform working area. In these early works, the proposed solutions are not suitable for experimental application

in real situations. Moreover, they focus on investigating the prediction capabilities rather than on taking advantage of the optimization approach of MPC. A similar approach was used in **[Bas1]** with application to the design of the MC algorithm for an innovative, small size driving simulator platform. The results presented in **[Bas1]** were based on simulations. In the present work, starting from the results of **[Bas1]**, a real time implementation of an MPC-based motion cueing strategy for the same driving simulator platform as in **[Bas1]** is described. Performance of the implemented algorithm is evaluated on the field by professional test drivers. In particular, it is shown that the MPC-based approach gives satisfactory performance even in the case where no prediction of future driver's behavior are available, it allows to effectively handle the platform working area, to limit the presence of those platform movements that are typically associated to driver motion sickness, and to devise simple and intuitive tuning procedures.

The paper is organized as follows. The experimental platform is first described, and the motion cueing design problem is stated. For the sake of readibility and self containedness, basics of MPC control applied to the design of MC algorithms are briefly reviewed. In particular, the performance index, the optimization algorithm to be used to solve the MPC problem and the model of the human vestibular system are described. Operation and tuning of the motion cueing algorithm are then discussed by means of experimental results.

Problem Statement

In Fig. 1 the platform considered in this study is represented. Its peculiarity is in the mechanical structure. By using linear actuators instead of the classic hexapodal structure, it is possible to achieve satisfactory results in physical simulation with a relatively small size hardware, that can fit standard laboratories environments, whereas traditional, large dimensional, hexapodal platform require dedicated hangars.

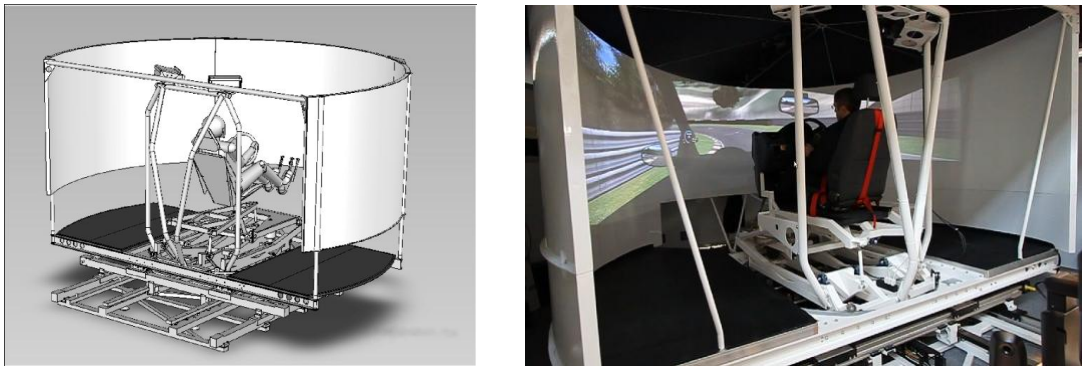

Fig. 1: Experimental platform : schematics and picture.

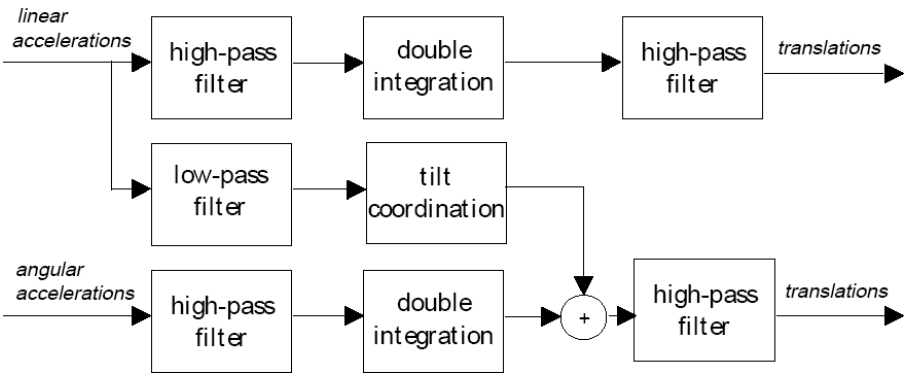

Fig. 2: Classical Motion Cueing (Washout).

The architecture is based on three completely decoupled degrees of freedom (DOFs, longitudinal and lateral axis, and yaw), and three partially coupled DOFs. The simulator kernel, i.e. the vehicle dynamics physical engine, has been developed and extensively tested on the field and provides a highly reliable representation of the real vehicle behavior. The screen covers more than 180 deg and moves in agreement with the platform to guarantee full immersion of the driver in the virtual environment. Finally, force feedback on the steering wheel and the braking system enhances the “driver's feeling” of the vehicle behaviour.

The platform dynamic performance reported in Tab. 1 highlights the limitations of the operational space, with maximal linear excursions of 1 m. This fact makes the role of the MC algorithm crucial.

Table 1. Platform performance.

Range	Position	Velocity	Acceleration
x	1m	1.3m/s	3.3m/s^2
y	1m	1.3m/s	3.6m/s^2
z	0.3m	0.9m/s	4.9m/s^2
Roll	30deg	112deg/s	600deg/s^2
Pitch	24deg	61deg/s	600deg/s^2
Yaw	50deg	61deg/s	240deg/s^2

The MC strategy has to provide the displacement references to the control system of the platform, which is assumed to be able to perfectly track the reference signals, with a fixed time delay. The conceptual scheme of the MC procedure is shown in Fig. 3, and is composed by the following steps:

1. obtain the current useful vehicle states d, i.e. translational acceleration and angular velocities calculated on the driver's eye-point, from the simulation software;
2. obtain the *perceived* acceleration r by filtering d via the vestibular system model, thus generating the reference signal for the MPC algorithm;
3. compute via MPC the displacement signal p passed to the platform control system in order to achieve the desired behavior on the eye-point.

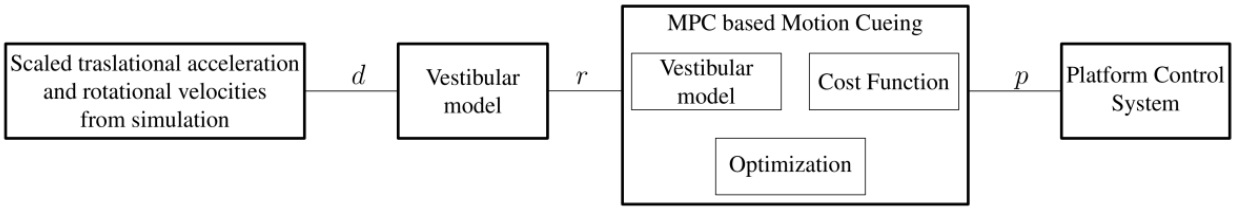

Fig. 3: Scheme of motion cueing strategy.

Model Predictive Control

Model Predictive Control (MPC) is an advanced control technique widely used in industrial applications **[Wan1]**, **[Mac1]** since the 1980s. In recent years, robust and efficient implementations have been developed, as well as software tools in standard computational environments that ease the design of MPC algorithms. The main advantages of MPC can be summarized as follows:

- its underlying idea is simple and intuitive to understand;
- it's the only generic control technique that efficiently deals with constraints;
- it can handle Multi-Input Multi-Output (MIMO) systems without formally increasing the complexity of the problem;
- it can handle non linearities in both the model and the constraints.

MPC Basics

Assume (discrete-time problem) that at time k a reference trajectory $r(t|k)$, $t \geq k$ and a current measure of the output $y(k)$, are available. Note that the current input is *not yet computed*. Now, suppose to have a model of the process to be controlled and that the state of the system (or its estimate) is available. We can therefore predict the future output $y(k+i|k), = 1, \dots, N_p$ corresponding to the input sequence $u(k+i|k), = 0, \dots, N_p - 1$ in a time-window of length N_p, where N_p is the prediction horizon length (Fig. 4). The idea is to compute the input sequence $\hat{u}(k+i|k)$ that minimizes a cost function, e.g. a function of the tracking error

$$\varepsilon(k+i|k) = r(k+i|k) - y(k+i|k),$$

while respecting a set of constraints. The input to be applied at time k is chosen as

$$u(k) = \hat{u}(k|k);$$

at time $k+1$ a new output $y(k+1)$ is measured and the algorithm is iterated applying only the first element of the computed optimal input sequence.

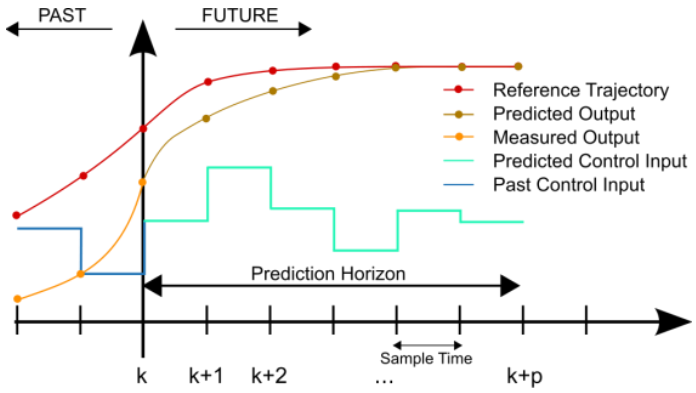

Fig. 4: Representation of MPC principle.

Process Model

In the literature, different implementations of the MPC principle have been proposed, with different model structures. In the application we are considering, the real-time constraints and the MIMO structure of the model are well described by a linear discrete state space model (sampled version of the continuous process) of the form

$$x_m(k+1) = A_m x_m(k) + B_m u(k)$$
$$y(k) = C_m x_m(k).$$

We assume that the input does not have a direct effect on the output (strictly proper system). State-space models are particularly well suited to design state estimators by using well-established tools of statistical filtering theory.

In our case, as proposed by Wang **[Wan1]**, we consider as the element to be optimized the *input difference* $\Delta u(k) = u(k) - u(k-1)$: considering also the state difference $\Delta x_m(k)$, we can write a new state equation

$$\Delta x_m(k+1) = A_m \Delta x_m(k) + B_m \Delta u(k).$$

Considering the output difference

$$y(k+1) - y(k) = C_m A_m \Delta x_m(k) + C_m B_m \Delta u(k)$$

and defining a new, augmented state $x(k) := [\Delta x_m(k)^T (k)^T]^T$, we obtain a new model

$$x(k+1) = \begin{bmatrix} A_m & 0 \\ C_m A_m & I \end{bmatrix} x(k) + \begin{bmatrix} B_m \\ C_m B_m \end{bmatrix} \Delta u(k)$$
$$y(k) = [0 \quad I] x(k)$$

where the control input is $\Delta u(k)$.

Cost function and state estimation

The optimal input sequence $\Delta\hat{u}(k+i|k)$, $i = 0, \dots, N_p - 1$ is computed by minimizing a cost function of the form **[Wan1]**

$$J(t) = \sum_{j=1}^{N_p} \delta(j)(y(t+j \mid t) - r(t+j))^2 + \sum_{j=0}^{N_c-1} \lambda(j) u(t+j)^2 + \sum_{j=0}^{N_c-1} \gamma(j) \Delta u(t+j)^2; \qquad (1)$$

$J(t)$ is quadratic, and takes into account the error between the predicted trajectory and the future reference in the prediction window of size N_p, and the future inputs and *input difference* in the control horizon N_c: in the specific case $N_c < N_p$ (as often done in the MPC framework). In this form, $J(t)$ has to be minimized over $u(t)$ and $\Delta u(t)$. Observe that weights on $\Delta u(t)$ are included in (1). In fact, as will be shown in the next Section, among the system inputs there are *longitudinal accelerations*, that are high-frequency, discontinuous signals. It is therefore convenient to have the possibility to act on their (approximate) derivative, to achieve a certain degree of regularity in the control signal, thus avoiding and excessive stress of the actuators.

The cost function can be rewritten in order to depend only on the input difference ΔU, obtaining the classic, matricial formulation of a *quadratic problem* (QP) **[Wan1]**, that is,

$$J = \frac{1}{2} \Delta U^T H \Delta U + \Delta U^T F.$$

To deal with *constraints*, limitations on the system inputs and outputs can be written in terms of constraints on the input variations ΔU **[Wan1]**

$$A \cdot \Delta U \leq b\,.$$

As a consequence, the QP becomes a *constrained* QP, for which a variety of solving algorithms are available in literature. This is a key step to ensure that the control problem, and consequently the MC algorithm, can be solved in real time.

Optimizer

From the implementation point of view, the Quadratic Programming solver is the core of the MPC algorithm. In the application at hand, there are strict real-time requirements, since fast dynamics (control frequency of 100 Hz) call for small computation times, and this leads to the use of *online QP solvers* which iteratively calculate the result at each sample time, without off-line precalculations.

After having analyzed different solutions, an Active Set method **[Wan2]** has been chosen to deal with the MPC problem described in this paper. The AS algorithm has been proposed by Ferreau, Bock and Diehl in **[Fer1]** and implemented in the tool qpOASES **[qpO1]**. qpOASES freeware C++ implementation provides a ready-to-use package with real-time capabilities that well fit the MPC-based motion cueing algorithm to be implemented in the driving simulator. In particular, the package offers some useful solutions for matching different real-time requirements, as the tunable limitation of the maximum number of active set recalculation per sample step and heuristics to assess the time required to complete the current optimization calculation, while limiting the possibilities of infeasibility if the procedure is stopped before reaching the optimum.

The Vestibular System

The vestibular system is located in the inner ear and is composed by the semicircular canals and the otolith organs. The former sense the angular rotation and the latter linear motion. Accurate mathematical models of the two systems have been derived starting from the '70s for application to MC of flight simulators. Zacharias **[Zac1]**, in a survey written in the 1979, reported most of the results nowadays available. Telban and Cardullo in 2005 **[Hou1]**, **[Tel1]** published a simplified transfer function model with estimates of the corresponding parameter values. For the semicircular canal, the transfer function that can best relate the sensed angular velocity to the acceleration stimulus in a MC control problem is the following:

$$W_{SCC}(s) = \frac{\hat{\omega}(s)}{\omega(s)} = K_{SCC}\frac{s^2}{(1+T_{SCC,1}s)(1+T_{SCC,2}s)} \qquad (2)$$

The otoliths are described in terms of the following transfer function that relates the sensed response to the specific acceleration stimulus:

$$W_{OTH}(s) = \frac{\hat{a}(s)}{a(s)} = K_{OTH}\frac{1+T_{OTH,1}s}{(1+T_{OTH,2}s)(1+T_{OTH,3}s)} \qquad (3)$$

Tilt coordination

An important component of perception in a dynamic simulator is given by tilt coordination. Otoliths are not capable to discriminate between gravitational and longitudinal forces. Hence, by using a non-zero pitch (roll) angle and without any other visual reference, it is possible to provide the driver in the simulator with a “fake” longitudinal (lateral) acceleration sensation. Such approach goes under the name of *tilt coordination*. Taking into account this effect is crucial to reproduce low frequency behavior with a reduced range working area. In the perception model, because of linearization, tilt coordination is nothing but a further contribution in the otoliths model $W_{OTH}(s)$ due to the pitch angle θ in the longitudinal direction and to the roll angle ϕ in the lateral direction: being $a = [a_x \;\; a_y \;\; a_z]^T$ the acceleration the driver has to be provided with, by using tilt coordination it suffices to generate the *specific acceleration*

$$\tilde{a} = \begin{bmatrix} a_x + g\sin\theta \\ a_y - g\cos\theta\sin\phi \\ a_z - g\cos\theta\cos\phi \end{bmatrix} \approx \begin{bmatrix} a_x + g\theta \\ a_y - g\phi \\ a_z - g \end{bmatrix}, \qquad (4)$$

using the small-angle linearization.

The complete model

In order to use the perception models in the MPC approach, state space realization of $W_{OTH}(s)$ and $W_{SCC}(s)$ are obtained and coupled with the tilt coordination contribution for all the 6 DOFs. The resulting system can be written as

$$\dot{x} = A_{VEST}x + B_{VEST}u$$
$$y = C_{VEST}x + D_{VEST}u$$

where the input u is composed by the three applied longitudinal accelerations and the three angular velocities, i.e $u = [a_x \;\; a_{y_z} \;\; \dot{\theta} \;\; \dot{\phi} \;\; \dot{\psi}]^T$. The overall state vector x is

$$x = [x_{SCC} \;\; x_{OTH} \;\; v_x \;\; p_x \;\; v_y \;\; p_y \;\; v_z \;\; p_z \;\; \theta \;\; \phi \;\; \psi]^T \qquad (5)$$

where the actual angles, positions and velocities are obtained by integration from the inputs u, and x_{OTH} and x_{SCC} are the state variable for the dynamical systems associated with the otoliths and semicircular canals. To impose a

set of constraints in a simple manner we choose $y = [\hat{\omega}\ \hat{a}\ v_x\ p_x\ v_{y_y}\ v_z\ p_z\ \theta\ \phi\ \psi]^T$, where $\hat{\omega}$ and $\hat{a}$ are the vectors of perceived angular velocities and longitudinal accelerations along all the DOFs.

Remarks on the operation and tuning of the MC algorithm

As can be seen by analyzing the structure of (1), it is necessary to produce reference trajectories for each of the output variables. This can be done by using the simulation environment, where perceived transactional accelerations and angular rates are generated, and then scaled prior to be used in the MPC algorithm. To keep the platform within its operational limits, as an alternative to the classical washout action, constant zero references for the position of the all six DOFs and for the velocities of the longitudinal ones are used. The weights in (1) are the tuning parameters to achieve a satisfactory trade-off between an accurate reproduction of the perceived in the simulated vehicle and the compliance with the platform working area.

By integrating the gravity effect inside the model as described in the previous Section, the low-frequency tilt coordination correction is automatically achieved giving an important contribution to the tracking of the perceived simulation signals. This fact can be seen as one of the major advantages of the MPC approach to the design of the motion cueing algorithm, namely, a tilt coordination correction can be obtained as the result of a model based optimization procedure.

As far as the design of the MPC algorithm is concerned, it would clearly be convenient to make use of the widest prediction/control window possible, if reliable information on the future driver's behavior is available. However, hard real-time constraints and the possible lack of capability to predict the driver's behavior may limit the length of the prediction/control window in practical situations. For these reasons, to design a general purpose Motion Mueing algorithm, it is preferable to first provide an effective algorithm where information about the future driver's behavior is not required and where a small prediction window is used. In the proposed solution, the MPC is designed to keep the reference trajectory constant along the prediction interval, and the length of the window becomes a tunable parameter that can be varied to obtain the desired tracking performance (a common strategy in MPC-based tracking problems for system with slow dynamics). In such conditions the low-frequency component of the desired perception signal is covered by tilt coordination and the high-frequency component is reproduced by using the translational DOFs. The tuning of the algorithm consists in choosing the weights, the length of prediction and control window, and the scaling factors to obtain satisfactory performance of the overall system, in terms of realistic sensations and effective usage of the platform working area. Due to the limited number of pages permitted we do not report the values of the tuning parameters in ditail.

Results

In this Section, some experimental results obtained during a professional driver training session on the platform are reported. The simulated vehicle is a sports-class car, and the virtual test track is a digital version of the Calabogie track. Since the considered model is almost decoupled for all the 6 DOFs, results on longitudinal dynamics only are reported, namely, the longitudinal acceleration and the pitch velocity of the vehicle, that have to be reproduced as faithfully as possible (in terms of driver sensations) by operating the platform with longitudinal and pitch motions.

The motion cueing algorithm is tuned so that the platform working area in the longitudinal direction is exploited at best, while avoiding motion sickness due to the tilt coordination correction. In Figure 5, tracking of the perceived accelerations and velocities, longitudinal platform displacement and angular displacement are shown. It can be seen that the platform actually exploits at best its operational area. It is worth noticing that this is achieved *w*ithout any filtering action, as would be required in a classical, washout filters-based approach. Also, the perceived acceleration is tracked almost perfectly. Focusing on the pitch displacement, tilt coordination correction can clearly be seen and has a peak value of 0.08 radians. As a consequence, the angular velocity contains low frequency disturbances. The frequency analysis of pitch and longitudinal contributions to the global perception in the platform, reported in figure 6, shows that the displacement is responsible of the low frequency contributions only. The tuning procedure followed to achieve such results is very intuitive and it is based on the ``natural interpretation'' of the weights in the cost function.

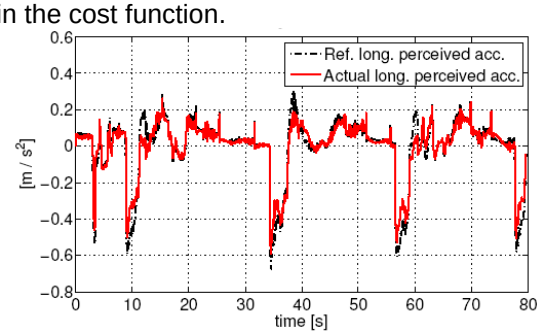

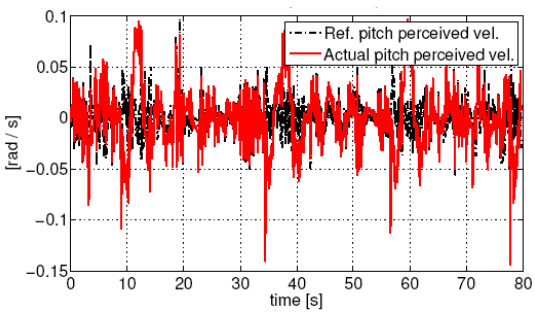

(a) Perceived longitudinal acceleration.

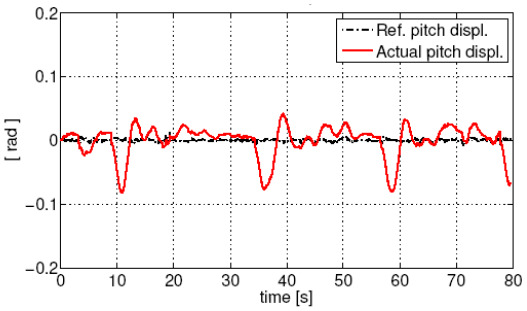

(b) Perceived pitch velocity.

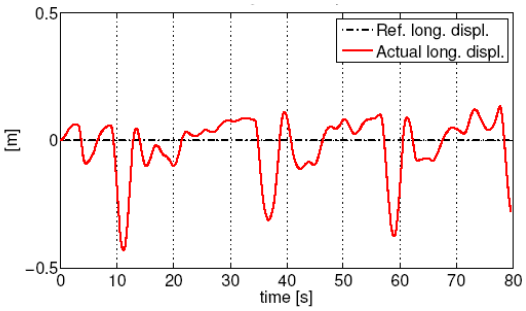

(c) Pitch position.

(d) Longitudinal position.

Fig. 5: Tracking based on MPC approach.

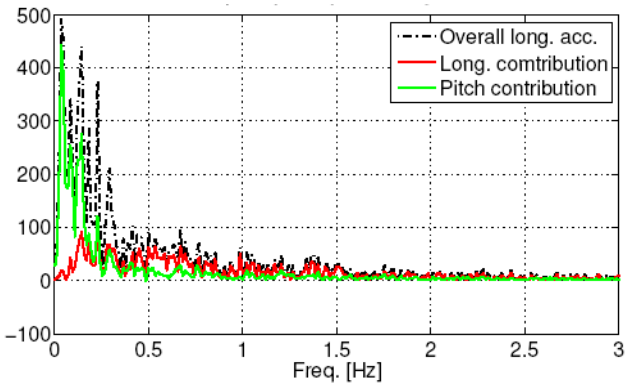

Fig. 6: Frequency comparison of the longitudinal and pitch contribution to the longitudinal acceleration

As a further example of the effects of manipulating the weights in (1) can be seen by increasing the values concerning the angular velocity of the platform and by modifying the scaling factor. A reduction of the overall pitch displacement for the platform is achieved, as shown in Figure 7. This operation allows to reduce the tilt coordination effect which is one of the main causes of motion sickness in a dynamic simulator, hence adapting quickly to different drivers' attitude.

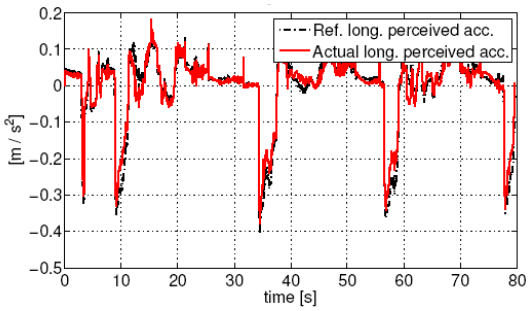

(a) Perceived longitudinal acceleration.

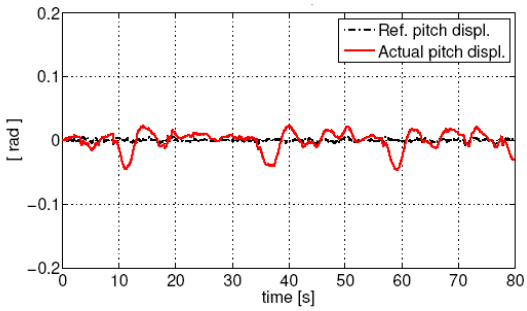

(b) Pitch displacements.

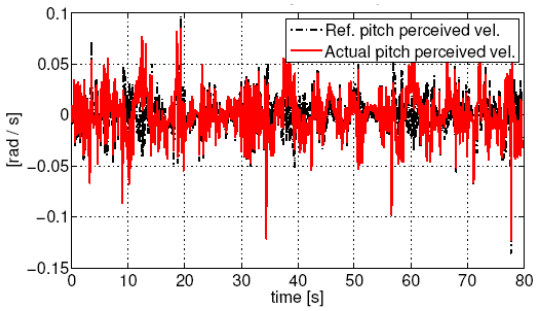

(c) Perceived pitch velocity.

Figure 7: Comparison of tracking performance with different exploitation of the platform.

Conclusions

In this paper we describe the experimental design of a MC algorithm for a small size dynamic driving simulator, based on MPC techniques. The proposed algorithm represents a novel approach to motion cueing that completely changes the classic paradigms of washout filters: tilt coordination and working area constraints are handled through an optimization procedure without the employment of any filter. This procedure results to be easily tunable and robust. It is worth noting that, given the high system dimension, although implementing a real time MPC procedure is not a trivial task, our algorithm is working at 100 Hz control frequency. Next step will be using a virtual driver tool to provide reliable driver's behavior prediction and hence extending the proposed algorithm capabilities.

References

[Aug1] Augusto, B.D.C. and Loureiro. Motion Cueing in the Chalmers Driving Simulator: A Model Predictive Control Approach. Master's thesis, Chalmers University of technology, 2009.

[Bas1] M. Baseggio, A. Beghi, M. Bruschetta, F. Maran, and D. Minen, "An MPC approach to the design of motion cueing algorithms for driving simulators," in Intelligent Transportation Systems (ITSC), 2011 14th International IEEE Conference on, oct. 2011, pp. 6926-97.

[Dag1] Dagdelen, M. and Reymond, G. and Kemeny, A. and Bordier, M. and Mazi, N. Model-based predictive motion cueing strategy for vehicle driving simulators. *Control Engineering Practice*, 17(9): pp. 995-1003, 2009.

[Fer1] H.J. Ferreau and H.G. Bock and M. Diehl. An online active set strategy to overcome the limitations of explicit MPC. *International Journal of Robust and Nonlinear Control*, 18(8): pp.816-830, 2008.

[Hou1] Houck, Jacob A and Telban, Robert J and Cardullo, Frank M. Motion Cueing Algorithm Development: Human-Centered Linear and Nonlinear Approaches. *NASACR*, 213747(May), 2005.

[Mac1] Maciejowski, J.M. *Predictive control: with constraints*. Pearson education, 2002.

[Nah1] Nahon, MA and Reid, LD. ''Simulator Motion-Drive Algorithms: A Designer's Perspective''. *J. Guidance*, 13(2), 1990.

[qpO1] qpOASES website, www.kuleuven.be/optec/software/qpOASES.

[Tel1] Telban, R.J. and Wu, W. and Cardullo, F.M. and Langley Research Center. *Motion Cueing Algorithm Development: Initial Investigation and Redesign of the Algorithms*. National Aeronautics and Space Administration, Langley Research Center, 2000.

[Wan1] Wang, L. *Model predictive control system design and implementation using MATLAB*. Springer Verlag, 2009.

[Wan2] Wang, Y. and Boyd, S. Fast model predictive control using online optimization. *Control Systems Technology, IEEE Transactions on*, 18(2): pp. 267-278, 2010.

[Zac1] Zacharias, G.L. Motion cue models for pilot-vehicle analysis. Technical report, bolt beranek and newman inc Cambridge ma control systems dept, 1978.

Effects of Yaw Motion on Driving Behaviour, Comfort and Realism

Jeroen Hogema[1], Mark Wentink [2], Gary Bertollini [3]

(1) TNO, Kampweg 5, 3769 DE Soesterberg, The Netherlands. E-mail: jeroen.hogema@tno.nl
(2) Desdemona BV, Kampweg 5, 3769 DE Soesterberg, The Netherlands, E-mail: mark.wentink@desdemona.eu
(3) General Motors Research and Development, VDR Laboratory, 30500 Mound Rd., Warren, Michigan, USA, E-mail: gary.p.bertollini@gm.com

Abstract *– The use of large displacement yaw cueing is becoming more common as a part of the motion cueing in driving simulators. It is expected that driving behaviour, comfort and realism will be positively affected by adding a yaw table, especially during low-speed turning manoeuvres.*

We used TNO's advanced motion platform Desdemona to explore the effects of yaw motion during highway and urban turning manoeuvres: 14 participants drove the simulator with and without yaw motion.

Questionnaires results showed that the simulation was rated as quite realistic. Effects of yaw motion on the subjective ratings were not found. In terms of driving behaviour, we found statistically significant effects of yaw motion in curve driving, especially in small-radius curves. With yaw motion present, driving behaviour became more cautious, and (compared against the literature) more realistic. This suggests that adding yaw motion to a driving simulator improves the external validity for low-speed corner driving manoeuvres.

Key words: *driving simulator; yaw table, motion cueing, driving behaviour.*

Introduction

In driving simulators, the simulation of cornering manoeuvres is considered particularly challenging, especially in city environments, where the curve radius is typically small [Wen1]. The discrepancy between the high yaw rates in the car and the lack thereof in the simulator, plus the associated mismatch in lateral acceleration, often cause disorientation or even motion sickness [Ken2]. This explains the growing interest in the use of large displacement yaw cuing platforms in driving simulators, such as those at the University of Tokyo [Yam3], the US National Advanced Driving Simulator [Sch4] and Toyota [Toy5].

Such yaw cueing systems would ideally generate yaw rates and displacements corresponding to the real car yaw dynamics. It is believed this may reduce simulator disorientation effects during low speed turning manoeuvres as typically encountered in city intersection scenarios. See e.g. [Mou6], who reported beneficial effects of yaw motion compared to no motion. Consequently, it is expected that driving behaviour, comfort and realism will be positively affected by this new yaw motion capability. We investigated the effects of adding yaw motion to other motion components by means of a driving behaviour experiment.

Method

The Desdemona simulator was utilized for the experiment. Desdemona is a moving-base research simulator located at TNO (Soesterberg, The Netherlands). It was built in close co-operation with AMST (Ranshofen, Austria). The simulator has 6 Degrees of Freedom (DoF). The cabin (see Fig.1) is mounted in a gimballed system (3 DoF, >2π radians), which as a whole can move vertically along a heave axis (1 DoF, ±1m) and horizontally along a linear arm (1 DoF, ±4m). This structure can rotate as a whole around a central axis to facilitate centrifugal motion (1 DoF, <3G).

For the current experiment, the Desdemona cabin was equipped with a generic car cockpit (see Fig.1). The cockpit contained force feedback on steering wheel, and on gas and brake pedals. Direct drive electrical motors generated the control loading for the steering wheel and pedals. The out-the-window visuals were projected at a screen in the cabin by three projectors. The driver was approximately 1.5 meters away from the central screen, which had a field-of-view of 120 degrees horizontally and 32 degrees vertically. Driving sounds were not simulated in this experiment.

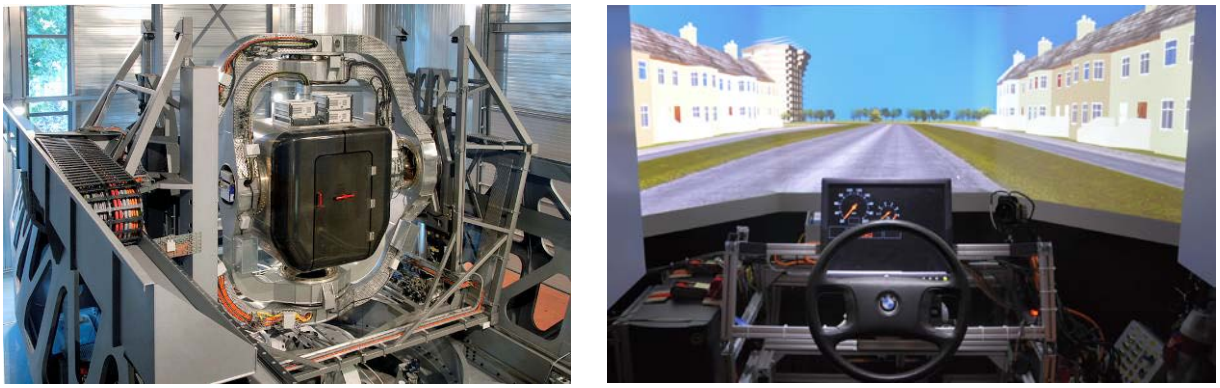

Figure 1 The Desdemona research simulator (left); the interior of the car cabin (right).

The motion cueing consisted of the following elements.

- A yaw component: the yaw motion of the vehicle model was simulated by yaw motion of Desdemona. This component could be switched on or off, and was used as an independent variable (the 'yaw motion' versus 'no yaw motion' condition). The participant's head position was 0 to 20 cm behind the yaw axis (dependent on the chair position).
- A 'road rumble' signal on the heave and the roll axis, consisting of a low-pass filtered noise signals.
- A pitch component that followed the pitch angle of the vehicle model (i.e. no tilt coordination)
- A roll component that followed the roll angle of the vehicle model (scaled by 50%).

The vehicle dynamics were representative for the dynamics of a C-Class Hatchback with automatic gear shift. The steering feedback torque was based on a spring-damper characteristic.

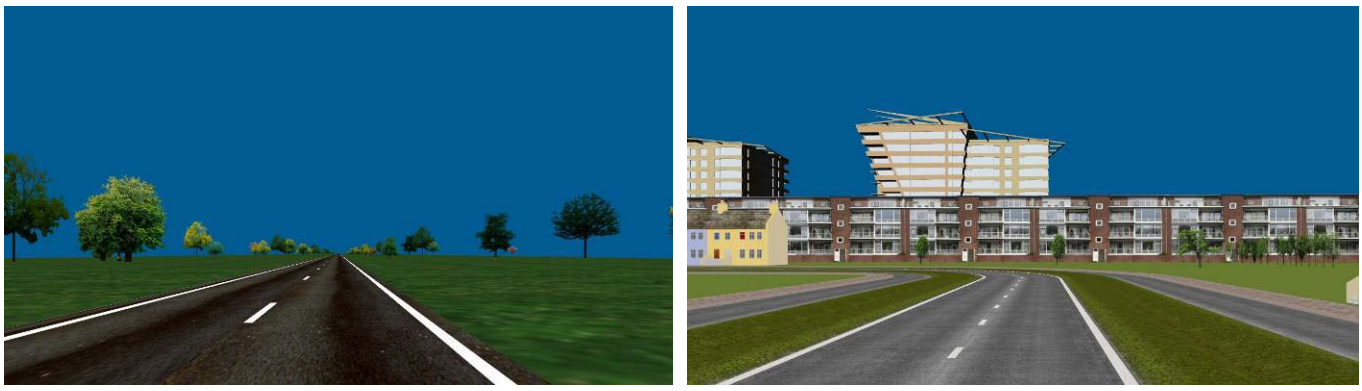

Figure 2 Straight road (left picture); curve to the left (right picture).

Two persons participated in blocks of two hours: while one was driving, the other one was resting. Each participant completed two runs. Each run consisted of two parts that were presented in a fixed order.

1. Lane changing on the straight road: four pairs of lane changes with, and four without yaw motion. The first was a straight road, which had 2 lanes with a standard lane width of 2.75 m. There were continuous lane markings on the outside and dashed markings on the centre line. The road was entirely straight. The vehicle's speed was limited at 82 km/h. Participants were instructed to press the gas pedal fully to ensure they would drive at a constant speed. They were instructed to carry out the lane changes manoeuvres swiftly.
2. Curve driving in an urban environment (four curves with, and four curves without yaw motion). In this environment the focus was on two types of corner driving such as that experienced in a tight curve and at an intersection crossing. The urban square circuit road had straight segments of 150 meters each and four 90 degrees corners. Two of these corners, in diagonally opposite corners, were curves with a radius of 20 m. The

other two were intersection crossings with rounded shoulders (radius of the rounded shoulders: 8.5 m). Participants were instructed to turn left on each corner / crossing, and not to exceed a speed of 50 km/h.

After a familiarisation procedure, the participant conducted four pairs of lane change manoeuvres, which typically took about two minutes in total. Then the participant was asked to stop the vehicle. After that, questionnaires were completed. These consisted of six questions about the experienced level of realism of the simulator (Likert scales). For motion sickness, we used the misery scale (MISC), developed and validated at TNO [Wer7]. A MISC score of 7 or higher (nausea – medium) was used as a termination criterion: if this level was reached, the run would be terminated and the participant would be excluded from the experiment. Then, the motion condition was changed and the second set of four lane changes was completed. Again the participant stopped the vehicle and the questionnaires were completed. This time a forced-choice selection of the most realistic simulation (first or second block) was asked as well.

Next, the set-up was changed to the urban environment. With the first motion condition operational, participants had a brief familiarisation run to get used to the task, the vehicle dynamics and the motion. After a brief stop, they conducted four curve driving manoeuvres, which typically took about two minutes. Then they were asked to stop the vehicle and give their ratings. Then the motion condition was changed and a second set of four curves was completed. Again the participant stopped the vehicle and the questionnaires were completed. This time a forced-choice selection of the most realistic simulation (first or second block) was asked as well.

In total, 14 subjects participated in the experiment (7 males, 7 females). Their average age was 40 years (s.d. 12). They had an average driving experience of 20 years (s.d. 11). They drove 15,000 km / year on average (9,3000 s.d.).

During the runs, driver input and vehicle state variables were logged with a frequency of 50 Hz.

The following dependent variables were derived for each lane change:

- maximum (absolute) steering wheel angle (^{o})
- the maximum lateral position (with respect to centre of new lane, in m)
- maximum yaw rate (^{o} /s)
- maximum lateral acceleration (m/s^2)
- SRR (Steering wheel Reversal Rate, s^{-1})
- percentage of time that any part of the vehicle was outside the lane (%)

In addition, the following the following dependent variables were determined for each corner:

- maximum braking pedal input (normalised)
- maximum deceleration (m/s^2)

Results

Motion sickness

In 89% of all observations, the MISC remains at 0 ('no problem at all'). In 10% of the cases, a MISC of 1 was given. The highest value that occurred, only once, was 2 (0.9% of observations). Thus, motion sickness was not an issue in this study.

Forced choice preference

After each pair of motion conditions, the participant was asked which of the two runs was perceived as most realistic. In total, the without yaw was selected 30 times (55%), and with yaw 25 times (45%). A Chi-square test showed no difference [$\chi 2 = 0.45$, $p=0.50$].

The preferred motion condition was with yaw in 44% on the straight road and 46% on the urban road. A Chi-square test showed no significant relationship between environment and preferred motion condition [$\chi 2=0.02$, $p=0.88$].

Thus, there is no indication that environment/task was related to preference of yaw motion.

Level of realism of the simulation

The results from the Likert scale questions were averaged over replications for each participant. Next, the results were analysed in separate ANOVAs, with two independent variables: environment (straight = lane changing task; urban = curve driving task) and yaw motion (without, with).

The results are shown in Table 1 and in Table 2 in terms of the main effects. The effect of yaw motion never reached statistical significance (see Table 1).

Table 1. ANOVA results: main effect of yaw motion (scale minimum 1; scale maximum 7).

Question	Without	With	Main effect significance
Q1: Felt like I was really driving	6.13	6.18	F(1,13)=0.1, p=0.74
Q2: I drove as I normally would	6.02	5.88	F(1,13)=0.8, p=0.40
Q3: I adjusted my driving to simulator	3.00	3.13	F(1,13)=0.5, p=0.48
Q4: I executed the task well	5.88	5.80	F(1,13)=0.2, p=0.68
Q5: motion and forces helped control the car	4.61	4.77	F(1,13)=0.1, p=0.82
Q6: motion and forces felt realistic	5.16	5.21	F(1,13)=0.0, p=0.84

As Table 2 shows, there were significant effects of the road environment. On the straight road, compared to the urban road:

- participants felt more like really driving a car,
- more like driving as normal,
- had to adjust their driving to the simulator to a lesser extent,
- had a higher rating of their task performance, and
- found that the forces and motion were more realistic.

Table 2. ANOVA results: main effect of environment/task (scale minimum 1; scale maximum 7).

Question	Straight / lane change	Urban / curve driving	Main effect significance
Q1: Felt like I was really driving	6.45	5.86	F(1,13)=6.0, p=0.03
Q2: I drove as I normally would	6.61	5.29	F(1,13)=16.6, p=0.002
Q3: I adjusted my driving to simulator	2.29	3.84	F(1,13)=12.2, p=0.004
Q4: I executed the task well	6.66	5.02	F(1,13)=34.3, p<0.001
Q5: motion and forces helped control the car	4.77	4.61	F(1,13)=0.3, p=0.57
Q6: motion and forces felt realistic	5.68	4.70	F(1,13)=11.5, p=0.005

Objective data: lane changes

Since no effects of replication were found, we averaged results over both replications before conducting the ANOVA.

Independent variables were yaw motion (off/without – on/with) and direction (to the left – to the right). The main effect results of yaw motion are summarised in Table 3. The effect of yaw motion never reached statistical significance. Thus, these results give no indication that yaw motion was of influence on driving behaviour in this part of the experiment.

Table 3 ANOVA results: main effect of yaw motion for lane changes.

Variable	Mean without	Mean with	Units	Effect yaw motion
max steering wheel angle	7.95	7.84	^{o}	F(1,13)=0.2, p=0.66
maximum lateral position	0.013	-0.002	m	F(1,13)=1.3, p=0.27
maximum yaw rate	2.05	2.05	^{o}/s	F(1,13)=0.0, p=0.98
max lateral acceleration	0.90	0.90	m/s^2	F(1,13)=0.0, p=0.99
Steering Reversal Rate	0.67	0.68	/s	F(1,13)=0.1, p=0.79
percentage outside road	2.45	2.26	%	F(1,13)=0.1, p=0.74

Objective data: curve driving

Initial analyses revealed several effects of corner type (curve or crossing), as did [Val8]. Therefore, this variable was included in the final analysis as reported here. An ANOVA was conducted for each dependent variable, using the independent variables yaw motion (off/without – on/with) and corner type (curve - crossing).

Table 4 ANOVA results: main effect of yaw motion for curve driving.

Variable	Mean without	Mean with	Units	Effect yaw motion
maximum steering wheel angle	201.9	188.1	^{o}	F(1, 13)=9.6, p=<0.01
Steering reversal rate	0.93	0.87	/s	F(1, 13)=1.7, p=0.21
Maximum path deviation	1.97	1.89	m	F(1, 13)=2.6, p=0.13
Maximum yaw rate	32.4	29.5	^{o}/s	F(1, 13)=21.0, p<0.001
Maximum lateral acceleration	5.6	4.8	m/s^2	F(1, 13)=13.8, p=0.01
average speed	30.4	29.0	km/h	F(1, 13)=11.9, p<0.01
Maximum braking	30	25	%	F(1, 13)=11.4, p<0.01
Maximum deceleration	4.4	4.0	m/s^2	F(1, 13)=3.38, p=0.088

The results revealed several effects of corner type, reflecting the smaller radius of the intersection crossing compared to the curve:

- Maximum steering wheel angle [F(1, 13)=273, p<0.001]: averages of 237 degrees on the crossing and 153 degrees in the curve.
- Maximum path deviation [F(1, 13)=12.7, p=0.01]: averages were 2.03 m on the crossing and 1.84 m in the curve.
- Maximum yaw rate [F(1, 13)=120.7, p<0.001], showing a higher yaw rate on the crossing (35.1 ^{o}/s) than on the curve (26.8 ^{o}/s).
- Maximum lateral acceleration [F(1, 13)=9.3, p<0.01]: the mean on the crossing was higher than on the curve (5.5 m/s^2 and 4.9 m/s^2, respectively)
- Average speed [F(1, 13)=74.2, p<0.001]: in the crossing, the average speed was 26.9 km/h, and in the curve 32.5 km/h.
- The maximum braking [F(1, 13)=52.2, p<0.001]: the on the crossing more braking was applied than in the curve (means 34% and 21%, respectively).

Several significant interactions were found between yaw motion and corner type. This was the case for the maximum steering wheel angle [F(1, 13)=11.9, p<0.01] and for the maximum yaw rate [F(1, 13)=19.7, p<0.001]. As Fig. 3 and Fig. 4 show, the effect of yaw motion was only present on the crossing, not in the curve.

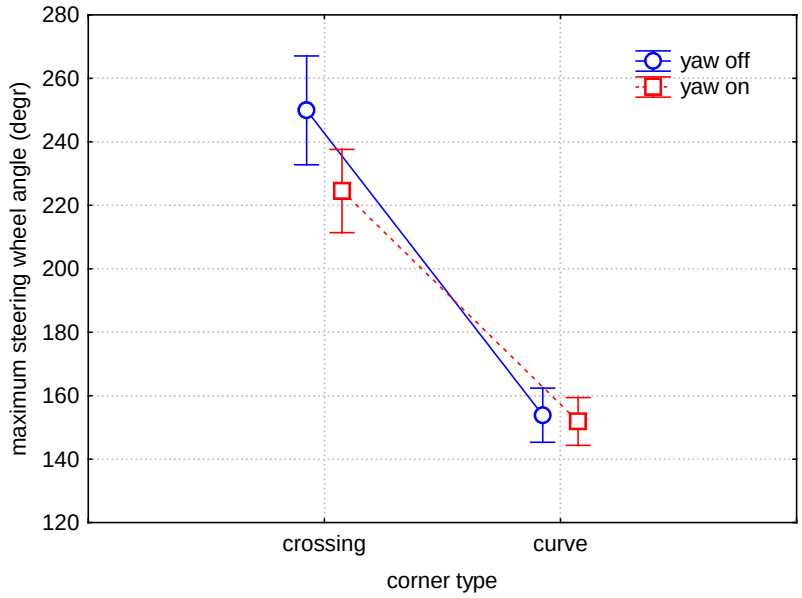

Figure 3: Maximum steering wheel angle as a function of yaw motion and corner type (means and 95% confidence interval).

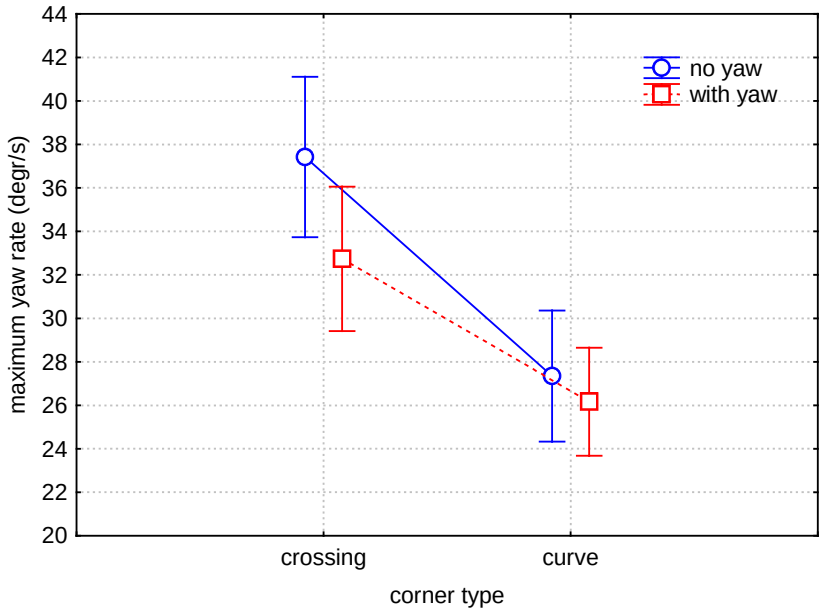

Figure 4: Maximum yaw rate as a function of yaw motion and corner type (means and 95% confidence interval).

Discussion and conclusions

The two combinations of task and environment (lane changing on the straight road, and corner driving in the urban environment) were deliberately designed to cover a wide range of lateral acceleration and yaw motion. The objective data confirmed that they did differ strongly. The maximum lateral acceleration was 0.9 m/s^2 in lane changing, and 5.2 m/s^2 in curve driving. The difference was even larger in terms of yaw rate: 2 $^o/s$ in lane changes, and 31 $^o/s$ in curve driving.

Reviewing the results of the questionnaires, it can be stated that the overall simulation was rated as quite realistic. Motion sickness was not an issue in this experiment. Typically, participants felt like they were "really driving a car", and "drove as they normally would" (scores above 6 on a scale from 1 to 7). Questions that focused on the motions and forces ('they helped', and 'felt realistic', respectively) scored a bit lower (4.7, and 5.2, respectively), but still clearly in the upper half of the scale. In informal debriefings, it became apparent that some subjects based their scores for these questions more on steering wheel forces rather than the forces associated with vehicle motion.

A statistical analysis showed that the ratings for the lane changing manoeuvres on the straight road were better than those for the cornering manoeuvres on the urban road. This illustrates the difficulty of simulating cornering manoeuvres in city environments.

In total, the questionnaires did not reveal effects of the yaw motion component (neither on the Likert scales, nor on the forced-choice preference). Informal debriefings showed that there were some participants who correctly identified the runs that had an 'extra' motion component, and some of them specifically stated that they felt this motion was not correct (e.g., 'felt like my rear wheels were steering', or 'felt as if I was driving a forklift').

When looking at the objective data of the lane change task, no differences were found between the conditions with and without yaw motion. In the corner driving task, several significant effects of yaw motion were found. With yaw motion present, we observed:

- smaller steering wheel amplitude (only on the crossing, not in the curve),
- smaller yaw rate amplitude (only on the crossing, not in the curve),
- smaller lateral acceleration amplitude,
- lower average speed,
- lower maximum braking, and
- lower maximum deceleration

All these effects show more cautious driving behaviour in the presence of yaw motion. This is in line with [Cor9] who found more cautious driving due to motion feedback in (more extreme) slalom driving in Desdemona. They concluded that with motion feedback, subjects drove more carefully and had better control of the car; therefore they could anticipate the car dynamic behaviour better and were not that surprised when the car did crash. Still, this was in rather extreme slalom driving. More in line with the current experimental setting, [Val8] reported a study in Desdemona, using the same urban environment as we did. There results showed that maximum deceleration levels were lower with their one-to-one yaw motion condition compared to rumble-only motion. Again, this is in line with the current results, i.e., showing more cautious behaviour with yaw motion present.

Now that we have found more cautious curve driving behaviour due to yaw motion, the question remains if this is an effect 'in the right direction', i.e. more towards driving behaviour in reality. [Fel10] reported test track results on speed choice and lateral accelerations on horizontal curves. In their smallest curve (R=16m), and under a comfortable driving instruction, the lateral acceleration levels were in the order of magnitude of 3 m/s^2. In the current experiment, we found maximum lateral accelerations of 4.8 m/s^2 with, and 5.6 m/s^2 without yaw motion. Thus, compared against the results from [Fel10], adding yaw motion appears to elicit more realistic driving behaviour.

In the urban environment, several differences were found between steering through the curve (R=20 m) and through the crossing (R=8.5 m). When the curve radius was smaller, we found:

- larger steering wheel angles,
- lower speed, and
- higher lateral accelerations.

These effects of curve radius are in line with the literature, see e.g. [Win11], [Fel10]. Furthermore, an earlier experiment in Desdemona in the same urban environment showed similar differences between the curve and the crossing [Val8].

In conclusion, the experiment has shown that adding yaw motion to the simulation changed driving behaviour in curve driving. With yaw motion present, driving behaviour became more cautious, and (compared against the literature) more realistic, especially in small-radius curves. This suggests that adding yaw motion to a driving simulator improves the external validity for corner driving manoeuvres.

Acknowledgements

This work was supported by General Motors.

References

[Cor9] Correia Grácio, B., Wentink, M., Feenstra, P.J., Mulder, M., Van Paassen, M.M., Bles, W. "Motion feedback in advanced driving manoeuvres". *Proceedings of the Driving Simulation Conference DSC2009.* Monaco: 4-6 February 2009.

[Fel10] Felipe, E., Navin, F. "Automobiles on horizontal curves: experiments and observation". *Transportation Research Record,* 1998, *1628,* 50-56.

[Ken2] Kennedy, R.S., Fowlkes, J.E., Berbaum, K.S., Lilienthal, M.G. "Use of a motion sickness history questionnaire for prediction of simulator sickness". *Aviation Space and Environmental Medicine,* 1992, *63,* 588-593.

[Mou6] Mourant, R.R., Yin, Z. "A Turning Cabin Simulator to Reduce Simulator Sickness". *Proceedings of SPIE - The International Society for Optical Engineering,* 2010, *7525, art. no. 752503.*

[Sch4] Schwarz, C., Gates, T., Papelis, Y. "Motion characteristics of the national advanced driving simulator". *Proceedings of the North American Driving Simulation Conference,* Michigan: October 8-10, 2003

[Toy5] Toyota "*Toyota Develops World–Class Driving Simulator".* News release November 26, 2007. http://www.toyota.co.jp/en/news/07/1126_1.html.

[Val8] Valente Pais, A.R., Wentink, M., van Paassen, M.M., Mulder, M. "Comparison of three motion cueing algorithms for curve driving in an urban environment". *Presence: Teleoperators and Virtual Environments,* 2009, *18* (3), 200-221.

[Win11] Van Winsum, W., Godthelp, J. "Speed choice and steering behaviour in curve driving". *Human Factors,* 1996, *38,* 434-441.

[Wen1] Wentink, M., Valente Pais, R., Mayrhofer, M., Feenstra, P., Bles, W. (2008). "First curve driving experiments in the Desdemona simulator". *Proceedings of the Driving Simulation Conference DSC2008.* Monaco: 31 January - 1 February 2008.

[Wer7] Wertheim, A.H., Ooms, J., De Regt, G.P., Wientjes, C.J.E. "Incidence and severeness of seasickness: Validation of a rating scale" 1992, Tech. Rep. No. IZF 1992 A-41, Soesterberg, Netherlands: TNO Human Factors.

[Yam3] Yamaguchi, D., Suda, Y., Onuki, M., Shimoyama, O. "Approach to Improvement of Realistic Sensation on Universal Driving Simulator". *Proceedings of the Driving Simulation Conference DSC 2010.* Paris, France: 9-10 September 2010.

Investigating Human Lane Keeping through a Simulated Driver

Sebastian Noth[1], Iñaki Rañó[1], Gregor Schöner[1]

(1) Institut für Neuroinformatik, Ruhr-Universität Bochum, 44780 Bochum, Germany, E-mail : {inaki.rano, sebastian.noth, gregor.schoener}@ini.rub.de

Abstract *– Human driving behaviour modeling is an active and exciting research field with many applications for the automotive industry, ranging from safety to driving automation. Lane keeping is a well-studied problem, but formal models of human driving for this task are scarce. This paper implements a methodology to obtain naturalistic driver models through Systems Identification techniques. We obtain two different representations for individual human driver controllers based on their driving in a simulated environment. The models capture the way humans steer cars and can generate stable trajectories when controlling a simulated vehicle.*

Key words: *lane-keeping model, systems identification, driver model.*

Introduction

Lane keeping for autonomous driving is a well-studied problem, and many good solutions can be found in the literature. Moreover, lane departure warning systems (LDW) and lane keeping systems (LKS) can be already found in several commercial cars nowadays. While LKS function by using some kind of bang-bang controller, many others actually work continuously in time implementing lane keeping mechanisms. However, most of the existing lane- keeping controllers try to keep the car in the centre of the lane through standard control techniques. Therefore these mechanisms might not match the criteria used by human drivers when keeping the car in the lane and result in unnaturalistic driving from the user point of view. Having a mechanism that mimics human driving has many other advantages like: detection of abnormal driving, teaching and training of drivers, substitution of human driving in tests or experiments, among others. This paper presents a novel approach to obtain naturalistic driver controller models based on data from real drivers.

Like humans do, many of the lane-keeping systems found in the literature rely on visual information from the road, since it is relatively easy to obtain and provides adequate information to feed into a controller. The pioneering works on visually guided vehicles go back to the early 90s (see [Dic1] and references therein), and therefore, an exhaustive review of the relevant works in this area would need to be quite extense. An elegant analysis of the effect of the look-ahead distance is presented in [Kos1], where a vision-based lane keeping controller is implemented. Moreover, by analysing the root locus of the system, they prove that a larger look-ahead distance helps stabilising the motion of the vehicle. In [Cer1] another vision-based controller is presented and designed using loop-shaping, a frequency domain technique that, among others, keeps the vehicle within some specified lateral position and velocity constraints. Since their vehicle works at high velocities, they need to account for the steering actuator and parameter uncertainty of the car. In some cases visual information is used jointly with other sensors to perform lane keeping, like the work presented in [Mar1]. The authors implement a double loop controller based on vision and a gyroscope measuring the yaw rate of the vehicle. The internal loop is a PI controller of the yaw rate while the external loop provides the reference yaw rate based on the visual system and a PID controller. Their controller is robust to changes in relevant parameters of the model like, among others, the vehicle speed and mass.

A common feature among the vision-based lane keeping mechanisms is that they rely on the deviation from the centre of the lane at a single point. If we intend to mimic or model the way humans perform that task, it seems appropriate to use the same sort of information humans use. In fact, it is well known that humans use two reference points to steer a car [Lan1], and, therefore, we will focus on two point based lane keeping mechanisms. While the car is kept in the centre of the lane mainly using an angular reference to a point right in front of the car (near point), the alignment with the road is performed using a point of the road close to the line of the horizon (the far point). The first two-point model for lane keeping that can be found in the literature is presented in [Sal1]. This work compares the behaviour of the proposed model with real drivers and demonstrates that their lane keeping model captures accurately the way humans drive. However, the parameters of the model are empirically adjusted to qualitatively

match the drivers' behaviour and, therefore, their estimate is just an approximation. Another work relying in a two-point controller to imitate human driving is presented in [Sen1]. There the authors use the standard car model presented in [Ack1] and propose an improved driver model derived from one of the earliest works in driver modelling [Hes1]. Even though the parameters of their model are adjusted through system identification techniques, they only use data obtained from simulated drivers implemented through optimal control techniques, and therefore their work does not represent human drivers' behaviour.

The standard way of modelling the car for a constant forward velocity is through a linear approximation of the car dynamics, and therefore several linear control models have been proposed in the literature to model human driving. A PD controller is used in [Hes1] with a single reference point, while a phase-lead and a proportional controller are used for the near and far points respectively in [Sen1]. A PI and a proportional controller are used for the far and near point respectively in [Sal1]. However, none of these works really compares the theoretical results of the control systems with known empirical findings of human driving [Lan1]. This paper contributes to the modelling of human drivers in several ways. First, we present a new perception model for the driver that allows to use a two point steering control mechanism in the same way humans do. Second, we fit data obtained from human drivers with system identification mechanisms to produce human equivalent linear controllers that can generate naturalistic driving. Our long term goal is to integrate this lane keeping system in a general driver model that includes modelling of human decision taking [Pel1].

The rest of the paper is organised as follows: The next section presents the car and driver models jointly with the setting used to gather the data needed to train the models. The experimental procedure and results are shown in the following section, while the last section accounts for the conclusions and future work.

The Car and Driver Models Integrated Within the Simulator

This section first presents the car model we used, a model that includes a new human-like output equation for the far angle. We then present the chosen potential models of human lane keeping behaviour, and finally, we describe the driving simulator used to gather human driving data.

The Car-Perception Model

Our model for the vehicle dynamics is adapted from [Sen1], though we discard the wind force as a disturbance since our focus is modelling human driving under normal conditions. The car model consists of a linear state space representation where the state of the car is described by the vector $x^T = [\beta, r, \psi_L, y_L, \delta_d, \dot{\delta}_d]$, with β representing the slip angle, r the yaw rate, ψ_L the relative yaw angle, y_L the lateral offset from the centre of the lane and δ_d and $\dot{\delta}_d$ the steering wheel angle and velocity respectively. The driver input u to the model is the torque Γ applied to the steering wheel, while, as already stated, we will consider the road curvature ρ as the only disturbance input w. Therefore, the dynamics of the vehicle is described by the equation:

$$\dot{x} = Ax + B_u u + B_w w, \qquad (1)$$

where matrices A and B_u are the same as in [Sen1], whilst the perturbance matrix B_w is in our case:

$B_w^T = [0\ 0\ -v\ 0\ 0\ 0]$, v being the linear velocity of the car. The numerical parameters of the simulated car are presented in table 1.

Table 1. Parameters of the car model.

C_r	C_f	l_f	l_r	m	I_z
60000	47000	0.88	1.5	867	1146

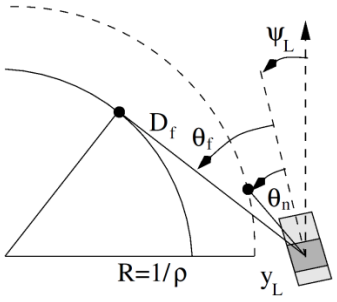

Fig. 1. Reference system of the model variables.

Since humans use near and far angles to steer a car (see Figure 1), the output equation should provide values for such variables. However, the existing works [Sen1] [Kos1] model the perception of the near (or far) point without accounting for the road curvature. While the near point angle (θ_n) can be computed from the near distance (D_n), yaw angle (ψ_L) and lateral position of the vehicle (y_L) as, $\theta_n = \frac{1}{D_n} y_L - \psi_L$, the far angle has to be computed using the road radius. The far point angle can be computed from the road radius (R), the car lateral position relative to the middle of the road and the yaw angle as:

$$\theta_f = asin\left(\frac{D_f^2 + y_L^2 + 2Ry_L}{2D_f(y_L + R)}\right) - \psi_L, \qquad (2)$$

where we neglected the width of the lane compared to the radius of the curve. Linearizing this equation around the middle position of the lane ($y_L = 0$) and a straight road, we obtain the output equation for the approximated far point angle:

$$\theta_f = \frac{1}{D_f} y_L + \frac{D_f}{2}\rho - \psi_L, \qquad (3)$$

where $\rho = 1/R$ is the curvature of the road and D_f is the distance to the far point. Therefore, matrices C and D for our output equation $y = Cx + D_w w$ can be stated as:

$$C = \begin{bmatrix} 0 & 0 & -1 & 1/D_n & 0 & 0 \\ 0 & 0 & -1 & 1/D_f & 0 & 0 \end{bmatrix}$$

and

$$D_w^T = [0 \quad D_f/2 \quad 0],$$

where the output vector is $y^T = [\theta_n \quad \theta_f]$. Even though the perception is carried out by the driver, it is convenient to consider it as an output from the car/road system, such that it can be directly fed into the controller model.

The Driver Model as a Black-Box Model

Systems identification techniques have been used as a tool to model controllers, for instance in robotics [Aka1], for complex tasks. This methodology presents a set of desirable features. On the one hand, it provides a way of obtaining controllers that perform appropriately under real world circumstances, as their parameters are estimated from real data and therefore robustness to noise is already accounted for. On the other hand, they provide a way of obtaining controllers through a process of learning by demonstration if the system is guided by a teacher while the training data is gathered.

Following a similar approach, we consider human drivers' lane keeping behaviour can be properly modelled by ARX models [Lju1] with the perceived near (θ_n) and far angles (θ_f) as an input and the torque (Γ) acting on the steering wheel as an output. This means we need to identify two ARX models simultaneously from the data, one for each input variable of the driver. Since the car model is a linearization and the driver is modelled also as a linear system, standard techniques can be applied to analyse the whole car-driver dynamical system once the controller is learned. Moreover, this approximation assumes no interaction between the near and far controllers, i.e. the global output comes from two independent contributions.

As we already explained in the introduction, some works model the driver as a state-space model of dimension five [Sen1]. This represents a grey-box model that imposes constraints to the internal control mechanism that generates human driving, constraints which may not be appropriate. In order to grasp a deeper insight of the internals of the lane keeping control mechanism, we decided to compare the ARX models with state-space black-box models that impose no restrictions to the controller form. This would allow to investigate whether there is an internal interaction between the near and the far point controller through some state-space variable.

The Driving Simulation Lab

To gather data from real drivers, we used our Driving Simulator Lab, which has seats for up to ten drivers in individual driving cabins as shown in Figure 2. The cabins are equipped with a force feedback steering wheel and a pedal console of a throttle and brake pedal. A realistic virtual environment is rendered to a 24" computer screen mounted in front of the subjects at an approximate distance of 60 cm, generating a field of view of 43°. For every cabin, the simulation software, TrafficSimulation [Not1], a commercial, fully customisable software with different modules and plug-ins, is run on a standard PC. For the present experiment, two adjacent cabins were used with simulators running in standalone-mode, such that drivers could drive in couples while talking to each other, therefore, instead of only focusing on the simulated environment, a rather automatic driving behaviour is induced.

Fig. 2. Two cabins of our driver lab.

Since the steering wheel used in our lab does not provide an accurate force feedback, the steering column generates a torque proportional to the angular displacement. Therefore, the torque the user needs to apply on the steering wheel is proportional to the angle, and the parameters on the car model, equation (1), are set accordingly to account for this drawback of our system. Apart from this issue, the simulator software runs the car model presented earlier in this section in a configurable simulation environment, which includes, among others, traffic signs, buildings or trees.

Experiments and Identification Results

This section presents the experimental identification setting and process, and it also includes the results and analysis of the obtained models.

Data Acquisition Procedure

In order to sample driving behaviour under different conditions, we created a specific road layout for the simulated environment. The test track is, after a 9 km long accommodation stretch, subdivided into 3 parts, each of which has a different speed limit (80, 100 and 120 km/h), which was indicated to the driver through traffic signs alongside the road. Every part contains sections of different curvatures, alternatingly 5 right and 5 left turns. Curves are separated by 300 m long straight stretches to let the drivers stabilise the car to the centre of the lane. Additional 500 m long straight stretches are inserted between the parts for the required speed adjustment. The five different curvatures are logarithmically equidistant steps, ranging from light curves of 8 km radius to rather sharp curves of 800 m radius. The track consists of two 3.8 m wide lanes. The ride takes altogether about 20 minutes. The DataWrite plug-in for TrafficSimulation allowed us to record driving data at a rate of 25 Hz, specifically the system state data recorded are steering wheel torque Γ, lateral position y_L, relative yaw angle ψ_L, yaw rate $\dot{\psi}_L$, track position s, and velocity v.

Prior to driving, subjects were asked to fill out a small questionnaire about their driving habits. We asked them when they received their driving license and some general personal questions. For some of the subjects the screen distance, seat height and distance to the pedals had to be adjusted. Subjects were recruited among the staff of the Institut für Neuroinformatik. Eleven subjects were accomplishing the driving task, 5 females and 6 males. Average age was 35.9 years with a minimum of 27 and a maximum of 56 years. Subjects held their licenses for 17 years on average, and reported to be driving 12120 km per year on average, thereof 5760 km on highways. The accommodation part was excluded from the recorded data in order to properly train the models.

Model Fitting

Since the TrafficSimulation software provides us with the state in time for all the trajectories, we used the already presented output equations to compute the inputs to identify the driver model. The model output was actually obtained from the steering wheel. For every subject, the data was resampled at a frequency of 5 Hz after being filtered in order to avoid aliasing problems. The two point lane keeping model requires distances of the far and the near point, D_f and D_n. We assume $D_f = 75$ m and $D_n = 5$ m. From the lateral position, the relative yaw angle and

the track position, we can compute the far and the near angle, θ_f and θ_n, which are used as inputs to the driver model.

A key problem when trying to identify a system using a black-box methodology is to identify the system structure and its order. As we already stated, we decided to use a black-box state-space representation and an ARX model, but the corresponding orders needed to be selected. We tested a large range of possible dimension for the state-space model and a set of possible parameters for the ARX model. Specifically the range of state-space dimensions was from 2 to 15, while for the ARX model we tested values for the number of poles (n_a) from 2 to 10 and several values for the number of zeros (n_b) for both inputs, always taking into account that the controller model has to be causal, i.e. the number of poles has to be higher or equal to the number of zeros. Figure 3 shows the average result of the computed mean square errors for different models trained with the data set of 11 drivers, jointly with bars indicating the standard deviation of the model error from the mean. In the case of the state-space models (right figure) we can see a global decreasing trend in the error mean as we increase the number of dimensions. However, as there is a trade-off between the descriptive capability of the model and its complexity, we decided to use a state-space representation of dimension 5, which coincides with the dimension of existing models [Sen1]. Since the ARX models include three parametric dimensions (the number of poles and the number of zeros for both inputs), we only represent the case in which both transfer functions had only one zero in figure 3 (right). In the case of the average error for the ARX models, the decreasing trend is not so clear, since, in fact, it seems to stabilize for a number of poles higher than 5. Theoretically the two representations, the state-space and ARX model, should be equivalent, and therefore it is normal that the optimal dimension and the best number of poles are the same, moreover, the mean square average errors for the eleven drivers is similar in both cases.

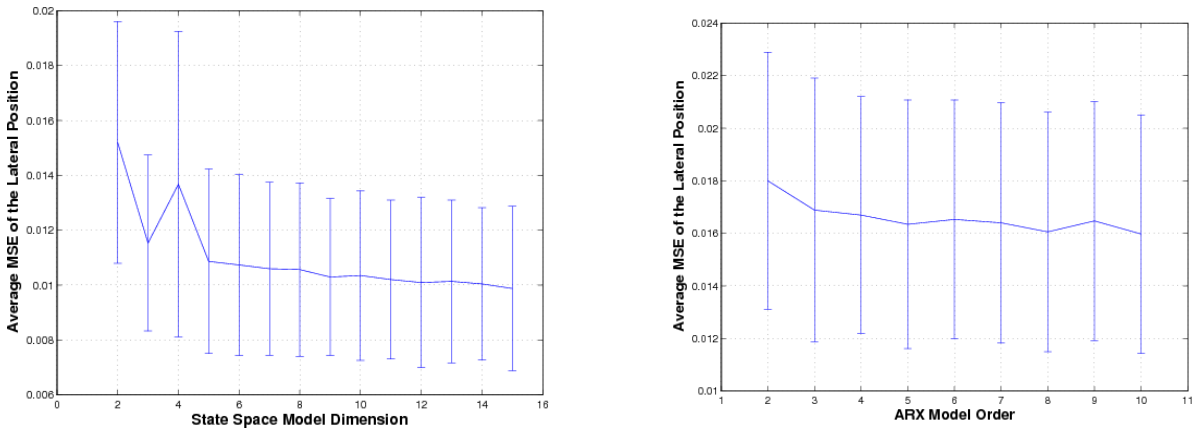

Fig. 3. Mean square errors for different state-space and ARX models.

The least-square errors were computed by simulating the obtained models fed with the corresponding near and far angles from the data recorded from the simulator and comparing the output of the model with the actual response of the driver under the same conditions. This corresponds to an open-loop simulation of the models, which is shown in Figure 4. The left part of the figure represents the inputs, near and far angle, while the right part plots the outputs of the state-space and the ARX model superposed to the actual command of the driver (the steering torque). The figure corresponds to a 160 seconds chunk of the experiments carried out by driver Dr04. As it can be seen, the range of variation for the near angle input is bigger that for the far angle. This is a joint effect of the near and far distance combined with the relatively small curvature of the road (even though the plot shows a section including a curve with small radius). On the other hand, the figures on the right show how both models capture the general shape of the steering torque generated by the user, but with a much less oscillatory behaviour. This will become more evident in the next section were closed-loop simulations are presented. In general it can be claimed that both models capture the global tendency of the driver, though they probably do not have enough descriptive capacity to account for the small details of the driving, i.e. high frequency signals.

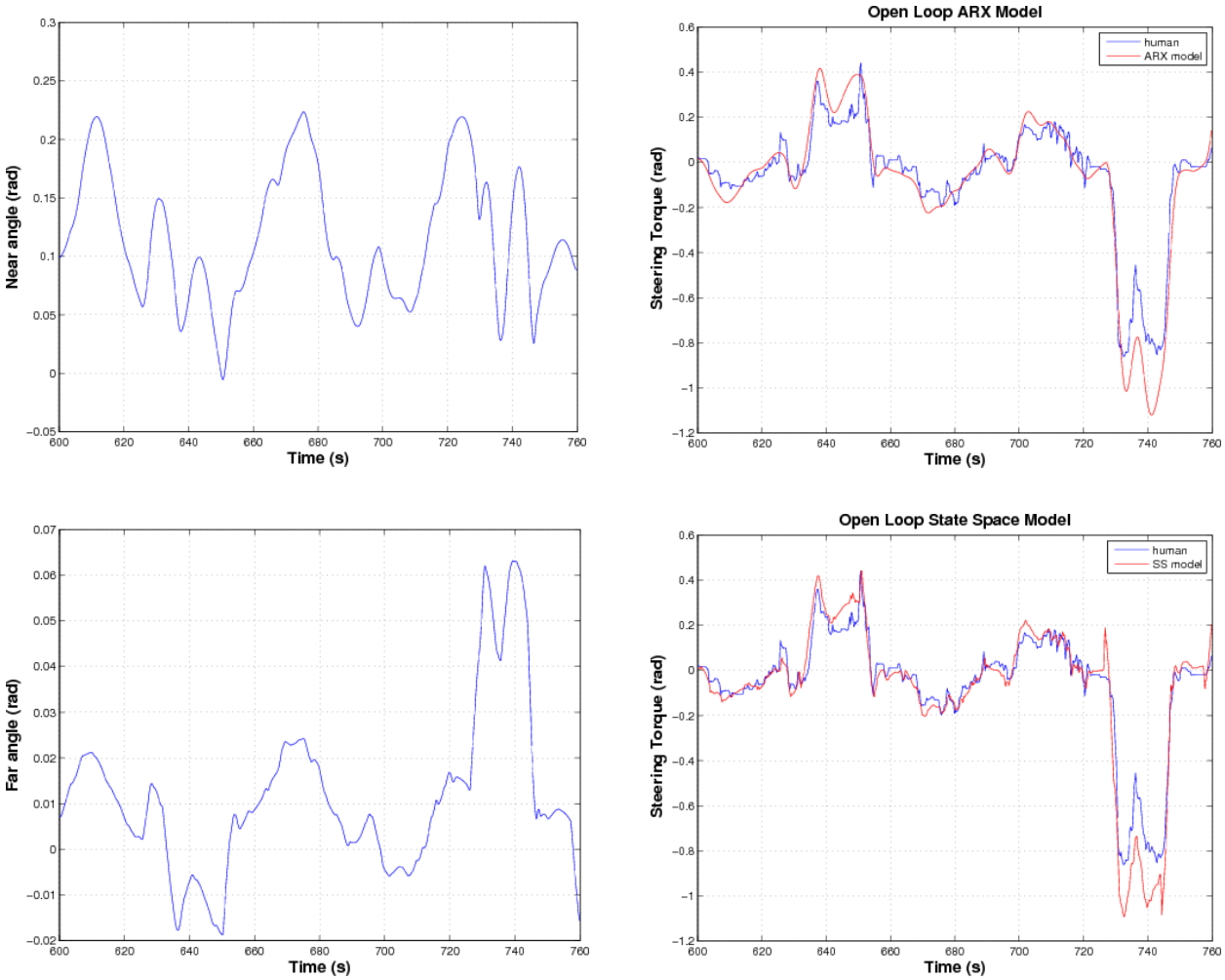

Fig. 4. Near and far angle based on recorded data, recorded steering torque output data and open-loop simulation based on the near and far angle

Closed-Loop Simulations of the Model

In order to test the real performance of the lane keeping controller models obtained, we need to test them in a simulated environment where they evolve to keep a car centered on the lane. First, we tested the stability of the whole driver model/car system beforehand, and we saw that all the learned controllers trained in the previous section were stable in closed-loop. Figure 5 shows the result of two models obtained from driver Dr03 superposed to the actual driver-car trajectories. The learned controllers were tested in an identical setting as the real drivers, actually obtained from the road specifications used on the session recorded using the driving simulator. Even though the models were simulated in Matlab, the configuration parameters of the car were identical to those in the simulated car. As it can be seen in the left figure, both controllers, the state-space and ARX models, capture the general trends of the driver Dr03, but they cannot cope with the fast variations present in the steering torque generated by the human driver. This can be interpreted as the model not having enough degrees of freedom to cope with these variations, but the most plausible reason is that the actual control mechanism used by the human drivers is non-linear. In fact, it is quite plausible that humans do not actually try to keep the car perfectly centered in the lane, but use instead some range where they do not control the steering wheel, a bang-bang controller for the near point. This could be modelled as a dead-zone in the controller models, but obviously it cannot be captured by a purely linear model. The right figure shows the actual lateral trajectory followed by the driver and the models. As it can be seen, there is a bigger difference between the real trajectory and those generated by the models. This is due to the dynamics of the car integrating and amplifying the small variations of the controllers, since what it was minimized during the training phase is actually the error on the steering toque and not on the lateral position of the car.

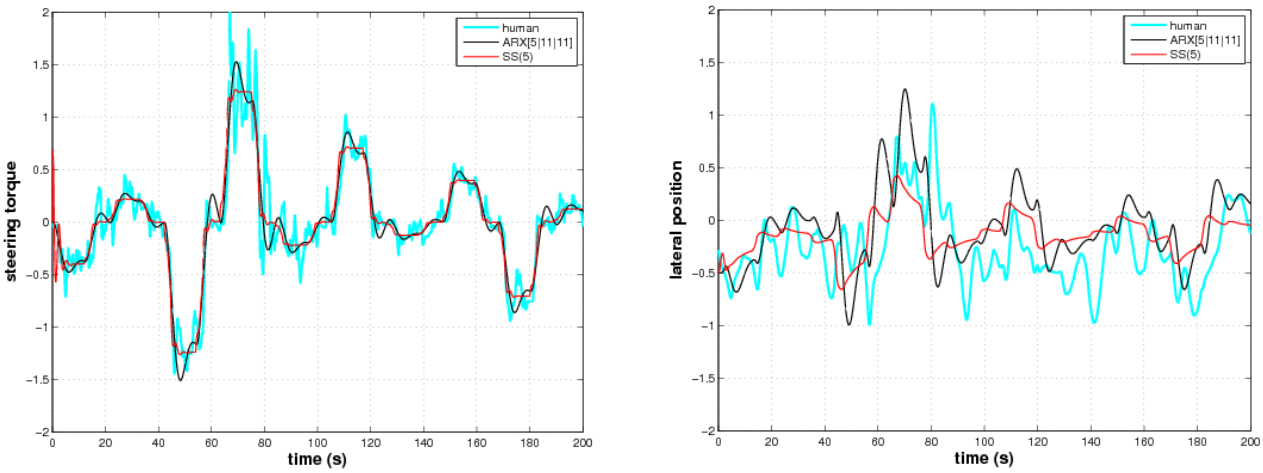

Fig. 5. Steering torque generated by the ARX and state-space model fitted with data from driver Dr03 and the resulting lateral position, compared to data from the driver.

Conclusions and Future Work

This paper presents a novel approach to obtain naturalistic driving controllers through the use of Systems Identification techniques with data recorded from human drivers. Existing works either did not fit real driving data or used heuristic methods to obtain the controllers, therefore, to the best knowledge of the authors, this represents the first time a formal identification technique is used to model human lane keeping. As already stated, all the works proposing linear models present limitations since they cannot cope with non-linear effects like dead-zones in the control variables. However, some extra simulations we performed switching off one of the models obtained, matched the known results from humans driving only using the near or the far point [Lan1]. This is an interesting topic which deserves a deeper analysis outside the scope of the present work.

Further analysis needs to be carried out using the state-space representation to test the hypothesis of total independence on the near and far controllers, since the output torque is computed from the five dimensional state-space vector which dynamically links the near and far input variables. Another important issue is that humans can adapt their driving to different cars, and, therefore, the robustness of the driver model to change on some parameters (like velocity or car model parameters) has to be assessed. Finally, we plan to integrate this mechanism as a part of a driver model that reaches the tactical level of driving.

References

[Aka1] Akanyeti O., Rañó I. “An application of Lyapunov stability analysis to improve the performance of NARMAX models”. *Robotics and Autonomous Systems*, 2010, 58(3), pp. 229-238.

[Ack1] Ackermann J., Bartlett A., Kaesbauer D., Sienel W., Steinhauser R. “Robust control: Systems with uncertain physical parameters”. *Springer*, 1993.

[Cer1] Cerone V., Chinu A., Regruto D. “Experimental results in vision-based lane keeping for highway vehicles”. *Proceedings of the 2002 American Control Conference*, 2002, pp. 869-874.

[Dic1] Dickmans E. “Vehicles capable of dynamic vision”. *Proceedings of the International Joint Conference on Artificial Intelligence*, 1997, pp. 1577-1592.

[Hes1] Hess R., Modjtahedzadeh A. “A Control Theoretic Model of Driver Steering Behavior”. *IEEE Control Systems Magazine*, 1990, 10(5), pp. 3-8.

[Kos1] Kosecká J., Blasi R., Taylor C., Malik J. "Vision-based Lateral Control of Vehicles". *Proceedings of the IEEE Intelligent Transportation Systems Conference*, 1997.

[Lan1] Land M., Horwood J. "Which parts of the road guide steering?". *Nature*, 1995, 377, pp. 339-340.

[Mar1] Marino R., Scalzi S., Orlando G., Netto M. "A Nested PID Steering Control for Lane Keeping in Vision Based Autonomous Vehicles". *Proceedings of the 2009 American Control Conference*, 2009, 9(2), pp. 2885-2890.

[Not1] Noth S., Edelbrunner J., Iossifidis I. "A Versatile Simulated Reality Framework: From Embedded Components to ADAS". *International Conference on Pervasive and Embedded and Communication Systems*, 2012.

[Pel1] Pellecchia A., Igel C., Edelbrunner J., Schöner G. "Making Driver Modeling Attractive ". *IEEE Intelligent Systems*, 2005, 20(2), pp. 8-21.

[Sal1] Salvucci D., Gray R. "A two-point visual control model of steering". *Perception*, 2004, 33, pp. 1233-1248.

[Sen1] Sentouh C., Chevrel P., Mars F., Claveau F. "A Sensoriomotor Driver Model for Steering Control". Proceedings of the 2009 IEEE International Conference on Systems, Man and Cybernetics, 2009, pp. 2462-2467.

[Lju1] Ljung, L. "System Identification: Theory for the User". *Prentice Hall*, 1999.

Perceptual Load in Central and Peripheral Regions and Its Effects on Driving Performance With and Without Collision Avoidance Warning System

Hadas Marciano[1] and Yaffa Yeshurun[1]
(1) University of Haifa, Psychology Department, Haifa, Israel {hmarcia1@univ.haifa.ac.il; yeshurun@research.haifa.ac.il }

Abstract *– A driving simulator study was conducted to test the influence of Collision Avoidance Warning System on drivers' performance. Perceptual load on the road (e.g., vehicles' congestion) and its sides (e.g., pedestrians' number) were manipulated, while critical events occurred on the road (e.g., a leading car suddenly slowed down) or initiated from its sides (e.g., a pedestrian crossed the road unexpectedly). Each participant drove in four different scenarios: two with the warning system and two without. We found that at least in one condition (low levels of load in both regions) the system acted like a two-edged sword: On the one hand it decreased accidents with entities on the road, but on the other hand it increased accidents with entities arriving from the road sides. These findings demonstrate the importance of a systematic manipulation of perceptual load across the visual field and the critical events' location when evaluating drivers' behavior.*

Key words: *Perceptual load; In-Vehicle Warning System; Attention; Driving Simulator;*

Introduction

As we drive, information from different regions of the visual scene continuously reaches our eyes. Only some of it is relevant for safe driving. The ability to allocate attention only to the relevant information is a crucial factor in many car accidents. [Lav8] claimed that this ability is affected by the perceptual load in the scene. With high perceptual load, selectivity is high and attention is allocated only to the relevant information, but with low perceptual load selectivity is low and irrelevant information is also processed. Most of the studies which tested the perceptual load model manipulated load only in central regions of the visual field, leaving the load at more peripheral regions quite minimal (e.g., [Lav7]; [Lav9], see [Lav8] for a review). However, using simple letter stimuli, we [Mar13] orthogonally manipulated the levels of load in both relevant (central) and non-relevant (peripheral) regions. The results showed that increasing peripheral load deteriorated performance, but only with low levels of central load. Recent studies conducted in our lab have shown that when participants were asked to perform an additional second task at the periphery, and therefore had to allocate attention not only to the central region but also to more peripheral regions, additional resources could be recruited. This result has clear implication for driving behavior, as it suggests that drivers can (and do) allocate some attentional resources to the peripheral regions while driving, even under high levels of road load.

Several studies explored the influence of warning systems on drivers' behavior (for a review see [Gre6]). For instance, some of the studies that explored Collision Avoidance Warning Systems (like the one investigated in the current study) have shown an overall benefit for the employment of the system, especially concerning avoiding dangerous headways (e.g., [Ben2]; [Mal12]; [Shi15]). Other studies focused on comparing different modes of the systems. For example, [Abe1] compared three different kinds of timing of the alarm (early: 0.05 sec, middle: 0.64 sec, and late: 0.99 sec after the leading vehicle brakes) and found that a more appropriate response was related to the early alarm compared with either the middle or the late alarms. Another example is [Lee11] who compared different alert modalities (haptic vs. auditory) and different strategies (graded vs. single-stage). They found that graded haptic alerts might be preferable. Interestingly, a number of studies have shown that under some conditions the Collision

Avoidance Warning System may impair or may not benefit performance. For instance, [Bro4] claimed that overestimating the speed of human response can lead to a system which will not allow enough time for collision avoidance, and [Yam16] showed that an imperfect reliability of the system might lead to a reduction in drivers' performance instead of improvement.

However, none of the former studies explored in a systematic way the influence of warning system under different conditions of perceptual load, as was done in the current study. We employed two levels of perceptual load at two locations, the road itself and the sides of the road. The load levels on the road and on its sides were orthogonally manipulated to create four distinct combinations: high load on the road with low load on its sides, low load on the road with high load on its sides, low load in both regions, and high load in both regions. Critical events that required a rapid response (e.g., a pedestrian crossing the road) were also manipulated, half of them occurred on the road and half of them were initiated from its sides (see also [Mar15]). In addition, we compared driving without a Collision Avoidance Warning System to driving with such a system, in order to test whether the system improves driving performance, and if so whether this improvement is manifested in all load by event location combinations.

Method

Participants:

20 participants, 6 women and 14 men, average age 25.75 years (ranging from 22 to 31) took part in the experiment for monetary reward. All were students of the University of Haifa, and had driving experience of at least five years (with an average of 7.85 years).

Tools:

The experiment took place in a partial driving simulator using STISIM Drive™ software (Fig. 1). A Logitech steering system, which included steering wheel and two pedals – gas pedal and brake pedal – was used. The participant sat 2.5 m in front of a wide screen (2.3x3 m). This viewing distance was calculated to ensure that the perceived objects would have a similar visual angle to that in real life. Moreover, given the size of the screen and this viewing distance, critical events that were initiated from the sides of the road initiated from an eccentricity of 31º of visual angle (i.e., when the driver is fixating the middle of the road) which is also similar to real life. A speaker, providing background sounds, was placed behind the participant.

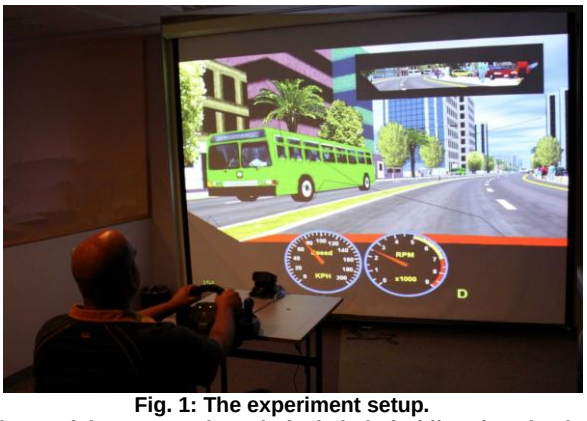

Fig. 1: The experiment setup.
The participant seats in a clerical chair, holding the wheel. The scenario is presented on a wide screen in front of the participant.

Scenarios:

Four different 23 km long scenarios were programmed. These scenarios simulated a suburban road with two lanes in each direction separated by a road median area. Each scenario consisted of four distinct different combinations of load on the road and on its sides: low load in both road and sides regions (LL, Fig. 2a), high load on the road with low load on its sides (HL, Fig. 2b), low load on the road with high load on its sides (LH, Fig. 2c), and high load in both road and sides regions (HH, Fig. 2d). The order of these four different load segments was balanced across the four different scenarios.

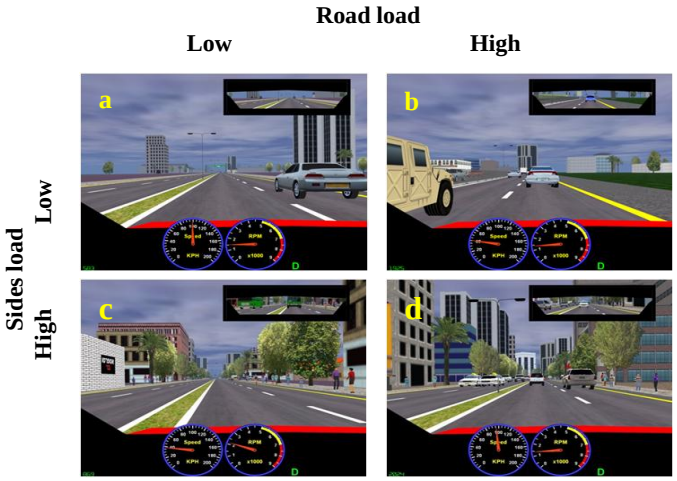

Fig. 2: Illustrations of the different load combinations in the experiment: a) LL: low load in both regions;
b) HL: high load on the road, low load on its sides;
c) LH: low load on the road, high load on its sides;
d) HH: high load in both regions.

The load on the road was manipulated via the number and congestion of the vehicles. The load on the sides of the road was manipulated via the number of pedestrians, the density of the buildings, the presence of parked vehicles, etc. In each scenario 16 critical events were included, eight occurred on the road (e.g. a leading car suddenly slowed down), and eight were initiated from the sides of the road (e.g., a

pedestrian crossed the road unexpectedly). Event location was balanced within the load conditions; in each load combination two events occurred on the road and the other two were initiated from its sides.

Collision Avoidance Warning System:

The warning system was programmed within the simulator. The criterion for its alarm activation was 2.5 seconds "time to collision" with a leading vehicle. This timing was chosen because pilot studies revealed that using it led to enough occurrences of the warning signal, but not too many, which might induce distrust in the system. The signal itself was an auditory signal of a brief pulsing tone.

Procedure:

Each participant came to the Lab for three meetings. In the first meeting the participant drove in a practice scenario of about 30 minutes, in order to get used to the simulator setting. The next two meetings included the experimental sessions and each lasted about one hour. In each experimental session the participant drove in two different scenarios. One of these scenarios included the activation of the Collision Avoidance Warning System, while the other scenario did not. The order of the scenarios' presentation and the order of the activation of the warning system within a session were balanced across participants.

In order to encourage the participants to drive at a speed that resembles real life driving, instead of slowing down to prevent accidents, they were informed that a monetary bonus would be given upon driving quickly. However they were also warned that each violation of the traffic regulations would result in a monetary penalty.

Results and discussion

Whole scenario analysis

For every load condition in each scenario of each participant the vehicle's median velocity and maximum velocity were calculated. These measures assessed the drivers' behavior in the whole scenario. Analysis of driving behavior that is constrained to the pre-planned events is presented later.

Vehicle's median velocity:

A three-way repeated measures Analysis of Variance (ANOVA) was conducted on the mean median velocity data. It included the variables of road load (low vs. high), sides of the road load (low vs. high), and the presence of a warning system ('with warning system' vs. 'without warning system'). The main effect of the road load variable was statistically significant [$F(1, 19) = 722.60$, $p < 0.0001$]; with low load on the road the median velocity was higher than with high load (70.1 kph vs. 48.3 kph, respectively). The main effect of the variable of sides load was also statistically significant [$F(1, 19) = 65.71$, $p < 0.0001$]; with low load on the sides of the road the median velocity was higher than with high load (61.3 kph vs. 57.1 kph, respectively). These findings demonstrate the effectiveness of the load manipulation, as increasing the levels of load resulted in slower driving.

The two-way interaction between the variables of road load and sides load reached statistical significance [$F(1, 19) = 30.51$, $p < 0.0001$]. As can be seen in Fig. 3 and confirmed by Least Square Difference (LSD) post hoc analyses, the increase in the perceptual load at the sides of the road led to reduction in the mean median velocity in both low and high road load conditions. However, the effect of sides load was modulated by the manipulation of road load, as this reduction was smaller and non-significant when the road load was high (low road load: 73.4 kph vs. 66.8 kph, $p < 0.0001$, for LL and LH conditions, respectively; high road load: 49.1 kph, vs. 47.4 kph, $p = 0.1406$, for HL and HH conditions, respectively). Because the road load involved central regions of the visual field and the sides load involved peripheral regions, this interaction is similar to the interaction between central and peripheral load found with simple letter stimuli in Experiments 1, 2a, and 2b in a former study we conducted [Mar13]. All these cases could be accounted for by the same explanation: With high levels of central load less attentional resources are available for the processing of peripheral information, resulting in a smaller effect of the load level at these peripheral regions. All other effects did not attain statistical significance ($F < 1$).

Note that the notion of the periphery here refers not only to the periphery of the visual field. This notion is also more conceptually driven, because when driving a car the road is often at the central focus of attention, while the sides of the road get less intentional resources. Therefore the sides of the road can be conceptualized as a more peripheral task.

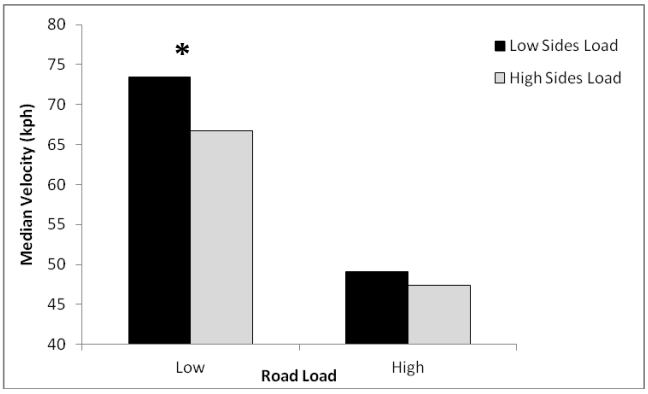

Fig. 3: Mean median driving velocity in the whole scenario as a function of road load and sides load.
The symbol '*' indicates a significant effect of the simple pairwise comparisons.

Vehicle's maximum velocity:

The same ANOVA was conducted on the mean maximum velocity data. The main effect of the road load variable was statistically significant [$F(1, 19) = 101.12$, $p < 0.0001$]; with low load on the road the maximum velocity was higher than with high load (91.5 kph vs. 84.5 kph, respectively). The main effect of the sides load variable was also statistically significant [$F(1, 19) = 119.86$, $p < 0.0001$]; with low load on the sides of the road the maximum velocity was higher than with high load (93.0 kph vs. 83.0 kph, respectively). As before, these significant effects of load indicate that the manipulation of load was successful. The main effect of the presence of the warning system was also statistically significant [$F(1, 19) = 5.55$, $p < 0.03$]; driving with the warning system reduced the maximum velocity compared to driving without such a system (88.7 kph vs. 87.4 kph, for the 'without warning system' and 'with warning system' conditions, respectively). Although the reduction in maximum velocity is quite small it implies that the Collision Avoidance Warning System may be an effective tool for reducing driving speed.

The two-way interaction between road load and sides load reached statistical significance [$F(1, 19) = 21.03$, $p < 0.0003$]. As can be seen in Fig. 4 and confirmed by LSD post hoc analyses, the interaction is similar to that found with median velocity. The perceptual load at the sides of the road significantly reduced the mean maximum velocity in both low and high road load conditions, but this reduction was smaller when the road load was high (low road load: 98.0 kph vs. 85.1 kph, for LL and LH conditions, respectively, $p < 0.0001$; high road load: 88.1 kph vs. 80.9 kph, for HL and HH conditions, respectively, $p < 0.0001$).

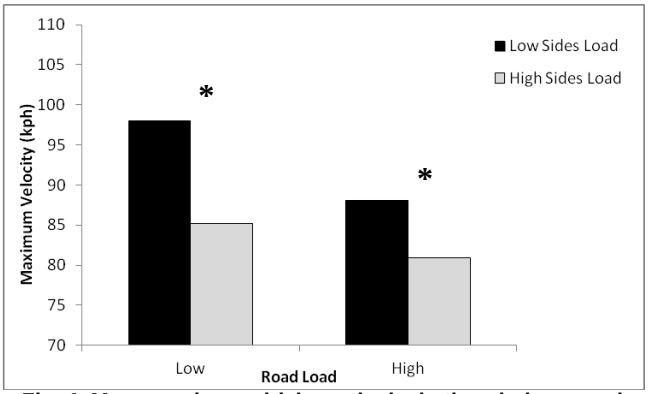

**Fig. 4: Mean maximum driving velocity in the whole scenario as a function of road load and sides load.
The symbol '*' indicates a significant effect of the simple pairwise comparisons.**

The three-way interaction between road load, sides load, and the presence of the warning system also attained statistical significance [$F(1, 19) = 4.44$, $p < 0.05$]. LSD post hoc analyses showed that the effect of the warning system on maximum velocity was manifested in two different conditions of load combination (Fig. 5 and Table 1): LH ($p = 0.0734$) and HL ($p < 0.04$). In these two conditions the presence of the warning system decreased the maximum velocity compared with driving without such a system. When load was either low or high in both regions (LL and HH) no difference was found between driving with and without the warning system.

The lack of warning system effect in the LL and HH conditions may reflect ceiling and floor effects, respectively. When the load in both regions is low, one feels safe to drive as fast as possible regardless of the presence of the warning system. Yet, when the levels of load are high in both regions one may adopt more careful driving, and the result would be lower velocities with or without the warning system.

Table 1: Mean median velocity, maximum velocity, and number of accidents, in the whole scenario, in the various load x presence of warning system (WS) conditions.

		The presence of a WS	
Condition/Measure (kph)		Without WS	With WS
LL	Median velocity	73.5	73.4
	Maximum velocity	98.3	97.6
LH	Median velocity	67.1	66.4
	Maximum velocity	86.3	83.9
LH	Median velocity	49.1	49.2
	Maximum velocity	89.5	86.7
HH	Median velocity	47.7	47.0
	Maximum velocity	80.6	81.3

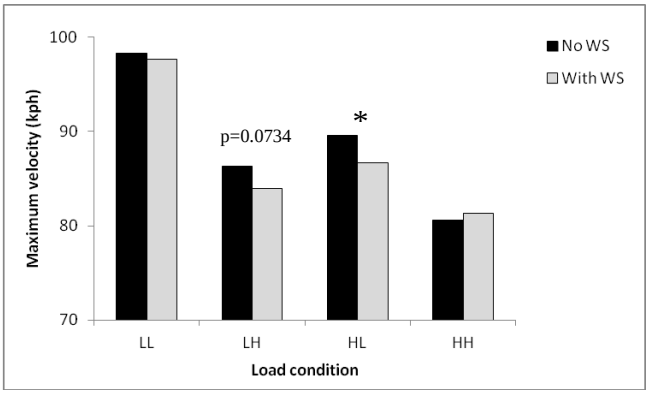

**Fig. 5: Mean maximum velocity in the whole scenario as a function of road load, sides load, and the presence of Warning System (WS).
The symbol '*' indicates a significant effect of the simple pairwise comparisons.**

Although the presence of the warning system did not have dramatic effects on driving velocity, which was more affected by the load conditions on the road and on its sides, it did reduce significantly the maximum velocity that the drivers were ready to adopt. This reduction in maximum velocity implies that the presence of the warning system encouraged a more careful driving, probably because the participants tried to avoid its activation by maintaining

a safer distance from a leading car. All other effects did not attain statistical significance (F<1).

Analysis of reactions to critical events: Proportion of accidents

The analysis presented in this section includes only accidents that occurred after a critical event (up to about 10 seconds after the event occurred). These are accidents that most likely were caused by the critical events. If an accident occurred for a specific event it was coded as 1 and if no accident occurred for that specific event it was coded as 0. These values were then averaged across all events of a specific condition. Hence, this measure represents the proportion of accidents that occurred per a specific condition.

A four-way repeated measures ANOVA was conducted on the mean proportion of accidents. It included the variables of road load (low vs. high), sides of the road load (low vs. high), event's location (road vs. sides of the road), and the presence of a warning system ('with warning system' vs. 'without warning system'). The main effect of the road load variable was statistically significant [$F(1, 19) = 8.62$, $p < 0.009$]; with low load on the road the proportion of accidents was higher than with high load (0.27 vs. 0.20, respectively). This effect might be due to the higher velocities adopted when the road load was low. The main effect of the event location variable was also statistically significant [$F(1, 19) = 23.00$, $p < 0.0001$]; when the event took place on the road the proportion of accidents was lower than when it was initiated from the sides of the road (0.16 vs. 0.30, respectively). This effect suggests that more attentional resources were allocated to the road than to its sides. The main effect of the warning system variable attained marginal significance [$F(1, 19) = 3.85$, $p = 0.0664$]; the proportion of accidents was lower when driving with the aid of the warning system compared to driving without such a system (0.21 vs. 0.26, respectively), suggesting that the warning system encouraged more careful driving.

The two-way interaction between the variables of road load and event location reached statistical significance [$F(1, 19) = 8.15$, $p < 0.02$]. LSD post hoc analyses revealed that the increase in the level of perceptual load on the road reduced the proportion of accidents, but only for events that were initiated from the sides of the road (road events: 0.17 vs. 0.16, sides events: 0.37 vs. 0.24, for low and high road load, respectively, $p < 0.0001$;Fig. 6). As mentioned above, when the levels of load on the road were high driving velocity was relatively low. This lower velocity helped the participants to avoid accidents when the events were initiated from the sides of the road – a less attended region of the visual field. When the events took place on the road itself, driving velocity probably did not play an important role. That is, when the load levels on the road were low and the event occurred on the road, it was relatively easy to spot the critical event and avoid an accident even with the high velocity adopted under low load conditions. Hence, there was no difference in the proportion of accidents for low and high road load for such events.

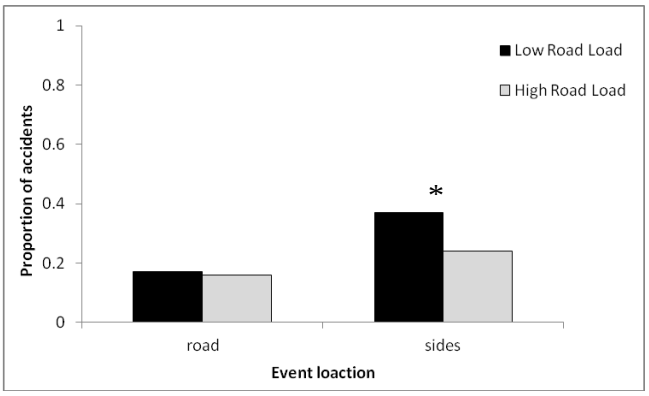

Fig. 6: Mean proportion of accidents following critical events as a function of road load and event location. The symbol '*' indicates a significant effect of the simple pairwise comparisons.

The two-way interaction between the variables of side load and event location was also statistically significant [$F(1, 19) = 5.24$, $p < 0.04$]. LSD post hoc analyses revealed that the increase in the level of perceptual load on the sides of the road significantly increased the proportion of accidents when the critical events initiated from the sides of the road (0.26 vs. 0.35 for low and high side load, respectively, $p < 0.002$; Fig. 7) but not when the events took place on the road itself (0.18 vs. 0.15 for low and high side load, respectively). This effect suggests that the higher levels of load on the sides of the road impaired the participants' ability to detect events initiating from the sides, resulting in a slower reaction to such unexpected yet relevant peripheral events. In fact, this finding suggests that some of these events were missed altogether and ended in accidents. In contrast, when the events occurred on the road, their detection was easy, regardless of load levels.

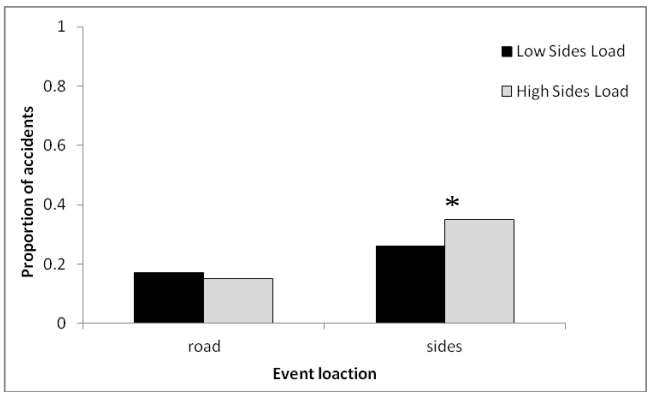

Fig. 7: Mean proportion of accidents following critical events as a function of sides load and event location. The symbol '*' indicates a significant effect of the simple pairwise comparisons.

The four-way interaction between the variables of road load, sides load, event location, and the presence of a warning system was marginally significant [F(1, 19) = 3.55, p = 0.0748]. As can be seen in Fig. 8 and in Table 2, and further confirmed by LSD post hoc analyses, when the event took place on the road the reduction in the proportion of accidents with the aid of the warning system was significant only in two load conditions: LL ($p < 0.005$) and HH ($p < 0.02$). It is possible that the warning system only helped in these two conditions because in the other two conditions – LH and HL – the proportion of accidents was already low even when driving without a warning system. More specifically, when there were more accidents while driving without the warning system, either because of high velocity (LL) or because of high levels of load at all regions (HH), the drivers could benefit from the presence of the warning system and a reduction in the proportion of accidents was found. Interestingly, for events that were initiated from the sides of the road there was a marginally significant opposite effect of the warning system: In the LL condition, the proportion of accidents was higher when driving with the warning system than without it ($p = 0.0768$). This finding suggests that with the warning system the drivers might allocate more attention to the road and therefore sometimes miss events that are initiated from the sides of the road. This seems to be particularly so when driving fast, as was the case in the LL condition. All other effects did not attain statistical significance.

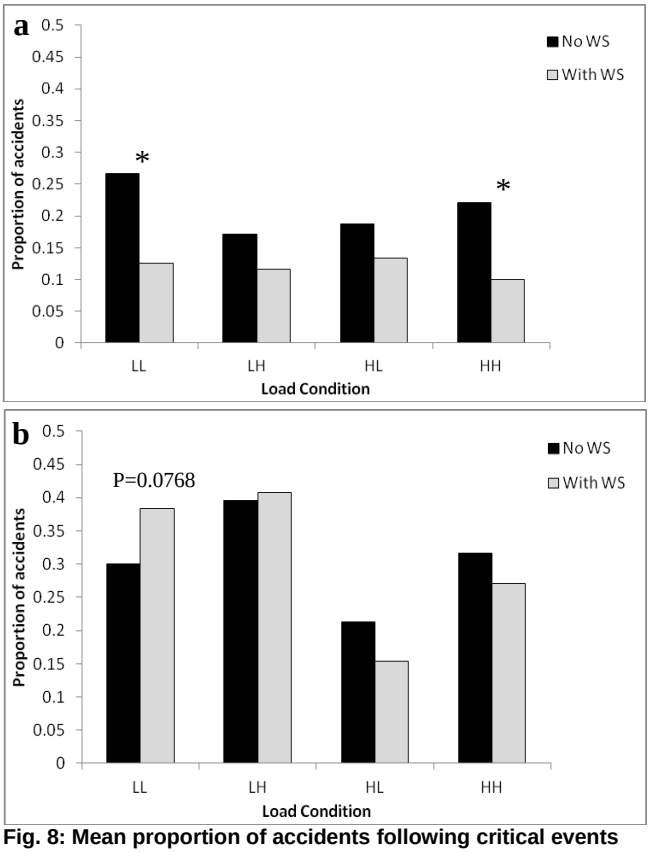

Fig. 8: Mean proportion of accidents following critical events as a function of road load, sides load, event location, and the presence of the warning system.
a) Events on the road; b) Events from the sides of the road. WS=Warning System.
The symbol '*' indicates a significant effect of the simple pairwise comparisons.

Table 2: Mean proportion of accidents in the various load x event location x presence of warning system (WS) conditions.

	Road events		Sides events	
Cond.	Without WS	With WS	Without WS	With WS
LL	0.27	0.12	0.30	0.38
LH	0.17	0.12	0.39	0.41
HL	0.19	0.13	0.21	0.15
HH	0.22	0.10	0.32	0.27

General Discussion

This study examined the effects of perceptual load on driving performance in a driving simulator. Additionally it tested the relevance of this setting – driving under varying levels of load in different regions of the visual field – for the evaluation of in-car warning systems, particularly a Collision Avoidance Warning System. Accordingly, the results will be discussed in relation to these two different issues.

Effects of perceptual load:

The degree of perceptual load and its location – on the road (central) vs. on road sides (peripheral) – played an important role in determining driving velocity. When the levels of load were low, particularly with load on the road, the participants adopted a higher driving velocity than when the levels of load were high. It is likely that the participants assumed that under low levels of load they can maintain adequate driving performance even when

driving fast. It is important to note that the speedometer was clearly visible and that the average velocity in the LL condition was around 70 kph (which was the legal velocity limit for such roads). These two facts suggest that the participants were aware of their velocity, and therefore the higher velocity they adopted cannot be attributed to a simulator artifact. What is more, although in the LL condition the load on the sides of the road was low, there were nevertheless objects on the sides of the road (such as buildings, trees, parked cars, etc.). Therefore the peripheral cues, which might help the driver to estimate her own velocity in this condition, were not different from any other condition in the experiment.

The faster velocity driving strategy with low loads had considerable ramifications on the proportion of accidents, mainly with regard to events initiating from the sides of the road. For these peripheral events more accidents occurred when the level of the road load was low. Adopting high driving velocity when load levels were low was less detrimental for events that occurred on the road, probably because they were indeed easy to detect when the road load was low. Still, the danger involved in such a driving strategy is evident when considering just the data without the warning system (Fig. 8a). It is clear that the condition with the highest proportion of accidents is the one that may appear the easiest to drivers: low levels of load in both regions (LL).

The level of perceptual load at the sides of the road had a somewhat different effect on driving performance. Similar to the effect of road load, low levels of load on the sides of the road encouraged the participants to adopt a higher driving velocity, though this effect of sides load was modulated by the road load: The effect of sides load on velocity was larger when the road load was low than when it was high. Hence, the results in this natural setting experiment replicate our more controlled setting employed in a previous study [Mar13]. However, because with high levels of side load the detection of critical events, particularly those initiating from the sides of the road, was considerably harder, the overall effect of sides load on driving performance was different than that of road load. Specifically, unlike the road load conditions, higher proportion of accidents was found for sides events when the level of side load was high than when it was low.

Evaluation of the Collision Avoidance Warning System:

The effects of the warning system found in this experiment were rather small, but they nevertheless suggest that this kind of Collision Avoidance Warning System probably has some merit. On some of the load conditions, the presence of the warning system lowered the maximum velocity of the vehicle and decreased the proportion of accidents that involved events occurring on the road. Similar effects of warning system on mean velocities were reported by [Bir3]. However, the effects of the warning system in the current study were not always beneficial. When the levels of perceptual load were low in both regions of the visual field, driving with the warning system resulted in a higher proportion of accidents that involved sides' events than driving without the system. This finding may reflect an effect of the warning system on the pattern of attentional allocation. Specifically, the warning system may lead to withdrawal of attentional resources from the sides of the road for the purpose of reallocating them to the road itself. This strategy is likely adopted to avoid the activation of the system's alarm, but it also results in decreased ability to detect events that initiate from the sides of the road. Although this detrimental effect of the warning system was only marginally significant it underscore the importance of evaluating such warning systems under varying levels of load at different regions of the visual field and with different types of critical events, as was done in the current study.

Because the effects of the warning system were relatively small, further research, with finer tuning of the implementation of the system in the simulator, is required to reach any strong conclusions. However, the pattern of results found in this study implies that the presence of the Collision Avoidance Warning System might act like two-edged sword**:** On the one hand it enhanced driving safety by preventing accidents with a leading car on the road. But on the other hand, in some conditions, it increased the probability of accidents when the critical events initiated from peripheral regions, compromising the safety of different entities located on the sides of the road.

Finally, we would like to discuss the possible limitations of the simulator. We are aware, of course, that driving in real life is not the same as driving in simulators. However, we believe that many variables that govern performance in the simulator also affect driving in real life, especially when the focus is on higher cognitive processes (such as attention which was the main process we considered). [Lee10] and [Dew5] are two examples that demonstrate the validity of driving simulators to real road performance. Both studies found high correlations between their participants' performance in the simulator and their performance in real driving tasks.

To sum, this study demonstrates the importance of the experimental paradigm employed here for the research of driving behaviour. The paradigm controls the load on the road and on its sides and also controls the location of critical events. Without these manipulations the current study would have suggested that the warning system is always beneficial. However, the load by event location

manipulation revealed that this is not always the case.

References

[Abe1] Abe, G., & Richardson, J." The effect of alarm timing on driver behaviour: an investigation of differences in driver trust and response to alarms according to alarm timing". *Transportation Research*, 2004, F7(4-5), 307–322.

[Ben2] Ben-Yaacov, A., Maltz, M., & Shinar, D. "Effects of an invehicle collision avoidance warning system on short and longterm driving performance". *Human Factors*, 2002, 44, 335–342

[Bir3] Birrell, S.A., & Young, M. S., "The impact of smart driving aids on driving performance and driver distraction". *Transportation Research*, 2011, F(14), 484–493.

[Bro4] Brown, T. L., Lee, J. D., & McGehee, D. V. "Human performance models and rear-end collision avoidance algorithms". *Human Factors*, 2001, 43, 462–482.

[Dew5] de Winter J. C.F., de Groot, S., Mulder, M., Wieringa, P. A., Dankelman, J., & Mulder, J. A. "Relationships between driving simulator performance and driving test results". *Ergonomics,* 2009, 52(2), 137-153

[Gre6] Green, P., Sullivan, J., Tsimhoni, O., Oberholtzer, J., Buonarosa, M.L., Devonshire, J., Schweitzer, J., Baragar, E., & Sayer, J. "Integrated vehicle-based safety systems (IVBSS): Human factors and driver-vehicle interface (DVI) - Summary report". *Report to National Highway Traffic Safety Administration*, 2008.

[Lav7] Lavie, N. "Attention, distraction, and cognitive control under load". *Current Directions in Psychological Science*, 2010, 19(3), 143-148.

[Lav8] Lavie, N. "Perceptual load as a necessary condition for selective attention". *Journal of Experimental Psychology: Human Perception and Performance*, 1995, 21, 451-468.

[Lav9] Lavie, N., & Cox, S. "On the efficiency of attentional selection: Efficient visual search results in inefficient rejection of distraction". *Psychological Science*, 1997, 8, 395-398.

[Lee10] Lee, H. C. "The validity of driving simulator to measure on-road driving performance of older drivers". *Transport Engineering in Australia*. 2003, 8(2), 89-100.

[Lee11] Lee, J. D., Hoffman, J. D., & Hayes, E. "Collision warning design to mitigate driver distraction". *Proceedings of the SIGCHI conference on Human factors in Computing Systems*, 2004, 65-72, Vienna, Austria.

[Mal12] Maltz, M., & Shinar, D. "Imperfect in-vehicle collision avoidance warning systems can aid drivers". *Human Factors*, 2004, 46(2), 357–366.

[Mar13] Marciano , H. &Yeshurun, Y. "The effects of perceptual load in central and peripheral regions of the visual field". *Visual Cognition*, 2011, 19(3), 367-391.

[Mar14] Marciano , H. &Yeshurun, Y. "Perceptual load in central and peripheral regions and its effects on driving performance: Advertizing billboards", *Work: A Journal of Prevention, Assessment and Rehabilitation*, 2012, 41, 3181-3188.

[Shi15] Shinar, D., & Schechtman, E. "Headway feedback improves inter-vehicular distance: A field study". *Human Factors*, 2002, 44, 474–481

[Yam16] Yamada, K. & Kuchar, J. K. "Preliminary study of behavioral and safety effects of driver dependence on a warning system in a driving simulator". *IEEE Transactions on Systems, Man, and Cybernetics - Part A: Systems and Humans,* 2006, 36(3), 602-610. http://ntl.bts.gov/lib/30000/30200/30257/14433_files/14433.pdf

Acknowledgments

This study was supported by THE RESEARCH FUND ON INSURANCE MATTERS to Y. Yeshurun, and by THE ISRAEL NATIONAL ROAD SAFETY AUTHORITY doctoral fellowship to H. Marciano

Towards the development of a user interface to model scenarios on driving simulators

Ghasan Bhatti[123], Jean-Pierre Jessel [3], Roland Bremond [2], Guillaume Millet[1], Fabrice Vienne[2]
(1)OKTAL SA**.** 19, Boulevard des nations unies, 92190, MEUDON, FRANCE
E-mail: {ghasan.bhatti, guillaume.millet}@oktal.fr
(2) Université Paris-Est, IFSTTAR, IM-LEPSIS**.** 58 Boulevard Lefebvre, 75732, PARIS, FRANCE
E-mail: {roland.bremond, fabrice.vienne}@ifsttar.fr
(3) IRIT, Université Paul Sabatier, 118 Route de Narbonne, 31062 TOULOUSE, FRANCE
E-mail: jessel@irit.fr

Key words: *Driving Simulator, Experiment Builder, Template Builder, Scenario Modeling and User Interface.*

Introduction

Scenario Modeling on driving simulators require careful consideration and controlled environment (depending on the research objectives) to achieve the desired goal of the experiment. It is one of the critical steps while designing and implementing an experiment on a driving simulator. It specifies where and what happens in the simulator by specifying, where to place the virtual objects and what those objects will be doing during the experimental trials. But the complex and technical nature of driving simulator makes it difficult for the end-users (behavioral researchers/trainers) to design and execute and experimental protocol.

Scenario Modeling includes specifying and controlling the ambient traffic, simulation conditions and manipulating the real-world traffic situations [Pap2003]. It is sometimes used to specify both the layout and activities during the experimental trial. Some authors use the term “Scene” to specify the layout (driving environment/terrain) and the term “Scenario” to specify critical events [Fis2011].

In the case of scenario programming on driving simulators, there are two main factors, which make scenario modeling a difficult problem [Fis2011]. First, the driving behavior is complicated and not well-understood; this makes it difficult to simulate realistic traffic. Second factor is the variability of human driving behavior, as they change their speed position, tactical decisions with the time during the trial, which leads to variance in drivers’ behavior to be studied.

Different approaches, systems and interaction environments have been proposed and used in the past for modeling scenarios on driving simulators. In SCANeR [Rey2000], scenario objects are placed directly on the map and use condition/action pair for scripting. In ARCHISIM [Esp1994], specification of objects positions and construction of script (condition/ action pair) is done using textual statements in a text editor like ‘Notepad’. In STI SIM [Par2011] objects and scenarios are specified by the route traveled by the driver during the simulation trial. A Tile-based approach [Pap2003] is also used, where tiles are configured with objects and then integrated. But these systems still do not fill the gap between user skills and objectives; they want to achieve with simulator.

In order to address the above mentioned problem, we have conducted a user survey [Bha2011], in which we interviewed 19 driving simulator users with various backgrounds about their problems requirements and the help they take from the technical persons while modeling scenarios. During this survey, users have described their problems as well as have given some ideas.

Proposed Approach

Traditionally, in order to configure an experimental protocol, a user (technical person or researcher) uses the functions offered by the simulator software to model scenarios regardless of what level of his programming skills. In the proposed design, we have split the scenario modeling activity by dividing the Interface into 3 sub-interfaces based on the set of skills and the roles users have to perform to implement an experiment protocol. The 3 roles *Experiment Operator*, *Template Designer* and *Experiment Designer* will correspond to the skills that users have, to design and implement the experimental protocol. We can explain this new interface using an example scenario to study drivers’ behavior. The scenario contains two situations. i.e. *Accident (Vehicle ‘A’ crosses the participant vehicle and apply brakes in front of the participant)* and *Pedestrian Crossing (A Pedestrian crosses the road as the participant vehicle approaches the Intersection)*. The proposed UI with an example is described in Fig 1.

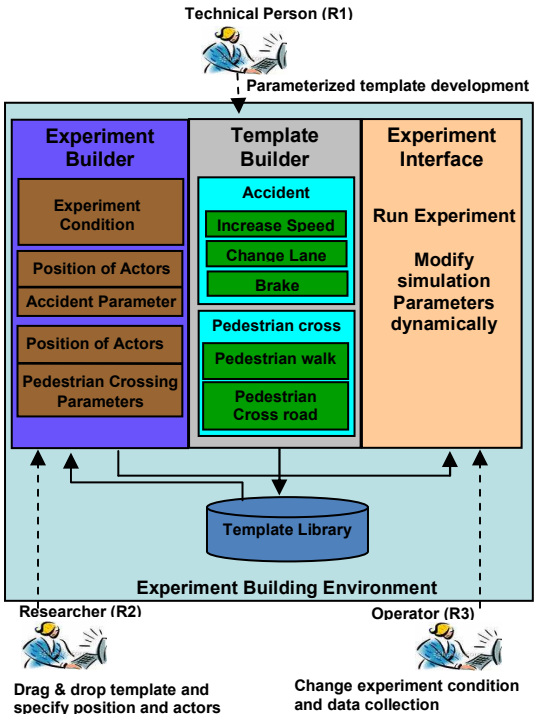

Fig 1: Experiment development process

Template Builder

This sub-interface will be used by technical persons performing role R1. R1 will design the GUI (Graphical user Interface)-based parameterized templates of the scenario events. Template builder will let R1 to use existing functions offered by the scenario-modeling environment of the driving simulator. For example, at back-end of the template "Accident", Template Builder will let R1 to program a vehicle 'A' to cross the participant vehicle, changes the lane and applies brakes in front of the participant vehicle and same for the "Pedestrian crossing". At the front end, there would be different text fields to specify the parameters for "Accident" and "Pedestrian crossing" actions.

Experiment Builder

This sub-interface will be used by researcher/trainer performing role R2 having no or low programming skills. R2 will specify the conditions of the experiment along with the data to be collected and studied to answer the research questions. R2 will access the Template library already developed using Template builder. R2 will drag and drop the templates on the experiment builder Interface. As described in the figure 1, using the experiment designer sub-interface, R2 will specify the position and actors involved in the templates "Accident" and "Pedestrian crossing" besides the template parameters. In this way, R2 person can quickly and easily develop the experimental protocol.

Experiment Interface

Experiment Operator will be used by researcher performing role R3. Using this interface, R3 will load and execute the scenario on the driving simulator. R3 can change the parameters of the scenario or template (if needed), and finally collect the data.

Conclusion

We have focused on the problem of one class of users (Behavioral researchers), who are primary users of driving simulators. The objective is to fill the gap between user skills and the goals they want to achieve in an efficient way. As we are working on user-centered design, we are developing a prototype of this interaction concept that will be evaluated by the users. In the near future, we are looking forward to implement this concept after user evaluation.

Acknowledgement

This work has received funding from the European Community's 7th Framework Program (FP7) under grant agreement n°238833/ADAPTATION project.

References

[Bha2011] Bhatti, G., Brémond, R., Jessel, J.-P., Millet, G., and Vienne, F. (2011). User requirements to model scenarios on Driving Simulators. *Proceedings of 5th International Conference on Driver Behavior and Training (ICDBT)*, Paris, France, 29-30 November, 2011

[Esp1994] Espié S., Saad F., Schnetzler B., and Burlier, F. (1994) Microscopic traffic simulation and driver behavior modeling: the ARCHISIM project. *Proceedings of the Strategic Highway Research Program and Traffic Safety on Two continents*, Lille, France.

[Fis2011] Kearney, J. K., and G. Timofey F, (2011). *Scenario Authoring. Handbook of Driving Simulation for Engineering, Medicine, and Psychology*. D. L. Fisher, Rizzo., Matthew, Caird, Jeff k., Lee, John D. Boca raton, FL, CRC Press/Taylor & Francis

[Pap2003] Papelis, Y., Ahmad, O., and Watson, G. (2003). Developing Scenarios to Determine effects of Driver Performance: Techniques for Authoring and Lessons Learned. *Proceedings of the Driving Simulation Conference North America 2003*. Dearborn, Michigan, USA.

[Par2011] Park, G. D., Allen, R. W. and T., Rosenthal, J. (2011) Flexible and Real-time Scenario Building for Experimental Driving Simulation Studies. *Presented at CHI 2011*, Palo Alto, CA, February 13-16, 2011

[Rey2000] Reymond, G., Heidet, A., Canry, M., and Kemeny, A. (2000). Validation of Renault's dynamic simulator for Adaptive Cruise Control experiments. *Proceedings of the Driving Simulation Conference, Paris*, September 2000

Autonomous Local Manoeuvre and Scenario Orchestration Based on Automated Action Planning in Driving Simulation

Zhitao Xiong[1], Anthony G. Cohn [2], Oliver Carsten [3], Hamish Jamson [3]
(1) Institute for Transport Studies and School of Computing, 38 University Road, University of Leeds, Leeds, UK, LS2 9JT, E-mail: tszx@leeds.ac.uk
(2) School of Computing, University of Leeds, Leeds, UK, LS2 9JT, E-mail: a.g.cohn@leeds.ac.uk
(3) Institute for Transport Studies, 38 University Road, University of Leeds, Leeds, UK, LS2 9JT, O.M.J.Carsten@its.leeds.ac.uk, A.H.Jamson@its.leeds.ac.uk

Abstract *– Techniques for orchestrating scenarios with autonomous vehicles in driving simulation are not abundant and three problems are still open: Actor Management, Actor Preparation and Scenario Orchestration. Moreover, "failures" still happen in scenarios. In this paper, a decision-making algorithm based on automated action planning called NAUSEA(autoNomous locAl manoeUvre and Scenario orchEstration based on automated action plAnning) is proposed for the cognitive layer of a driver model called SAIL (Scenario-Aware drIver modeL). Autonomous drivers equipped with SAIL/NAUSEA can make decisions according to their memories of scenario instructions and personal features (e.g., personalities), so as to make their controlling vehicles not only follow the scenario requirements and perform pre-defined actions, but also tolerate interferences and endow the scenario with rich behaviours as permitted. An experiment was used to evaluate NAUSEA and its implementation. It shows that NAUSEA is working properly but the implementation needs improvement.*

Key words: *Scenario Orchestration, Driving Simulation, Automated Planning, Temporal Reasoning*

1. Introduction

In driving simulation, a scenario[1] is a pre-defined environment that experimenters need a participant or simulator driver to experience; it includes the physical scenes, pre-defined traffic flow, interactions with other vehicles and measures that need to be collected. There are two basic requirements regarding scenarios: 1) the simulated vehicles in driving simulation should behave in a natural and realistic manner and 2) the scenario in the driving simulation should be reproducible. Researchers always put a focus on the second requirement and materials about how to satisfy the two requirements in the meantime are still not rich, that is, the following three questions are still open: 1) Which vehicles should interact with the participant? (Actor management problem); 2) How should those vehicles go to their proposed position? (Actor preparation problem) and 3) How should those vehicles be instructed what to do when interacting with participants? (Scenario orchestration problem).

In [Kea1], an actor manager was included in their HTPS-based architecture but no detail of actor management was mentioned. In [Ols1], Johan Olstam discussed the actor preparation and actor management problems with a focus on producing reproducible start conditions of plays in his algorithm. In [Pap1], autonomous vehicles can be directed to perform specific actions by receiving orders from an external director object, in which case humans handle scenario orchestration and scenarios may fail, e.g., the vehicle fails to follow the scenario instructions of overtaking because of some trigger failure and the whole scenario may be destroyed.

In order to find a solution for the three problems above and deal with failures, a "The Matrix" metaphor has been taken to design a driver model for driving simulation (see [The1] for a description of the film trilogy "The Matrix"). In short, this research separates the (virtual) driver from the vehicles. Drivers are treated as "Agent Smith" [Age1], and vehicles in the simulation are treated as "simulated humans" in "The Matrix" (at least one of them is driven by a participant). More details about this metaphor can be found in [Xio1]. A driver model called SAIL (Scenario-Aware drIver modeL) is therefore proposed to create a (virtual) driver that can:

1) Take control of one vehicle or a flock of vehicles dynamically by using Role Matching (solution to problem 1 and in section 2.2);

[1] In driving simulation literature, terms may have different meanings, e.g., "scenario", so in this paper/research terms are defined in order to be consistent and unified, not to be accurate. The Ontology for Scenario Orchestration mentioned later is trying to standardize the definitions and scenarios among different groups and different platforms.

2) Understand the scenario instructions and navigate any vehicles to the proposed Formation[2] Position needed for the scenario (solution to problem 2 and in section 2.3);

3) Follow the scenario instructions intelligently with a general plan and the ability of replanning in order to deal with failures (solution to problem 3 and in section 2.1) and

4) Cooperate with other (virtual) drivers so several drivers can run in parallel and coordinate.

SAIL uses OSO (Ontology for Scenario Orchestration) [Xio1] as its data source, which is stored in SDF (Scenario Definition File). OSO can also standardize scenario procedures, descriptions and concepts. SAIL uses an algorithm called NAUSEA (autoNomous locAl manoeUvre and Scenario orchEstration based on automated action plAnning) to make decisions. SAIL and NAUSEA have been implemented in a program called Smith. The vehicle or flock Smith is controlling are termed as "ego-vehicle" or "ego-flock" respectively.

This paper will introduce NAUSEA in SAIL including an experiment and results. It is organised as follows: Section 2 will first have a description of NAUSEA followed by Section 3 that is dedicated to show the experiment and results. Section 4 will include a conclusion and a discussion about future research and enhancement.

2. Algorithm Description - NAUSEA

SAIL is derived from ECOM architecture [Eng1] and illustrated in Fig. 1. The Perception layer is used to sense the outside environment and make necessary interpretation. The Cognition layer is used to maintain Memory and make decisions. Memory includes the Individual Features (e.g., personalities) and the World Model (e.g., the logical road network, previous Memory of World Model etc.). More details about SAIL can be found in [Xio1]. NAUSEA is based on temporal reasoning proposed in [Had1] and works in the Decision-Making layer in the Cognition (see Fig. 1). In order to adopt not only the temporal constraints[3] but also triggers including monitors (pre-conditions), success conditions (post-condition) and failure conditions(post-condition), extra procedures have been added. NAUSEA is described in Fig. 2 and procedures of Plan Evaluation, Role Matching and Regulating are elaborated as follows:

2.1 Plan Evaluation Procedure

NAUSEA maintains a General Plan $\boldsymbol{Gr_\alpha}$ to guide Smith through a scenario. Before introducing $\boldsymbol{Gr_\alpha}$ and its evaluation procedure, three concepts are given first: ***Action, Assignment*** and ***Recipe***.

An ***Action*** can be an Assignment-action or a pre-defined action described in the next paragraph: $\boldsymbol{\alpha, \beta_0, \beta_1, \beta_2}$ and $\boldsymbol{\beta_3}$. It can be a High-Level Action or a Low-Level Action[4] (which are complex action and basic action in [Had1] respectively; the names have been changed in order to reflect the hierarchical architecture of SAIL). Each action is associated with the following parameters: ***ID, d, D, r, s, f***. ***ID*** represents the name/id of the ego-vehicle/flock. ***d*** represents the deadline of the action. ***D*** represents the duration of the action. ***r*** represents the release time of the action. ***s*** and ***f*** represent the start time and finish time of the action. Moreover, each action has a type and an action profile, e.g., "change desired speed to 10 mph" is an Assignment-action whose type is "Low-Level" and "Adapt-Speed" and whose action profile is "Desired Speed" with a value of "10.0" (mph).

Assignments are stored as Motivations in the Memory layer and specify what Smith needs to do in a scenario. An ***Assignment*** has four main components: monitors, success conditions, failure conditions and Assignment-actions. Monitors are used to trigger the corresponding Assignment-actions and success/failure conditions are used to check if the Assignment-actions have succeeded or failed respectively. Assignment-actions are what Smith should do in scenarios and can be driving behaviours or non-driving behaviours such as "request new vehicle", etc.

In every scenario, each Smith needs to finish a top High-Level Action $\boldsymbol{\alpha}$ that can be either ***Perform-scenario*** or ***Free***. ***Free*** makes Smith ignore any Assignment and autonomously navigate the world, in which case route or a destination will be randomly chosen. ***Perform-scenario*** has only one ***Recipe***[5] that contains four sub-actions, namely, $\boldsymbol{\beta_0, \beta_1, \beta_2}$ and $\boldsymbol{\beta_3}$ (Fig. 4). $\boldsymbol{\beta_0}$ (Get-to-the-initial-state) adopts initial state (e.g., initial speed, initial target speed etc.). $\boldsymbol{\beta_1}$ (Generate-formation) means that Smith should "drive" the ego-vehicle(s) to the proposed Formation Position in an unsuspicious manner [Ols1] in order to perform the corresponding Assignment-actions, which is the process called Autonomous Local Manoeuvre in NAUSEA. Because the recipe of $\boldsymbol{\beta_1}$ will change according to the dynamic environment, this action will not be further divided into sub-actions, but it will be monitored throughout the scenario in order to make sure that the ego-vehicle(s) can get to the position in time or on time. $\boldsymbol{\beta_2}$ means Perform-assignment Action, and can be further divided into several Assignment-actions, which are represented as $\boldsymbol{\gamma_0}$

[2] A Formation is a set of pre-defined local positions around the simulator driver/participant. Vehicles in driving simulation always interact with the participants at these Formation Positions. See figure 3 for further information.

[3] They include metric and precedence constraints, e.g., "action α ***Before*** action β" is a precedence constraint and "***the start time of*** β – **the finish time** of $\alpha \leqslant 100$ (seconds)" is a metric constraint. Details can be found in [Had1].

[4] A Low-level action is defined as an action that can be only performed in one way, one sequence and by one vehicle/flock.

[5] A Recipe is a set of actions that specifies how to perform a complex/High-Level Action. Recipe is a term borrowed from [Had1].

through γ_n (n is the number of Assignment-actions a Smith needs to perform). Each Assignment-action (γ_0 through γ_n) is contained in the Assignments stored in Memory. β_3 (Clean-up) should be specified by experimenters as an Assignment-action in most circumstances; however, it can be an autonomous action by changing it to the top-action of Free. At present, Smith always ignores Clean-up/β_3 and Get-to-the-initial-state/β_0 when constructing or evaluating Gr_α.

By using the start time ***s*** and finish time ***f*** of every action in the recipe of ***Perform-scenario*****,** Smith, or specifically, NAUSEA can generate a General Plan in Memory - a temporal constraint graph Gr_α [Had1], so ***s*** and ***f*** are represented as nodes in the graph Gr_α. The plan evaluation procedure uses the Floyd-Warshall algorithm to check the consistency of Gr_α, which is to check if there is any conflict regarding temporal constraints. When Smith is making decision and trying to finish the Assignment-actions specified in β_2, it may change: 1) performer(s) of the action (***ID*** of the ego-vehicle/flock); 2) Assignment-actions and 3) the action ***Recipe*** of β_1. Change of performer(s) may lead to the change of temporal constraints if permitted. Change of Assignment-actions will lead to the change of the temporal constraints and nodes in Gr_α. Change of the action ***Recipe*** of β_1 is caused by any failure in β_2 and Smith may need to navigate the ego-vehicle(s) to the proposed Formation Position first. It will lead to the change of nodes in Gr_α, as it will add or delete actions. In such a case the temporal constraints will not be changed but Smith needs to predict how long it will take for the ego-vehicle(s) to get to the Formation Position (duration and proposed finish time of β_1) and check if the duration and proposed finish time of β_1 are consistent with the temporal constraints in Gr_α.

2.2 Role Matching Procedure

Role Matching has three steps: Matching of Formation Position (Fig. 3), Matching of vehicle model and Matching of Gr_α. When Smith needs to find a vehicle/flock to perform some Assignments, he will first find a vehicle that is near the proposed Formation Position (flocks are usually used for ambient traffic flow). There are now two versions of Formation Position available for Smith. Fig. 3a is the original version for all circumstances while Fig. 3b is the version for rural road. For instance, if an Assignment needs a leader, the "Formation Position" of that Assignment will be specified as "L" in SDF (according to Fig 3b). Smith will try to find a vehicle that is near position "L", which means that he will first try to find a vehicle in position "L"; if no vehicle is found, then try "LL", "NSL" etc. Smith will then match the vehicle model with specified parameters regarding its model, its manufacturer, its max speed etc. If he can find a right vehicle in "L", it will proceed to Matching of Gr_α, if not, he will try other near positions such as "NSL" or "LL" until he finds one. If Smith fails in finding a vehicle/flock, it will broadcast "Failure" or request vehicles from SMM (Scenario Management Module), which will be discussed in section 4. The last step is the Matching of Gr_α, which is to use the values of vehicle parameters to re-evaluate the time Smith needs to navigate the ego-vehicle(s) to the proposed position and see if the time is consistent with Gr_α.

2.3 Regulating Procedure

At present, only three behaviours are adopted: lane changing, overtaking and speed adaption. Lane changing is used to get to the lane that the Formation Position requires while overtaking is used to overtake slower vehicles and get to the Formation Position in time. Speed adaptation is mainly used to make Smith obey the speed limit and maintain a realistic speed trajectory when performing a turning movement. The Regulating procedure is only active in the phase of β_1, which is to generate formation for Assignment-actions. In the phase of β_2, which is to perform Assignment-actions, lane changing and overtaking are both forbidden while speed-adaptation is allowed if there is no speed requirement in Assignment-actions.

3. Experiment and Results

An experiment was designed to see if NAUSEA can provide proposed output and if the implementation – Smith - can work properly and stably. The desktop version of UoLDS (University of Leeds Driving Simulator) [Jam1], which is called Babysim has been used to conduct the experiment. A laptop is used to run Smith. It is equipped with an Intel® T2130 CPU and 2GB of memory and runs Ubuntu Linux 11.10 32bit. Communication between Babysim and Smith is based on a wired 10Mb hub. A video camera is also used to record the animation of the screen so that the driving activities can be recorded, which are needed for future examination or papers/presentations. The experiment contains one scenario and two phases, which are described in the following sections.

3.1 Experiment Description

3.2.1 Scenario Description

The scenario contains a 13.7 miles long (22 km) rural road with some curved road segments. There are three villages and five junctions along the road. The speed limit on the open road is 60 mph but in villages the speed limit is 30 mph. Assignments of "**Coherence**", "**Layby**" and "**Gap Acceptance**" are supposed to provide measurements regarding driver's behaviours but for the purpose of this experiment, these measures have been ignored. Because

participants may sabotage Assignments and Smith can generate extra actions to compensate the Assignments, participants may experience less than or more than three Assignments, which depends on whether or not the failed Assignment can cause the whole scenario to fail and whether it can be reattempted. Moreover, the temporal constraints of the scenario are generated by manual estimation at present. Assignments that a participant could experience are listed below and illustrated in Fig. 5.

- Assignment of **Acc-BL**: **Acc-BL** is short for "Accelerate and Be Participant's Leader". It is the first Assignment that participants experience. This Assignment needs a Formation Position of "L", so vehicle with the id "1" is chosen in the beginning as the ego-vehicle. Smith will accelerate vehicle 1 and maintain speed of 30 mph;
- Assignment of **CL-BL**: **CL-BL** is short for "Change Lane and Be Participant's Leader". It is actually an action generated by the Regulating Layer in order to navigate vehicle 2 to the position of "L" so that the participant can have a leader after he/she has failed **Acc-BL**. Vehicle 2 is the ego-driver in this Assignment. The failure of **CL-BL** will lead to the failure of the whole scenario;
- Assignment of "**Coherence**": After the adoption of a leader by performing **Acc-BL** or **CL-BL**, the **Coherence** Assignment will start and last for 50 seconds[6]. During this period, the ego-vehicle (vehicle 1 or vehicle 2) will be the leader and varies its speed according to a sinusoid. The participant will be told to match the leader's speed and maintain his/her favoured distance to the leader. Two sub-Assignments can be generated: **Coherence1** and **Coherence2**, which are short for "**Coherence** performed by vehicle 1" and "**Coherence** performed by vehicle 2" respectively. The failure of **Coherence** will lead to the failure of the whole scenario;
- Assignment of "**Free Traffic Flow**": This Assignment is used to generate a traffic flow in order to prevent the participant from overtaking but because the traffic flow is of low density, the participant can still have chance to overtake. This Assignment starts with "**Coherence**" and stops in "**Layby**" that is elaborated next;
- Assignment of "**Layby**": In this Assignment, Smith needs to find a vehicle and then pull it out suddenly without indication, in which case the participant may accidently overtake the vehicle. Vehicle 3 is chosen as the ego-vehicle first and if it fails, vehicle 4 will be chosen, so two sub-Assignments can be generated as well: **Layby-V3** and **Layby-V4**, which are short for "**Layby** performed by vehicle 3" and "**Layby** performed by vehicle 4" respectively. The failure of **Layby-V4** will lead to the failure of the whole scenario;
- Assignment of "**Gap Acceptance**": After the **Layby** Assignment, the participant will arrive at a junction with oncoming vehicles whose gap is increasing; he/she is instructed to turn right if the gap is considered safe by him/her. This Assignment is not supposed to fail so the participant will be instructed to turn right.

If we call a Test Case a set of Assignments that a participant will experience or sabotage and the corresponding information Smith receives, there are in total 9 Test Cases in this experiment. This number is generated by considering all the combinations of the seven Assignments and the fact that 1) failures of **Coherence1/Coherence2/Layby-V4/CL-BL** will lead to the failure of the whole scenario and 2) some Test Cases are actually the same, for instance, in order to perform **CL-BL**, **Acc-BL** should be failed first. Hence, the Test Case of "fail **Acc-BL** and then fail **CL-BL**" is actually the Test Case of "fail **CL-BL**". See Table 3 for all the 9 Test Cases and corresponding desired output. From Table 3, we can see that in the normal Test Case, **Acc-BL** should be triggered (M: √) and succeed (S: √). Failure condition of **Acc-BL** should not be triggered (F: ×). **Coherence1** should be triggered and succeed by considering its duration (S: D). Failure condition of **Coherence1** should not be triggered. **Layby-V3** should be triggered and succeed by considering its duration. Failure condition of **Layby-V3** should not be triggered. **Gap Acceptance** and **Free Traffic Flow** should both be triggered and since there are no success or failure condition in this Assignment (S: N; F: N), Smith will not check the status of the Assignment after they are triggered. Moreover, in the Normal Test Case, **CL-BL**, **Coherence2** and **Layby-V4** are not triggered.

3.2.2 Phase One

In Phase one, five participants were recruited within the Institute for Transport Studies (ITS) to act as software testers. All of them are male and four of them have taken part in a driving simulation experiment before. Every participant will drive in the scenario twice or three times in two rounds. In round one, the participant will try Test Case 1, which means the participant should drive normally and experience **Acc-BL**, **Coherence1**, **Layby-V3** and **Gap Acceptance** in sequence. In round two, the participant will try two other Test Cases randomly in two sections and overtaking the leader may be allowed according to the requirement of each Test Case. The participant may try Test Case 3, 4, 7 in section one and 2,5,6,8,9 in section two, so two participants will not try any Test Case in section one. The rule is that the Test Case that has been tried by the last participant will not be considered for the next participant. The Test Cases each participant has tried can be found in Table 1. The input to Smith, which is the information of every vehicle in the Babysim was recorded in a Data-Log during each participant's drive.

3.2.3 Phase Two

[6]It has been set to 70 seconds in temporal constraints in order to make sure that Smith has enough time to monitor the Assignment and will not trigger failure accidentally. 50 seconds is used in the Assignment definition for success condition.

In Phase two, an automatic software test is performed by using the Data-Log recorded in Phase one. In this phase, every record of Test Case is played by a Log player in order to re-construct every participant's drive. Every log has been played 10 times, so there are in total 90 tests (9 × 10). Test of the Normal Test Case used the Data-Log of participant one in round one. The time that Smith makes the decision has been recorded in each test and is termed "Order Release time".

3.2 Results

Increase in the number of Assignments and the number of action ***Recipe*** for a high-level action will certainly make Smith slower and may cause failure due to the complexity of the Plan Evaluation Procedure. However, Assignments can be distributed to several Smiths and the number of action ***Recipe*** can be restricted, so we can safely ignore the size effect. Although the time spent on decision-making is platform-dependent, it can still reflect whether Smith is working stably as in a specific platform with the same scenario, Smith should spend almost the same time to trigger the same Assignment so that every participant can experience the same context when the same Assignment is triggered.

3.3.1 Can Smith Generate the Desired Output? (Is the Algorithm Working?)

In Phase one, Smith generated the desired output (13 Participant-based tests) and in phase two, Smith generated the desired output with a success rate of 100% in all the 90 tests. Moreover, the plan evaluation procedure is also working properly and its output can be found in Fig. 6, Fig. 6a shows the output in the Normal Test Case and Fig. 6b shows the output when Acc-BL fails (Test Case 2,3,7,8,9). Numbers in the graph are temporal constraints, e.g., 255 means that "Coherence1"/ "Coherence2" should start before 255 seconds from the start of the simulation.

3.3.2 How well did Smith Generate the Output? (Is the Implementation Good?)

Order lag is measured in Phase one by using the time that Babysim receives an order from Smith to minus the time when Smith makes the decision. The latter is the time stamp of the package that makes the monitor become true and Action Execution procedure is evoked. The result is shown in Table 2 and shows that Smith needs 2 ± 1 frame(s) to make decisions, which is supposed to be a reference as the time is a platform-dependent value.

3.3.3 Is Smith Stable?

The statistics description of the results is shown in Table 4 and the time value is all Babysim-based, e.g., a time value of 300 means 300 seconds after the start of the Babysim simulation. It shows that Smith is not stable enough, as the time point when he makes decision in the same test varies a lot from less than 1 frame to more than 10 frames compared to the mean order release time. Since there is no difference regarding algorithm or data structure when performing the same Assignment on the same machine, the cause of the variance is the communication mechanism used between the Perception and Cognition layers.

3.3.4 Comments from Participants

Participants were encouraged to give some general comments after their drive. Some of them have noticed that 1) in Coherence1 and Cohehence2, the acceleration rate of the leader is relatively high; 2) vehicle 3 or vehicle 4 in Layby-V3 or Layby V4 pulls out without advance indications (although they are designed to be a surprise Assignment) and 3) Lane changing trajectory of the vehicle is not smooth enough.

Hence, SAIL/NAUSEA is working properly as desired but the implementation of Smith needs enhancement regarding the communication mechanism between the Perception and Cognition layers. Moreover, the behaviours need enhancement as well although Smith is not responsible for the low-level trajectory generation, e.g., the trajectory of lane changing.

4. Conclusions

In this paper, a decision-making algorithm called NAUSEA has been designed for SAIL to solve the three problems and deal with "failures". SAIL/NAUSEA is working properly with a 100% success rate but the implementation needs enhancement. This driver model is a component of a framework called SOAV (Scenario Orchestration with Autonomous simulated Vehicles), which is designed to be an architecture that can orchestrate scenarios with autonomous vehicles, so that participants can experience rich, appropriate and reproducible scenarios. For scenario description, OSO and SDF can standardize scenarios and make them shareable among different simulators; for scenario interpretation, the driver model can naturally combine autonomous actions and scenario actions; for scenario execution, a Scenario Management Module (SMM) is proposed to cooperate with the driver and meet any macroscopic requirement, including traffic flow generation and vehicle creation/destruction.

A further experiment will be carried out in order to test SOAV. The enhancement for the next experiment will be: 1) adoption of a new communication mechanism between Perception and Cognition; 2) adoption of multi-triggers so that Smith can monitor more than one state variable in the simulation; 3) adoption of a Scenario

Management Module (SMM) so that vehicles can be added/destroyed dynamically according to traffic flow or Assignment requirements, in which case actor preparation can be tested dynamically and 4) adoption of dynamic temporal constraints based on the work from [Ols1].

SAIL adopted a goal-oriented hierarchical architecture, which can be used to assist the design of in-vehicle devices and adopt findings in related areas, such as driver model, driving behaviour, psychology etc. NAUSEA can also be used when self-management is needed for goal-oriented decision-making. All data in this experiment including OSO, SDF, videos and original data logs are available upon request.

5. Acknowledgement

Thanks to China Scholarship Council and University of Leeds for funding this research and to people in ITS (alphabetically): Dan Gillett, Daz Hibberd, Mojtaba Moharrer for their kind help before the experiments. Special thanks to Tony Horrobin (ITS) who gave me many suggestions ranging from scenario preparation to software test.

6. References

[Age1] Agent Smith(2011). Agent Smith. Retrieved October 16, 2011. http://en.wikipedia.org/wiki/ AgentSmith

[Eng1] Engström, J. and Hollnagel, E. (2007). A General Conceptual Framework for Modelling Behavioural Effects of Driver Support Functions. In Cacciabue, P. C (Editor), Modelling Driver Behaviour in Automotive Environment (pp. 61 - 84). Springer.

[Had1] Hadad, M., Kraus, S., Gal, Y. and Lin, R.(2003).Temporal Reasoning For A Collaborative Planning Agent In A Dynamic Environment. Annals of Mathematics and Artificial Intelligence, vol37, pp. 331-379.

[Jam1] Jamson, A. H., Horrobin, A. J., and Auckland, R. A.(2007). Whatever Happened to the LADS? Design and Development of the New University of Leeds Driving Simulator. In Proceedings of Driving Simulation Conference America (DSCNA), DSC'2007.

[Kea1] Kearney, J., Willemsen, P., Donikian, S., Devillers, F., de Beaulieu, C., and Rennes, F. (1999). Scenario languages for driving simulation. In Proceedings of Driving Simulation Conference,DSC'99, pages 377–393.

[Ols1] Olstam, J., Espi, S., Mardh, S., Jansson, J. and Lundgren, J. (2011) An algorithm for Combining Autonomous Vehicles and Controlled Events in Driving Simulator Experiments. Transportation Research Part C: Emerging Technologies, Elsevier.

[Pap1] Papelis, Y., Ahmad, O., and Schikore, M. (2001). Scenario definition and control for the national advanced driving simulator. In International Conference on the Enhanced Safety of Vehicles (ESV). SAE International.

[The1] The Matrix (franchise) (2011). The Matrix (franchise).Retrieved on February 2, 2012. http://en.wikipedia.org/wiki/The_Matrix_(franchise)

[Xio1] Xiong, Z., Carsten, O., Cohn, A.G. and Jamson, H. (2012). Driving with Smith: A Scenario-Aware Driver Model for Driving Simulation. To appear in the Proceedings of BRIMS 2012, March 2012.

1. Initialization Procedure: Read SDF and store relevant information into Memory; build a General Plan Gr_α according to the Recipe in Figure 4 and Scenario Assignments from Memory along with metric and precedence constraints;
2. Manoeuvre Loop: Run the following procedure until the end of Gr_α:
   (a) Plan Evaluation Procedure: If a new plan is found, check it's consistency. If it's consistent, continue, if no, go to 2b;
   (b) Role Matching Procedure: if a vehicle/flock is needed, do role matching and if a vehicle/flock can be found, update Gr_α and go to 2a; if no, go to 4;
   (c) Targeting Procedure: find the shortest route in length between current position and destination, if a route is found, continue; if failed, go to 2b;
   (d) Regulating Procedure: Autonomously navigate the local area, and go to the formation position according to the temporal constraints in Gr_α; if failed, go to 2b;
   (e) Situation Assessment Procedure:
      i. Assignment Checker Procedure: Check if some Assignment has been triggered sequentially or according to its monitor, set the online release time r_β^{online} of its corresponding Assignment-action β and add the Assignment to Action Execution Queue;
      ii. Action Execution Procedure: Check if there is any Assignment in Action Execution Queue, if true, check if r_β^{online} of its Assignment-action is consistent with Gr_α, if yes, execute the Assignment-action whose r_β^{online} is earlier than or equal to present time by evoking 3, delete the Assignment from the Action Execution Queue and add it to Action Monitor Queue; if no, go to 2b;
      iii. Action Checker Procedure:
         - check postconditions of any Assignment in Action Monitor Queue, if true, set the adjusted deadline of its Assignment-action β: d_β^{adj}; if d_β^{adj} is consistent with Gr_α, delete the Assignment from the Action Monitor Queue and related nodes from Gr_α, set corresponding Assignment Status if necessary; if it's not consistent, go to 2b;
         - if the Assignment-action did not finish after its duration, set the corresponding Assignment to "Failure" and go to 2b;
         - Check if there is some "Failure" conditions regarding the Assignment, if yes and it becomes true, set the Assignment to "Failure" and go to 2b;
3. Action Procedure: Send out Orders, if success, go to 2;
4. Failure Broadcast procedure: Broadcast "Failure".

Fig.2 Algorithm Description of NAUSEA

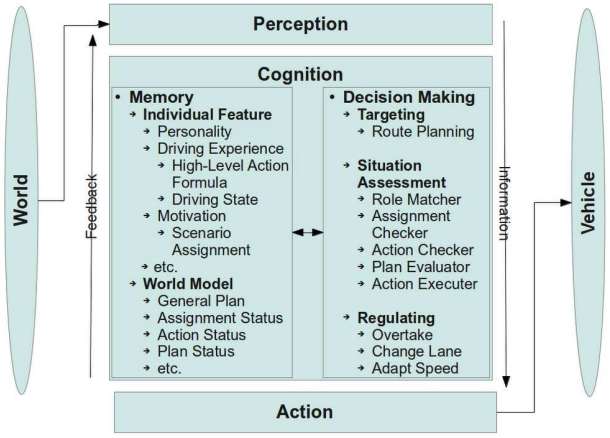

Fig. 1. Scenario-Aware Driver Model

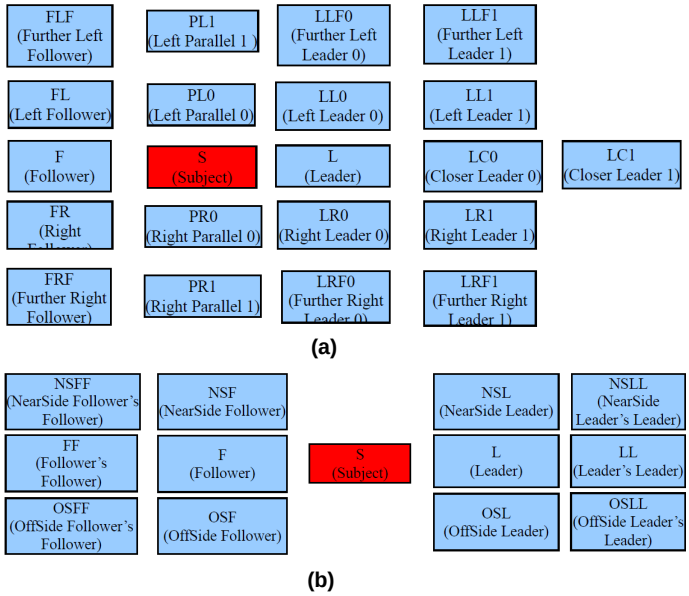

Fig. 3. Formation Position in SAIL/NAUSEA

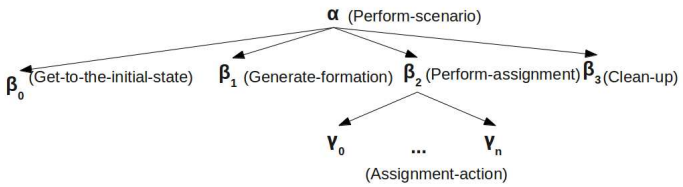

Fig. 4. Action Recipe for Smith (Perform-sceanrio)

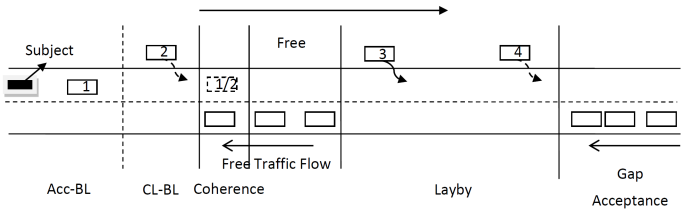

Fig. 5. Illustration of Scenario

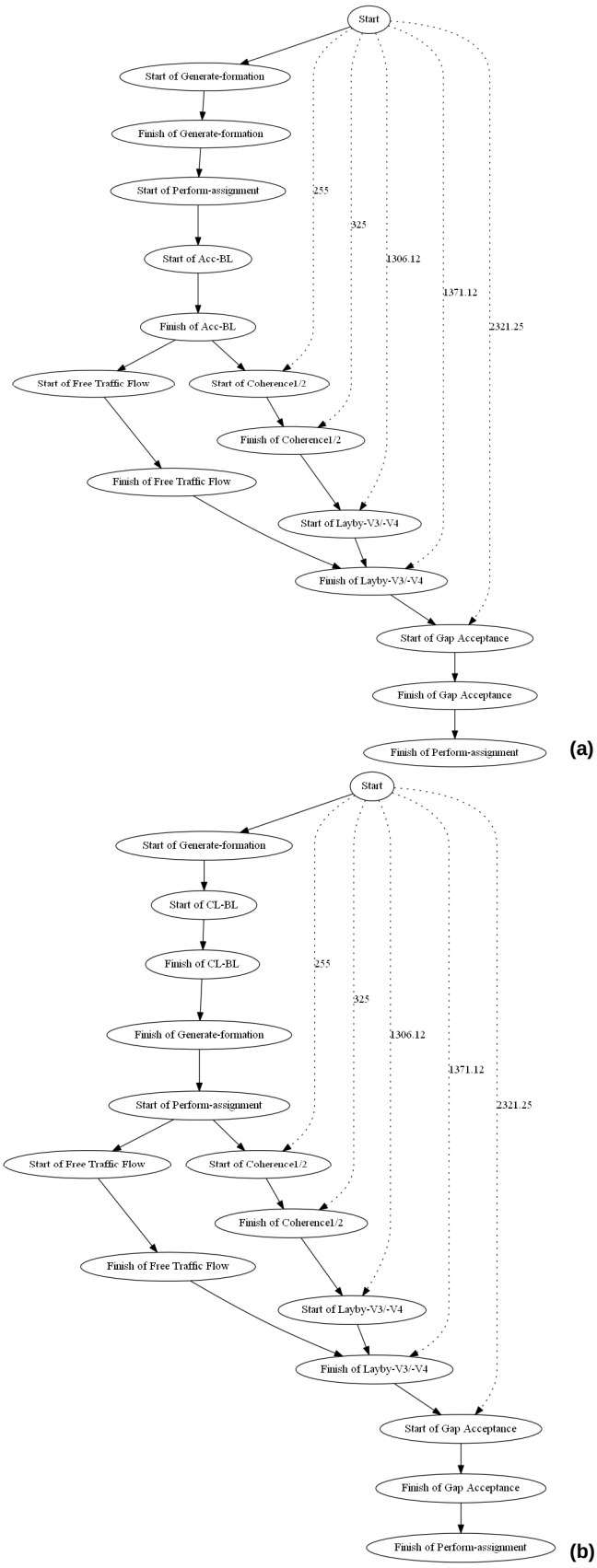

Fig. 6. Output of Plan Evaluation Procedure in Normal (a) and Failure (b) Test Case

Participant No.	Test Case in Round One	Test Case in Round Two	
		Section One	Section Two
1	1	7	9
2	1		8
3	1	4	2
4	1		6
5	1	3	5

Table 1. Test Case Tried by Every Participant

Table 2. Statistics of Order Lag in Phase One

Minimum	Maximum	Mean	Std. Deviation
.0000163	.1000000	.031511634	.0148830995

Table 3. Desired Output of Each Test Case

Table 4. Statistics of Order Release Time in Phase Two

Test Case		Total Trigger Number/ Order Number	Acc-BL			CL-BL			Coherence1			Coherence2			Layby-V3			Layby-V4			Gap Acceptance			Free Traffic Flow		
			M	S	F	M	S	F	M	S	F	M	S	F	M	S	F	M	S	F	M	S	F	M	S	F
1	Normal	6/5	√	√	×				√	D	×				√	D	×				√	N	N	√	N	N
2	Fail **Acc-BL**	8/6	√	×	√	√	√	×				√	D	×	√	D	×				√	N	N	√	N	N
3	Fail **CL-BL**	4/2	√	×	√	√	×	√																		
4	Fail **Coherence(1)**	5/3	√	√	×				√	×	√													√	N	N
5	Fail **Layby-V3**	8/6	√	√	×				√	D	×				√	×	√	√	D	×	√	N	N	√	N	N
6	Fail **Layby-V4**	8/5	√	√	×				√	D	×				√	×	√	√	×	√				√	N	N
7	Fail **Acc-BL** and **Coherence2**	7/4	√	×	√	√	√	×				√	×	√										√	N	N
8	Fail **Acc-BL** and **Layby-V4**	10/6	√	×	√	√	√	×				√	D	×	√	×	√	√	×	√				√	N	N
9	Fail **Acc-BL** and **Layby-V3**	10/7	√	×	√	√	√	×				√	D	×	√	×	√	√	D	×	√	N	N	√	N	N

M: Monitor

S: Success Condition

F: Failure Condition

√ : Triggered

× : Not Triggered

N **: Not Available**

D **: Duration-Based Success Condition**

Test Case	Coherence1				Coherence2				Layby-V3				Layby-V4				Gap Acceptance			
	Min	Max	Mean	Std. Deviation	Min	Max	Mean	Std. Deviation	Min	Max	Mean	Std. Deviation	Min	Max	Mean	Std. Deviation	Min	Max	Mean	Std. Deviation
1	247.067	247.183	247.108	0.037					710.400	710.433	710.414	0.012					869.350	869.367	869.361	0.009
2					200.350	200.917	200.541	0.177	661.467	661.567	661.500	0.031					822.350	822.383	822.365	0.012
3																				
4	244.000	244.333	244.074	0.103																
5	238.317	238.533	238.386	0.070					699.617	699.650	699.627	0.011	808.500	808.533	808.511	0.011	853.533	853.583	853.564	0.015
6	238.933	239.033	238.971	0.038					693.333	693.367	693.342	0.012	796.250	796.267	796.258	0.009				
7					181.317	181.983	181.574	0.194												
8					215.167	215.800	215.352	0.186	674.783	674.833	674.794	0.015	795.033	795.067	795.042	0.012				
9					195.817	196.583	196.147	0.269	662.850	662.917	662.882	0.020	784.533	784.633	784.562	0.030	829.533	829.683	829.618	0.040

Simulated traffic and auditory information: The impact on street crossing in young and old adults.

Jérôme RODRIGUES [1], Maria PINTO [1], Aurélie DOMMES [1], Viola CAVALLO [1] & Fabrice VIENNE [2]

(1) Laboratoire de Psychologie de la Conduite (LPC), Institut Français des Sciences et Technologies des Transports, de l'Aménagement et des Réseaux (IFSTTAR), 25 allée des marronniers, F-78000 Versailles – Satory. E-mail: jrmrdrgs@gmail.com (corresponding author); {maria.pinto, aurelie.dommes, viola.cavallo}@ifsttar.fr

(2) Laboratoire Exploitation, Perception, Simulateurs et Simulations (LEPSIS), Institut Français des Sciences et Technologies des Transports, de l'Aménagement et des Réseaux (IFSTTAR), 58, Boulevard Lefebvre, F-75732 Paris cedex 15. E-mail: fabrice.vienne@ifsttar.fr

Abstract

This study aimed at investigating the influence of auditory information and ageing on street-crossing decisions, using a virtual environment. Four auditory contexts were tested: (1) no sounds at all; (2) only the sounds from the simulated vehicles; (3) only an ambient auditory context composed of traffic sounds; and (4) the sounds from the simulated vehicles + the ambient context. Young and older participants were evaluated on their performance regarding the safety margins during the simulated street-crossing task. The results indicated that a full privation of auditory information significantly increased the participants' unsafe behaviour. They also point to a global benefit from auditory information on the participants' decisions, irrespective of its type. Finally, no age-related differences were observed. The findings support the idea that auditory information is an important experimental factor when simulating traffic and investigating street crossing in virtual environments. The results are discussed regarding the psychological notion of *presence*.

Key words: *Simulated traffic, auditory information, street crossing, ageing, presence.*

Introduction

To cross a road safely, pedestrians have to select appropriate gaps in traffic. To do so, they have to estimate the *time to arrival* (TA) of oncoming vehicles [Hec15]. TA judgments have been shown to depend on both visual [DeL6] and auditory [But4] information. For example, It has been demonstrated that multiple visual sources of information, such as pictorial [DeL7] or motion-based [Kai19] cues, can help TA judgements. Similarly, multiple auditory indicators can be used to estimate the TA of oncoming vehicles [But4]. Jenison argued that TA judgments are dependent on the observer's motion, and that interaural time delays, Doppler shift, and average sound intensity are relevant variables used to specify TA information [Jen18]. In the same way, papers reported that the listener-to-source distance can be estimated using spectral changes in the emitted sounds [Ros29], as well as the rate of change in sound pressure [Ash1]. Among the multiple auditory indicators, it seems that rising sound intensity is one of the most used and important auditory cues in TA judgments [Neu25, Sei31].

In most ecological situations, vision and audition are simultaneously used in TA judgments, and the multimodal integration generally helps the coupling of perceptions and actions. Auditory information seems therefore important to estimate the TA of oncoming vehicles, especially because it allows compensating for deficits in visual processing [Gus14, Sch30]. Regarding street crossing, auditory information could then be especially beneficial to vulnerable pedestrians, such as the elderly.

Regarding transport activities, the global decline with age creates safety problems for both older drivers [Cla5, Dob8, Sha32], and older pedestrians [Dom9, Fra13, Lob20, Lob21, Oxl27, Oxl28, Spa36]. Street-crossing studies have shown that the elderly tend to adopt more unsafe behaviours compared to young adults [Lob20, Lob21, Oxl28]. These unsafe behaviours were particularly observed in constraining circumstances, such as complex road traffic [Oxl27] or high vehicle speeds [Lob20, Lob21, Oxl28]. Increased unsafe behaviours in older individuals compared to younger pedestrians can be explained by the tendency to rely on simplified distance-based heuristics, leading to a less efficient use of the visual information, and, thus, to more unsafe decisions [Lob20, Lob21, Oxl28]. In this context, it can be assumed that, similarly to visually impaired individuals [Sch30], older pedestrians could benefit from the presence of auditory information to compensate their deficient use of visual cues in TA judgments.

Virtual environments are more and more often used as experimental tools to conduct street-crossing studies [Dom9, Lob20, Lob21, Nei23, Nei24, Oxl28, Sim35]. Although auditory information seems important in TA judgments, this factor was not really considered in previous studies which used virtual environments. Some studies provided their participants with auditory information, but this factor was not manipulated and not analyzed regarding its potential influence on street-crossing performance [Dom9, Lob20, Lob21, Oxl28]. In other studies, audition was neglected by the authors, as no acoustic information was given to the participants during the experiments [Nei24, Nei25]. In few papers, no information about this parameter was even presented to the readers [Hol17, Sim35]. In simulated tasks, as well as in real situations, auditory information can be assumed to contribute to TA judgments, and, more generally, to performance. This assumption is supported by the TA literature but also by many papers dealing with virtual reality, and showing the importance of auditory information in simulated activities [Bor2, Hen16, Nam22]. Actually, several studies indicate that auditory information generally increases task performance in virtual environments [Nam22], and that behaviours can be modified by both relevant and irrelevant auditory sources [Bor2].

In this context, the aim of the present study was to investigate the influence of auditory information on TA judgments and street-crossing performance, but also to determine whether a potential effect of auditory information depends on the participants' age. Three hypothesises were made: (1) a full privation of auditory information is detrimental to street-crossing safety; (2) the type of auditory context influences the participants' performance differently; and (3) auditory information is particularly beneficial in older pedestrians.

Material & Methods

Participants

Forty participants took part in the study: 20 young people (20-35 years old; M = 28.5, SD = 5.1) and 20 older individuals (60-80 years old; M = 68.0, SD = 4.7). Each age group was composed of 13 men and 7 women. All the older participants were living on their own at the time of the experiment, without any medical assistance. All the participants went through a series of control tests aimed at eliminating subjects with visual, auditory, or motor deficient skills. Moreover, the older participants were tested using the Mini Mental State Evaluation (MMSE) [Fol11] to be sure that none of them were suffering from pathological ageing. Finally, an informed consent form was signed by the participants before starting the experiment.

Experimental set up

The street-crossing simulation device used in the experiment was based on the INRETS Sim^2 driving simulator [Esp10]. The device included a portion of experimental street (4.2-m wide, materialized on the ground), 3 large screens (2.70m x 1.90m each), an image-generation system including 3 video projectors, and a computer connected to a spatial sound-rendition system and a movement-tracking apparatus (Fig. 1, bottom). This computer was dedicated to the emission of the auditory contexts and data recording. The sound-rendition system was composed of five speakers: 2 in front of the participants, 2 in the back, and one subwoofer which was placed aside. This configuration allowed emitting the auditory contexts stereophonically, and, therefore, with spatial variations. Regarding the movement-tracking apparatus, it was composed of a locometer linked to the participants by the mean of a cable attached to their waist. Each time the participants moved forward to cross the experimental street, distance and time were recorded.

The setup provided the participants with a horizontal visual field between 90° (at the departure sidewalk) and 140° (in the middle of the experimental road), and a vertical visual field of 40°. The images were calculated at a refresh rate of 30 Hz. Image generation and projection took the participants' eye height into account; the simulated viewing angle was aimed the vanishing point of the modeled street. By way of a cable attached to the participants' waist, the movement-tracking system interactively updated the visual scenes according to their motion, and all their movements were simultaneously recorded.

The visual scenes represented a one-way street, 4.2-m wide sidewalk-to-sidewalk (Fig. 1, top). Traffic consisted of three vehicles: a motorcycle followed by two identical cars. All vehicles were moving at a constant speed from left to right in reference to the participants' position on the departure sidewalk. At the beginning of each scene, the motorcycle was 1.5 seconds away from the participants, and the first car was 1 second away from the motorcycle. Given that the visual scenes were updated according to the participants' position, oncoming vehicles were displayed on the central screen when crossing was accepted, but the vehicle approach ended on the right screen when the participants rejected crossing.

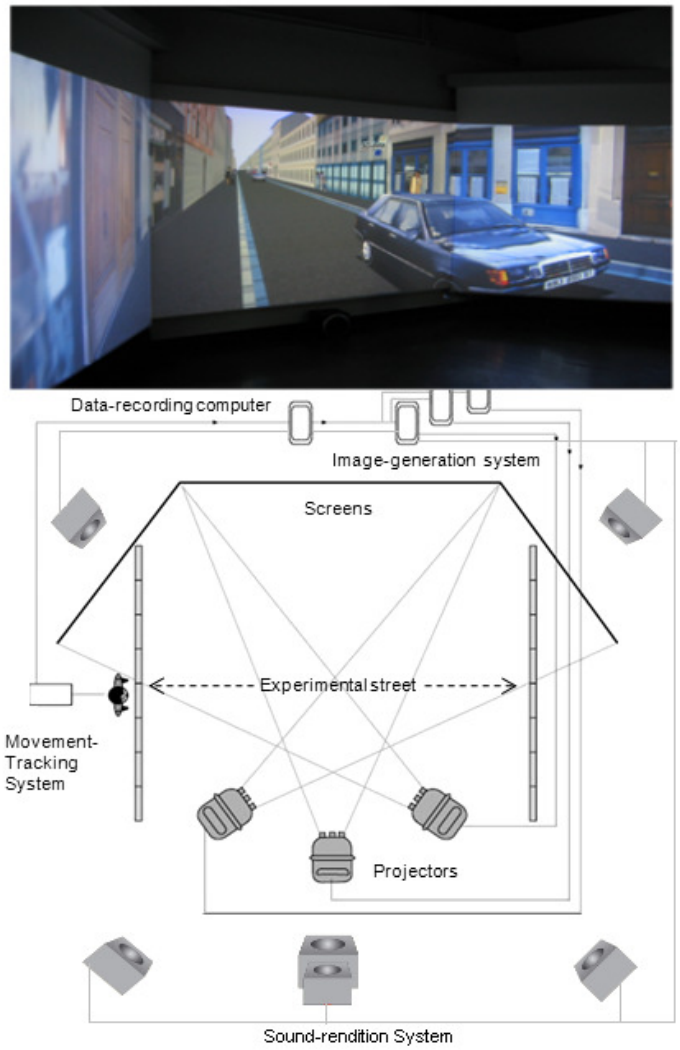

Fig. 1. Picture representing a scene from the participant's point of view at the departure sidewalk (Top). Top-down schematic view of the experimental setup (Bottom). **(© IFSTTAR, 2010)**

Experimental design

Four auditory conditions were used to investigate the role of auditory information in street-crossing: (1) no sounds at all (i.e., "no-sound" condition); (2) only the sounds from the simulated vehicles, that is to say engine, tires, and air displacement (i.e., "vehicle-sound" condition); (3) only an ambient auditory context composed of traffic sounds with no relations with the simulated vehicles (i.e., "ambient-sound" condition); and (4) sounds from the simulated vehicles to which was added the ambient context (i.e., "full-sound" condition). Considering conditions 2 and 4, the sound level from the vehicles was proportionally decreasing as a function of the distance between the considered position of the vehicle in the virtual environment and the crossing line, where was standing the participants and crossing the experimental street. The maximum sound level was therefore reached when the vehicle passed the crossing line, and the minimum vehicle-sound level (actually inaudible by the participants) corresponded to the vanishing point of the modeled street.

Four experimental blocks were distinguished, corresponding to the four possible auditory contexts. In each experimental block, 2 vehicle speeds were used (i.e., 40 and 60 km/h), and the time gap between the two cars varied from 1 to 7 s. The speeds were chosen to be representative of urban areas in France (i.e., speed limit = 50 km/h). Time gaps were chosen so that all of the participants, regardless of their age, would be confronted with both favorable (i.e., gap ≥ 4 s) and unfavorable (i.e., gap < 4 s) street-crossing situations. The number of repetitions per time gap differed according to their probability of being accepted for crossing. In fact, as it has been shown in previous studies, the shortest gaps are systematically refused and the longest gaps systematically accepted (e.g., Lobjois & Cavallo, 2007). Therefore, time gaps of 1 and 7 s were presented once, time gaps of 2 and 6 s twice, and the "critical" time gaps of 3, 4, and 5 s three times, making 15 trials in all. Using 15 trials for each vehicle speed leads to 30 trials per experimental bloc, that is to say 120 trials considering the whole experiment.

Procedure

Participants were tested individually on the street-crossing simulator. They were positioned at the edge of the sidewalk facing the experimental road and had to look to the left at the virtual environment and the approaching simulated vehicles. For each trial, participants were instructed to cross the street between the two cars when they thought it was safe to do so, by walking at any pace but not running. They were also told that they did not have time to cross in front of the approaching motorcycle, or between the motorcycle and the first car.

Before beginning the experiment, the participants performed some practice trials until they told the experimenter they fully understood the task. Thereafter, they performed the 120 experimental trials divided, as indicated above, in 4 experimental blocks of 30 trials each. Presentation order of the blocks was counterbalanced between the participants for each age group, and, in each experimental bloc, the presentation order of the trials was randomized. The participants' decisions to cross or not to cross and their motion until the end of the visual sequence were recorded on each trial. The complete session lasted approximately 45 minutes, and a 5-minute break was proposed in the inter-bloc intervals to the participants (especially for the older ones) to prevent fatigability.

Data Analysis

All trials were marked according to the participants' decision to accept or reject gaps to cross the street. For each accepted trial, the safety margin (SM) was computed. The SM corresponds to the time between the moment when the participants were completely over the edge of the arrival sidewalk and when the second car passed through the crossing line. Therefore, SM was negative if the participant was still on the road when the front of the second car passed the crossing line. For each participant, mean SM was computed for each auditory condition and each vehicle speed. Thereafter, the mean SM were input into a 4 (auditory contexts) x 2 (vehicle speeds) x 2 (age groups) mixed analysis of variance (ANOVA) with the significant level set at .05. The effect size (η^2) was also computed, and significant effects were further examined using Fisher's PLSD post hoc test.

Results

The participants' performance is presented in Table 1. The ANOVA on mean SM first revealed a significant effect of the auditory context, $F(3,114) = 3.09$, $p < .05$, $\eta^2 = .08$. The post hoc test indicated that the "no-sound" condition (M = 1.59s) induced a significant decrease of the SM, compared to all of the other auditory conditions ("vehicle-sound": M = 1.65s; "ambient-sound": M = 1.72s; "full-sound": M = 1.70s).

Similarly, the ANOVA revealed a major effect of the vehicle speed, $F(1,38) = 38.78$, $p < .0001$, $\eta^2 = .51$, yielding to greatly decreased SM while simulating cars moving at 60 km/h (M = 1.44s) compared to 40 km/h (M = 1.88s). In contrast, no significant effects of the age factor were observed, $F(1,38) = 2.22$, $p = .14$, $\eta^2 = .05$, indicating no overall differences on SM between the young (M = 1.76s) and the elderly (M = 1.56s) participants.

Regarding interactions, the *Speed×Age* interaction was close to significance, $F(3,114) = 2.79$, $p = .08$, $\eta^2 = .07$. Examination of the means and the post hoc test showed that the SM of each group were significantly decreased while increasing the vehicle speed, but that the decrease tended to be higher in the elderly (M = -0.57s) than in the young (M = -0.32 s) participants. No other interactions were significant.

Table 1. Mean safety margins (expressed in seconds) depending on the age group, the auditory context, and the vehicle speed. Standard deviations are indicated in parentheses.

Auditory context	Vehicle speed	Young participants	Old participants
« No-sound » condition	*40 Km/h*	1.8 (0.6)	1.9 (0.7)
	60 Km/h	1.5 (0.7)	1.2 (0.5)
« Vehicule-sound » condition	*40 Km/h*	1.9 (0.7)	1.7 (0.6)
	60 Km/h	1.6 (0.5)	1.3 (0.4)
« Ambient-sound » condition	*40 Km/h*	2.0 (0.5)	2.0 (0.5)
	60 Km/h	1.6 (0.4)	1.3 (0.5)
« Full-sound » condition	*40 Km/h*	2.0 (0.7)	1.9 (0.5)
	60 Km/h	1.7 (0.6)	1.3 (0.4)

Discussion

In the context of a simulated street-crossing task using a virtual environment, the present study indicates that full privation of auditory information tends to decrease the safety of the participants' decisions. SM were actually increased when auditory information was added to the visual scenes, compared to the conditions in which auditory information was not present. From this result, it can be concluded that auditory information was useful to the

simulated street-crossing task and that auditory-visual information seemed to help the increase of the participants' performance. This conclusion is in accordance with previous papers reporting the benefit from auditory-visual information on TA judgments [But3, But4, Gus14, Sha33]. One observation moderates however the conclusion.

Analyzing the SM variations in the different auditory conditions, it was observed that, although they were statistically significant, these variations ranged only between 0.06 and 0.13 s. The variation range being relatively small, it is therefore difficult to estimate the impact of such variations in real conditions. Although auditory-visual information seemed to help the participants in the simulated street-crossing task, compared to the visual condition only, the results have however to be taken with careful considerations before generalizing the findings to reality. Transposition to a real street-crossing task seems even more premature as the explanation of the results needs to be clarified.

In the present experiment, the results do not seem to indicate that the benefit from auditory-visual information on the participants' performance can be explained by the use of relevant auditory cues (i.e., the specific sounds of the oncoming simulated vehicles) helping the participants to estimate the TA of the vehicles during the task. Actually, If this had been the case, a significant difference would have been observed between the auditory conditions where only the vehicles sounds or only the ambient context were available. The absence of such a difference tends to indicate that the improved performance when auditory information was available cannot be explained by the auditory cues specifically involved in TA estimation.

The present results could be explained instead by referring to the field of virtual reality (VR). Many studies reported that auditory information is an important experimental factor in simulated tasks as it increases the participants' *sense of presence* [Bor2, Hen16]. Applied to virtual environments, presence refers to experiencing the computer-generated environment rather than the actual physical location [Wit38]. Studies in the field of VR have demonstrated that the extent of sensory information transmitted to the participants in virtual environments determines the strength of the sense of presence [She34]. Concerning auditory information, Hendrix and Bartfield have shown in a free-navigation task that auditory-visual conditions increase the sense of presence, compared to visual conditions alone [Hen16]. According to Bormann's work, this observation seems true even when the auditory information is not relevant for the to-be-performed task [Bor2]. Increasing the sense of presence generally leads to increased performance in a simulated task [Nam22]. Actually, presence and attention are intimately linked [Fon12]: increased presence is related to increased attentional focus, and, thus, to greater performance.

In line with the VR literature, it can be assumed that the auditory information available in the present experiment increased the sense of presence in the participants, compared to the "no-sound" condition, leading to an increased attentional focus and, thus, to better performance in the simulated street-crossing task. Our results seem then to confirm Bormann's findings [Bor2], as an ambient auditory context (i.e., irrelevant information) had as much impact on the participants as the specific sounds of the simulated vehicles (i.e., relevant information). Further investigations should address the influence of presence in simulated street-crossing tasks, using dedicated questionnaires [Nic26, Tro37, Wit38].

Regarding ageing, no age differences were observed in this experiment when comparing the two groups of participants on the simulated street-crossing task. In our previous studies, the results showed that, considering normal ageing, some cognitive differences appeared when comparing the data of young and older participants. Precisely, regarding visual cues, it was showed that older individuals seem to rely more on distance-based heuristics than young subjects to estimate the time-to-arrival of oncoming vehicles. Similarly to visual cues, we expected that age-related differences could be revealed regarding the utilization of auditory information by young and older pedestrians in a street-crossing task. This hypothesis was obviously not confirmed. One explanation of this unexpected result could be that our old participants may actually have been too "young". In the street-crossing literature, it was demonstrated that ageing effects on performance tend to appear particularly in "old-old" participants (i.e., > 75 years old), but in a less important manner in "young-old" participants (i.e., 60-70 years old) [Lob20, Lob21, Oxl28]. In our study, the average age of the older participants was 68 years old, and only three of them were over 75 years old. It can therefore be assumed that the older group did not exhibit important age-related declines, and that the consequences on street-crossing safety remained limited. The present results therefore support the idea that the effects of age on street-crossing safety seem to especially concern pedestrians aged above 75 years old. Further investigations should be done to test the effect of auditory information in a simulated street-crossing task in "old-old" pedestrians.

In conclusion, the present study indicates that auditory information influences behaviours and contributes to increase the safety of decisions in the context of a simulated street-crossing task. Despite the limits of our experiment, the findings underline the fact that auditory information is an important factor when simulating traffic and investigating street crossing in virtual environments. Consequently, the studies which neglected this experimental parameter may appear questionable [Hol17, Nei24, Nei25, Sim35].

References

[Ash1] Ashmead D.H., Davis D.L., Northington A. "Contribution of listeners' approaching motion to auditory distance perception". *Journal of Experimental Psychology: Human Perception and Performance*, 1995, 21(2), pp. 239-256.

[Bor2] Bormann K. "Presence and the Utility of Audio Spatialization". *Presence: Teleoperators and Virtual Environments*, 2005, 14(3), pp. 278-297.

[But3] Button C. "The effect of removing acoustic information of ball projection on the coordination of one-handed ball-catching". In K. Davids, G. Salvelsberg, S. Bennett & J. van der Kamp (Eds), *Interception Actions in Sport: Information and Movement* (pp. 184-194), 2002, Taylor & Francis: London.

[But4] Button C., Davids K. "Acoustic information for timing". In H. Hecht & G. J. P. Savelsburgh (Eds.), *Advances in psychology (Vol. 135): Time-to-Contact* (pp. 355-369), 2004, Elsevier-North-Holland: Amsterdam.

[Cla5] Clarke D.D., Ward P., Bartle C., Truman W. "Older drivers' road traffic crashes in the UK". *Accident Analysis & Prevention*, 2010, 42(4), pp. 1018-1024.

[DeL6] DeLucia, P.R. "Multiple sources of information influence time-to-contact judgments: Do heuristics accommodate limits in sensory and cognitive processes?" In H. Hecht & G. J. P. Savelsburgh (Eds.), *Advances in psychology (Vol. 135): Time-to-Contact* (pp. 243-286), 2004, Elsevier-North-Holland: Amsterdam.

[DeL7] Delucia P.R., Novak J.B. "Judgments of relative time-to-contact of more than two approaching objects: Toward a method". *Perception & Psychophysics*, 1997, 59(6), pp. 913-928.

[Dob8] Dobbs A.R., Heller R.B., Schopflocher D. "A comparative approach to identify unsafe older drivers". *Accident Analysis & Prevention*, 1998, 30(3), pp. 363-370.

[Dom9] Dommes A., Cavallo V. "The role of perceptual, cognitive, and motor abilities in street-crossing decisions of young and older pedestrians". *Ophthalmic and Physiological Optics*, 2011, 31(3), pp. 292-301.

[Esp10] Espié S. "Vehicle-driven simulator versus traffic-driven simulator: the INRETS approach". In Proceedings of the *First Driving Simulation Conference Europe* (pp. 367–376), 1999, Paris, France.

[Fol11] Folstein M.F., Folstein S.E., McHugh P.R. "Mini-mental state: A practical method for grading the cognitive state of patients for the clinician". *Journal of Psychiatric Research*, 1975, 12(3), pp. 189-198.

[Fon12] Fontaine G. "The experience of a sense of presence in intercultural and international encounters". *Presence: Teleoperators and Virtual Environments*, 1992, 1(4), pp. 482-490.

[Fra13] François M., Morice A.H.P., Blouin J., Montagne G. "Age-related decline in sensory processing for locomotion and interception". *Neuroscience*, 2011, (172), 366-378.

[Gus14] Guski R. "Acoustic Tau: An Easy Analogue to Visual Tau?" *Ecological Psychology*, 1992, 4(3), pp. 189-197.

[Hec15] Hecht H., Savelsbergh G.J.P. "Advances in Psychology: Time-to-contact". 2004, Elsevier North Holland: Amsterdam.

[Hen16] Hendrix C., Bartfield W. "The sense of presence within auditory virtual environments". *Presence: Teleoperators and Virtual Environments*, 1996, 5(3), pp. 290-301.

[Hol17] Holland C., Hill R. "Gender differences in factors predicting unsafe crossing decisions in adult pedestrians across the lifespan: A simulation study". *Accident Analysis & Prevention*, 2010, 42(4), pp. 1097-1106.

[Jen18] Jenison R.L. "On Acoustic Information for Motion". *Ecological Psychology*, 1997, 9(2), p. 131.

[Kai19] Kaiser M.K., Mowafy L. "Optical specification of time-to-passage: Observers' sensitivity to global tau". *Journal of Experimental Psychology: Human Perception and Performance*, 1993, 19(5), pp. 1028-1040.

[Lob20] Lobjois R., Cavallo V. "Age-related differences in street-crossing decisions: The effects of vehicle speed and time constraints on gap selection in an estimation task". *Accident Analysis & Prevention*, 2007, 39(5), pp. 934-943.

[Lob21] Lobjois R., Cavallo V. "The effects of aging on street-crossing behavior: From estimation to actual crossing". *Accident Analysis & Prevention*, 2009, 41(2), pp. 259-267.

[Nam22] Nam C.S., Shu J., Chung D. "The roles of sensory modalities in collaborative virtual environments (CVEs)". *Computers in Human Behavior*, 2008, 24(4), pp. 1404-1417.

[Nei23] Neider M.B., Gaspar J.G., McCarley J.S., Crowell J.A., Kaczmarski H., Kramer A.F. "Walking and talking: Dual-task effects on street crossing behavior in older adults". *Psychology and Aging*, 2011, 26(2), pp. 260-268.

[Nei24] Neider M.B., McCarley J.S., Crowell J.A., Kaczmarski H., Kramer A.F. "Pedestrians, vehicles, and cell phones". *Accident Analysis & Prevention*, 2010, 42(2), pp. 589-594.

[Neu25] Neuhoff J. "An Adaptive Bias in the Perception of Looming Auditory Motion". *Ecological Psychology*, 2001, 13(2), pp. 87-110.

[Nic26] Nichols S., Haldane C., Wilson J.R. "Measurement of presence and its consequences in virtual environments". *International Journal of Human-Computer Studies*, 2000, 52(3), pp. 471-491.

[Oxl27] Oxley J., Fildes B., Ihsen E., Charlton J., Day, R. "Differences in traffic judgements between young and old adult pedestrians". *Accident Analysis & Prevention*, 1997, 29(6), pp. 839-847.

[Oxl28] Oxley J., Ihsen E., Fildes B.N., Charlton J.L., Day R.H. "Crossing roads safely: An experimental study of age differences in gap selection by pedestrians". *Accident Analysis & Prevention*, 2005, 37(5), pp. 962-971.

[Ros29] Rosenblum L.D., Wuestefeld A.P., Saldaña H.M. "Auditory looming perception: Influences on anticipatory judgments". *Perception*, 1993, 22(12), pp. 1467 – 1482.

[Sch30] Schiff W., Oldak R. "Accuracy of Judging Time to Arrival: Effects of Modality, Trajectory, and Gender". *Journal of Experimental Psychology: Human Perception and Performance*, 1990, 16(2), pp. 303-316.

[Sei31] Seifritz E., Neuhoff J.G., Bilecen D., Scheffler K., Mustovic H., Schachinger H., Elefante R., Di Salle F. "Neural Processing of Auditory Looming in the Human Brain". *Current Biology*, 2002, 12(24), pp. 2147-2151.

[Sha32] Shanmugaratnam S., Kass S.J., Arruda J.E., 2010. "Age differences in cognitive and psychomotor abilities and simulated driving". *Accident Analysis & Prevention*, 2010, 42(3), pp. 802-808.

[Sha33] Shaw B.K., McGowan R.S., Turvey M.T. "An acoustic variable specifying time-to-contact". *Ecological Psychology*, 1991, 3(3), pp. 253-261.

[She34] Sheridan T.B., "Musings on Telepresence and Virtual Presence". *Presence: Teleoperators and Virtual Environments*, 1992, 1(1), pp. 120-125.

[Sim35] Simpson G., Johnston L., Richardson M. "An investigation of road crossing in a virtual environment". *Accident Analysis & Prevention*, 2003, 35(5), pp. 787-796.

[Spa36] Sparrow W.A., Bradshaw E.J., Lamoureux E., Tirosh O. "Ageing effects on the attention demands of walking". *Human Movement Science*, 2002, 21(5-6), pp. 961-972.

[Tro37] Tromp J., Bullock A., Steed A., Sadagic A., Slater M., Frécon E. "Small Group Behavior Experiments in the Coven Project". *IEEE Computer Graphics and Applications*, 1998, 18(6), pp. 53-63.

[Wit38] Witmer B.G., Singer M.J. "Measuring Presence in Virtual Environments: A Presence Questionnaire". *Presence: Teleoperators and Virtual Environments*, 1998, 7(3), 225-240.

Principle other Vehicle Warning

Jonas Jansson [1], Birgitta Thorslund [1], Mattias Brännström [2], Jonas Andersson Hultgren [1]

(1) Swedish Road and Transport Research Institute, SE-581 95 Linköping, Sweden, E-mail : {jonas.jansson, birgitta.thorslund, Jonas.andersson.hultgren}@vti.se
(2) Volvo Car Corporation, SE- 405 31 Göteborg, Sweden, E-mail : {mbranns3}@volvocars.com

Abstract – *This study aims at providing basic understanding of driver responses to headlight and sound warning coming from another vehicle, in a critical situation. A possible application is the implementation of systems for automatic activation of the warnings. A simulator study of a critical frontal collision situation was conducted in order to examine usefulness of four different warning modalities (light, sound, sound and light, no warning) from a principal other vehicle (POV). The posted speed was 70 km/h and the critical situation was created using a secondary task and simultaneously turning the vehicle towards the oncoming POV.*

In total, 48 participants drove 30 km while performing the secondary task, announced by a vibration in the seat, and experiencing light and/or sound warnings from oncoming traffic. The behavioural results of the simulator study indicate tendencies that the warning provides an increased safety by making the driver respond, in a proper manner, to the dangerous situation. Some of the indications for this were faster response time in the critical situation, shorter glance time away from the road and degraded performance in the secondary task. The combined warning, where both the horn and headlight is used, had a larger effect than the light or sound warnings alone. The participants are generally positive towards the warning and the warning modalities; 65% are positive towards auditory warning, 75% towards visual warning and 85% towards the combination warning of sound and light.

Considering automatic activation of the warnings; the current scenario represent a situation which is at the limit of what available sensing system is capable of i.e. a warning is issued 2,8 second before collision, which yields a distance of ~110 meters at 140 km/h relative velocity.

Key words: *driving simulator, horn sound, headlight, warning system, head-on collision.*

Introduction

Systems for automatic activation of brakes and steering are currently entering the market. These systems use proximity sensors to monitor the state of surrounding road users. Depending on the specific situation the effort/possibility to avoid or mitigate an accident may differ significantly between the principle road users of a pending collision, e.g. one road user may easily avoid a collision while a second may not be able to do so. The only possibility for the second road user to avoid a collision in such a situation is to issue a warning to the first, so that he/she may take evasive actions. Connecting the horn and the headlight to already existing sensor system, for automatic warning activation, is a cost effective means to provide such a warning. The aim of this project is to evaluate the effectiveness of such a warning and also to validate if the warning between the road users is experienced as intended and whether the warning is an effective countermeasure for avoiding accidents. A second objective of this study was to develop simulation technology for a realistic sensation of headlight glare and horn sound of an oncoming vehicle.

There is limited research on how to design warning signals to avoid collision. In a simulator study auditory collision warnings with increasing intensity have been shown more effective than other types of auditory warnings [Gra1]. According to research regarding warning signals in general, auditory warnings should, if possible impart the nature of the events to the user. [Edw1]. It has also been shown that people can match the frequency with which they respond to alarms to the false alarm rate, that increasing the perceived urgency of an alarm decreases reaction time and that increasing the number of modalities in which a warning is presented decreases reaction time [Edw2].

Experimental setup

Field measures and implementation

Field measurements where performed in cloudy daylight conditions to meet light conditions of daylight in the simulator. Pictures were taken and luminance levels measured on both full and half beam from a Volvo V70 model

year 2007 every tenth meter from 100 meters distance. To replicate the full beam in the simulation the size of the lights was enlarged. The blinks were accomplished by activating and deactivating the full beam of the encountering vehicle, see Figure 1. At critical events there was a pulsed warning signal of 0,3 seconds full beam presented 5 times with pauses of 0,04 seconds between. At non-critical events there were two blinks of 0,15 seconds with 0,10 seconds between. Additionally a line of led lights at the roof of the simulator cabin was lit simultaneously with the full beam.

Figure 1: Photos of full and half beam are displayed for 20 meters distance along with an implementation in the simulator of a critical event with light warning thru a pulsed headlight from the POV.

The horn signal was recorded at a distance of 1,7 meters with a Svantek 955 Class 1 with a signal to noise ratio of 55 dB(A). The recording was adjusted according to an airborne sound transmission in a SAAB 9-3 cabin. At critical events there was a pulsed sound warning signal analogous to the light warning. Horn signals of 0,3 seconds were presented 5 times with pauses of 0,05 seconds. These signals were increasing in intensity as the principle other vehicle came closer, see Figure 2 for the acoustic signals.

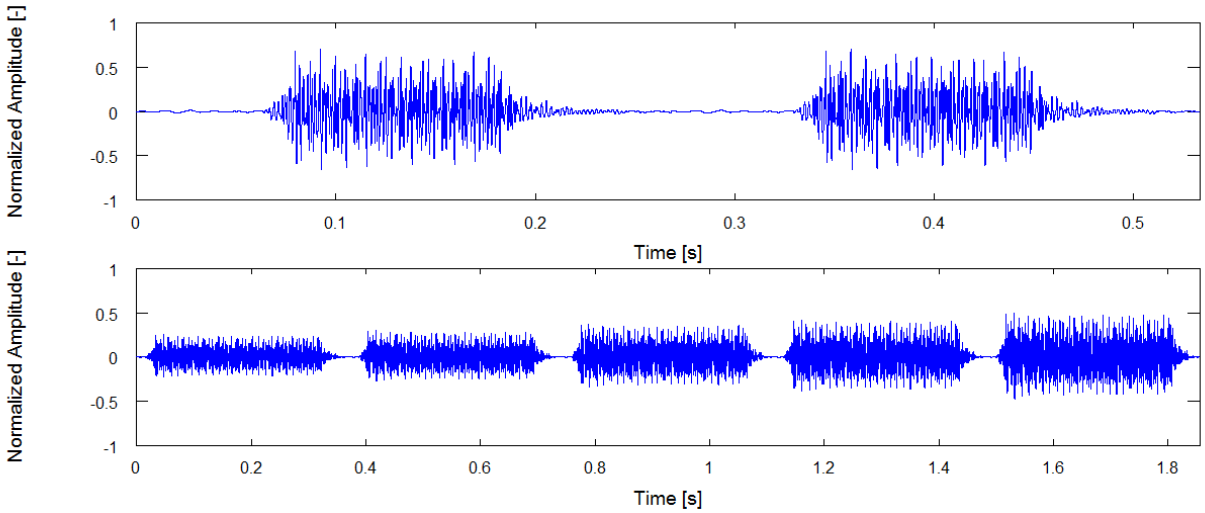

Figure 2: Sound signals at non-critical events (above) and critical events (below).

Method

A within subject design with four experimental warning conditions were used to evaluate the modality of the warning signals. The number of test participants was 48, 25 men and 23 women with a mean age of 62 years (SD = 7,5). The participants drove the Subject Vehicle (SV) and experienced the critical event 5 times with different

warning signals; *No warning, Light, Sound* and *Light+Sound*. The warning coming from the encountering vehicle was given at TTC 2,8 seconds, where the horn and/or the lights of the POV were triggered. The warning signals were presented in balanced order. To investigate learning effects, the signal presented at the first event was repeated at the fifth event.

Non critical noise and light signals from other vehicles were presented in the gaps between critical events. These signals represent a greeting or a wish to make the driver aware of the headlight. Compared to the pulsed critical signals, these are shorter and meant to be experienced as friendly. The purpose of the non-critical signals is to evaluate if the driver understands the difference between the critical and the non-critical.

The driving scenario was a rural road (70 km/h speed limit) where the driver was distracted by a visual distraction task. The participants were instructed to drive as he or she usually does and to put a lot of effort into the secondary task. This consisted of reading and remembering four letters and after they have been displayed saying them out loud, see Figure 3. A vibration in the seat was used to prompt the participant to perform the letter task. At critical events a yaw movement was introduced to the simulator while the participant was looking down to perform the letter task.

The study used VTI's driving simulator III, see Figure 3. This is equipped with a Saab 9-3 cabin and an advanced motion system for realistic simulation of forces felt when driving [Nor1]. The main projection screen has a 120 degrees field of view, and three lcd-displays simulate the rear-view mirrors.

Figure 3: VTI´s driving simulator III and the position of the visual distraction task display.

Measurements and Performance indicators

Measurements used to monitor driver behaviour were measured in a time window (16 sec) before and after each critical event. These are lateral distance, time to line crossing (TLC), time to collision (TTC), steering wheel reversal rate, driver reaction time (in terms of steering wheel correction, brake pedal response and time to look up) and eyes off road (total time, number of glances and longest glance). The objective measures were also accompanied by subjective ratings during and after the test drive. These aim at evaluating the realism of the simulated event and the usefulness of the warning provided by the meeting vehicle. The questionnaire included both yes/no-questions (*e.g: did you experience any warning?*) and 5 point scales, where 1 was "not at all" and 5 was "very much" (*e.g: how realistic did you experience the simulator?*)

Analysis

A mixed linear model was used and the Factors were *Participant*, *Warning type* and *Gender*, while *Order of warning* was a covariate. There was a separate analysis of the first event due to expected learning effects and realism. The participants were expected to be more shocked by the first critical event since this is not what they have expected. This event is also more realistic since these critical situations are not that likely to happen. In the secondary task, dependent variables were *Amount Correct, Amount skipped* and *Amount correct ignoring order* which will all be numbers between 0 and 4. The questionnaire was analyzed with logistic regression.

Results

Although the instruction was to consider the secondary task as important, several participants were not comfortable looking away in the situation of an encountering vehicle. This led to 12 % of the secondary tasks during events being skipped and there was no effect of order. Further analysis was carried out only on events where the secondary task was performed. A fast response was defined as when the driver have made either a steering wheel correction, brake response or have looked up within one second after the warning was issued. Looking at frequencies of fast responses reveal that 34% of all warnings gave a fast response. Of these fast responses (N=63) the most (32%) where at light+sound warning.

In the present study, the majority of all events did not lead to any incident or near crash situation, here defined by TTC < 1s with a lateral clearance < 0.5 m, see Figure 4. A warning was triggered at TTC = 2.8s, equivalent to a distance of about 110 m between the vehicles. At this stage, the SV is still positioned in its original lane and has a lateral velocity less than 0.5 m/s.

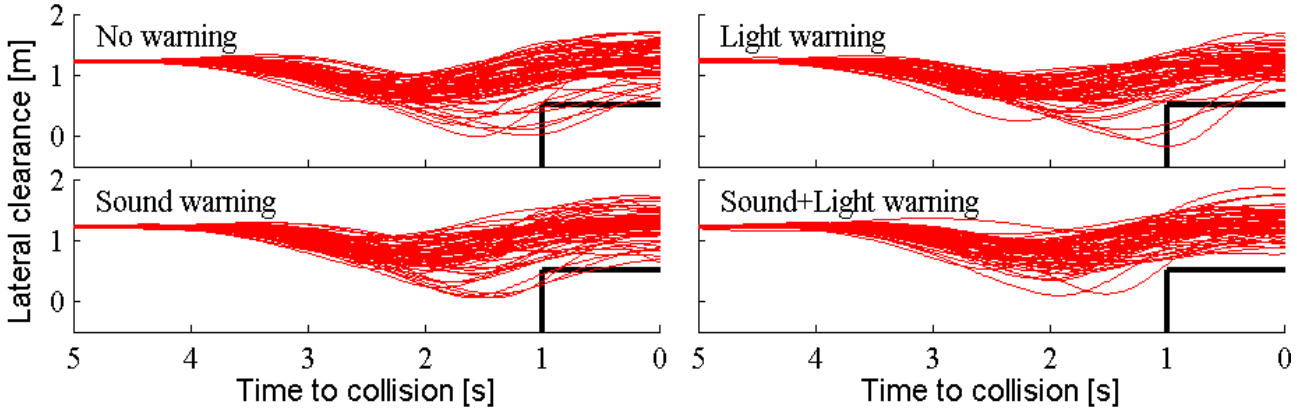

Figure 4: Lateral clearance and TTC (if no evasive action is taken) for the four warning types, respectively. Trajectories that pass through the rectangular area (thick solid line) are defined as incidents (TTC < 1s and lateral clearance < 0.5 m). Five incidents were detected for 'No warning', three for 'Light warning', four for 'sound warning' and zero for combined warning.

Of all performance indicators and measures only those who reveal significant effect of the warning are presented. This was examined by comparing the measures from a time window of 16 seconds before and after the warning respectively. The first critical event is treated separately, due to possible learning effects.

First critical event

There was a decrease in the standard deviation for the lateral position for all warning types (including no warning) after the first critical event. This means that the critical event decreased the wobbling. The effect was significantly larger for light+sound warning compared to both no warning, t(34) = 2,51, p = 0,019 and light warning t(34) = 2,13, p = 0,044. Only 88% (N = 42) performed the first task, showing the unwillingness to look away although no critical event has happened so far. Mean values, standard deviations and numbers of cases for each warning modality are shown in Table 1.

Table 1: Change in standard deviation (SD) for the lateral position after first critical event

Type	Mean (m)	SD	N
No warning	-0,010	0,068	13
Light	-0,025	0,034	10
Sound	-0,067	0,072	10
Light+sound	-0,070	0,077	9

Eye tracking revealed that the Longest Glance away from the road decreased in duration as an effect of the critical situation, for all warning types except for no warning. The effect was significantly larger for light+sound than for no warning, t(34) = 1,57, p = 0,047. For mean values, see Table 2.

Table 2: Change in Longest Glance after first critical event

Type	Mean (s)	SD	N

No warning	0,26	0,44	13
Light	-0,01	0,63	10
Sound	-0,06	0,31	10
Light+sound	-0,21	0,62	9

The steering activity measured by SWRR increased for all warning types (including no warning) after the first critical event. The increase was larger for light+sound, however this was not significant. See Table 3.

Table 3: Change in SWRR after first critical event

Type	Mean (n)	SD	N
No warning	1,31	3,06	13
Light	2,00	2,40	10
Sound	1,80	2,97	10
Light+sound	2,77	2,17	9

There was an increase in TLC for all warning types (including no warning) and the increase was significantly larger for light+sound than for no warning, $t(34) = 1,56$, $p = 0,028$. For mean values, see Table 4.

Table 4: Change in TLC after first critical event

Type	Mean (s)	SD	N
No warning	0,29	0,42	13
Light	-0,05	0,19	10
Sound	-0,04	0,31	10
Light+sound	-0,47	0,34	9

Following Critical events (2-5)

For the following critical events SWRR (Steering wheel reversal rate) increased for all warning types (including no warning). The increase was largest, however not significant, for light+sound warning, see Table 5.

Table 5: Change in SWRR for event 2-5

Type	Mean (n)	SD	N
No warning	0,33	2,89	45
Light	1,10	2,25	42
Sound	0,61	3,14	38
Light+sound	1,30	2,78	37

Secondary task

Performance on secondary task is an alternative measure of warning effectiveness. There was a significant effect of warning type on the amount skipped letters. At each task four letters were displayed, thus maximum four letters could be skipped. The more skipped letters the more effective was the warning. Light+sound warning resulted in most skipped letters while no warning and greetings resulted in least skipped letters, see Table 6.

Table 6: Mean and SD for amount skipped on secondary task.

	Mean (n)	SD	N
No warning	1,00	1,10	61
Light warning	1,49	1,27	59
Sound warning	1,65	1,46	60
Sound+Light warning	1,90	1,39	60

Light Hello	0,60	0,98	48
Sound Hello	1,00	1,29	48

Questionnaire after driving

A questionnaire regarding for example experienced warning modalities, usefulness and realism was filled in by the participants after the experimental drive. Almost all participants, 94% (N=45), have experienced warnings during the drive. Among those, 98% have experienced sound warnings, 87% light warnings and 71% the combination warning of sound and light. Only few, 31%, have experienced greetings. Among those, 21% have noticed light greetings, 31% have noticed sound greetings and 8% have noticed a combination of sound and light. The general realism in the simulator was rated high (M= 3,7; SD = 0,7) and men experienced the simulator as significantly more realistic(OR=17). The usefulness of warning was rated shortly above average (M=3,2; SD = 1,2).

The participants were positive to the way of announcing the secondary task thru seat vibration (M=4,60; SD=0,68). The difficulty of secondary task was rated shortly above average (M=3,3; SD = 0,8). The participants are generally positive towards the warning system and the warning modalities; 65% are positive towards auditory warning, 75% towards visual warning and 85% towards the combination warning of sound and light.

Discussion

Many (12%) skip the secondary task in a situation with an encountering vehicle. There was no effect of order, which means that even though the participants are not prepared of any critical events they are unwilling to take the eyes off the road. This is probably related to the high ratings of reality in the simulator making the participants uncomfortable with performing the task.

The level of criticality of the event was a major design issue for this experiment. Since the participants where to experience several events, having a collision was not desirable. No collisions occurred during the test. There were relatively few significant results among the performance indicators and measures, indicating that the critical event possibly could have been made more critical. However this could also lead to even more participants skipping in the secondary task.

In the beginning of the project running the test in low light conditions (dusk or night) was considered. This would have required a different simulator set-up (with an external light source, e.g. as was used in [Bol1], and presumably the effects of the warning under such circumstances would have been larger.

Among all warnings at critical events, 34% were useful according to the definition of leading to a fast response (< 1s). The first critical event is regarded as the most interesting and also most relevant, since the participants are totally unprepared of the situation. This is also were most significant results appeared. Although not overwhelmingly many, they are consistent. The combination of sound and light warning significantly decrease both wobbling and glances off the road and significantly increases time to line crossing. There is also a tendency of increase for steering activity.

When evaluating the possible effect of different warnings, it is important to create events that are critical enough. It would have been desirable to have more incidents. On the positive side, the combined sound and light warning eliminated all incidents. However, since few incidents were detected in the 'No warning' case, these results indicate that the warning has a positive effect. More critical events need to be created and evaluated to draw strong conclusions.

Detecting that the vehicles are on collision course before the SV enters the POV's lane (lateral clearance about 0.6 m) is highly challenging for the sensor system, which may, e.g., be camera and radar based. Furthermore, providing warnings to vehicles that still did not enter the POV's lane, and possible never enter the lane, may be disturbing for the driver of the SV. Realistic suitable sensor system may be able to detect if the SV enters the POV's lane at distances of up to 80 – 120 m, in this study equivalent to 2 – 3s TTC. Camera based sensor systems may be able to do so by detecting the lane markings and detecting if any part of the SV is placed inside the POV's lane. Such actions by the driver of SV may also motivate a warning, hence reducing the risk of triggering disturbing warnings during normal traffic conditions.

Greetings are experienced as less critical than warnings indicating that this new use of horn and headlight would not affect reactions to non-critical warnings or greetings. Participants are generally positive towards this warning system and most positive toward a combined sound and light warning.

A consistent significant main effect of warning modality emerged from the results of the secondary task. When performance on task is low, the driver's attention has effectively been drawn from the secondary task. This indicates that some warning modalities are more effective in alerting the driver. The greetings have the highest scores, which again points to a distinction between these two signals (warning and greeting).

Conclusions

The results of this study indicate that light and sound warnings, issued in a critical situation, are useful to the driver, and have an effect that increase safety. This type of countermeasure is the only feasible solution to avoid an accident in certain situation e.g. when the own vehicle is standing still and being struck by an oncoming vehicle. Correct autonomous activation of the signals is dependent on the capabilities of the vehicles proximity sensors and data processing. The effect may also degrade at higher relative velocities because of the increased distance at which a warning needs to be issued. Both horn and head light warnings have been shown to have an effect in critical situations, with a combination of these two leading to more fast responses than horn or light warning alone. Participants were positive towards having automated warnings from encountering vehicles in critical situations.

References

[Edw1] Edworthy, J. (1995a). "A user-centred approach to the design and evaluation of auditory warning signals: 1. Methodology". *Ergonomics* 38(11), 2262-2280.

[Edw2] Edworthy, J. (1995b). "Warnings in research and practice". *Ergonomics*, 38(11), 2145-2154.

[Gra1] Gray, R. (2011). "Looming Auditory Collision Warnings for Driving". *Human Factors*, 53(1), 63-74.

[Nor1] Nordmark, S., Jansson, H., Palmkvist, G., & Sehammar, H. (2004). "The new VTI Driving Simulator - Multi Purpose Moving Base with High Performance Linear Motion". Driving Simulator Conference, Paris.

[Bol1] Bolling, A., Sörensen, G. (2010). "Simulating the Effect of Low Lying Sun and Worn Windscreens in a Driving Simulator". Driving Simulator Conference, Paris.

THE REALIZATION OF A MEGACITY ENVIRONMENT IN THE DRIVING SIMULATION OF BMW GROUP RESEARCH AND TECHNOLOGY

Martin Strobl [1]
(1) BMW Group Research and Technology, 80788 Munich, Germany, E-mail: martin.strobl@bmw.de

Abstract *– For many emerging advanced driver assistance systems and driver information systems investigations in the area of megacities are required. Therefore, a project was set up for implementing this new and challenging environment in the driving simulation of BMW Group Research and Technology. This paper describes the different phases of definition and realization of the megacity. Aspects like the identification of typical complex crossings and the type and density of surrounding buildings are covered as well as an extensive performance tuning. Beside the graphical part, the behaviour and the control of traffic in the megacity is discussed. Different adaptations and extensions had to be done to get a realistic behaviour in this environment and to improve the setup possibilities for achieving a huge number of cars in the close surrounding. Finally, the advantage of the new megacity environment is shown in the context of a driving simulation study about contact analogue navigation.*

Key words: *Database Modelling, Megacity, Traffic Simulation, Contact Analogue Navigation, Head-Up Display.*

Introduction

Driving simulators are used in the automotive industry to develop and test new car systems such as advanced driver assistance systems or driver information systems [Hue1]. Due to the worldwide launch of these systems they also need to be investigated in the area of megacities. On the one hand the behaviour of the driver in such an environment must be considered. On the other hand the systems must be compatible with these big cities or are even designed for this highly complex area. For these reasons BMW Group decided to develop a megacity environment for its driving simulators.

The reproduction of a megacity in a driving simulator comprises many challenging aspects. At first a 3D database with a complex road network and many high buildings is required. In addition to this static environment traffic plays a very important role. High amounts of cars, bikes and pedestrians occur in the streets. These static and dynamics contents of the megacity have very high demands on the performance of the computer hardware in the area of number crunching and visualization. But not only vision, also sound from the engines of the cars and bikes, talking people, construction sites and horns account for a holistic impression. To complete this list even the smell of the city area would have to be considered.

At a first step BMW Group concentrated on the development of the 3D database and traffic for the megacity. An experienced supplier in the field of databases was chosen for cooperation to enter this new demanding area. Due to existing very advanced solutions for cars and pedestrians the main focus in the field of traffic was put on these road users.

Megacity Database

The development and modeling of the 3D database was split into different parts. First of all basic issues and requirements had to be defined to ensure that the aims from the application point of view would be achieved. Then realization was done with a lot of testing and performance tuning. Additionally, an optimization of the rendering software was necessary to process this very complex content in high frequency.

Definition Part

What is a megacity or, to be more precise, what are the typical characteristics of a megacity? Actually, each city is unique and there are as many types of megacities as there are megacities in the world. A megacity in the driving simulation should therefore be representative for all of them in terms of road types, surrounding buildings and traffic. It should provide a generic test environment for new car systems regardless of the location and the specific attributes of the different real cities.

What is the challenging part of these cities' road networks? First, a large number of lanes leading to varying destinations and ending at sometimes very complex intersections. Second, a large number of different intersections within small areas. And third, long roads with moderate deflections providing a far viewing plane.

Complementing the road infrastructure the overall appearance of the 3D environment had to be consistent. Characteristic buildings (i.e. skyscrapers) in high density, accompanying infrastructure (e.g. parking areas, pedestrian areas and advertising billboards) and vegetation were further features to be considered.

In the road network, special emphasis was put on the design of the intersections. If you look at aerial imagery, you will clearly see that there are typically few very large intersections within megacities, many major ones and an almost uncountable number of small ones. Each of these types demands varying (usually high) numbers of driving lanes in complex sequence – within the intersection and on the adjacent roads – many traffic lights and even more traffic signs (many of them lane-specific).

The 3D environment envisaged for the driving simulation was supposed to reflect all of these characteristics. Additionally, the proven tile-based-concept for databases was applied which means that actual databases are composed on the basis of tiles according to a specific study's requirements. In this way, high flexibility and reusability of database tiles is guaranteed.

Three main tiles in the style of a megacity were designed, each consisting of a road network with a very large intersection, partially accompanied by major and smaller ones. The large intersections reflect three different basic types: one roundabout (derived from an aerial image of Sao Paolo, Brazil), one inner-city motorway interchange (derived from a situation in Shanghai, China) and a complex crossing (derived from Potsdamer Platz in Berlin, Germany).

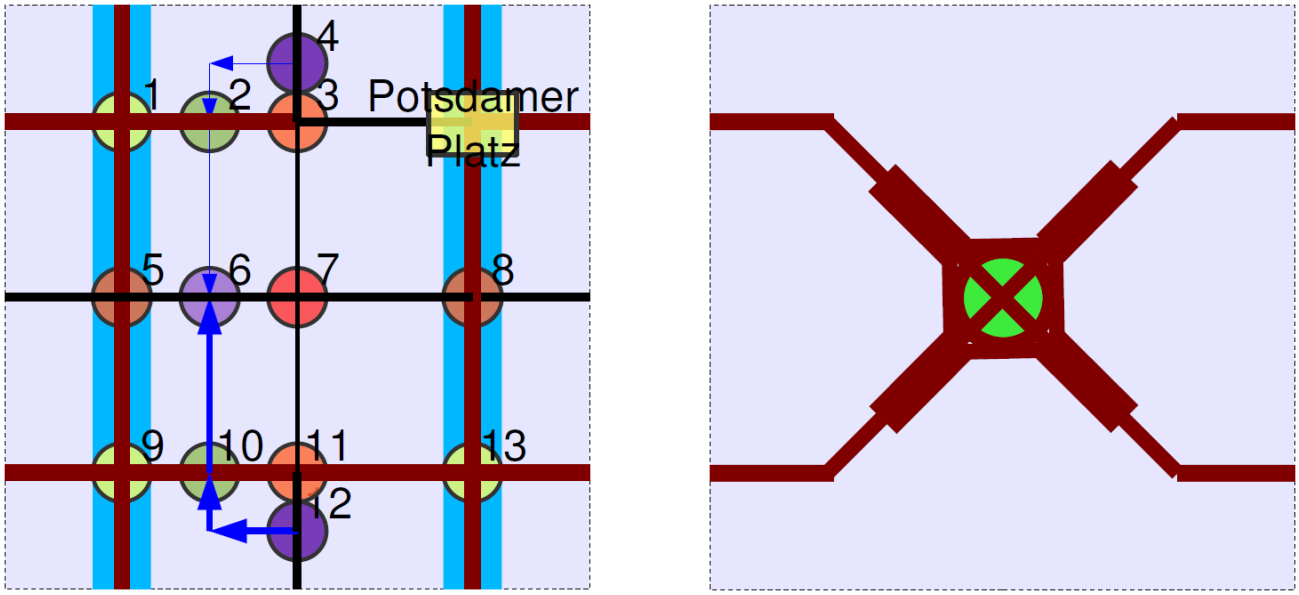

Fig. 1: Tiles with crossings and interchanges derived from real constructions (Potsdamer Platz in Berlin, Germany and interchange in Shanghai, China)

Complementing the three main tiles, a series of further tiles was designed to provide various connections and transitions to smaller road networks. Road and landscape cross-sections had to be harmonized at the interfaces so that the tiles could be arranged as flexible as possible.

Software Optimizations

Modeling database tiles with the mentioned complexity has to go along with performance considerations if they are intended for real-time driving simulation. Achieving the desired visual complexity requires that the image generation software provides a large polygon, material and object count budget.

Previous profiling results showed that the performance depends heavily on the number of distinct objects to be rendered and that the dependence on the number of polygons is weaker. This observation led to specific optimization techniques that reduce the number of objects without decreasing the perceived visual quality.

Occlusion culling is one of these techniques and a city environment is a very good candidate for its application because buildings in a street hide everything behind them. Therefore, performance can be improved without any loss of visual quality. There are two main possibilities for occlusion culling: hardware occlusion culling or using manually placed occlusion planes. The definition of these planes tells the render software not to draw any objects

that are fully masked by them from the current point of view. Early tests showed that manually placed occlusion planes provide a better performance so that the database creation and rendering tool-chain was adapted accordingly.

Another optimization technique is based on the fact that there are many objects in the viewing frustum that cover only a very little amount of pixels in the screen area. Detecting such objects and preventing their rendering is called “Small Feature Culling”. This technique was applied successfully in this project since the complex city environment contains many small or distant objects.

An easy method to reduce the object and polygon count is limiting the far plane distance. Objects behind the far plane aren’t regarded by the rendering software. There are two problems with this technique:

- Objects that enter the visible area become suddenly visible which is easily detected by the human eye.
- There is a visually empty area after the visibility distance, covered by sky instead of buildings and street.

Traditionally, far planes are positioned far from the observer to solve these problems. However, addressing these problems with other techniques allows reducing the far plane distance, which means a significant amount of reduction in rendered object count.

A distance based fade-in method was used to prevent the sudden appearance of objects when they enter the visibility region. First, they are rendered completely transparent (i.e. invisible) but as their distance to the eye becomes smaller, they gradually get visible. To alleviate the problem with the empty area, a 2D background image showing buildings was placed behind the actual 3D world. These two methods helped to reduce the far plane improving performance.

Realization of Database

With the target content and structure of the databases being as complex as laid out in the definition part of the project, the realization was a demanding task: large roads providing room for a vast number of vehicles, large intersections with many individually controlled traffic lights, a populated environment and high buildings along straight, wide roads.

In order to minimize the expected effort of performance tuning a gradual approach was chosen: the layout of the intersections and lanes was designed first and in accordance with the requirements of future studies. All other features were introduced step by step and recurring tests were performed on the actual simulator hardware (IG and projection system). This approach helped to identify basic performance killers (e.g. occluded geometry) early and develop appropriate solutions.

Extensive tests of the scenarios in all driving directions and from the respective eye-points were very time-consuming. The performance analysis led to further optimizations of the static database (e.g. by introducing additional occlusion planes) and with regard to dynamic elements like vehicles and pedestrians. Especially dynamic entities were crucial since the clear aim was to simulate a traffic environment as dense as possible.

The following images will give an impression of the database complexity that was achieved:

Fig. 2: Complexity of road network and graphical content

Traffic Simulation

The simulation of traffic is one of the main aspects if you aim to reproduce a megacity in your simulation. In a first step the major focus was put on three components, each of them emerging in high numbers and used in a complex context: traffic lights, pedestrians and in particular, vehicles.

Configuration of Traffic

In order to reduce the time and effort to configure huge traffic scenarios, appropriate parts can be implemented as re-usable template configurations for single tiles. A transformation mechanism transforms a template definition to a certain instance of the associated tile within a bigger road network. The transformation is done for positions and directions, and also for object names. The transformation of names guarantees unique names if the same tile with the same traffic template is used twice.

The switching of traffic lights is implemented separately for each tile. Each intersection with all corresponding traffic lights is configured considering the individual aspects of turn lanes. Furthermore, the traffic lights of consecutive intersections on main roads are phase-shifted to get long road sequences of green lights (green wave).

In addition to individuals for graphical decoration pedestrians are also used for specific test situations. Therefore, it is possible to define for each pedestrian route, type of movement and speed. The interaction with other road users is part of the simulation software.

Vehicles are the most important road users in driving simulation because they interact with the driver of the simulator at most. From configuration point of view there are three different groups of vehicles in the simulation to consider:

- Vehicles on parking lanes: Parked vehicles are necessary to get a realistic appearance of urban traffic.
- Moving vehicles for heavy traffic: It is important and quite tricky to control vehicles in a way to get heavy traffic around the viewer but not to use as many instances that performance drops.
- Vehicles with special reproducible behavior: These individually programmed vehicles are used for the special situations that a simulator experiment requires.

Behaviour of Vehicles

Multi-lane urban roads with large intersections require some special strategies for driving behaviour to achieve a realistic traffic flow. With regard to megacities, some mechanisms were added and optimized in the driving simulation software [Str1]:

- Approaching a large intersection with red traffic lights, vehicles should decide only once which lane to use to line up and perform this single lane change maneuver.
- Because of small distances between intersections, several driving lanes and heavy traffic it is necessary to change early to a suitable lane for a future left or right turn. Already some intersections before, this has to be concerned with regard to lane change decisions (see fig. 3).

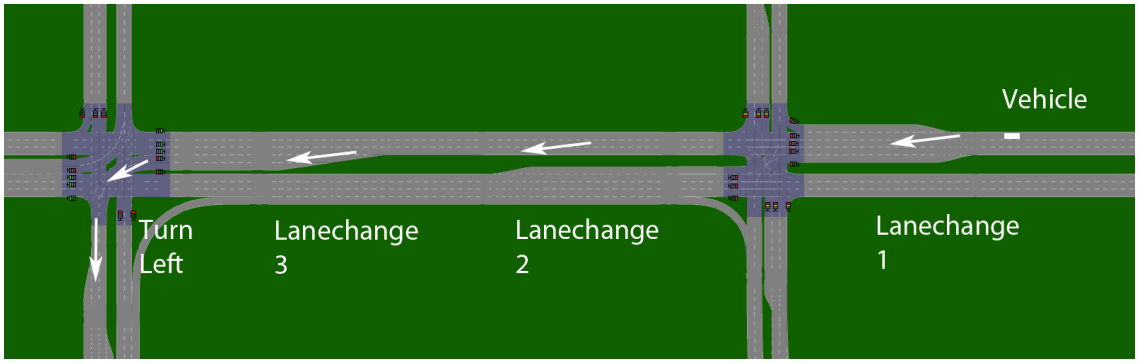

Fig. 3: Multiple lane changes in short distance

- If vehicles turn left while traffic lights are green, in a first step they should drive into the intersection until short before the conflict area with oncoming traffic starts. Then they should recognize when the oncoming traffic stops, and afterwards finish the left turn maneuver immediately.
- Park and unpark maneuvers occur very often in city environments and are an important factor for traffic flow. These maneuvers must work with all parking lanes in the megacity database.

Traffic Control

To create the impression of dense traffic around the driver of the simulator – what he expects from a megacity – and not to run into any performance penalties, vehicles must be activated and deactivated in a tricky way. The aim is to get a certain amount of vehicles at the right time and position.

With the definition of single individually controlled vehicles this would be too much effort. A traffic bubble in which vehicles are created at a certain distance in front or behind the driver of the simulator works well at linear courses like highways or country roads, but is not suitable for megacities with dense road network layout. For this reason two new features were implemented in the driving simulation software:

- The activation or deactivation of vehicles on basis of occlusion conditions. In this way vehicles can be activated e.g. in a crossing road very close to the intersection, while they can't be seen by the viewer. The advantage of this approach is that activated vehicles get very close to the viewer in a short time and cannot be delayed e.g. by red traffic lights on their way to him. An ideal approach to test the visibility is the usage of occlusion planes which are created mainly for the rendering system.
- The introduction of "traffic sources". A traffic source has a defined location, e.g. close to an intersection, and one or more routes starting from it, e.g. leading straight, left and right over the intersection area. Detailed parameters can be specified, e.g. the total number of vehicles per traffic source or the percentage of vehicles per route. With these parameters the traffic can be trimmed easily.

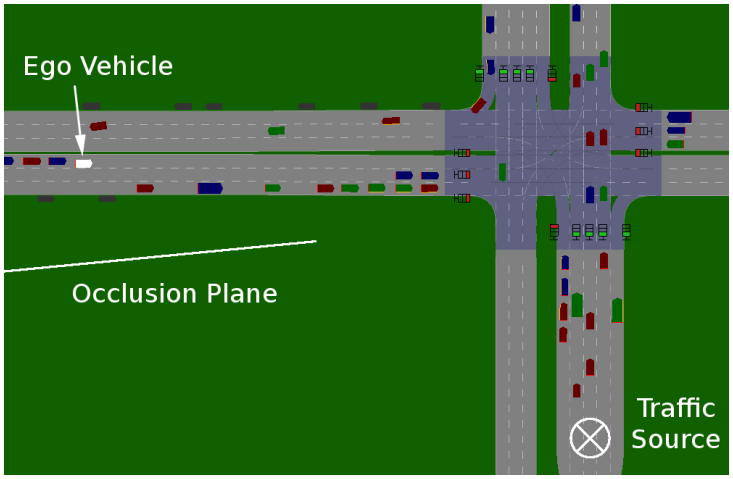

Fig. 4: Occlusion plane to check visibility of traffic source

Result

With the realization of the discussed extensions in vehicle behaviour and traffic control the traffic flow and density could be improved a lot and the aim to provide realistic vehicle traffic for studies was achieved. The traffic density can be easily adjusted and the scenarios are well reproducible even if the drivers of the simulator behave differently. The efficient setup method for vehicles and the overall performance tuning allow simulating traffic on a level that provides a good megacity impression. In fig. 5 a scenario is shown where 200 vehicles in the close surrounding of the viewer are computed.

Fig. 5: Complexity of traffic. Left: Driver's view.
Right: Observer's view; driver is in white BMW X1 close to the middle of the picture.

Application: Contact Analogue Navigation in Head-Up Display

The new possibilities emerging from the developed megacity environment could be proven in first driving simulation applications. One of these was a study about a new navigation concept in the head-up display of cars. In contrast to the classic approach with symbols, lane based navigation information was displayed contact analogue. This means, that the information is positioned and formed so that it appears to be attached to real objects in the scene from the driver's perspective (fig. 6). By means of the study the potential of such a contact analogue navigation should be tested.

Fig. 6: Contact analogue lane marking and realization of head-up display in driving simulation

A special setup in the simulator was necessary to realize a head-up display with big horizontal (20°) and vertical (5°) field of view. As shown in fig. 6 a combiner screen was installed in front of the driver which reflected the image of a 50”-Monitor on the roof of the cabin to the driver’s eyes. With this setup the driver had the impression that the information shown on the monitor was located at a specific position in front of him. In comparison to directly render the head-up information in the driving scene the shown setup provided a much more realistic impression of a head-up display due to the separated display technique.

The new navigation concept in this study consists of sequences with symbolic and contact analogue information to mark the lanes which should be used to drive in the recommended direction at intersections ahead. Details can be read in [Jan1]. A database with multiple lanes per driving direction and complex intersections in short sequence is an important requirement for such a kind of study. Therefore, the developed megacity was an ideal environment for testing the navigation system.

Additionally, the requirements on the visualization were very high in terms of field of view as well as spatial and temporal resolution. On the one hand the driver had to be able to look into crossing roads and be aware of the exact position of the own car in the street. On the other hand, traffic signs, road markings and other important contents had to be displayed clear and sharp even if they were small due to the distance. For these reasons, the study was conducted in a simulator with 220° horizontal (120° left and 100° right) and 45° vertical field of view and a resolution of 4’ / OLP [Hue2].

Rendering the megacity in such a high resolution configuration with 60Hz was one of the big challenges of performance tuning.

The result of the conducted study can also be read in [Jan1]. In general, the new contact analogue concept for lane based navigation was preferred in many aspects in comparison to a classic solution.

Conclusion and Outlook

The reproduction of a megacity environment in the driving simulation needed a lot of effort, but the results are convincing. The envisaged aims of BMW Group Research and Technology were achieved and first studies already have been conducted on basis of this new environment. Still not all aspects of a megacity are realized. Among others two major key aspects can be identified for further development.

First, traffic simulation must be enhanced with the typical behaviour and density of motor bikes and bicycles. They play an important role to reproduce the high dynamics of traffic in an urban area and to provide a further type of road users with specific properties.

And second, an extension of the sound simulation is necessary. Not only sound from the own or other vehicles can be heard in cities, also walking and shouting people, construction sites and music from open stores generate noise, which is characteristic for megacities.

References

[Hue1] Huesmann A., Ehmanns D., Wisselmann D. “Development of ADAS by Means of Driving Simulation”. *Proc. Driving Simulation Conf. DSC Europe,* 2006, pp. 131-141

[Hue2] Huesmann A., Strobl M. “Heading Towards Eye Limiting Resolution – Display Systems in Driving Simulation”. *Proc. Driving Simulation Conf. DSC Europe,* 2010

[Jan1] Jansen A., Israel B., Spiessl W. ”Augmented Reality Navigation in zukünftigen Head-Up Displays - Prototypenaufbau und erste Bewertung mittels Probandenstudie“. *VDI Conf. Optische Technologien in der Fahrzeugtechnik*, 2012, Karlsruhe

[Jan2] Jansen A., Spiessl W., Franz G. ”Besser als die Wirklichkeit - Reale und virtuelle Welt verschmelzen zu einer neuartigen Fahrerlebniswelt“. *Elektronik Automotive*, 12/2011, pp. 38-42

[Str1] Strobl M., Huesmann A. “High Flexibility – An Important Issue for User Studies in Driving Simulation”. *Proc. Driving Simulation Conf. DSC Europe*, 2004

The Influence of the feedback control of the hexapod platform of the SAAM dynamic driving simulator on neuromuscular dynamics of the drivers

Baris Aykent [1], Damien Paillot [1] , Frédéric Mérienne [1] , Andras Kemeny [1,2]
(1) Arts et Métiers ParisTech, CNRS, Le2i Institut Image, 2 Rue T. Dumorey, 71100 Chalon-sur-Saône, France,
E-mail : b.aykent@gmail.com
(2) Technical Centre for Simulation, RENAULT, Guyancourt, France

Short Summary

Multi sensorial cues (visual, auditory, haptic, inertial, vestibular, neuromuscular) [Ang2] play important roles to represent a proper sensation (objectively) and so a perception (subjectively as cognition) in driving simulators. For a similar situation, the driver has to react in the same way as in reality in terms of 'self motion'. To enable this behavior, the driving simulator must enhance the virtual immersion of the subject in the driving situation. The subject has to perceive the motion of his own body in the virtual scene of the virtual car as he will have in a real car. For that reason, restituting the inertial cues on driving simulators is essential to acquire a more proper functioning [Kol15]. Simulation sickness has been one of the main research topics for the driving simulators. It has been assessed between dynamic and static simulators [Cur5], [Wat24]). For a braking maneuver; [Sie22] stated that if the motion platform is activated, the bias in reaching increased levels of decelerations was reduced strongly comparing to inactivated platform case. However, there have been a few publications of vehicle-vestibular cue conflict based illness rating approach and its correlation with the neuromuscular dynamics for that kind of research. In order to reduce the simulator sickness, the difference between the accelerations through the visual and the vestibular cues have to be minimized (cost function minimization via model reference adaptive control, in this paper). Because of that fact, this paper addresses the simulator motion sickness as a correlated function of this deviation for the both cues with the perception questionnaires as well as the EMG analysis results for the subjects who joined in those experiments. Due to the restricted workspace, it is not possible to represent the vehicle dynamics continuously with scale 1 to 1 on the motion platform [Moo17]. Nevertheless, the most desired aim is to minimize the deviation of the sensed accelerations between the represented dynamics as realistic as possible depending on the driving task. This research work has been performed under the dynamic operations of the SAAM driving simulator as an open-loop and a closed-loop controlled tracking of the hexapod platform of the SAAM dynamic driving simulator. The dynamic simulators are being used since the mid 1960s (Stewart platform) [Ste23] firstly for the flight simulators, then the use has spread to the automotive applications. The dynamic driving simulator SAAM (Simulateur Automobile Arts et Métiers) involves a 6 DOF (degree of freedom) motion system. It acts around a RENAULT Twingo 2 cabin with the original control instruments (gas, brake pedals, steering wheel). The visual system is realized by an approximate 150° cylindrical view. Within the cabin, the employment of extensive measuring techniques (XSens motion tracker, and Biopac EMG (electromyography) device [Acq1]) are equipped, which have been already used with numerous attempts such as sinus steer test, NATO chicane, etc.

The visual accelerations of translations (longitudinal X, lateral Y and vertical Z axes) as well as the visual accelerations of roll and pitch, which correspond to the vehicle dynamics, have been taken into account for the control. Then the platform positions, velocities and accelerations have been controlled and fed back to the vehicle level, in order to minimize the conflict between the vehicle and the platform levels. The research question about this paper explains a comparative study between an open and a closed loop controlled platform in order to determine the spent power by the muscles to maintain the vehicle pursuing among the pylons with real time controls of the platform at a longitudinal velocity of 60 km/h.
This research has indicated that the vehicle to vestibular level's representation is near to 1:1 with an adaptive controlled platform. And also; the peak values for dizziness, eye strain, eyes trouble and headache for the classical strategy have coincided greater values which mean a higher level of sickness. Accumulated EMG total power analysis denotes that; the minimum, mean and the maximum cumulative EMG RMS (root mean square) total powers have been reduced from the proposed classical washout to our adaptive control drastically. Having a closed loop feedback control of the platform has decreased the IR level with respect to the open loop controlled platform. Pearson's *r* depicts that having a classical algorithm (open loop control) causes more discrepancy (sensorial conflict) in multisensory interaction (vestibular-vehicle) compared to the adaptive control. When evaluating the association of the EMG total power with psychophysics, a Pearson's *r* differences which are more

than 0.1 are the *significant* characteristics; vomit, nausea, cold sweat, eye strain, mental pressure, having tired. Only for the eye strain, the classical algorithm is agreeable. Because it has coincided the bigger oscillations with respect to the adaptive strategy. Because of the decreasing discrepancy in multisensory cues for the closed loop control; the orientation related (vomit, nausea) and emotions related (cold sweat, mental pressure, tired) sicknesses are more agreeable whereas the eye strain has been worse in the case of adaptive control which might be exerted by having a less conflict in multisensory, so that the participants could have been more related with the visual environment. As prospective, we will report and publish different coupling and decoupling variations with different types of degrees of the freedom (7 and 8 DOF) and their effects on the drivers' as well as the passengers' behaviors.

References

[Acq1] Acq*Knowledge*® 4 Software Guide For Life Science Research Applications, Data Acquisition and Analysis with BIOPAC MP Systems Reference Manual, for Acq*Knowledge*® 4.1 Software & MP150 or MP36R Hardware/Firmware on Windows® Vista or Mac OS® X 10.4-10.5, pp.309-310.
[Ang2] Angelaki D. E., Gu Y. and DeAngelis G. C., "Multisensory integration: psychophysics, neurophysiology, and computation", Current Opinion in Neurobiology 2009, 19: pp 452-458.
[Ben3] Benson A J: (1988). Motion Sickness. Aviation Medicine, second ed. pp 318-338, London
[Che4] Chen, D., Hart,J., and Vertegaal, R., "Towards a Physiological Model of User Interruptability", IFIP International Federation for Information Processing 2007, INTERACT 2007, LNCS 4663, Part II, pp. 439 – 451, 2007.
[Cur5] Curry, R.; Artz, B.; Cathey L.; Grant, P. & Greenberg, J., "Kennedy SSQ results: fixed- vs motion-based FORD simulators", Proceedings of Driving Simulation Conference 2002, pp. 289-300.
[Dic6] Dichgans, J. & Brandt, T., 1973 . Optokinetic motion sickness and pseudo-coriolis effects induced by moving visual stimuli. Acta Otolaryngologica, 76, pp. 339-348.
[Diz7] DiZio, P., & Lackner, J R., 1988**.** "The effects of gravitoinertial force level and head movements on post-rotational nystagmus and illusory after-rotation", Experimental Brain Research, Volume 70, Number 3, pp. 485-495, DOI: 10.1007/BF00247597
[Diz8] DiZio, P., & Lackner, J R.**,** "Perceived self-motion elicited by postrotary head tilts in a varying gravitoinertial force background", *Perception & Psychophysics*, 1989, Volume 46, Number 2, 114-118, DOI:10.3758/BF03204970
[Gri9] Griffin, M.J., "Handbook of Human Vibration"., Academic Press Limited, London, 1990
[Hal10] Hall J.,R, "The need for platform motion in modern piloted flight training simulators", October 1989, Tech Mem, FM 35.
[Ioa11] Ioannou, P.A and Sun, J., 'Robust adaptive control'. Prentice-Hall Inc, 1995.
[Iso12] ISO 2631-1:1997, "Mechanical vibration and shock -- Evaluation of human exposure to whole-body vibration -- Part 1: General requirements".
[Kem13] Kemeny A. and Panerai, F.,"Evaluating perception in driving simulation experiments", TRENDS in Cognitive Sciences, Vol. 7 No. 1, 2003, pp 31-37.
[Kim14] Kim M.S. et al, "Partial range scaling method based washout algorithm for a vehicle driving simulator and its evaluation", International Journal of Automotive Techno-logy, Vol. 11, No. 2, pp. 269−275 (2010).
[Kol15] Kolasinski E., M., 'Simulator Sickness in Virtual Environments', Army Project Number 2O262785A791, Education and Training Technology, May 1995.
[Mes16] MeSH Electromyography, National Library of Medicine - Medical Subject Headings, 2011 MeSH, (http://www.nlm.nih.gov/cgi/mesh/2011/MB_cgi?mode=&term=Electromyography), reached on 13th March 2012.
[Moo17] MOOG FCS, 6 DOF Motion System, "Motion Drive Algorithm (MDA) Software Tuning Manual Version 1.0", Document No: LSF-0468, Revision: A, Date: June 21, 2006.
[Neh18] Nehaoua L, Arioui H., Espié S.and Mohellebi, H., **"**Motion Cueing Algorithms for Small Driving Simulator", IEEE International Conference in Robotics and Automation (ICRA06), Orlando, Florida.
[Per19] Persson R., "Motion sickness in tilting trains: Description and analysis of the present knowledge", Literature Study, ISBN 978-91-7178-680-3, 2007.
[Pic20] Pick, A.,J. , "Neuromuscular Dynamics and the Vehicle Steering Task", PhD thesis, St Catharine's College, Cambridge University Engineering Department, December 2004.
[Rea21] Reason J & Brand J: (1975). "Motion sickness". London: Academic press. London.
[Sie22] Siegler, I., Reymond,G, Kemeny, A. & Berthoz,A.,"Sensorimotor integration in a driving simulator: contributions of motion cueing in elementary driving tasks", Proceedings of Driving Simulation Conference 2001, pp 21-32.
[Ste23] Stewart D., "A platform with six degrees of freedom," Proc. Inst. Mech. Eng., Vol.180, partI(15), 1965-1966, pp.371-386
[Wat24] Watson, G., S., "A synthesis of simulator sickness studies conducted in a high fidelity driving simulator", Proceedings of Driving Simulation Conference 2000, pp. 69-78.

Effects of driving experience depending on simulated driving task's difficulty

Freydier, C [12], Berthelon, C [1], Bastien-Toniazzo, M [2], Aillerie, I, [1]
(1) French Institute of Science and Technology for Transport, Development and Networks (IFSTTAR) – Salon de Provence , chloe.freydier@ifsttar.fr , catherine.berthelon@ifsttar.fr , isabelle.aillerie@ifsttar.fr
(2) National Center for Scientific Research (CNRS), UMR 6057 – Aix en Provence, mireille.bastien@univ-amu.fr

Abstract –

Young drivers are overrepresented in road accident linked to driver distraction. We experimentally tested the hypothesis of an interaction between driving experience and distraction with a dual-task paradigm. The interference between simple task and dual task was assessed for three groups of drivers with different driving experience. Results showed that response time (braking) and standard deviation of lateral position decreased with driving experience, conversely the percentage of correct responses increased. Results are interpreted in terms of psycho-socio-cognitive differences.

Key words: *Driving experience; Novice driver; Distraction; Dual-task.*

1. Introduction

Driving is a dynamic complex task which implies to simultaneously perform several sub-tasks, like looking for the information in the visual scene and keeping lane. So, drivers are often in situation of divided-attention, notably when a secondary task (for example using mobile phone) distracts them. Thus attentional processes play an essential role in driving activity which is confirmed by the fact that driver distraction is an important factor of road-crashes. Distraction is present "whenever a driver is delayed in the recognition of information needed to safely accomplish the driving task, because some event, activity, object, or person within [or outside] his vehicle, compelled or tended to induce the driver's shifting of attention away from the driving task" (Treat, 1980, pp. 21, in Reg[1]). More recently, Hoël (2010) define the distraction as the interference between the driving task and a secondary motor or visuo-spatial task. Many researches were interested in the effects of various distractive tasks on driving behaviour but only few investigated the influence of moderating factors like attentional requirement of the task and the amount of free and available resources to carry out the task.

Firstly, we assumed that the higher the task's attentional requirement, the higher the effects of distraction would be. Secondly, as the processes necessary to safely drive become automatic with the practice, the more the drivers is experienced, the more they have free resources to process the information necessary to succeed the driving task. We thus postulated that experienced drivers had more available attentionnal resources than novice drivers to perform a secondary task. These resources must progressively increase depending on driving experience.

2. Method

2. 1. Subjects

Three groups of drivers: young novice (18 years, 4 months of driving license), young experienced (21 years, 36 months of driving license which corresponds, in France, to the end of the period of probationary license), more experienced (30 years, at least 8 years of practice).

2.2. Experimental design

Participants were submitted to a dual-task paradigm in a driving simulator. It consisted in performing a car-following task combined with a numbers identification task. In the main task, drivers had to maintain a fixed distance (30 meters) with a lead vehicle which speed varied. The secondary task consisted in the identification of odd or even numbers in the central or in the peripheral visual field. Performance in the car following task was assessed by objective measures (inter-vehicular distance, standard deviation of lateral position on the lane (SDLP), response time that is press on the brake pedal when the lead vehicle decelerated, time to reach the same speed that the lead vehicle). Performance in the numbers identification task was measured by response accuracy and response times.

2.3. Statistical analyses

Dependent variables were submitted to ANOVA with repeated measure as a function of driving experience (3 groups) and task (simple vs dual).

3. Results

ANOVA revealed a significant main effect of the task attentionnal requirement. The analyzes highlighted an impairment of performance in dual task compared to car-following single task on the time necessary to reach the same speed that the lead vehicle ($F(1,31) = 8.85$, $p < 0.005$, respectively m = 11.04 s and 10.34 s) and on the mean inter-vehicular distance ($F(1,31) = 4.61$, $p < 0.05$, respectively 54.92 m and 50.08 m). The percentage of correct responses ($F(1,31) = 24.87$, $p < 0.001$) also decreased (respectively m = 87% , m = 91.2%) and the percentage of omission increased ($F(1,31) = 24.87$, $p < 0.001$, respectively m = 6.1% and m = 2.9%) on dual task. An interaction between task and numbers location (central vs peripheral) (correct responses $F(1,31) = 12.77$, $p <0.005$ and omissions $F(1,31) = 11.33$, $p < 0.005$) showed that these impairments in dual task occurred only when the numbers appears in peripheral vision.

ANOVA also revealed a significant decrease of time to brake and of standard deviation of lateral position (SDLP) ($F(2,31) = 8.22$, $p < 0.005$) with driving experience (Figure 1). Conversely, the percentage of correct responses ($F(2,31) = 4.91$, $p < 0.05$) increased with driving experience (86.2% after 4 months of practice, 90% after 36 months, and 91.4% after 8 years).

4. Conclusion

Just licenced drivers seem to distribute their attentionnal resources in an inappropriate way. This outcome is consistent with previous research on distraction among young novice drivers (Stu[3], 2001; Met[4], 2011). Attentional abilities after 36 months of practice don't seem differ significantly from those after 8 years of licensing. In an applied viewpoint, the training to divide the attention of novice drivers in driving simulator could have benefits on the driving behaviour.

Figure

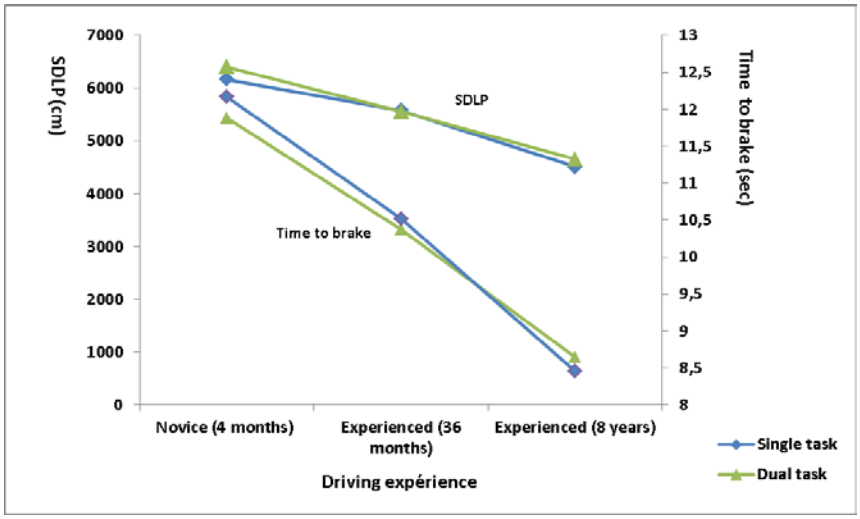

Fig.1. SDLP and time to brake as a function of task and driving experience.

References

Hoel, J., Jaffard, M., Van Elslande, P. "Attentional competition between tasks and its implications." Paper presented at the European Conference on Human Centred Design for Intelligent Transport Systems (29–30 April 2010). Retrieved from http://www.conference2010.humanist-vce.eu/.

Metz, B. Schömig, N. Krüger, H.P. "Attention during visual secondary tasks in driving: Adaptation to the demands of the driving task". *Transportation Research Part F,* 2011, 14, pp. 369-380.

Regan, M., Hallett, C., Gordon, Craig P. "Driver distraction and driver inattention: Definition, relationship and taxonomy". *Accident Analysis and Prevention,* 2011, 43, pp. 1711-1781.

Stutts, J. C., Reinfurt, D. W., Staplin, L., & Rodgman, E. A. "The role of driver distraction in traffic crashes." 2001. Washington, DC: University of North Carolina

Optimum Utilization of a Motion System by Offline Motion Cueing and its Applications

Sebastian Granzow

BMW Group Research and Technology, 80788 Munich, Germany
sebastian.granzow@bmw.de

In the driving simulation of BMW Group Research and Technology the requirements of the application field vehicle dynamics are increasing. In a simulator with motion base dynamics variables for different vehicle types are evaluated on the basis of selected standardized maneuvers. An optimal evaluation requires an unmodified representation of movement. This requirement is contrary to the limited motion space of existing motion systems. For this reason an extension or redesign of classical motion cueing algorithms is necessary.

The purpose of a motion cueing algorithm is to transform accelerations of a vehicle into movements of a platform of a motion system. To achieve a realistic driving experience the complete motion space of the system needs to be used optimally. A pass through the limits of available space degrades the impression of movement and of driving.

The scaling of the vehicle accelerations as well as an integrated safety (buffer) and a superimposed drift back into the neutral center position (washout) avoid running against these limits. Thereby the unpredictable behavior of a driver, especially in the longitudinal dynamics is taken into account.

Usually, with these techniques the actual potential of the motion system is not completely exhausted. One way to solve this problem is to put the driver out of the loop (open loop), i.e. he cannot drive interactively, but experiences a predefined maneuver. The advantage is that over the entire time of this maneuver all accelerations are already known. Thus, either the maneuver can be integrated in the available movement space optimally (Maximum Scale) or it can be designed such that no scaling is required.

The evaluation of configurations in the chassis design takes place by the use of standardized maneuvers. Usually, they are created on software systems which are independent from the driving simulation software. The outcome of these software tools is the basis for the mentioned open loop driving simulation.

The objective is to provide the user a tool that can be used without having the knowledge of the motion cueing algorithm. Anyway, he must be able to achieve the optimum utilization of motion space of the simulator. The algorithm is controlled by the parameters of the implemented FIR filters with regard to the perception thresholds. In order to simplify the use of the Offline Motion Cueing (OMC), the algorithm is enhanced by an intelligent optimizer. This optimizer fits the maneuver perfectly into the motion envelope and additionally reduces the computing time.

Additionally, it considers the limits of movement space and the motion perception barriers while taking into account first the translational motion and then the rotary motion. It automatically checks whether a scaling of the movements is avoidable.

The application of the OMC Algorithm allows a significant increase of displayable maneuvers and of issues that could previously not be investigated. The simple application of the optimizer and the resulting possibilities of Offline Motion Cueing lead to a wide acceptance of the approach and respectively to many different applications.

This methodology is suitable for objectification of human perception barriers in terms of driving dynamics. In particular the knowledge of perception thresholds for certain maneuvers and driving conditions is important. It allows to identify and to scale degrees of freedom which are not important for the dynamics perception and the holistic impression of the maneuver.

The open loop mode, which is based on the presented Offline Motion Cueing Algorithm, comes along with some restrictions. Without modification test persons have no knowledge of important input variables like steering angle or accelerator pedal position. With the additional implementation of force feedback steering and accelerator pedal the driver experiences the input variables and performs a more extensive evaluation.

Further research and investigations have to be done to reinstate an interactive driver for a standardized driving dynamics maneuver. This needs a combination of algorithms from Classic and Offline Motion Cueing.

Roll rate thresholds and perceived realism in driving simulation

Alessandro Nesti[1], Carlo Masone[1], Michael Barnett-Cowan[1], Paolo Robuffo Giordano[1], Heinrich H. Bülthoff[1], Paolo Pretto[1]

(1) Max Planck Institute for Biological Cybernetics, Tübingen, Germany; Department of Human Perception, Cognition and Action; E-mail: {alessandro.nesti, carlo.masone, mbc, paolo.robuffo-giordano, heinrich.buelthoff, paolo.pretto}@tuebingen.mpg.de

Abstract: Due to limited operational space, in dynamic driving simulators it is common practice to implement motion cueing algorithms that tilt the simulator cabin to reproduce sustained accelerations. In order to avoid conflicting inertial cues, the tilt rate is kept below drivers' perceptual thresholds, which are typically derived from the results of classical vestibular research where additional sensory cues to self-motion are removed.
Here we conduct two experiments in order to assess whether higher tilt limits can be employed to expand the user's perceptual workspace of dynamic driving simulators. In the first experiment we measure detection thresholds for roll in conditions that closely resemble typical driving. In the second experiment we measure drivers' perceived realism in slalom driving for sub-, near- and supra-threshold roll rates.
Results show that detection threshold for roll in an active driving task is remarkably higher than the limits currently used in motion cueing algorithms to drive simulators. Supra-threshold roll rates in the slalom task are also rated as more realistic. Overall, our findings suggest that higher tilt limits can be successfully implemented in motion cueing algorithms to better optimize simulator operational space.

Key words: motion cueing, tilt coordination, perceptual threshold, driving simulation, motion perception

Introduction

Motion based driving simulators have a limited physical workspace. One method to perceptually expand this workspace is to simulate sustained linear acceleration by a combination of translation and tilt (tilt coordination). Indeed, when the tilt occurs below perceptual threshold our vestibular system cannot distinguish between the effects of linear acceleration and gravity [Mac8]. This leads to practical motion cueing solutions in which the results of vestibular research on perceptual thresholds are used to limit simulators tilt [Zai19]. However, these limits might be too conservative for an ecological driving simulation, as several works have shown that increasing the complexity of the stimulation affects the perception of motion. Indeed, vestibular thresholds increase for motion with multiple degrees of freedom (e.g. pitch threshold increases with heave motion intensity [Zai19]). Tilt perceptual threshold varies as well when visual cues are also provided (see [Gro4], [Val18] for reviews). Finally, there is evidence that the mental load induced by complex tasks such as flying increase threshold values [Hos5].
Active driving simulation provides a variety of complex visual and vestibular cues as well as demands on attention which vary with task difficulty. It is thus important to measure motion perceptual thresholds in conditions that closely resemble typical driving to determine how the variability of these thresholds can contribute to the sensation of realistic driving. This will allow for tilt coordination in which the tilt/translation ratio is based on perceptual threshold variability, leading to more optimized simulated driving.
We conducted an experiment to measure roll rate detection threshold in a curve driving simulation, where drivers experience multisensory stimuli such as vestibular and visual information and cognitive load. The detection threshold indicates the lowest level at which a stimulus can be detected, i.e. the lowest roll rate at which the tilt is noticed by the driver. The measured thresholds are then compared with the tilt rate detection threshold found in literature [Gro3] to assess the effect of an active driving task. A second experiment was also conducted which relates these thresholds to slalom driving preferences using a paired comparison design in order to determine which roll rate values are most appropriate for driving simulators so as to present the most realistic driving experience. In addition, whether sub- or supra-threshold tilt coordination interferes with preferred motion during driving simulation was assessed.
We hypothesised that: *i.* roll rate thresholds increase during active driving; *ii.* subjective preferences in the slalom task are similar as long as tilt-coordination roll rates remain sub-threshold; *iii.* realism drops for supra-threshold tilt-coordination.

Method

Apparatus and Visual Stimuli

Two experiments were performed using the MPI CyberMotion simulator (Figure 1a): a six degrees-of-freedom anthropomorphic motion simulator derived from an industrial heavy load robot manipulator [Teu16], [Kuk6], [Bar1], [Ber2]. This simulator allows for accelerations up to 4 m/s^2 and rotatory ranges of ± 58 deg pitch and infinite roll and yaw. A driving cockpit was mounted at the end effector, providing drivers with an immersive virtual environment for visual feedback. The simulated vehicle was controlled by the driver through a Sensodrive force-feedback steering wheel and pedals. The visualization was done on a cylindrical projection screen mounted in front of the seat with a horizontal FoV of 90 deg and a vertical FoV of 45 deg. A video projector displayed an image of 1152x450 pixels with refresh rate of 60 Hz at a distance of approximately 70 cm from the driver's eyes. The visual environment resembled a typical slalom course and presented a 4m-wide sinusoidal path (2m amplitude and 125m period), outlined by pylons on both sides (Figure 1b). In the first experiment only one curve of the path was presented; whilst in the second experiment nine curves were provided, for a total length of 501.3 m.

In both experiments, each trial was started by pressing the gas pedal until the vehicle reached 70 km/h. Then, the driver's speed control was disabled to keep the speed constant throughout the remainder of the trial.

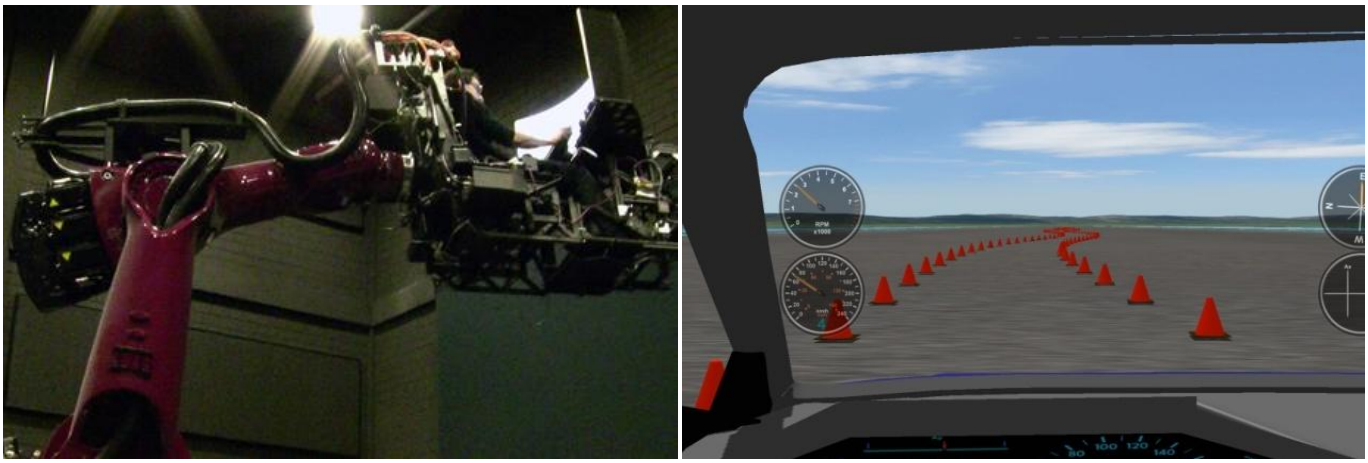

Fig. 1. MPI CyberMotion Simulator (a) and visual environment as seen from the driver (b).

Motion rendering and experimental manipulations

Vehicle motion, generated by CarSim mid-sized hatchback car model, was transformed into simulator motion using an extension of the well-known classical washout filter [Rei11], [Rei12], [Rei13] designed in cylindrical coordinates [Rob14]. In the classical motion algorithm accelerations are high-pass filtered, so that the high-frequency components are reproduced by actual translation of the simulator in the direction of the vehicle motion (onset cue). The low-frequency components are achieved by properly orienting the gravity vector in the driver's frame, so to reproduce the illusion of persistent acceleration in a given direction (tilt-coordination). In our experiments, tilt-coordination was operated on roll motion.

Roll rate was manipulated in order to determine how fast the driver can be rolled in simulated sustained lateral acceleration without noticing the roll component of the tilt-coordination technique. In the first experiment, roll rate was systematically saturated according to whether or not the rotation was perceived by the drivers. In the second experiment, roll rate was saturated according to the individual detection thresholds measured in the previous experiment (see the experiment procedures for further details).

In a typical simulation the driver experiences a combination of roll provided by the suspensions model of the vehicle and roll output by the tilt coordination algorithm [Nah9]. In these experiments the former was set to zero in order to fully control the total amount of roll presented to the driver.

Participants

Seven male participants with normal or corrected-to-normal vision and no history of vestibular dysfunctions, aged from 25 to 53 years (mean 30), took part in both experiments. All had a valid driving license and gave their informed consent to the study.

Experiment 1 procedure

Drivers were asked to complete one curve section of the path without leaving the borderlines, as if they were driving on a real track.

In each trial, as soon as the vehicle passed the end of the curve, the screen turned black and the question "did you feel tilted? (yes/no)" appeared. The participant provided the answer by button press. The simulator was then repositioned to the starting position and after a pause of 10 seconds the participant start the next trial by pressing the gas pedal. Written instructions explicitly asked

participants to answer the question relying on the sensation they felt while negotiating the curve, i.e. when the lateral motion occurred, and not before or after the curve.

A psychophysical two-alternative forced-choice procedure (2-AFC) with two adaptive staircases (one ascending and one descending, using the "2-down, 1-up" rule) was used to set the saturation value for roll rate at every trial, according to the driver's previous answers [Lev7]. The saturation in the first trial was set to 0 and 12 deg/s for the ascending and descending staircases respectively. Every two consecutive "yes" answers (felt tilted) the saturation was decreased by a predetermined step size.

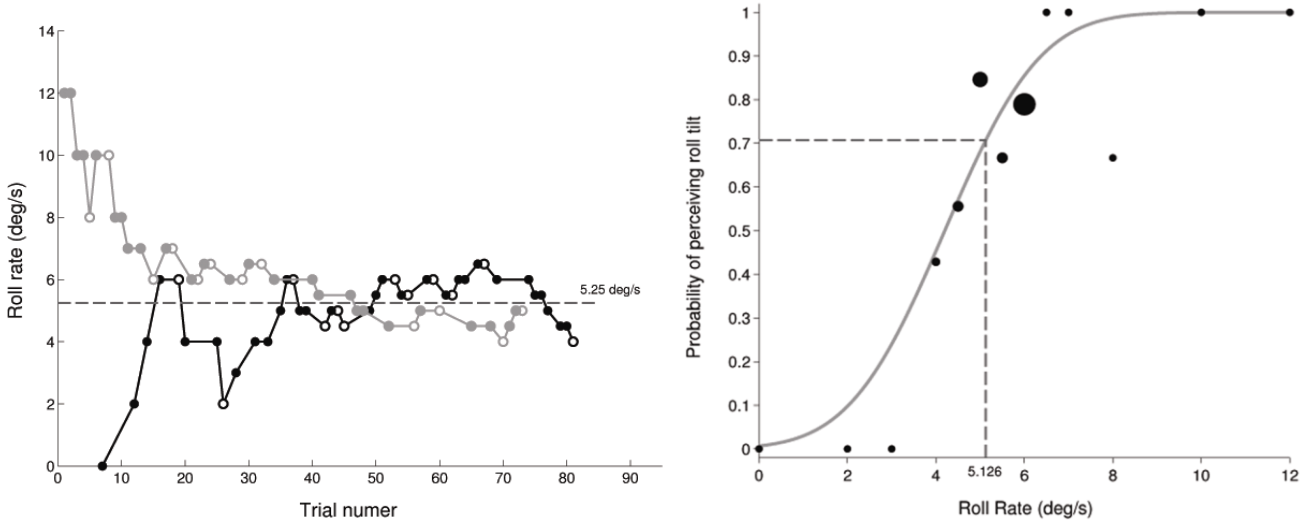

Fig. 2. Adaptive staircases (a) and corresponding psychometric function (b) for one participant. The horizontal line in (a) indicates the detection threshold calculated from the average of the last 5 reversals in both staircases (white dots). This average value, resulting from a "2-down, 1-up" tracking rule, corresponds well with the theoretical 70.7% probability of perceiving roll tilt when fit with a psychometric function (b).

Similarly, every "no" answer (did not feel tilted) the saturation was increased by the same step size. The step size was initially set to 2 deg/s and halved every seven trials to a minimum of 0.5 deg/s, in order to allow for fine estimation when detecting near-threshold values. The experiment was finished when both staircases reversed in direction 12 times (see Figure 2a, white dots). The detection threshold was then calculated by averaging values over the last five reversal points in both staircases. In this procedure the stimulus (roll rate) oscillates around an asymptotic value representing where the participant's detection is equal to chance. At that point, the probability *P* of providing a wrong answer (1-up) equals the probability *P* of providing two correct consecutive answers (2-down), so that *P* = 0.5. Therefore, the "2-down, 1-up" staircase targets a roll rate value that is perceived with a probability of 0.707 (square root of 0.5). For each participant we also calculated the corresponding psychometric function (Figure 2b), which describes the probability of perceiving the tilt on a continuous scale. We assumed the psychometric function to be a cumulative Gaussian distribution and we fit this model to our data by minimizing the sum of squared errors (SSE).

A typical experimental session for one participant is shown in Figure 2. Each session lasted approximately 40 minutes and required between 78 and 98 trials to complete. Participants had breaks every 15 minutes. A training session of six consecutive curves, with roll rate saturation values similar to the staircases first trial, allowed drivers to familiarize with the simulated motion range and the commands before the experiment.

Experiment 2 procedure

Drivers completed a slalom course driving within the pylons, as if they were driving on a real track. Different roll rate saturation values were selected in the motion filters according to the individual results of the previous experiment. For each participant, we defined sub-, near- and supra-threshold roll rate saturation values to be employed in the slalom driving task (see Table 1, experiment 2). A training session of six consecutive slalom courses allowed drivers to familiarize with the simulator commands and learn how to drive smoothly as required by the instructions. To avoid possible influences on the experiment, drivers experienced in this phase all the three roll rate conditions, in random order.

The paired comparison method was used as a subjective measure to produce a scaling of preferred roll rates. This method allows the construction of a standardized interval-type scale [Tor17] from which a preferred roll rate can be obtained. In this study, the

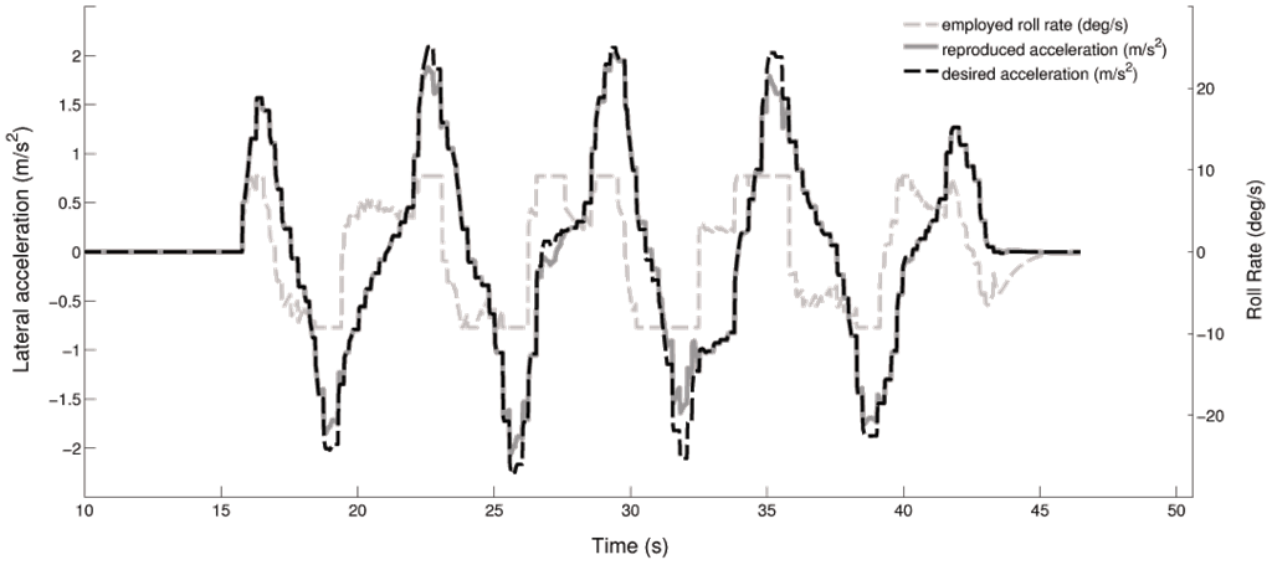

Fig. 3. Example of lateral accelerations (left y-axis) and roll rate output by the tilt coordination (right y-axis) during slalom driving. The lateral acceleration output by the vehicle model (desired acceleration) is provided to the driver as a combination of linear acceleration and roll tilt relative to gravity (reproduced acceleration). In the example, the roll rate was limited to 10 deg/s, causing the reproduced acceleration to occasionally be lower than desired.

preferred value corresponds to the roll rate that provides the most realistic lateral motion. In each trial, two slalom courses with different roll rate saturations were presented consecutively, and then the question "Which slalom felt more realistic? (First/Second)" was displayed on the screen. The participant provided the answer by button press. The simulator was then repositioned to the starting position and the next trial began. Written instructions invited drivers to compare the two previously completed slaloms to the sensation of lateral motion that they would feel in a real car on a similar path. All possible combinations were tested twice for a total of 6 pairs of slaloms for each driver.

A typical experimental session lasted approximately 15 minutes. The lateral accelerations produced during a slalom run and the effects of roll rate saturation on the reproduced motion are shown in Figure 3 for one participant.

Results

Experiment 1

Roll rate perceptual thresholds were calculated using the adaptive procedure described in the method (Table 1, experiment 1). The average perceptual threshold among all participants was 6.3 deg/s (s.d., 2.8 deg/s; Figure 4).

A one-sample t-test executed on the measured detection thresholds compared to the tilt rate saturation value commonly used in many simulators (3 deg/s) showed a significant difference ($t(6) = 3.17$ $p < .01$). This result constitutes a main finding of the study and shows that there is a strong influence of motion and task complexity on perceptual thresholds. No signs of motion sickness were aroused during this experiment and no session had to be interrupted.

Table 1. Experiment 1: Roll rate detection thresholds in deg/s. Experiment 2: roll rate (in deg/s) values used in the slalom.

Experiment 1				Experiment 2		
Participant	Roll rate threshold	Standard error		Roll rate 0.5*threshold	Roll rate threshold	Roll rate 2*threshold
1	2.05	0.2409		1	2	4
2	9.75	0.6292		5	10	20
3	8.5	0.8913		4.5	8.5	15
4	5.85	0.4537		3	6	10
5	5.25	0.2911		2.5	5.5	10
6	8.8	0.4163		4.5	9	20
7	4.2	0.4422		2	4	8.5

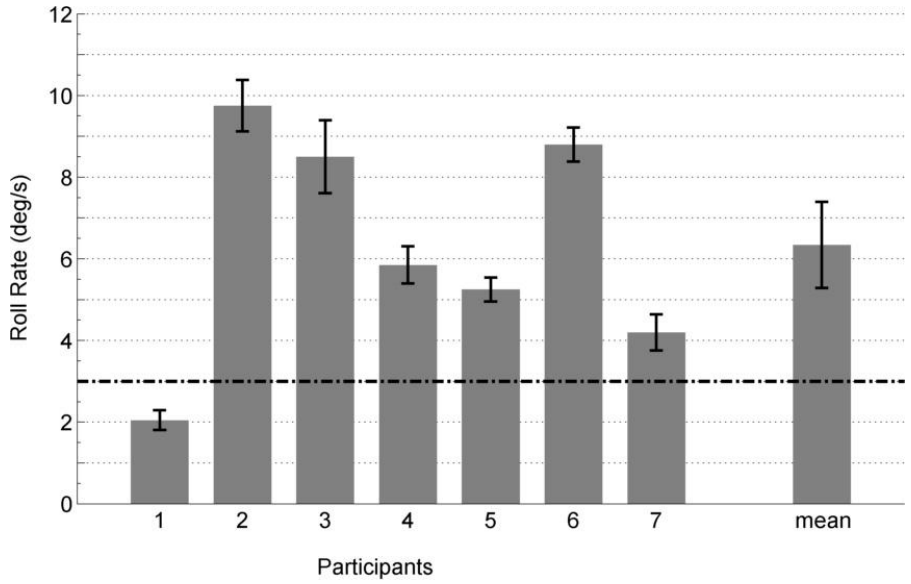

Fig. 4. Individual detection thresholds for roll rate. The dashed line indicates the roll rate saturation value suggested by Groen and Bless (2004) and commonly used in many motion cueing algorithms [Gro4], [Str15]. Error bars indicate the standard error of the mean.

Experiment 2

All participants were able to complete the experiment, but three of them required a break due to dizziness symptoms. The observed preferences counts (Table 2) were converted into proportions and then transformed into standardized scores. (Fig. 5).

Table 2. Preference count for different roll rates in the slalom task. The value on each cell indicates the number of times that the corresponding condition in row has been preferred over the condition in column. The last column reports the preference count for each roll rate condition.

Roll rate condition	sub-threshold	near threshold	Supra-threshold	Total
sub-threshold		7	5	12
near threshold	7		5	12
Supra-threshold	9	9		18

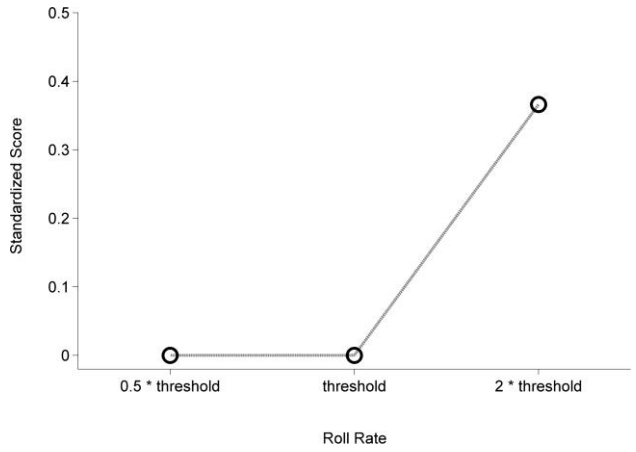

Fig. 5. Standardized scores of the preferred roll rate. The method of paired comparison transforms preference counts into standardized scores, providing a representation of the perceived difference between the roll rate conditions.

As expected, no difference resulted between sub- and near-threshold values, as confirmed by a chi-square test of the preference count ($\chi^2(1) = 0.57$; $p = 0.45$). Data showed higher preference for driving simulation with supra-threshold roll rate, although the difference to sub- and near-threshold values were not statistically significant ($\chi^2(1) = 1.43$; $p = 0.23$).

Discussion and conclusions

We have shown that the detection threshold for roll in an active driving task (6.3 deg/s) is remarkably higher than the threshold reported in literature (3 deg/s) and commonly used in motion cueing algorithms to drive simulators [Gro4], [Str15]. As reported by [Gro3], the presentation of visual stimuli during vestibular measurements on pitch detection increased the perceptual threshold from 0.5 deg/s to about 3 deg/s. In line with this, our results show that in an active driving task the cognitive workload and the complex motion stimuli lead to even higher perceptual threshold [Hos5], [Zai19]. Indeed, despite large individual differences, only one participant revealed a detection threshold lower than 3 deg/s. Our findings suggest then that roll rates similar to the thresholds we have measured can be employed in motion cueing algorithms to better optimize simulator operational space. This would lead to a subjective expansion of the perceptual workspace of dynamic simulators by allowing more intense motion to be reproduced in the same physical workspace.

In addition to being able to increase the amount of roll during tilt coordination, our results show that supra-threshold roll rates are judged as more realistic. This is surprising considering that tilt coordination is expected to fail for roll rates above perceptual threshold, as it evokes the sensation of tilt in addition to a linear acceleration smaller than expected. It is possible, however, that our

participants attributed this tilt component to the effect of vehicle suspension, which would provide a more natural feeling of vehicle roll movement when driving around a curve. Supporting evidence for this can be found from previous work by [Pre10], who found that a lateral motion gain smaller than one was preferred in a similar slalom driving simulation. Another explanation could be that the fraction of lateral acceleration lost for low roll rate saturation values is too big, and significantly compromises the realism of the simulation.

Our results show that roll rate saturation values close to detection threshold in an active driving task can be employed for driving simulations without losing motion fidelity. For applied purposes it is unpractical to use filter parameters individually tuned for each driver taking part in a simulation. Therefore, we suggest to implement in tilt-coordination a roll rate saturation of about 6 deg/s, i.e. a value close to the mean of the detection thresholds measured in experiment 1. Even if this choice might lead in some cases to inefficient tilt-coordination, results from experiment 2 show that perceived realism will not be impaired.

During the experiments some participants reported that they could not disentangle physical from visual roll, i.e. whether they were physically tilting or whether the image on the screen was tilting. Unlike physical roll, visual roll was always consistent with the output of the vehicle model. This caused sometimes a tilt of the visual environment even though there was no physical tilt, and more generally a mismatch between visual and physical roll. This might have induced the illusion of being tilted even when the physical roll was not perceivable. Without such an illusion, the individual detection thresholds we measured in the experiment could have been even higher.

Overall, our work shows that higher tilt limits are tolerated by simulators users and can be effectively employed in tilt coordination techniques without impairing the realism of the simulation. The development of more optimized motion cueing algorithm will need to take this into account.

References

[Bar1] Barnett-Cowan, M., Meilinger, T., Vidal, M., Teufel, H., Bülthoff, H. H. (2012) MPI CyberMotion Simulator: Implementation of a novel motion simulator to investigate multisensory path integration in three dimensions. *J. Vis. Exp.*, e3436, DOI: 10.3791/3436

[Ber2] Berthoz, A., Bles, W., Bülthoff, H.H., Correia Gracio, B.J., Feenstra, P., Filliard, N., Huhne, R., Kemeny, A., Mayrhofer, M., Mulder, M., Nusseck, H.G., Pretto, P., Reymond, G., Schlüsselberger, R., Schwandtner, J., Teufel, H., Vailleau, B., van Paassen, M.M., Vidal, M., Wentink, M. (2012). *High-performance motion cueing for driving simulators*. IEEE SMC – part a. (In press)

[Gro3] Groen, E. L., & Bles, W. (2004). How to use body tilt for the simulation of linear self motion. Journal of Vestibular Research: Equilibrium & Orientation, 14(5), 375–385.

[Gro4] Groen, E. L., & Wentink, M. (2006). *Motion Perception Thresholds in Flight Simulation*. Presented at the AIAA Modeling and Simulation Technologies Conference and Exhibit, American Institute of Aeronautics and Astronautics.

[Hos5] Hosman, R. J. A. W., & van der Vaart, J. C. (1978). *Vestibular models and thresholds of motion perception. Results of tests in a flight simulator* (No. LR-265). Delft University of Technology, Department of Aerospace Engineering.

[Kuk6] Kuka AG. (2010). Kuka AG. Retrieved from http://www.kuka-entertainment.com/en/.

[Lev7] Levitt, H. (1971). Transformed Up-Down Methods in Psychoacoustics. The Journal of the Acoustical Society of America, 49(2B), 467. doi:10.1121/1.1912375.

[Mac8] MacNeilage, P. R., Banks M. S., Berger D. R. and Bülthoff H. H. (2007). A Bayesian model of the disambiguation of gravitoinertial force by visual cues. *Exp. Brain Res.* 179: 263–290.

[Nah9] Nahon, M., & Reid, L. (1990). Simulator Motion-Drive Algorithms: A Designer's Perspective. Journal of Guidance, Control, and Dynamics, 13(2), 356–362.

[Pre10] Pretto P, Nusseck H-G, Teufel H and Bülthoff H.H. (2009). *Effect of lateral motion on drivers' performance in the MPI motion simulator*. Proceedings of the Driving Simulation Conference – Europe 2009, 121-131.

[Rei11] Reid, L. D., and Nahon, M. A. (1985). *Flight simulation motion-base drive algorithms. Part 1: Developing and testing the equations* (Tech. Rep. No. 296). Toronto: University of Toronto Institute for Aerospace Studies (UTIAS).

[Rei12] Reid, L. D., and Nahon, M. A. (1986a). *Flight simulation motion-base drive algorithms. Part 2: Selecting the system parameters* (Tech. Rep. No. 307). Toronto: University of Toronto Institute for Aerospace Studies (UTIAS).

[Rei13] Reid, L. D., and Nahon, M. A. (1986b). *Flight simulation motion-base drive algorithms. Part 3: Pilot evaluations* (Tech. Rep. No. 319). Toronto: University of Toronto Institute for Aerospace Studies (UTIAS).

[Rob14] Robuffo Giordano P., Masone C., Tesch J., Breidt M., Pollini L. and Bülthoff H.H. (2010). *A Novel Framework for Closed-Loop Robotic Motion Simulation - Part II: Motion Cueing Design and Experimental Validation 2010.* IEEE International Conference on Robotics and Automation (ICRA 2010), IEEE, Piscataway, NJ, USA, 3896-3903.

[Str15] Stratulat, A., Roussarie, V., Vercher, J., & Bourdin, C. (2011). Improving the Realism in Motion-Based Driving Simulators by Adapting Tilt-Translation Technique to Human Perception. SciencesNew York, 47–50.

[Teu16] Teufel, H. J., Nusseck, H.-G., Beykirch, K. A., Butler, J. S., Kerger, M. and Bülthoff, H. H. (2007) *MPI Motion Simulator: Development and Analysis of a Novel Motion Simulator*. AIAA Modeling and Simulation Technologies Conference and Exhibit 2007, American Institute of Aeronautics and Astronautics, Reston, VA, USA, 1-11.

[Tor17] Torgeson, W. S. (1958). *Theory and Methods of Scaling*. New York: John Wiley & Sons.

[Val18] Valente Pais, A. R., Mulder, M., van Paassen, M. M., Wentink, M., & Groen, E. L. (2006). *Modeling Human Perceptual Thresholds in Self-Motion Perception*. Presented at the AIAA Modeling and Simulation Technologies Conference and Exhibit, American Institute of Aeronautics and Astronautics.

[Zai19] Zaichik, L., Rodchenko, V., Rufov, I., Yashin, Y., & White, A. (1999). Acceleration perception. Collection of Technical Papers, edited by AIAA Modeling and Simulation Technologies Conference, 4334, 512–520.

Effects of motion parallax in driving simulators

Jonas Andersson Hultgren [1], Björn Blissing [1], Jonas Jansson [1]
(1) Swedish National Road and Transport Research Institute, E-mail : {jonas.andersson.hultgren, bjorn.blissing, jonas.jansson}@vti.se

Abstract *– Motion parallax due to the driver's head movement have been implemented and tested in VTI Driving Simulator III. An advanced camera-based system was used to track the head movements of the driver. The output from the tracking system was fed to the simulation software, which used low-pass filtering and a forward prediction algorithm to calculate an offset. The offset was then used by the graphics software to display the correct image to the driver.*

The effects of driving with motion parallax in the simulator were also observed by an initial study. During the experiment, the subjects caught up with several slower vehicles which forced the driver to make an overtaking maneuver. Oncoming traffic forced the subject to search for a suitable gap for overtaking. The study also included a speed perception test. The results from the study showed no difference in lateral positioning when running behind a slower vehicle nor in speed perception with and without motion parallax.

Key words: *driving simulator, motion parallax, depth cues, distance perception, speed perception*

Introduction

Motion parallax has been shown to be an important source of depth information, both when the observer makes lateral movement relative to an object as well as when an object moves relative to a stationary observer [Rog1].

In modern driving simulators most relevant visual depth cues are available, such as relative size, occlusion and shadows. However, cues like motion parallax due to the driver's head movement and stereoscopic view are often missing because of the additional cost and complexity of such systems [Kem1]. The absence of such visual cues might be a reason why different driving behaviour is observed in driving simulators compared to real-life driving. It has been suggested that motion parallax arising from driver head movement might be necessary for improved depth perception in driving simulators [Kem1].

The aim of the project was to implement motion parallax due to driver's head movement in the VTI simulation system. A small study was performed, mainly focusing on distance perception. This was done to evaluate if the additional depth information affects driving behaviour in a driving simulator.

It is commonly known that distances are underestimated in virtual environments and that people tend to drive faster in simulators than in real life [Bau1][Boe1]. Because of this a speed perception test was also included in the study.

Methods

In this project VTI Driving Simulator III was used (Figure 1).

Figure 1. VTI Driving Simulator III

The simulator features a high-performance linear motion system for simulation of realistic lateral forces experienced when driving [Nor1]. The motion system also includes roll and pitch movements of the whole simulator

platform, as well as a vibration table for simulating road roughness and bumps. The vibration table is located under the passenger car cabin installed in the simulator, and provides vibration movement relative to the projection screen. The driving environment is presented to the driver on the projection screen by three projectors, each with a resolution of 1280x1024 pixels, providing 120 degrees field of view, as well as in three rear view mirrors. Image rendering is performed in 60 Hz. The driver is located three meters in front of the projection screen.

Head movement tracking equipment

An advanced camera-based tracking system was used for measuring the driver's head position while driving [And1]. The tracking system is capable of measuring, among other things, the driver's head position, head rotation and gaze direction in three dimensions. For this project a four-camera tracking system was used. The cameras were located about 80 centimetres from the driver's head (depending on seat adjustments), allowing maximum lateral head movements of 15 to 20 centimetres in each direction from the centre point without losing tracking. The camera placement in the simulator cabin can be seen in Figure 2. The tracking system provided new data at approximately 100 Hz.

Figure 2. Camera placement in simulator cabin. Cameras highlighted by red markers.

Implementation of motion parallax algorithm

The basic flow of the algorithm can be seen in Figure 3. The simulation software reads the output from the head tracking system, filters the signal and then calculates a new output position using a forward prediction algorithm. The output is then sent to the graphics software which changes the viewpoint from which the image is rendered according to this data. Special consideration had to be made when tracking was lost and later regained. The different parts of the algorithm are explained in more detail below.

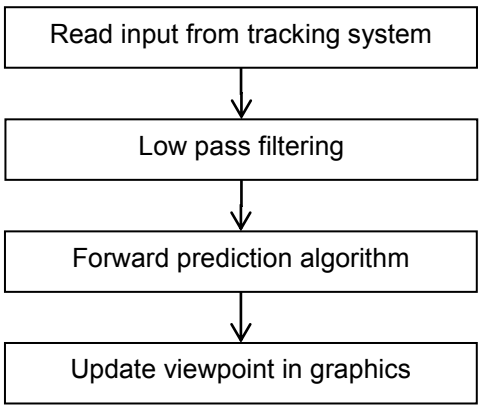

Figure 3. The basic flow of the motion parallax algorithm.

When motion parallax is activated during simulation, the current head position of the driver is used as origin for future calculations, as the driver most often is not located in the origin of the tracking system's coordinate system.

In the first step of the algorithm, the input from the head tracking system is passed through a low pass filter before being fed to the forward prediction algorithm. Each dimension is filtered separately, with potentially different cut-off

frequencies, to accommodate the different needs for filtering. This would however introduce more time delay into the system, so it was important to keep the filtering to a minimum, particularly for lateral head movements which are most common for a driver. The rear view mirrors were particularly susceptible to noise due to their position close to the driver and further low pass filtering was added for them specifically.

In the second step, a forward prediction algorithm is used to compensate for the time delays in the simulation system and make the motion parallax algorithm responsive on the driver's head movements. For this implementation Double Exponential Smoothing-based prediction (DESP) is used [LaV1].

Special considerations had to be made when tracking was lost, which for instance could happen if the driver left the cameras' detection zone, or if the face was obstructed by an object. As it is difficult to anticipate how and where the driver moves when tracking is lost, and to avoid that the visual presentation "drifts away", the motion parallax algorithm stops producing new outputs and stays in the last position until tracking is resumed. When tracking is resumed, a smooth transition is made from the old position to the new position to avoid jerks in the visual presentation.

The motion parallax algorithm is based on the driver's head position only. In the planned scenarios the head rotations were expected to be minimal and thus head rotation was not taken into consideration. The algorithm produces output in all three dimensions.

Calculating the parallax effect on the screen

Given that the observer moves in parallel with the screen and have gaze direction perpendicular to the screen surface, triangle similarity can be used to calculate the amount of displacement caused by the parallax effect (see Figure 4 and Table 1).

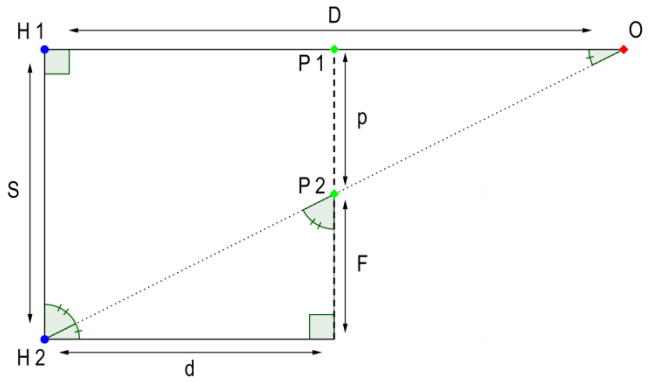

Figure 4. Geometry for calculation of parallax effect.

Table 1. Symbols for calculation of parallax effect.

Symbol	Description
O	Object in simulator world
D	Distance to the object (H1, O)
d	Distance to the screen
S	Distance between observer positions (H1, H2)
p	Distance between the projected object (P1, P2)

Triangle similarity can be used to describe the relationship between the distances:

$$\frac{F}{d} = \frac{S}{D} \qquad (1)$$

From Figure 4 the following correlation can be derived:

$$S = F + p \qquad (2)$$

Inserting Eq. 2 into Eq. 1 produces:

$$\frac{S-p}{d} = \frac{S}{D} \qquad (3)$$

Solving Eq. 3 for p:

$$p = S - \frac{Sd}{D} \quad (4)$$

Considering an object at infinite distance:

$$\lim_{D\to\infty}\left(S - \frac{Sd}{D}\right) = S \quad (5)$$

Eq. 5 shows that an object at infinite distance will be moved in sync with the observer, i.e. the object will be perceived as standing still relative to the observer.

Objects closer than infinity will not move in sync with the observer which will result in the parallax effect. This effect is the difference between the movement of the projected object (P1, P2) and distance the observer has travelled (H1, H2):

$$F = \frac{Sd}{D} \quad (6)$$

Calculating the limit of the parallax effect

There is a limit on how far humans can perceive the parallax effect. This limit depends on two factors; the visual acuity of the eye and the motion of the observer. Visual acuity is defined as $^1/_A$, where A is the response in line pair/arc-minute. The human eye has a visual acuity of 1.7 [Art1][Hec1], which corresponds to 0.59 arc-minute/line pair.

The simulator screen used in the study has a resolution of 4.2 arc-minute/line pair [VTI1], which limits the effect further. The simulator cabin also limits the motion of the observer. In our study we recorded an average range of lateral motion of the observer of 0.1 meter.

The limit of the parallax effect can be defined as the distance at which an object remains at the same position on the screen relative to the observer's position. When the parallax effect results in a projected movement less than the projected line pair width, the object is perceived as being at infinite distance from a parallax point of view. The projected line pair width can be calculated by Eq. 7 and Eq. 8 below. Symbols descriptions are listed in Table 2.

Table 2. Symbols for calculating the limit of the parallax effect.

Symbol	Description
L	width of line pair projected at screen
d	distance to screen
v	arc-minute / line pair
r	radians / line pair

$$r = \frac{v}{60}\cdot\frac{\pi}{180} \quad (7)$$

$$L = d\tan^{-1} r \quad (8)$$

Eq. 6 and Eq. 8 can be used to calculate the distance where the parallax movement is equal to the projected line pair width, i.e. the limit of the parallax effect.

$$D = \frac{Sd}{F} = \frac{Sd}{L} = \frac{Sd}{d\tan^{-1} r} = \frac{S}{\tan^{-1} r} \quad (9)$$

Inserting the values from the simulator study limits the parallax effect to roughly 80 meters. If projectors were available that could reach the same resolution as the human eye, the driver should be able to see the parallax effect of objects almost 600 meters away.

Evaluation study

Finally, a small study was conducted to evaluate the system in the simulator. 22 participants (twelve men, ten women) were recruited for the study and they were between 22 and 63 years old (average 43.4). Each subject drove the same scenario twice, once with motion parallax enabled and once disabled. The order was fairly balanced (nine enabled first and 13 disabled first) between the participants. They were not made aware that motion parallax would be available.

The driving scenario in the study consisted of three overtaking situations of slower vehicles including a car, a bus and a truck (Figure 5) on a 24 kilometer long single-track rural road. The road had a posted speed limit of 90 kilometers per hour, while the slower vehicles traveled at a speed of 70 kilometers per hour. In each situation, oncoming cars forced the participant to search for a suitable gap to safely complete the overtaking maneuver. The gaps between the oncoming cars increased for each vehicle and were the same for all three situations. Eight gap sizes were used; 100, 150, 200, 300, 300, 400, 400 and 600 meters. After each situation the subjects were asked to judge how difficult it was to find a suitable gap for overtaking the preceding vehicle. The order of the overtaking situations was balanced between the subjects and the same subject never had the same order in both parts. There was no traffic on the road between the different overtaking situations. Participants were encouraged to overtake slower traffic.

In addition to the overtaking situations, a speed perception test was included at the end of each run. The speed limit on the road was lowered first to 70 kilometers per hour, and then to 50 kilometers per hour and the participants were asked to stay as close to the speed limit as possible. Before reaching the first speed limit change, the speedometer and tachometer were turned off. The participants were informed before the experiment that this would happen and also reminded after the final overtaking situation. Also, the road marks were changed to solid white lines to eliminate the road marks as a speed perception cue. The length of the 70-zone was 750 meters, while the 50-zone was 500 meters. After this part of the experiment, the subjects were asked to judge how difficult it was to estimate their own velocity.

Figure 5: Overtaking situation involving a truck.

Results and discussion

The primary measurement in this study was the lateral positioning of the own vehicle when searching for a suitable gap for overtaking. This measurement was calculated by taking the average lateral position from the point in time when the driver got within 50 meters of the vehicle in front, until the driver initiated the overtaking maneuver. Each kind of overtaking situation (car, bus, truck) was analyzed on its own, as well as bus and truck combined since they obscured the driver's view equally. No significant differences driving with and without motion parallax was found in neither case.

Secondly, the raw data from the head tracking system was analyzed to find differences in the subjects' head movements with and without motion parallax. It was observed that the subjects did move their head when running behind preceding vehicle trying to get a better view of the oncoming traffic. The same behaviour was observed regardless of the use of motion parallax.

Finally, the data from the speed perception test was analyzed, including average velocity and lateral positioning of the vehicle. The measurements were calculated over the whole 70- and 50-zones respectively, but no significant differences were found. The measurements from the study are shown in Table 3.

For the subjective measurements collected through questionnaires, we could not see any trends regarding neither the difficulty to find a suitable gap for overtaking nor for the self-speed perception.

Likewise, no increase in simulator sickness in relation to the use of motion parallax could be observed. This was also based on subjective measurements from the subjects through questionnaires. There were no discontinued test drives due to simulator sickness. Also, most subjects failed to notice any difference between the two runs.

Table 3. Mean value and standard deviation for study measurements.

Type	Situation	Motion parallax	No motion parallax
Lateral positioning relative to road center [m]	Overtaking car	1.56 ± 0.21	1.50 ± 0.20
	Overtaking bus	1.36 ± 0.22	1.32 ± 0.23
	Overtaking truck	1.32 ± 0.23	1.39 ± 0.21
	Overtaking bus + truck	1.34 ± 0.22	1.35 ± 0.22
Speed perception test [kph]	50-zone	52.6 ± 7.8	54.3 ± 11.7
	70-zone	65.9 ± 8.0	66.2 ± 8.3

In conclusion, we do not see any significant effects on the driving behaviour, i.e. vehicle lateral lane position, speed perception and driver head movements, in this study.

We have considered why we couldn't see any significant effects and have the following theories. One theory is that motion parallax due to head motion is not used by drivers to estimate distances in the types of scenarios included in the study. An interesting comparison would be to perform the alignment and bisection tasks used in [Bau1] where subjects are required to position their own car at predefined positions relative to other vehicles.

Another theory could be that the image resolution in the simulator is too low to give a realistic parallax effect.

Inter-scenario learning effects during the experiment could also be a potential error source. Since the subjects experience the same situations several times, their driving behaviour might change over the course of the experiment, e.g. they might be keener on overtaking the preceding vehicle in the first situation while taking a more cautious approach in subsequent situations knowing that they won't be able to overtake right away.

References

[And1] Andersson Hultgren, J. "Methods for improved visual perception in driving simulators". Master Thesis, Linköping University, Linköping. 2011.

[Art1] Arthur, K. "Die Abhängigkeit der Sehschärfe von der Beleuchtungsintensität". Berlin: Akad Wissensch Berlin, 1897.

[Bau1] Baumberger, B., Flückinger, M., Paquette, M., Bergeron, J., Delorme, A."Perception of relative distance in a driving simulator". *Japanese Psychological Research*, 2005, 47(3), pp. 230-237.

[Boe1] Boer, E. R., Yamamura, T., Kuge, N., & Girshick, A. "Experiencing the Same Road Twice: A Driver Centered Comparison between Simulation and Reality". *Driving Simulation Conference*, 2000.

[Hec1] Hecht, S. "The Retinal Processes Concerned with Visual Acuity and Color Vision". Howe Laboratory of Ophthalmology, Harvard Medical School, 1931, Bulletin No. 4. Cambridge: Harvard University Press.

[Kem1] Kemeny, A., & Panerai, F. "Evaluating perception in driving simulation experiments". *Trends in Cognitive Sciences*, 2003, 7(1), pp. 31-37.

[LaV1] LaViola Jr., J. "Double Exponential Smoothing: An Alternative to Kalman Filter-Based Predictive Tracking". *Eurographics Workshop on Virtual Environments*, 2003, pp. 199-206.

[Nor1] Nordmark, S., Jansson, H., Palmkvist, G., & Sehammar, H. "The new VTI Driving Simulator - Multi Purpose Moving Base with High Performance Linear Motion". *DSC Europe, Paris*, 2004.

[Rog1] Rogers, S., Rogers, B. J. "Visual and nonvisual information disambiguate surfaces specified by motion parallax". *Perception & Psychophysics*, 1992, 52(4), pp. 446-452.

[VTI1] VTI's driving simulators. Retrieved from http://www.vti.se/en/research-areas/vehicle-technology/driving-simulation/vtis-driving-simulators/. 2012.

The multi-driver simulation as a new method for researching driver behavior and traffic

Dominik Mühlbacher [1] & Florian Fischer [2]
(1) WIVW GmbH, Raiffeisenstraße 17, 97209 Veitshöchheim, E-mail : muehlbacher@wivw.de
(2) WIVW GmbH, Raiffeisenstraße 17, 97209 Veitshöchheim, E-mail : fischer@wivw.de

Abstract *– The aim of this poster is to present the multi-driver simulation as a new tool in traffic research. With this linked driving simulation, several drivers can be analyzed in the same situation at the same time under controlled conditions. The use of this method is shown in three studies: Study 1 demonstrates possibilities for the investigation and description of driving behavior at intersections. In study 2, a hazard warning system is evaluated. Study 3 analyzes the effects of various penetration rates (i.e. percentage of equipped vehicles in a traffic system) of a traffic light assistant. These studies show several possibilities and requirements of the multi-driver simulation. In particular, methodological aspects during the various stages of experimental research, which are necessary when using this simulation, will be discussed.*

Key words: *multi-driver simulation, methodology, driver behavior, evaluation, driver assistance systems.*

Introduction

Various disciplines of traffic sciences (e.g. traffic psychology and traffic engineering) are researching to enhance traffic safety and traffic efficiency. Besides observational techniques, crash data analyses and driver inquiries, experimental studies are conducted for this purpose. Up until now, three experimental methods are mainstream: (1) traffic flow simulation, (2) driving simulation and (3) studies in real traffic

Each of these three methods has advantages and disadvantages. The use of several human drivers in the same simulated environment helps to combine the various advantages of these methods and is realized in the multi-driver simulation which is presented by means of this poster.

Multi-driver simulation

The multi-driver simulation consists of five driving stations that are used by the subjects to drive through the same virtual environment. There is one subject at each driving station and she/he controls her/his simulated vehicle. In the virtual environment, the drivers are able to see the other vehicles and can react to the other subjects' behavior.

The visual system of each driving station provides a horizontal field of view of 150 degrees which is shown on three 22" size LCD-displays with a pixel resolution of 1680x1050. The left, right and inside mirrors are shown in the front view. The simulator is run by a software called SILAB which was developed by the Würzburg Institute for Traffic Sciences (WIVW GmbH).

The drivers control their vehicle via a high-quality PC-game-steering wheel with force feedback and pedals. They wear a headset which enables them to hear sounds of the simulated vehicle and its environment. Furthermore, the drivers are able to communicate via the headset in two possible modes which can be controlled by the operator: (1) The operator is able to communicate with one driver or with all drivers simultaneously. (2) The drivers are able to communicate with the operator or with all drivers and the operator.

Examples for studies in the multi-driver simulation

Study 1: Description of driving behavior at intersections

Study 1 was an explorative study to describe driving behavior at intersections. For this purpose, n=4 drivers absolved a country road course which consisted of several intersection elements. After the start in platoon formation, the driver group was divided in two parts at a first turn-off. While two drivers followed the left road, the other two drivers followed the right road. After that, the drivers crossed the intersection, were merged at the same road and met at a stop sign in platoon formation again. From here, the drivers approached to the next intersection. By means of time-way diagrams, this multi-driver scenario can be pictured descriptively.

Study 2: Evaluation of a hazard warning

Study 2 evaluates the effects of a driver assistance system that warns the driver in a platoon that a hazard is likely to emerge (hazard warning). For this purpose, four test drivers had to follow a simulated leading vehicle in platoon formation. In test situations, the leading vehicle made a sudden braking maneuver from 83 km/h down to 47 km/h. The hazard warning was realized via a virtual danger sign on top of the roof of the leading vehicle. Three different experimental variations (early warning, late warning, no warning) were studied.

The analysis shows that only the first driver in the platoon reacts on the early warning. The first driver following the lead car increases its time headway by 0.7s, whereas the drivers on the other positions are not influenced by the early warning in a significant way. Due to the larger headway after the early warning, the drivers on the first position have to brake less compared to both other conditions (analysis of the maximum braking after the sudden deceleration). The last drivers benefit also from the early warning: The benefit of the early warning increases with the posterior positions in the platoon. Regarding the late warning, the braking reactions of the drivers on the first and second position have the same size compared to braking without warning. The drivers on posterior positions, however, benefit from the late warning in similar way as from the early warning. Also concerning the early warning, the benefit increases with the posterior positions in the platoon.

This study demonstrates that a hazard warning has the potential to increase road safety. Especially early and anticipatory warnings seem to provide great benefits.

Study 3: Evaluation of a traffic light assistant

Study 3 analyses the effects of a traffic light assistant with various penetration rates. While approaching a traffic light, this system informs the driver via a message on the HMI display about the optimal speed to pass while the lights are green or about how long the red light will remain. Therefore, it is possible that a driver gets a recommendation to drive 30km/h, although the current speed limit is 50km/h. In particular, possible negative effects for following drivers without this system should be evaluated.

In each session, n=4 drivers took part. Within the group in each session, different penetration rates were realized:

(1) 0%: All four participants drove without system (=control group)

(2) 25%: One participant drove with system (=experimental group), three participants without system

(3) 50%: Two participants drove with system, two participants without system

(4) 75%: Three participants drove with system, one participant without system

(5) 100%: All four participants drove with system

The participants had to absolve an urban course with 18 traffic lights at intersections. At each intersection, the platoon was split into different directions which were displayed in each driver's navigation system. After a few hundred meters, the drivers were merged again at a stop-sign to approach also the next traffic light in platoon formation. This method was used to shuffle randomly the positions in the platoon.

The results show influences of the penetration rate. Within the control group, the anger about other drivers increases with the penetration rate. However, the judgments of the drivers with system are not affected by the penetration rate. Similar, in runs with higher penetration rates (50%, 75%), the drivers without system judge to be obstructed by the other drivers in an higher degree compared to the lower penetration rates. The ratings of the experimental group are not influenced by the penetration rate.

These results indicate that the launch of a traffic light assistant on the market might lead to anger at drivers without this system. Especially higher penetration rates hold this danger.

Conclusion

This paper presents the multi-driver simulation as a new tool for traffic research using the examples of three studies: Using traditional methods in experimental traffic research, these studies would be impossible or difficult. In traffic simulation, subjective data as in study 3 cannot be generated. For the studies 1 and 2 the traffic simulation needs well developed driver models which consider driving behavior and reactions of other drivers. Similarly, in the driving simulation with one driver, the driver models of the simulated surrounding traffic have to take other drivers into account. In real traffic, study 3 would be very complex and expensive. Study 2 and possibly also study 1 are too dangerous for tests with real vehicles.

Therefore, with the multi-driver simulation it is possible to analyze new research questions in an experimental way. However, due to the participation of several drivers at the same time, the test situations vary in a higher degree which might impair the internal validity. On the other hand, this increased variability leads to enhanced external validity: Because of non-standardized behavior of surrounding traffic the situations are similar to situations in real traffic. Besides the requirements concerning study design, conduction and analysis, these specifics concerning internal and external validity have to be considered in further studies using the multi-driver simulation.

Virtual reality for real driving: a tool to fill the gap between simulators and test tracks

Vincent JUDALET [1], Sébastien GLASER [1], Vincent KOCHER [2], David CHARONDIERE [2]
(1) IFSTTAR/IM/LIVIC, 14, route de la minière, 78000 Versailles, tel : +33 1 40 43 29 08, email : firstname.lastname@ifsttar.fr
(2) OKTAL, 19, Bd des nations unies, 92190 Meudon, tel: +33 1 46 94 93 53, email: firstname.lastname@oktal.fr

In order to conduct driving test, researchers and engineers have two possibilities, which are simulators, either static or dynamic, or test in a real car, on a test track or on open traffic roads. Each solution has its own advantages but they both have several drawbacks to deal with:

- Simulators: static simulators are too limited to represent haptic feedbacks and impact of acceleration. Dynamic simulators allow a larger range of feedbacks. Moving base simulators can even reproduce acceleration over a long period [Kem1]. However, they make the driver develops a self adaptation : his acceptable level of risk become higher than on real vehicle [Sah1]. They also can induce sickness [Joh1]. Moreover, the price of this kind of simulator may be a limiting factor.
- Real test: even on a test track, acceleration feedback is realistic. However, the safety of the vehicle and the driver, limits the range of test. The test on test track may also be limited because of the environment : less traffic and less interaction with the environment, it is difficult to represent specific situations and to reproduce them.

The solution that we present, allows tests on a real car but with a virtual environment [See Bock reference in Las1], as known as vehicle in the loop simulation. In a few words, the driver sees a simulated environment using a head mounted display (HMD) that masks the real environment, and acts on the steering wheel and pedals of a real car which is moving. In order to display the virtual environment in the helmet, the system must locate the vehicle on the track, must locate the position of the head in the car and must allow a control of the simulator using these data. All these functions have to be robust according to the specific environment of the car. The data frequency must be high enough to allow smooth and accurate movement display. And the transport delay must be minimized as much as possible to avoid simulator sickness.

In this paper, we focus on the architecture of the system. We have developed a data bus that allows fast transfer between the different part of the simulator and with the environment sensing process. Moreover, we specifically address the localization of the HMD with a reliable and low cost process that fits with the requirements of the environment. The application have been tested and demonstrated during the final of PARTAGE French project.

The authors would like to thanks the French project PARTAGE (ANR-VTT-09) for the funding of this research.

[Joh1] David M. Johnson, "Introduction to and review of simulator sickness research", US Army Research Institute for the behavioral and social sciences, research report 1832, april 2005

[Kem1] Kemeny A., "Driving simulation for virtual testing and perception studies", Driving Simulation Conference 2009, Monaco, February 2009

[Las1] Laschinsky, Y., von Neumann-Cosel, K., Gonter, M., Wegwerth, C., Dubitzky, R., Knoll, A. Evaluation of an active safety light using virtual test drive within vehicle in the loop, 2010 IEEE International Conference on Industrial Technology (ICIT)

[Sah1] Sahami S. "Modeling adaptation behavior to driving simulators and effect of experimental practice on research validity", Ph D. Thesis, University of Columbia (Vancouver), 2011

[Wel1] Welch G., Bishop G. "An introduction to the kalman filter", Technical Report 95-041, Department of Computer Science, University of North Carolina, 2006

Building a Driving Simulator as an Electric Vehicle Hardware Development Tool

Dirk Kok [1], Michael Knowles [1], Adrian Morris [1]
(1) Institute for Automotive and Manufacturing Advanced Practice (AMAP), University of Sunderland, Colima Avenue, Sunderland, SR5 3XB, UK, E-mail : {Dirk.Kok, Michael.Knowles, Adrian.Morris}@sunderland.ac.uk

Abstract *– Driving simulators have been used to support the development of new vehicle systems for many years. The rise of electric vehicles (EVs) as a means of reducing carbon emissions has lead to the emergence of a number of new design challenges related to the performance of EV components and the flow of power under a variety of circumstances. In this paper we describe the integration of an EV drive train test system with a driving simulator to allow the performance of EV systems to be investigated while under the control of real drivers in simulated scenarios. Such a system offers several potential benefits. The performance of EV drive trains can be evaluated subjectively by real world users while the electrical and mechanical properties can be tested under a variety of conditions which would be difficult to replicate using standard drive cycles.*

Key words: *Driving Simulation, Hardware testing, Electric Vehicles, Simulator Control, Vehicle Design*

Introduction

As the world faces ever growing pressures to reduce carbon emissions, Electric Vehicles (EVs) are seen as a potential replacement for conventionally fuelled vehicles. First generation mass produced or converted electric vehicles are now on the market and are receiving widespread recognition. Many drawbacks remain, however, and it is crucial that improvements are made to make the next generation of vehicles to suit the requirements of users. The driveability of vehicle as experienced by the user is a particular area of concern.

Alongside the experience gathered from current EV models and trials, we believe that driving simulators have a major part to play in ensuring human factors are given appropriate consideration in the design process. The key technical requirements for future EV development include thermal management, range optimisation, control strategies and transmission design. Alongside these technical considerations Crolla et al [Cro1] have identified 3 areas for additional research to ensure EVs are viable and attractive in real world conditions:

1. Driveability – optimisation research should be based upon realistic driving conditions rather than standard patterns.
2. Braking behaviour – regenerative braking means energy can be recovered but such systems should not compromise safety.
3. Practical design – research currently done leaves many implementation issues; e.g. some methods for control are just too computationally intensive.

Research and development in these areas makes extensive use of the hardware-in-the-loop (HIL) methodology where hardware can be combined with simulated elements to achieve HIL tests (c.f. [Bou1], [Ros1]). Zha and Zong [Zha1] describe the use of an electric motor to act as a dynamometer for simulating the inertia of an electric vehicle. Jun Liu et al [Jun1] describe the use of an electrical load for simulating the motor in drive train experiments. Such activities utilise drive cycles which consist of a pattern of use in terms of vehicle speed through time. At present much of the power system simulation and modelling work is based on standard drive cycles. This has the advantage of providing a snapshot of performance and allowing easy comparison. The usefulness of standard drive cycles is, however, restricted by the accuracy of the assumptions upon which it is based. In order to achieve greater realism it is necessary to look for more realistic drive cycles [Saj1][Ado1] and a variety of techniques are beginning to receive attention to address these [Wal1][Hiw1].

In this paper we will describe an architecture for using a driving simulator as a control mechanism for HIL tests creating a new development platform capable of supporting Human-in-the-Loop (HuL) testing. A bespoke dynamometer developed at the University of Sunderland [Kno1] will be integrated with a Forum8 3D driving simulator to allow hardware to be tested under the direct control of a driver travelling around a real route.

The remainder of the paper is structured as follows. The motivation for the test system is summarised in the following section. This is followed by a description of the two major system components: the dynamometer and the driving simulator. The integration strategy for these two components is then discussed followed by a section considering the ongoing work to realise such a system.

Motivation

An integrated hardware test system controlled by a realistic immersive driving simulator has many potential benefits. Electric vehicle (EV) design issues listed above can be evaluated and improvements developed using realistic driving patterns. Furthermore feedback can be obtained on the performance of traction system configurations by drivers without the need to create expensive test vehicles. The effect of control strategies on driver behaviour can also be investigated in real time using easily varied control systems. Finally, the driving simulator software can be used to create different test routes which can be either designed specifically to investigate certain aspects of performance or which recreate real road systems, the latter will also allow for cross validation with data captured from test vehicles driven around standard laps. It is our contention that the development of such a system has much to offer EV research and development programmes.

Driving simulator

The University of Sunderland driving simulator laboratory was established in 1999 and has been used to support research in a variety of areas relating to vehicle design and human factors (c.f.[Mid1][Mid2][Mid3]). The laboratory presently houses two driving simulators. The system which has been utilised for these experiments is the most recent system which has been used for a variety of work including eco-driver training [Sco1] and assessment of driving style [Kno2].

The hardware component of the simulator is a Forum8 Driving Simulator and is illustrated in Figure 1. The hardware is based around a vehicle cockpit comprising all the usual controls including steering wheel, transmission selector, parking brake, accelerator and brake. Instruments include speedometer and engine speed measurement. The display consists of three 32 inch LCD screens, each with a resolution of 1024x768 pixels and a fourth, smaller 8.4 inch LCD TFT screen with a resolution of 800x600 pixels which can be used for display of navigational information or other data to the driver.

Fig.1. Forum8 driving Simulator

This simulator has been selected for the work for the following reasons:

- The ease with which simulated versions of real routes can be created using GPS or mapping data using the LandXML data format for import.
- The provision of a plug-in based architecture allowing bespoke software components to be developed giving access to the appropriate internal data structures.

Dynamometer

The Dynamometer which will be used for the test system was rebuilt in 2011 to provide bespoke test facilities for EV drive train components. The system consists of a Froude Hofmann EC38TA (Eddy Current) dynamometer, shown in figure 2, which is controlled from a Texcel V4 ECE/HE controller, shown in figure 3.

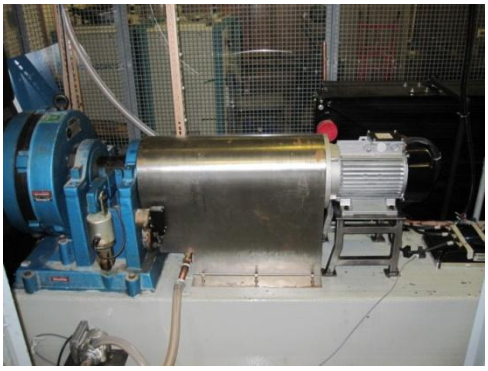

Fig. 2. Dynamometer hardware

Fig.3. Dynamometer control and datalogging equipment

The dynamometer is currently fitted with an EV drive train which consists of:

- A 15kW (30kW peak) induction motor controlled through a Curtis motor controller. The Curtis motor controller can be programmed and controlled via CAN bus.
- A Lithium-ion phosphate pack of 29 3.2V 90Ah cells (8.352 kWh 100% discharged) with individual battery management cell controllers and overall battery management monitoring module with CAN connector.

These drive train components can be fully or partially replaced with any system which requires testing. Other components currently available for testing include alternative lithium-ion power cells and a variety of hydrogen fuel cells.

In terms of instrumentation and control, the system features a Murphy Power View (PV)750 display which features 3 separate CAN ports, 3 analogue I/O ports and internal memory for data logging. In its current configuration two options exist for controlling the system:

1. Manually through a linear actuator, much like a throttle pedal in a vehicle. This option is primarily used for testing purposes.
2. Programmed operation via the Murphy display. The PV750 can be loaded with a drive cycle and when started it will control the motor controller and the dynamometer, while recording data.

The data capture system currently consists of 4 parts:

1. A 4 band digital oscilloscope which is connected to a computer for data logging. This system is used to record electrical transients in the motor power system with high speed recording.
2. Two CAN connections allow for data logging from the motor controller (voltages, current, motor and controller temperature) and BMS (cell number of highest voltage, cell number of lowest voltage and temperatures of respective cells).
3. A USB connection from the Battery Management System (BMS) to computer for capturing voltages, temperatures and state of charge (SoC) for cells within the battery pack.
4. Analogue data capture from the dynamometer controller via the Murphy PV750 of torque and speed.

Both the CAN connections (2) and analogue data capture (4) are done through the PV750 at a maximum speed of 50Hz.

The current system has been designed primarily to investigate the electrical behaviour of EV drive systems, however it should be emphasised that the instrumentation and data capture system can be easily customised using the reprogrammable nature of the Murphy display unit and the Curtis motor controller.

Integration design

Control of the test motor on the dynamometer will be achieved using data captured from the simulator controls. The mechanical load imposed by the dynamometer will be based around the mechanical characteristics of the vehicle as well as surface properties of the road and aerodynamic factors and the gradient upon which the simulated vehicle is travelling [Lar1]. The speed at which the motor turns under that load will be measured from the dynamometer and fed back via an inverse vehicle model to the simulator to control the speed of the simulated vehicle. The proposed system structure is illustrated in figure 4 below.

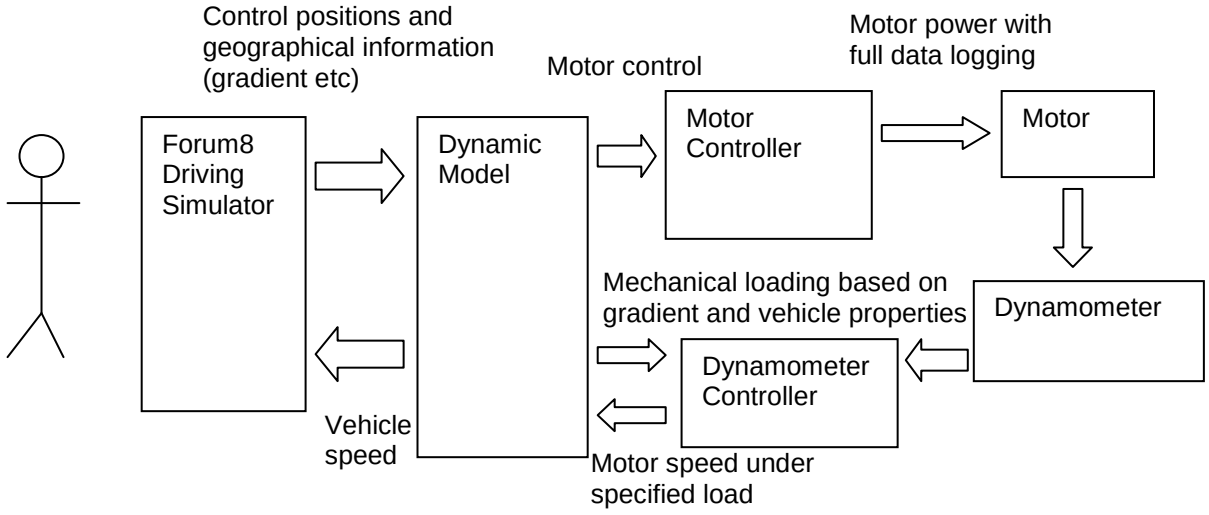

Fig. 4 System structure illustrating data flow

A number of key requirements for the system have been determined. These will be discussed in the following sections.

Data rate

One of the key considerations for the system viability is the speed and latency of the system such that the dynamometer system reacts to changes in throttle position and feeds back speed changes fast enough to ensure that the driver feels the experience is realistic. The effect of 'transport delays' has been widely investigated over a number of years (c.f. [Lee1]). The frame update rate offered by the simulator is 20 Hz (under current development conditions) so the objective for this integration is for the total round trip communication time to be within the time period of the frame update i.e. 50ms.

Safety

The primary safety concern for the dynamometer is a stall condition since this will be detrimental to the motor and controller potentially causing extensive, costly to repair damage. Also, sudden stall could lead to a break in the drive shaft. Such a condition should therefore be avoided at all times. In addition to standard safety features already installed on the dynamometer such as cut out switches and temperature monitoring, the following additional safety protocols have been identified as being necessary:

- Upon detection of both a brake and a throttle signal, the brake signal will be passed on to the controller while the throttle signal will be set to zero. This practise is used inside the Curtis motor controller as well.
- All values sent to the motor and dynamometer controller will be capped at their respective minimum or maximum values
- Upon switching off the simulator or if the connection with the simulator is lost the control signals to the motor will be set to zero.

Simulator control

As discussed previously, a plug-in software component is under development for the driving simulator. This will fulfil a dual role:

- Data will be extracted from the simulation regarding the throttle and brake controls, as well as the gradient on which the vehicle sits.
- Data from the dynamometer will be used to control the speed of the simulated vehicle.

The plug-in is under development in the Delphi programming language using the Forum8 UC-Win Road SDK version 5.02.04.

Dynamic model

The dynamic model of vehicle properties is based upon that proposed by Larminie and Lowry [Lar1]. This model is used in the first instance to determine the mechanical torque which must be applied to the motor to simulate the tractive effort required to propel the vehicle. This will depend on a number of factors including the gradient of the road – if the vehicle is travelling uphill more effort is required.

The tractive effort F_{te} is the sum of four distinct factors:

$$F_{te} = F_{rr} + F_{ad} + F_{hc} + F_{la} \qquad (1)$$

The four factors are:

1. Rolling road resistance. This is caused by the effect of frictional forces acting at the wheel/road interface and is dependent on the coefficient of rolling friction μ_{rr}:

$$F_{rr} = \mu_{rr} * m * g \qquad (2)$$

Where m is the mass of the vehicle and g is the acceleration due to gravity.

2. Aerodynamic drag. This is the frictional effect of the vehicle moving through the air:

$$F_{ad} = \frac{1}{2}\rho * A * C_d * v^2 \qquad (3)$$

Where ρ is the density of air, A is the vehicle frontal area and C_d is the drag coefficient, a value based on A.

3. Hill climbing force. This is the mechanical effort required to overcome a gradient, expressed as an angle, α. If the vehicle is travelling downhill then this will become negative:

$$F_{hc} = m * g * sin\,(\alpha) \qquad (4)$$

4. Lateral Force. This force represents the inertia of the vehicle and its rotating components and is estimated on the basis the inertia as a percentage of the vehicle mass, I and the vehicles acceleration a.

$$F_{la} = I * m * a \qquad (5)$$

Since the dynamometer is not connected to the motor by a final drive gearbox it is necessary to account for this. Therefore the torque to be applied at the dynamometer is give by τ:

$$\tau = F_{te} * \frac{r}{G} \qquad (6)$$

Where r represents the vehicle's wheel radius and G is the overall gear ratio between the motor and the wheels.

The throttle/brake demand is communicated directly from the control position in the simulator to the motor controller. This throttle / brake command will cause the motor to respond which results in a speed measured by the dynamometer. The controller manages the throttle and brake inputs and allows for tweaking of input response. Based on the above model a new torque value is calculated and sent to the dynamometer. The start torque is derived directly from the rolling resistance since this is the only force at no speed.

The power applied to the motor will cause it to work against the torque applied by the dynamometer. The speed of the resultant rotation will be recorded and used to update the dynamic model and will be converted to vehicle speed which will be communicated back to the simulator.

System Implementation

Implementation of the system is underway. The following activities have been completed:

- Communications between the simulator and the dynamometer control systems is achieved via a TCP connection operating over a Local Area Network.
- Dynamometer control is achieved using National Instruments' PCI-MIO-16E-4 real-time data acquisition card. This card operates its own operating system and Virtual Instruments (VI's) can be downloaded to the card through LabVIEW 7 RT.
- Bi-directional communication has been achieved with 2 computers running LabVIEW software. The first computer contains the I/O card and runs the real-time VI. The second computer runs as a TCP/IP server

and sends required data to the first computer and receives the data sent from the first computer. This Setup allows simple testing and improves development speed.

- Communications between Simulator and Dynamics computer have been tested and validated

The Dynamic Model has been implemented in LabVIEW as a VI running on the I/O card. A screenshot of the interface where the model properties are configured is shown in figure 5.

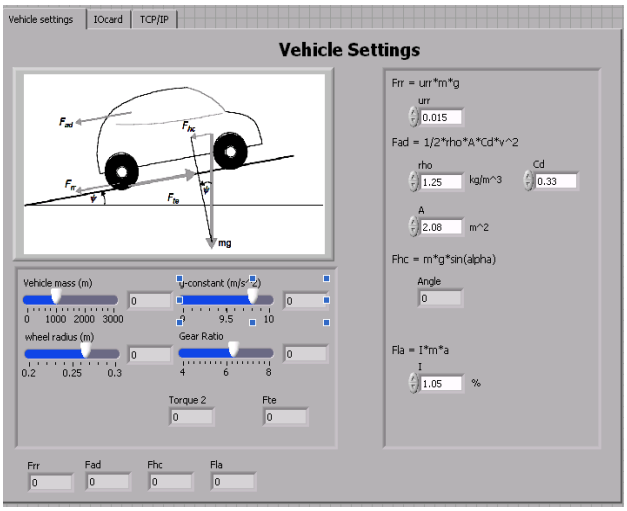

Fig.5. Dynamic model screenshot

Conclusions and future work

The benefits and difficulties involved in connecting a driving simulator to an EV hardware test system to allow human control of hardware tests have been described. Work is ongoing to achieve successful integration and proof of the concept of human-in-the-loop hardware testing. Once the concept is proved it will be necessary to develop suitable test strategies to ensure the maximum benefit is achieved from the system.

References

[Ado1] Adornato B. Patil R. Filipi Z. Baraket Z. Gordon T. "Characterizing naturalistic driving patterns for Plug-in Hybrid Electric Vehicle analysis". *IEEE Vehicle Power and Propulsion Conference*, 2009. VPPC '09. Pp 655 – 660.

[Bou1] Bouscayrol A. "Different types of hardware-in-the-loop simulation for electric drives". *IEEE International Symposium on Industrial Electronics,* 2008, pp 2146 – 2151.

[Cro1] Crolla, D. A., Ren, Q., Eldemerdash, S. & Yu, F. "Controller design for hybrid vehicles - state of the art review". *Vehicle Power and Propulsion Conference*, 2008. VPPC '08. IEEE. Harbin, China.

[Hiw1] Hiwatari R. Ikeya T. Okano K. Yamamoto H. Ito T. Takagi M. Iwafune Y. Yamaji K. "A New Approach to Analyze Effectiveness of Charging Infrastructure for Electric Vehicle by Road Traffic Simulator". *SAE Technical Paper*, http://papers.sae.org/2011-39-7216

[Jun1] Jun Liu, Li Fang Wang "Research of a Novel Bi-Directional Flexible Load for Electric Vehicle Test Bench". *Applied Mechanics and Materials*, 2011, pp55-57, 512

[Kno1] Knowles M.J. Kok D. Baglee D. And Morris A.C. "Design and Development of an Electric Vehicle Drive Train Test Bed". *To appear in Proceedings of The Ninth International Conference on Condition Monitoring and Machinery Failure Prevention Technologies (BINDT CM 2012)* June 2012

[Kno2] Knowles M.J Scott H. Baglee D. “The effect of driving style on electric vehicle performance, economy and perception”. Submitted to *International journal of electric and hybrid vehicles*, April 2012

[Lar1] Larminie J. and Lowry J. “Electric Vehicle Technology Explained”. John Wiley and Sons. 2003 0-470-85163-5.

[Lee1] Lee, Woon-Sung. "Compensation of Transport Delay in Driving Simulator," *American Control Conference, 1991*, pp.1050-1055, 26-28 June 1991

[Mid1] Middleton, H., Litchfield, D., and Westwood, D., "Driving performance and gaze behaviour of younger and older drivers at a simulated junction" *26th International Congress of Applied Psychology,* Athens,Greece, 2006.

[Mid2] Middleton, H., Litchfield, D. & Westwood, D., “Gaze transitions of young novice, young experienced and older experienced drivers at a simulated junction,” *Vision-in-Vehicles 11*, Dublin, Ireland, 2006.

[Mid3] Middleton, H., Westwood, D., Robson, J. & Kok, D. “Assessment and decision criteria for driving competence in the elderly” In G. Underwood (Ed.). *Traffic and Transport Psychology* (pp. 101-113) Elsevier Ltd. UK.

[Ros1] Rosario L.C. “Power and Energy Management of Multiple Energy Storage Systems in Electric Vehicles”. *PhD Thesis, Cranfield University*. 2007.

[Saj1] Sajith A.H. Nagendra Babu S. Vinay Kumar and Prakash R. “Optimisation of an Electric Drive Train for “On Road” Electric Vehicle”. *SAE Technical Paper. 2009*. http://papers.sae.org/2009-26-0041

[Sco1] Scott H. Knowles M. Morris A. Kok K. “The role of a driving simulator in driver training to increase fuel economy”. Submitted to *Driving simulator conference 2012,* Paris, September 2012.

[Wal1] Waldowski P. Schuppel F. Schindler V. “Battery Optimisation in Electric Vehicles and Range Extended Electric Vehicles based on Measured Individual Operational Profiles”. *VDE Kongress 2010 – E-Mobililty*. Leipzig.

[Zha1] Zha H. and Zong Z. “Emulating Electric Vehicle’s Mechanical Inertia Using an Electric Dynamometer”. 2010 *International Conference on Measuring Technology and Mechatronics Automation*. Changsha, China

Perception of longitudinal acceleration on dynamic driving simulator

Anca M. Stratulat [1], Vincent Roussarie [1], Jean-Louis Vercher [2] , Christophe Bourdin [2]
(1) PSA Peugeot Citroën, Centre Technique de Vélizy, Route de Gizy 78943 Vélizy-Villacoublay Cedex FRANCE, E-mail : {ancamelania.stratulat, vincent.roussarie}@mpsa.com
(2) UMR 6233 « Institut des Sciences du Mouvement », CNRS – Aix-Marseille Univ, Faculté des Sciences du Sport, 163, avenue de Luminy - CP 910, 13288 Marseille cedex 09 FRANCE, E-mail : {jeaan-louis.vercher, christophe.bourdin}@univ-amu.fr

Abstract – *Classical washout algorithm for driving simulators doesn't take into account the non-linearity of human sensory systems. Our previous work showed that the most realistic tilt/translation ratio for the simulation of braking during passive driving depends on the level of deceleration. However, the interpretation of previous results cannot be extended to acceleration. Therefore, a new experiment was developed in order to determine if the best tilt/translation ratios found for braking are also valid for acceleration. The present results suggest that the acceleration is generally overestimated directly proportional to the level of acceleration, but contrary to what was observed for deceleration, the variation of tilt/translation ratio doesn't seem to have an impact on the final perception of motion. As a conclusion, the simulation of deceleration and acceleration on a dynamic driving simulator should be considered separately.*

Key words: *dynamic driving simulator, motion perception, longitudinal acceleration, multisensory integration.*

Résumé - *L'algorithme Washout utilisé pour les simulateurs de conduite ne prend pas en compte la non-linéarité caractéristique des systèmes sensoriels humains. Nos travaux antérieurs montrent que le rapport basculement/translation le plus réaliste afin de simuler un freinage durant la conduite passive dépend du niveau de décélération à produire. Toutefois, ces résultats ne peuvent pas être appliqués stricto sensu au cas de l'accélération. Dans ce cadre, nous avons conduit une nouvelle expérimentation pour déterminer si le meilleur rapport basculement/translation trouvé pour freinage est également le meilleur pour restituer l'accélération. Nos résultats démontrent que l'accélération est généralement surestimée. Cette surestimation est directement proportionnelle au niveau d'accélération à produire. Mais contrairement à ce que nous avions pu montrer dans le cas de la décélération, les différents rapports basculement/translation proposés ne semblent pas produire des différences dans la perception finale de l'accélération. En conclusion, la simulation d'accélération et décélération sur simulateurs doivent être considérées séparément.*

Mots clés: *simulateur dynamique de conduite, perception du mouvement, accélération longitudinale, intégration multisensorielle.*

Introduction

Driving simulators have become an important tool in the automotive research. They bring great advantages in the upstream phases of the development of the car. Thanks to their complexity, they allow the exploration of certain areas of research that are difficult to reach in normal conditions, like the study of the interaction of multiple sensory cues during driving (visual, auditory, vestibular, somesthetic, etc.). However, the driving sensation on a dynamic simulator is sometimes reported by the subjects as unrealistic, especially for braking and turning situations. As a result, during the last decade, the driving simulation community started to concentrate their research on the motion perception and driver's behavior.

As showed by studies in driving simulation domain and in human motion perception, the addition of motion (basically tilt and translation) to static simulators may consistently improve the sensation of motion during driving simulation. From the motion point of view, it seems that using tilt extensively improves the perception of linear accelerations through the use of tilt-coordination technique (inclination of the simulator in order to orient the driver's head relative to gravity in a way similar to how the gravito-inertial acceleration (GIA) is oriented in the real vehicle during acceleration), even if the rotation of the simulator slightly exceeds the detection thresholds of the vestibular system (i.e. semicircular canals) [Gro; Ber]. Even so, this technique limits the maximum level of linear acceleration that can be simulated, due to the detection of rotation by the subject (beyond 3.7 deg/s of angular velocity [Ben] and 6 deg of inclination [Bri]). Therefore, new techniques were applied, like the addition of surge linear accelerations used at the beginning of the motion, which seems to support the visual simulation of larger motions. Unfortunately, small surge motions do not improve consistently the perception of the overall motion [Ber]. Still, many of the modern driving simulators possess motion-based platforms to produce longer translations to physically simulate stronger linear accelerations. These longer accelerations are commonly used in combination with tilt (tilt-coordination technique) in order to extend the range of "simulable" linear accelerations.

Background

In the framework of a collaborative project between PSA Peugeot-Citroën and the Institute of Movement Sciences of Marseille, we studied the processes underlying motion perception on PSA's dynamic simulator SHERPA². The first results of this collaborative work have shown that the combination of tilt and large translation determines the perception of acceleration in the case of passive braking [Str1; Str2]. In order to perceive the desired deceleration, the combination of tilt and translation must be adapted to the level of braking: for strong decelerations, more translation is needed, for weak decelerations, more tilt is needed [Str2]. Therefore, the best perceived tilt/translation ratio depends on the level of deceleration, suggesting that the motion cueing algorithms of the simulators should not only use gain factors, but also be adapted to this non-linearity. But on a dynamic driving simulator, the braking is simulated by forward tilt and backward translation, while the acceleration is simulated by backward tilt and forward translation. Studies on perception of acceleration/deceleration [Sch] or forward/backward motion [Bri] showed that, even if the two opposite motions are identical from the physical point of view (except direction), there are external factors that partly determine the final perception of motion, like speed (visual cues through optic flow), previous motion information, context or sense of familiarity [Hol1; Hol2; Hes].For example, Bringoux et al. [Bri] showed that the threshold for the perception of a body tilt is dependent on the direction of tilt. The thresholds were lower for forward tilt than for backward tilt. Moreover, Hess and Angelaki [Hes] observed a difference between eye movement latencies (translational VOR) during forward-backward displacement in rhesus monkeys. During forward movement, a shorter VOR latency was observed compared to backward motion. The authors considered that this difference could be due to the functional adaptation of vestibular system to forward movements, which are met more often compared to backward motions. This could also be related to Holly's works. Holly and colleagues have developed a theory on the construction of self-motion perception, in which the familiarity plays an important role [Hol1; Hol2]. The results of these studies suggest that perception of acceleration may be based on different signals and/or on different processes than the perception of deceleration.

As a consequence, the objective of the present study is to evaluate if the perception of acceleration also depends on the way tilt and translation are coordinated on a dynamic driving simulator. Therefore, we developed an experiment carried on the dynamic driving simulator SHERPA² that allows us to produce a large range of motions (up to 10 m on longitudinal translations).

Fig. 1. PSA Peugeot Citroën's dynamic driving simulator SHERPA².

Methods

SHERPA² is a dynamic driving simulator equipped with a hexapod and an X-Y platform (10 x 5 m) [Cha]. The cell placed on the hexapod contains a half-cab Citroen C1 fully-equipped (2 front adjustable seats, seat belts, steering wheel, pedals, gearbox, rearview mirror and side-view mirrors) where the driver is sitting. The motion limits of the hexapod are ±5 m, ±2.75 m and ±20 cm, on X, Y and Z respectively. The rotational movements are limited to ±18 deg, ±18 deg and ±23 degrees, on pitch, roll and yaw respectively. The X-Y motion platform can reproduce linear movements of 10 and 5 meters. The maximum acceleration is 5 m/s².

For this study, 26 volunteers (6 women and 20 men), aged between 21 and 47 were submitted to a passive acceleration (they did not control the motion of the car). The visual scene consisted in a straight two-lane road surrounded by an empty green field, with grass texture. The subject's car was advancing on the left lane, while a second car travelled a few meters forehead on the right lane of the road. Both cars were advancing towards a finish line at constant speed (50km/h). At a given distance from the finish line, the subject's car started to accelerate and the second car instantly disappeared. The acceleration lasted exactly 3 seconds, until the subject's car crosses the finish line. In order to evaluate perception of acceleration, we used a 2AFC paradigm. The moment the subject's car passed the finish line, the subject was asked to answer to the following question: "Who crossed the finish line first?", also using a certainty level from 1 to 6, where 6 was used to express a strong certainty of the answer, while 1 was used for uncertain answers.

The acceleration of the subject's car was precisely adjusted to pass the finish line in the same time than the other car. This was possible because the second car travelled at constant speed for all time, even after it has disappeared from the screen. The subject was informed about the constancy in speed of the second car, but not about the synchronous arrival of the cars. The dynamic stimulation, controlling the physical motion of the car, consisted in simulating the acceleration through tilt and translation. Three levels of acceleration were tested (1.0 m/s², 1.5 m/s² and 2.0 m/s²). Each of the 3 accelerations was dynamically simulated on 5 combinations of tilt and translation (tilt/translation ratios). The ratios were composed of inverse-proportional percentages of tilt and translation (from 100 / 0 % tilt/translation to 0/100 % tilt/translation with a 25% step) presented in Table 1. The decelerations followed a cosine curve with the maximum peak corresponding to the 3 levels of acceleration.

The performance of the task was analyzed in terms of acceleration perception errors. Each time the subjects responded that they won the race (understand they thought to cross the finish line in first position), their answer was matched to a value of 1, corresponding to an overestimation of the acceleration. When they answered the other car won the race, the answer was matched to a value of -1, corresponding to an underestimation of acceleration. A repeated-measures analysis of variance (ANOVA) and a post-hoc Duncan test were conducted in order to determine the influence of the level of acceleration, tilt/translation ratio and the interaction between the two variables. The p-values calculated during ANOVA represent the probability of error that is involved in accepting our observed result as valid, that is, as "representative of the population" [Bro]. We chose p=0.05, indicating that there is a 5% probability that the relation between the variables found in our sample is a chance occurrence. Therefore, p-value should be smaller than 0.05 in order to observer a significant effect of the tested variable. The post-hoc Duncan test consists of looking at the data for patterns that were not specified a priori.

Table 1 - Dynamic simulation of three levels of acceleration through 5 different combinations of tilt and translation.

Acceleration 1.0 m/s²				
Distance between cars: 6.11 m				
Acceleration distance: 34.14 m				
Condition	Translation		Tilt	
	m/s²	m/s²	deg/s	deg
1	0	1	6.12	5.85
2	0.25	0.75	4.6	4.38
3	0.5	0.5	3.06	2.92
4	0.75	0.25	1.53	1.46
5	1	0	0	0

Acceleration 1.5 m/s²				
Distance between cars: 7.24 m				
Acceleration distance: 34.84 m				
Condition	Translation		Tilt	
	m/s²	m/s²	deg/s	deg
1	0	1.5	9.2	8.8
2	0.375	1.125	6.9	6.58
3	0.75	0.75	4.6	4.38
4	1.125	0.375	2.3	2.2
5	1.5	0	0	0

Acceleration 2.0 m/s²				
Distance between cars: 8.37 m				
Acceleration distance: 35.54 m				
Condition	Translation		Tilt	
	m/s²	m/s²	deg/s	deg
1	0	2	12.3	11.76
2	0.5	1.5	9.2	8.8
3	1	1	6.12	5.85
4	1.5	0.5	3.06	2.92
5	2	0	0	0

Results

At the end of the test, all participants reported that they were exposed to different levels of acceleration and that there were different distances between the two cars and different distances to the finish line. Interestingly, none of the subjects reported the use of different tilt/translation ratios, even if, for the pure tilt simulations, they did felt the tilt and considered it as unnatural, especially for high values of acceleration. Moreover, for all trials, they were not aware to cross the line in the same time as the other car.

The responses of the subjects represented an overestimation (passing the finish line before the other car) or an underestimation (passing the finish line after the other car) of the perceived acceleration. The levels of certainty (from 1 to 6) used to evaluate their perception of motion describes their level of overestimation/underestimation or error perception. The variation of this level of certainty for each of the 5 tilt/translation ratios and for each of the level of acceleration is presented in figure 2.

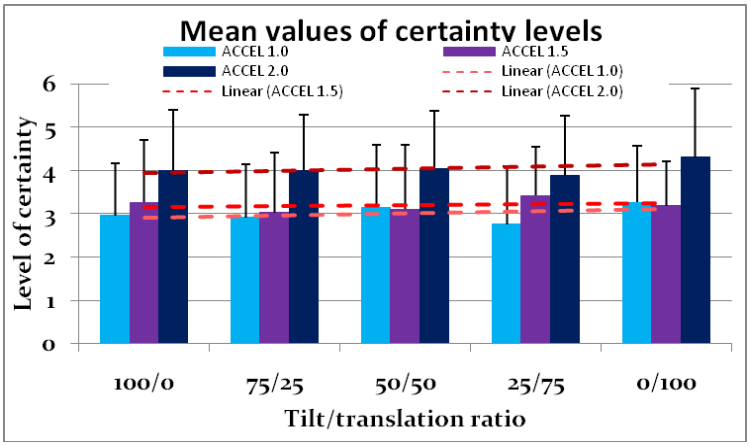

Fig. 2. Mean values of certainty level depending on the level of acceleration and on the tilt/translation ratios. The maximum value (6) represents a 100% certainty, while the minimum value (1) represents a 0% certainty. The dashed lines represent the linear tendencies for the 3 levels of acceleration.

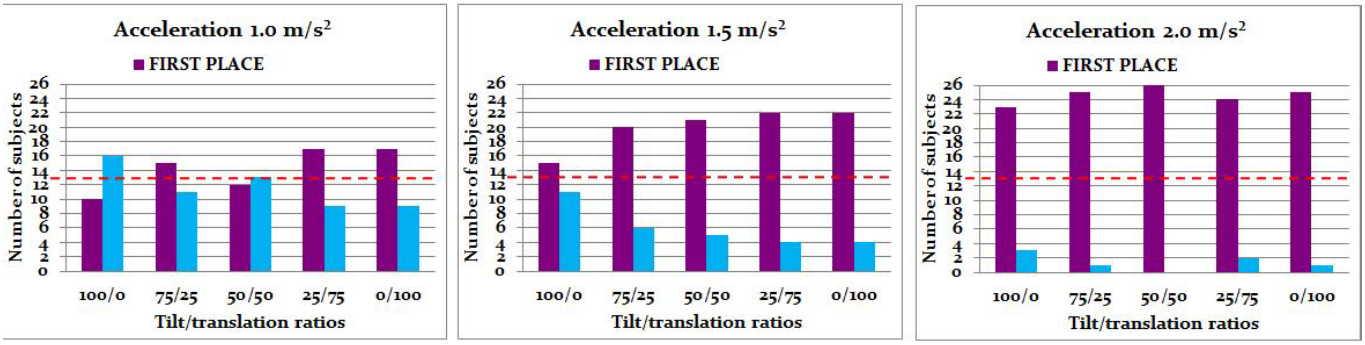

Fig.3. Number of subjects that overestimated (blue) or underestimated (purple) the acceleration, for each level of acceleration and for each tilt/translation ratio. The red line represents the case when 50% of the subjects overestimated the acceleration and 50% of them underestimated it. Under this line we talk about underestimation, over the line we talk about overestimation of the acceleration.

Interestingly, the results show no differences between the 5 tilt/translation conditions for the same level of acceleration, also confirmed by an ANOVA test (p=0.753). But the ANOVA yielded a significant effect of level of acceleration (p=0). The post-hoc Duncan showed a similarity between acceleration of 1.0 m/s² and 1.5 m/s², both different from acceleration of 2.0 m/s². Therefore, the error perception is higher in the case of 2.0 m/s² (the subjects are surer that they passed first the finish line).

If we compare the number of subjects overestimating/underestimating the acceleration, the results show an increased overestimation of the acceleration proportional to the level of acceleration (fig.3, ANOVA p=0). Moreover, as there is no significant difference between tilt/translation ratios for the same level of acceleration (ANOVA p=0.662).

Discussion

The experiment was designed to test the influence of the variation of tilt/translation ratio on the perception of positive longitudinal accelerations. The results showed no significant difference between the 5 tilt/translation ratios. This means that one level of acceleration can be simulated by any of the 5 tilt/translation ratios, without influencing the final perception of acceleration. Interestingly, these observations are in contrast with the results obtained for braking scenarios, where the perception of deceleration was greatly influenced by the use of tilt/translation ratios [Str1; Str2]. In addition, our results also showed that acceleration is mainly overestimated and the overestimation of acceleration seems to be direct proportional with level of acceleration (greater certainty levels for 2.0 m/s²). Nonetheless, given that the values of physical motion presented in this study are greater than the values used for braking situation, it is possible that the acceleration is underestimated for motions under 1.0 m/s².

However, as shown by the previous studies and the present study, there is a perceptual difference between acceleration and deceleration even on a driving simulator, which is in agreement with other previous studies [Sch; Bri]. This may be due to the fact that drivers are more used to forward motion [Hol2] or simply because the perceptual thresholds for tilt are lower for forward tilt than for backward tilt [Bri]. Nonetheless, it seems that, in our case, the tilt was detected by the subjects only for conditions with pure tilt (ratio 100/0%), even if most of the conditions that are including tilt have an angular velocity greater than the semi-circular canals' threshold of 3.7

degrees/s [Ben]. This suggest that the addition of translational motion to tilt could facilitate the perception of overall motion as linear acceleration, which is in correlation with other studies that used surge translations in combination with tilt [Ber]. This phenomenon may explain the linearity of acceleration perception throughout the 5 tilt/translation ratios, but it does not justify entirely the perceptual differences between acceleration and deceleration. In the case of our experiments, this difference may also be due to the presence or lack of visual cues: there were no visual cues during braking (no texture on the fields or the road, in order to avoid self-positioning in the space of the subjects), while they were present during latter. As a consequence, the presence of optic flow produced by the texture of the field and road may have produced, for one level of acceleration, constant visual information for all 5 tilt/translation ratios (the same displacement speed and traveled distances - even though there were no consecutively identical conditions). This may also explain the constancy of perceived linear acceleration along the tilt/translation ratios for the same level of acceleration. Therefore, even if physical motion represents an important cue in the simulation of linear accelerations on driving simulators, their weight in the process of motion perception could be influenced by non-vestibular cues. Viewed from the perspective of Bayesian framework [Zup], the non-inertial cues seems to change the reliability of the inertial cues (the semicircular canals' and otolith cues), giving more weight to the later, to the expense of semicircular canals.

As a result, motion cueing algorithms should use a gain factor that changes with the level of acceleration (for higher simulated accelerations we need smaller gain factors).However, which gain factors we need to use for each level of acceleration is still to be determined.

Conclusion

The perceptual differences between braking and acceleration during passive driving on a simulator suggest that the motion cueing algorithms should take into consideration the context of simulation (forward/backward motion), but also the influence of non-inertial cues (e.g. visual cues). Therefore, they must be adapted to the non-linearity of the human sensory systems in order to provide the tomorrow’s simulators.

References

[Ben] Benson, A. Sensory functions and limitations of the vestibular systems. In *Perception and control of self motion*, L. E. Ass. (Ed.). R. Warren and A.H. Wertheim, 1990, 145-170.

[Ber] Berger, D. R., Schulte-Pelkum, J., Bülthoff, H. H. Simulating believable forward accelerations on a stewart motion platform. *ACM Transactions and Applied Perception*, 2010, 7, 5:1-5:27.

[Bri] Bringoux, L., Nougier, V., Barraud, P.-A., Marin, L., Raphel, C. Contribution of somesthetic information to the perception of body orientation in the pitch dimension. *Quaterly Journal of Experimental Psychology Section A - Human Experimental Psychology*, 2003, 56 (5), 909-923.

[Bro] Brownlee, K.A. *Statistical theory and methodology in science and engineering*. Wiley Ed. 1960.

[Cha] Chapron,T., Colinot, J.-P. The new PSA Peugeot-Citroën Advanced Driving Simulator. Overall design and motion cue algorithm. *Proceedings of Driving Simulation Conference, 2007*.

[Gro] Groen, E. L., Bles, W. How to use body tilt for the simulation of linear self motion. *Journal of Vestibular Research* , 2004, 14 (5), 375-385.

[Hes] Hess, B. J. M. Angelaki, D. E. Vestibularcontributions to gaze stability during transient forward and backward motion. *Journal of Neurophysiology*, 2003, 90, 1996-2004.

[Hol1] Holly, J. E., McCollum, G. Constructive perception of self-motion. *Journal of Vestibular Research*, 2008, 18 (5-6), 249-266.

[Hol2] Holly, J. E., Vrublevskis, A., Carlson, L. E. Whole motion model of perception during forward- and backward-facing centrifuge runs. *Journal of Vestibular Research*, 2008, 18(4):171-186.

[Sch] Schlack, A., Krekelberg, B., Albright, T. D. Speed perception during acceleration and deceleration. *Journal of Vision*, 2008, 8 (8), 9.1-11-9.1-11.

[Str1] Stratulat, A. M., Roussarie, V., Vercher, J-L., Bourdin, C. Does tilt/translation ratio affect perception of deceleration in driving simulators? *Journal of Vestibular Research*, 2011, 21(3), 127-139.

[Str2] Stratulat, A. M., Roussarie, V., Vercher, J-L., Bourdin, C. Improving the realism in driving simulators by adapting tilt-translation technique to human perception. *Proceedings of IEEE Virtual Reality, 2011*.

[Zup] Zupan, L. H., Merfeld, D. M., & Darlot, C. Using sensory weighting to model the influence of canal, otolith and visual cues on spatial orientation and eye movements. *Biological Cybernetics*, 2002, 86 (3), 209-230.

The role of a driving simulator in driver training to improve fuel economy

Helen Scott [1], Michael Knowles [1], Adrian Morris[1] Dirk Kok [1],
(1) The Institute for Automotive and Manufacturing Advanced Practice (AMAP), University of Sunderland, The Industry Centre, Enterprise Park West, Colima Avenue, Sunderland, SR55 3XB, UK. E-mail :{Helen.Scott, Michael.Knowles, Adrian.Morris, Dirk.Kok}@sunderland.ac.uk

Abstract *– The use of driving simulators in driver training has become widespread. With the global push to reduce C02 emissions and achieve greater fuel economy, driving simulators are now being used in initiatives aimed at training drivers in Eco-Driving techniques, with varying levels of success. The Institute for Automotive and Manufacturing Advanced Practice (AMAP), at the University of Sunderland, UK, has recently used a Forum 8 driving simulator to deliver and evaluate a new Eco-Driving course for safe driving. Thirty participants took part in the study in the age range 20-64 years. Half were trained in Eco driving (intervention group) and half took part in two simulated drives without training (control group). The results indicate lasting positive effects of the training intervention on fuel economy. Results also highlight a positive role for driving simulation in the evaluation and delivery of Eco-Driving training.*

Key words: *Driving Simulator, Eco-Driving, Fuel Economy, C02 Emissions, Driver Training.*

Introduction

Driving simulators have become widely used in driving research and driver training over the past two decades [Abo1] [Bla1] [ESR1]. In comparison, the application of driving simulators in the field of Eco-Driving research and training is relatively new, applying various methodologies with varying levels of success [CAR1; Vir1].

Research has shown that fairly simple modifications to driving style can improve drivers fuel economy and C02 emissions [Aut1] [Bar1] [Ber1] [FIA1] [Gos1] [Van1] and many organisations now offer recommendations on driving style, and training in techniques to help driver's to refine their driving in order to reduce fuel consumption, wear and tear on the vehicle and cut C02 emissions [IAM1] [Ene1] [Gos1] [Aus1]. A variety of titles have been used for such techniques according to the extent to which safety is a consideration. Possibly the most commonly used term to describe energy efficient use of vehicles is 'Eco Driving' [ECO1].

The Institute for Automotive and Manufacturing Advanced Practice (AMAP) [AMA1], at the University of Sunderland, UK, has recently used a Forum 8 driving simulator [For1] in the delivery and evaluation of a new Eco-Driving course for safe driving. The course, named the DROPLET Course (Driver Optimisation for Low Emissions Transport), is based on a theoretical model of driver training, Goals for Driver Education (GDE) by Hattaka et al (2002) [Hat1]. Hatakka [Hat1] provides a comprehensive framework for goals and content of driver education. A driving simulator, classroom-based, and on-road driving techniques were used to modify driver behaviour. This paper reports on the rationale and methodological approach underpinning the course. Procedures, accompanying research, and results are discussed, and the role of driving simulators in the delivery of such courses is considered.

The aim of the DROPLET course is to raise individual's awareness of how to modify their driving to achieve optimum safety and fuel economy, and to start the process of implementing it. Research has shown that it is possible to optimise fuel economy by applying a smooth and progressive driving style [FIA1]. The DROPLET course combines best practice from the research on how drivers interact [Ful1] with methodologies, and advice from existing driver training initiatives [IAM1] aimed at maximising drivers attentional and observation skills, the ability to anticipate what will happen, and plan safe, timely, controlled responses through smooth application of vehicle controls. Components of best practice in Eco-Driving applications were mapped to the GDE model of driver training [Hat1] and applied within the course methodology, according to the most appropriate method of delivery for each. The mapping of the various pieces of advice and techniques to the different levels of the GDE model are shown in table 1.

Table 1. GDE/DROPLET Matrix

Goals for Driver Education (GDE) Model	DROPLET Course Content
Goals for Life & Skills for Living (general) • Importance of cars in driving & to self development • Skills & self-control • Driver preconceptions	General awareness of social and personal benefits of Eco - Driving and available Low Carbon Vehicle (LCV) technologies. Skill enhancement awareness Self awareness and evaluation
Goals & Context of Driving (trip related) Purpose, Environmental, Social context, Company	Plan ahead before driving. Consider using alternative modes of transport. Avoid short journeys. Plan the most direct route. Drive during off peak times if possible. Check tyres (inflation/tread depth etc.). Avoid carrying unnecessary luggage around. Only fill the fuel tank with the necessary amount of fuel. Consider turning the engine off if stuck in traffic. Close windows to reduce drag. Turn air conditioning off unless it is necessary.
Mastering Traffic Situations • Adapting to the demands of the situation at hand.	Use appropriate observation, anticipation and planning. Leave space and time to react, between yourself and other road users. Obey speed limits. Avoid stop starting in traffic. Reverse into parking bays if possible. Do not over rev the engine when conducting manoeuvres.
Vehicle Manoeuvring • Controlling speed, direction and position of the car.	Use smooth and gradual acceleration. Change gear early and keep the revolutions low. Use the correct gear for the speed and control, using block changing where and when appropriate. Maintain a constant cruising speed once the target speed is reached, when and where it is safe to do so. Use gradual and smooth braking to slow, making maximum use of engine braking. Then apply the brakes gently to stop.

Research involving two groups of volunteers was conducted to evaluate the effectiveness of the training course. One group took part in the training course (intervention group). This group drove a short route in the driving simulator before and after taking part in the DROPLET driver training course. The other group received no training (control group) and drove the same short route in the simulator, on two occasions. It was proposed that participants in the training condition would show a greater reduction in fuel consumption and C02 emissions on their second drive in the simulator, compared to the control group.

Method

Participants

From an original sample of thirty three participants, data for three of the participants was discarded due to difficulties adapting to using the driving simulator. The study therefore utilised data for thirty participants in the age range 20-64 years. The intervention group consisted of fifteen participants in the age range 31 – 64 years (mean age 47.53 years, SD 11.154; mean estimated annual mileage 10,667 miles, SD 3,266; mean duration since obtaining full driving licence 27 years, SD 12). Of these 12 were male and 3 were female. The control group consisted of fifteen participants in the age range 20-63 years (Mean age 44.07 years, SD 11.310; mean estimated annual mileage 13,567 miles, SD 9,081; mean duration since obtaining full driving licence 24 years, SD 11) of which 11 were male and 4 were female. All participants were members of the general public or staff from the University of Sunderland who had volunteered to take part in an Eco-Driving study. All volunteers had a full and valid UK driving licence, had been driving for at least three years, and reported having normal or corrected-to-normal eyesight.

Apparatus

A Forum 8, fixed base driving simulator was used for the lab based element of the study [For1]. The hardware component of the simulator is illustrated in Figure 1. The hardware is based upon a typical vehicle cockpit comprising all the usual primary and secondary controls including steering wheel, automatic transmission selector, parking brake, accelerator and brake. Instruments include directional indicator, speedometer and engine revolution counter. The display consists of three 32 inch LCD screens, each with a resolution of 1024x768 pixels and a fourth, smaller 8.4 inch LCD TFT screen with a resolution of 800x600 pixels which can be used for display of navigational

information or other data to the driver. The simulation runs at a 20 Hz frame rate (50 mS), which is also the data sampling rate. Real time information on speed km/h and fuel consumption km/L, in bar format, is also displayed in the bottom right hand corner of the central display screen. The simulator currently runs the Uc-win/Road Plug-in [Ucw1], which has an Eco-Drive module for calculating carbon footprint. A Dell Latitude D505 lap top computer was also used to display video clips of driving scenarios for the classroom element of the course.

Materials

Simulated road user scenarios

Three scenarios requiring the driver to interact with other road users were included in the simulated drive. The first scenario occurred at cross roads, in an urban setting, during a right turn manoeuvre and involved moving and stationary opposing traffic (cars, buses and lorries). The next scenario involved an opposing motorcycle passing through the junction. This was followed by a child on a bicycle crossing the road into which the driver was turning. The final scenario involved heavy traffic flow (cars and lorries) travelling in the same direction as the driver during a merge manoeuvre on a dual carriageway road.

Fig.1. Forum 8 driving simulator

Video clips

A series of five video clips was developed. The video clips lasted for one minute each and were filmed from the drivers perspective during real world, on-road driving. Two of the video clips were designed specifically to help participants to contrast the effects of poor driver observation techniques with those of an effective and efficient observational technique, two were designed to enhance driver's anticipation skills and one provided a demonstration of safe, fuel efficient, cornering techniques.

Questionnaires and interview materials

A driver perception questionnaire was developed for pre course, post course and follow up use. This contained five questions requiring responses on a five point Likert scale, The questions were designed specifically to tap driver's perceptions of their own ability on a series of dimensions that have been shown to be important in Eco-Driving. More specifically, the questions were designed to tap driver's perceptions of their own ability with regards to concentration, observation, anticipation, keeping a safe distance from other vehicles, and Eco-Friendliness while driving. A set of ten structured interview questions was also used in the follow-up study which took place three months after the course. The questions were designed to investigate the extent to which any improvements in driving style were maintained over time.

Procedure

Lab session 1

One participant at a time took part in the study. Each participant was taken to the lab and provided with an explanation of what their participation in the course would involve. After a driving documentation check, they were then asked to complete a participant consent form and pre-course driver perception questionnaire before being asked to sit in the driving simulator. The participant was then shown how to adjust the seat and asked to make them self comfortable assuming their usual driving position. They were then given an explanation of the primary and secondary controls and instructed to turn the ignition key to start the engine. The participant took part in a short 1.23 km drive on the simulator to capture a pre-training baseline measure of Eco-Driving performance. A plan view of the route and surrounding simulated environment, with numbered feature points, is shown in Figure 2.

The simulated drive started with the drivers vehicle stationary in the left hand lane of an urban dual- carriageway (start point [1]), with a 50 km/h speed restriction, on the approach to crossroads (which were situated at 0.09 km from start [2]). The driver was instructed to turn right into a triple-carriageway road. The participants view from within the vehicle, at the starting point, is shown in Figure 3.

Fig.2. Plan view of the route and surrounding environment

The driver was required to move across into the right hand lane in order to carry out the right turn junction manoeuvre. The driver then had to navigate the various road user scenarios, turning right when safe to do so. Upon turning right the driver had to get over to the far right hand lane so that they could exit the triple-lane carriageway via a single lane slip road on the right of the carriageway (situated at 0.25 km from start [3]). The slip road followed a steep incline then levelled out (at 0.55 km from start [4]) onto a short dual carriageway strip of road in which the left hand lane was closed with a series of cones. The driver was then faced with two toll booths (at 0.74 km from start [5]) and instructed to go through the one on the right hand side. Upon approach the toll booth barrier opened to allow the driver to pass. Shortly after the toll booth, the driver was required to merge with heavy traffic to join a dual carriageway on the left. The dual-carriageway continued until reaching a fork in the road (at 1.15 km from start [6]). At the fork, the driver was required to branch left and drive for a short distance before a sign appeared on the screen signifying the end of the simulated drive (at 1.23 km from start [7]).

Fig.3. The drivers view at the start of the simulated drive

No feedback on performance was given to the participant at this initial stage. In instances where a participant had difficulty in adapting to driving the simulator, a minimal amount of practise drives were allowed to enable the participant to adapt.

On-road driving session

Following the first drive in the simulator each participant took part in an on-road drive. For this part of the course, the participant was first introduced to a qualified Advanced and Fleet Driver Training, DfT Safed Trainer [Fle1] who explained what would be happening during the on-road training. The trainer used a combination of recognised on-road fleet training techniques [SAF1] combined with the relevant 'Mastering Traffic Situations' level and 'Vehicle Manoeuvring' level DROPLET course content according to the GDE model [Hat1]. The on-road element of the course lasted for approximately ninety minutes, starting and ending at AMAP, and involved driving on a standardised route including a variety of dual-carriageway and urban roads in the Sunderland area. Upon completion of the on-road element the participant returned to the lab to take part in the classroom session and second simulated drive.

Classroom session

The classroom session began with a general discussion and opportunity to reflect upon what had been learnt during the on-road session. In particular, the participant was given further advice and reinforcement on how to

implement and continue improving on the various GDE 'Mastering Traffic Situations' and 'Vehicle Manoeuvring' level Eco-Driving techniques. During the classroom session the participant was also given general strategic advice and advice on attitudes to driving, according to the specified course elements for the 'Goals for Life and Skills for Living' and 'Goals and Context of Driving' levels of the GDE model [Hat1]. Participants were then shown a series of videos to reinforce further what had been taught and discussed during the on-road session and earlier part of the classroom session.

Lab session 2

Following the classroom session, the participant was reminded how to implement all of the 'Mastering Traffic Situations' level and 'Vehicle Manoeuvring' level Eco-Driving techniques they had been taught during the course. They were then asked to take a final drive in the simulator, this time putting into practise everything that they had learnt during the course. The procedure and content of the second simulated drive was the same as for the first except the participant was given feedback on their performance upon completing the drive, according to on-screen feedback as shown in Figure 4. The participant's scores on fuel consumption and C02 emissions were compared for the first and second drive in order to demonstrate any improvements. Where a participant wished to work on gaining further improvement they were allowed to have further practise on the driving simulator, but in every case data from the first and second drive only were saved for use in the analysis. Finally, the participant was asked to complete a post-course driver perception questionnaire. Participants in the control group drove the simulator on two occasions but did not take part in any of the training interventions. However, feedback on individual's Eco-Driving performance was provided, following the second drive in the simulator.

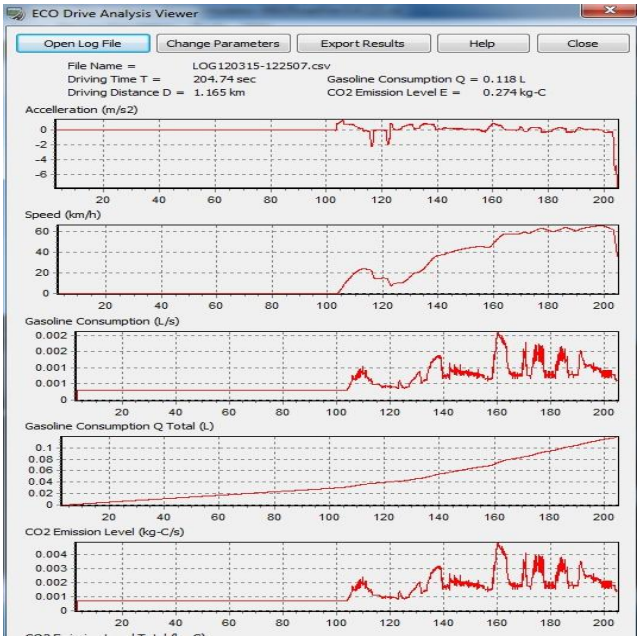

Fig.4. Screenshot of Eco-Drive performance feedback. The graphs show acceleration, speed, fuel consumption and CO2 emissions plotted against time.

Debrief

All participants were thanked for taking part in the study and given an opportunity to comment on the course. They were also asked if they would be willing to be contacted three months after taking part in the training study, to take part in a follow-up interview, and to complete a follow-up driver perception questionnaire.

Results

Using an Eco-Drive module located in the UC-win/Road tools menu and using the 'Calculate Carbon Footprint' function, results showing values for travel Time (T), Travel Distance (D), Fuel consumption (Q), and Carbon Footprint over time are displayed and can be output as a CSV file for use with Microsoft Excel and other statistical packages. Fuel consumption and carbon footprint across a journey, with a vehicles carbon dioxide emission is assumed to be proportional to its fuel consumption, and is estimated using the model proposed by Oguchi, Ktakura and Taniguchi (2002) [Ogu1] as described in equation 1 below.

$$Q = 0.3T + 0.028D + 0.056\sum_K \delta_k\left(v_k^2 - v_{k-1}^2\right) \quad (1)$$

Where Q is the fuel consumption in cubic centimetres, T is the travel time in seconds, D is the travel distance in meters, K is the number of measurements, δ_k=1 when the current speed is greater than the previous speed or 0 otherwise, v_k is the speed at point k in ms^{-1}.

Data on fuel consumption and C02 emissions captured using the UC-win/Road Eco-Drive module, was exported to IBM Statistical Package for the Social Sciences (SPSS) for further analysis. Fuel consumption and C02 emission is linearly related therefore only the results for fuel consumption are reported below. All results are reported according to standard statistical notation, where t is a statistical measure of how many standard errors the coefficient is away from zero, df is degrees of freedom (the number of values in the final calculation of a statistic that are free to vary), and p is the level of marginal significance.

Intervention group

A paired samples T-Test was used to compare driver's fuel consumption (L) before (Drive 1) and after training (Drive 2). Fuel consumption was significantly lower after training than before training for drivers in the intervention group. ($t = 6.578$, $df = 14$, $p<0.0005$)

Control group

A paired samples T-Test was also used to compare fuel consumption (L) for the first and second simulated drive (Drive 1 and Drive 2), for drivers in the control group. Results are shown in table 2.Fuel consumption was also significantly lower for the second drive compared to the first drive for drivers in the control group. ($t = 6.037$, $df = 14$, $p<0.0005$)

Table 2. Mean fuel consumption (L/km) for drive 1 and drive 2 for the two experimental groups [standard deviations of means are shown in brackets].

Group Measure	Intervention Fuel	Control Fuel
Drive 1	0.119 *[0.02]*	0.102 *[0.014]*
Drive 2	0.085 *[0.011]*	0.084 *[0.007]*

Intervention group versus control group

The difference between pre and post-training scores (Drive 1 & Drive 2) was calculated for each participant in the intervention group, and the difference between scores for the first and second simulated drive (Drive 1 & Drive 2) was calculated for each participant in the control group. An independent groups T-test was then conducted to compare the relevant differences between the two groups and to establish whether or not there was a significant effect of training intervention. The results show that the reduction in fuel consumption for the intervention group was significantly greater than that for the control group. Results are shown in table 3. ($t = 2.663$, $df = 28$, $p = 0.013$)

Table 3. Mean difference in fuel consumption (L/km) and percentage improvement (%) between drive 1 and drive 2 for the two experimental groups [standard deviations of means are shown in brackets].

Group Measure	Training Fuel	Control Fuel
Difference Between Drive 1 & Drive 2	0.034 *[0.009]*	0.018 *[0.007]*
Improvement	(28.57%)	(17.65%)

Analysis of data for the driver perception questionnaires and follow-up interviews is currently on-going and is not reported in-depth in the current paper. However, an initial review of content suggests general improvements in driver perceptions on elements of driving associated with Eco-Driving following participation in the DROPLET course. Furthermore, these improvements appear to be reasonably well maintained over time.

Discussion and Conclusion

Participants first drove a short un-instructed route in the driving simulator to obtain a baseline measure of Eco-Driving performance. They then took part in some on-road and classroom based training. Following participation in the training course, drivers were required to take a final drive in the simulator, following the same route as for the baseline drive. This time drivers were asked to put into practise everything they had learned on the course, and Eco-Driving related scores for the first and final drive were compared to evaluate the effects of training. Participants completed pre-course, post-course and follow-up driver perception questionnaires. Follow-up interviews were also conducted three months after participants took part in the course, to investigate the extent to which any effects of the training were durable over time. Results from the control group were used to examine and control for exposure related learning effects associated with simulated driving. The results show a significant reduction of 28.57 % in driver's fuel consumption following participation in the DROPLET driver training course. As fuel consumption and C02 emissions is linearly related, this is also assumed to indicate a significant reduction in driver's C02 emissions as well as general improvement in driver's application of Eco-Driving techniques. Nevertheless, data for the control group also shows a significant reduction of 17.65 % in fuel consumption between the first and second simulated drive, and although this reduction is 10.92% less than that for the training condition, it highlights the fact that there may be some Eco- related benefits associated with simply being exposed to simulated driving practise. This is something that could be exploited in future studies.

The results of the present study highlight the important role of driving simulators in the research and evaluation of Eco-Driver training. Furthermore, the results indicate that there are benefits to providing drivers with the opportunity to practise improving upon their driving techniques in a driving simulator. Driving simulators do not require fuel and do not produce C02 emissions. Driving simulators also provide experimental control and guarantee safe driving conditions, something that can not be achieved with on-road driving. One limitation of the current study however, is the simple fuel consumption formula currently used for the Eco-Drive module of the UC-win/Road tool of the Forum 8 driving simulator. While this formula makes it possible to discriminate between different accelerator behaviour (for example, aggressive high speeds and inconsistent speed will be penalised), it is not possible to infer many of the manoeuvre specific consumption factors such as gear changes and the use of smooth and gradual acceleration to an optimum and stable engine speed, with the current calculation. While previous studies have indicated that this model is adequate for the current study, future work will involve the application of a more realistic fuel consumption model based on engine physics. More extensive road networks and road user interaction driving scenarios should also be developed for use in the Forum 8 driving simulator. This would enable a predominantly simulator based Eco-Driving course and research study to be developed, utilising and expanding upon Modules from the GDE Matrix. Initial results from the driver perception questionnaires and follow-up interviews indicate lasting benefits of participation in the course. Further analysis is being conducted and results will be reported in a future paper.

Acknowledgements

The DROPLET study and Forum 8 driving simulator were funded by The Regional Development Agency ONE NORTH EAST, as part of the Zero Emissions Transport (ZET) Programme. We would like to thank David Whiting of Fleet Technique for conducting the on-road training element of the course.

References

[Abo1] Abou-Zeid, M., Kaysi, I., & Al-Nagtu, H. Measuring Aggressive Driving Behaviour using a Driving Simulator: An Exploratory Study. 3rd International Conference on Road Safety and Simulation. September 14-16, 2011. Indianapolis, USA. http://onlinepubs.trb.org/onlinepubs/conferences/2011/RSS/1/Abou-Zeid,M.pdf Accessed 15/03/2012.

[AMA1] AMAP, The Institute for Automotive Manufacturing and Advanced Practice. http://www.sunderland.ac.uk/university/factsandfigures/universitystrengthsandoverview/amap/ Accessed 15/03/2012.

[Aus1] Australian Energy Agency Eco-Driving Europe Project http://www.aatas.com/files/eco_driving.pdf Accessed – 01/02/2012.

[Aut1] Automobile Association [AA] eco driving advice http://www.theaa.com/motoring_advice/fuels-and-environment/drive-smart.html Accessed 02/02/2012

[Bar1] Barkenbus, J.N., 2010. Eco-driving: An overlooked climate change initiative. *Energy Policy,* V 38 (2), 762-769.

[Ber1] Berry, M.I (2010). The Effects of Driving Style and Vehicle Performance on the Real-World Fuel Consumption of US Light-Duty Vehicles, Thesis submitted in Partial Fulfilment of the Requirements for the Degrees of Master of Science in Mechanical Engineering and Master of Science in Technology and Policy, Massachusetts Institute of Technology. http://web.mit.edu/sloan-auto-lab/research/beforeh2/files/IreneBerry_Thesis_February2010.pdf. Accessed 15/03/2012.

[Bla1] Blana,E.(1996). Driving Simulator Validation Studies: A Literature review. Institute of transport Studies, University of Leeds. White paper. 480. http://eprints.whiterose.ac.uk/2111/1/ITS169_WP480_uploadable.pdf Accessed 15/03/2012.

[Car1] CARNETSOFT.COM
http://www.carnetsoft.com/index.html?gclid=COq8q6mG6q4CFc4LtAodYE3MKw Accessed 15/03/2012.

[ECO1] ECOWILL, What is Ecodriving? http://www.ecodrive.org/en/what_is_ecodriving-/Accessed 02/02/2012

[ENE1]Energy Saving Trust: Fuel Efficient Driving http://www.energysavingtrust.org.uk/Transport/Consumer/Fuel-efficient-driving Accessed 19.01.2012

[ESR1] ESRA Consulting Corporation (2005). Driving Simulators: Yesterday and Today http://www.esracorp.com/559DRIVINGSIMULATORS.pdf Accessed 15/03/2101

[FIA1] FIAT eco: Drive (2010), Eco-Driving Uncovered: The benefits and challenges of eco-driving, based on the first study using real journey data.
http://www.lowcvp.org.uk/assets/reports/Fiat_Eco-Driving%20Uncovered.pdf Accessed 01/02/2012

[Fle1] Fleet Technique. http://www.fleettechniquetraining.com/ Accessed 15/03/2012.

[For1] Forum8 http://www.forum8.com/ Accessed 15/03/2012.

[Ful1] Fuller, R. (2005) Towards a general theory of driver behaviour. Accident Analysis and Prevention, Vol. 37, pp461-472.

[Gos1] Gosford City Council project report for the Local Air Education Project (2011)
http://www.gosford.nsw.gov.au/environment/education/documents/Economic%20Driving_Ver2.pdf
Accessed 01/02/2012.

[Hat1] Hatakka, M., Keskinen, E., Gregersen, N.P., Glad, A, Hernetkoski, K., (2002). From control of the vehicle to personal self-control: broadening the perspectives to driver education, Transportation Research Part F 5 (2002) 201-215.

[IAM1] IAM, The Institute of Advanced Motorists (2007). Advanced Driving the Essential Guide, How to be a better driver, Motorbooks, China.

[MIT1] MITei (2010). Electrification of the Transportation System. *An MIT Energy Initiative Symposium. April 8, 2010.* http://web.mit.edu/mitei/docs/reports/electrification-transportation-system.pdf Accessed 10/02/2012

[Oug1] Ouguchi, T., Kytakura, M., & Taniguchi, M. (2002). Carbon Dioxide emission model in actual urban road vehicular traffic conditions, Journal of Infrastructure Planning and Management (JSCE), No.695/IV-54, pp. 125-136

[SAF1] SAFED Safe & Fuel Efficient Driving http://www.fleetnews.co.uk/fleet-management/safed-for-vans/35928/ Accessed 15/03/2012.

[UCw1] UC-win/Road Eco-Drive Plug-in http://www.forum8.co.jp/topic/up78-p11-e.htm Accessed 14/03/2012.

[Van1] Van Mierlo, J.V., Maggetto, G., van de Burgwal, E., & Gense, R. Driving style and traffic measures – influence on vehicle emissions and fuel consumption. Proceedings of Institute of Mechanical Engineers, Vol. 218 Part D: Journal of Automobile Engineering – DI 3902 IMechE: 2004.

[Vir1] Virage Simulation. Driving Simulation Based Ecodrive Training Presentation. Sustainable Communities Conference and trade Show, 2011. http://www.fcm.ca/Documents/presentations/2011/SCC2011/Driving_Simulator_based_Ecodrive_Training_EN.pdf Accessed 15/03/2012.

Construction of Riding Simulator for Two-wheeled Vehicle Handling

Atsushi Watanabe [1], Ichiro Kageyama [2], Yukiyo Kuriyagawa [3]
(1) Department of Mechanical Engineering, College of Industrial Technology, Nihon University, 1-2-1 Izumicho, Narashino-shi, Chiba 275-8575, Japan
E-mail: ciat11036@g.nihon-u.ac.jp
(2) Nihon University, 1-2-1 Izumicho, Narashino-shi, Chiba 275-8575, Japan
E-mail: kageyama.ichiro@nihon-u.ac.jp
(3) Nihon University, 1-2-1 Izumicho, Narashino-shi, Chiba 275-8575, Japan
E-mail: kuriyagawa.yukiyo@nihon-u.ac.jp

Abstract – This paper describes the development and evaluation of a riding simulator (RS) for two-wheeled vehicles to analyze rider control behavior from the viewpoints of human factors and control engineering. In simulator development, sense of realism is divided into riding sensation and handling feeling. In addition, they are governed by the motion equation and the required pseudo-experience. In this study, we show the effectiveness of wide-angle change and stereoscopic vision in the front visual information. Also, we show that we could lower the degree of freedom of the system in normal travelling conditions. After that, we ensured the equation of motion could be stable at all speed ranges. Through these measures, we were able to reproduce the sense of a real vehicle's riding feeling and handling feeling. Since this simulator is able to generate a higher sense of presence than conventional RS, we were able to create a tool for analyzing the behavior of rider steering.

Key words: *Simulator, Two-Wheeled Vehicle, Human Factor, Stereoscopic, Control Engineering.*

Introduction

This paper describes the development and evaluation of a riding simulator (RS) for two-wheeled vehicles to analyze rider control behavior from the viewpoints of human factors and control engineering.
The number of two-wheeled vehicles continues to increase, especially in developing countries, for such reasons as price, operating costs, and user-friendliness. Therefore, research on two-wheeled vehicle handling is important for safety and usability. Since such vehicles tend to be small and light and have inherent balance requirements, the action of the rider's body greatly influences the vehicle behavior. Therefore, we need to clarify two-wheeled vehicle behavior with human two-wheeled vehicle systems. In this field, however, theoretically analyzing the multi-control action of riders for two-wheeled vehicles is impossible because we need human-vehicle systems using experimental vehicles. In such field tests, riders are sometimes at risk. Attaching experimental instruments is also difficult because of the small carriers on the vehicles. In addition, at this stage, we cannot experimentally identify these inputs, especially the weighting factors of each input, their timing, and a reproducible method. One solution to these problems is to use a simulator of a two-wheeled vehicle for handling. In this study, we developed a riding simulator to investigate not only such human factors as mental workload and distraction but also a rider control algorithm. A system was constructed for RS and is shown in Figure 1.

Composition of simulator system

Motion Simulator Device

This riding simulator comprised of three degrees of freedom. They are roll-axis, pitch-axis, and steering-axis. At each of this axis, a servo motor is placed to operate and control the vehicle body movement. The angles, which are controlled by AC servo motors, are set to have movable range of ±15° for pitching angle, ±20° for rolling angle, and ±10° for steering angle.

Visual Simulation System Device

The front-view images are generated by a computer and then projected onto a screen installed in front of the system. 3D graphics development software called omega-space is used to generate these images.

Sound simulation system

The sound simulation system is meant to reproduce engine sound, which will act as engine sound feedback for the rider. The sound simulation system reproduces the different sound of engine by changing the frequency of the sampled sound relative to the revolution of engine.

Wind Simulator / Skin-sensation simulation system / Wind Generator Device

A system of blower is set in the under screen to give a virtual feelings of travelling wind to the rider. The amount of wind depends on the speed simulated at that moment. The blower emplacement is decided only after carefull consideration of the wind strength, range, and the rider's vision range. With the inclusion of this blower system the rider feels a more realistic riding experience.

Calculation and Control Devices

Motion information, rider's input and movement of the servo motor are all programmed to be controlled by computers.

Control System

A program called for Digital Signal Processor (DSP) was installed, in order to tune the model's parameters online in real time. This means when the simulator is running, the program allows the parameters to be altered and sees the result in real time.

Construction for front visual field screen images

RS needs to represent real vehicle feeling and handling feeling when we analyze a rider's handling action in it. Riders recognize and estimate a vehicle's feeling through kinesthetic sense, eyesight, hearing, and cutaneous feeling. Also, riders give control input to the simulator to achieve the desired vehicle motion. Thus, RS needs to increase information capacity and information quality for increased handling feeling. Also, we checked quasi-body sensory information for construction of front visual field screen images and a traction wind model. This paper describes construction for front visual field screen images as quasi-body sensory information. Previously, Morita considered rider's eyesight when steering a two-wheeled vehicle [TAK1]. This report showed that when handling a two-wheeled vehicle, a rider's gaze distribution is greater compared with a four-wheeled vehicle. Goshima noted that view-angle increase impacts the driver's sense of speed [You2]. In this study, experiments were performed to examine the needed view angle of a two-wheeled vehicle rider. As a result, we confirmed an increase in the feeling of speed from an increase in the view angle.

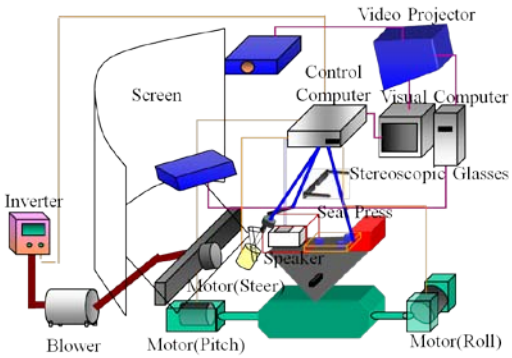

Fig.1 Outline of simulator system

Study on wide-angle changes

Experiments were performed to examine feeling of speed in the RS. The simulated course used a two-lane highway model. Figures 2 and 3 show the course that was used. The animation ran for 60 seconds as set by the experimenter, and the subject was informed of the time limit. As auditory information, we provided sounds sampled from a real vehicle engine. The experimental procedure included the following steps, and each experiment was carried out once. Subjects were three people with motorcycle licenses. We did informed-consent to them. There were four view angle conditions.

View angle condition 1: Horizontal view angle 100 [deg], Vertical view angle 45 [deg]

View angle condition 2: Horizontal view angle 100 [deg], Vertical view angle 87 [deg]

View angle condition 3: Horizontal view angle 207 [deg], Vertical view angle 45 [deg]

View angle condition 4: Horizontal view angle 207 [deg], Vertical view angle 87 [deg]

The five speed conditions were 45, 60, 65, 75, 85 [km / h].

Figure 4 shows the results of the experiment about wide-angle changes. In addition, Figure 5 shows the error rate about Figure 4 from the results of the experiment. It was confirmed that, with the increase of angle of view, sense of speed also increased. Table 1 shows the test of significant difference in experimental conditions. The results were obtained by the method of Dunnett. The'○' means that a significant difference could be confirmed. In addition, the '×' means that a significant difference could not be confirmed. The red color means the same condition on the vertical angle of view, and these show a significant difference on horizontal angle of view. The blue color means the same condition on the horizontal angle of view, and these show a significant difference on vertical angle of view. From these results, it is found that the under vertical view angle has greater influence than the horizontal view angle for feeling of speed.

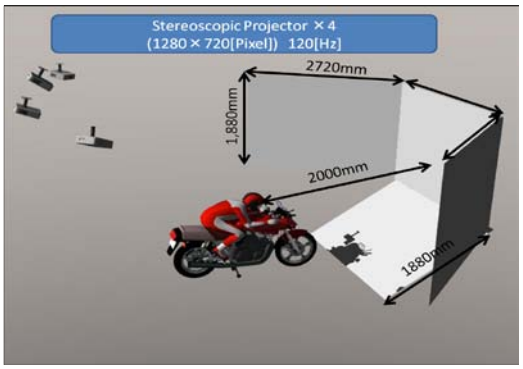

Fig. 2 Screen Image

Fig. 3 Scene of riding simulator

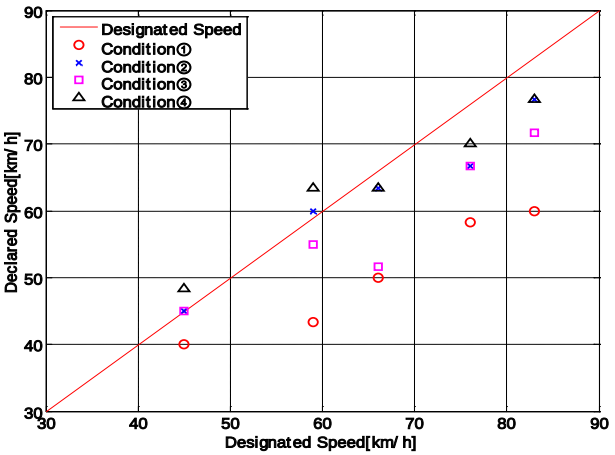

Fig. 4 Relationship between Designated Speed and Declared Speed

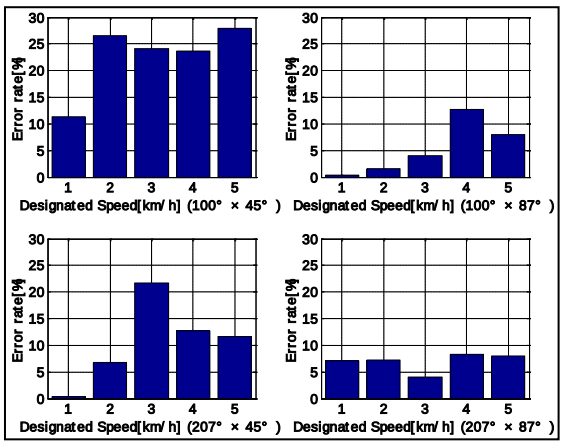

Fig. 5 Relationship between Designated Speed and Error rate

Table1 Test of significant difference

	Horizontal 100° × Vertical 45°	Horizontal 207° × Vertical 45°	Horizontal 100° × Vertical 87°	Horizontal 207° × Vertical 87°
Horizontal 100° × Vertical 45°		○	○	○
Horizontal 207° × Vertical 45°	○		×	○
Horizontal 100° × Vertical 87°	○	×		×
Horizontal 207° × Vertical 87°	○	○	×	

Study on impact of stereoscopic vision

Subsequently, we introduced stereoscopic vision into the image system to improve the feeling of distance. We used the "omega space" as a graphic tool [SOL3]. This tool can easily create stereoscopic vision through various methods. We used the LCD shutter method (refresh rate 120 Hz) to change the rider's perspective. A PC and an infrared emitter were connected to stereoscopic glasses and synchronized. Figure 6 shows the experimental environment. Experiments were performed to examine feeling of distance in the RS. The simulated course used a two-lane highway model. Figures 2 and 3 show the course that was used. First, they was enough practice running. Second, they watched running animation. And,We were asked to report to them at a specified distance. We will calculate the declared distance on the traveling time that has been reported. It then calculates the distance reported by subtracting the distance traveled from the first distance. We compare the declaration distance and the set distance, to makes an assessment of the sense of distance.

The experimental procedure included the following steps, and each experiment was carried out once.

Subjects were three people with motorcycle licenses. We did informed-consent to them. Evaluation was carried out on the Simulator (SSQ)[Ken4]. There were total of 18 conditions.

View Angle Condition：Horizontal view angle about 100 [deg], Vertical view angle about 87 [deg]

Velocity Condition: 60 km/h, 90 km/h,120 km/h

Visual condition: Planar vision or Stereoscopic vision

The experimental results were shown in Figures 7. Figure 8 shows the error rate on experimental results shown in figure 7. In addition we performed the test of significant difference. The one-sample t-test method was used as a significant difference test. Results of significance test, we confirmed the significant differences in the conditions which is the 20 meters. The stereoscopic vision method has binocular disparity and is effective primarily within a range of 20 metres. As a cause of distance feeling improvement, it is considered such as stereoscopic vision and a factor increase in the vertical viewing angle.

Next, we confirmed that visually-inducted motion sickness may occur with the increase of stereoscopic feeling. Figure 9 shows influence of the sickness. We confirmed that visually-inducted motion sickness may not occur by the increase of stereoscopic feeling.

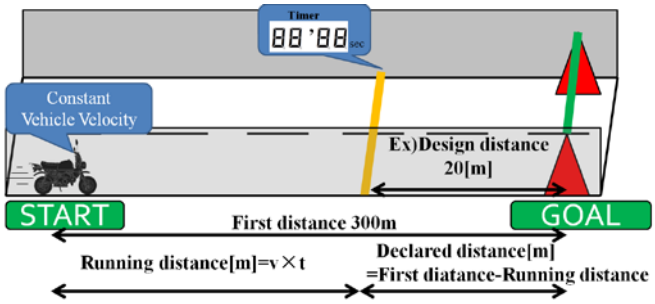

Fig. 6 Experimental Envernment

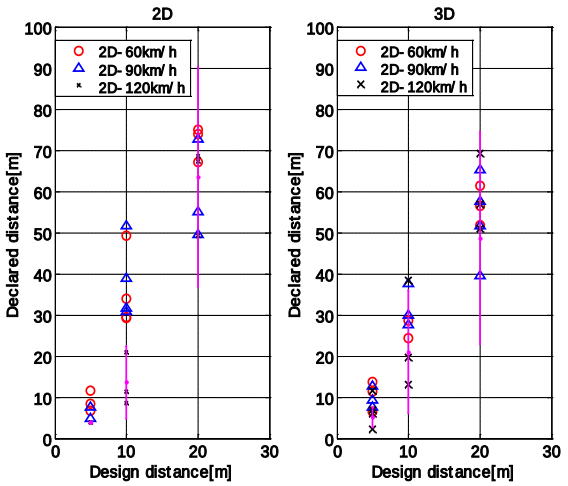

Fig. 7 Relationship between Designated Distance and Declared Distance

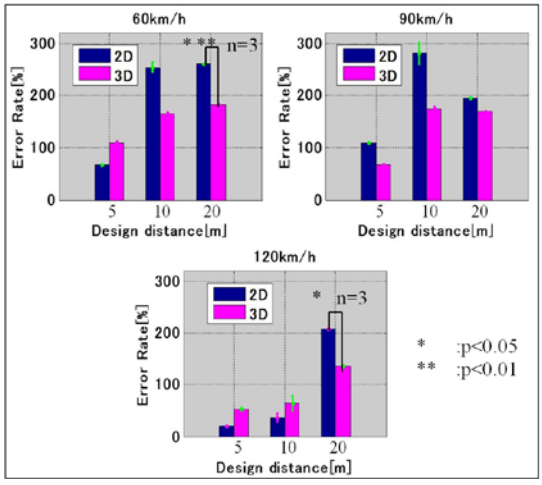

Fig. 8 Relationship between Designated Distance and Error Rate

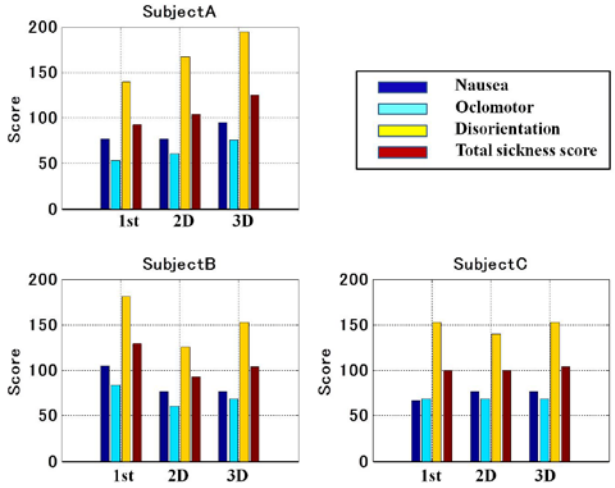

Fig. 9 SSQ Result (Stereoscopic condition influence)

System design

Determination of main control input

We have carried out an experiment to examine how the vehicle's main input control should be adopted to the RS. We conducted a double-lane change test and a pulse response test. We used the step reaction force, steering-torque and the seat-moment as control inputs of the riders. We used the yaw rate and roll rate as a response indicating the motion of the two-wheeled vehicles. From this result, yaw rate is seen to have the largest impact on the steering torque. In addition, the roll rate is seen to influence the change of attitude angle around the x-axis, and the steering torque is large. Thus, we found that steering torque is greatest in the control input of the rider for the motorcycle. As the second input, we changed the attitude angle around the x axis. Thus, we used these control inputs as the primary control input.[Oow5]

Determination of degree of freedom

We have measured the rotational center axis of motion for a real vehicle. Also, we investigated lowering the degree of freedom of the system.

We established the experimental vehicle accelerometer at 1.15 m and 1.45 m height. We conducted a slalom and acceleration-deceleration experiment. During the experiment, we measured the vehicle speed, acceleration and roll rate. The calculation results of the instantaneous center of rotation show the rotation center distance from the ground contact face. The negative value indicates the rotation center is located under the ground. These results indicate that we can lower the degree of freedom of the system in normal travelling conditions by setting it underground 0.5m, 0.9m from the instantaneous center of rotation about the roll axis and pitch axis. Thus, the degrees of freedom of the RS are three: roll axis, pitch axis, plus the handling axis that is the rider's interface during the simulation.

Lateral movement models

Stability limit of two-wheeled vehicle movement model

At present, most motion equations of a two-wheeled vehicle use models comprised of four degrees of freedom. By using Sharp's analysis method, it is known that three-vibration mode controls most of the movement of a two-wheeled vehicle, and these vibration modes are called 'capsize', 'weave', and 'wobble'. Weave has a natural frequency of 1 - 4 Hz; while on the other hand Wobble has a high frequency of 6 - 10 Hz.
Therefore, it is impossible for the rider to control a two-wheeled vehicle when such high-frequency wobble vibrations occur, especially while the vehicle is traveling at high speed and tends to be unstable. [Sha6]
After comparison to other motion equations that have been published, it is known that under the occurrence of such high-frequency vibration, especially at a certain speed range, erratic and violent vibrations are most likely to occur. These motion equations can express the characteristic of a real vehicle relatively well, but not perfectly. Thus, by

using Eigenvalues and then correcting them, these motion equations can be used as lateral directional motion models for the simulator.
To simulate lateral movements and ultimately best express the characteristics of a two-wheeled vehicle, and also to construct models that could run stably at various speeds, in this research various motion equations' roots are revised to evaluate their characteristics.[Kag7]

Lateral motion model construction

The first step is construction of basic lateral movement motion equations.
These equations are created to find the 'transfer function'. Even though these equations do not represent the exact actual movement of the vehicle, these equations could give a rough image of what the motion would be like in a real situation. At this point, there is a need to consider other forces such as cornering force, camber thrust, self-aligning torque, and gyro-moment. In terms of degrees of freedom and simulation, other factors that need to be considered are steering-angle, roll-angle, yaw-rate, and four degrees of freedom lateral speed.
The next step would be deriving Eigenvalues from the motion equation from which an approximate value of (ω_n), damping ratio (ζ), time constant (T), and gain (K) can be found. These values are then rounded up.
To stabilize the system, the values of damping ratio (ζ) and time constant (T) are corrected.
Upon achieving that, each value is calculated using appropriate equations, and the roots of the equation are also corrected so that unstable values become stable. After these processes, a model of a two-wheeled vehicle that is stable at variable speeds and has all the basic characteristics of a two-wheeled vehicle are completed.
Using the coefficients derived from the above process, the transfer functions for the simulator are then determined. Factors such as steering angle (δ), simulator body rolling angle (Φ_w), computer graphic rolling angle (Φ_c), yaw rate (ω), and lateral velocity (V_y) are required to simulate a two-wheeled vehicle. Most of them are inputs by the rider. In addition to these, the vibration modes are then further improved. This is due to the fact that these factors would greatly affect the output variables (the angle of the handle: wobble ; rolling angle: weave and capsize ; yaw rate: weave ; and lateral speed: capsize). The transfer functions are shown as the following.

$$\frac{\delta}{T_h} = \frac{K_\delta}{s^2 + 2\zeta_1\omega_{n1}s + \omega_{n1}{}^2} \quad (1)$$

$$\frac{\phi_w}{T_h} = \frac{K_{\phi_w}}{s^2 + 2\zeta_2\omega_{n2}s + \omega_{n2}{}^2} \quad (2)$$

$$\frac{\phi_c}{T_h} = \frac{K_{\phi_c}}{T_1 s + 1} \quad (3)$$

$$\frac{\omega}{T_h} = \frac{K_\omega}{s^2 + 2\zeta_2\omega_{n2}s + \omega_{n2}{}^2} \quad (4)$$

$$\frac{V_y}{T_h} = \frac{K_{V_y}}{T_1 + 1} \quad (5)$$

$$\text{Thus, } K_\delta = \{-0.3 + 5.2\times10^{-2}\times log(V+1)\}^3 \times 1.82 + \{2.3\times10^{-2} - 3.9\times10^{-3}\times log(V+1)\} \quad (6)$$

$$K_{\phi_w} = \{-7.5\times10^{-4}\} \quad (7)$$

$$K_{\phi_c} = \{-1.2\times10^{-2}\} \quad (8)$$

$$K_\omega = \{-3.0\times10^{-2} + 3.2\times10^{-3}\times log(V+0.1)\} \quad (9)$$

$$K_{V_Y} = \{-2.25\times10^{-3}\times V - 4.0\times10^{-2}\} \quad (10)$$

$$V = velocity \quad (11)$$

Using the velocity derived from the calculations above, stability examinations of the lateral movement models could be performed. As mentioned, the models consist mainly with three main values such as 'capsize', 'weave' and 'wobble'. After some experiments, it is proven that the model is able to maintain stability at any speed.
By examining for certain changes in the load, changes in center of gravity of the simulator rider can be figured out. This can be achieved and calculated after placing a 'load-cell' in the inner compartment of the simulator. To calculate the input value of the simulator, there is a need to change input several variables' values into the

equations. These variables consist of 'seat-torque' and addition of steering-torque ; also after consideration of first-order lag factors, the equation can be written in the following form:

$$Input = T_{st} \times \dot{M}_{st} + M_{st} + T_s \qquad (12)$$

In this equation, T_{st} is first order lag time constant, while M_{st} symbolizes seat-torque. After some subjective assessments, the time constants in the system are adjusted such that the rider is able to operate the simulator easily and experience more comfortable feeling. [Kag8]

Lateral Motion Simulation

At this part of the paper, there will be explanations on the lateral simulation model that involves factors such as calculations of yaw-angle, roll-angle, and the resultant yaw-motion.
First, yaw motion is simulated by using images and calculated by using the lateral motion model.
At the next step, the value of the yaw angle is then entered into the 'visual computer' for further processing.
Unlike the real two-wheeled vehicles, the riding simulator does not produce much centrifugal force, which could give an unrealistic feeling for the rider.
To overcome this problem, plenty of visual screen images and roll-motion are used to give the rider as realistic a feeling as possible. Moreover, to simulate a realistic capsize motion, light shaking of screens is used. The systems are further adjusted so that the rider would not feel any discomfort or experience any hazards by excessive screen vibrations. In regard to realistic motion for the simulator, only simulating capsize motion is not sufficient ; thus, by utilizing the simulator body vibration, weave motions were also generated. We using target roll angle and can be calculated the lateral movement model. Then the differences of the present roll-angle and the target roll-angle are again further processed by using PD control, in which the AC servo-motor output will be controlled by the PD control system.

Control System Design

A program called Digital Signal Processor (DSP) was installed to be able to monitor the model's parameters and tune it when it is offline or online in real time. This means even when the simulator is running, the program allows the parameters to be altered and sees the result in real time. Additional benefits of this software are: (1) the riding simulator allows the system designer to quickly change and tune the initial design of the system by just changing parts of the system block diagram, and (2) the software allows changes even when the simulator is running, which allows instant feedback from the rider. Thus effective parameter tuning could be achieved in shorter time. [Kus9]

Evaluation of simulator system

This simulator can produce a higher sense of realism than conventional RS, and we were able to create a tool for the analysis of rider steering action. This simulator is very effective in the analysis of control behavior in a certain limited range, but all speed ranges are not reliable. In addition, this simulator can represent different characteristics to implement two different types of motorcycle chassis. In this paper, by using the RS developed by experiment and analysis, we constructed a two-wheeled vehicle simulator that humans can control. Thus, this simulator can analyze steering action in a limited range. In addition to the steering action analysis, it would be possible for use in human-machine interface (HMI) and the development of an advanced safety vehicle (ASV). In the future, we will describe applications of the RS.

Conclusion

In this paper, we developed a motorcycle simulator that humans can control by experiment and analysis. In a simulator, realism is particularly important. In simulator development, the sense of realism is divided into riding sensation and handling feeling. In addition, they are governed by the motion equation and the require pseudo-experience. The results are summarized as follows.

1) As the improvement in a sense of speed, it is important to adopt the wide viewing angle, especially around a front wheel.

2) We introduced stereoscopic vision to improve the sense of distance. From this experimental condition, stereoscopic vision is able to verify the improved distance feeling. Therefore, it is concluded that the stereoscopic vision is effect to improve the sense of distance.

3) Steering torque is the biggest input to the motorcycle to control by the rider. As the second input, we need to adopt the attitude angle around the x axis.

4) We performed the experiments and analysis on degrees of freedom. Analysis results indicate that we can lower the degree of freedom of the system in normal travelling conditions by setting it underground 0.5 m, 0.9 m from the instantaneous center of rotation about the roll axis, pitch axis. Thus, the degrees of freedom of the RS are degrees of freedoms of three: the roll axis, pitch axis, plus the steering axis that is the rider's interface during the simulation.

5) We examined the lateral model in the two-wheeled vehicle's equation of motion. We derived Eigenvalues from the motion equation from which an approximate value of (ωn), damping ratio (ζ), time constant (T), and gain (K) can be found. To stabilize the system, the values of damping ratio (ζ) and time constant (T) are corrected. Using the coefficients derived from the above process, the transfer functions for the simulator are then determined. In addition to these, the vibration modes are then further improved. This is because these factors greatly affect the output variables (the angle of the handle: wobble; rolling angle: weave and capsize; yaw rate: weave; and lateral speed: capsize). After some experiments, the ability to maintain stability at any speed has been demonstrated.

6) By examining for changes in the load, changes in the center of gravity of the simulator rider can be figured out. This can be achieved and calculated after placing a 'load-cell' in the inner compartment of the simulator. Furthermore, we add that sheet-moment as the handling-torque moment was measured from the load cell, and was treated as the first-order lag element.

7) We constructed a Control System using the Digital Signal Conditioner (DSP) to improve steering feeling. As a result, tuning in real time becomes possible, and efficient design has become possible to detail. Thus, the discomfort of the rider can be lessened.

Through these measures, we were able to reproduce the sense of a real vehicle's riding feeling and handling feeling. This simulator generates a higher sense of presence than conventional RS, and we were able to create a tool for analyzing the behavior of the rider steering. In the future, we will use an available advanced safety vehicle (ASV) and human-machine interface (HMI) in addition to the analysis of steering behavior, and describe the applications of the RS.

References

[Tak1] TAKANOBU.M. "ON VISUAL INFORMATION SEEKING OF MOTERCYCLISTS". Department of Human Science Osaka University Bulletin, 4, p.239-265, 1978

[You2] Youichi GOSIMA, et al, "Improvement of Driver's Feeling to a Driving Simulator". Japan Society of Mechanical Engineers, No.03-8, 8th ''Motion and Vibration Control'', (in Japanese with English summary).

[SOL3] SOLIDRAY CO., LTD.''**http://www.solidray.co.jp/product/omega/index.html'' .**

[Ken4] Kennedy, N.E., Lane, K.S., Berbaum, K.S., and Lilienthal, M.G. 1993 Simulator sickness questionnaire: An enhanced method for quantifying simulator sickness. The International Journal of Aviation Phychology,3 ,203-220.

[Kat5] Katuyuki OWADA, et al, "A Study of a Rider Model for Two Wheeled Vehicle Handling". JSAE,No.942,pp.41-44 (1994).

[Sha6] R.S. Sharp; THE STABILITY AND CONTROL OF MOTERCYCLE, JOURNAL MECHANICAL ENGINEERING SCIENCE, pp.316-329,1971,Vol.13 No.5

[Kag7] Kageyama, et al, Development of riding simulator for two wheeled vehicle, Proceeding of 9th Trans-Log Meeting of JSME, No.00-37, 2000(in Japanese with English summary).

[Kag8] Kageyama, et al, Development of riding simulator for two-wheeled vehicle, Trans, JSAE 23 , 2002.

[Kus9] Kusakari, et al, Fundamental Study on HMI for Advanced Safety Vehicle on Indication Method of Information for Active Safety of Two-wheeled Vehicle, Trans. JSAE 38 (4) , 2007

Toward predicting the subjective assessment of ESC in a driving simulator

Thomas Denoual[1, 2], Franck Mars[2], Jean-François Petiot[2], Andras Kemeny[1,3]
(1) RENAULT, Technical Center for Simulation, 1 avenue du golf – 78288 Guyancourt, France, E-mail : andras.kemeny@renault.com
(2) LUNAM Université, CNRS, Ecole Centrale de Nantes, IRCCyN (Institut de Recherche en Communications et Cybernétique de Nantes), 1 rue de la Noë, BP 92101, 44321 Nantes Cedex 3, France, E-mail : {thomas.denoual, franck.mars, jean-francois.petiot}@irccyn.ec-nantes.fr
(3) Arts et Métiers ParisTech, Institut Image, 2, rue Thomas Dumorey 71100 Chalon-sur-Saône, France

Abstract *– Previous works have sought to develop an evaluation method to describe loss of adherence episodes by means of subjective indicators and to propose a predictive model of the subjective evaluations. This study presents the use of the presented model and predicted evaluations when ESC is triggered. The results confirm the capabilities of the model and the potential of the presented methodology to evaluate and characterize ESC on a driving simulator in the early stages of the engineering design. However further studies will be necessary to improve the robustness of the model and its use in various situations.*

Key words: *Sensory evaluation, ESC, Driving simulators, Model prediction, Virtual engineering.*

Introduction

Loss of adherence (LOA) can lead to loss of vehicle control, a major factor in many accidents. Electronic Stability Control (ESC) is an advanced driving assistance system (ADAS) that dynamically corrects the vehicle trajectory according to the driver's intentions in emergency situations. It is useful in particular in case of loss of adherence (LOA) in bends due to excessive speed or alteration of road grip, which can lead to loss of vehicle control. Using electronic stability control (ESC) can limit the consequences of these situations [Lie1] [Erk1]. The calibration and validation processes of ESC are time consuming and require the use of physical prototypes and expert drivers at specific test sites, especially for very low-adherence situations. Consequently, driving simulators are being used to study LOA episodes and ESC performance [Wat1] [Pap1]. Driving simulators are useful tools in vehicle design and perception studies. They allow the safe exploration of critical situations with naive drivers and without environmental bias [Kem1]. The present study is a step of a research program that is aimed at understanding how drivers perceive and react to trajectory perturbations and to the intervention of an ESC system. This could be useful for using driving simulators to develop the engineering specifications of ESC and to evaluate how actual drivers perceive different system configurations.

Previous works [Den1] [Den2] have sought to develop an evaluation method to describe LOA episodes by means of subjective indicators using a non-structured-scaled questionnaire [Str1] and to determine to what extent objective and subjective indicators were related. In this paper, an explicative and predictive model of driver subjective assessment in LOA situations has been proposed. It is based on objective measurement of vehicle behaviour such as lateral acceleration, heading speed or slip angle [Den3]. The present study evaluated the influence of ESC activation on subjective ratings and the predictiveness of the model for ESC triggering cases in LOA situations.

An experiment was conducted on the high fidelity dynamic ULTIMATE simulator using the SCANeR©Studio software package with a real-time version of the MADA (Advanced Modelling of Vehicle Dynamic) vehicle dynamic software, developed by RENAULT. The intensity (0.1 to 0.3 adherence coefficient) and duration (250ms to 750ms) of the simulated LOA in the bend were manipulated as independent variables on the four wheels. Situations of LOA inducing a significant modification on the vehicle without involving a brutal road departure were chosen. ESC availability (on or off) was the third independent variable. All subjects experienced the same LOA situations with and without ESC assistance. They were not aware of the presence of the assistance.

The objective of the study is to evaluate the accuracy of the developed model on a new data set, with and without the presence of an ESC system. The first results show a good accuracy of the predictive model on the data set without ESC. ESC triggering seems to slightly perturb the model prediction. Although further experiment will be necessary to improve the robustness of the model and enlarge to various applications, the methodology proposed seems to have a strong potential to evaluate ESC strategy in the early steps of engineering design.

Method

Participants

Four female and ten male drivers between 27 and 59 years old (mean age of 43.6) participated in the experiment. They had held a driving licence for 20.6 years on average and drove between 1000 and 20000 km per year (mean = 13400). All of them had normal or corrected-to-normal vision.

Apparatus

The experiment was conducted on the high-performance dynamic Ultimate simulator [Dag1] at Renault Technical Center for Simulation (Fig. 1). It consists of a compact size passenger car based on a real Laguna interior design. The cab is mounted on a large X-Y table and a hexapod motion system to render physical accelerations and rotations. Transmission is carried out using a manual gearbox. A system of sound synthesis is used to reproduce engine noise and the audio environment for an interactive vehicle. Active steering force feedback is computed by a proprietary model and reproduced by a TRW electric power steering system.

The SCANeR© Studio software package was used with a real-time version of the MADA (Advanced Modelling of Vehicle Dynamic) vehicle dynamic software, developed by RENAULT. The visual environment was displayed on a cylindrical screen (radius 1.9 m) by three single-chip DLP projectors, each with a resolution of 1024 x 768. The system covers a visual angle of 150°.

Figure 1. Ultimate Renault driving simulator

The graphics database reproduced an open countryside driving environment (Fig. 3). Behavioural measures (lateral position, steering angle, lateral acceleration, etc.) were recorded during the trials at 20 Hz. All trials were performed on a short section of the driving environment, which comprised a straight line followed by a bend (total distance: 700 m; mean radius in the bend: 111 m) without traffic (Fig. 2).

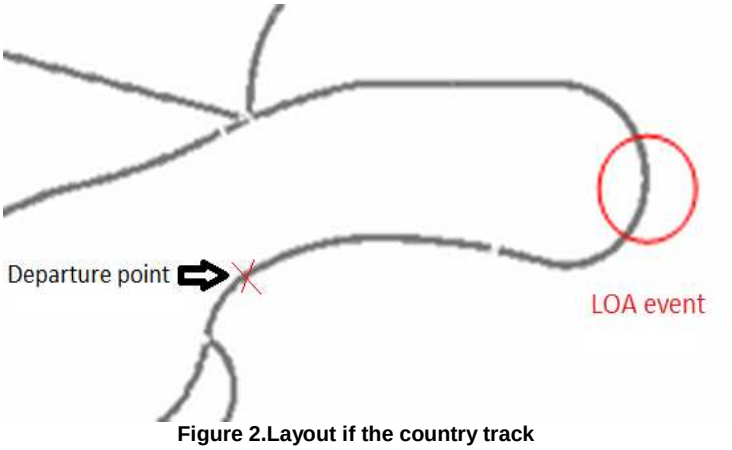

Figure 2.Layout if the country track

Figure 3. Visual environment in the bend

A software-in-the-loop generic ESC system was used (Fig. 4). The system was set up with the characteristics of the simulated vehicle, but the tuning did not reflect the supplier tuning mounted on the real car. The complex proprietary control laws to handle the vehicle stability will not be detailed.

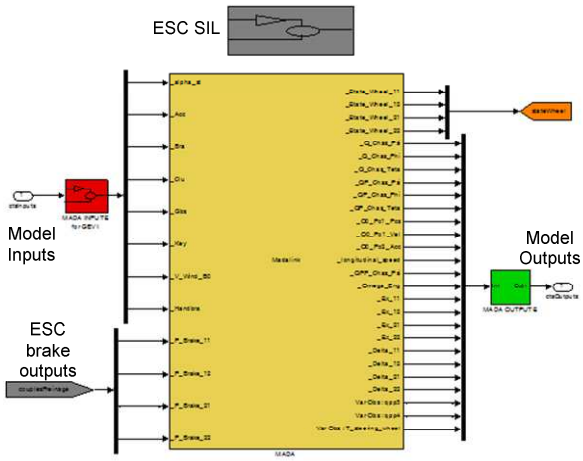

Figure 4. ESC software model integrated in the MADA vehicle dynamics model

Procedure

LOA was simulated by modifying the adherence under the wheels when the vehicle reached a defined point in the bend. The intensity (adherence coefficient) and duration of the simulated LOA in the bend were manipulated as independent variables (IV). An adherence coefficient decrease corresponds to an increase in the intensity of LOA. ESC availability (on or off) was the third independent variable. These values of intensity and duration were chosen to induce perceptible but controllable LOA simulated on four wheels (Table 1). The LOA situation induced a skid towards the outside of the bend. The environment did not give clues about a potential LOA (such as snow, rain or a mark on the road). Subjects faced each of the four conditions two times, with and without ESC. A Williams Latin Squares design [Wil1] was adopted to control rank and carry-over effects. After each experimental condition, the subject was asked to assess the LOA on a continuous unstructured scale according to 3 descriptors: perceived intensity, control feeling, danger.

Participants were asked to keep to their lane without cutting the corner, even if there was no oncoming traffic. After a 10-minute practice session, they drove around the test bend at a predefined speed (75 km/h). Subjects received verbal assistance from the person conducting the experiment in order to maintain a constant speed and stay focused on steering control. Four trials without any LOA were performed in order to allow the subjects to familiarize themselves with the task.

Table 1. LOA conditions

Conditions	C1	C2	C3	C4
Adherence coefficient	0.1	0.1	0.3	0.3
Duration (ms)	250	750	250	750

Data Analysis

Data were sorted out to identify situations where ESC has actually triggered. Predictive subjective responses were computed with a perception evaluation model of LOA situations that was developed previously by [Den3]. The models for each subjective descriptor (Yj) are reminded below (Eq. 1, 2 & 3). Actual subjective responses Yj were then compared with the values of the model $\hat{Y}_j$ in order to assess its accuracy as a function of ESC activation.

Perceived intensity = -17.90 + 6.62 lateral acceleration + 3.57 heading speed *(1)*

Control feeling = 26.64 - 0.86 slip angle - 6.90 heading speed *(2)*

Danger = - 13.57 + 4.71 lateral acceleration + 2.50 steering wheel angle *(3)*

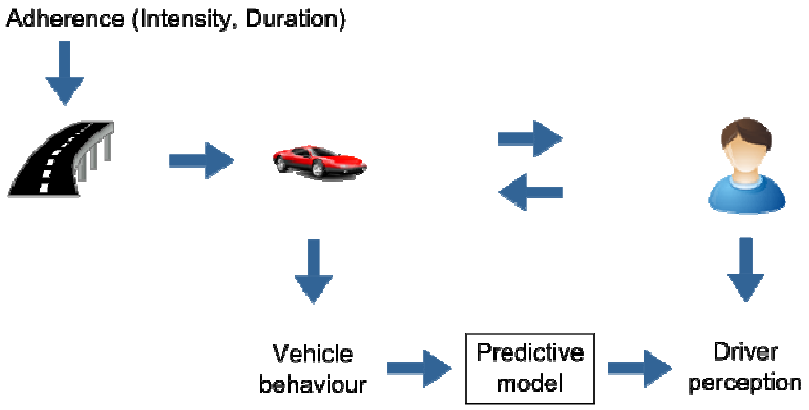

Figure 5. Input and Output data

Table 2: Input and output data for the predictive model

Input (objective indicators)	Output (subjective descriptors)
Lateral acceleration ($m.s^{-2}$)	Perceived intensity
Heading speed ($deg.s^{-1}$)	Control feeling
Slip angle (deg)	Danger
Steering wheel angle (deg)	

Two indicators were used to evaluate the predictions errors:

- The mean absolute error (MAE). It represents the forecast accuracy of the model (equation 4): the smaller the *MAE*, the better the forecast accuracy.

$$MAE = \frac{1}{N}\sum_{k=1}^{N}\left|\hat{Y}_{kj} - Y_{kj}\right| \qquad (4)$$

where N is the data sample size

- The root mean square error (RMSE)

In order to evaluate the quality of the predictions, we also computed the Pearson coefficient correlation (r) between the predicted values $\hat{Y}_j$ by the models and the actual observed values Y_j.

Results

The followings tables give the results of the MAE, the RMSE and the correlation coefficients between predicted and actual values for each descriptor, without (table 3) and with ESC triggering (table 4). Situations where ESC has not triggered were excluded for the analysis. In order to have same data sample size for both group (ESC vs. no ESC), we also excluded the paired data in the "without ESC" group. Finally, we had 18 situations in each group.

Table 3. RMSE, MAE and correlation coefficients for model forecast without ESC triggering

Yj	RMSE	MAE	r
Intensity perceived	1.08	0.90	0.81
Control feeling	1.9	1.61	0.65
Danger	1.47	1.19	0.65

Table 4. RMSE, MAE and correlation coefficients for model forecast with ESC triggering

	RMSE	MAE	r
Intensity perceived	1.39	1.07	0.60
Control feeling	2.39	1.64	0.52
Danger	1.58	1.24	0.60

Figure 6 and 7 represent the correlation between observed and predicted scores for subjective indicators with and without ESC activation for the data sample.

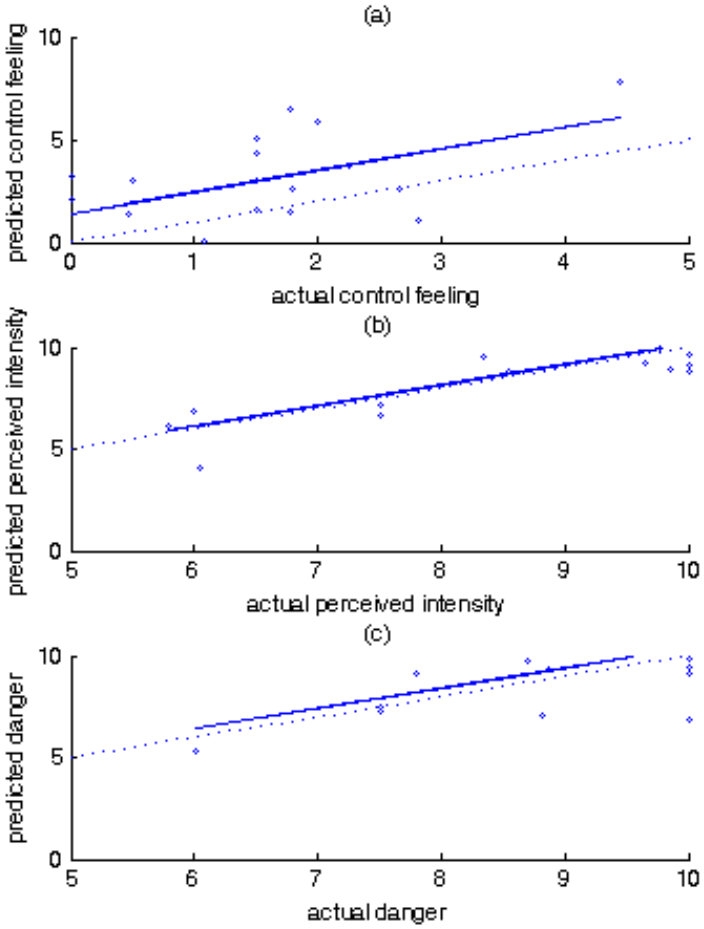

Figure 6. Correlation between actual and predicted scores for control feeling, perceived intensity and danger without ESC triggering (n=18). Solid line: actual correlation, dotted line: perfect correlation

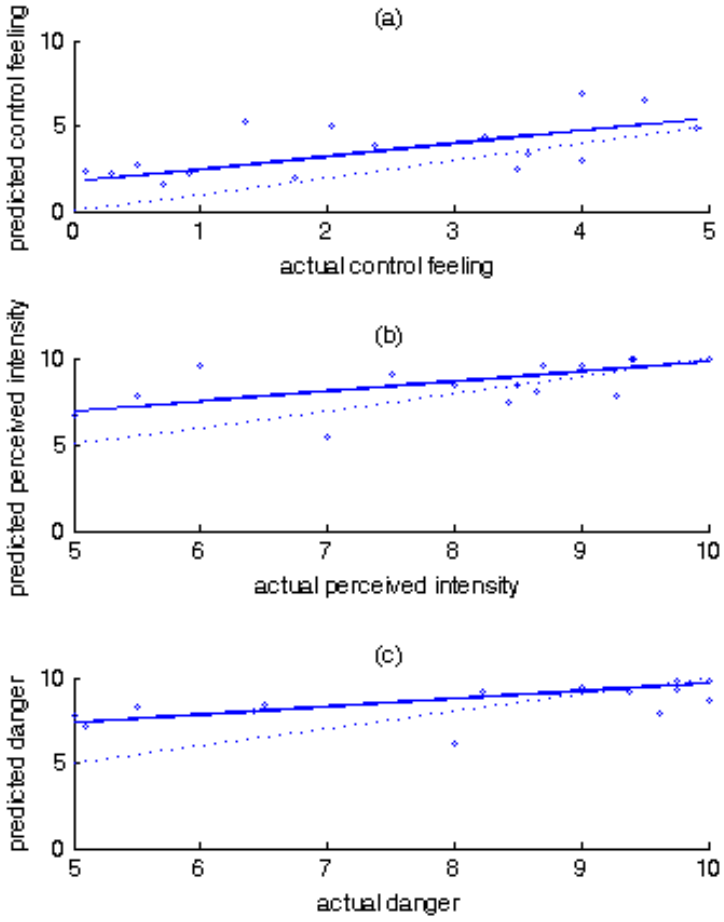

Figure 7 Correlation between actual and predicted scores for control feeling, perceived intensity and danger with ESC triggering (n=18). Solid line: actual correlation, dotted line: perfect correlation

Fisher's tests perform on the subjective variables show no significant effect of ESC triggering on "Danger" (F=1.209, p=0.28), "intensity perceived" (F=0.47, p=0.50), and "control of feeling" (F=1.58, p=0.22)

Fisher's tests perform on the objective variables show no significant effect of ESC triggering on maximum lateral acceleration (F=0.42, p=0.52), maximum steering wheel angle (F=2.12, p=0.15), maximum heading speed (F=0.32, p=0.58) and maximum slip angle (F=0.02, p=0.88).

Discussion

The present study shows the use of multiple linear models to predict driver subjective assessment in LOA situations with and without ESC triggering. For the data set without ESC, we observed good predictions of the models in the same range as seen as previously [Den3]. This confirms the capabilities of the model with a different panel of participants, which validates the methodology we used.

The same model was applied to characterize different situations in which ESC triggered. Results show that the prediction errors were more important with ESC activated. In this case, the predictive evaluations were also less correlated with the actual subjective evaluations. This probably means that the model parameters need adjustments to fit with the action of ESC. The correlation plots seem to show that the model overestimated the subjective evaluations compared to the observations. Unfortunately, results do not show a significant effect of ESC on subjective evaluation. This could be explained by the tuning of our ESC that provided limited trajectory corrections. Further investigations will be made on this question with different tuning of ESC and different LOA situations.

A traditional problematic with subjective evaluation on simulator is the simulation rendering fidelity compared to real perception. In our case, for obvious safety reasons, it would be difficult to reproduce the same experiment on a real track with non-expert drivers and compare the results. However, the global fidelity of a simulator can be estimated indirectly. On the Ultimate simulator, subjective evaluation campaign has been performed by Renault expert drivers. They have notably rated steering wheel, heading and pitch as "Satisfying" for a 0.2Hz / 0.2G slalom manoeuvres on Laguna simulation [Dag2]. We can also identify and compensate for the simulator motion cueing delays [Fan1] and adjust scale factor for lateral and yaw motion rendering [Fil1]. Moreover, the fidelity of the

simulator has been evaluated within the framework of the Eureka Moves European Project [Ber1]. Thus, we are confident on the level of fidelity of Ultimate for this application.

This study shows the strong potential of this methodology to evaluate and characterized ESC with the help of a driving simulator, in particular in the early stage of the development process when no physical prototypes are available. It also adds the possibility to evaluate ESC system from a non-expert point of view, which may complement traditional methods. However, further studies are necessary to improve the quality and robustness of the model. A similar method could be applied on new projects like electrical vehicle [Fan2] for which drivers' reactions are not well known.

Conclusions

A model presented in this paper allows predicting subjective evaluations of loss of adherence in driving simulator experiments. Further studies will allow improving the robustness of the model and its application in various situations. This study shows the strong potential of this methodology to evaluate and characterized ESC on a driving simulator in the early stages of the engineering design.

References

[Ber1] Berthoz A., Bles W., Bülthoff H.H., Correia Gracio B.J., Feenstra P., Filliard N., Huhne R., Kemeny A., Mayrhofer M., Mulder M., Nusseck H.G., Pretto P., Reymond G., Schlüsselberger R., Schwandtner J., Teufel H., Vailleau B., van Paassen M.M., Vidal M., Wentink M. High-performance motion cueing for driving simulators. Submitted *to IEEE Transactions on Systems, Man, and Cybernetics--Part A: Systems and Humans*

[Erk1] Erke A., Effects of electronic stability control (ESC) on accidents: A review of empirical evidence. *Accident analysis and prevention*, 2008, vol. 40, n°1, pp. 167-173.

[Dag1] Dagdelen, M., Berlioux, J.C., Panerai, F., Reymond, G. and Kemeny A., "Validation process of the ULTIMATE high-performance driving simulator," *Proceedings of DSC Europe Conference 2006*, Paris, pp. 37-48.

[Dag2] Dagdelen, M. Comportement Dynamique du Simulateur de Conduite ULTIMATE mi-2007, Internal Technical Note, Renault, 2007, pp. 1-31

[Den1] Denoual, T., Mars, F., Petiot, J.-F., Reymond, G. and Kemeny, A., Drivers' perception of simulated loss of adherence in bends. *Trends in driving simulation design and experiments*, 2010, A. Kemeny, F. Merienne, & S. Espié, eds., Les collections de l'INRETS, Paris, pp. 43-53.

[Den2] Denoual, T., Mars, F., Petiot, J.-F., Reymond, G. and Kemeny, A., Drivers' perception of loss of adherence in bends: influence of motion rendering. *Journal of Computing and Information Science in Engineering*, 2011, Vol. 11 / 041004-7

[Den3] Denoual, T., Mars, F., Petiot, J.-F., Reymond, G. and Kemeny, A., Predicting the subjective evaluation of vehicle behaviour in a driving simulator. *Engineering Systems Design and Analysis conference*, 2012, Nantes, France.

[Fan1] Fang Z., Reymond G.and Kemeny A. Performance identification and compensation of simulator motion cueing delays. *Trends in driving simulation design and experiments*, 2010, A. Kemeny, F. Merienne, & S. Espié, eds., Les collections de l'INRETS, Paris, pp. 111-120.

[Fan2] Fang Z., Alirand M., André S., Denoual Th., Kemeny A., Reymond G and Jansson A. Multi objective analysis on a driving simulator applied to an electric vehicle: vehicle stability, handling and drivability Proceedings SIA 2011, *Vehicle Dynamics Congress*, 5-6 Oct. 2011, Mulhouse, France, R-2011-04-18.

[Fil1] Filliard N, Vailleau B, Reymond G. and Kemeny A. Combined scale factors for lateral and yaw motion rendering. *Proceedings of DSC Europe Conference 2009*, Monte-Carlo, pp. 161-172.

[Kem1] Kemeny, A., Driving Simulation for Virtual testing and perception studies. *Proceedings of DSC Europe Conference 2009*, Monte-Carlo, pp. 15-23.

[Lie1] Liebemann E.K., Meder K., Schuh J. and Nenninger G., Safety and Performance Enhancement: The Bosch Electronic Stability Control (ESP). *SAE,* 2004, Paper No. 2004-21-0060.

[Pap1] Papelis, Y.E., Watson, G.S. and Brown, T.L., An empirical study of the effectiveness of electronic stability control system in reducing loss of vehicle control. *Accident Analysis & Prevention*, 2010, **42**(3), pp. 929-934.

[Str1] Strigler F., Touraille C., Sauvageot F., Barthélémy J. and Issanchou S. « Les épreuves » dans *évaluation sensorielle : manuelle méthodologique*, 1998, sous la direction de SSHA, Depledt F., Strigler F. Ed. Lavoisier.
[Wil1] Williams, E.J., "Experimental Designs Balanced for the Estimation of Residual Effects of Treatments," *Australian Journal of Scientific Research*, *Series A: Physical Sciences*, 1949, **2**, pp. 149-168.

[Wat1] Watson, G., Papelis, Y. and Ahmad, O., Design of Simulator Scenarios to Study Effectiveness of Electronic Stability Control Systems. *Transportation Research Record*, 2006, (1980), pp. 79-86.

Motion cueing algorithms for a real-time automobile driving simulator

Zhou FANG, Andras KEMENY
RENAULT, Technical Center for Simulation, TCR AVA 0 13, 1 avenue du Golf, 78288 Guyancourt, France
e-mail : zhou.fang@renault.com, andras.kemeny@renault.com

Abstract

The MCA (Motion Cueing Algorithm) for driving simulator takes into account the simulator's workspace limits and the driver's motion perception thresholds to reproduce simulated vehicle's accelerations. For the motion based driving simulators, the most applied MCAs are the classical and the optimal filters. This paper presents a new algorithm, called MPC (Model Predictive Control) explicit algorithm. Compared with the filters' algorithms, the MPC integrates directly the system constraints into its optimization process, and then gives a real optimal solution and hardly needs the tuning process to check the workspace limits and the driver's perception thresholds. The reported MCA studies based on MPC implicit algorithm need high computational costs which can destroy the stability properties of optimal MPC in a real-time system. The proposed workspace limit condition improves significantly the MPC optimal stable condition for its application in MCA. The current MPC algorithm can achieve the complicated 2dofs optimization.

Key words: *Motion cueing algorithm, explicit MPC algorithm, washout filter, tilt technique, real-time simulator.*

I. Review of motion cueing algorithms

A. Classical filter algorithm

The classical filter is a rapid prototype method to develop motion cueing algorithm. By taking the road information as workspace limit, the car's lateral dynamics in a straight road can be realistically reproduced in a driving simulator [Gra1, Fis1]. Using different 1st and 2nd order HP filter parameters, for the 8 dofs simulator, Fischer et al. [Fis1] proposed to decompose the linear acceleration signal into high, middle and low components, i.e. linear hexapod, linear x, y rails and tilt angle command signal. The idea is worth being studied. However, the actuators' performance limits and the different transfer functions between rail system and hexapod could make the tuning task very difficult without modern control theory. The authors have also introduced a lane-signal feedback loop which allows applying rather optimally the tilt coordination technique for lateral motion cues. This information is in fact very useful to choose the best strategy for MCA [Cha1]. We think that the way of taking into account road information and driver's attention in MCA is an interesting research issue in order to reduce the false cues. The table 1 summarizes the classical filters' roles and the corresponding conventional parameter settings.

Table 1: classical filters and corresponding parameter settings

Filter Type	Motion rendering for	Filter transfer function: H(s)	Conventional pulsation, ω_n, and damping ratio, ξ, values [Fis1, Ron1]	Final position to step input signal: $y(t \to \infty)$
1st order HP	Rotational rate	$\frac{k.s}{(s+\omega_b)}$	ω_b = 0.2	$\frac{k}{\omega_b}$
2nd LP	Tilt technique	$\frac{k.\omega_{n2}}{(s^2+2\xi.\omega_{n2}.s+\omega_{n2}^2)}$	ω_{n2} = 0.65~1.02, ξ=1 ω_{n2} = 1.2~2.5, ξ=1	
2nd HP	Linear acc.	$\frac{k.s^2}{(s^2+2\xi.\omega_{n1}.s+\omega_{n1}^2)}$	ω_{n1} = 2.5~4.0, ξ=1~1.4	$\frac{k}{\omega_{n1}^2}$
Washout	Linear acc.	$\frac{k.s^3}{(s^2+2\xi.\omega_{n1}.s+\omega_{n1}^2).(s+\omega_w)}$	ω_w = 0.1 ~ 0.5	0

The filter's parameters should be designed with the worst case: a unit step acceleration whose corresponding position is: $X(s) = 1/s^3$. The simulator final steady position, y(t) can be evaluated by:

$$\lim_{t\to\infty} y(t) = \lim_{s\to 0} s.H(s).X(s) = \lim_{s\to 0} \frac{ks^2}{\left(s^2 + 2\xi.\omega_{n1}.s + \omega_{n1}^2\right)s^2} = \frac{k}{\omega_{n1}^2} \qquad (1)$$

To avoid the workspace violation, the parameters should be determined by:

$k/\omega_{n1}^2 \le k_p.x_{max}$, if $\xi_1>1$, $k_p=1$ otherwise $k_p<1$and max(gain. $\ddot{x}(t)$) = k.

B. Adaptive filter algorithm

As the classical filter needs to be designed in the worst case, the available workspace is often badly used. Another issue is the false cues generated by this simple technique which can be considered as a main cause for the occurrence of motion sickness.

UTIAS and NASA [Tel1], Nahon and Reid [Nah1], suggested an adaptive washout algorithm with a similar formulation as the classical filter in the time domain. The parameters are self-tunable and determined by optimizing a quadratic cost function (the acceleration difference between simulated vehicle and platform within the performance limits). The proposed algorithm with tilt technique involves 8 weight tuning parameters for 2dofs optimization. The main issue of this algorithm is its stability and the difficulty to determine the best range of adaptive parameters P_{xi}. The non-significantly improved results given by this algorithm seem much compromised with the complexity of the calculation effort. We can also observe that the lack of tilt acceleration constraint could be critical for applying the tilt coordination technique in a vehicle driving simulator (see fig. 14). A LP filter or additional weight parameter for tilt acceleration seems necessary to limit the false cues level within the human motion perceptual threshold. The adaptive filter for 2dofs MCA proposed by UTIAS and NASA is given by [Tel1]:

$$\ddot{x}_s(t) = P_{x1}.\gamma_{xveh}(t) - K_{x1}.\dot{x}_s(t) - K_{x2}.x_s(t) \qquad (2)$$
$$\dot{\theta}_s = Lim\left(P_{x2}.\gamma_{xveh}(t)\right) + P_{x3}.\dot{\theta}_{veh}(t)$$

where P_{x1}, P_{x2} and P_{x3} are the adaptive parameters and K_{x1}, K_{x2} are equation constants. The P_{xi} and the cost function are determined by:

$$P_{xi} = -G_i \frac{\partial J_x}{\partial P_{xi}}$$

$$J_x = 0.5[\left(\gamma_{xveh} - \ddot{x}_s\right)^2 + W_{x1}\left(\dot{\theta}_{veh} - \dot{\theta}_s\right)^2 + \rho_x\left(W_{x2}.\dot{x}_s^2 + W_{x3}.x_s^2 + W_{x4}.\dot{\theta}_s^2 + W_{x5}.\theta_s^2\right) + W_{x6}\left(P_{x1} - P_{x10}\right)^2 + W_{x7}\left(P_{x2} - P_{x120}\right)^2 + W_{x8}\left(P_{x3} - P_{x30}\right)^2]$$

C. Optimal filter algorithm

The optimal filter taking into account models for vestibular system was proposed by Sivan et al. [Siv1]. This algorithm uses techniques of optimal control and minimizes the driver's perception error between the vehicle and the simulator. Chen and Fu [Che1] have studied the algorithm based on different techniques (optimal, fuzzy compensation) to find a better optimal solution. In the formulation of Chen [Che1] and Telban[Tel2], the input signal is [$d\theta/dt$ $u_{s\ lin}$]. It has been found impossible to control the tilt acceleration level without introducing $d^2\theta/dt^2$ into input signal. Nevertheless, as we will discuss in paragraph (§-II.E), the control of tilt acceleration level is very important for tilt technique in vehicle driving simulator. So in our future research, a modified state-space model, as reported in [Tel1], by using tilt acceleration instead of tilt rate as input signal will be proposed and analysed for explicit MPC algorithm.

D. Model Predictive Control algorithm

Dagdelen [Dag1] and Augusto [Aug1] have studied an implicit MPC algorithm for MCA application. The authors' works are based on on-line MPC optimization technique. Due to the real-time requirement (step time in milliseconds), this technique would be limited by the predictive horizon time and iterative number. Morari et al. [Mor1] indicated that a limit on the online computation time can destroy the stability properties of optimal MPC. The explicit MPC algorithm is developed to rise above this weakness.

Both implicit and explicit MPC algorithms are based on the same optimization principle. A more detail explication is introduced in next paragraph. Due to the direct integration of the simulator's limits into MPC optimization strategy, the MPC algorithm is considered better than any other motion cueing strategy [Dag1, Aug1]. Unlike the classical filter algorithm, the MPC algorithm is a non delayed algorithm.

II. Explicit MPC algorithm

A. Principle of explicit algorithm

The MPC algorithm aims at finding an optimal control law, based on minimizing (or maximizing) the value of a cost function, for the following state-space model:

$$\begin{aligned} X_k &= A.X_{k-1} + B.U_{k-1} \\ Y_k &= C.X_{k-1} \\ H_x.X + H_u U &\le K \end{aligned} \qquad (3)$$

where $A \in R^{nxn}$, $B \in R^{mxn}$, $C \in R^{pxn}$. $U_k \in R^m$, $X_k \in R^n$, $Y_k \in R^p$ are the input, state and output vectors respectively. The constraints given by $H_x \in R^{qxn}$, $H_u \in R^{qxm}$, $K \in R^q$ define a polyhedral region containing the origin in their interior, and the pair (A,B) is assumed stabilizable.

The optimal control law for current state, X_k, can be obtained by means of multi-parameter programming algorithm with a quadratic cost function defined by:

$$J_N^*(X_k) = \min_{u_0,u_1,\ldots,u_{N-1}} \|X_N\|_{Q_N}^2 + \sum_{i=0}^{N-1} \|U_i\|_R^2 + \sum_{i=0}^{N-1} \|X_i\|_Q^2 \qquad (4)$$

subj. to: $X_i = A.X_{i-1} + B.U_{i-1}$, $X_0 = X_k$, $1 \le i \le N$, $X_N \in T_{set}$ $H_x.X_i + H_y.U_i \le K$, $0 \le i \le N-1$

with weighting matrices $R > 0$, $Q \ge 0$, $Q_N \ge 0$ and $(Q^{1/2},A)$ is detectable.

At each sampling time, the current state X_k is used to find an open-loop control sequence: $K_{opt\,k} = [u^T_{0|k}, u^T_{1|k},\ldots,u^T_{N-1|k}]^T$ where only the first element is applied for the plant system control and the procedure is repeated by following a "receding horizon control" principle. Thereby, the plant state evolution can be considered as a result of close-loop system. The future reference trajectory, updated at each moment, *t*, is generally supposed as constant (cf. fig. 1).

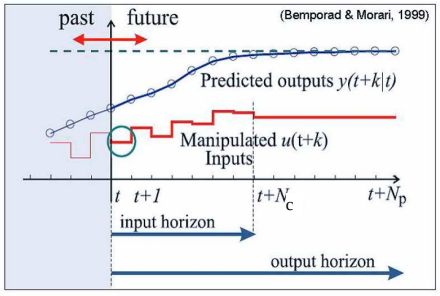

Fig. 1: Principle of MPC algorithm [Bem1]

For the explicit MPC with multi-parameter Quadratic Programming (QP) algorithm, the optimal control law, $U^*_0(X)$, can be deduced from an affine function [Kva1]:

$$U_0^*(X) = F_i.X + G_i, \text{ for } X \in R_i, \qquad (5)$$

where R_i is a polyhedral region in R^n.

The parameters F_i and G_i are given by the MPT (Multi-Parametric Toolbox) developed by the Automatic Control Laboratory of ETH, Zürich (http://control.ee.ethz.ch/~mpt/) for Matlab. The principle of explicit algorithm is recited as follows: By multi-parametric programming, a linear or quadratic optimization problem is solved off-line. The associated solution takes the form of a piecewise affine state feedback law. In particular, the state-space is

partitioned into polyhedral sets and for each of those sets the optimal control law is given as one affine function of the state.

The main on-line computational time is consumed for finding the appropriated region by the test: $|H_i.X(k) - K_i| <$ numerical error tol. (e.g. = 10^{-7}). Hence the maximal computation cycle time can be evaluated by the test over all regions during MPC algorithm design phase.

B. Reference Tracking model

Compared with the regulation problem where the reference state is fixed, the reference tracking optimization is to treat a time varying reference problem. The reference signal, r, is described by following model [Pek1]:

$$\begin{aligned} z_{k+1} &= A_r.z_k \\ r_k &= C_r.z_k \end{aligned} \qquad (6)$$

where: $r_{min} \le r_k \le r_{max}$

We can define an augmented state space model in order to transform the optimization tracking problem to a standard regulation optimization:

$$\begin{aligned} \hat{X}_{k+1} &= A_m.\hat{X}_k + B_m.u_k \\ \hat{Y}_k &= C_m\hat{X}_k + D_m.u_k \end{aligned} \qquad (7)$$

where:

$$\hat{X}_k = \begin{bmatrix} X_k \\ z_k \end{bmatrix}, \quad A_m = \begin{bmatrix} A & 0 \\ 0 & A_r \end{bmatrix}, \quad B_m = \begin{bmatrix} B \\ 0 \end{bmatrix}, \quad C_m = \begin{bmatrix} C & -C_r \end{bmatrix}, \quad D_m = \begin{bmatrix} 0 \\ 1 \end{bmatrix}$$

In driving simulator with A_r=1, C_r=1, the tracking reference is the acceleration signal for the linear acceleration rendering or the angular position for the tilt coordination technique.

C. Algorithm stable condition

Bemporad and Morari et al. [Bem1, Bem2], have summarized different stability conditions for MPC algorithm of which we briefly review those related to the present study. The stability conditions can be classified into two categories: using a cost function to minimize the command sequence at each moment *t* as a Lyapunov function and those shrinking the state in some norm to guarantee future feasible solution:

- End constraint is imposed by forcing the predictive end state to equal its origin,
- Invariant terminal set (the idea is to relax terminal constraints into set-membership constraints, where the feedback gain, K_{LQ}, corresponds to the invariant set under LQ regulation and the constraints are fulfilled inside it).

For motion cueing algorithm, the second condition is more profitable, because it gives a more efficient exploitation of simulator workspace for the same predictive horizon steps. Thanks to the work of different automatic experts [Bem1] and MPT group, an algorithm determining automatically the LQ terminal set is implemented in MPT. For MCA and 1dof optimization, this technique can provide an appropriated real-time solution. But for 2dofs optimization, it's difficult to achieve a convergent solution, which is the reason why this paper developed a new special MCA invariant set to overcome the encountered difficulty.

Our stable condition is based on the following assumption:

If the simulator can provide a large enough available workspace, it performs the acceleration or angle tracking task. When the simulator approaches its workspace limit, the simulator should be slowed down to reach its saturated position or to be turned back to some fixed point (washout process). To apply the washout process or not depends on the simulated scenario. For instance, the former one is more suitable for slalom profile test, whilst the washout is more adapted for a free driving test.

For the convenience of demonstration, we first suppose that the simulator approaches its limit with a constant deceleration. The workspace restriction can be described by:

$$|x_i + v_i.T + u_i.T^2/2| \leq x_{max} \quad (8)$$

To avoid any violation of the simulator workspace boundaries and to keep a non conflicting perceived acceleration, it is necessary in terminal braking stage to pass a zero velocity state. Thereby:

$$u_i = -v_i/T \quad \text{with } u_i \leq u_{thd} \quad (9)$$

which leads to the following relationship between T and u_{thd} :

$$T = \sqrt{\frac{2(x_{max} - x_i)}{|u_{thd}|}} < 2\sqrt{\frac{x_{max}}{|u_{thd}|}} \quad (10)$$

Supposing x_{max} = 2.6m and x_i = 0, u_{thd} = 0.2m/s², it produced: T_{max} = 5.1s

Theoretically, the T_{max} is the minimal horizon (for a constant horizon) to explore the optimal solution in the whole workspace range. Even so, such horizon time remains too large to be applied in a real time system in practice. Consequently, other conditions such as terminal invariant set have to be used to guarantee the stability condition. In the following paragraphs, is proposed a new stable condition particularly efficient for MCA which can guarantee the stability condition even with a short horizon. The concept is to add an appropriated workspace limit condition instead of imposing terminal invariant set in the MPC optimization process.

In the MPC algorithm, the relation (8) is checked at each sampling time step. For an open-loop, it describes the condition $x(t+T) \leq x_{max}$. But MPC algorithm actually gives a close-loop optimal result due to its feedback state information. During braking phase of motion cues, i.e., (8) lies at its equality restriction, the input acceleration, u, should be written as a time-variant signal as well as the simulator state:

$$x_i(t) + v_i(t).T + u_i(t).T^2/2 = x_{max} \quad (11)$$

Eq. (11) is an unstable condition for simulator, because the temporal signal x(t) can exceed the limit value x_{max} before reaching its final steady value x_{max} which will be proved later. Concerning the stability of equation (11), we introduce a modified condition:

$$x_i(t) + c_v.v_i(t).T + c_u.u_{thd}(t).T^2/2 = x_{max} \quad (12)$$

whose corresponding Laplace function is :

$$x_i(s) = \frac{\left[s^2.(x_0/x_{max}) + s.(v_0 + 2\xi.\omega_n.x_0)/x_{max} + \omega_n^2\right].x_{max}}{s.(s^2 + 2\xi.\omega_n.s + \omega_n^2)} \quad (13)$$

This is a typical second order time-invariant system with the step input x_{max}/s, system natural frequency $\omega_n = [2/(c_u.T^2)]^{0.5}$ and damping ratio: $\xi = c_v/(2\ c_u)^{0.5}$, x_0 and v_0 constitute the last tracking vehicle state from which the braking process slows down or the washout process starts.

The steady value can be evaluated by:

$$\lim_{t\to\infty} x(t) = \lim_{s\to 0} s.x_i(s) = x_{max}$$

Naturally, the $v(t\to\infty) = 0$.

According to the second-order system (13), if $\xi<1$, the oscillation in response of x(t) around x_{max} appears. Hence, the condition (11) is not a stable condition. To avoid the overshoot phenomenon during the future coming time, the necessary and sufficient condition is: $c_v^2/(2c_u) \geq 1$.

Like some classical filters, it's possible for the MPC to take $\xi<1$, but the final steady position should be reduced in consequence.

The evolution of acceleration is given by the following formulation:

$$u_i(t) = A_1.\exp(-k_1.\xi.\omega_n t) - A_2.\exp(-k_2.\xi.\omega_n t) \qquad (14)$$

$$with \quad A_1 = \frac{\omega_n\left(v_0 - 2k_1.v_0.\xi^2 - k_1.x_0.\xi.\omega_n + k_1.\xi.\omega_n.x_{max}\right)}{\xi(k_1 - k_2)}$$

$$A_2 = \frac{\omega_n\left(v_0 - 2k_2.v_0.\xi^2 - k_2.x_0.\xi.\omega_n + k_2.\xi.\omega_n.x_{max}\right)}{\xi(k_1 - k_2)}$$

$$k_1 = 1 - \sqrt{1-\xi^{-2}}, \qquad k_2 = 1 + \sqrt{1-\xi^{-2}}$$

Note that the simulator's restriction on velocity is not yet taken into account in above analysis. An exponential asymptotic law can be adopted to restrict the maximal velocity: $v(t) = (v_0 - v_{max}).\exp(-t/T_v) + v_{max}$ or in term of its corresponding acceleration limit: $u_{lim\ v}(t) = [v(t) - v_{max}]/T_v$. Finally, the $\max\{u_i(t), u_{lim\ v}, -u_{lim\ perf}\}$ or $\min\{u_i(t), -u_{lim\ v}\ u_{lim\ perf}\}$ should be sent as simulator input signal.

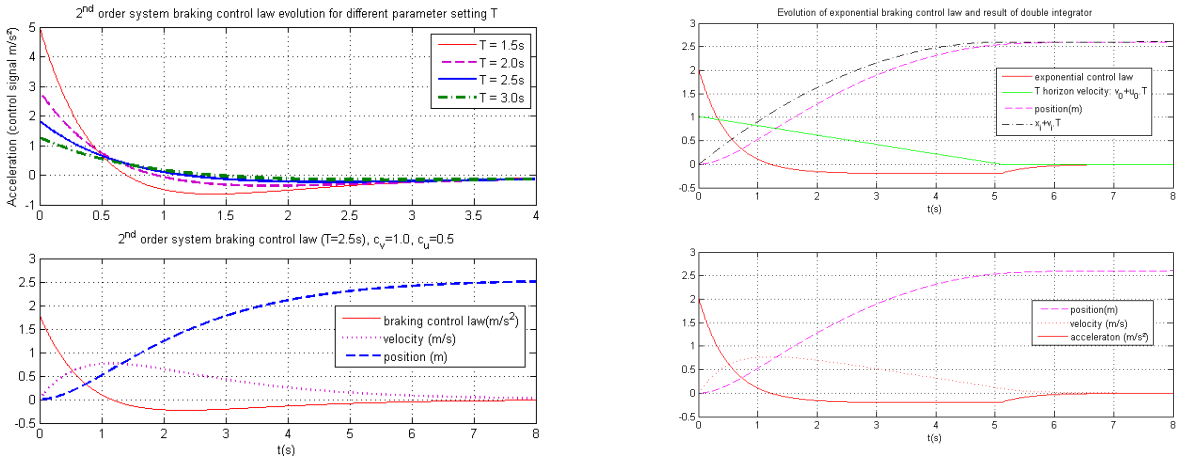

Fig. 2 : Simulator state evolution after x_0=0m v_0=0m/s and $u_s(t_0)$=2m/s² (left for eq. (14), right for table 2)

The tracking process associated with the developed braking law (eq.-12~14) can be considered as a special adaptive filter. Actually, the equation (12) is an invariant set and a workspace limit condition for MPC used only if the relation (12) is fulfilled. Here come the questions like whether it is possible to keep the braking deceleration as a constant value, e.g. equal to u_{thd}? In fact, such control law can result from a new assumption as follows:

$$u_i(t) = (u_0 + u_{thd}).\exp(-t/T_a) - u_{thd} \qquad (15)$$

The deduced control laws are in fact very simple. They are summarized in table 2 and shown in the right of fig.2.

Table 2: constant u_{thd} washout law for ideal simulator

	if $v_i + u_i.T \geq 0$	else ($v_i + u_i.T < 0$)
$v_i>0$	$u_{lim\ x\ sup} = \frac{\sqrt{2u_{thd}(x_{max} - x_i - v_i.T)} - v_i}{T}$	$u_{lim\ x\ sup} = -v_0/T$
$v_i<0$	$u_{lim\ x\ inf} = -v_0/T$	$u_{lim\ x\ inf} = \frac{-\sqrt{2u_{thd}(x_{max} + x_i + v_i.T)} - v_i}{T}$

Although this proposed braking law (15) cannot be directly used as the MPC explicit algorithm workspace limits condition, this control law can be efficiently applied to 1dof MCA application, if the state-space model is an ideal simulator (double integrator).

D. State space model of driving simulator

For a cost-effective MCA, using the simulated plant to represent a real disturbed system is preferable, because a non symmetric driving scenario such as braking or mountain road lasts hardly over 15mn. At the end of a test of

such duration, the simulated position is very close to simulator's real position. Actually, non symmetric scenario can produce more derivation than a symmetric maneuver e.g. sinus if one takes a first order system transfer function [Fan1] for the simulator. The benefit of using non disturbed system lies in the fact that the control law acts on acceleration, u, rather than on its differential term, du which is normally used to avoid the offset-free tracking. Thus, we can reduce the state-space equation dimension, which is important in order to develop explicit MPC real-time algorithm and to facilitate parameters' tuning.

In the current paper, the simulator is supposed to be an ideal one, i.e., the actuator manufactory controller is perfect. The figure 3 illustrates the scheme of MPC algorithm integration in the simulator.

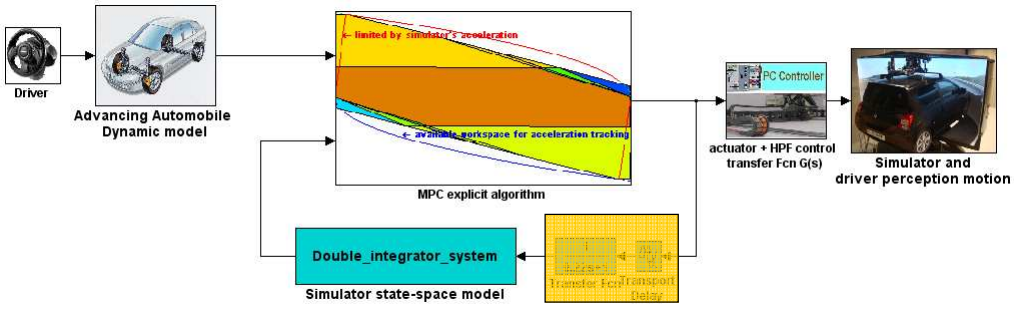

Fig. 3: Simulator model and MPC algorithm integration

The ideal simulator corresponds to a double integrator. With the proposed condition (12), the equation for MPC algorithm optimization can be formulated by:

$$\hat{X}_k = \begin{bmatrix} x_k \\ v_k \\ \theta_k \\ \omega_k \\ r_k \end{bmatrix}, \quad A_m = \begin{bmatrix} 1 & dt & 0 & 0 & 0 \\ 0 & 1 & 0 & 0 & 0 \\ 0 & 0 & 1 & dt & 0 \\ 0 & 0 & 0 & 1 & 0 \\ 0 & 0 & 0 & 0 & 1 \end{bmatrix}, \quad B_m = \begin{bmatrix} 0.5dt^2 & 0 \\ dt & 0 \\ 0 & 0.5dt^2 \\ 0 & dt \\ 0 & 0 \end{bmatrix}$$

$$C_m = \begin{bmatrix} 1 & 0 & 0 & 0 & 0 \\ 0 & 0 & 1 & 0 & 0 \\ 0 & 0 & sign.g & 0 & -1 \end{bmatrix}, \quad D_m = \begin{bmatrix} 0 \\ 0 \\ 1 \end{bmatrix} \quad U_m = \begin{bmatrix} \dot{v}_k \\ \dot{\omega}_k \end{bmatrix} \qquad (16)$$

$$sign = 1,\ for..x..and..sign = -1..for..y[].$$

$$J_N^*(\hat{X}_k) = \min_{u_0,u_1,\ldots,u_{N-1}} \left\| \hat{X}_N \right\|_{\hat{Q}_N}^2 + \sum_{i=0}^{N-1} \|u_i\|_R^2 + \|x_i\|_{\hat{Q}x}^2 + \sum_{i=0}^{N-1} \|(u_i - r_i)\|_{Qu}^2$$

$$subject \quad to:$$

$$\left| x_k + T_1.v_k + \frac{T_1^2}{2}.u_k \right| < L_{x,y\,\lim}/2 \qquad |x_k| \le x_{\max} \quad |v_k| \le v_{\max} \quad |\dot{v}_k| \le \dot{v}_{\max}$$

$$\left| \theta_k + T_1.\omega_k + \frac{T_2^2}{2}.d\omega_k/dt \right| < \theta_{pitch,roll\,\lim}/2 \qquad |\theta_k| \le \theta_{\max} \quad |\omega_k| \le \omega_{\max} \quad |\dot{\omega}_k| \le \dot{\omega}_{\max}$$

E. Motion perception threshold

As mentioned in published results of Max Planck Institute [Bey1], human self-motion perception involves the contribution of different sensory systems and central mechanisms: the visual, vestibular, tactile and kinesthetic sensors along with brainstem and higher cortical processing. One of the interesting results reported is that the linear acceleration perception threshold can be described by a power law (cf. figure 4).

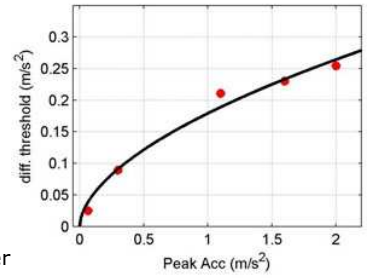

Fig. 4: Differential threshold for vertical translation increases with stimulus intensity in accordance with Steven' power law (from [Bey1])

According to the result of figure 4, the linear motion perceptual threshold increases with the acceleration level. Compared with our braking law (14), this allows us to choose the best T parameter based on the simulator performance and simulation requirements. The figure 5 gives an example for tuning T and u_{thd}.

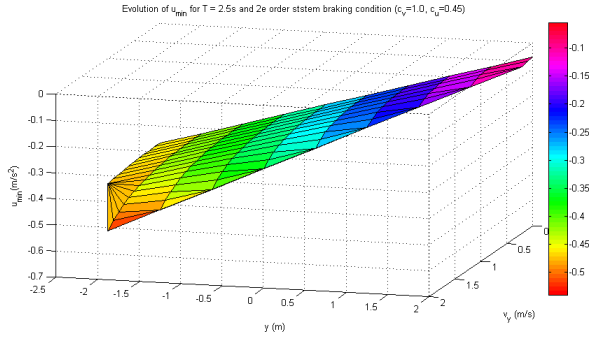

Fig. 5: Evolution of u_{min} from (14) in function of lateral position, y_0, and velocity, v_{y0}, for T = 2.5s and c_v=1, c_u=0.45

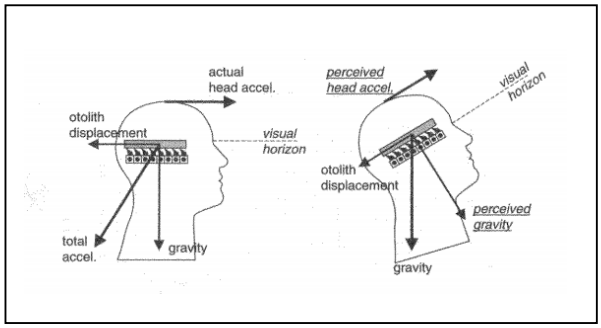

Fig. 6: Tilt coordination principle (from [Rey1])

$\gamma_{tilt} = g.\sin\theta \cong \gamma.\theta$ for $|\theta| < 0.2$ rad

Although the rail system can provide a satisfied acceleration level for slalom or sinus test, for rendering a sustained acceleration, the tilt coordination technique is necessary. This technique is based on the fact that the vestibular system cannot distinguish between inertia force produced by a linear acceleration and the effect of gravity (cf. fig. 6).

Distortions of the subjective vertical sensation may occur when the tilt angle exceed 20~30° (Aubert effect) [Rey1], therefore sustained acceleration simulated by tilt coordination should not exceed 0.5 g.

Since the driver is very sensitive to the tilt rate or the tilt acceleration [Rey1], the tilt rate should be within driver's perception threshold. Generally, it is found that the tilt rate is about 2~4°/s. However, in a driving simulator, this value is too limited to reproduce a realistic driving simulation. In practice, the tilt detection thresholds may be significantly raised above the theoretical level. For example, the PSA subjective tests at VTI simulator [Cha1] have provided higher tilt rate thresholds which increase with the linear motion level and are given in the following table:

Table 3: parameter settings From PSA paper [Cha1]

Perception threshold	$\gamma_{x, y}$ linear acceleration	
	0 m/s²	**1m/s²**
Linear acceleration	0,15m/s²	0,15m/s²
Tilt rate	2°/s	6°/s
Tilt acceleration	8°/s²	11°/s²

In a subjective ratings study of a 6dofs simulator, Fisher et al. [Fis2] have found that, for an emergency braking maneuver, the participants ratings of realism were better in high tilt rate (30°/s) condition than in low tilt rate (3°/s) one.

For 8dofs simulator, it's better to perform with the hexapod only the tilt motion, given that the system delay between rail and hexapod could be different, e.g., Renault's simulator ULTIMATE has 200ms for rail system and 80ms for hexapod at 0,2Hz [Fan1]. To exploit completely the performances of hexapod and rail systems for rendering a linear acceleration, we have to integrate the different actuator systems in the state-space model. This is a new future subject that we can treat with the MPC technique. The tilt rotation axe based on the head position can produce a close equivalent acceleration due to the human's tilt-translation ambiguity. But this rotational motion will also generate a linear motion at the seat position. The driver can detect this acceleration, given by $h.d^2\theta/dt^2$, if its level is high enough, where h is the distance between head and seat and θ, the tilt angle. For tilt acceleration threshold of 11°/s², its corresponding linear acceleration in seat is about to 0,2m/s² (with h=1m e.g.). This value may be found by chance in accordance with vestibule or self-motion detection thresholds. As the first tuning parameters, we have fixed: $|\theta| < 12°$; $|d\theta/dt| < 6°/s$; $|d^2\theta/dt^2| < 11°/s^2$.

Some special constraints can be added to adapt the driver perception threshold with linear acceleration level.

III. Simulation and experimental results

A. 1 DOF simulation result

Figure 7 illustrates the workspace exploited by MPC algorithm using proposed invariant set with N=5 and Nc=2. With a bigger number N (>200), the available workspace can be almost covered. Whilst with the standard LQ invariant set method provided by MPT, the N should be superior to 500 to reach an acceptable workspace (see fig. 8).

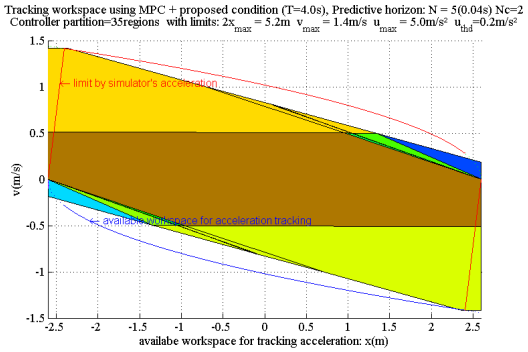

Fig. 7: Workspace used by MPC algorithm based on proposed law (N=5 and Nc=2)

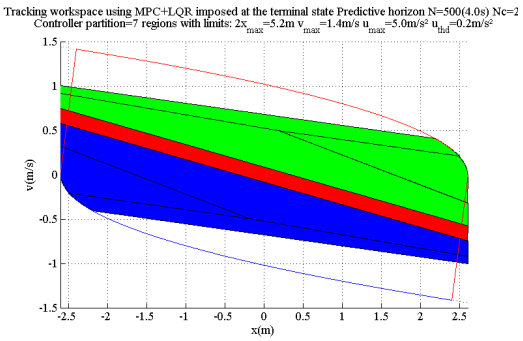

Fig. 8: Workspace covered by MPC algorithm based on standard LQ invariant set (N=500 and Nc=2)

Figure 9 shows an example of motion cues for lateral acceleration given by MPC algorithm. The reference signal measured from slalom driving test is quite well restituted.

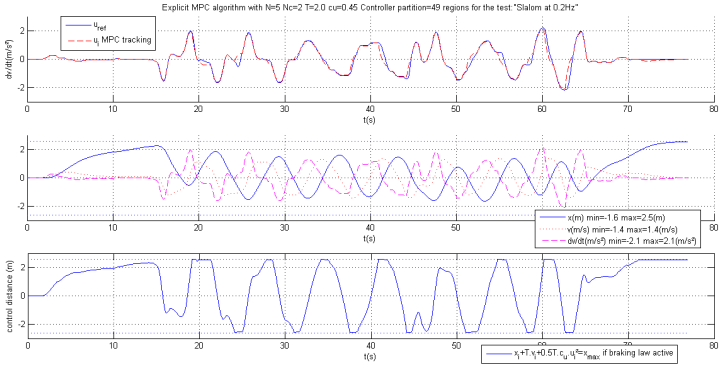

Figure 9: Illustration of lateral acceleration rendering for slalom test (top: rendering acceleration; middle: simulator state; bottom: braking control law is activated if blue line is statured)

Fig. 10 illustrates the motion cues given by the explicit MPC algorithm designed for different parameter settings T.

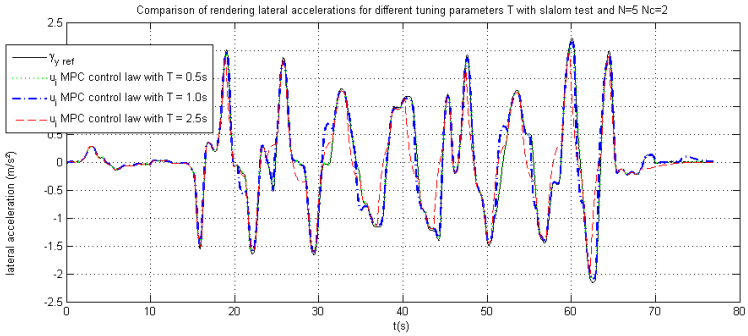

Fig. 10: Slalom test motion cues given by different parameter settings, T

For the current test, the rendering acceleration, given by the parameter setting T=0.5s, is superposed with the simulated car one. For the rendering result obtained with T=1.0s, 2~3 false conflicting cues are observed. In the case of the algorithm designed with T=2.5s, the braking phases appear more frequently, but the big conflicting false cues are reduced. Generally, the lower the value of T is, the lower the error between the restituted and the simulated acceleration is, but also the riskier it is to have big false cues.

Figure 11 displays a conventional tracking result: the pursuit of tilt angle. The reference signal from the paper [Cha1, PSA] corresponds to a lateral acceleration. It results from a double lane change maneuver followed by a 100m radius curve with vehicle speed of about 70km/h. The scenario is difficult to render with a universal algorithm without road information. The original authors have done a theoretical analysis through non delay classical filter (off-line simulation) and proposed an algorithm switching to render the first part of high-frequencies signal by rail's linear acceleration, whereas the second part by the combination of the tilt technique with the linear acceleration. We can find that the classical filter and the optimal filter provide very similar rendering results and have important delay. The MPC algorithm can provide non delay rendering result. Note that for the rapid acceleration signal, the false cues are also evident for the MPC algorithm owing to the tilt rate limit. However, as LP and HP filters' combination method, these false cues can be removed by using the linear rendering MPC algorithm for high frequencies signal and the tilt technique MPC algorithm for remaining signal. But it should be more reasonable to perform the motion cueing optimization with 2dofs motions at the same time. The next paragraph will discuss this issue.

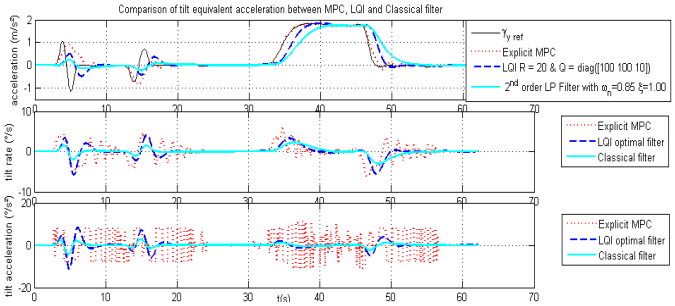

Fig. 11: Tilt equivalent acceleration from MPC, LQI and classical filter

B. 2 DOF simulation results

The motion cues for vehicle's x,y,z linear accelerations associated with corresponding rotation motions can be treated independently with simulator's corresponding linear motion and tilt rotation, here called 2dofs optimization for which a corresponding MPC explicit algorithm is developed. Using the same reference signal of PSA mentioned in the above paragraph, we compared the performances of classical filter, adaptive filter, optimal filter, and explicit MPC algorithm.

The classical and the optimal filters have been tuned only for the concerned reference signal, thus leading to an ideal theoretical result. They have not been validated for a free driving test. On the contrary, the explicit MPC algorithm is a general algorithm, applicable for free driving tests.

The classical filter gives a bad motion cueing result with some distortion phase for the first part and relatively important phase delay for the second part (cf. fig. 12). The UTIAS adaptive filter uses a cost function without tilt acceleration limit. According to the simulated result (see fig. 13), it is necessary to introduce this constraint. The rendering result with this technique is similar to that of classical filter for the first part of high frequencies signal and is better than the classical filter for the second part of low frequencies signal. But this conclusion may be wrong if the tilt acceleration constraint is taken into account.

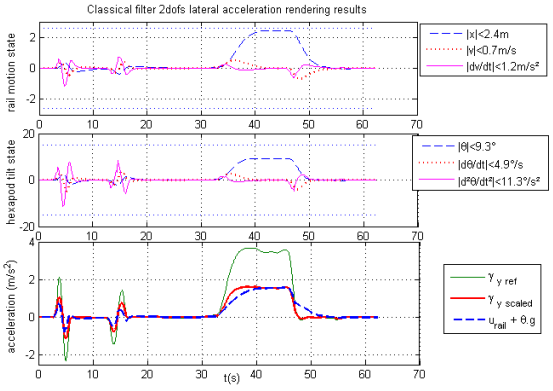

Fig. 12: Classical filter lateral acceleration rendering results

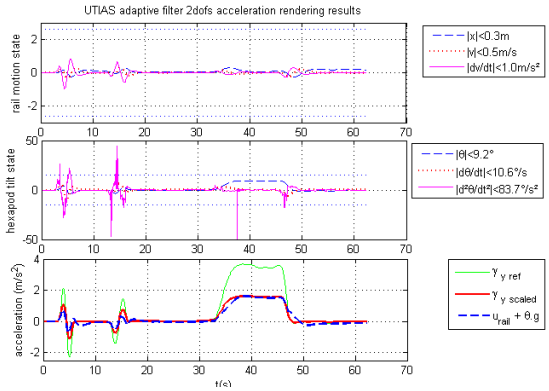

Fig. 13: Adaptive filter acc_y rendering results

The optimal filter gives an interesting result (see fig.14). But the tilt acceleration level is not acceptable. It's difficult and probably impossible to find the appropriated weight matrices to respect the tilt acceleration limit without it in the input signal. The figure 15 presents explicit MPC algorithm acceleration rendering results for which the tilt acceleration is actually controlled under the human perceived threshold limit. The result is better than the optimal filter one.

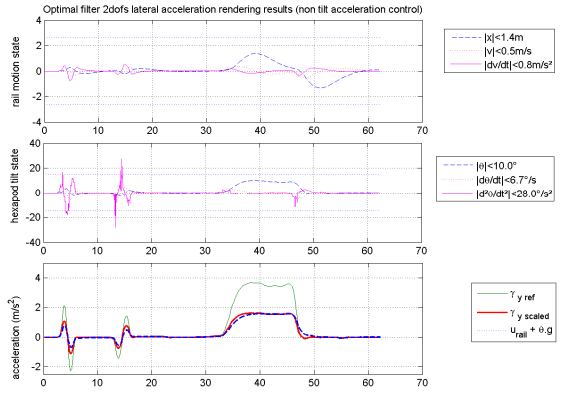

Fig. 14: Optimal filter 2dof γ_y rendering results

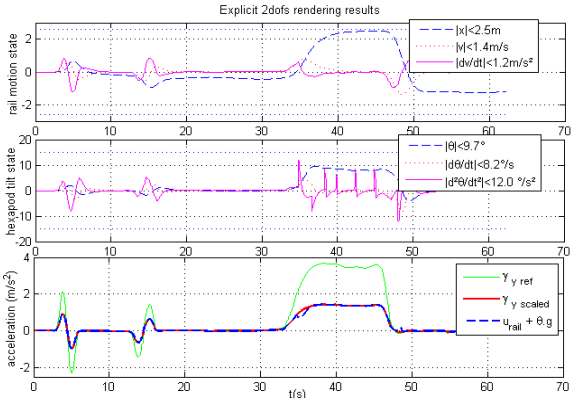

Fig. 15: Explicit MPC 2dof γ_y rendering results

In practice, we can adapt the algorithm for each scenario, e.g., using the pre-position technique like that analysed by Chapron et al. [Cha1] to optimize the simulator's workspace. This technique can be easily treated in the cost function. This corresponds to the tuning process task, not discussed here.

C. Driving test results

The first tuning of the MPC algorithm has been evaluated with an unlimited tilt acceleration control. The effect of tilt acceleration is obviously perceived by the driver and measured by CrossBow inertial system, fixed under platform. The weight coefficient for tilt rotation is not optimized. The second tuning MPC algorithm is prototyped by tilt acceleration control, i.e. $|d^2\theta/dt^2| < 11°/s$, $|d\theta/dt| < 8°/s$, $|\theta| < 12°/s$. The weight coefficients for linear acceleration input signal and for tilt rotation are modified. The effect owing to the tilt acceleration is considerably reduced. The driver feeling is improved. The evaluation of different tunings is planned in our future work.

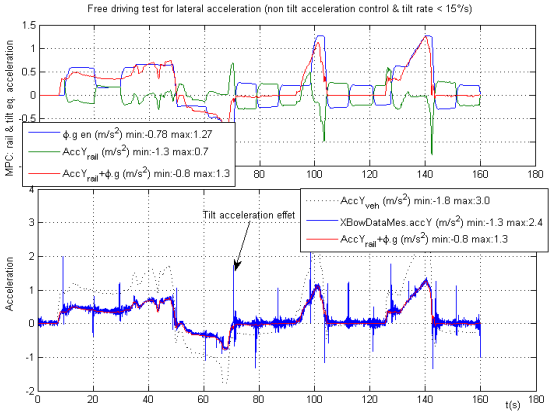

Fig. 15: Free driving test for sustained γ_y
(bad tuning parameters & high tilt acc. threshold: $|d^2\theta/dt^2|<60°/s^2$)

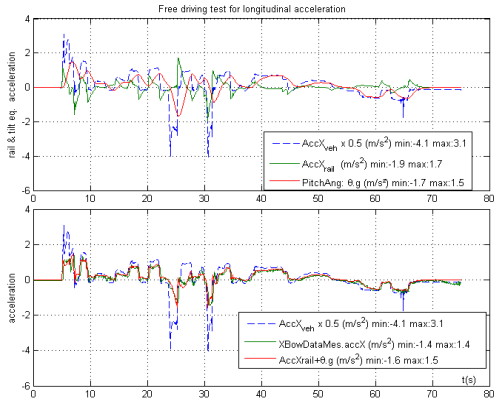

Fig. 16: Free driving test for γ_x
(improved tuning paramete rs)

IV. Conclusions

This paper presents a novel algorithm, called MPC explicit algorithm. An appropriated workspace limit condition, or in other words, a special adaptive filter is proposed, which can achieve the complicated 2dofs optimization by MPC explicit algorithm, so it reveals a new way to develop future MPC motion cueing algorithm. In comparison with the MCA used in flight simulators by NASA, Thales, TNO (optimal filter or in-line optimal filter) or in driving simulator (VTI, PSA, TNO, Ford, NADS etc., classical filter and optimal filter), the MPC algorithm possesses one important advantage: the ability of integrating the simulator's performances and the driver's perception threshold constraints into its optimization process. In such way, real optimal motion cueing results can be reached. Compared with classical filter method, the MPC algorithm can significantly reduce the distortion phase and the delay. In terms of tuning, it is also much easier than with the optimal method.

The first driving tests showed an interesting result. In combination with other information such as road situation and driver's attention, we can still improve the performance of the algorithm. We will prepare a series of test scenarios to evaluate the performance of the proposed algorithm and the optimal filter.

The relatively high number regions for some complicated constraints of the algorithm may provoke high computational costs, although the calculation formulation is very simple. Finding efficient algorithm to reduce polyhedral states-space, or using a parallel algorithm will promote this technique application in the field of driving simulator.

References

[Gra1] Grant P., Artz B., Blommer M., Cathey L., Greenberg J., "A paired comparison study of simulator motion drive algorithm" , DSC Europe 2002 Proceedings, Paris pp. 75-88

[Fis1] Fischer M., Sehammer H. and Palmkvist G., "Motion cueing for 3-, 6- and 8-degrees-of-freedom motion systems", DSC Europe 2010 proceedings, Paris, France

[Fis2] Fischer M. and J. Werneke, "The New Time-Variant Motion Cueing Algorithm For The DLR Dynamic Driving Simulator", DSC 2008, Monaco

[Cha1] Chapron T., Colinot J.P., "The new PSA Peugeot-Citroën Advanced Driving Simulator – Overall design and motion cue algorithm", DSC North America 2007 proceedings, Iowa City

[Ron1] Ronald A. Hess. " Prediction of aircraft handling qualities using analytical models of the human pilot", J. NASATM84 233, 1982, 1-16

[Tel1] Telban Robert J., Weimin Wu, and Frank M. Cardullo, " Motion Cueing Algorithm Development: Initial Investigation and Redesign of the Algorithms", NASA /CR-2000-209863

[Tel2] Telban Robert J. and Frank M. Cardullo, "Motion Cueing Algorithm Development: Human-Centered Linear and Nonlinear Approaches", NASA /CR-2005-213747

[Nah1] Nahon M.A., L.D. Reid and J. Kirdeikis, "Adaptive Simulator Motion Software with Supervisory Control", Journal of Guidance, Control, and Dynamics, vol.15, no.2 pp.376-383, 1992

[Siv1] Sivan R., Ish-Shalom J., and Huang J. K., "An Optimal Control Approach to the Design of Moving Flight Simulators", IEEE Transactions on Systems, Man, and Cybernetics, 1982. 12(6): p. 818-827

[Che1] Chen S.H., and Li-Chen Fu, "An Optimal Washout Filter Design with Fuzzy Compensation for a Motion Platform", 18th IFAC World Congress Milano, Italy August 28 - September 2, 2011

[Dag1] Dagdelen M., G. Reymond, A. Kemeny, M. Bordier, and NadiaMaýzi (2009). "Model-based predictive motion cueing strategy for vehicle driving simulators", Control Engineering Practice, Vol. 17(No. 9), 2009, pp. 995–1003

[Aug1] Augusto B.D.C., "Motion Cueing in the Chalmers Driving Simulator: An Optimization-Based Control Approach", Master of Science Thesis, 2009

[Kva1] Kvasnica M., "Real-Time Model Predictive Control via Multi-Parametric Programming: Theory and Tools", VDM Verlag (October 29, 2009)

[Pek1] Pekar J., V. Havlena, "Design and analysis of model predictive control using MPT ToolBox", http://dsp.vscht.cz/konference_matlab/matlab04/pekar.pdf, 2004

[Bem1] Bemporad A. and M. Morari, "Robust Predictive Control: A Survey", Robustness in Identification and Control, vol. 245, pp. 207-226, 1999

[Bem2] Bemporad A., M. Morari, V. Dua, E.N. Pistikopoulos, "The explicit linear quadratic regulator for constrained systems", Automatica 38(2002) 3-20

[Mor1] Morari M. & Jones C. et al., "Real-time Optimization for Distributed Model Predictive Control", 2010, Automatic control Laboratory, ETH Zürich

[Bey1] Beykirch K, Barnett-Cowan M, Zaichik L, Bos J, Ledegang W., "Human Motion Perception" http://www.kyb.tuebingen.mpg.de/research/dep/bu/motion-perception-in-vehicle-simulation/human-motion-perception.html

[Rey1] Reymond G, Kemeny A., "Motion Cueing in the Renault Driving Simulator", Vehicle System Dynamics, 34(2000), pp. 249-259

[Fan1] Fang Z., Reymond R., Kemeny A., "Performance identification and compensation of simulator motion cueing delays", DSC Europe 2010 proceedings, Paris, France

Electric vehicle's stability study on low friction road based on driving simulator

Z. Fang[1], A. Kemeny[1,2], C.S. Guo[2], R. Deborne[1], Th. Denoual[1,3], M. Alirand[4]

[1]: RENAULT, Technical Centre for Simulation, 78280, Guyancourt, France, zhou.fang@reanult.com, andras.kemeny.@renault.com, renaud.deborne@renault.com

[2]: Arts et Métiers Paris Tech, 2 rue Thomas Dumorey, Chalon-sur-Saône, France, chunshi.guo@ensam.eu

[3]: IRCCyN, 1 rue de la Noë, BP 92101, 44321 Nantes Cedex 3, France, thomas.denoual.renexter@renault.com

[4]: LMS Imagine, 42300, Roanne, France, marc.alirand@lmsintl.com

***Abstract**: This paper presents an overview of EV driving simulation development work on ULTIMATE simulator of Renault, Technical Center for Simulation (TCS). A user case of driving on packed snow road is developed in order to analyze the stability of the EV with regenerative brake on the one hand and to prepare the future ESC tuning scenario on the other hand. The real-time vehicle's dynamics model and the tyre model on low friction road are the prerequisites for achieving the realistic driving simulation. First of all, a process from Adams/Car multi-body dynamics to real-time functional model, such as MADA (internal vehicle dynamics model) or AMESim, is developed by TCS. Secondly, a special adjusted Pacejka internal model based on packed snow road measures is used in the vehicle's model. As the result, the precise modelling associated with a tilt coordination explicit MPC motion cueing algorithm gives a close fidelity of driving simulation.*

***Keywords**: EV stability, regenerative brake, packed snow driving, driving simulator, low friction tyre model*

I. Introduction

The design of electric vehicle has brought new challenges into the driving dynamics and drivability domains. The high torque dynamics of electric motors lead to particular problems such as motor oscillation in the transmission, torque splitting between the standard hydraulic braking system and the regenerative brake, or the stability problem in case of slippery roads. For instance, it is well known that Split-μ and tip-out in curves are typical manoeuvres under which the electric motor response has a great influence on vehicle stability.

During vehicle development, the indispensable different validation tests are currently carried out with physical prototypes and different configurations of ADAS systems for fulfilling the requirements of security, handling, drivability, durability etc.. These tests not only bring about high costs but also influence the project development cycle, among which the vehicle handling and stability behaviours evaluation on low friction road is a significantly costing one for different purposes (ESC tuning and validation, vehicle's stability, security study etc…). Generally, these tests are achieved by professional testers. However, as mentioned by van Zanten et al [Zan1], "The concept of the vehicle including the tires and the suspension should very strongly account for the normal human behavior", it is because the reaction of a normal driver is very often different in critical low friction situation compared with that of a professional tester. The driving simulator could be considered as an interesting test platform to accomplish these tasks. Actually, simulators are used as efficient virtual test platforms for the security evaluation [Pap1, Wat1, Bro1] and the subjective evaluation for optimizing the chassis design and ESC tuning [Wus1].

What's more, due to shorter time and more economic constraints, it becomes more and more important to expand the numerical simulation technique into the vehicle development process. Therefore, it is crucial to develop the robust numerical simulation to assess vehicle's dynamics behaviours. RENAULT's idea is to perform driving simulation in early stage of the vehicle development and integrate the driver in loop in order to highlight the stability problem and ESC tuning validation. The objectives of the RENAULT TCS are: (1) developing almost 100% numerical process for vehicle dynamics by using driving simulator, (2) performing driving simulations in the early stage of vehicle projects for engineering applications and studies of driver perception or behaviour.

The above concerns conduct us not only to develop a simulator engineering application: electric vehicle stability evaluation on low friction road, but also to redevelop the processes for driving simulation (The visual rendering of the simulation is considered here as a relative achieved technique):

- dynamics model integration process
- new motion cueing algorithm for 8 dofs simulator [Fan1]
- new feedback force control systems for steering wheel system and accelerator pedal

II. Development of a real-time vehicle's dynamics model

The vehicle's dynamics modelling plays a key role in driving simulation. Currently, the Adams/Car multi-body dynamics model, as well as other car's dynamics functional model, are used in Renault during vehicle's project development. The Adams/Car simulation results are compared with those of a real car and at this basis the model is improved if needed during its validation phase. Thus, the Adams/Car's model can be considered as the reference for the validation of vehicle's functional model used in simulator real-time environment. MADA (Modèle Avancé de Dynamique Automobile, Renault's internal model) and AMESim (LMS commercial software), both using suspension look-up tables provided either by K&C test rig or Adams/Car simulation, are integrated in SCANeR Studio™ software. This chapter describes the efforts made by TCS on building such models. The tyre model has a critical effect on packed snow road simulation results. Thanks to the work of internal vehicle's dynamics team, a well adjusted internal Pacejka model based on packed snow road measures was integrated in the vehicle's dynamics model. As for the steering system, a simplified real-time system model is proposed and the parameters are tuned by means of the comparison with a real car's feeling. A powerful Sensodrive steering wheel was recently installed in ULTIMATE to improve the steering wheel force feedback rendering.

Due to the AMESim modularity, its collection of physical model libraries and its rapidity for prototyping numerical development, it is chosen as current EVs dynamics integration platform (see fig. 1). Note that the process to build the functional model is similar in AMESim as in MADA.

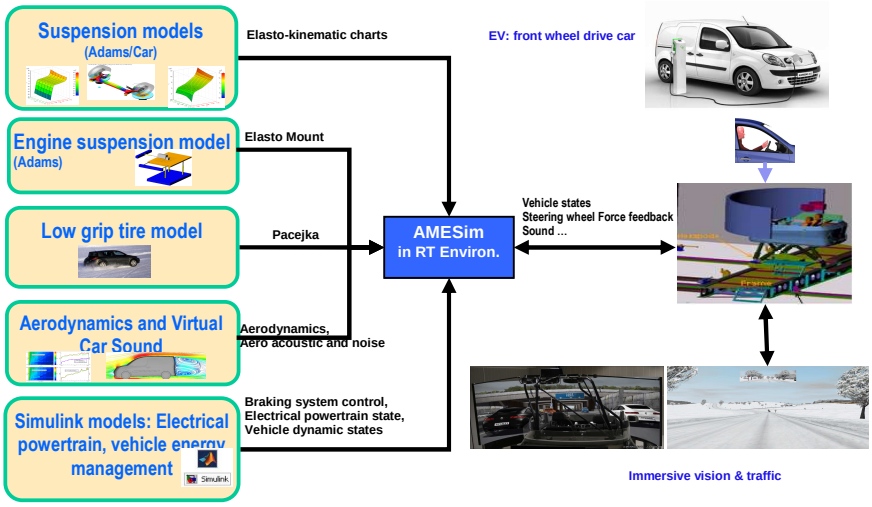

Fig. 1: Electrical vehicle models development & integration on the simulator

II.1. Vehicle's sub-system models development

a. Steering and Suspension model

The current EV suspension model is based on ADAMS/Car™ which has been validated with K&C measurements. Some important lateral suspension parameters are presented in Table 1 under the standard RENAULT index.

Table 1: Correlation ADAMS vs K&C measurements

Axle	Method	Wheel Steering angle induced by roll	Camber angle induced by roll
Front	Adams/Car	-9,3%	75%~82%
	K&C rig	-9,6%	82%
Rear	Adams/Car	3~6%	59%
	K&C rig	2%	58%

To obtain accurate suspension parameters, the flexible bodies (front sub-frame, suspension arm, stabilizer bar etc.) for front and rear axles are introduced into the ADAMS/Car™ model thanks to NASTRAN™. The bushing parameters (stiffness and damping) come from experimental measurements.
Starting from this, the suspension of the AMESim vehicle model is adapted by taking into account the suspension kinematic as well as the elasto kinematic (bushing contribution). The suspension kinematics are in form of look-up tables and the deformation of the suspension under five tyre forces are evaluated by a first order coefficient matrix

(see equation 1), all provided by ADAMS/Car™. The elastic contributions of the suspension bushings are considered as quasi static phenomenon on the one hand and as a compliance to correct the wheel centre location and the wheel orientation under tire forces and torques on the other hand.

$$\begin{bmatrix} \Delta x \\ \Delta y \\ \Delta \varepsilon \\ \Delta \eta \\ \Delta \delta \end{bmatrix}_{elas} = \begin{bmatrix} C_{xFx} & C_{xFy} & C_{xTx} & C_{xTy} & C_{xTz} \\ C_{yFx} & C_{yFy} & C_{yTx} & C_{yTy} & C_{yTz} \\ C_{\varepsilon Fx} & C_{\varepsilon Fy} & C_{yTx} & C_{\varepsilon Ty} & C_{\varepsilon Tz} \\ C_{\eta Fx} & C_{\eta Fy} & C_{\eta Tx} & C_{\eta Ty} & C_{\eta Tz} \\ C_{\delta Fx} & C_{\delta Fy} & C_{\delta Tx} & C_{\delta Ty} & C_{\delta Tz} \end{bmatrix} \begin{bmatrix} F_x \\ F_y \\ T_x \\ T_y \\ T_z \end{bmatrix} \quad (1)$$

The suspension vertical stiffness and the associated damper in damper directions (damper rate and its ratio to convert vertical velocity into damper velocity) as well as the roll stabilizer are taken into account with tables as shown in Figure 2., which is the standard solution in RENAULT to model a suspension for functional design. A special Adams2AMEsim suspension conversion tool is developed to generate automatically the elasto-kinematic tables.

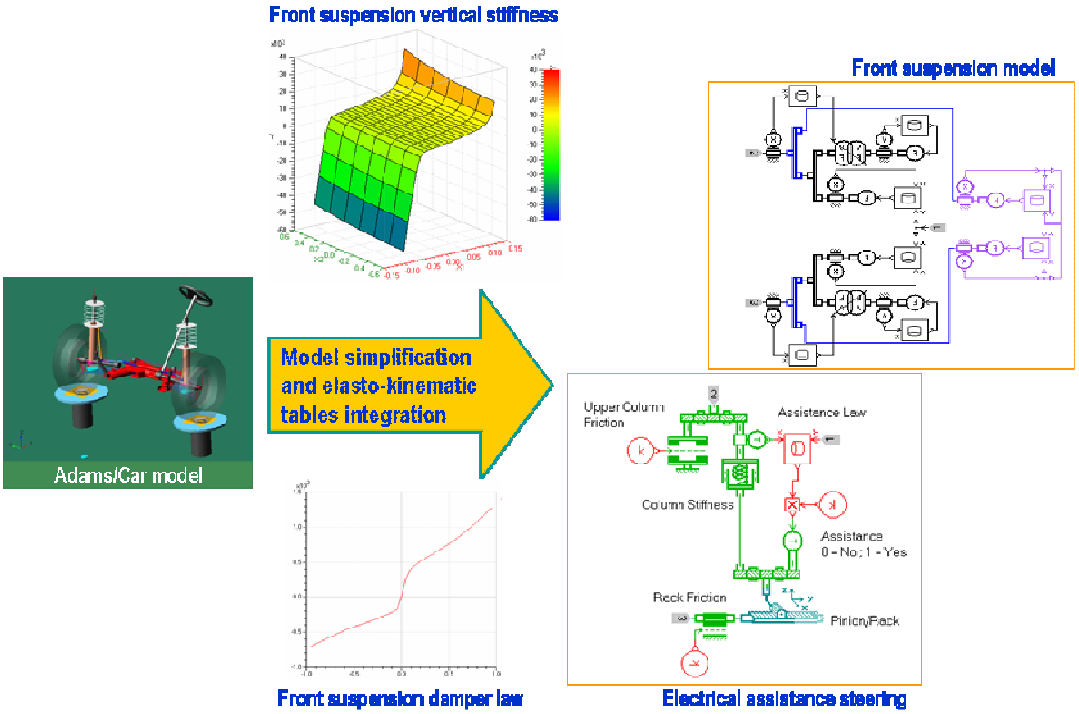

Fig. 2: Suspension and steering models from Adams/Car to AMESim functional model

An electrical assistance steering system is modelled with rack friction non linear model. The assistance law is obtained from available similar system, which is a function of vehicle's speed and measured steering torque. A powerful sensor driver (30N.m) system is newly equipped in ULTIMATE to improve the steering wheel force feedback rendering.

b. Power-train model and regenerative brake controller

The studied EV is based on existing thermal engine vehicle whose thermal engine is replaced by an electric motor with its inverter. The mass of these components is as important as that of the thermal engine. The motor suspension system including these components and motor mounts may greatly influence the drivability and ride comforts in some range of frequencies. In Renault's numerical process, they are modelled by ADAMS/View™ for the engine workspace, mounts durability evaluation and suspension design (kinematics and bushings). The model built here inherits from this simulation tool since most of the parameters are from ADAMS™.
The details of engine's dynamic model, as well as the corresponding Adams model, are illustrated in figure 3 where the flywheel of the motor is included into the "engine" icon representing the engine bloc (see fig. 3).

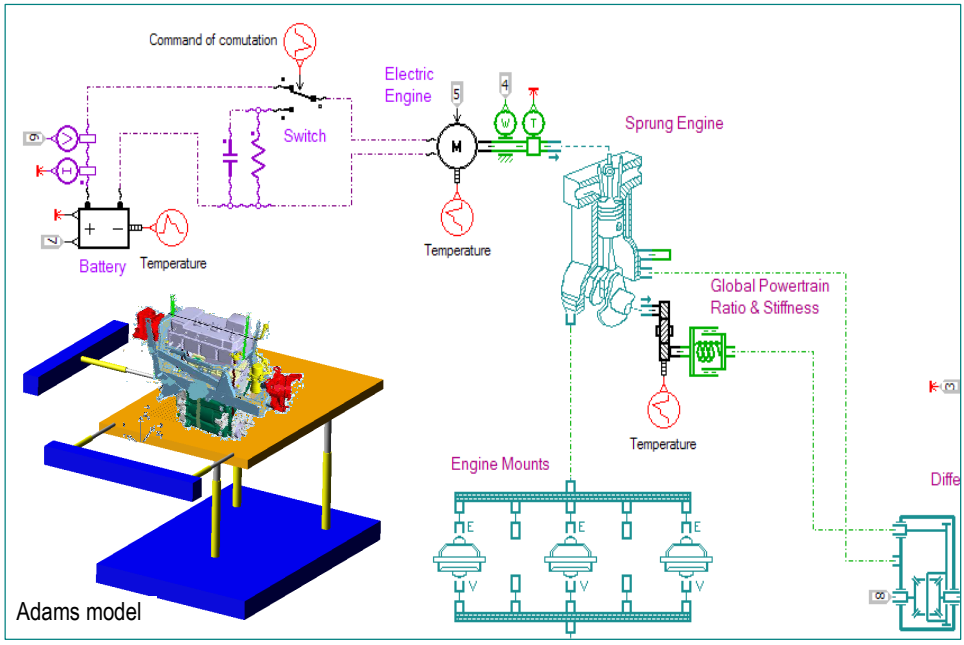

Figure 3: Motor adaptation and ADAMS model

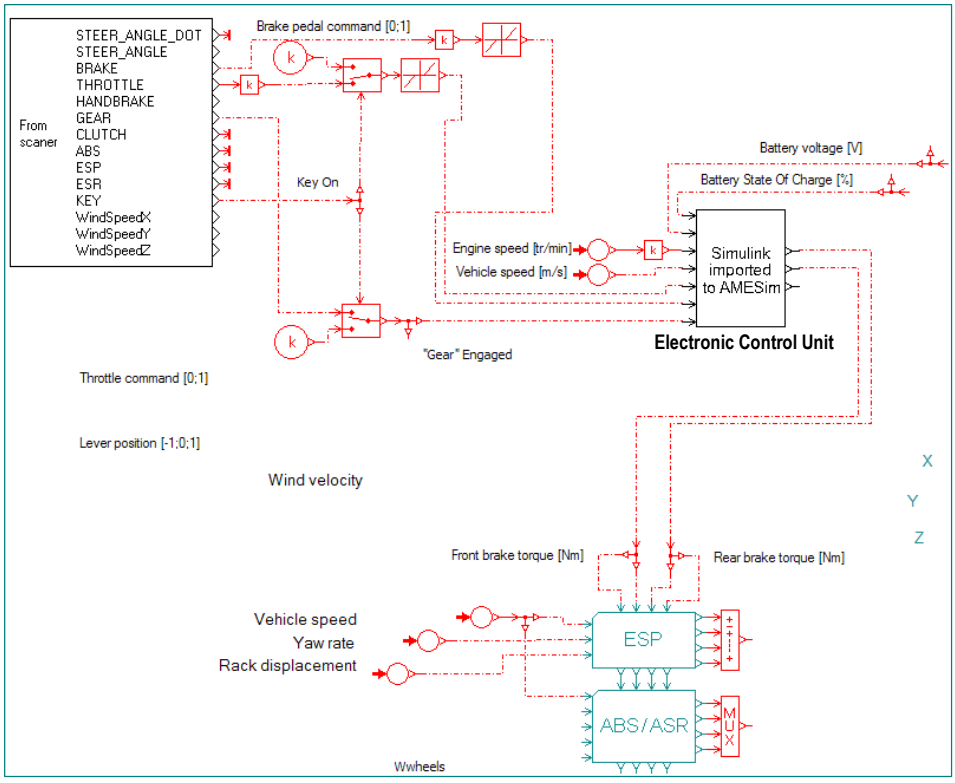

Figure 4: Connection for the Simulink imported model of the regenerative brake controller

Regenerative braking is an integral part of hybrid and electric vehicles. Regenerative braking re-captures and stores part of the kinetic energy during the stopping (at least deceleration) process that would otherwise be lost into heat and then utilizes it to recharge the electric batteries within driver's acceptable disturbed level. It is a truism to say that only the driven axle(s) can capture the regenerative brake energy.

As to the control logic of the regenerative brake, the internal Electronic Control Unit (ECU) in Simulink model [Ell1] has been integrated directly in AMESim thanks to its compatibility with RTW as an equivalent C code (see fig. 4).

This was done in order to produce only one *.rtdll for the ULTIMATE environment under control of SCANeR Studio™, thus making the integration much simpler.

c. Tyre model on low friction road

It is well known that the fast response of the electric motor influences the drivability as well as the driving dynamics aspects. Split-μ and tip-out in curves are typical manoeuvres under which the electric motor response has a great influence on vehicle stability. In order to highlight the stability problems, some efforts have been made on tire parameters to represent low adherence surface, mainly packed snow.

The Pacejka magic formula is a standard for vehicle dynamics simulation. For a low grip road such as packed snow or icy road, the standard model deduced from high adherence test rig cannot be extrapolated to these low grip roads. According to [Lac1], the magic formula model is not well suited for vehicle parameter analysis on vehicle stability performance if snow and ice are considered on the road surface. Despite this restriction, RENAULT has elaborated a procedure for parameter identification that works well for packed snow road. Figure 5 shows a comparison among experiments, a representative physical model presented in [Lac1] and the RENAULT's Pacejka model estimation based on the similar commercial car tyres.

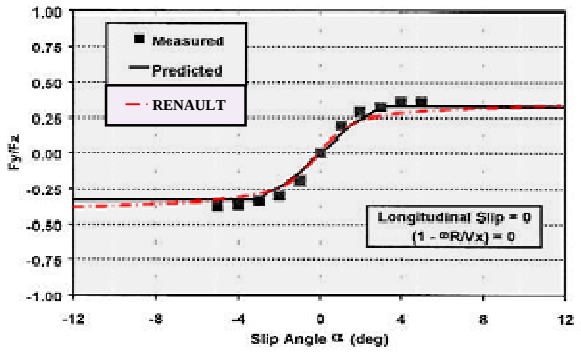

Fig. 5: Comparison between brush tire model [Lac1] and Renault's Pacejka model on packed snow road

d. Aerodynamics model

Based on the experiences and theoretical analysis, the aerodynamic resistance can be evaluated by a simple relation valid for turbulent flow:

$$F_{aero\ i} = 0.5.SC_i(\theta).\rho.V^2 \qquad \text{with i = \{x, y, z for resistance force components and l, m, n for moment components\}}$$

For personal cars, when the vehicle speed is between 80~90km/h, the longitudinal aerodynamic force is at the same magnitude order of mechanical resistance. It rises quickly as the velocity increases, e.g., twice as much as that of the mechanical resistance for a highway driving. The aerodynamic effects have been considered for the driving simulator by using a table of SC_i in function of air flow~vehicle incident angle, θ.

The coefficients from CFD (Computational Fluid Dynamics) simulation are validated in experiments in wind tunnel. The values are demonstrated in Figure 6.

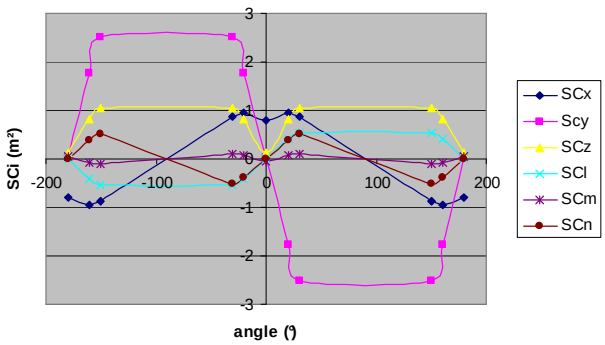

Figure 6: aerodynamics tables

II.2. Vehicle sound's model

Based on LMS Virtual Car Sound software and real car's acoustic measures, a VCS model is tuned to reproduce as closely as possible the EV's noise. The principle of audio synthesis is based on linear frequencies interpolation (see fig. 7). The aero-acoustic effect is not yet taken into account in the current model at the absence of the complementary measures.

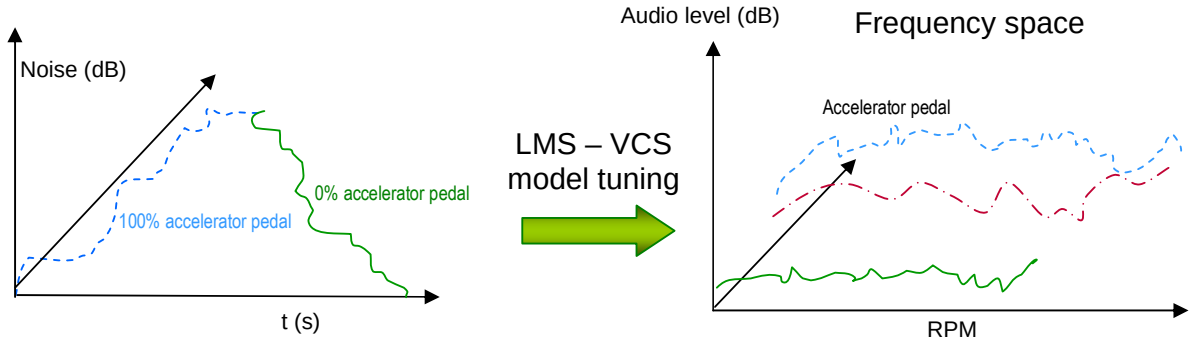

Fig. 7: Principle of audio synthesis

II.3. RTX real-time model generation and its performance evaluation

We use AMESim and RTX™ (http://www.intervalzero.com) to generate a real-time dynamic model. Runge-Kutta (R-K) algorithm is used in solving system equations. The calculation errors with different orders and time steps are evaluated to deduce the optimal combination set of the parameters involved.

a. RTX real-time model generation

The environment of a driving simulator is generally very specific. The ULTIMATE environment is based on RTX and consequently, some AMESim adaptations have been required for its integration and industrial use, including: a new developed interface with SCANeR software, the compatibility of AMESim with RTX, the improved C code optimization and compilation to allow including in one file all the modelling aspects of the vehicle inside the driving simulator, the improved start and stop features for the tire model, protections considering boundary limits of the Pacejka formulation and multi points contact handling for tire/road interaction.

b. Model's real-time performance evaluation

An analysis has been carried out to find the most efficient solver for the considered model. This analysis is based on the best compromise choice between the precision of calculation and CPU running time which are the function of time step and R-K algorithm's order. The reference values are calculated with the adaptive time step AMESim algorithm and the minimal error of simulated results for each order is given by a low fixed time step (=0.1ms) algorithm. The best compromise solution was order 2 R-K method with 1 ms as time step as shown in Figure 8.

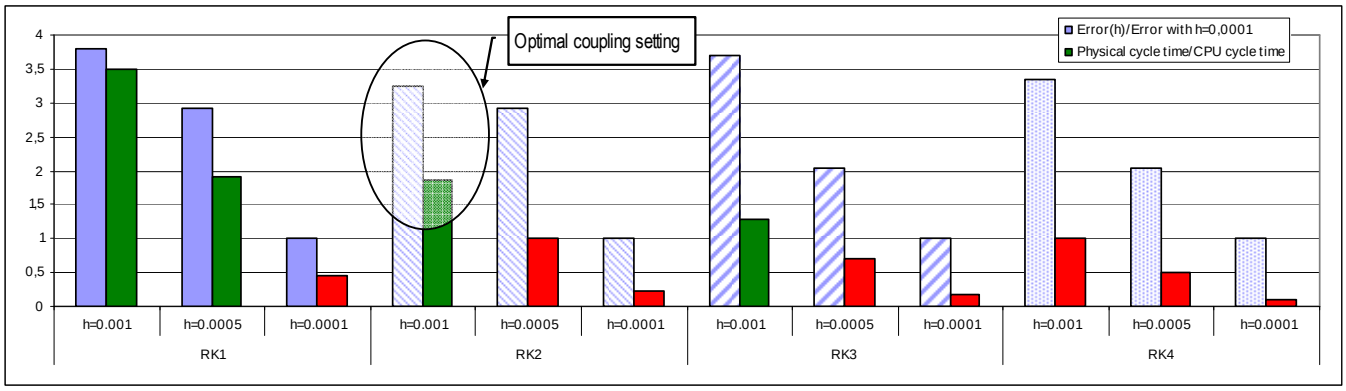

Figure 8: Comparison of the performances for different R-K algorithm's step sizes and orders

III. The ULTIMATE driving simulator's tests

II.1. The performance and limits of ULTIMATE

ULTIMATE is a high performance driving simulator based on an X-Y rail actuator system combined with a 6 degrees of freedom hexapod (Stewart platform). The driving simulator is used for vehicle dynamics engineering applications in the early phase of the vehicle design process. The motion system is driven in position by SCANeR Studio™ via a predictive motion cueing algorithm. Table 2 presents the linear motion performance limits due to actuator capability and the workspace of the simulator building.

Table 2: ULTIMATE linear motion performance limits

	X_{rail}	Y_{rail}	$X_{actuat.}$	$Y_{actuat.}$	$Z_{actuat.}$
Excursion(m)	±2,6	±2,6	±0.20	±0.20	±0.20
Velocity(m/s)	±2	±3	±0.70	±0.70	±0.40
Acceleration(m/s²)	5	6	6	6	5

The apparent lag motion feedback was deemed by some expert drivers as a disturbing factor for the subjective assessment of transverse dynamics especially under faster manoeuvres. Another problem is the attenuation of acceleration amplitude due to the system transfer function. The results from the driving simulator shown in Figure 9 illustrate this defect. The red line in Figure 9 corresponds to the simulation result, the blue dot line to the simulator's platform lateral acceleration simulated with its transfer function.

The simulator's delay (transport delay and phase delay due to its transfer function), one of the main factors for motion sickness is also measured and can be compensated by a PID controller [Fan2] or other more efficient state-space MPC algorithm (in coming). The delay between the simulation and the driving simulator around 200 ms can lead to perception troubles. In Figure 9, the green line corresponds to the result after compensation using a PID controller with better fitting (no delay).

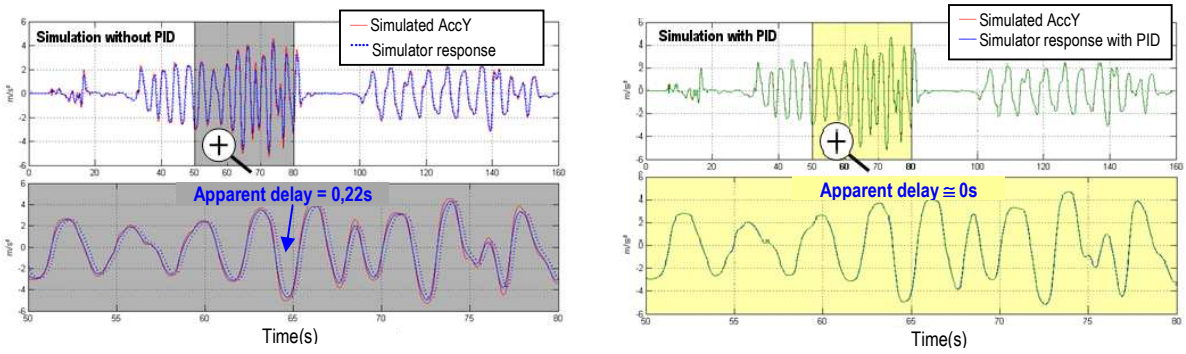

Figure 9: Slalom test with (right fig.) and without (left fig.) PID correction

II.2. Driving simulator tests

The strategy between regenerative brake and others ADAS systems should be coordinated in order to avoid conflicting decision during critical situation, such as driving in curves and losing the adherence. The driver's behaviour, as illustrated in figure 10, could influence directly the stability of vehicle in these situations. This application aims to reproduce as closely as possible the real car's behaviour to perform different tests discussed as follows:

- Tip-in and tip-out
- Low grip road with cornering maneuvers
- slalom

In scale 1 to 1, the tip-in and tip-out tests are quite difficult to be performed on ULTIMATE due to the already presented limitations (workspace and simulator performances). However for a tip-in or a tip-out with limited time schedule and with a driver having a good experience in driving simulator, the test is feasible. The first tests with professional drivers reveal that they can feel the real acceleration levels and are interested by the driving simulator.

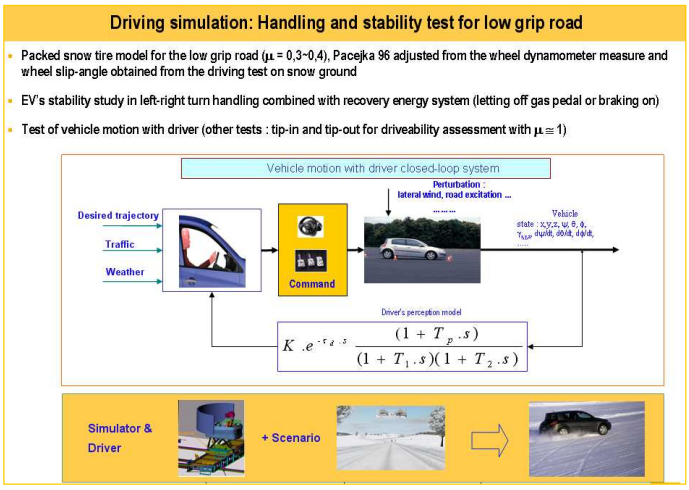

Figure 10: driving simulation on packed snow road

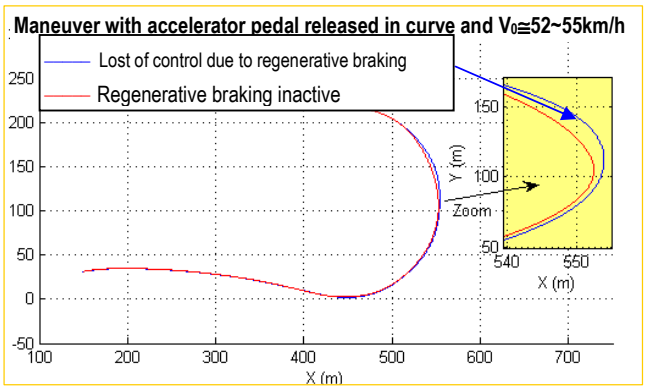

Figure 11: Vehicle trajectory in packed snow road with driver in loop

Packed snow road test aims to analyze the stability of the EV with regenerative brake on the one hand and to prepare the future ESC tuning scenario on the other hand. Note that the ESC control logic is not activated for the presented tests. Figure 11 shows the under steering phenomena in curve when releasing the gas pedal (back out or better said tip-out), with regenerative brake compared to a normal driving. Qualitatively, it can be explained by a limited adherence on the tires of the front axle since the regenerative brake is acting. The electric motor solicits more the longitudinal Fx forces and owing to the tire coupling, it reduces the lateral tire force Fy, hence leading to an under steering effect.

Figure 12 shows the decrease in lateral acceleration at time 35 seconds when the accelerator pedal is released and regenerative brake is activated. However in Figure 13 for regenerative brake disabled, even if the release of the accelerator pedal (t=20,5s) conduces a decrease in lateral acceleration, this decrease is less impressive. Note that the change in lateral acceleration may also be caused by the change in steering wheel angle.

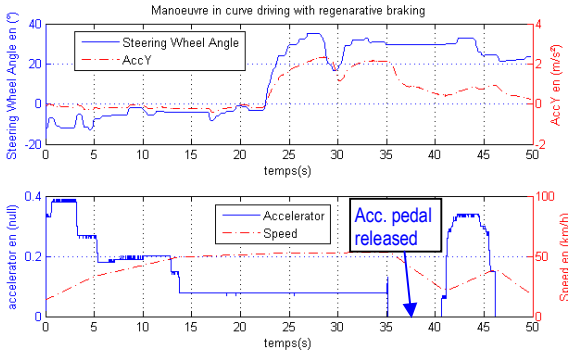

Figure 12: Tip out in curve with regenerative brake

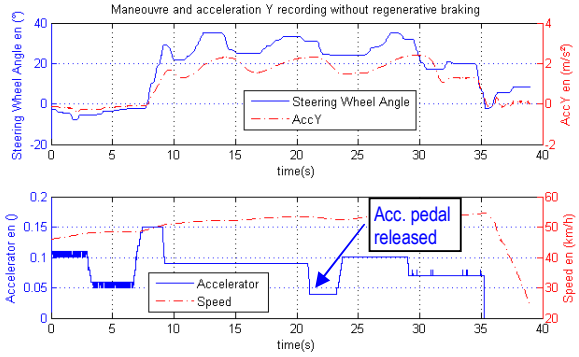

Figure 13: Tip out in curve without regenerative brake

Up to now, the regenerative brake alone has been explored within the driving simulator. As mentioned before, it is the first step to explore what can be the contributions of the driving simulator in the domain of EVs. Combining the ESC and the regenerative control laws is another foreseen task. The actual works on motion cueing algorithm adaptation and the improvement of modelling steering, braking, and powertrain systems received the promising feedbacks from RENAULT internal users of this complete virtual simulation tool (models and driving simulator).

IV. Conclusions

The feasibility to build a complete electric vehicle model from Adams/Car and Simulink controller to AMESim, able to treat with drivability, ride and handling and vehicle stability has been proven by means of running in the real time within the ULTIMATE environment. Even if the 3D vehicle model is mainly dedicated to ride and handling analyses, its adaptation as well for drivability aspects has been demonstrated.

The improvement of the model of the vehicle dynamics on low friction road and of the motion cueing algorithm has significantly ameliorated the driving simulation fidelity for the studied scenario on the ULTIMATE simulator. Promising feedbacks have already been reported by RENAULT internal users on this complete virtual simulation tool.

References

[Zan1] van Zanten A., Erhardt R. and Pfaff G., "*VDC, The Vehicle Dynamics Control System of Bosch*", SAE paper, n°. 950759

[Pap1] Y.E. Papelis, T. Brown, G. Watson D. Holtz, W. Pan, "*Study of ESC Assisted Driver Performance Using a Driving Simulator*", NADS, Iowa University, 2004

[Wat1] G.S. Watson, Y. E. Papelis, O. Ahmad, "*Design of simulator scenarios to study the effectiveness of electronic stability control systems*", NADS, Conference paper, 2005,

[Bro1] T. Brown, C. Schwarz, J. Moeckli & D. Marshall, NHTSA, "*Heavy Truck ESC effectiveness Study Using NADS*", November 2009

[Wus1] Klaus Wüst, Daimler AG, CAE Commercial Vehicles, "*Electronic Stability Program (ESP) for Trucks on the Daimler Driving Simulator*", SIMPACK News, September 2010

[Fan1] Fang Z. and Kemeny A.; "*Motion cueing algorithms for a real-time automobile driving simulator*", DSC Europe 2012, Paris, France

[Fan2] Fang Z., Reymond G., Kemeny A.: "*Performance identification and compensation of simulator motion cueing delays*", DSC Europe 2010, Paris, France, 2010, pp 111-120.

[Ell1] Eller B., Hetet J.F., André S., Hennequet G.: "*Electric vehicle platform for drivability analysis*", 8th IEEE International Conference on Control and Automation, Xiamen, China, June 2010, pp 2251-2257

[Lac1] Lacombe J: "*Tire model for simulations of vehicle motion on high and low friction road surfaces* ", SCS Proceedings of the Winter Simulation Conference, San Diego, CA, USA, 2000, pp 1025-1034

Validation of fuel consumption calculated by a driving simulator

Christoph Rommerskirchen, Thomas Müller, Klaus Bengler
Institute of Ergonomics – Technische Universität München,
Boltzmannstr. 15, 85747 Garching, Germany
rommerskirchen@lfe.mw.tum.de, tmueller@lfe.mw.tum.de, bengler@lfe.mw.tum.de

Abstract *– The driving simulator is one of the main tools for development and investigation of driving behaviour and new assistance systems. To investigate the impacts of the driver behaviour on fuel consumption in a driving simulator a validated fuel consumption calculation is needed. This work describes the validation of fuel consumption calculated by a driving simulator. Two approaches were done. One method is to compare the calculated fuel consumption with a real car. For this the New European Driving Cycle (NEDC) was rebuild in the simulator to assess the fuel consumption and to compare it with a real car. The big advantage of the NEDC is that the test is repeatable and is obligatory for every car in Europe, so comparable data is available. It can be shown that the driving simulator has a comparable fuel consumption in the NEDC to a real car. The other approach in this study was to compare the distribution of fuel consumption of real car drivers with the distribution from drivers in the simulator. The results of a study with 30 participants in the simulator showed that the resulting fuel consumption is good comparable to real car data.*

Key words: *fuel consumption, validation of driving simulation*

Introduction

The evaluation and development of driver assistance systems to reduce fuel consumption is one of the main research topics at the Institute of Ergonomics at the Technische Universität München e.g. in the project eCoMove. The goal of many studies is to identify fuel savings potential for individual drivers as well as for different situations and to develop driver assistance systems for fuel saving. The main research tool for these topics is the driving simulator with its well-known advantages. Therefore it is required to have a driving simulator which measures not only individual differences for example in acceleration or speed but also in fuel consumption. Although many driving simulators calculate fuel consumption in many cases the data still has to be validated.

Two approaches to validate the fuel consumption were done. One is to compare the fuel consumption of the driving simulator with real cars. For this approach the New European Driving Cycle (NEDC), which every new vehicle model in the European Union has to pass [CEC1], was chosen. The other approach is to compare the distribution of fuel consumption data of different car drivers from real drives with a comparable drive in the simulator. The goal is to have a simulation with which it is possible to estimate differences in fuel consumption between different assistance system or different drivers. It is not goal to simulate the exact amount of fuel on a given route because that depends in reality of the type of car, weather conditions, traffic conditions etc.

Driving simulator

In the following the driving simulator and the simulation model of the fuel consumption is described.

Hardware and simulation software

The fixed base driving simulator which needed to be validated is located at the Institute of Ergonomics at the Technische Universität München, Germany. The simulator has three projection screens for the front view with a 180° field of view. For the rear-view mirrors projection three additional projection screens are implemented. The Mock-Up is a complete BMW 6 convertible (E64) with automatic gear shift. The CAN-Bus from the Mock-Up is connected to the simulation. The standard instrumental cluster of the car was replaced by a free-programmable TFT-Display.

Fig. 1. Panorama view from inside of the driving simulator of the Institute of Ergonomics

The simulation software used is SILAB from WIVW GmbH (www.wivw.de) which allows a precise and flexible creation of driving situations as well as full control over the simulated traffic. SILAB is connected to the software CarSim in the version 7.11 from Mechanical Simulation (www.carsim.com). CarSim is responsible for the vehicle dynamics simulation including the calculation of the fuel consumption. All data from the simulation is recorded at a frequency of 100 Hz.

Simulation of fuel consumption

The simulation of the fuel consumption is part of the vehicle dynamics simulation and done by the software CarSim. It was decided to model a compact class car because it is the most common vehicle class and therefore it is the most suitable to use for comparison. Therefore a model was created with the size, weight and other parameters so that it represents a typical compact class car. A 75 kW engine model was used for simulation. It was adapted from an 150 kW engine model which is included in CarSim. This again was derived from a real car. The simulation calculates a fuel flow rate through a fuel-consumption map. The fuel consumption in liter per 100 km is calculated through the fuel flow rate, time and distance.

Validation Methods

The following chapters describe the validation of fuel consumption by using driving cycles and a driving simulator study.

Validation with Driving Cycles

The standardized measurement of fuel consumption for new vehicle models is done normally through driving cycles. A driving cycle consists of a given sequence of different speeds for a given duration and defined accelerations and decelerations. It is performed on a roller bench. The measurement is done under predefined conditions like for example outside temperature and vehicle specific conditions like cold motor in the beginning and full battery. Vehicles in Europe for example have to pass the New European Driving Cycle (NEDC) [CEC1] whereas for USA and Japan other cycles exist. The big advantage for measuring fuel consumption through driving cycles is the repeatability of the test and defined conditions which leads to a good comparability between different cars.

The New European Driving Cycle (NEDC)

The NEDC is the cycle used in Europe. Therefore it was chosen to measure the fuel consumption of the simulation with it. It is specified in the directive 70/220/EC of the Council of the European Commission. For each new car model in Europe it is obligatory to pass the test to specify the fuel consumption. The NEDC includes an urban scenario and an extra-urban scenario which are combined to the full cycle [CEC1]. The figures published from the cycle are the urban, the extra-urban and the overall fuel economy. Figure 2 shows the speed profile of the full cycle.

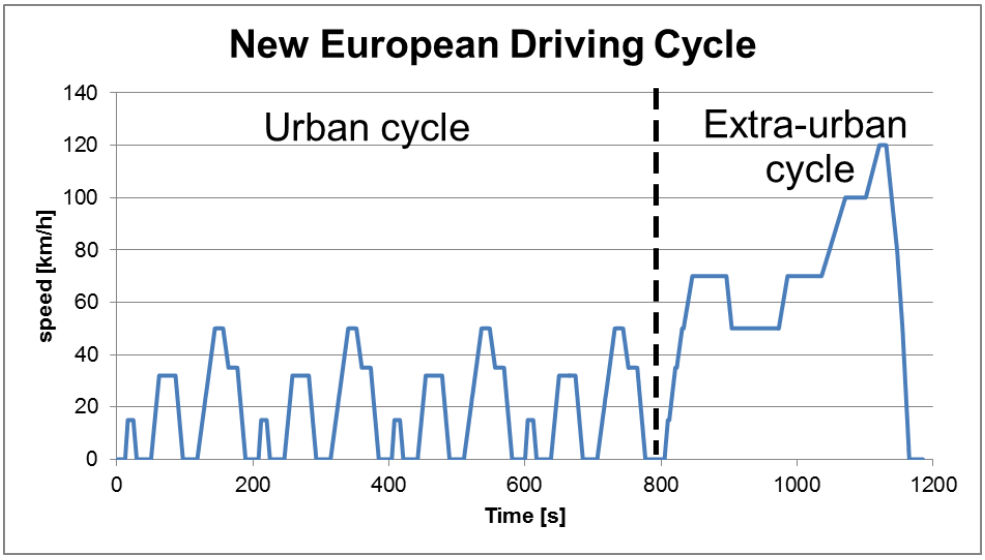

Fig. 2. Velocity profile of the full New European Driving Cycle

Newspapers and magazines (e.g. [FOC1]) often criticize the NEDC because the published fuel consumption is very often lower than the typical fuel consumption experienced during normal driving. Reasons for this are amongst others that the accelerations and the maximum speeds in the NEDC are lower than in reality and additional electrical consumers like air-conditioning or heating are switched off during the test [BAS1]. Although the NEDC does not represent the typical driving behaviour and therefore typical fuel consumption. But it is still due to the fact that the test is standardized and repeatable one of the best ways to compare different vehicles.

The NEDC in the driving simulator

The NEDC for real cars is normally performed on the roller bench. There a trained test driver gets the actually driven speed and the target speed displayed. The NEDC allows a tolerance of ±2 km/h of the defined speed [CEC1].

Fig. 3. The NEDC performed on a roller test bench with a monitor showing the target speed [FOC1]

In the driving simulator there is naturally no roller bench, so a long, straight and plain road was implemented for the test. Additionally a visualization of the NEDC was implemented in Adobe Flash and displayed in the instrument cluster. The visualization helps the test driver by showing actual speed, actual and upcoming target speed and tolerances (Fig. 4). With its support of it was possible for a test driver to perform the NEDC also correctly in the driving simulator.

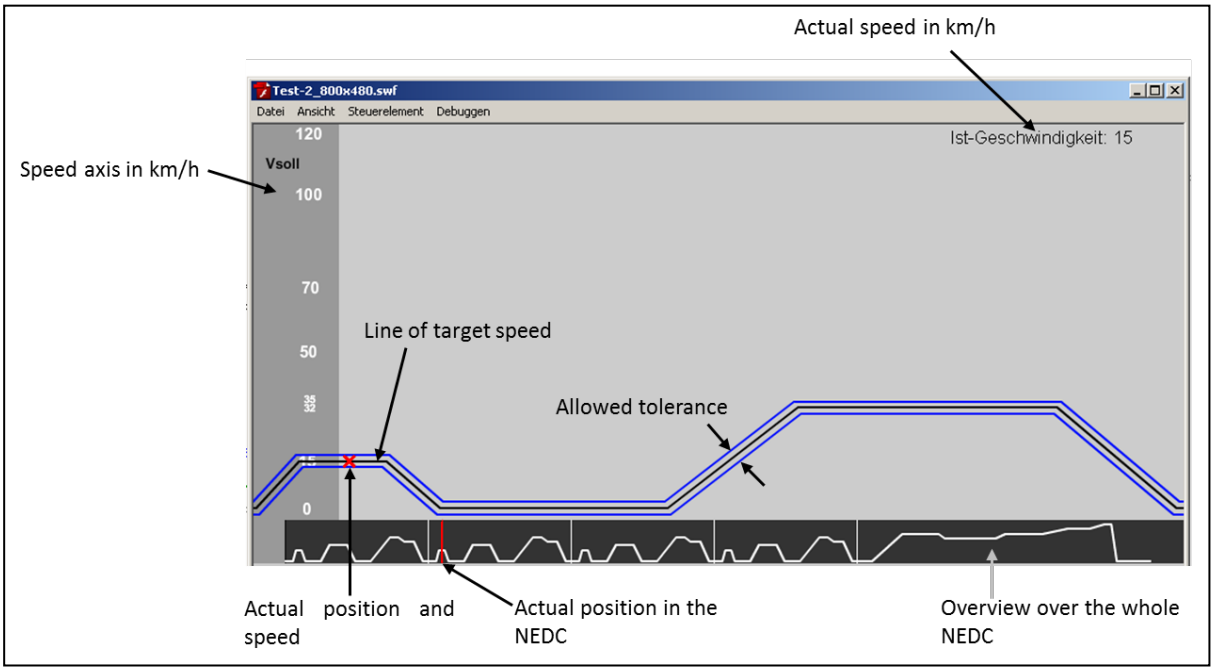

Fig. 4. Visualization displayed in the instrument cluster for performing the NEDC

Results of the NEDC

As it was described earlier a compact class car with 75 kW is modelled in the vehicle simulation. Therefore a Volkswagen Golf IV one of the best-selling cars in Europe with an 1.6 l engine and 75 kW was chosen for comparison. The data for the fuel consumption was extracted from the official brochures for this car [VW1]

The NEDC was carried out and checked multiple times in the simulator to guarantee that it was performed correctly. Figure 5 shows the results of the NEDC for the simulator compared to the Volkswagen. It can be shown that the fuel consumption of the simulation is although not identical to the Golf it is quite good comparable. This is a first indication that the fuel simulation is quite good.

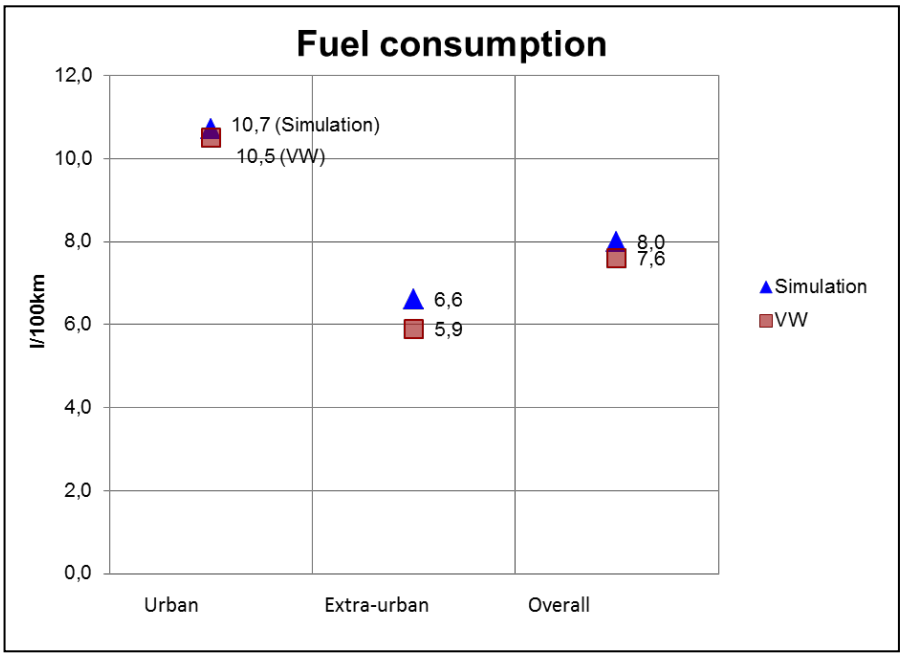

Fig. 5. NEDC fuel consumption of the simulation compared to the VW Golf IV

But the goal is not to get exactly the same fuel consumption as the VW. The target is to simulate a comparable characteristic of the fuel consumption during acceleration, deceleration and different speeds. Therefore a comparison of the fuel consumption trends of simulation and the Volkswagen Golf VI [VW2] during the NEDC was done (Fig. 6). Although the overall fuel consumption at the end of the NEDC is different, the graphs show that the

behaviour of the simulation (black graph) and of the measured Golf (green and blue graph) is very good comparable. This proves that the results of the fuel simulation are very good in the case of using the NEDC.

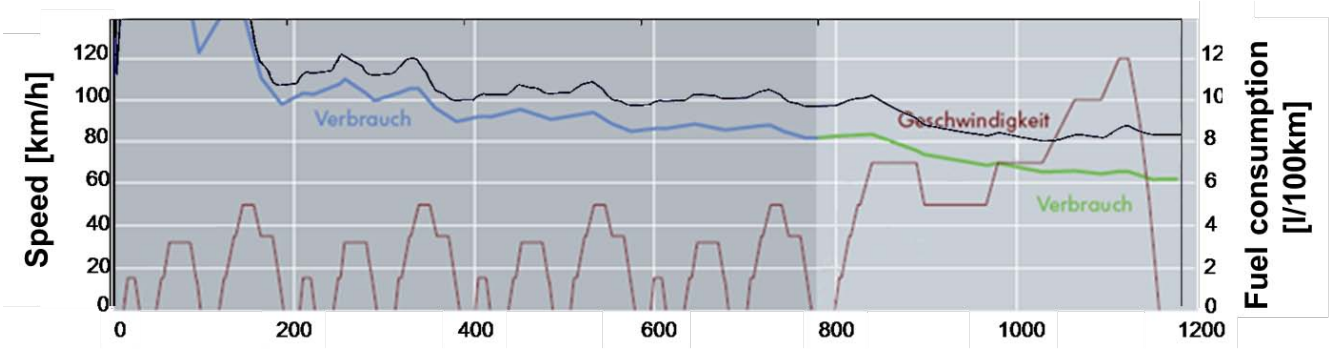

Fig. 6. Fuel consumption during the NEDC from simulation (black graph) and Volkswagen Golf (blue and green graph) [VW2]

Validation through driving tests in the simulator

In the previous chapters it could be shown that the results of the driving simulation are very good if the NEDC is used. But the problem of the NEDC is that it does not represent the typical driving behaviour. In the NEDC the accelerations are lower than under usual driving conditions and it has very long parts of constant speed which is not usual under normal driving conditions [GAS1]. Therefore a method was needed to validate the fuel consumption also for real driving conditions. A literature research for fuel consumption under real driving conditions was already done by Dorrer [DOR1]. The main results of his research were that the distribution of fuel consumption between different drivers lies between 25% and 62% of minimum fuel consumption. Also typical is that the distribution of the fuel consumption is asymmetric (Figure 7). On highways the fuel consumption depends mostly of the driven speed whereas in urban areas the fuel consumption is independent of the speed. There, in the city, differences of up to 50% can be observed. The idea for the following study was to look if the results Dorrer found for real driving scenarios can be repeated in the driving simulator.

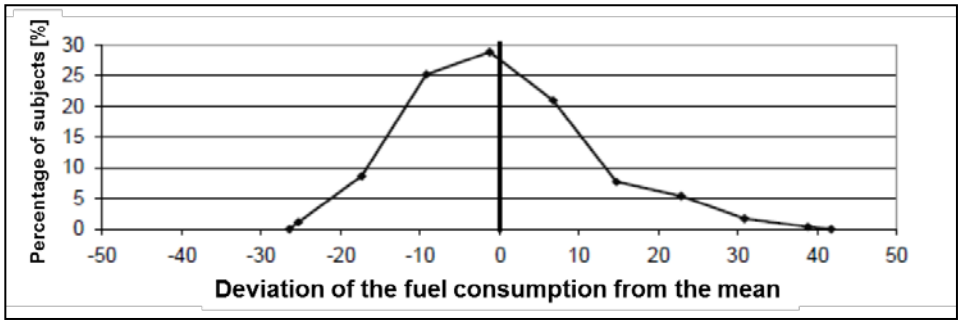

Fig. 7. Typical asymmetric distribution of fuel consumption for car drivers derived from a consumer questionnaire [DOR1]

Experimental design for the driving tests

The length of the test course is about 31 km. It includes 5 km of urban and 16 km of rural roads as well as 10 km of a highway. Different situations like traffic lights, different crossings, different speed limits and traffic conditions were implemented to have a typical driving scenario.

30 subjects aged between 19 and 57 (Mean: 24 years, SD: 7 years) took part in the experiment. The 17 male and 13 female drivers all held a valid driver's license. Five participants drove less than 5,000 km per year, four more than 20,000 km and the rest between 5,000 and 20,000 km per year. For most of the participants it was the first driving simulator study.

After an introduction and a practical drive in the simulator each subject had to do the test course. The participants got the advice to drive like they would do with their real car. They got no information or hint before they did the test drive about the goal of the study. After the test they were informed about the objective of the study they took part in.

Results of the driving tests

As not the absolute figures of the fuel consumption is of interest the mean fuel consumption of all participants is defined as 100%. The minimum fuel consumption reached by a participant for the whole drive is 74%, the maximum is 141%, the standard deviation 18.2%. Figure 8 compares the distribution of the fuel consumption for the simulation and for real world data. Although the data from the simulation was accessed through driving tests

and the distribution for the real world is an outcome of consumer questionnaires no big differences between both distribution can be observed. Not only the minimum and maximum fuel consumption is the same, also between 25% and 30% of the participants of both studies have about the mean fuel consumption. The only conspicuous difference which cannot be explained is that at 30% over the mean fuel consumption in the simulation the percentage of subjects which have this fuel consumption is higher than expected.

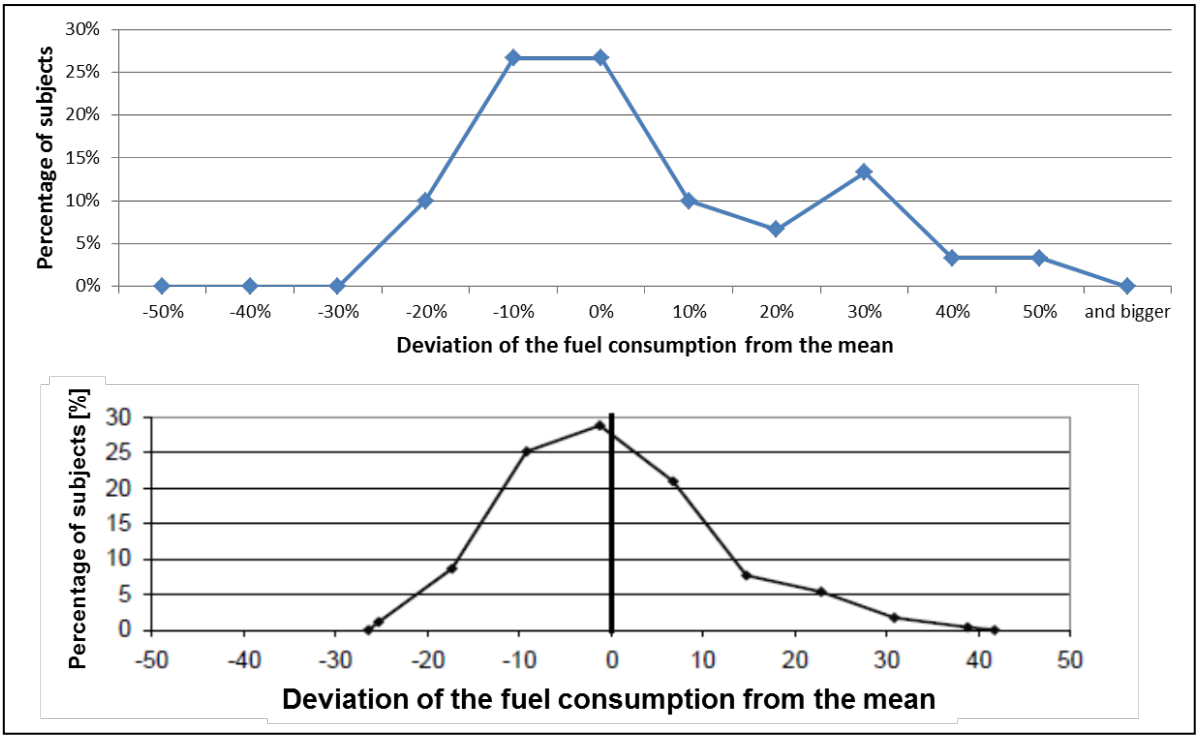

Fig. 8. Distribution of fuel consumption for simulation (top figure) and real world (bottom figure [DOR1])

According to Dorrer [DOR1] the fuel consumption on highways is mostly influenced by the speed. The regression analysis of the fuel consumption on 3 km free driving on a highway is highly significant. There a minimum fuel consumption of 43% and a maximum fuel consumption of 220% can be observed. Two urban scenarios where analysed as well. One was passing a roundabout in the city and one was passing a red traffic light. In both situations the regression analysis showed no significance between mean, maximum or minimum speed and fuel consumption. But the difference between maximum and minimum fuel consumption is over 42% (roundabout) and 28% (traffic light). This is consistent to the results of Dorrer [DOR1].

Fig. 9. Roundabout and traffic light scenario

Summary

The goal of the validation was to show that the driving simulator can estimate differences in fuel consumption for different driving behaviours. Two approaches were done to validate the simulation. The NEDC showed that the absolute fuel consumption of the simulation is not exactly identical to the for the comparison used VW Golf. But the comparison of the fuel consumption trend during the NEDC shows no big differences. Due to the fact, that the NEDC does not represent normal driving behaviour a second approach for validation was done. A study on a representative test route in the driving simulator with 30 subjects showed the distribution of the fuel consumption of the different drivers in the simulator is nearly identical to drives in the real world.

Overall it can be stated that for future studies differences in fuel consumption can be good measured. But it has still to be kept in mind that the fuel consumption depends not only on the individual driving behaviour, it also depends for example on the type of car, different environmental conditions etc.

References.

[BAS1] Basshuysen, R. “Handbuch Verbrennungsmotoren”, Wiesbaden, Germany, 2010, ISBN: 978-3834806994

[CEC1] The Council of the European Communities. “Council directive of 20 March 1970 on the approximation of the laws of the Member States on measures to be taken against air pollution by emissions from motor vehicles”, 70/220/EEC, 1970

[DOR1] Dorrer, “Effizienzbestimmung von Fahrweisen und Fahrerassistenz zur Reduzierung des Kraftstoffverbrauchs unter Nutzung telematischer Informationen“, Dissertation, Renningen, Germany, expert Verlag, 2004, ISBN 3-8169-2384-4

[FOC1] Focus (newspaper) 24th July 2007, “Porsche Cayenne - E-Motor plus 280-PS-V6” Accessed 12th March 2012, http://www.focus.de/auto/neuheiten/studie/tid-6937/porsche-cayenne_aid_67691.html

[GAS1] Gaßmann, S. “Untersuchungen zum Einfluß von Fahrzeug, Fahrer und Verkehr auf Betriebsweise und Kraftstoffverbrauch eines Pkw im realen Stadtverkehr“. Düsseldorf, Germany, VDI-Verlag, 1991, ISBN 3-18-145512-1

[VW1] Volkswagen AG, „Technische Daten und Ausstattungen Golf IV“, Brochure of the Volkswagen AG, 1998

[VW2] Volkswagen AG, „Effizient unterwegs. Spritspartipps für Profis“, Brochure of the Volkswagen AG, 2010

Driving Characteristics and Development of Anticipation of Experienced and Inexperienced Drivers When Learning a Route in a Driving Simulator

Kalermo, J.[1], Nurkkala V-M. [1], Koskela K. [1] and Järvilehto T.[1,2]

(1) Kajaani University of Applied Sciences, P. O. Box 52, FI-87101 Kajaani, Finland, {jonna.kalermo; veli-matti.nurkkala; kyosti.koskela}@kajak.fi; tjarvile@gmail.com
(2) Helsinki University, Department of Behavioural Sciences, P.O. Box 9, FI-00014 University of Helsinki, Finland

Abstract *– The driving behaviour is clearly different when the driving route is unfamiliar in comparison to the situation in which the driving route is known. However, the details of the critical behavioural and physiological parameters during the development of the mastering of the driving are not well known. It is possible that the development of the anticipation in different phases of the driving plays a critical role in the learning of the driving skills. It is as well possible that the critical differences between experienced and inexperienced drivers will be found in their anticipatory processes. In the present study, we examine driving characteristics and development of anticipation in inexperienced and experienced drivers when learning a new driving route through an unknown city in the driving simulator. The present paper presents preliminary results from nine subjects. The results show that significant differences were found in braking activity and driving speed when comparing the groups of different driving experience levels. Also, the development of anticipation was more pronounced with the experienced drivers as indicated by the driving parameters.*

Key words: *Anticipation, driving simulator, driving behaviour, simulator data, learning task*

1. Introduction

It is obvious that the driving behaviour is different when the driving route is unfamiliar in comparison to the situation in which the driving route is known, i.e. when the route is well-mastered. However, the details of the critical behavioural and physiological parameters during the development of the mastering of the driving are not well known. It is possible that the development of the anticipation in different phases of the driving plays a critical role in the learning of the driving skills (see e.g., [Jar3]). It is as well possible that the critical differences between experienced and inexperienced drivers will be found in their anticipatory processes. Such differences could be seen in the temporal activation of muscles (EMG) in relation to the phases of driving, in the indicators of the activation of the autonomic nervous system (heart rate, heart rate variability and galvanic skin response), in changes in perception and attention (e.g., eye movements, see [Gar1] and [You7]), in the amount of driving errors (failed attention to traffic signs, breaking the traffic rules, over-speeding, breaking the lane borders, etc.) and in changes of driving controls (movements of the steering wheel, throttle, brake, etc.).

Anticipatory driving is considered essential in successful and quick acting in sudden occurrences. It is also related to economical driving, which reduces the harmful CO_2 emissions. But how to explicate what anticipation is in the driving behaviour? We approach this question with a psychophysiological perspective. The theoretical approach of our research is based on a systemic anticipation model of the theory of the organism-environment system [Jar2]. According to the model, anticipation is not a process for waiting for stimuli, but an active process of preparation for results of action, which develops during learning. The anticipatory process proceeds towards the result of action, and it is this process that determines which parts of the environment can be used as "stimuli", i.e. as necessary constituents in the realization of actions. In the present study, we examine, by recording changes in driving behaviour and in electrophysiological indices of performance, how anticipation develops in inexperienced and experienced drivers when learning a new driving route through an unknown city in the driving simulator. The present paper presents preliminary analysis of changes in driving controls (simulator data) from nine subjects when learning a new route in a simulated city.

2. Methods

The experiments were carried out in a low-cost driving simulator. The task of the subject was to navigate and learn a shortest route through an unknown virtual city.

The base for the simulator and the driving control system are manufactured by Frex GP (Osaka, Japan). The system consisted of two degrees of freedom motion platform, high quality steering wheel and pedals. Blinkers as well as a middle console with a gear shifter and a hand brake from a Volvo S60 were added to the simulator in order to increase the realistic driving feeling. Also a high impact speaker was installed inside the driver's seat in order to add a feeling of vibration while driving. Logitech Z-5500 high quality speaker system was used for creating the driving sounds. Two high performance desktop computers were used to run the driving simulator. An in-house designed 220 degree curved display with radius of 2.5 meters was constructed (10 x 1.9 meters; 3840 x 720 pixels). For combining the image from three different projectors and making the view look seamless, a program called Nthusim was used. rFactor was selected as the main simulator software for several reasons. It is inexpensive, but also highly modifiable, and it supports custom-made driving scenarios and enables recording telemetry data with an in-house programmed plug-in. Lastly, the control program for the actuators was a program called X-Sim which was also used to show gauge values (speed, RPM, etc.) in a small display and to send a trigger pulse to other research equipment to start recordings. [Kos5] The simulator is presented in Figure 1.

Figure 1 The driving simulator

The research equipment included a number or measurement devices, including NeurOne (EMG), EyeLink II (eye tracker), Polar S810i heart rate monitor (RR-interval), and a simulator data capturing system.

22 male subjects (Ss) participated in the experiments. 17 of the subjects were policemen and five were university students.

In this paper, we present preliminary results of the study that consist of the data from nine Ss. The nine Ss were divided into three groups (N=3 in each): 1) inexperienced drivers (university students, age 21–34 years, driving license max three years, mileage 0-4000 km/year), 2) experienced drivers (policemen, age 23–33 years, driving license 6–16 years, mileage 10000–55000 km/year), and 3) very experienced drivers (policemen, age 47–51 years, driving license 29–32 years, mileage 15000–30000 km/year).

Before the experiments, the Ss were interviewed to collect the background information, as well as information of the driving experience and driving behaviour. Driving experience was classified according to the time the S had received their driver's license and on the basis of driven km per year. In addition, questions related to simulator and motion sickness were asked. The Ss filled in the SSQ form [Ken4] before and after the experiments. The experiment was part of a larger study, in which we also explored simulator sickness by using SSQ and TMSS-methods [Nur6], and how drivers performed in unexpected driving tasks. The present analysis is based on the temporal changes of driving controls (steering wheel, pedals). During the experiments, also electrophysiological data were recorded for deeper analysis.

The navigation task in the virtual city started from a parking place at one side of the city. The task of the S was to find the shortest driving route through the city to a skyscraper that could be seen at the other side of the city from the starting place. The S had a limit of five minutes in trying to find the route, after which the trial was stopped. After each trial, the S got feedback of his driving task (e.g., "after the bridge there is a shorter route"), and another trial began. When the S had found the shortest route, he was asked to drive twice the same route. The average amount of trials to find the route was 3.8 (minimum 2 and maximum 6 trials).

The data from each S was divided for the examination of the development of the anticipatory processes in two sections: 1) driving the unfamiliar route (the first and the second trial) and 2) driving the known route (the last two drives).

The changes in driving behaviour were explored by looking at changes in driving parameters in relation to a fixed point on the road (time control point), which was static and could be precisely detected in each trial (e.g., the front part of the vertical white line on the road before the zebra crossing, see Fig. 2). The changes in driving behaviour were examined by looking at temporal changes between the trials in driving speed, the starting moment of braking and loosening the throttle, and the starting moment of

steering movement. The subjects were advised to obey the traffic rules, e.g., comply with speed limits.

The five situations, in which the driver had to make decisions concerning the route selection, were chosen to explore the possible changes in driving activity. These situations were

1) the first intersection when arriving to the city centre (turning right prohibited),
2) an intersection with a yield-sign (left, right or straight),
3) an intersection with a STOP-sign that could easily be detected rather early (turning left or right),
4) an intersection (left or straight), and
5) an intersection with a yield-sign (left or right).

Figure 2 Situation 5: the time control point is the front part of the vertical white line on the road in front of the zebra crossing

The changes in the use of throttle, braking, steering and speed were studied from the simulator data. The time interval between starting to press the brake pedal and crossing the time control point is referred as braking delay. Similarly, the time interval between starting to steer and crossing the time control point is referred as steering delay. The use of the throttle is detected from the moment the S starts to loosen the throttle or alternatively pressing the throttle pedal in comparison with passing the time control point. Finally, the data was analysed with SPSS 20.0 statistical analysis software (IBM) by using t-test and one-way ANOVA.

3. Results

The results are based on the preliminary analysis of nine subjects (inexperienced, experienced and very experienced). Changes in driving behaviour are approached from three points of view. First, we examine the dependence of driving parameters on driving experience by concentrating on the differences related to experience in situations in where the route is known. Second, we examine the dependence of driving parameters on the development of anticipation during the route learning task. Finally, we explore the dependence of the development of anticipation in relation to driving experience in order to find what differences can be detected between the groups during learning.

3.1 Dependence of driving parameters on driving experience

We examined the dependence of driving parameters on driving experience when the driving route was learned (the last two trials). Experienced drivers started braking significantly later (see Fig. 3) than less experienced and inexperienced drivers (One-way ANOVA; p<.001; F=11,871; df=2,40). Parameters related to steering and the use of throttle did not show any significant differences.

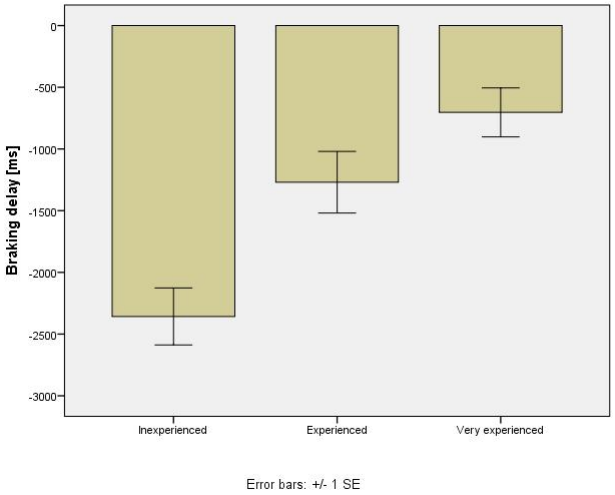

Figure 3 Braking delay of the subjects with different driving experience when the driving route was known

Significant differences were also found in the driving speed. The driving speed was higher with very experienced drivers (48,9 km/h) in comparison to inexperienced drivers (38,6 km/h) (One-way ANOVA;p<.01; F=4,612; df=2,82).

3.2 Dependence of driving parameters on the development of anticipation during the route learning

We explored how anticipation develops during the learning of the route through the city. The changes in driving parameters were analysed when the route was unknown (first two trials) as well as when it was known (last two trials). The analysis shows that the beginning of braking starts later (avg. 1,3 s. later) when the route has been learned (t-test, p<.001; t=-3,697; df=52,458). Additionally, as the route became familiar, the driving speed increased significantly (t-

test, p<.05; t =-2,099; df =162). No significant differences were seen in loosening the throttle pedal.

For more detailed analysis, we studied situations 4 and 5. In these situations the subject had to turn the steering wheel in order to drive the car correctly in an intersection. The results show a significant effect of learning in the steering delay (t-test, p <.05; t=2,335; df=59) when the driving route became known. The steering started earlier in the last two trials i.e. when the route was known. The change in the steering delay is presented in Figure 4.

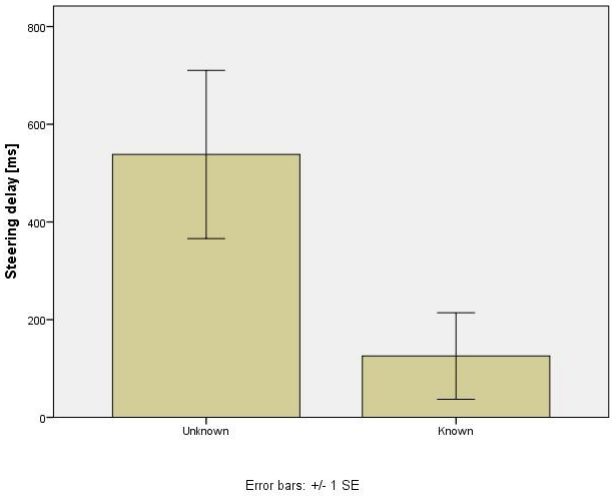

Figure 4 Comparison of steering delay with unknown and known driving route, situations 4 and 5

3.3 Dependence of development of anticipation in relation to the driving experience

Finally, the dependence of development of anticipation was examined in relation to driving experience between the groups (inexperienced, experienced and very experienced drivers) as indicated by the driving parameters.

The braking delay showed significant differences in experienced and very experienced drivers during the learning of the driving route (see Fig. 5). The beginning of braking moved 1.7 s. later in experienced drivers (t-test, p<.01; t=-3,156; df =31), and 1.5 s. later in very experienced drivers (t-test p<.05; t=-2,453; df=9,881). No significant difference was found in inexperienced drivers.

Driving speed increased in every group when the route became known, significant difference was found in very experienced drivers (t-test, p<.05; t=-2,305; df=55).

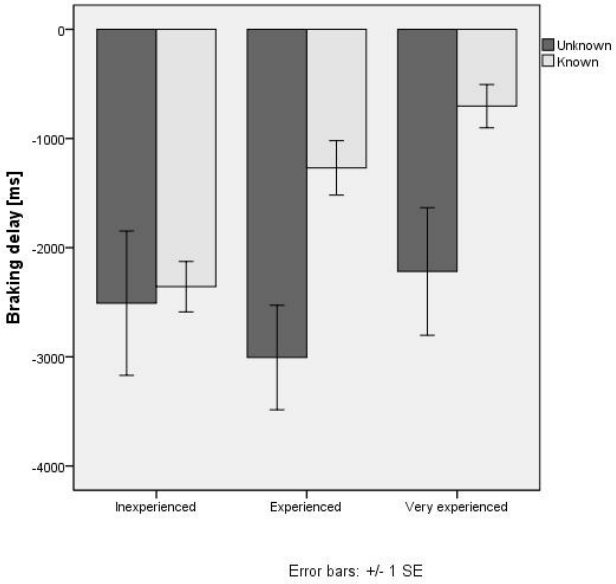

Figure 5 The difference in braking delay with unknown and known driving route for the subjects with different driving experience.

4. Conclusions and future work

The preliminary results on the analysis of driving parameters of experienced and inexperienced drivers show that in a driving simulator some interesting features can be seen during learning of a shortest driving route through an unfamiliar simulated city. The results show how anticipation develops with familiarisation of the route. The driving experience was reflected in some driving parameters, the indications of the development of anticipation during learning were seen, and this development was more pronounced with more experienced drivers.

In general, with the learning of the driving route, the driver performance became more goal-oriented and smooth. The Ss reduced the amount of unnecessary use of brakes, controlled better the speeding but also drove faster.

In the present analysis only several driving parameters were examined, but the analysis of bioelectrical data (EMG and heart-rate) may help to determine in more detail how anticipation develops during learning. Exploring how anticipation develops in certain driving situations enables us to understand driving behaviour better. The findings from our study may provide information that can be utilised in developing driver's training for novice drivers, as well as training of, for instance, economical driving.

Acknowledgements

This research was funded by European Regional Development Fund, the Joint Authority of Kainuu Region, and Sunit Oy. We are grateful for the support. Special thanks to all the subjects who took part in the study.

References

[Gar1] Garay, L., Fisher, D.L. & Hancock, K.L. (2004) Effects of Driving Experience and Lighting Condition on Driving Performance. Proceedings of the Human Factors and Ergonomics Society Annual Meeting September, Vol. 48, no. 19: 2290-2294.

[Jar2] Järvilehto, T. (1998) The theory of the organism-environment system: I. Description of the theory. Integrative Physiological and Behavioral Science, 33, 321-334.

[Jar3] Järvilehto, T. (2010) Anticipation as the main principle of brain function and mastering of skills. In: Thomson, K, and Watt, A. (Eds.) Connecting paradigms of motor behavior to sport and physical education. Tallinn: TLU Press, 16-33.

[Ken4] Kennedy R. S., Lane N. E., Berbaum K. S., & Lilienthal M. G. (1993) Simulator Sickness Questionnaire: An Enhancement Method for Quantifying Simulator Sickness, International Journal of Aviation Psychology, 3(3), 1993, pp. 203 – 220.

[Kos5] Koskela, K., Nurkkala, V-M., Kalermo, J. & Järvilehto, T. (2011) Low-cost Driving Simulator for Driver Behavior Research. Proceedings of the 2011 International Conference on Computer Graphics and Virtual Reality, CGVR'11, July 18-21, 2011, Las Vegas, Nevada, USA.

[Nur6] Nurkkala, V-M, Koskela, K., Kalermo, J., Järvilehto, T. & Honkanen, R. (2012) A Method to Evaluate Temporal Appearances of Simulator Sickness during Driving Simulation Experiments. Submitted

[You7] Young, K. & Regan, M. (2007) Driver distraction: A review of the literature. In: I.J. Faulks, M. Regan, M. Stevenson, J. Brown, A. Porter & J.D. Irwin (Eds.). Distracted driving. Sydney, NSW: Australasian College of Road Safety. Pages 379-405.

Multisensory interaction – A comparative study on driving sound evaluation in moving base and fixed base driving simulators

Sabrina Skoda, Jochen Steffens, Joerg Becker-Schweitzer [1]
(1) Institute of Sound and Vibration Engineering, Duesseldorf University of Applied Sciences, Josef-Gockeln-Str. 9, 40474 Duesseldorf, Germany, sabrina.skoda@fh-duesseldorf.de

Abstract – Perception and evaluation of comfort and quality in a passenger car is strongly influenced by the noise and vibration behaviour of the vehicle and always happens in the context of multiple sensory impressions which are consciously and subconsciously processed in the human brain. The interaction mechanisms of sensory perception are highly complex and raise several scientific questions. In order to investigate the mutual influence of acceleration forces and driving sounds a comparative listening study was conducted in two different driving simulators, one moving base simulator offering longitudinal acceleration forces and one fixed base simulator without motion. During the listening test different vehicle interior sounds and different accelerations were evaluated by 52 non-expert test participants. Afterwards the evaluations from both driving simulators were compared. This comparison didn't bring up any general differences in evaluation between the two different test environments but small effects concerning single items. Based on the results from the study the mutual influence of driving sounds and longitudinal acceleration will be discussed in this contribution.

Key words: *multisensory interaction, sound evaluation, acceleration perception, moving base simulator, fixed base simulator*

1 Introduction

The evaluation of vehicle interior sounds is strongly dependent on the context, in which the sounds are presented [Pau7]. If the results from a listening study shall be assigned to everyday life conditions, the test environment has to reproduce a great degree of reality as well. On the one hand, this means that the test participant has to interact with the vehicle like in everyday life. On the other hand, also non-acoustical sensory stimuli have to be presented during the test in order to take account of the complex interaction processes between multiple sensations that complement one another to form an overall impression of the perceived environment.

The combinations of auditory, visual, haptic, olfactory and somatosensory information being processed consciously and subconsciously by the human brain contribute to judgement formation as well as cognitive processes like attention focusing during a driving scenario and multitasking [Bro3, Kah4]. With these facts in mind, the use of a driving simulator for listening experiments appears to be quite obvious.

The driving simulators used by the vehicle manufacturers become more and more complex and today's computer technology allows real-time simulation of vehicle dynamics and virtual environments with high precision. However, the multitude of sensations and environmental factors affecting a person under everyday driving conditions never can be fully represented in a physically limited driving simulator. Thus the reproduction of realistic driving situations in such a test environment always involves compromises. This raises the question which sensory stimuli are crucial to a high degree of subjectively perceived reality and how these stimuli have to be presented in the driving simulator. Regarding the interaction of visual and auditory perception valuable insights have been obtained during the past years and there are also a number of theories about the auditory-tactile interaction. Perceptual aspects have been investigated in previous studies [Bau1, Mer5] as well as the influence of vibrations on the evaluation of comfort and quality in a vehicle [Bel2, Sko8]. In contrast, the connection between auditory and somatosensory perception remains largely unexplored. Nevertheless, this part of perceptual research is of high importance if a driving simulator shall be used as an appropriate test environment for listening experiments. In the course of this, the question arises how acceleration forces in a moving-base simulator influence the evaluation of vehicle interior sounds. And how do driving sounds affect the sensation and evaluation of longitudinal acceleration? These considerations lead to the more practice oriented question if there is a difference in driving sound evaluation using a moving-base simulator compared with a driving simulator that doesn't offer any motion.

2 Listening study

In order to explore the interaction mechanisms of sound and acceleration perception a comparative listening study was conducted in cooperation with the company Daimler AG using two different driving simulators.

2.1 Test environment

2.1.1 Moving base simulator

The first test environment was the moving base driving simulator owned by the company Daimler AG in Sindelfingen. This simulator consists of a large dome offering space for a full vehicle. In this study a mid-range vehicle was used. The inner wall of the dome is a curved projection screen where the virtual environment is projected onto in 360°. The dome itself is placed on a Stewart platform offering motion in six degrees of freedom. In addition, this construction is flexibly mounted on a guide rail with a movement range of 12 m.

Fig. 1. Moving base simulator (Daimler AG).

The fast linear motors of the electric drive are able to generate translational accelerations up to 1 G. According to the orientation of the vehicle in the dome lateral or longitudinal vehicle dynamics can be simulated with a high degree of realism. The perceived acceleration inside the vehicle is a combination of translation on the guide rail, hexapod movement and pitch. By using different motion cueing algorithms the ratio of translational and rotational movement can be varied. In the course of this listening study the participants should be exposed to inertial forces as strong as possible. Thus a motion cueing algorithm with great amount of translation and moderate pitch was chosen. Since the study was focused on longitudinal acceleration the vehicle in the dome was positioned along the guide rail and moved and pitched forwards and backwards according to the driving manoeuvers. In the course of this, the vehicle dynamics of a mid-range vehicle with automatic transmission was simulated. The driving sounds were presented to the test participants via headphones inside the vehicle.

2.1.2 Fixed base simulator

In the second test environment, a fixed base simulator without any motion cueing, the control group performed the driving test under the same conditions as the treatment group. The test environment was designed equally to the moving base simulator and also the vehicle used in the test was the same. So the only variable to be modified was the “acceleration”. Due to the missing movement the subjective impression of acceleration was just a virtual one.

Fig. 2. Fixed base simulator (Daimler AG).

2.2 Test design

The listening test was subdivided into two parts and took about 45 minutes in total.

In the first part of the test the participants had to drive the vehicle themselves. They had to follow a leading vehicle keeping a distance as constant as possible and imitating the driving manoeuvers of the leading vehicle. The test drive took place on a straight country road during daytime and there were no other traffic participants on the road besides the leading vehicle. Two different driving scenarios each with two accelerations had to be passed. The first scenario consisted of two part-throttle accelerations and the second one of two full-throttle accelerations. Each scenario was presented five times with five different vehicle interior sounds. Thus every test person had to drive ten times in total and carry out an evaluation after each run by filling out a questionnaire. The questionnaire consisted of a 7-step Semantic Differential and the test persons first had to rate the driving sound in terms of the items *Pleasantness, Sportiness, Loudness, Timbre, Powerfulness, Quality.* Beyond that, they were asked to evaluate the vehicle acceleration on the basis of the items *Strength, Realism* and *Familiarity*.

In the second part of the test the driving simulator was set into replay mode and the test persons had to remain passive in the vehicle. Ten short driving scenarios of equal length, which had been recorded previously, were presented one by one to the test persons. The scenarios were composed of three different kinds of acceleration to specified target speeds (80 km/h, 95 km/h, 110 km/h) and three variations of a vehicle interior sound respectively combined with each other. The resulting nine driving scenarios were randomized in order and one scenario was additionally repeated for reliability reasons. After each run the test persons had to carry

out their evaluation again using a 7-step Semantic Differential with the items *Sportiness (of the vehicle)*, *Acceleration strength* and *Pleasantness (of the vehicle sound).* In addition, the questionnaire contained questions about the participants' driving experience. The test persons were asked about their annual mileage and the type of vehicle they use regularly.

Before performing the listening test the participants were not informed about the objectives of the experiment. This should avoid a distortion of test results possibly caused by artificial attention focussing. Besides the quantitative evaluation during the test drive narrative interviews were conducted subsequent to the listening test, so the participants could express their impressions and associations concerning the experiment. This kind of explorative evaluation approach gives the opportunity to record the test persons' individual evaluation strategies and frames of reference which can be a valuable addition to the quantitative assessments in the questionnaire [Muc6]. In the course of the interviews the test persons finally were informed about the objectives of the listening study.

2.3 Stimuli

The vehicle interior sounds in the first part of the listening test were five different engine sounds all with the same wind and road noise. In order to cover a wide range of sound characteristics the engine sounds of a diesel vehicle, three gasoline vehicles (sports sedan, mid-range and large executive car) and an artificially designed electric vehicle sound were presented in randomized order.

In the second part of the listening test the interior sound of the mid-range car was presented in three different versions: the original sound and two parameter variations, one of which was a volume increase (+5dB), and the other a level increase in low-frequency range with a cut-off frequency of 280 Hz. The aim of this approach was to investigate if the variation of single sound parameters, e.g. volume, has an effect on the subjective impression of acceleration.

All sounds were generated by a HEAD 3D Sound Simulation System (H3S) and presented to the test persons in randomized order.

2.4 Test participants

52 persons were invited to the listening test and equally distributed by age and gender into a treatment group and a control group. Every test person had to pass the test in only one of both driving simulators (Between Subject Design) in order to avoid learning effects, that would be caused by repetition of the test in the respective other simulator, and to achieve independence between the two experiments. The participants were non-technical employees of the Daimler Company and external persons from the company's test pool aged between 19 and 69 years. The mean age was 38 years with a standard deviation of 13.3 years. 57% of the test persons were male and 43% were female.

3 Results

Subsequent to the listening test the judgements from both driving simulators were evaluated and compared with each other. The results were analysed first with regard to figure out potential differences in evaluation between the two driving simulators and second to investigate mutual effects of vehicle interior sounds and acceleration.

3.1 Sound evaluation

A one-way MANOVA was performed on the sound evaluation results from the first part of the test using Pillai's Trace. There was no statistically significant difference between the ratings from both driving simulators in total ($F = 9.75$, $p = 0.25$, $\alpha = 0.05$). However, additional tests of between-subjects effects revealed a couple of significant differences, so the results were analysed more in detail.

The two most interesting results, the evaluation of the items *Pleasantness* and *Loudness* have been chosen and will be discussed below. Fig. 3 exemplarily depicts the arithmetic means of the item *Pleasantness* in the full-throttle scenario for all five vehicle interior sounds with standard error.

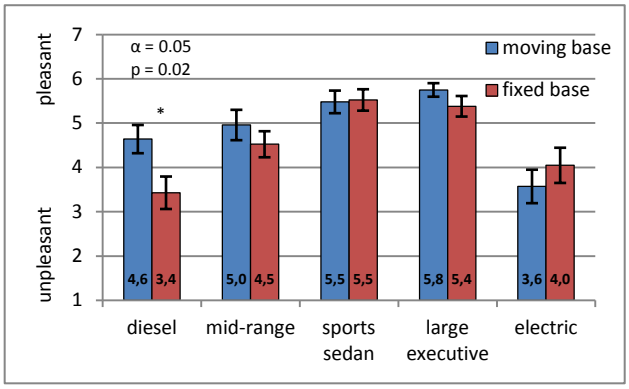

Fig. 3. Ratings of the item *Pleasantness* (full throttle scenario).

A t-test performed on the judgements from both samples on a level of significance of 5% indicates a statistically significant difference in evaluation only for the first sound, the diesel vehicle. This sound obviously was evaluated as more pleasant in the moving base simulator. Concerning the other sounds differences in evaluation are not significant. However, the small number of test participants and the choice of a Between Subject Design decrease the statistical certainty of the test. The coefficient of determination is $R^2 = 0.55$ so that 45% of not explained variance between the samples remains. This can be explained by the composition of the sample or influence factors in the test environment.

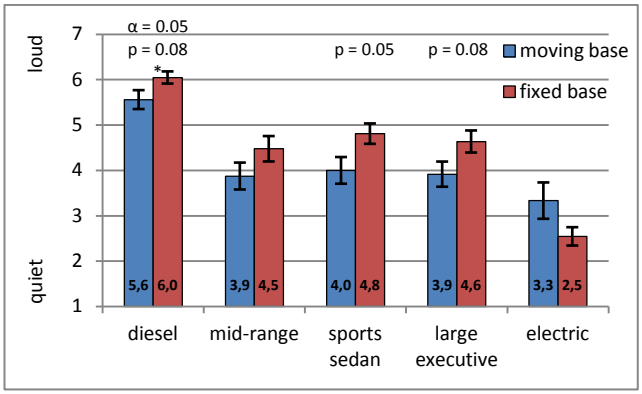

Fig. 4. Ratings of the item *Loudness* (full throttle scenario).

Fig. 4 displays the evaluation of the item *Loudness* in the full-throttle scenario. The arithmetic means are presented with standard error.

There is an offset between the mean values from the moving base simulator compared to those from the fixed base simulator. Although the t-test does not reveal any statistical significance the p-values are close to the significance threshold in three cases. Thus the vehicle sounds in the moving base simulator were evaluated as quieter than in the fixed base simulator.

3.2 Acceleration evaluation

In the next step the influence of vehicle interior sounds on the subjective evaluation of acceleration was investigated. Fig. 5 shows the average judgements of the item *Acceleration strength* in the full-throttle scenario of test part one in the moving base simulator with standard error.

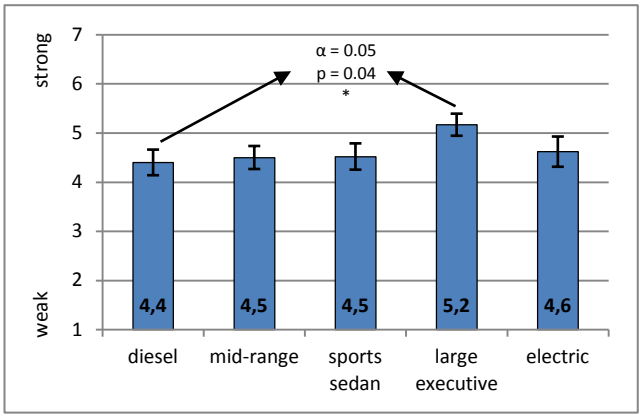

Fig. 5. Ratings of the item *Acceleration strength* (full throttle)

The results show a significant difference in evaluation between the best rated and the worst rated sound. These are the diesel vehicle and the large executive gasoline vehicle. The other sounds were rated similarly.

In Fig. 6 the arithmetic means of the judgements of the item *Acceleration Strength*, now from the second part of the test, are depicted with standard error. The nine different driving scenarios are plotted on the abscissa, labeled by the three target speeds and the corresponding sound variations, where the index *n* represents the normal version, *l* the level variation and *b* the low-frequency variation. The vertical axis shows the seven steps of the Semantic Differential.

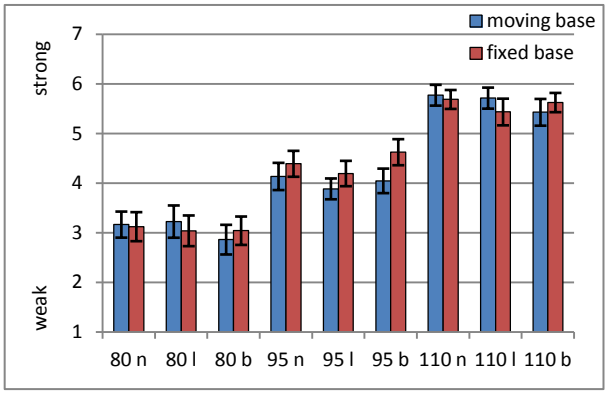

Fig. 6. Ratings of the item *Acceleration strength* (test part II).

The results show no significant difference between the evaluations in the moving base simulator compared to the fixed base simulator. Furthermore, the three sound variations for each acceleration scenario were rated similarly. So there is no influence of the sound variations on the evaluation of the acceleration strength. Only the three different acceleration scenarios were correctly distinguished by the test persons.

In contrast, the judgements on the sound item *Pleasantness* show differences in the evaluation of the three sound variations within one acceleration scenario. The arithmetic means of the ratings are depicted in Fig. 7 with standard error. The labelling of the horizontal axis is the same as in Fig. 6.

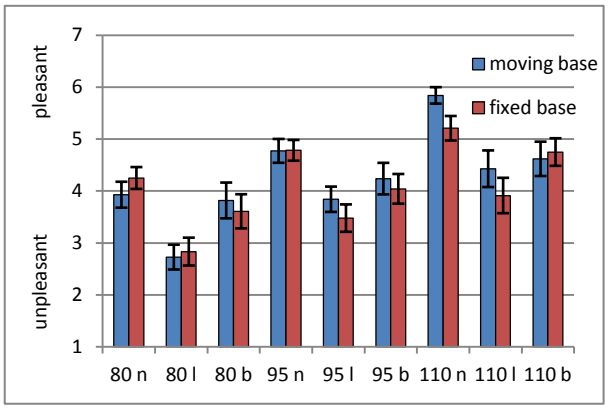

Fig. 7. Ratings of the item *Pleasantness* (test part II)

The volume increase was rated worst in all three acceleration scenarios and also the low-frequency variation has lower mean values than the normal sound. The driving scenarios with the target speed of 110 km/h were rated as more pleasant than the lower accelerations. There is no significant difference in evaluation between moving base and fixed base simulator ($R^2 = 0.86$).

4 Discussion

Concerning single items, the evaluation of the vehicle sounds from the first part of the test conducted in the moving base simulator is slightly different than in the fixed base simulator. There is an offset in the loudness ratings indicating that the vehicle sounds were evaluated as more quiet in the moving base simulator. One possible explanation to this finding is that attention processes in the moving base simulator are different due to the presence of inertial forces as additional stimulus. The test persons might be more deflected from the vehicle sounds because of the superposition of multiple sensory impressions whereas in the fixed base simulator the attention probably is more focused on the sounds when no motion takes place. The item *Pleasantness* among other items also was evaluated differently in both simulators although the differences are very small. Therefore a suggested influence of acceleration on sound evaluation seems to be quiet obvious. It is conspicuous that the electric vehicle was evaluated differently than the other sounds. This finding, together with the fairly wide variety in the results, might be explained by competing frames of reference occurring when test persons evaluate less familiar sounds. The artificial sound character of the electric vehicle has an impact on the test participants' evaluation strategies and also demands more attention from the driver than the well-known sound of a traditional combustion engine.

Although there were only two different driving scenarios in the first part of the test and only the vehicle sounds changed, the evaluation of the acceleration strength in the full-throttle scenario reveals a difference in ratings between the diesel vehicle and the large executive vehicle. These two sound characteristics differ from each other to a large extent. Hearing one of these sounds forms an association with a certain type of vehicle and its acceleration behavior. This means that expectations and prior experiences of the test persons play an important role. These factors apparently have an influence on the subjective estimation of acceleration and the evaluation of the acceleration strength as well.

The test persons' statements in the interviews indicate an interaction of acceleration and sound. For example, many people talked about a stronger impression of acceleration when the vehicle sound gets louder.

However, in the second part of the test the sound variations didn't have any effect on the evaluation of acceleration. Although the test persons clearly distinguished between the different sound variations in the *Pleasantness* rating, the acceleration strength was judged similarly for each target speed scenario. The change of single sound parameters obviously doesn't comprise to a modified acceleration rating. One reason could be the test persons' frame of reference from the first part of the test, where the sound characteristics of the sports sedan, the large executive and the diesel car offer a wider range for the evaluation of *Acceleration Strength* and *Sportiness* than the sound of the mid-sized car with its variations does.

In addition to that, the test persons had several different evaluation strategies except for the auditory stimuli to identify the real differences in acceleration such as the virtual sense of acceleration perceived by the visual system, the real inertial forces sensed in the moving base simulator and the frequency gradient in the vehicle sound. So other perceptual aspects may have been taken into account as indicators for changes in acceleration prior to sound.

Comparing the results from both simulators regarding the second part of the test no significant difference in evaluation could be shown. The coefficients of determination are $R^2 = 0.94$ for the item *Acceleration Strength* and $R^2 = 0.86$ for the item *Pleasantness*. Despite the presence of inertial forces in the moving base simulator both items were not rated differently than in the fixed base simulator.

As a main difference compared with the first part of the listening test, the participants remained passive in the second part and didn't interact with the vehicle. This could explain the different results from both parts of the test.

Moreover, the driving scenarios with the highest target speed (110 km/h) were rated as most pleasant. The coefficient of determination between the items *Pleasantness* and *Sportiness* is $R^2 = 0.55$ and there is a highly significant correlation between the items *Sportiness* and *Acceleration Strength* ($R^2 = 0.96$). The test persons obviously preferred the driving scenario with the highest target speed. This might be associated with particular personality traits of the participants from the company's test pool.

To sum up, the first part of the test indicates small interaction effects between acceleration and sound evaluation although the MANOVA shows no statistically significant difference between both driving simulators. In the second part of the test these effects could not be confirmed. As a consequence, the data from this study reveal no clear empirical evidence of a benefit of using moving base simulators in listening tests. However, the acceleration in the moving base simulator represents only 30% of a real vehicle's acceleration. So the listening study should additionally be conducted in a real vehicle. Furthermore, the role of driving behaviour has to be investigated in detail. Therefore, further research on this topic is of great interest.

5 References

[Bau1] Baumann I., Bellmann M.A., et al. „Wahrnehmungs- und Unterschiedsschwellen von Vibrationen auf einem Kraftfahrzeugsitz“. *Fortschritte der Akustik - DAGA 2001,* Hamburg-Harburg, 2001, p. 292.

[Bel2] Bellmann M.A., Baumann I., et al. „Wirkung von Sitz- und Lenkradvibrationen auf den Komfort im Fahrzeug“. *K.Becker (ed.), “Subjektive Fahreindrücke sichtbar machen II”*, *Expert-Verlag*, Renningen, 2002, pp. 99-114.

[Bro3] Broadbent D. E. “Perception and communication”. *Pergamon Press*, Oxford, 1969.

[Kah4] Kahneman D. “Attention and effort”. *Prentice-Hall,* New Jersey, 1973.

[Mer5] Merchel S., Altinsoy M.E., Leppin A. „Multisensorische Interaktion im Fahrzeug: Audio-taktile Intensitätswahrnehmung“. *Fortschritte der Akustik - DAGA 2010,* Berlin, 2010, Pt. 2, p. 871.

[Muc6] Muckel P., Ensel L., Schulte-Fortkamp B. “Exploration of associated imaginations on sound perception AISP: A method for helping people to describe and to evaluate their sound perceptions”. *Journal of the Acoustical Society of America,* 1999, Vol. 105, No. 2, Pt. 2, p. 1279.

[Pau7] Paul S., Schulte-Fortkamp B., Genuit K. “Explorative Sound Evaluation“. *Journal of the Acoustical Society of America*, 2004, Vol. 116, No. 4, Pt. 2, p. 2641.

[Sko8] Sköld A., Västfjäll D. “Vibrational influence on Product Sound Quality in cars“. *Proceedings of the Forum Acusticum 2005*, Budapest, 2005.

A Method to Evaluate Temporal Appearances of Simulator Sickness during Driving Simulation Experiments

V.-M. Nurkkala[1], K. Koskela[1], J. Kalermo[1], S. Nevanperä[2], T. Järvilehto[1,2], and R. Honkanen[3]

(1) Kajaani University of Applied Sciences, P. O. Box 52, FI-87101 Kajaani, Finland, {veli-matti.nurkkala; kyosti.koskela; jonna.kalermo; timo.jarvilehto}@kajak.fi
(2) Helsinki University, Department of Behavioural Sciences, P.O. Box 9, FI-00014 University of Helsinki, Finland
(3) Kajaani University Consortium, CEMIS Oulu, University of Oulu, P. O. Box 51, FI-87101 Kajaani, Finland, risto.t.honkanen@gmail.com

Abstract *– Driving simulator is an important tool for driver's training and driving behavior studies. A driving simulator offers a safe and replicable virtual driving environment, but on the other hand causes simulator sickness for many drivers. Our motivation was to study what kind of simulator sickness symptoms subjects will have in our driving simulator with stereoscopic driving view. Simulator Sickness Questionnaire (SSQ) offers a valuable tool for the evaluation of the appearance of simulator sickness. It does not give, however, temporal information on the levels of nausea or on the exact instant of the appearance of different adverse symptoms during driving. In this paper, we present a method for studying the time course of the appearance of nausea and different symptoms during a driving experiment (TMSS, Temporal Method for Simulation Sickness). The method is based on periodically asking the driver on the intensity of possible nausea or other symptoms during driving. According to the present study, the method reveals that driver's level of nausea may vary a lot during a single simulation experiment, and in many cases it does not correlate with the results of Simulation Sickness Questionnaire. TMSS is also a useful tool in determining factors related to the appearance of nausea and other symptoms of simulator sickness.*

Key words: Simulator sickness, Driving simulator, Motion base, Stereoscopic view, SSQ

1. Introduction

Driving simulation is an invaluable tool for research, training, and product development in driving studies. Not only can it produce scenarios that are ethically, logistically, and financially impossible in the real world, but it also eliminates risks associated with performing dangerous tasks in the real world [1]. Driving simulators also offer human-computer interaction (HCI) researchers distinct advantages over real vehicles in terms of repeatability. By keeping a simulation scenario exactly the same from trial to trial or from subject to subject, one can study differences between in-car devices or interfaces with fewer complications, confounds and consumed time [14].

Although simulation can eliminate crash risks associated with on-road research, the use of simulation induces a symptom known as the simulator sickness. This malady, similar to motion sickness in the real world, can potentially confound the data, limit the effectiveness of training, and influence drop-out rates of the participants of a simulation test.

Simulator Sickness Questionnaire (SSQ) has been frequently used method in the evaluation of the driver's simulator sickness after it was published by Kennedy et al. in 1993 [8]. An SSQ form is usually filled before and after the driving examination or training. The SSQ gives a score for the subject's level of simulator sickness, based on weighted symptoms [8]. However, the SSQ method does not offer any temporal information on the level of nausea or on the instant of the appearance of different symptoms.

The aim of the present work was to develop a method to determine how much and when simulator sickness occurs and to study factors that may be related to the appearance of the simulator sickness. This kind of information may be crucial in order to decrease subject's drop-out rate in the future experiments.

In this study, we developed the Temporal Method for Simulation Sickness (TMSS). In order to use the TMSS method, the subjects were advised to use a

scale from 1 to 5 when estimating the level of the nausea during the driving task. The estimation was prompted with a frequency of 1/min. Additionally, the subjects were advised to inform immediately if the level of nausea changed or if any other simulator sickness symptoms occurred during driving. An SSQ form was also filled before and after each simulation experiment. According to our studies, driver's level of sickness may vary a lot during a single simulation experiment and sometimes does not correlate with the results of SSQ.

Simulator sickness was initially reported by Havron and Butler in 1957 in a helicopter trainer [Häk5]. It was documented to be similar to motion sickness, but it could occur without any actual motion of the subject. The most common symptoms of simulator sickness are a general discomfort, apathy, drowsiness, headache, disorientation, fatigue, sweating, salivation, stomach awareness, nausea, retching, and vomiting [8]. Postural instability and flashbacks (sudden recurrence of symptoms) have also reported to occur [10].

According to Mollenhauer and Romano, symptoms of simulator sickness can affect driver's performance in a variety of negative ways causing inappropriate behaviour, loss of motivation, avoidance of tasks that are found disturbing, and distraction of the normal attention allocation processes [12].

Even though a driver is able to experience driving during a simulation with the help of visual and audio cues, psychological studies have revealed the importance of vestibular sensations in the driving experiment [7]. In a fixed-based simulator, the subject has the experience of visual motion while the corresponding vestibular stimulation is missing [4]. This conflict is believed to lead to simulator sickness in a fixed-based driving simulator.

In comparison with fixed-based driving simulators, simulator sickness has been reported to be less frequent in motion-based driving simulators [3], [16]. Slob even states that the main reason why a motion system is important is the prevention of simulator sickness [15]. Nevertheless, the level of motion-base inaccuracy or conflicts between the two different inputs (e.g., visual and vestibular) are known to be related to increased simulator sickness rates [1].

One of the first tools for measuring motion or simulation sickness was the Pensacola Motion Sickness Questionnaire (MSQ) by Kellogg et al. [6]. An MSQ is a self-report form divided in 23 symptoms. Symptoms are estimated on a 4-level severity scale [10]. Because of the slight difference in symptoms as well as their lower incidence and severity, an improved questionnaire was needed. Some symptoms included in the scoring of MS are irrelevant for SS, and several are misleading [8]. The SSQ was designed especially for simulator purposes and soon replaced previously prevailing MSQ. An SSQ form consists of a list of 16 symptoms which are estimated by the subject on a 4-level scale [1], [10].

Other frequently used questionnaires are the Motion Sickness Assessment Questionnaire (MSAQ) [1] and Revised Simulator Sickness Questionnaire (RSSQ) [9].

The SSQ has also been used in order to evaluate simulator sickness during driving. The SSQ was filled every 5 minutes during the driving experiment [13]. However, it is probable that asking a series of 16 questions during a driving experiment influences the driver's behaviour and may, therefore, affect the results of the study.

Chen et al. [2] proposed a joystick-based method for continuously reporting passenger's nausea in a scale from 1 to 5 during driving simulation. The subjects were sitting in a motion-based driving simulator as passengers and a joystick was used to continuously report the level of nausea**.** However, this kind of method is not suitable for the study of the simulator sickness when the subjects are driving themselves.

2. Methods

2.1 Driving simulator with the motion-base

The base for our simulator and the driving control system are manufactured by Frex GP (Osaka, Japan). The system consists of two degrees of freedom (2 DOF) motion platform, high quality steering wheel, pedals, and gear shifter. We used a single high performance laptop to run the simulator environment. The computer, Sager NP8120, has an Intel 1,6 GHz i7 720QM quad core with 8 GB DDR3 RAM memory and Windows 7 operating system. We used two nVidia GTX 285M graphic adapters for the video output. These graphic adapters provide the 3D view for 3D Projector (Acer H5360) in scalable link interface (SLI) parallel processing mode. The resolution of the projected image was 1280x800, and it was projected on a 3x3 meter flat canvas. The size of the projected image was 2.2 x 1.375 m. Subject's distance from the centre of flat canvas was 1.9 meters. nVidia 3D Vision Home kit with a shutter glass technique was selected for the presentation of stereoscopic 3D view (refresh rate 120hz).

We added a number of details from real cars to the simulator in order to increase the realistic driving experience. These include a middle console with a gear shifter, a hand brake and a seat from Volvo, and a high impact speaker installed inside the driver's seat for adding a feeling of vibration while driving. We used a Logitech Z-5500 high quality 5.1 speaker system for creating realistic driving sounds. A small display including gauges for speed, RPM, fuel level and engine temperature was added behind the steering wheel to create an illusion of real car indicators. A further developed version of the driving simulator is presented by Koskela et al. [11].

2.2 Temporal Method for Simulator Sickness

Motivation for our studies was to develop a temporal method for simulator sickness (TMSS) 1) to study how much the new driving simulator derives nausea and other simulator sickness symptoms during driving, 2) to study factors that may be related to appearance of simulator sickness (driving view, motion base movements etc.), and 3) to study the relation between the appearance of symptoms and severity of simulator sickness for different subjects.

We considered a number of published methods to measure simulator sickness during driving. Unfortunately, none of them directly met our needs. We saw it important that the method would interfere as little as possible with the subject's driving.

The TMSS questionnaire consists of a scale indicating the level of nausea (1 = none, 2 = mild, 3 = mediocre, 4 = strong, and 5 = severe). The nausea level is asked with one minute intervals during simulation. The subjects are also advised to inform immediately if the nausea level changes. When the nausea level changes, the subjects are asked to describe the symptoms they have (headache, stomach ache, dizziness, blurriness of eyes, nausea, and general discomfort).

We evaluated two parameters describing the overall level of sickness of subjects during driving. The parameters are

1. TMc, defined as the cumulative sum of the symptom values given by a subject during the simulation experiment.

2. TMm, defined as the maximum among the symptom values given by the subject during the simulation experiment.

We also studied the relation between the SSQ score and TMSS values TM_c and TM_m. Therefore, we used both methods in the experiments.

2.3 Measurements

SSQ method: Before and after both drives the Ss filled a simulator sickness questionnaire (SSQ) in order to evaluate different simulator sickness symptoms on a scale of none to severe (16 questions dealing, e.g. with the distraction of eyes or dizziness). The answers were calculated together to compose a general score using the conversion table by Kennedy et al. [8].

TMSS method: Before the driving task, the Ss were shown the nausea scale. The Ss were advised to use these numbers in the estimation of their nausea level during the driving task. The nausea level was asked with one minute intervals. Before each driving task, we introduced the subject with different kinds of symptoms. All changes in nausea level or any other feelings the subject informed were written down minute by minute into a measurement protocol note. In addition, every driving session was recorded by using two video cameras (one recording the driver and another recording the driving view).

Telemetry: We collected a number of telemetry data indicating the state of the simulation such as the distance from the start, speed, acceleration, wheel position, throttle and brake positions. The data was recorded with accuracy of one millisecond. The recorded data was used to study the relation of distance information to the S's nausea level.

2.4 Subjects

Twelve subjects (Ss) (6 men and 6 women, aged from 22 to 32 years, mean 25.8) participated in the experiments which consisted of two driving situations (Drive 1 and 2). One subject got too sick at the first driving session and suspended the second session. All Ss were in good general health, and they were instructed to come well rested and abstain from alcohol 12 hours before testing. All Ss had a normal or a corrected-to-normal vision. S's background, driving experience, and sensitivity to motion sickness were filled out. None of them had previous experience of driving simulator. All Ss were informed about the scope and design of the study, and they gave their written consent for participation.

2.5 Experimental protocol

The two parts of the experiment (Drive 1 and 2) were carried out during different days. Drive 1 consisted of driving on an asphalt road with some hard turns and fast straights (ADAC 24h). In Drive 2 the Ss had to drive on a very lumpy and rough gravel road which changed into winding asphalt after four kilometres of driving (Lienz Rally Hillclimb).

Before Drive 1 each subject filled out a subject's background questionnaire, heart rate monitor was attached, and the driving position was adjusted. The SSQ-form was filled. Thereafter, the Ss were given instructions of the driving task. All subjects drove with automatic shift and used 3D-glasses. Subjects were also informed that they are free to abort driving if they are feeling too sick to continue. Subjects were also advised to start carefully and then drive a speed they feel comfortable. Subjects were instructed that driving would last about 15 minutes. The simulator and the heart rate monitor were synchronized by pressing on the simulator and the Polar wrist computer's lap key at the same time. The temporal method was applied as presented in the previous section. After the driving task the subjects were free to relax for a couple of minutes before the SSQ-form was filled out. Lastly, the heart rate recording was stopped.

3. Results

The data gathered in this study consisted of the SSQ data of subjects collected before and after each experiment and the temporal sickness data (TMSS) collected during each driving simulator experiment. Additionally, we stored telemetry information of simulator experiment consisting of, e.g., the distance from the start point at the road, the time used for driving, and the speed of vehicle.

We first studied subject's tendency for simulator sickness. In the analysis, the subjects were divided, on the basis of the appearance of nausea, in three groups:

1. Subjects who got severe symptoms
2. Subjects who got moderate and varying nausea levels
3. Subjects who did not have any symptoms

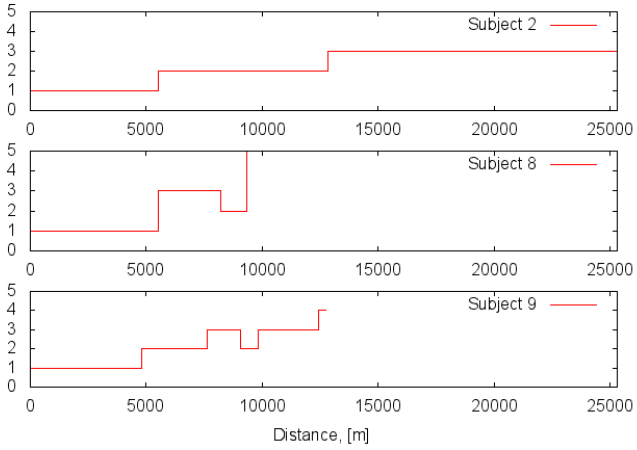

Figure 1. The appearance of nausea (scale in the ordinate) as a function of the section of the road (distance) during driving (group of subjects with severe symptoms).

Subjects belonging to the Group 1 got symptoms quite quickly after the start of the simulation. On the other hand, the level of their sickness grew rather quickly and led to an interruption in two cases out of three. Results for the group getting severe symptoms are presented in Figure 1.

Subjects belonging to the Group 2 reported the first symptoms later than the subjects belonging to the Group 1. We originally assumed that the level of sickness should monotonically increase with the increasing distance from the beginning of simulation. The findings did not support this hypothesis as can be seen in the results for the Group 2 (Fig. 2). It was also interesting to find out that the level of nausea could both increase and decrease during the experiment.

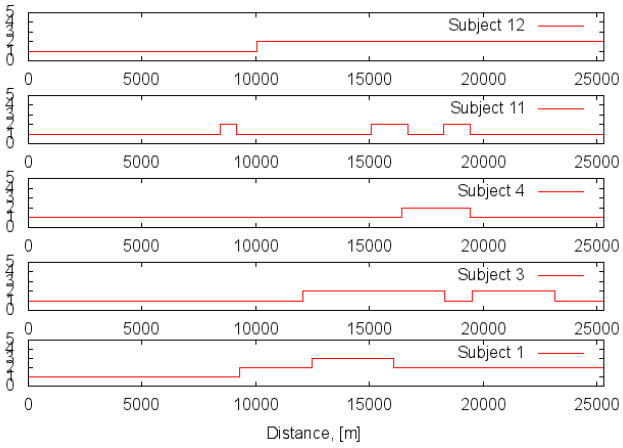

Figure 2. The appearance of nausea (scale in the ordinate) as a function of the section of the road (distance) during driving (group of subjects with average symptoms).

We then studied subject's sensitivity for simulator sickness with respect to the distance from the starting place of driving. For each subject, we calculated distances at the road where the subject's symptoms changed their value or state for the first time.

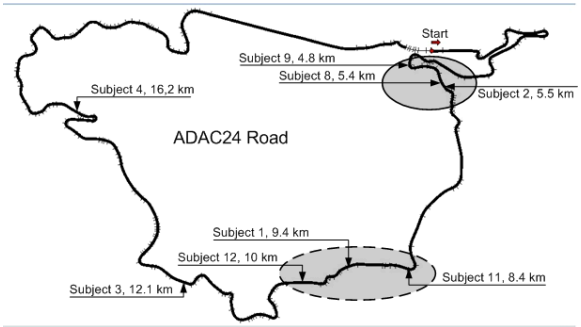

Figure 3. Profile of ADAC24 road and two areas where nausea appeared for the most of subjects.

The profile of ADAC24 road is presented in Figure 3. The starting point of Drive 1 is located in the right-up corner of the figure. Figure 3 also presents the sections of the road (grey areas) where the subjects expressed their increasing nausea levels at the first time. At the oval rounded by solid line, subjects 2, 8, and 9 got their first nausea symptoms. Respectively, the oval rounded by the dashed line indicates the area of the first nausea symptoms for subjects 1, 11, and 12. According to the results, the subjects that had increasing symptom levels at the early stage of the experiment also suffered from the most severe symptoms. We also noticed that six subjects had the first appearance of nausea immediately after a series of steep curves with red-and-white coloured curbs (see the section of the road with continuous line in Fig. 3). Also many of the subjects reported short period of dizziness symptoms (2-5 sec) in steep curves and downhills.

The results of SSQ questionnaire were computed using the scoring procedure table by Kennedy et al.

[Ken8]. We compared the results of our TMSS method with the results obtained by SSQ forms. SSQ_d is defined as the difference between the sum of values of the SSQ before and after a simulation experiment. We evaluated TM_c by adding together values of 15 evenly distributed samples of symptom values. After that, TM_c was normalized to start from 0 by subtracting 15 from the cumulative value.

Table 1. Comparison of SSQ and TMSS. SSQ_d: difference in SSQ values, TM_c: cumulative value of temporal method, TM_m: maximum value of symptom levels (Q = quitted from the experiment).

	Drive 1			Drive 2		
Subject	***SSQ_d***	***TM_c***	***TM_m***	***SSQ_d***	***TM_c***	***TM_m***
1	11.5	11	3	3.0	5	2
2	23.0	17	3	23.3	23	4
3	5.8	6	2	6.8	0	1
4	14.3	2	2	18	2	2
5	1.0	0	1	1.0	0	1
6	-1.0	0	1	4.8	0	1
7	28.5	0	1	42.8	0	1
8	41.3	Q	5	-	-	-
9	21.3	Q	4	19.3	Q	4
10	23.8	0	1	21.8	0	1
11	4.5	2	2	8.8	0	1
12	27.8	9	2	10.5	0	1

On the basis of the comparisons in Table 1 the subjects were divided in two groups:

1. Group “consistent”: Subjects who had high SSQ value and high TM values OR low SSQ value and low TM values.
2. Group “inconsistent”: Subjects who had high SSQ value, but low TM values

Subjects belonging to the Group “consistent” were subjects 1, 2, 3, 5, 6, and 8. Subjects having high SSQ_d value, but low TM_c and TM_m values belonging to the Group “inconsistent” were 7, 10, and 12. Also subjects 4 and 11 showed inconsistent values in drive 2. Reason to this is possibly that SSQ measures simulator sickness changes before and after drives. In many cases the symptoms of simulator sickness may increase or decrease quickly after the experiments and before the post SSQ form is filled. TMSS offers a more accurate method to analyse simulator sickness during driving.

4. Conclusions and future work

In this paper, we have presented the temporal method for simulation sickness (TMSS) for the study of the time course of the appearance of nausea during a simulation experiment. We also have compared TMSS and SSQ methods.

We divided the subjects in three groups according to the severity of the symptoms they had. We noticed that the subjects having the most severe symptoms got their first nausea symptoms much earlier than the others. Most of the subjects got their first nausea symptoms after a series of steep curves with red-white curbs. We noticed that the TMSS and SSQ tools do not correlate in many cases.

The present results indicate that the TMSS provides a useful tool for exploring nausea levels and other unpleasant symptoms during a driving experiment. The TMSS can be used to specify simulation related factors that may cause simulator sickness. This information can be used in further development of simulators in order to decrease the drop-out rates of subjects.

By using the TMSS we can evaluate both the driving distance and the driving time in relation to the appearance of nausea. We can also determine changes in the nausea levels of a subject during the experiment. Our results show that the level of nausea may vary a lot during a simulation experiment. Furthermore, the method offers the possibility to evaluate the severity of nausea and other symptoms during simulation.

The TMSS can also be utilized in preliminary tests as an analysis tool for the evaluation of the subject’s sensitivity to simulator sickness. Subjects having high TMSS values may be then excluded from the main experiment.

In the future, we aim to use the TMSS tool in order to study the relation between the simulator sickness and heart rate variability. Additionally, we will study whether the stereoscopic driving view increases/decreases the occurrence of simulator sickness.

Acknowledgements

This research is funded by European Regional Development Fund, the Joint Authority of Kainuu Region, and Sunit Oy. We are grateful for the support.

References

[1] Brooks J. O., Goodenough R. R., Crisler M. C., Klein N. D., Alley B. L., Logan W. C., Ogle J. H., Tyrell R. A., and Wills R. F., Simulator Sickness During Driving

Simulator Studies. *Accident Analysis and Prevention* 42, Elsevier, 2010, pp. 788 – 796.

[2] Chen Y.-C., Duann J.-R., Chuang S.-W., Lin C.-L., Ko L.-W., Jung T.-P., and Lin C.-T., Spatial and temporal EEG dynamics of motion sickness, *Neuroimage*, 49, 2010, pp. 2862 – 2870.

[3] Curry R., Artz B., Cathey L., Grant P., and Greenberg J., Kennedy SSQ results: fixed- vs. motion-based FORD simulators, *Proceedings of Driving Simulator Conference,* 2008, pp. 289 – 300.

[4] Havron, M. and Butler, L., *Evaluation of training effectiveness of the 2FH2 helicopter flight trainer research tool.* Naval Training Device Center, Port Washington, New York, NAVTRADEVCEN 1915-00-1, 1957.

[5] Häkkinen J., Pölönen M., Takatalo J., and Nyman G., Simulator Sickness in Virtual Display Gaming: A Comparison of Stereoscopic and Non-stereoscopic Situations, *Proceedings of the 8th conference on Human-computer interaction with mobile devices and services*, Stockholm, Sweden, 2006.

[6] Kellogg, R. S. and Gillingham, K. K., United States Air Force experience with simulator sickness, research and training. *Proceedings of the 30th Annual Meeting of the Human Factors Society*, 1986. vol. 1. pp. 427 – 429.

[7] Kenemy A. and Panerai F., Evaluating perception in driving simulator experiments, *TRENDS in Cognitive Sciences,* 7(1), 2003, pp. 31 – 37.

[8] Kennedy R. S., Lane N. E., Berbaum K. S., and Lilienthal M. G., Simulator Sickness Questionnaire: An Enhancement Method for Quantifying Simulator Sickness, *International Journal of Aviation Psychology*, 3(3), 1993, pp. 203 – 220.

[9] Kim, D.H., Parker, D.E., Park, M.Y. *A New procedure for measuring simulator sickness - the RSSQ.* Seattle, WA, USA 2004, University of Washington, Human Interface Technology Laboratory Technical Report R-2004-52.

[10] Kolasinski E. M., *Simulator Sickness in Virtual Environments,* Technical Report 1027, U. S. Armey Research Institute, Education and Training Technology, 1995.

[11] Koskela K., Nurkkala V.-M., Kalermo J., and Järvilehto T., Low-cost Driving Simulator for Driver Behavior Research. *The 2011 International Conference on Computer Graphics and Virtual Reality, CGVR'11,* July 18 – 21, 2011, Las Vegas, Nevada, USA, 2011.

[12] Mollenhauer M. A. and Romano R. A., The Evaluation of a motion Base Driving Simulator in a Cave at Tacom, *Proceedings for the Army Science Conference*, Orlando, Florida, 2005.

[13] Min B.-C., Chung S.-C., Min Y.-K., and Sakamoto K., Psychophysiological evaluation of simulator sickness evoked by a graphic simulator. Applied Ergonomics, 35, 2004, pp. 549 – 556.

[14] Rieber L. P., Seriously considering play: Designing interactive learning environments blending of microworlds, simulations, and games, *Educational Technology Research & Development,* 44(2), 1996, pp. 45 – 58.

[15] Slob J. J., *State-of-the-Art Driving Simulators, a Literature Survey*, DCT 2008.107, DCT report, Eindhoven University of Technology, 2008.

[16] Watson G., A Synthesis of simulator sickness studies conducted in a high fidelity driving simulator, *Proceedings of Driving Simulator Conference*, 2000, pp. 69 – 78.

Enhanced game mode for Eco-driving simulator

Beloufa Sabrina[1,2,3], Cauchard Fabrice[3], Vailleau Benjamin[1], Vedrenne Joël[2], Boucheix Jean-Michel[3], Kemeny Andras[1,2], Mérienne Frédéric[2]

[1]RENAULT, Technical Center for Simulation – TCRAVA 013 , 1 avenue du Golf 78288 GUYANCOURT
E-mail: sabrina.beloufa@renault.com, benjamin.vailleau@renault.com, andras.kemeny@renault.com

[2]Arts & Métiers Paristech – Institut image ENSAM – 2 rue Thomas Dumorey 71100 Chalon sur Saône
E-mail : frederic.merienne@ensam.eu, joel.vedrenne@ensam.eu

[3]LEAD, Université de Bourgogne - CNRS UMR 5022 - Université de Bourgogne Pôle AAFE - Esplanade Erasme - BP 26513 - 21065 Dijon CEDEX
E-mail : Jean-Michel.Boucheix@u-bourgogne.fr, Fabrice.cauchard@u-bourgogne.fr

Abstract

The use of driving simulators is part of RENAULT's approach for eco-driving development. The geDRIVER project objectives were to: develop ECO mode for all, taking into account eco-driving criteria; develop a training business offer and develop specific assistance HMI (Human Machine Interface).

In terms of driving simulation, this induced a need to develop a wide range deployment training tools integrating multisensorial feedback, enhanced gameplay for scenario design, and driving analysis tool into ECO² simulator.

Several experiments were carried out, in order to evaluate validity of simulation for an eco-driving training purpose.

Results show that visual indicators is the most appropriate and that the eco-driving rule "gear up at 2500 rpm" is the most efficient. At last, the simulator appears to be an efficient tool, to understand and integrate eco-driving rules, and to improve economies in terms of CO2 emissions.

Key words: Eco-driving, Driving simulation, Serious game, Learning, Human machine interface.

I. Introduction

Analysis of driver behavior has been the purpose of many studies for several years. This is linked with expansion of driving assistance systems in modern vehicles, as well as development of new systems and solutions. On the other hand, improvement in numerical technologies has enabled more detailed experimental studies conditions for behavior analysis with well controlled immersive driving situations (full-scale simulators, haptic feedback, designed scenarios, virtual reality, etc). However, only a few scientific studies focused on ecological behavior and fuel consumption (some applications of learning methods for truck drivers for example [KEM1]). Another new aspect, which was not often discussed in driver behavior studies, is learning processes.

This study was part of a double context:

- Environemental context: reduction of energetic consumptions and CO2 emissions transports has become essential, and the object of socio-economic global issues. Drivers' behavior should change to take into account environmental criteria
- Safety context: at the same time, European directive 2003/59 CE aimed to regulate qualification and learning for driver assigned to freight and passenger transportation, in terms of eco-driving and road safety.

Today, technologies in support of learning are evolving to accompany the implementation of this directive (e-Learning, simulators).

The objective was to design and provide tools and methods for eco-driving behavior learning, in order to enable driver to improve their eco-performance, in the respect of environmental and safety rules. With a strong practical experience, this project aimed to reinforce position and utility of driving simulation between theoretical and practical learning. The consortium of the project geDRIVER (green efficient driver), labeled by the French national pole System@tic, included industrial partners: Oktal (leader), Renault SAS and KDC (eco-driving school), and research partners: Arts et Métiers ParisTech, and LEAD University of Bourgogne.

II. Eco-driving Method

2.1 Eco-Driving Program

More and more companies are concerned with eco-driving, in order to reduce fuel consumption and CO2 emissions, and reduce accidents risks. Whether it is large companies equipped with fleets of vehicles, or smaller ones, whishing to make their employees aware of eco-driving benefits: optimize and reduce operating costs, harmonize mobility and environment, and protect them as part of the road risk prevention in enterprises ([Ana1]).

Renault has deployed an eco-driving program, illustrated with the label eco2[1], which takes different forms:

- Communication campaigns were conducted in several companies and organisms, with distribution of communication kits, and demonstration of small static driving simulators (fig 1).

Figure 1 : Static eco2 driving simulator

[1] For ecological and economic

- Embedded assistance systems are developed, with specific information feedbacks and dedicated HMI (Human Machine Interface), and active automatic systems having hand on vehicle performance and engine mapping.
- Learning modules are still distributed by KDC, with theoretic and practical phases, respectively with presentation of several driving "rules" and advice, and with driving sequences on open roads. These are based on successive evaluations, with analysis criteria, enabling to quantify eco-performance of candidates, as well as on long-term (several months) eco-performance evolution study.

According to Renault specifications (http://www.renault.com/fr/capeco2/eco-conduite/pages/eco-conduite.aspx), main rules and advice to remember for eco-driving are the following:

Advice 1: Optimize gear shift

Gear down near 1000rpm; gear up near 2000rpm for diesel vehicle, and 2400rpm for gasoline vehicle; select 4^{th} or 5^{th} gear at 50km/h.

Advice 2: Drive smoothly

Keep a steady speed (if >40km/h); use engine brake, and as little as possible brake pedal (natural deceleration cuts off fuel injection); drive at 50km/h in 5^{th} gear, release throttle 100m before the traffic lights.

Advice 3: Moderate accelerations

Up to 50km/h, it is better accelerating strong enough to be quickly in 5^{th} gear; above 50km/h, accelerations have to be moderate; gear up quickly to 5^{th} gear.

Advice 4: Manage climbs and descents

Keep speed in descent; slow down in climbs (without interfering with traffic), and stabilize if possible at a speed > 40km/h; release throttle in descents.

Advice 5: Use engine wisely

Stop engine from 30 seconds stops; do not preheat engine; start engine quickly after ignition.

These are part of the advice provided during eco-driving lessons. During practical session, it is applied and adapted to various situations with specific traffic and road configurations.

Main findings from Renault and KDC internal studies and learning results analysis showed that eco-driving enables generally consumption (and CO2 emissions) gains of 10 to 20%. Improvement is noticed immediately after learning. Unfortunately, eco-performance curve goes down over time, for a residual gain of about 5%.

Another drawback was that drivers often may not go to the end of the experiment, organized during several weeks if not coached by a trainer.

This led to necessity to improve some points: necessity to do periodic reminders, and to improve interest of drivers for exercises. This means a necessity to have appropriate learning tool and appropriate application integrated. Driving simulator could provide an interesting solution.

2.2 Eco-driving simulation

Driving simulators are mainly used for driving learning, experimental research on human behavior, and automotive engineering ([Par1], [Azz1], [Kem1]). With evolutions and improvements of simulation techniques, as well as the increasing popularity of some gaming technologies, simulators have gradually become testing tools that could be provided turnkey. These more accessible solutions enabled to focus on contents (teaching, scripting, realism, interactivity). Fidelity of simulation provided by these tools is useful for application such as eco-driving learning.

Experimental studies of the project geDRIVER required specific content in order to enable validation of simulator as a pertinent learning tool for eco-driving. Techniques derived from videogames enabled to reinforce interest of the experiment and of the learning sessions [Bou4]. Serious gaming is indeed now quite widespread for learning and awareness, and has been acknowledged as efficient and effective tool, with great attractivity, especially for the general public. In order to feed this content, analysis models for eco-driving, and performance monitoring were adapted to a learning context. New interactive guidance techniques based on ecologic and safety criteria were developed, and gameplay was enhanced with more interactive scripting techniques.

2.3 Eco-driving software architecture

As can be seen in Figure 1, the simulator was a one-person fixed-base simulator including an adjustable seat, a wheel, a gear stick, the clutch, gas and brake pedals. The player was immersed in the simulated environment by means of three LCD screens, audio speakers located in front and behind the seat, and vibrators embedded in the seat.

Simulation was based on SCANeR™ Studio v1.0, developed by Renault and Oktal and SCANeR™ DT v1.5 (training oriented version). Global architecture schema is represented in fig 2.

Software evolutions were made so that utilization of SCANeR™ tool could remain generic. Main developments concerned:

- Integration of new simulator cockpit specific acquisition module to Studio v1.0 and DT v1.5; integration of new I/O information from cockpit commands
- Industrialization on ECO-DS of the VEN interface (Virtual Extended Network), enabling communication and data exchange between distinct soft environments (vehicle data, driver evaluation variables, etc…)
- Improvement of the Training Manager module of SCANeR™ DT v1.5 to manage training session database and interface.

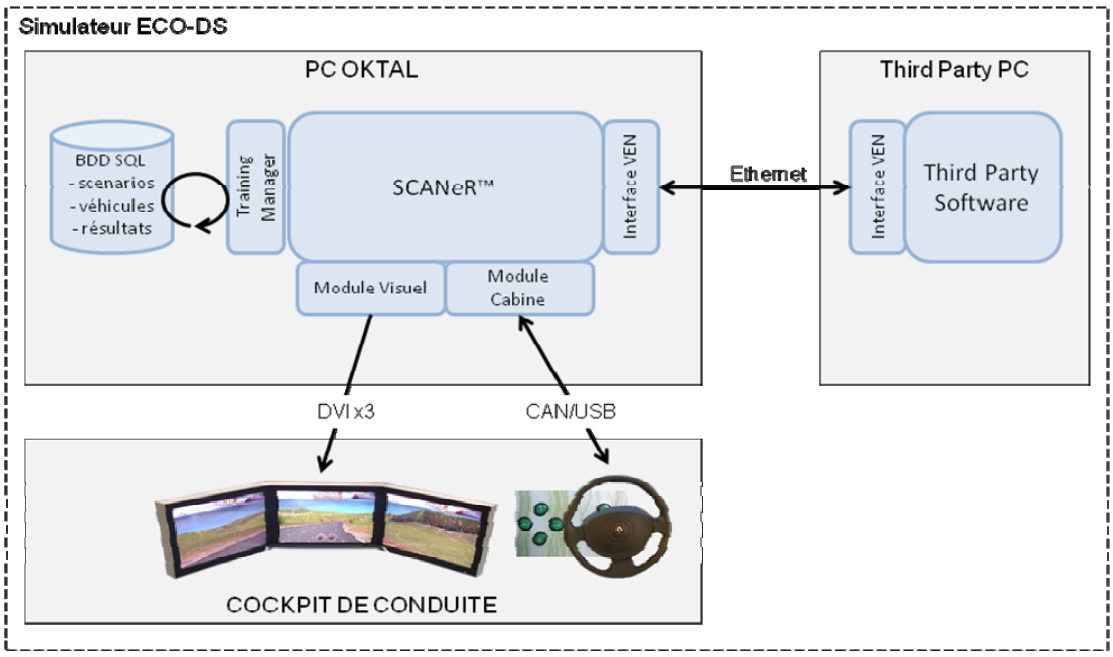

Figure 2: ECO-DS simulation architecture

The eye-tracking is a faceLAB apparatus and the eye-tracking data and the driving performance data are recorded at a frequency of 60 Hz.

Eco-driving analysis

A driving style measurement and analysis method was implemented and improved in order to adapt former measurement system and to validate this tool for simulated and real driving. A technical demonstrator was built in order to test interactions between SCANeR™ and KDC former tool. Each one runs on a dedicated PC and exchanging data through a network communication layer (cf. fig 2).

This tool analyses driving style with data based on driver actions on vehicle. These data acquisition system is implemented via a CAN bus interface and takes into account all vehicle and engine data (pedals position, acceleration, speed, rpm, distance, etc…). While comparing several identical driving courses data (for the same driver or for an eco-driving expert) it enables to determine global driving behavior (cumulated braking time, accelerations duration) and fuel consumption.

All this architecture was integrated into the cockpit of eco2 simulator shown on fig 1.

2.4 Interactive guidance techniques

Innovative interactive guidance techniques for eco-driving were built and implemented. A preliminary study was carried out, focusing on the guidance tools optimization, and the courses the subjects would have to drive on. The goal was to determine which sensory modality, or combination of modalities, was the most effective for each guidance dispositive. Then, the aim was also to see if the subjects could keep on using what they learned from this guidance dispositive when we removed it. Finally, we wanted to be sure that the guidance tools did not distub the driving behavior and activity.

The module was adapted to the simulation software and guidance dispositives integrated to the ECO² simulator. Global architecture is represented on fig. 3.

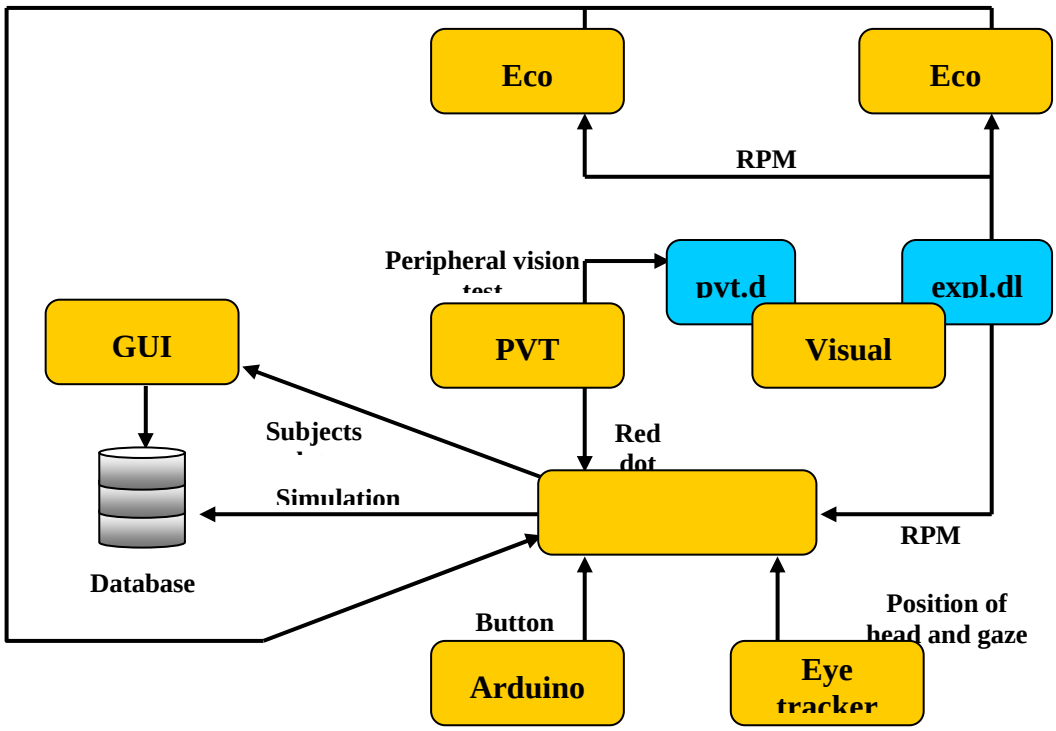

Figure 3: Metaphors restitution architecture

Metaphors had to be interactive, easy understandable and not too heavy in terms of cognitive load. They included visual messages, sounds and tactile feedbacks. These guidance metaphors were connected to vehicle data and acquisition module.

Visual information concerned CO2 emmissions, gearbox engaged, action expected on gearbox, RPM ideal level, limit speed, messages concerning clutch and brake pedals. Illustration of visual feedback is visible on fig. 4.

Sounds accompanied visual messages in the same situations of alerts, information, and were bips, spacialized 3D sounds, or vocal messages.

Haptic feedbacks were released through vibrations in the seat.

Figure 4: Visual feedback on the dashboard

Driving scenarios were designed, in order to evaluate different guidance techniques proposed.

2.5 Enhanced gameplay

In order to implement these functionalities, improve simulation conditions, simplify use of the simulator, and result in a serious game configuration, several gameplays were built. The gameplays defined game modes, evaluation processes, and scenario events. They were designed to ensure sensitization of the player to eco-driving, and security. The developments also consisted in making SCANeR™ environment more accessible to trainers for creation of their own driving scenarios, with a high level scenarization tool. This included building of a new dedicated graphic interface, adapted to preparation of players' profiles, datafiles, and measurements. This interface had to be user friendly and enable introduction of learning sessions.

The game mode used was made of successive levels, illustrating different eco-driving rules, with dedicated scenarios. In each scenario, several events required specific interventions from the driver, corresponding to one eco-driving rule, the performance of which was evaluated.

A debriefing was presented to the player after a session. A score was calculated according to his eco-performance, and a detailed analysis of his drive provided. Some explanations could also be given, with advice to improve his score. Fig. 5 illustrates a debriefing screen example.

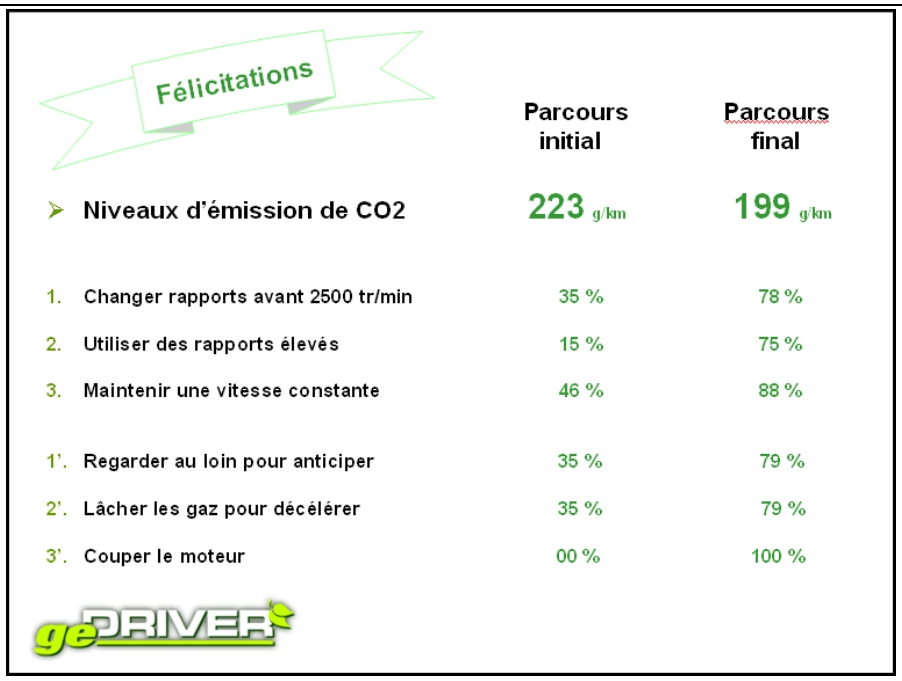

Figure 5: debriefing screen

III. Eco-Driving Simulator Experiment

Several studies focused on attention and guidance during activity ([Bou1], [Bou2], [Low1], [Low2], [Sch1], [Bou3]). The purpose of this study was to validate efficiency of geDRIVER learning, to quantify economies in CO2 emmissions, determine the respective contribution of each eco-driving rule to the achieved economy.The experiment was carried out in LEAD during July and August 2011. Subjects sample was composed of 72 persons, 45 males, and 27 females, aged 19 to 55 (mean age was 24). All of them had driving license for at least 1 year. They had driven 9000km in average during 12 last months (min 150, max 40000).

Progress of the geDRIVER learning was as following:

The player drove several dedicated courses, for learning or evaluation. Two of them were dedicated to learning, each one concerning a group of three eco-driving rules.

Rules were simplified versions of advices presented in the paragraph entitled Eco-Driving:

1: Gear up under 2500rpm

2: Drive with upper gearbox ratio possible

3: Maintain constant speed with clear road

1': Look far forward to anticipate decelerations

2': To decelerate: 1 release throttle, 2 gear down, 3 brake if necessary

3': Stop engine for more than 30sec stops

Experiment progress was:

Initial Evaluation (8 min)

Eco-drive lesson 1 (1min43) – rules 1,2,3

Training 1 (8min)

Eco-drive lesson 2 (2min10) – rules 1',2',3'

Training2 (10min)

Final evaluation (8min)

For all courses, dashboard provided following information: tachometer, speedometer, gearbox indicator, GPS.

Subjects were assigned to three groups: normal (with lessons and guidance system during training), control 1 (with lessons, without guidance), and control 2 (without lessons, without guidance).

In order to prevent from bias induced by difference in courses, or even habituation, a counterbalance system was used for initial and final courses between two half of subjects group. Courses were also equivalent in terms of curves, straight lines, specific events, etc…

The analysis performed on the CO2 emission with an ANOVA revealed a reliable Scenario x Group interaction, F (3, 69) = 8.54, p < .001. Results show a significant decrease of 10% in CO2 emissions in normal group, and of 7% in control 1 group. This indicates that interactive guidance systems help player to integrate focused eco-driving rules. In the control 2 group, no decrease is noticed, which indicates that differences noticed are indeed due to integration of eco-driving rules. Results are shown in fig. 6.

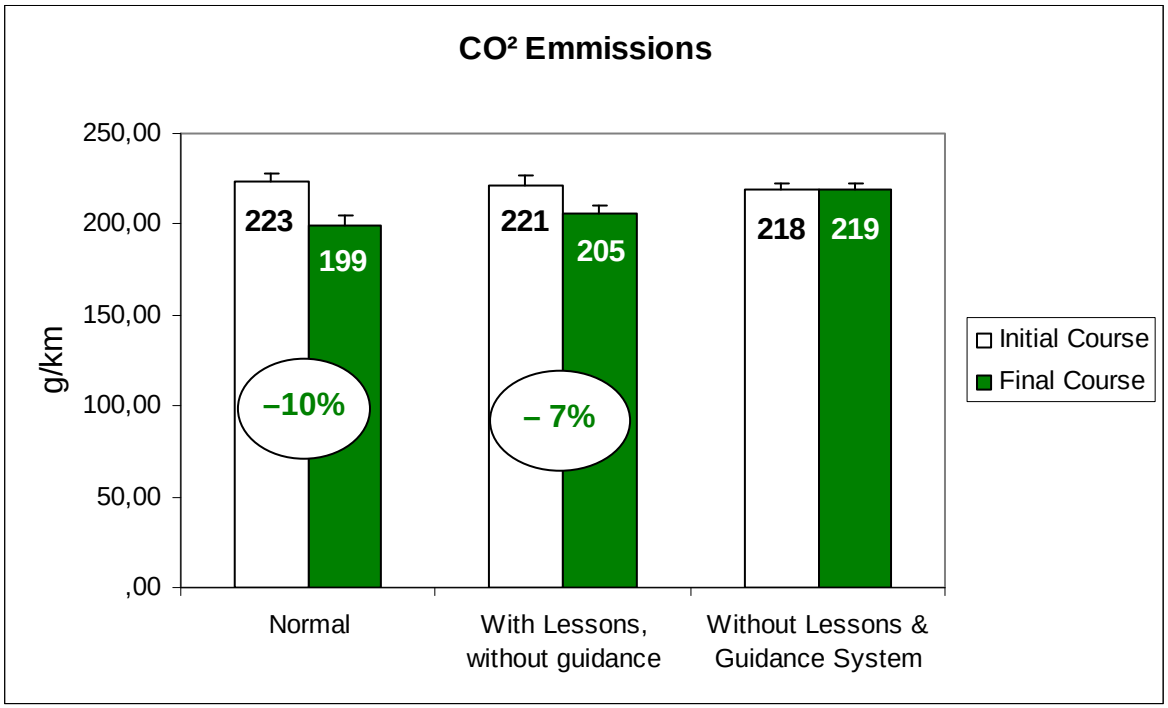

Figure 6: Levels of CO2 emmissions for initial (white) and final (green) courses in g/km

An important point is that no significant difference was noticed in driving time to achieve courses between normal and control 1 group. Irrespective of the groups the players were in, they took approximately the same time to drive the initial and final scenarios. This result showed that it is possible to modify one's own driving behavior in a way that reduces the CO2 emission level *without* losing any time in completing one's drive

Several indicators were analysed to evaluate driver behavior in terms of road safety : collisions, time leaving the road, safety distance,with other vehicles, eyes position, violation of highway rules, reaction time to dangerous events and ability to maintain the car in the middle of the lane. None of these indicators, showed a deficit in safety between two courses.

If we focus on respective contribution of different rules in CO2 emission decrease, results show first that all rules were generally integrated except rule 2. Players did not really use highest gearbox ratio.

Linear regression applied on results enables to estimate contribution of each rule to eco-performance. Two main conclusions can be enounciated: rules 1' and 2' seem to be the most efficient for CO2 emission decrease. Contribution of all other rules appears to be less evident.
This can be partly explained by the fact that rule 1 is not very clear to players. "Gear up under 2500rpm" may encourage player to gear up too early, which is unefficient. A more precise message, such as "Gear up near 2400rpm" should be better interpreted.
It's important to precise that mesures were also made to be sure that the learning of these rules has no effect on the travel times (by comparing the durations of initial and final courses), and security behavior of the subjects (by comparing several safety mesures between the initial and final couse).

Conclusion

Results confirm the hypothesis that driving simulators provide efficient solution for eco-driving learning, with greater interest than classic learning tools. Rules concerning anticipation and deceleration strategy seem to be the most efficient for gamers. But better definition of the rules might provide better results. For example, to help rule 1, visual indicators could target ideal rpm area for gearing up.
In driving simulation experiment, it may be difficult to anticipate stops, because traffic lights and stop panels are not necessarily visible until 200-300m distance. Higher screen resolution, traffic, or visual signs may provide an efficient solution.

Further studies are planned in collaboration between Arts et Métiers ParisTech, LEAD and Renault to learn more on eco-driving electric cars, especially for an efficient use in the best safety and comfort conditions with optimal road traffic autonomy.

References

[Par1] Parodi-Keravec A, Azzi S, Filliard N, Vailleau B, Icart E, Kemeny A, Mérienne F, Martinez JL. « Eco-driving performance assessment with in-car visual and haptic feedback assistance". *Proceedings of Virtual Reality International Conference (VRIC 2011),* 6-8 April 2011, Laval, France.

[Azz1] Azzi S, Reymond G, Kemeny A, Mérienne F. "Eco-Driving Performance Assessment With in-Car Visual and Haptic Feedback Assistance". *In Trends in driving simulation design and experiments, Proceedings of the Driving Simulation Conference* Europe 2010, pp. 181-190.

[Bou1] Boucheix, J.M. & Lowe, R.K. "An Eye Tracking Comparison of External Pointing Cues and Internal Continuous Cues in Learning with Complex Animations". *Learning and Instruction*. 2009. (Psychinfo).

[Low1],Lowe, R.K. & Boucheix, J.M.. "Learning from animated diagrams/ How mental models are built". *Diagrams, Lecture Notes in Artificial Intelligence.* 2008. 266-281. (ISI).

[Low2] Lowe , R.K. & Boucheix, J.M.. "Supporting relational processing in complex animated diagrams". *Diagrams, Lecture Notes in Artificial Intelligence.* 2008. 391-394. (ISI).

[Bou3] Boucheix, J.M. & Schneider, E. "Static and animated representations in learning dynamic technical processes". *Learning and Instruction.* 2008 (PsycInfo).

[Sch1] Schneider, E., & Boucheix, J.M. “Compréhension d’animations et mouvements oculaires : rôle du contrôle et de l’orientation de l’attention“. *L’année Psychologique*. 2008. (PsycInfo).

[Bou2] Boucheix, J.M., & Guignard, H. “Which animated illustration condition can improve science text comprehension in children? “ *European Journal of Psychology of Education*, 4, 2005. 369-388. (PsycInfo).

[Ana1] Anable J., Bristow A. L. “Transport and Climate Change”, *Supporting document to Climate Change Working Group of the Commission for Integrated Transport*, Sep. 2007.

[Kem1] Kemeny A., Kelada J.M. and Liano J.P. “Un simulateur de conduite pour la formation des conducteurs de véhicules poids-lourds". *Proceedings of the SIA Normandie*, Rouen, Oct. 1997

[Bou4] Boucheix, J.M. (2004). Multimedia Simulation and Comprehension Aid Tool for Complex technical documents. Advanced Learning Technology, ICALT, I.E.E.E, 898-900. (ISI, ISI Web of Science)

Evaluation of methods for measuring speed perception in a driving simulator

Martin Fischer, Lars Eriksson [1] and Katharina Oeltze [2]

(1) Swedish National Road and Transport Research Institute (VTI), Olaus Magnus Väg 35, 581 95 Linköping, Sweden, E-mail: martin.fischer@vti.se, lars.eriksson@vti.se

(2) German Aerospace Centre (DLR), Institute of Transportation Systems, Lilienthalplatz 7, 38108 Braunschweig, Germany, E-mail: katharina.oeltze@dlr.de

Achieving realistic sensation of longitudinal velocity and changes in velocity is a fundamental difficulty even for the most advanced driving simulators. It is also an aspect of great importance in many simulator studies. A stronger focus in recent years on driver assistance systems and CO2 issues, relating to driving style, further increase the need for realistic experience of speed and acceleration. This calls for investigation of the significance of different sensory cues to achieve realistic sensation and perception of especially longitudinal motion. A first step towards this goal was done by performing a study with the aim to explore different psychophysical methods for measuring speed perception in the context of driving simulation. The results of a conducted experiment indicate which of the evaluated methods are most suited for this task. Further, the presentation of a related literature study provides a broad overview on publications dealing with the topic of motion perception and motion cueing in driving simulation.

Keywords: *Speed perception, motion cueing, driving simulator, literature study*

Introduction

The driver's sensations and perceptions of acceleration, speed, and distance in driving simulators depend on several factors such as level of detail in the graphics, conveyance of sound and vibration, and degree of engaged peripheral vision [1]. If a motion platform is used, the strategies and control algorithms for its physical motions are of great importance in terms of experienced linear and angular accelerations [2]. The driver's abilities to appropriately accelerate, maintain speed, and decelerate all depend on the driver's sensations and perceptions. The basis for a realistic driving behaviour is realistic estimations of the driving speeds of the own and other vehicles because they directly affect performance indicators like time-headway, time-to-collision, and time-gap acceptance. However, it is a well-known problem that the driving speed is often severely underestimated in driving simulators [3], which implies that simulator studies aimed at evaluating certain driver assistance systems may be critically biased. A more realistic experience of acceleration and speed in driving simulators, that is, a perception in better correspondence with real driving, can be essential for certain types of simulator studies.

Although research has been done on how humans perceive motion (see [4-6]), more knowledge is needed on how much various sensory cues contribute to motion perception in driving simulators. In order to find ways to enable the driver to estimate the speed of the own vehicle, and other vehicles, in a similar manner as in real driving it is important to aim for quantification of the importance of different sensory cues to achieve realistic motion sensation. Based on this analysis, the following step must be the development of general methods and/or technologies to improve the motion sensation.

Method

With the aims stated above, a first step was to perform a literature study on motion perception and motion cueing aspects to obtain an overview of past research and existing knowledge. Based on this overview and several pilot tests in a driving simulator, an experiment was designed to evaluate several methods that seemed most suitable.

Literature study

For the estimation of distance, the visual impression is of highest importance (e.g. [7]). For the sensation of acceleration, the visual impression significantly adds to the sensation, but, as vision is a rather slow sense (e.g. [8, 9]) the vestibular system with its fast responses can be considered most important. However, the auditory and haptic impressions can add valuable information as well, i.e. through surrounding static or moving sound sources (e.g. [10]) or from vibrations or forces acting on the body (e.g. [11]). For the sensation of speed, all sensory cues

add to the final impression, although the visual can be considered dominant. Evaluating the absolute value of the driving speed based on auditory and haptic impressions is only possible based on driving experience and is always related to a certain vehicle type. Nevertheless, these cues give a strong indication for small velocity changes. Even though there are no vestibular cues for constant speed driving, perceiving velocity changes through vestibular motion cues adds to the ability of evaluating the current driving speed. Hence, it is more difficult to determine the actual importance of each sensory channel for speed perception because each one of them may be more or less equally important for the holistically realistic perception of speed.

Subsuming, all of the main sensory inputs are important for achieving the highest level of realistic motion perception. The results of the literature study were structured into four main categories of impression in accordance with the simulator's feedback channels to the driver:

- visual
- auditory
- vestibular
- haptic (including tactile)

An overview of the literature study results is provided below in Fig. 1, which shows the identified 49 factors that influence the perception of speed and acceleration in a driving simulator.

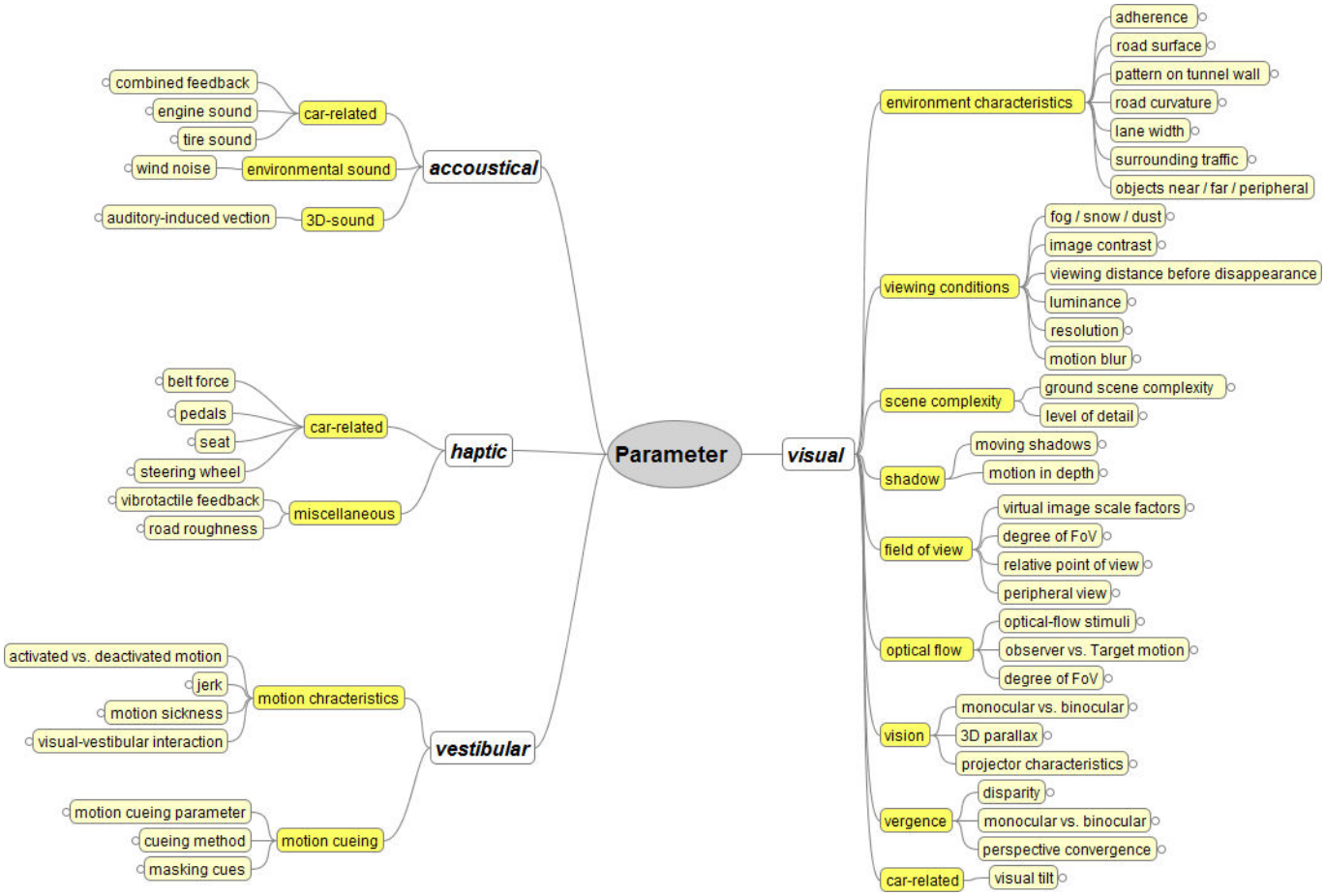

Fig. 1. Overview of parameters influencing the motion perception in driving simulators classified by motion cue type

The aim for the literature study was mainly to get a broad overview on publications about motion perception and motion cueing. Thus, the resulting listings (Tab. 1 - Tab. 4), which contains the most relevant articles examined during the study, is by no means to be treated as complete. For each referenced article, the main findings are shortly summarised. As the context of the gained results (facility, test subjects, applied method, etc.) is of high importance, the lecture of the original text is necessary for detailed interpretation of the results. However, the overview shall provide the reader a good base for understanding the different aspects of the topic and can serve as a base for deeper studies

Tab. 1: Visual cueing

ENVIRONMENT CHARACTERISTICS		
Adherence	drivers were able to discriminate different conditions of Loss of adherence (LOA) without vestibular feedback cues (fixed-base simulator); effect of intensity on duration, danger and intensity perception, fear and feeling of control significantly higher for longer LOA	[12]
Road surface	reaction time shorter with road markings; shorter intervals of road marking lead to longer response time; visual anticipation depends on visual cues included in road environment; environmental cues important for visual anticipation of collision & self-motion sensation	[13]
	realistic road roughness visualisation (coupled to corresponding acoustic and haptic feedback) improves perceived realism	[14]
	dot density of road texture has an significant influence on perceived speed; perceived speed with 10% dot density matches actual velocity best; perceived velocity more affected by image than sound information; perceived velocity improved by diversifying location of environmental objects	[15]
	higher chosen speed with abstract texture and no vertical markers present; no difference in simulator sickness and distance judgement; speed overestimation when driving without speedometer	[16]
Pattern on tunnel wall	no effect of pattern; more accurate estimation of TTC with higher approaching velocity	[17]
	pattern has no effect on lateral position or speed choice; no subjective favour for any pattern; access to speedometer had no effect	[18]
Road curvature	significant effect of curve radius on min. speed during curve negotiation; TLC as regulating mechanism for controlling speed (i. e. less experienced drivers compensate larger steering errors by choosing lower speed, so that constant TLC is maintained)	[19]
	lower speed with raised curve sharpness; correct subjective estimation of curve sharpness; left curves rated sharper than right curves; driving speed lower in left curves; no effect of age on ratings or speed selection	[20]
Lane width	visual feedback is used to control steering actions; variations in lane width and speed are compensated by steering choice in order to maintain certain safety margins	[21]
Surrounding traffic	general underestimation of distance; better position adjustments at higher speed; no effect on positioning error relative to distance between cars; performance better when targets did not move; performance improved with increase in speed and decrease in distance between vehicles; driving experience most important in differentiation of subjects' performances	[22]
	significant effects for vehicle type (motorcycle, compact car, full-size car, van) and viewing distance on time-to-arrival estimations before a left-turn; overall underestimation of time-to-arrival	[23]
	increased speed in surrounding traffic makes subjects drive faster during free driving on a highway	[24]
Objects near / far / peripheral	approaching peripheral stimulus appears slower than identical central stimuls; no effect of duration	[25]
VIEWING CONDITIONS		
Fog / snow / dust	no effect of fog on speed perception; overestimation of headway; headway perception improved by appropriate rear fog-light	[26]
	increase in the perceived distance of vehicles in fog as compared with normal visibility conditions; overall distance overestimation, effects reduced when using more than one light	[27]
	lower speed in foggy condition	[28]
	higher speeds in foggy condition	[29]
Image contrast	visual contrast between lead vehicle and road surface has larger impact on car following behaviour than field of view, motion or sound	[30]
	vehicle speed harder to discriminate and appears slower with reduced image contrast	[31]
Viewing distance	significant effects for vehicle type (motorcycle, compact car, full-size car, van) and viewing distance on time-to-arrival estimations before a left-turn; overall underestimation of time-to-arrival	[23]
Luminance	change of luminance has minor effect on the perception of motion-in-depth	[32]
	higher circular vection (CV) velocity and shorter latency with high luminance in the central vision field; CV velocity and CV latency depend on spatial frequency	[33]
Resolution	motion feedback and reduced blurred image leads to lowest simulator sickness; image quality is an important factor for reducing simulator sickness	[34]
	better sign readability with higher resolution; higher subjective ratings for environment clarity and realism	[35]
	increasing the spatial resolution leads to a significant increase in visibility; the level of spatial and temporal resolution has to be almost equivalent	[36]
	no significant effect of image resolution on validity of speed choice and lane position	[37]
	speed choice more closely matches the real world driving with a narrow FoV and high resolution; contrariwise lane position is closer to real world driving with wide FoV and low resolution	[38]
Motion blur	significant effect of motion blur on perceived speed; underestimation of speed decreases with motion blur	[39]
SCENE COMPLEXITY		
Ground scene complexity	increase of scene complexity leads to better performance in altitude control; estimates of altitude highly dependent on distance from impact point (more accurate estimating at closer distances and lower altitudes)	[40]
Level of detail	improved altitude judgements through level-of-detail constancy	[41]
SHADOWS		
Moving shadows	detection of an “approaching” target defined by moving cast shadows is faster than the detection of a “receding” target	[42]

	information provided by the motion of an object`s shadow overrides other strong sources of information and perceptual biases; natural constraint of shadow darkness plays a role in the interpretation of moving image patch as a shadow	[43]
Motion-in-depth	The visual system is more sensitive to expanding convex circles (impression of approaching objects) ; anisotrophy for the perception of motion in depth caused by shading cue	[32]
FIELD OF VIEW		
Virtual image scale factors	significant effect of visual scale factor; perceived speed increases with higher visual scale factors; modification of the geometric FoV (GFoV) remained unnoticed; perception of distances may be affected	[44]
	visual speed is underestimated for GFoV/FoV ratios of 1 or below; larger GFoV/FoV ratio leads to reduced errors in perceived speed	[45]
	both, minification and magnification of the image scale factor leads to greater sickness symptoms than in neutral condition; no effect of changes in time delay	[46]
Degree of FoV	FoV has less impact on car following behaviour than visual contrast between lead vehicle and road surface	[30]
	no effect of FoV on performance	[47]
	wide FoV (230 degrees) improves speed keeping and lane selection performance when compared to actual on road driving	[37]
	speed choice more closely matches the real world driving with a narrow FoV and high resolution; contrariwise lane position is closer to real world driving with wide FoV and low resolution	[38]
	strong underestimation of distances in observing proximal objects with reduced FoV; no effect of monocular/binocular vision on distance estimation	[48]
Relative point of view	with high eye height (relative to the road) subjects tend to drive faster with more variability and less consistent lane position keeping; no effect of eye height on following distance	[49]
	low vertical angle of the driver's view-point lead to a higher perceived velocity; minimized difference between actual and perceived velocity with a vertical angle of about -3 deg	[15]
Peripheral view	peripheral stimulus approaching subject appears slower than identical central stimulus; no effect of duration	[25]
OPTICAL FLOW		
Optical-flow stimuli	motion-in-depth information can bias perceived stereoscopic-based depth; with simulated motion towards the observer objects appear closer to observer than the depth signalled by disparity information; simulated motion away from the observer made it seem further away	[50]
	observers are more sensitive to contracting than to expanding patterns with large-field stimuli	[51]
	linear relationship of perceived and real distance, but consistent undershoot of absolute magnitude; motion simulation has no effect on distance judgement	[52]
	using a vertically oscillating display leads to more severe simulator sickness and stronger vection ratings	[53]
	drivers slow down with increased optic flow and speed up with slower optical flow	[28]
	perceived self-speed increases with stimulus area; perceived self-speed in central and peripheral conditions increase with circular border size; retinal image velocity strongly contributes to perceived self-speed	[54]
Observer vs. Target motion	dominant nature of the visual condition for the discrimination of forward linear translation	[55]
	perceived TTC shorter during observer motion; overestimation of actual TTC; significant interaction between motion type and closing speed; overestimation of TTC decreases as the proportion of observer motion increases	[56]
	objects perceived to have higher closing speed when self-motion and object-motion are in same direction; effect saturated with increase in ratio between the speeds of self- and object-motion; perceived direction of object-motion-in-depth (MID) shifted towards focus of expansion of the flow pattern	[57]
	overestimation of TTC, significant difference in the estimated TTC for observer vs. target motion only for high closing velocities	[58]
	saturated vection more robust for translations than for rotations; subjects didn't perceive any visual scene deceleration; subjects did perceive sudden changes in self- and visual scene velocity	[59]
Degree of FoV	visual flow perturbed spatial orientation, but effect varied as a function of the visual information provided; wide-angle display caused high levels of postural sway in the conditions of forward motion; omitted central field of 30° with added horizon-line effects at relatively high levels for y-translation and x-rotation; greater separation of peripheral screens from the central screen generated decreased display effectiveness	[60]
	strong underestimation of distances in observing proximal objects with a reduced FoV for both, real and virtual scenes; the more FoV is reduced the more underestimation can be observed	[48]
VISION		
Monocular vs. Binocular	no effect of monocular/binocular vision on distance estimation	[48]
	binocular information about MID helps to reduce biases in perceived speed and direction	[57]
	positioning errors smaller with monocular than binocular viewing; driver performance shows distance underestimation with monocular as well as with binocular vision; target cars were perceived farther in depth and more accurately using monocular vision in sections where significant performance differences occurred; alignment with static cars turned out to be easier than tasks with cars in motion	[61]
Projector characteristics	better driving performance using a projection system compared to usage of an head-mounted-display	[47]
	different technologies of projectors as they are relevant for the use in driving simulation are mentioned including their basic properties various testing procedures and gained experiences; the influence of spatial and temporal resolution is explained	[36]

	turning cabin and/or projectors while cornering; indication that not only the bodily sensation but the image quality is important factor in order to reduce simulator sickness	[34]
VERGENCE		
Disparity	conflict between disparity and perspective contributes to depth contrast	[62]
	vergence induced by disparity change is an effective cue for motion in depth; looming gives stronger cues when looming and disparity are in conflict	[63]
Perspective Convergence	the visual system uses perspective convergence to perceive slant and the effective use of convergence requires the presence of spectral components aligned with the tilt direction; in case of nearly frontal surfaces perspective convergence becomes the primary factor when available and has greater influence on perceived slant than the combined contributions of size, density, or other gradient texture cues	[64]
CAR-RELATED		
Visual tilt	adding visual tilt leads to better control and higher stopping accuracy of braking	[65]

Tab. 2: Acoustical cueing

CAR RELATED		
Combined feedback	sound has less impact on car following behaviour than visual contrast and vehicle dynamic cues	[30]
	only with combined high quality haptical, acoustical and visual feedback, extra strain on the driver is minimised and simulator experiments will produce reliable outcomes	[66]
	vehicle feedback is strongly associated with driver's situational awareness (SA) ; the addition of non-visual vehicle feedback increases SA above vision alone; drivers seem not to be self-aware of changes in the presence/absence of different feedback signals; significant effect of auditory feedback compared to visual only condition; effect of auditory feedback combined with tactile feedback (under-seat resonators) and steering wheel feedback on sensitivity and SA compared to visual feedback alone	[67]
Engine sound	perceived velocity is accurate when sound is applied; with mismatch of visual and sound information the perceived velocity is more affected by image information	[15]
	adding auditory feedback (engine and aerodynamics noise) leads to earlier onset braking, less, but longer braking and increasing number of inversions of deceleration profile	[65]
	addition of engine sound significantly affected participants sensation of illusory self-motion	[68]
Tire sound	subjective rating of tire/road noise variations for different road surfaces; all roads received high mean ratings according to realism	[14]
	no significant effect of screeching tires on braking and cornering driving behaviour; adaptation of maximum deceleration over runs when screeching sound was added; subjectively rated as useful for adaption of cornering speeds	[11]
ENVIRONMENTAL		
Wind noise	Adding auditory feedback (engine and aerodynamics noise) leads to earlier onset braking, less, but longer braking and increasing number of inversions of deceleration profile	[65]
3D-SOUND		
auditory-induced vection	An auditory aftereffect occurs from adaptation to visual motion-in-depth; adaptation to combined auditory and visual stimuli changing in compatible directions increases magnitude of aftereffect; sound intensity changes do not cause a visual aftereffect	[69]
	sound source characteristics (type) is a determinant of auditory-induced vection; type plays minor role when multiple sound sources are present, indication for an increase of vection by realistically rendered environment sounds; high probability that interaction between type of sound source and environment is of importance	[70]
	moving sound stimuli add to visual induced vection; no effect of non-moving/ambient sound sources; mono sound increased convincingness of self-motion illusion	[71]
	significant auditory after-effects following adaptation to unisensory auditory and visual motion in depth; auditory effects can fill-in sparsely sampled visual motion	[72]

Tab. 3: Haptic cueing

CAR-RELATED		
Belt force	effect of seatbelt tensioning system on braking behaviour: maximum decelerations are lower, earlier braking, better stopping position consistency, lower braking onset jerk; subjective rating showed that seatbelt force-feedback improved realism	[11]
Pedals	a stiffer brake pedal leads to better stopping consistency, lower maximum decelerations and lower onset jerk; rated as more realistic than soft pedal	[11]
Seat	effect of vibration seat on speed choice in curve driving; no effect of pressure seat	[11]
	vehicle feedback is strongly associated with driver's situational awareness (SA) ; the addition of non-visual vehicle feedback increases SA above vision alone; drivers seem not to be self-aware of changes in the presence/absence of different feedback signals; effect of auditory feedback combined with tactile feedback (under-seat resonators) and steering wheel feedback on sensitivity and SA compared to visual feedback alone	[67]
Steering wheel	small effect of vibrating steering wheel; vibrations lead to lower onset jerk	[11]
	effect of different steering feedback modalities on driver behaviour; only with combined high quality haptical, acoustical and visual feedback extra strain on the driver is minimised and simulator experiments will produce reliable outcomes	[66]
	vehicle feedback is strongly associated with driver's situational awareness (SA) ; the addition of non-visual vehicle feedback increases SA above vision alone; drivers seem not to be self-aware of changes in the presence/absence of different feedback signals; no effect of steering wheel feedback on increasing	[67]

	SA on its own; effect of auditory feedback combined with tactile feedback (under-seat resonators) and steering wheel feedback on sensitivity and SA compared to visual feedback alone	
	driver are able to adapt their behaviour to a range of different steering feedback configurations; control of vehicles in curves possible with both linear and non-linear torque feedback; driving almost impossible with zero torque or inverted torque feedback	[73]
MISCELLANEOUS		
Road roughness	Realisation of road roughness related vibrations; subjective rating of simulated vibrations caused by different road surfaces lead to high mean ratings according to realism	[14]
Vibrotactile feedback	clear improvement of response time due to the use of vibrotactile feedback; vibrotactile cues are slightly more efficient than sound	[74]

Tab. 4: Vestibular cueing

MOTION CHARACTERISTICS		
Activated vs. deactivated	motion feedback leads to improved altitude judgements; no effect on control of climb rate or descent rate	[41]
	with motion the braking duration is shorter and the onset of braking later; small additional longitudinal motion cues lead to higher stopping accuracy; significant interaction between speed and motion	[65]
	with motion feedback the drivers are closer to the optimal speed as compared to the no-motion condition; effect of a motion platform on speed choice strategy: greater safety margin, higher level of lateral acceleration; underestimation of driving 'danger' in the no-motion condition due to a poorer anticipation of lateral acceleration based on visual cues only	[75]
	motion feedback leads to more realistic deceleration levels; braking strategy remains stable in presence of motion cues; lateral cues influences the drivers choice of driving trajectory; longitudinal cues influences linear velocity in turns	[76]
	yaw motion cues have large impact on pilot performance; translational motion cues improves performance and increase fidelity; if translational motion was present, addition of yaw motion provided only little additional benefit to performance, workload, compensation or fidelity	[77]
	motion has less impact on car following behaviour than visual contrast and vehicle dynamic cues	[30]
	simulator translational motion had a larger impact on perceived motion fidelity and motion perception than yaw motion; simulator sway reduced control activity and therefore pilot workload	[78]
Visual-vestibular interaction	dominant nature of the visual condition for the discrimination of forward linear translation (heading) due to less uncertainty	[55]
	sensation of linear self-motion becomes more realistic when applying whole body tilt; tilt rate shall remain below 3 deg/s	[6]
	both visual and vestibular cues are used to estimate the self-motion	[79]
Jerk	both jerk and acceleration contribute significantly to the perceived strength of motion; rating of motion larger for some conditions with lower level of acceleration when presented jerk was larger	[80]
	strong effect of jerk on linear motion detection thresholds	[81]
Motion sickness	habituation greater for longer exposure and more severe motions; pitch and roll motion failed to increase motion sickness incidence	[82]
MOTION CUEING		
Motion cueing parameter	with large motion (high scaling, optimized filters) pilot-induced oscillation and handling qualities ratings matched flight data more closely; large motion feedback increased pilot confidence, reduced safety pilot interventions and lowered touchdown velocities	[83]
	roll and lateral motion gain variations have significant effect both on pilots perception of motion fidelity and on handling quality ratings; subjective and objective measures decreased for lower gains	[84]
	scaling around 0.45 is optimal according to controllability of the vehicle and perceptual rating of combined visual and motion feedback	[85]
	the preference for a certain motion cueing feedback is more depending on the parameter choice than on the applied motion cueing algorithm (comparing classical washout and lane dependant approaches); best performance and ratings are reached with a 0.5 scaling and a lane dependant approach	[86]
	different expert driver prefer different parameter settings	[87]
	tilt coordination is to be avoided if possible; if used, tilt with rather unrestrictive rate in order to avoid time lags in signal presentation; use the drivers head as tilting point; chose filter parameter such that the need to washout signals is reduced; preferably apply weak washout;	[88]
Cueing method	vector substitution vs. leaning vehicle method; with leaning vehicle method the motion were rated as more natural subjects judged curves more correctly	[89]
	With offline motion cueing it is possible to produce the best possible representation of a specific driving manoeuvre for a given motion system	[90]
	In order to get a well performing motion feedback, the difference between algorithms (classical, optimal, adaptive) is to a great extend the effort in getting a good parameterisation; the classical algorithm seems to be a good starting point; gradually introduction of adaptive elements should be advantageous	[91]
	When designing a motion cueing algorithm, consider to avoid tilt coordination, compensate for washout false cues and use the road position for lateral cueing	[88]
Masking cues	no significant effect of heave masking cue on pitch rate perception threshold frequency description	[92]
	motion detection performance may be expressed as a function of the signal-to-noise ratio; random motion can mask a sinusoidal signal; the masking is most effective when containing frequency components near the signal frequency	[93]
	mentally "loading" subjects with additional tasks considerably increases motion perception thresholds	[94]

The analysis of the literature study revealed two aspects with a strong need of more exploration:

1) Most of the examined studies mainly (or exclusively) used the chosen driving speed as criterion for the evaluation of perceived speed or perceived overall motion. This seems to be problematic as the final driving speed is not only depending on the perceived speed, but also on the gas and brake pedal characteristics of the simulator and the sensitivity of the vehicle model to driver inputs. In order to avoid this closed loop between driver action and motion perception, a method that presents a certain motion to the driver and focuses the driver's task on perception and estimation seems to be favourable. The chosen experimental approach, which aims for assessing different speed-perception evaluation methods, is explained in the following section.
2) Among the different types of cues, the field of visual perception has been most thoroughly investigated so far. The majority of the examined articles focus on the investigation of one or two single factors. Only a few discuss the visio-vestibular interaction (see Tab. 4). None is considering and comparing all four types of motion cues in the context of motion perception (Walker et al. [67] compare all cues, though with a strong focus on situation awareness). Thus, there is still a great need for understanding the overall relation between certain cues on speed perception. This problem shall be explored in a later study.

Simulator experiment design

An experiment was performed with the aim to evaluate primarily two methods for measuring driver's estimation of speed in a fixed-base driving simulator. Among several methods tested in simulator pilot-tests, prior to the experiment, the passive driving approaches "forced choice paired comparison" and "staircase paired comparison" were considered most suitable. The experimental sequence that was used in both methods, shown in Fig. 2, is adapted from a study on motion blur by Breithecker et al. [39]. The sequence uses masks to separate the presentation of two driving scenes with different speeds (i.e. different optical flow).

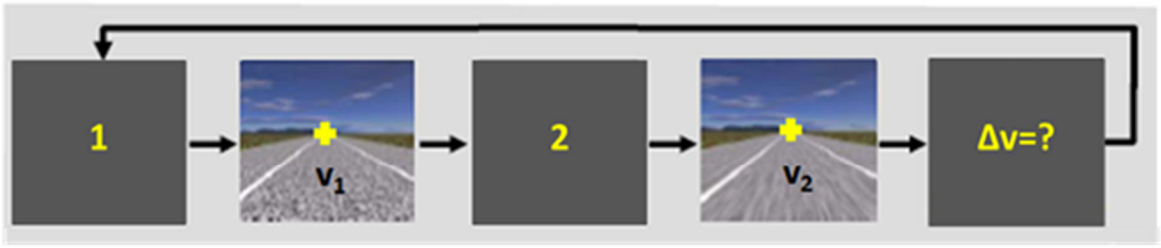

Fig. 2. Passive driving sequence (adapted from [39])

The used road was a normal straight road with no bricks or patches and without curves or intersections. The surroundings had no "regularities" at all (i.e. no dashed centre line, no delineators, no guide posts, no alley) in order to avoid cues that enable speed estimation based on counting seconds between certain objects or similar strategies. Only randomly distributed trees were placed in the surroundings to support the participant in the speed estimation tasks.

Besides the different speeds used, the main independent variable was the field-of-view of the visual presentation, which had two levels consisting of 45 and 180 degrees horizontally. Field-of-view has been shown to have an influence on speed choice and lane-keeping performance (e.g. [37, 38, 95]). We therefore hypothesised that the field-of-view could be used to reveal which speed estimation method is most sensitive. That is, if one of the methods shows levels of speed estimates dependent on the field-of-view the method would be judged more sensitive.

In the experimental scheme, shown in Fig. 3, the order of both the passive driving methods (PD) and the field-of-view settings (FoV) were balanced between participants.

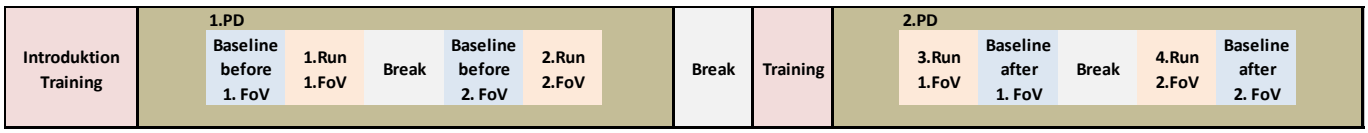

Fig. 3: Experimental scheme

Based on the experiences of the pilot tests we further hypothesised that the resulting speed perception threshold will vary with the direction of speed change, that is whether the second speed is higher (corresponding to an

acceleration) or lower (corresponding to a deceleration). More specifically, we expected higher thresholds for decreasing speeds. Only visual cues were presented (no sound, no physical motion, no haptic feedback).

A within-group design was used. The participants were 13 men and 3 women with a mean age of 42 years and a mean driving experience of 20 years. The speedometer was turned off during the whole experiment.

Forced choice paired comparison

In the forced choice paired comparison, successfully used by e.g. Haycock and Grant [80], either the first or the second scene is one of four base speeds (30, 50, 70 or 90 km/h). The other one shows an additional speed of +1, +5 or +10 km/h. For example, for the base speed of 30 km/h six different pairs of speeds are obtained including both increasing and decreasing speed: 30-31, 30-35, 30-40, 31-30, 35-30 and 40-30. The participant's task was to make a judgement of how the second speed of each pair differed from the first by responding with one of the six forced choice alternatives: -10, -5, -1, +1, +5, or +10 km/h. The total number of pairs of speeds was 24 (four base speeds with six pairs each) for each of the two levels of visual field, and each participant evaluated all 48 pairs. The presentation order of the pairs was varied over participants to avoid order effects.

Staircase paired comparison

In the staircase paired comparison, described by Ehrenstein and Ehrenstein [96], the participant also judges the speed difference between two different scenes. As opposed to the forced choice paired comparison, the staircase method requires the participant only to judge whether the presented velocities were different or not. If the response is "yes" (a difference), the speed difference is lowered for the next presentation of pair of speeds, and if the response is "no" (no difference) the speed difference is raised for the next pair. The aim of such a staircase method is to reach the threshold for perceiving a change of a given stimulus, which in this case is the speed difference to a certain base speed (Fig. 4, left). Ehrenstein and Ehrenstein propose to use two interleaved staircases were one initial stimulus is chosen to be below the expected threshold value and the other one above (Fig. 4, right). This reduces the risk that the participant notices the logic behind the staircase variation and thus increases the probability for establishing an unbiased threshold value.

Because this method is quite time consuming, the experiment design considered only two base speeds for the exploration of speed perception thresholds, which were 50 and 90 km/h. Each base speed included a fixed staircase sequence of 24 trials that was performed for both levels of visual field. A variable step size between the trials were used in order to be able to use a start value which is reasonable far away from the expected threshold range, to approach the threshold region with only a few trials, and then to have the major parts of the trials within the threshold range. Thus the step size was first set to 5 km/h and after the first changes of answer (i.e. previous answer was "yes" but actual answer is "no" or the other way round) it was reduced to 3 km/h, then 2 km/h and finally to 1 km/h. In the single staircase example given in Fig. 4, between trial 1 and 4 the step size would be -5 km/h, after trial 4 it would be +3 km/h, after trial 5 -2 km/h and in the following + or – 1 km/h. Furthermore, both starting stimuli were chosen to be above the expected threshold value, but with the lower speed presented first in one sequence (speed increase from scene 1 to scene 2) and the higher speed presented first in the other sequence (speed decrease). As mentioned above, differences in threshold values related to this condition (speed increase or decrease) were hypothesised based on the experience gained from the pilot-tests.

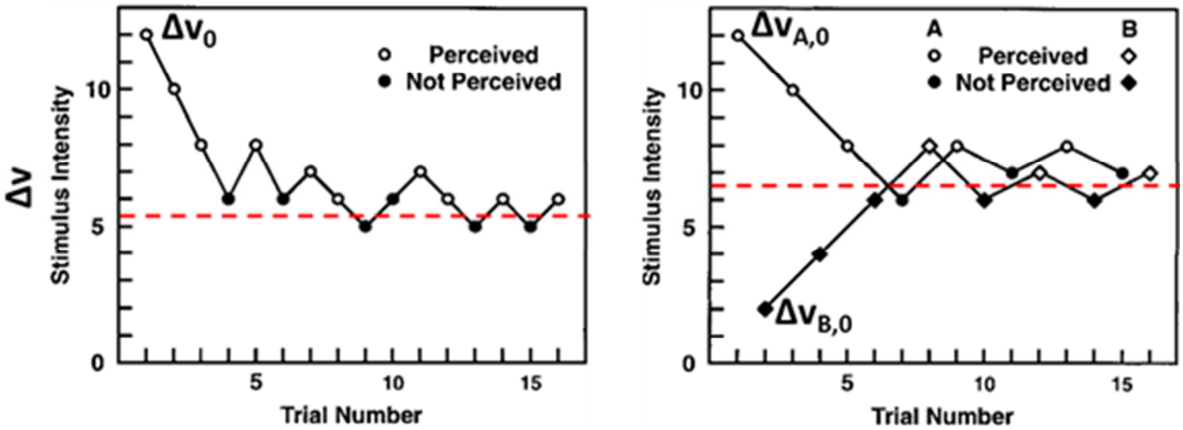

Fig. 4. Staircase method sequence in order to obtain a threshold for perceiving change of a certain stimulus (here: speed difference), Left: single staircase, Right: Two interleaved staircases. Adapted from Ehrenstein and Ehrenstein [96]

Baseline driving

A baseline task was performed to obtain indications of driver ability to estimate absolute speeds. The participant was passively accelerated and the task was to judge when a certain target speed was reached. The target speeds were 30, 50, 70 and 90 km/h. Each speed was estimated twice, once starting with an initial speed of 0 km/h (estimation during acceleration) and once with an initial speed of 120 km/h (estimation during deceleration), for each level of visual field. The participant indicated reached target speed by pressing a button on the steering wheel.

Questionnaires

Before and after the experiment, each participant answered a questionnaire about physical and mental states based on the simulator-sickness questionnaire (SSQ), described in Kennedy et al. [12], that includes a four-point rating scale for each of 16 stated symptoms. After the experiment, some additional questions were answered on 7-point rating scales:

- *How was the speed perception with the narrower/broader presentation field?*

Not at all realistic ☐ ☐ ☐ Neither … nor ☐ ☐ ☐ Very realistic

- *How good judgments/responses did you make with the narrower/broader presentation field?*
- *How good judgments/responses did you make when only responding by indicating whether there was a difference or not?* [Staircase paired comparison]
- *How good judgments/responses did you make when responding by indicating how large the difference was?* [Forced choice paired comparison]
- *How good judgments/responses did you make when responding by indicating when a specific speed was reached?* [Baseline driving]

Very bad ☐ ☐ ☐ Neither … nor ☐ ☐ ☐ Very good

Results

The following paragraphs show the results of the statistical analyses of the logged data from the simulator experiment as well as of the responses in the questionnaires filled in by the participants.

Forced choice paired comparison

An analysis of variance (ANOVA) for repeated measures was conducted with the design of field of view (2) × base speed (4) × speed sequence (6).

The ANOVA showed significant main effects of base speed, $F(3, 45) = 3.66$, $p < .025$, and speed sequence, $F(5, 75) = 52.28$, $p < .0001$, and a significant interaction effect of base speed by speed sequence, $F(15, 225) = 2.50$, $p < .01$, with no other significant effects. The interaction effect is shown to the left in Fig. 5.

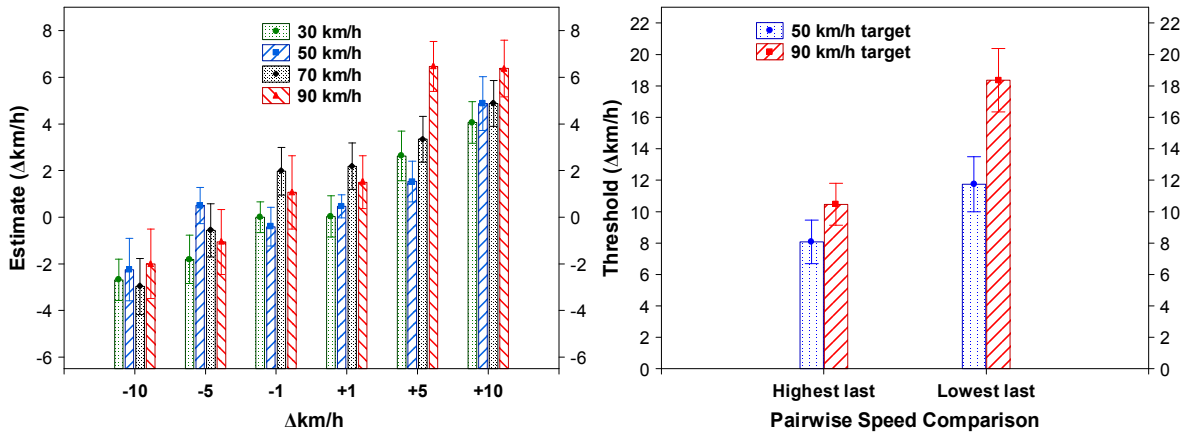

Fig. 5. To the left, the significant interaction effect of base speed by speed sequence with the forced choice paired comparison; to the right, the significant interaction effect of base speed by speed sequence with the staircase paired comparison

Staircase paired comparison

An ANOVA for repeated measures was conducted using the design of field of view (2) × base speed (target) (2) × speed sequence (2).

The ANOVA showed significant main effects of base speed, $F(1, 15) = 54.71$, $p < .0001$, and speed sequence, $F(1, 15) = 19.89$, $p < .001$, and a significant interaction effect of base speed by speed sequence, $F(1, 15) = 6.24$, $p < .025$, with no other significant effects. The interaction effect is shown to the right in Fig. 5.

Baseline driving

An ANOVA for repeated measures was conducted using the design of time (2) × field of view (2) × speed sequence (2) × speed (4). The time variable included the two conditions of baseline driving "before" and "after" using the respective paired comparison methods, the field of views were 45 and 180 degrees, speed sequence included the conditions of acceleration and deceleration phases, and the category speed referred to the target speeds of 30, 50, 70, and 90 km/h.

The ANOVA showed a significant main effect of speed, $F(3, 45) = 348.67$, $p < .0001$, and a significant interaction effect of speed sequence × speed, $F(3, 45) = 15.67$, $p < .0001$, with no other significant effects. The significant interaction effect is shown to the left in Fig. 7. However, there was also a tendency of a three-way interaction effect of field of view, speed sequence, and speed, $F(3, 45) = 3.31$, $p = .06$, which is shown to the right in Fig. 7.

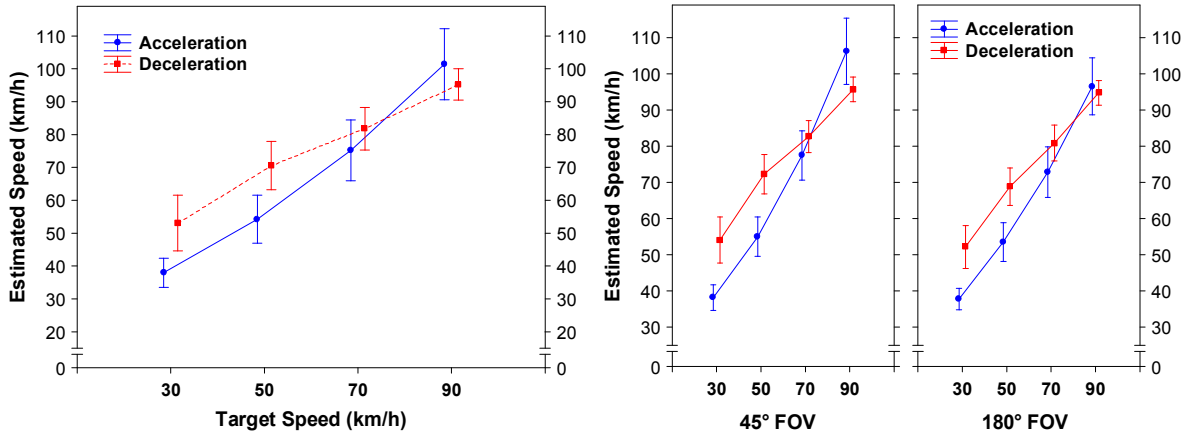

Fig. 6. To the left, the significant interaction effect of speed sequence by speed with the baseline driving. To the right, the tendency of a three-way interaction effect of field of view by speed sequence by speed with the baseline driving.

Questionnaires

The questionnaire data were analysed with several non-parametric Wilcoxon matched pairs test.

There was a significant difference in speed perception quality between the 45° and the 180° fields of view ($p < .01$). The broader 180° was considered to give a significantly more realistic experience of speed (to the left in Fig. 8). There was also a significant difference in positive speed perception quality between the 45° and the 180° fields of view ($p < .025$), showing that the 180° was considered to give a significantly more positive experience of speed (to the right in Fig. 8).

There was a significant difference in self-estimated response quality between the 45° and the 180° fields of view ($p < .05$) in which the 180° was considered to lead to significantly better speed perception estimations (to the left in Fig. 9). The difference in response quality between the forced choice paired and the staircase paired comparison methods was also significant ($p < .05$), with the staircase paired comparison method considered to enable significantly better speed perception estimations (to the right in Fig. 9).

Further, the significant difference in response quality between the forced choice paired comparison and the baseline driving methods ($p < .025$) shows that the baseline driving method was rated to enable significantly better speed perception responses (to the left in Fig. 9). (There was no significant difference in response quality between the staircase paired comparison and the baseline driving methods ($p = .083$).) Finally, there was no significant difference in total SSQ scores between before and after the experiment ($p = .06$). However, it indicates a tendency of a slight effect of simulator exposure on simulator sickness symptoms (to the right in Fig. 9).

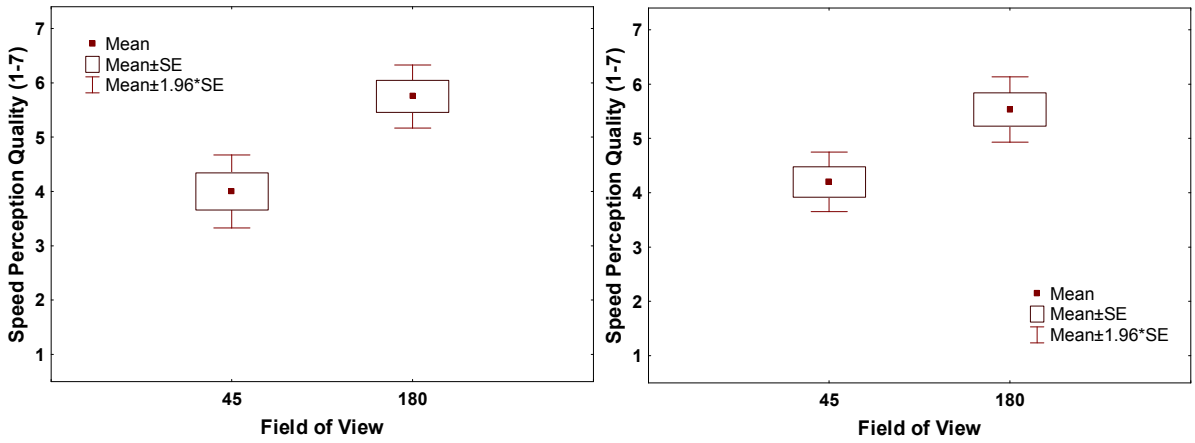

Fig. 7. To the left, the significant difference in realistic speed perception between the two visual fields. To the right, the significant difference in positive speed perception between the two visual fields.

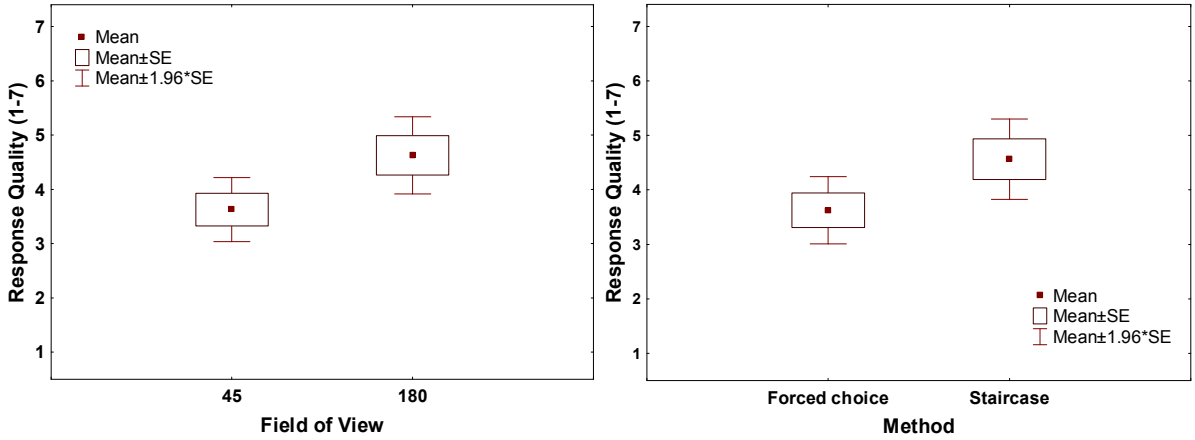

Fig. 8. To the left, the significant difference in judgment/response quality between the two visual fields. To the right, the significant difference in judgment/response quality between the forced choice paired comparison and the staircase paired methods.

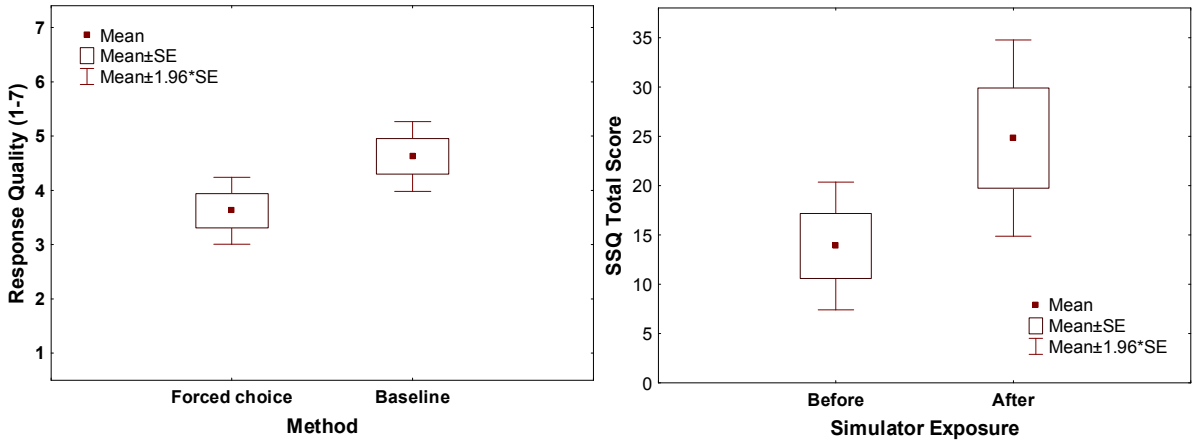

Fig. 9. To the left, the significant difference in judgment/response quality between the forced choice paired comparison and the baseline driving methods. To the right, the non-significant difference in SSQ total score between before and after simulator exposure.

Summary and conclusions

Presenting the lowest speed last in a paired speed comparison makes it more difficult to judge the difference correctly, as indicated by the results from both the forced choice paired comparison and the staircase paired comparison method. Hence, the threshold for perceived speed differences is substantially higher for decreasing speeds. In addition, the forced choice paired comparisons indicate that speed differences with the base speeds of 70 and 90 km/h are more correctly judged when the highest speed is presented last.

The staircase paired comparisons show that the threshold values for both base speeds, 50 and 90 km/h, are in the same range when the highest speed is presented last, whereas the threshold is significantly higher for 90 km/h when the lowest speed is presented last. However, the threshold values increase for both based speeds when applying a speed decrease compared to speed increase.

The results of the baseline driving show that the lower speeds of 30 and 50 km/h are more correctly judged when accelerating. At the higher speeds of 70 and 90 km/h there is no difference in speed judgement between accelerating and decelerating. The baseline driving results also indicate a tendency of an interaction effect including field of view, which may imply that at 90 km/h with the smaller field of view the speed may be more overestimated during acceleration than during deceleration.

The questionnaire results reveal that the larger field of view is preferred in terms of more realism, more positive experience, and better judgment/response quality of the speed perception. Both the methods of staircase paired comparison and baseline driving were rated to entail better judgment/response quality than the method of forced choice paired comparison. Finally, the SSQ total scores indicate a tendency of a slight effect (i.e. non-significant) of simulator exposure on simulator sickness symptoms.

Our conclusion is that the hypothesis of higher thresholds for speed differences with decreasing speeds was supported, whereas the influence of the size of the field of view was not supported. At least there was a tendency of an effect of field of view with the baseline driving, and the participants in fact considered the larger field of view better in terms of realism, positive experience, and judgment/response quality. The most probable explanation for the performance result is that the scene was too simplified (e.g. no mid-line, no guide posts) so that the larger field of view did not add significantly to the speed estimation ability.

There was no clear advantage of either method of pairwise comparison for judging speed differences. However, the staircase paired comparison method was preferred by the participants, and it also has the advantage of flexible levels of speed difference (i.e. no predefined speed differences) that can make the method more valid for measuring speed perception. Furthermore, considering the identified threshold levels by using the staircase method, places the results of the forced choice method into the region of chance, as the used pre-defined speed variations are mainly below these threshold levels. Of course, these two methods are fundamentally different, with the staircase method specifically designed for finding just noticeable differences (i.e. JNDs). As such, and in agreement with the overall results, the staircase method seems to be preferable and will be used within the following experiments.

The baseline driving method for establishing absolute judgements of speed perception seems to be a good complement to methods for measuring the perception thresholds of relative speed differences.

A coming experiment shall try to quantify the importance of different sensory cues. Different combinations of sensory cues of motion will be explored in order to evaluate their effect on driving behaviour and speed perception. Both a passive estimation task (staircase paired comparison) and an active driving task will be included.

Acknowledgments

The presented work has been performed within the MeMoS-project, financed through the Swedish competence centre for “Virtual Prototyping and Assessment by Simulation” (www.vipsimulation.se), and the related Eureka-project DrivObs (E! 5395).

References

[1] M. Pinto*, et al.*, "The development of driving simulators: Toward a multisensory solution," *Travail Humain,* vol. 71, pp. 62-95, 2008.

[2] G. Reymond*, et al.*, "Contribution of a motion platform to kinesthetic restitution in a driving simulator," in *Driving Simulation Conference* 2000.

[3] B. Sidaway*, et al.*, "Time-to-Collision Estimation in a Simulated Driving Task," *Human Factors,* vol. 38 (1), pp. 101-113, 1996.

[4] A. Kemeny and F. Panerai, "Evaluating perception in driving simulation experiments," *Trends in Cognitive Sciences,* vol. 7, pp. 31-37, 2003.

[5] M. Mulder*, et al.*, "Exploring the roles of information in the manual control of vehicular locomotion: From kinematics and dynamics to cybernetics," *Presence: Teleoperators and Virtual Environments,* vol. 13, pp. 535-548, 2004.

[6] E. L. Groen and W. Bles, "How to use body tilt for the simulation of linear self-motion," *Journal of Vestibular Research,* vol. 14, pp. 375-385, 2004.

[7] I. P. Howard and L. Childerson, "The contribution of motion, the visual frame, and visual polarity to sensations of body tilt," *Perception,* vol. 23, pp. 753-762, 1994.
[8] E. L. Groen*, et al.*, "Perception of self-tilt in a true and illusory vertical plane," *Perception,* vol. 31, pp. 1477-1490, 2002.
[9] R. J. A. W. Hosman, "Pilot's perception and control of aircraft motions," Ph.D., Delft University of Technology, Delft, 1996.
[10] A. Väljamäe*, et al.*, "Travelling without moving: auditory scene cues for translational self-motion," in *ICAD 05-Eleventh Meeting of the International Conference on Auditory Display*, Limerick, Irland, 2005.
[11] J. C. F. de Winter*, et al.*, "The search fo high fidelity in fixed-base driving simulation: six feedback systems evaluated," in *Driving Simulation Conference* Monaco, 2008.
[12] T. Denoual*, et al.*, "Drivers' perception of simulated loss of adherence in bends," *Driving Simulation Conference* 2010.
[13] C. Berthelon*, et al.*, "Environmental cues involved in the visual anticipation of a collision," in *IEA 2000/HFES 2000 Congress*, 2000.
[14] A. Bolling*, et al.*, "Shake - an approach for realistic simulation of rough roads in a moving base driving simulator," in *Driving Simulation Conference* Paris 2010.
[15] S. J. Kwon*, et al.*, "A study on the factors that improve the velocity perception of a virtual reality-based vehicle simulator," *International Journal of Human-Computer Interaction,* vol. 21, pp. 39-54, 2006.
[16] T. Luke*, et al.*, "The effect of visual properties of the simulated environment on simulator sickness and driver behaviour," in *Driving Simulation Conference*, Paris, 2006.
[17] M. P. Manser and P. A. Hancock, "Advanced simulation technology used to reduce accident rates through a better understanding of human behaviors and human perception," 1996, pp. 60-67.
[18] J. Törnros, "Effects of tunnel wall pattern on simulated driving behaviour," VTI Statens väg- och transportforskningsinstitut.", Linköping2000.
[19] W. Van Winsum and H. Godthelp, "Speed choice and steering behavior in curve driving," *Human Factors,* vol. 38, pp. 434-441. , 1996.
[20] K. Wochinger and K. Pecheux, "Driver perception of horizontal curves on a simulated two-lane rural highway," The Federal Highway Administration2001.
[21] W. Van Winsum*, et al.*, "Lane change manoeuvres and safety margins," *Transportation Research Part F: Traffic Psychology and Behaviour,* vol. 2, pp. 139-149, 1999.
[22] J. Bergeron*, et al.*, "A driving simulator study on the perception of distances in situations of car-following and overtaking," 2006, pp. 431-437.
[23] J. K. Caird and P. A. Hancock, "Perception of oncoming vehicle time-to-arrival," 1992, pp. 1378-1382.
[24] J. Olstam*, et al.*, "An algorithm for combining autonomous vehicles and controlled events in driving simulator experiments," *Transportation Research,* vol. C, 2010.
[25] K. Brooks and G. Mather, "Perceived speed of motion in depth is reduced in the periphery," *Vision Research,* vol. 40, pp. 3507-3516, 2000.
[26] V. Cavallo, "Perceptual distortions when driving in fog," 2002, pp. 965-972.
[27] V. Cavallo*, et al.*, "Distance perception of vehicle rear lights in fog," *Human Factors,* vol. 43, pp. 442-451, 2001.
[28] P. Pretto and A. Chatziastros, "Changes in optic flow and scene contrast affect the driving speed," in *Driving Simulation Conference*, Paris, 2006.
[29] L. Steeghs*, et al.*, "Speed perception fogs up as visibility drops," *Nature* vol. 392, 1998.
[30] E. R. Boer, "Driving simulator validation: car following gap controllability," in *Driving Simulation Conference*, Tsukuba, 2006.
[31] M. S. Horswill and A. M. Plooy, "Reducing contrast makes speeds in a video-based driving simulator harder to discriminate as well as making them appear slower," *Perception,* vol. 37, pp. 1269-1275, 2008.
[32] N. Shirai and M. K. Yamaguchi, "Asymmetry in the perception of motion-in-depth," *Vision Research,* vol. 44, pp. 1003-1011, 2004.
[33] Y. Yu and J. Wu, "Luminance effects on visual perception of self-rotation for development of driving simulator," 2007, pp. 2583-2586.
[34] Y. Asano and N. Uchida, "Effects of image quality and representation of somatic sensation on drive feeling " in *Driving Simulation Conference*, 2006.
[35] V. Govil, "A high-resolution wide-screen display for simulators and virtual reality," in *Human factors and ergonomics society* 2004.
[36] A. Huesmann and M. Strobl, "Heading towards eye limiting resolution – display systems in driving simulation," in *Driving Simulation Conference*, 2010.
[37] H. Jamson, "Image characteristics and their effect on driving simulator validity," in *First International Driving Symposium on Human Factors in Driver Assessment, Training and Vehicle Design* Snowmass, Colorado, 2001.

[38] H. Jamson, "Driving simulator validity: issues of the field of view and resolution," in *Driving Simulation Conference*, Paris, 2000, pp. 57-64.
[39] M. Breithecker*, et al.*, "Increasing perceived velocity by means of texture-based motion blur," in *Driving Simulation Conference DSC 2006.*, Paris, 2006.
[40] W. Barfield*, et al.*, "Relationship between scene complexity and perceptual performance for computer graphics simulations. ," *Displays: Technology and Applications,* pp. 79-185, 1990.
[41] W. W. Johnson and J. A. Schroeder, "Visual-motion cueing in the control of altitude," 1995, pp. 2676-2681.
[42] T. Imura*, et al.*, "Asymmetry in the perception of motion in depth induced by moving cast shadows," *Journal of Vision,* vol. 8, 2008.
[43] D. Kersten*, et al.*, "Moving cast shadows induce apparent motion in depth," *Perception,* vol. 26, pp. 171-192, 1997.
[44] F. Colombet*, et al.*, "Impact of geometric field of view on speed perception," *Driving Simulation Conference,* 2010.
[45] C. Diels and A. M. Parkes, "Geometric field of view manipulations affect perceived speed in driving simulators," *International Conference Road Safety and Simulation,* 2009.
[46] M. H. Draper*, et al.*, "Effects of image scale and system time delay on simulator sickness within head-coupled virtual environments," *Human Factors,* vol. 43, pp. 129-146, 2001.
[47] V. Grabe*, et al.*, "Influence of display type on drivers'performance in a motion-based driving simulator," *Driving Simulation Conference,* 2010.
[48] D. Paillé*, et al.*, "Stereoscopic stimuli are not used in absolute distance evaluation to proximal objects in multi-cue virtual environment," 2005, pp. 596-605.
[49] C. M. Rudin-Brown, "The effect of driver eye height on speed choice, lane-keeping, and car-following behavior: Results of two driving simulator studies," *Traffic Injury Prevention,* vol. 7, pp. 365-372, 2006.
[50] M. Edwards and D. R. Badcock, "Motion distorts perceived depth," *Vision Research,* vol. 43, pp. 1799-1804, 2003.
[51] M. Edwards and M. R. Ibbotson, "Relative sensitivities to large-field optic-flow patterns varying in direction and speed," *Perception,* vol. 36, pp. 113-124, 2007.
[52] H. Frenz and M. Lappe, "Absolute travel distance from optic flow," *Vision Research,* vol. 45, pp. 1679-1692, 2005.
[53] S. Palmisano*, et al.*, "Vertical display oscillation effects on forward vection and simulator sickness," *Aviation Space and Environmental Medicine,* vol. 78, pp. 951-956, 2007.
[54] K. Segawa*, et al.*, "Effects of visual field on perceived speed of self motion from optic flow," 2002.
[55] J. S. Butler*, et al.*, "Visual Vestibular Interactions for self-motion estimation," in *Driving Simulation Conference* Paris, 2006.
[56] G. A. Geri*, et al.*, "Simulating time-to-contact when both target and observer are in motion," *Displays,* vol. 31, pp. 59-66, 2010.
[57] R. Gray*, et al.*, "Long range interactions between object-motion and self-motion in the perception of movement in depth," *Vision Research,* vol. 44, pp. 179-195, 2004.
[58] R. P. Grutzmacher*, et al.*, "Time-to-contact estimates for observer versus target motion," 2000, pp. 419-423.
[59] F. A. M. Van Der Steen and P. T. M. Brockhoff, "Induction and impairment of saturated yaw and surge vection," *Perception and Psychophysics,* vol. 62, pp. 89-99, 2000.
[60] L. Eriksson, "Visual flow display for pilot spatial orientation " 2009.
[61] B. Baumberger*, et al.*, "Could a "monocular advantage effect" be measured in driving simulation?," *Ecological Psychology,* vol. 19, pp. 201-213, 2007.
[62] M. Sato and I. P. Howard, "Effects of disparity-perspective cue conflict on depth contrast," *Vision Research,* vol. 41, pp. 415-426, 2001.
[63] E. G. González*, et al.*, "Cue conflict between disparity change and looming in the perception of motion in depth," *Vision Research,* vol. 50, pp. 136-143, 2010.
[64] J. A. Saunders and B. T. Backus, "Perception of surface slant from oriented textures," *Journal of Vision,* vol. 6, pp. 882-897, 2006.
[65] M. Pinto*, et al.*, "The perception of longitudinal accelerations : what factors influence braking manoeuvres in driving simulators?," in *Driving Simulation Conference DSC* Paris, 2004.
[66] F. M. Reich*, et al.*, "Optimized haptical, acoustical and visual tuning with different vehicle dynamic models for the BMW driving simulator," *Vehicle System Dynamics,* vol. 29, pp. 648-654, 1998.
[67] G. H. Walker*, et al.*, "The ironies of vehicle feedback in car design," *Ergonomics,* vol. 49, pp. 161-179, 2006.
[68] A. Väljamäe*, et al.*, "Sound representing self-motion in virtual environments enhances linear vection," *Presence: Teleoperators and Virtual Environments,* vol. 17, pp. 43-56, 2008.
[69] N. Kitagawa and S. Ichihara, "Hearing visual motion in depth," *Nature,* vol. 416, pp. 172-174, 2002.

[70] P. Larsson*, et al.*, "Perception of self-motion and presence in auditory virtual environment," in *Seventh Annual International Workshop Presence*, Valencia, Spain, 2004, pp. pp. 252-58.
[71] B. E. Riecke*, et al.*, "Moving sounds enhance the visually-induced self-motion illusion (circular vection) in virtual reality," *Transactions on Applied Perception,* vol. 6, 2009.
[72] A. Väljamäe and S. Soto-Faraco, "Filling-in visual motion with sounds," *Acta Psychologica,* vol. 129, pp. 249-254, 2008.
[73] D. Toffin*, et al.*, "Influence of steering wheel torque feedback in a dynamic driving simulator," in *Driving Simulation Conference*, Dearborn, 2003.
[74] S. Cardin and D. Thalmann, "Vibrotactile jacket for perception enhancement," 2008, pp. 892-896.
[75] G. Reymond, Kemeny, A., Droulez, J., & Berthoz, A. (1999). "Role of lateral acceleration in curve driving: driver model and experiments on a real vehicle and a driving simulator." Human Factors. 43, 483-495 (2001). , "Role of lateral acceleration in curve driving: driver model and experiments on a real vehicle and a driving simulator.," *Human Factors,* vol. 43, pp. 483-495, 1999.
[76] I. Siegler*, et al.*, "Sensorimotor integration in a driving simulator: contributions of motion cueing in elementary driving task," in *Driving Simulation Conference*, Sophia Antipolis, 2001.
[77] P. R. Grant*, et al.*, "Effect of simulator motion on pilot behavior and perception," *Journal of Aircraft,* vol. 43, pp. 1914-1924, 2006.
[78] H. Smaili*, et al.*, "Pilot motion perception and control during a simulated decrab maneuver," 2007, pp. 951-961.
[79] G. L. Zacharias and L. R. Young, "Influence of combined visual and vestibular cues on human perception and control of horizon rotation," *Experimental Brain Research,* vol. 41, pp. 159-171, 1981.
[80] B. Haycock and P. R. Grant, "The influence of jerk on perceived simulator motion strength " in *Driving Simulation Conference* Iowa City, 2007.
[81] F. Soyka*, et al.*, "Does jerk have to be considered in linear motion simulation?," in *AIAA Modeling and Simulation Technologies Conference* 2009.
[82] M. E. McCauley*, et al.*, "Motion sickness incidence: exploratory studies of habituation, pitch and roll, and the refinement of a mathematical model," Canyon Research Group, Human Factors Research Division 1976.
[83] J. A. Schroeder and W. W. Y. Chung, "Simulator Platform Motion Effects on Pilot-Induced Oscillation Prediction," *Journal of Guidance, Control, and Dynamics,* vol. 23, pp. 438-444, 2000.
[84] J. A. Schroeder*, et al.*, "Effects of roll and lateral flight simulation motion gains on a sidestep task," 1997, pp. 1007-1015.
[85] E. R. Boer, Yamamura, T. & Kuge, N. (2001). "Affording realistic stopping behavior: a cardinal challenge for driving simulators". Proceedings of the 1st Human-Centered Transportation Simulation Conference, Iowa City, Iowa., "Affording realistic stopping behavior: a cardinal challenge for driving simulators," in *Human-Centered Transportation Simulation Conference*, Iowa City, Iowa, 2001.
[86] P. Grant, Blommer, M., Cathey,L., Artz, B. & Greenberg, J. (2003). "Analyzing classes of Motion Drive Algorithms Based on Paired Comparison." In Proceedings of the Driving Simulation Conference DSC 2003., "Analyzing classes of Motion Drive Algorithms Based on Paired Comparison," in *Driving Simulation Conference*, Dearborn, Michigan, 2003.
[87] M. Dagdelen*, et al.*, "DagdelenValidation process for the ultimate high-performance driving simulator," in *Driving Simulation Conference* Paris, 2006.
[88] M. Fischer*, et al.*, "Applied motion cueing strategies for three different types of motion systems," *Journal of Computing and Information Science in Engineering,* vol. 11 (4), 2011.
[89] J. A. Molino*, et al.*, "Motion cues for a 3-DOF driving simulator," in *Driving Simulation Conference*, North America Dearborn Michigan, 2003.
[90] J. Nauderer and A. Huesmann, "Progress in off-Line motion cueing and the application in automotive engineering as well as in the development of motion cueing algorithm," in *Driving Simulation Conference*, Monaco, 2009.
[91] M. A. Nahon and L. D. Reid, "Simulator Motion-Drive Algorithms: A designer's perspective.," *Journal of Guidance, Control and Dynamics,* vol. 13, pp. 356–362, 1990.
[92] A. R. V. Pais*, et al.*, "Modeling human perceptual thresholds in self-motion perception," in *AIAA Modeling and Simulation Technologies Conference and Exhibit*, Reston (VA), 2006.
[93] G. L. Greig, "Masking of motion cues by random motion: comparision of human performance with a signal detection model," University of Toronto Institute for Aerospace Studies, Toronto1987.
[94] R. J. Hosman and J. C. van der Vaart, "Vestibular models and thresholds of motion perception. Results of Tests in a Flight Simulator," University of Technology, Delft, Technical Report LR-265, 1978.
[95] B. Kappé*, et al.*, "Effects of head-slaved and peripheral displays on lane-keeping performance and spatial orientation," *Human Factors,* vol. 41 (3), pp. 453-466, 1999.

[96] W. H. Ehrenstein and A. Ehrenstein, "Psychophysical methods," in *Modern Techniques in Neuroscience Research*, U. Windhorst and H. Johansson, Eds., ed Berlin: Springer, 1999, pp. 1211–1241.

An optimisation of Classical motion cueing in the University of Leeds Driving Simulator

A. Hamish Jamson
University of Leeds Driving Simulator, Institute for Transport Studies, University of Leeds, LS2 9JT, U.K.
E-mail: a.h.jamson@its.leeds.ac.uk

Abstract *– This investigation examined the perception of self-motion in a research driving simulator, focussing on the dynamic cues produced by a motion platform. The study was undertaken in three stages, evaluating both subjective ratings of realism and objective measures of driver performance against two specific driving tasks involving braking and cornering. Using a Just Noticeable Difference methodology, Stage 1 determined that scale factors over 90% could not be perceptibly differentiated from unscaled motion. Stage 2 suggested that participants were also unable to perceive a change in the point in space at which platform translations and rotations were centred, however a position closer to the human vestibular system did result in marginally smoother braking. Stage 3 explored the perceptual trade-off between the specific force error and tilt rate. For both driving tasks, whilst slow tilt that remained sub-threshold was perceived as the most realistic, driving task performance was superior when a more rapid tilt was experienced. Several interactions were also observed, most notably between platform tilt rate and the availability of extra translational capability afforded by a XY-table.*

These interactions provide system design guidance research driving simulator motion cueing. Assuming accurate driving performance is a design goal, for simulators without significant extra translational capability, priority should be given to the minimisation of specific force error through motion cues, even if this means that cues at a presented at a perceptibly high tilt rate. However, large amplitude motion should be complimented by a slower tilt. Such a design supports accurate driving task performance whilst also accomplishing maximum perceived realism.

Key words: *motion cueing, classical algorithm, driving simulator.*

Introduction

Typically, driving is a much more challenging environment for motion cueing compared to commercial flight simulation. Significant longitudinal acceleration is not limited to a specific portion of the journey, i.e. take-off and landing. Laterally, turns are more frequent and uncoordinated, occupants sensing the side-slipping of a cornering vehicle as a specific lateral force, unlike the normally imperceptible heading changes of a commercial airliner. Rotationally, suspension characteristics need to be mimicked over a broad range of frequencies not experienced in controlled flight.

For specific individual driving manoeuvres, the perception of acceleration cues presented via the classical filter can be superseded by alternative algorithms (e.g. adaptive cueing [Par1], Model Predictive Control strategy [Dag1], Lane Position Algorithm [Nor1], Fast Tilt-Coordination [Fis1]). However, the flexibility, simplicity and elegance of the classical filter make it highly appropriate to cope with the expansive and varied nature of driving. Nevertheless, it suffers from the difficulties associated with tilt-coordination and the typical trade-off between specific force and tilt rate errors. Managing this trade-off is essential in the formation of an effective research driving simulator. Optimal parameter selection, or tuning, therefore now becomes the unenviable task of the simulator engineer.

Classical algorithm in driving simulation

In the example of driving simulation, the classical filter is applied to the six orthogonal accelerations generated from the vehicle dynamics model. These are the three linear accelerations of longitudinal acceleration (braking/accelerating), lateral acceleration (cornering) and the vertical acceleration (road roughness and bumps). These are supplemented by the three angular accelerations of pitch (suspension effects of braking/accelerating),

roll (suspension effects of handling) and yaw (actual yawing of the vehicle in a turn). The output of the classical filter describes the desired attitude that the motion platform should adopt [Con1; Rei2].

Consideration in the frequency domain of classical filter response to a control input allows the simulation engineer to assess the accuracy of the motion system's response in both gain (magnitude of the expected motion) and phase (timeliness of the motion). However, except in the case of very low accelerations or very small filter scale-factors, the transfer function of even a well-tuned classical algorithm is not flat. Transfer function fidelity criteria have been postulated in flight simulation (e.g. the "critical" Sinacori/Schroeder 1 rad/s motion fidelity criterion [Sch1]), but these do not yet exist in driving simulation.

The complementary nature of the classical filter allows independent control of high-frequency translational and low-frequency tilt-coordination channels. Flattening the transfer function by quickening the response of the tilt-coordination channel requires the development of tilt at a rate above perceptual threshold. Hence, an optimal solution, must be found solution between a platform response which is perceived as timely but with too much tilt (maximising specific force error at the expense of tilt rate error), or a response which feels lagged but without detectable tilt (maximising tilt rate error at the expense of specific force error).

Specific force error and tilt rate error trade-off

This trade-off between specific force errors and angular velocity errors is not new, having vexed researchers for some time in flight simulation (e.g. [Hos1]), but is governed predominantly by the flying task at hand. In their helicopter bob up/down simulator motion study with pilots undergoing a vertical tracking task of hovering to various target heights, [Sch2] suggested that flattening the transfer function by lowering high-pass onset filter cut-off frequency resulted in a greater degradation of tracking performance than by reducing the onset scale-factor. Additionally, in an evaluation of the perceived horizontal acceleration of a simulated a take-off run, [Gro1] observed a high correlation between the perceived discontinuity and the perceived magnitude of surge motion, indicating that pilots tolerate variations in filter natural frequency less than they do variations in filter scale-factor. Hence, in the design of commercial flight simulators, downscaling the specific force is commonly preferred over rapid tilt.

Influence of Motion Reference Point

Another design choice faced by the simulator engineer is the location of the motion reference point (MRP). The MRP denotes the point in space at which the platform translations and rotations are centred. Analogous to the design eye-point at which optimal viewing of a display system is achieved, in effect it is the point at which the perceived acceleration is ideally felt.

Since the vestibular system is located in the inner-ear, the ideal location for the MRP should be centred on the head of the observer [Rei1]. However, due to the geometric constraints of the hexapod, moving the MRP vertically upwards to this point requires significantly greater actuator strokes to achieve the same degree of tilt. Locating the MRP at the upper joint rotation points of a conventional hexapod will maximise the angular displacement capability and therefore the largest achievable specific force though tilt-coordination, but risks cue conflicts [see Fis1]. These false cues are at a maximum for at the lowest possible MRP.

[Fis1]'s study using the DLR driving simulator showed a subjective preference for a higher MRP (fewer false cues). However the geometry of the simulator's motion platform was an inverted hexapod, where the cab hangs below the main platform. Contrary to a traditional six degree of freedom motion platform, the inverted hexapod allows the MRP to be located above the driver's head without any loss of platform angular displacement. Hence, yet another compromise is faced by the simulation engineer who must decide, for a standard hexapod, whether the false cue or the loss of angular displacement capability is the lesser of two evils.

Influence of scale factor

Given an appropriately sized motion envelope, using a unity scale-factor where the onset acceleration of the motion platform directly matches that of the input may seem an intuitive choice. However, there is evidence that the selection of high scale-factors can lead to the perception of unrealistically strong motion cues. Based on their pilots' subjective response, [Gro1] observed the range of realistic motion parameters was centred around a scale-factor as low as 0.2 for the onset filter. Unity scale-factors were unanimously rejected as too powerful.

To achieve an acceptable perception of motion within the constraints of a typical motion platform, the onset filter scale-factor is typically set at a value around 0.7 [Rei2]. [Gra2] even observed accurate lane keeping and acceptable subjective ratings to a range of slalom steering manoeuvres undertaken by drivers of Ford's VIRTTEX simulator with a classical MDA onset filter scale-factor of 0.5. The manoeuvre used in this experiment was a double

lane change demarcated by a set of cones. However, decreasing the scale-factor still further to 0.3 resulted in a significant deterioration of driver performance and an accompanying worsening of subjective motion assessment. [Sch2] achieved improved vertical tracking task performance and better accepted motion perception with an onset scale-factor of 0.5 than with unity, a result they attributed to the reduction in the filter's scale-factor reducing its phase error.

Aims and objectives

The fundamental aim of the overall study was investigate how best to manage these trade-offs of specific force/tilt rate error, MRP location and scale-factor in order to achieve the best possible classical motion cueing in the University of Leeds Driving Simulator (UoLDS). It was undertaken in a three-staged approach.

Through a Just Noticeable Difference procedure, Stage 1 examined the maximum perceptible scale-factors of both pure translational and rotational motion platform movement. With knowledge of the maximum perceptible scale-factor, Stage 2 made use of maximally-scaled motion without needless platform excursion, examining the effects of relocating Motion Reference Point (MRP) and specific force/tilt rate trade-off. With the maximum perceptible scale-factor and most suitable MRP location established, it was possible in Stage 3 to make a more thorough evaluation of the perceptual trade-off of specific force and tilt rate errors.

Apparatus

University of Leeds Driving Simulator

The University of Leeds Driving Simulator (UoLDS) is the U.K's most advanced such research facility. Operational since early 2007, UoLDS is the second generation of driving simulators developed at the University. Its hardware is tuneable and its software, developed in-house, is fully flexible such that driving scenarios can be tailored to the needs of an individual research project.

UoLDS's vehicle cab is based around a 2005 Jaguar S-type, with all of its driver controls fully operational. The Jaguar is housed within a 4m diameter, spherical projection dome. A real-time, fully textured graphical scene of the virtual world is presented over eight visual channels. The five forward channels are front-projected providing a horizontal field of view of 250°. The three rear channels can be seen through the vehicle's central view and side mirrors.

The vehicle cab and dome are mounted on an eight degree-of-freedom (DoF) motion system, designed, manufactured and installed by Dutch company Rexroth Hydraudyne B.V. Systems & Engineering. The electrically-driven, synergistic EMotion-2500-8DOF-500-MK1-XY consists of a typical six DoF hexapod built upon a two DoF XY-table and can achieve a peak linear acceleration of 0.5g. The maximum excursion is 5m both longitudinally and laterally. The system's bandwidth is over 5.3Hz in all DoFs.

Implementation of the Classical Motion Drive Algorithm

The full block diagram of the implementation of the classical MDA in the UoLDS can be found in Figure 1, controlling the movement of the hexapod in translation and rotation along with the XY-table in translation.

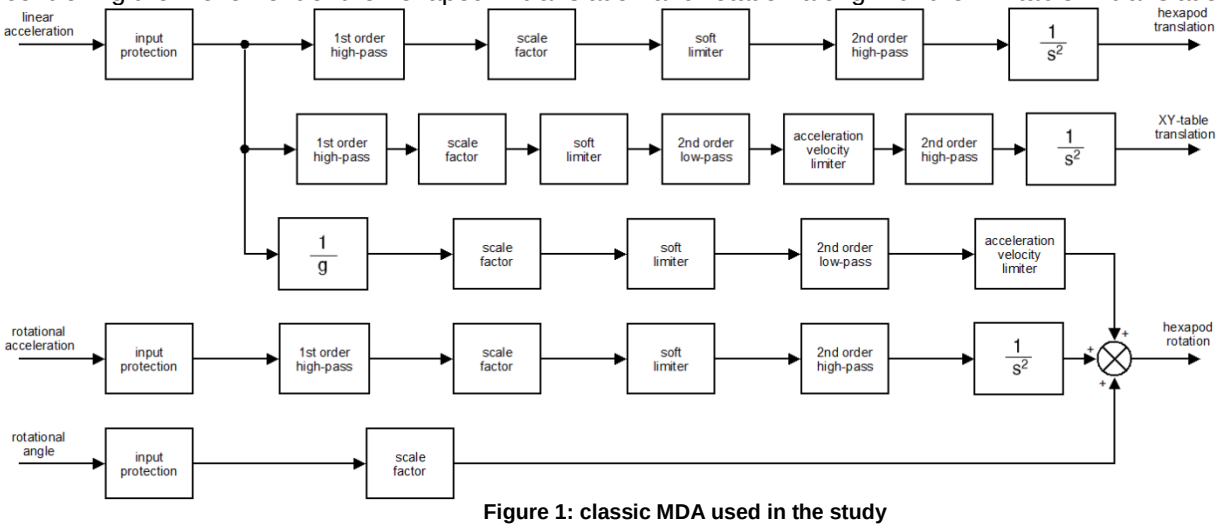

Figure 1: classic MDA used in the study

Experimental Stage 1: Just Noticeable Difference – maximum perceptible scale-factors in motion platform translation and tilt

The performance of the classical MDA to an acceleration input in each of the three linear and rotational vehicle degrees-of-freedom is characterised most easily in the frequency domain. The resultant transfer function is commonly illustrated by a Bode plot, the magnitude describing the system gain and the phase depicting the timing of the output with respect to the input. In terms of driving simulation, the system gain effectively describes the magnitude of the perceived acceleration: the extent to which the simulator achieves the required acceleration demand. The controllability of the simulator, on the other hand, is a direct result of the phase error between demanded and perceived accelerations. For a particular frequency of input, the mismatch can be expressed in units of time. Phase error affects the overall transport delay or latency of a driving simulator motion. Such latencies lead to handling difficulties [Rei2] and can contribute towards simulator sickness (see [Sta1] for a review).

In assessing only the maximum perceptible scale-factor, Stage 1 simply considered motion system gain. Participant drivers were not required to actively handle the simulator through the vehicle controls, simply to ride as observers to a pre-scripted series of control inputs. Dynamically, the performance of the simulator, including the update of the visual scene, was as though drivers had actually made those control inputs. The phase lag associated with motion filtering and the consequent issues of simulator controllability of the simulator was considered later in Stages 2 and 3.

Stage 1 was split into two phases; the first investigated maximum perceptible scale-factor error for motion platform translation (or more accurately the maximum perceptible scale-factor closest to unity). A second, complimentary phase deciphered the equivalent for platform tilt. Stage 1, therefore, required four driving scenarios, designed to assess the maximum perceptible scale-factor for platform translation and tilt for both longitudinal and lateral vehicle manoeuvres. Each trial consisted of a scenario pair, one for which motion was scaled and one for which it was unscaled (unity scale-factor), the order of which being presented randomly. Participants were required to indicate for which of the scenario pair they felt motion had been unscaled.

A Levitt 1 up / 3 down [Lev1] procedure was used to estimate the maximum perceptible scale-factor using a Just Noticeable Difference technique. The stimulus, therefore, was the error between the scaled and unscaled, “ideal” motion cue. Thus the perceptual threshold measured was the minimum error that could be sensed at the 79% probability level (c.f. [Gra2]).

Method

Scaling of motion platform displacement in translation

For platform translation, the simulation of linear acceleration was realised through raw, unfiltered cueing, using surge and sway generated only by the XY-table. Naturally, the greater the scale-factor, the larger the XY-table displacement required. Two scenarios were designed at a driver control input frequency of 1.35rad/s (0.215Hz) in order to remain comfortably inside the bandwidth of both XY-table surge and sway. The value of 1.35rad/s was selected to be close to the 1rad/s “critical” frequency suggested by the Sinacori / Schroeder motion fidelity criterion [Sch1] whilst also allowing the scenario to be achieved unfiltered and unscaled within the excursion limits of UoLDS’s XY-table.

Longitudinal translation driving scenario
The longitudinal translation scenario involved braking and accelerating during car following. The participant was seated in the vehicle cab viewing the visual scene as normal, but the display showed full white. Over a 1s period, the scene was faded-in to present a typical rural road with the participant “driving” at the speed limit of 60mph (96kph). Another vehicle, also travelling at 60mph was situated in front at a distance headway of 25m. After 10s the lead vehicle first slowed then sped up, its linear acceleration following one cycle of a continuous sine function. The peak of the sine wave was ±1.5m/s^2 at the selected frequency of 1.35rad/s (0.215Hz) implying a period of 4.65s to complete the “manoeuvre”. Simultaneously, pre-scripted vehicle control inputs were made on behalf of the driver.

Participants were instructed that their vehicle would behave in the same way as the lead vehicle. The main aim of the lead vehicle was to allow participants to form a concept of how the pre-scripted driving controls were handling their vehicle. To them, the scenario appeared as though they had gently applied the brakes in an attempt to keep a constant gap to the lead vehicle, before accelerating to close the gap and maintain a constant following distance to the lead vehicle. The speedometer in the simulator cab displayed the gentle speed reduction of approximately 5mph followed by its return to 60mph.

Lateral translation driving scenario
The achievement of unfiltered and unscaled motion within the excursion limits of UoLDS's XY-table, close to the Sinacori / Schroeder motion fidelity criterion, was equally desirable to assess the scale-factor for lateral translational platform excursion in sway. Hence, its scenario was also designed at the same driver control input frequency (steering) of 1.35rad/s (0.215Hz). Again, this demand fell well within the bandwidth of XY sway with no appreciable signal attenuation or phase error at this frequency. Participants were instructed that pre-scripted vehicle control inputs would be made on their behalf that allowed the vehicle to follow the short, S-shaped chicane, designed to achieve a peak linear lateral acceleration of ±1.5m/s^2 from the vehicle model.

Scaling of motion platform displacement in tilt

For the assessment of the maximum perceptible scale-factor in platform rotation, the simulation of linear acceleration was realised entirely through tilt-coordination, the input signal merely being low-pass filtered to command a corresponding platform angular position. Unsurprisingly, the greater the scale-factor in question, the larger the tilt displacement required.

In order for this tilt-coordination to remain below perceptual thresholds, the longitudinal and lateral driving scenarios were designed at a much lower control input frequency than for the previous assessment of translational scale-factor. The lower input frequency ensured that, even with a unity scaling, the specific force built up sufficiently slowly to demand only an imperceptibly low tilt rate and acceleration. This was managed by the selection of the cut-off frequency (1.5Hz) and damping ratio (1.0) of the low-pass filter. For the selected control input frequency, the filter demonstrated no appreciable modification of the input in terms of the magnitude or phase of its output. Hence, motion was effectively unfiltered, to all intents and purposes specific force demand directly affecting tilt angle.

Longitudinal tilt driving scenario
Similarly to motion platform translation, the longitudinal tilt scenario involved braking and accelerating during car following. Once more the linear acceleration of lead vehicle followed one cycle of a continuous sine wave with a peak of ±1.5m/s^2. However, this time it did so at the lower frequency of 0.333rad/s (0.0531Hz): a time period of 18.85s to complete the manoeuvre.

Lateral tilt driving scenario
A similar, slowly-developing motion platform rotation, but this time in roll, was also required to assess the scale-factor for lateral platform tilt. Hence, its scenario was also designed at the same driver control input frequency (steering) of 0.333rad/s. Like its lateral translation equivalent, the lateral tilt scenario involved a steering through a section of virtual test-track marked out by cones. However, the lower control input frequency called for a much longer, sweeping S-shaped curve as opposed to the short chicane.

Again, participants were instructed that pre-scripted vehicle control inputs would be made on their behalf that allowed the vehicle to follow the long, S-shaped curve. The amplitude of the sine steer at the wheel was 6.35° to achieve the designed peak linear lateral acceleration of ±1.5m/s^2.

Participants

Twenty drivers were recruited for Stage 1 with experience provisos that each had to have held a valid U.K. driving licence for at least five years and were currently driving at least 5000 miles (8000km) per annum. Seven of the sample were female. The demographics of the participants is shown in 1. Payments of £20 were made for participation in Stage 1.

Table 1: participant demographics

	age (♂/♀)	years licensed (♂/♀)	annual mileage (♂/♀)
mean	37.1 / 36.6	17.7 / 17.4	8846 / 9286
standard deviation	10.2 / 7.4	11.0 / 7.3	2968 / 1496

Procedure

The appearance of scaled and unscaled motion within a scenario pair was ordered randomly. The initial scale-factor was 0.5. In order to speed up convergence, a slightly modified version of the Levitt procedure was used such that each time the scaled motion was correctly identified, scale-factor was increased by a step size of 0.1. Once the first error was made, the step size was halved and the scale-factor reduced by 0.05. This was the point of the first reversal, where the direction of scale-factor modification changed sense. At this moment, standard Levitt 1 up / 3 down was used such that three consecutively correct responses had to be achieved before any further increases in

scale-factor were made. Any error led to a decrease in scale-factor by the 0.05 step size. The session was terminated after six reversals or thirty scenario pairs, whichever occurred first. The participant's threshold in motion scaling was estimated by taking the mean value of the third and subsequent reversals. [Gra1] used a similar Levitt Just Noticeable Difference technique to motion-visual phase error detection in a flight simulator.

Results

A repeated-measures ANOVA was undertaken, for two independent variables, each of two levels: Motion System Movement (translation / tilt) and Movement Modality (longitudinal / lateral). The assumptions of ANOVA were not violated in any way, with the resulting maximum perceptible scale-factor threshold (79% detection likelihood) shown in Figure 2. The error bars show the 95% confidence intervals of the means displayed.

Maximum perceptible scale factors were significantly higher in translation that in tilt, $F_{(1,19)}=4.56$, $p=.046$, $\eta^2=.20$ However, there was no significant effect of driving scenario modality ($F_{(1,19)}=0.098$) nor was there any significant interaction of motion system movement and scenario ($F_{(1,19)}=0.198$). Hence, for the consideration of maximally-scaled motion conditions in the upcoming experimental investigations of Stage 2 and Stage 3, the same scale-factors were used for both longitudinal and lateral motion, the mean of their respective values to two significant figures: 0.90 for motion platform translation movements and 0.87 for platform tilt.

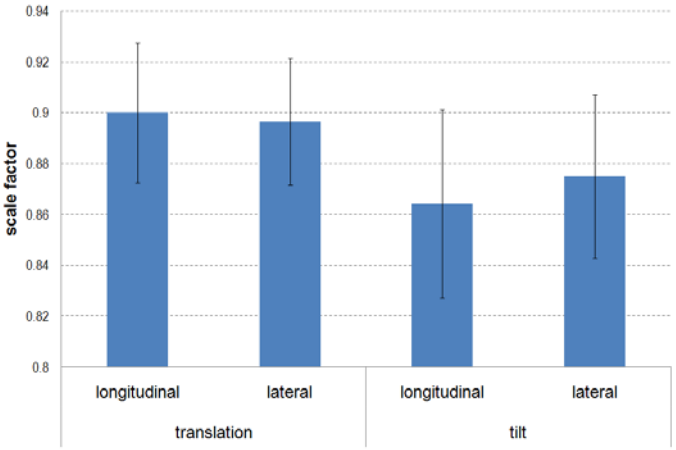

Figure 2: maximum perceptible scale-factors for motion system movements in translation & tilt for longitudinal & lateral driving scenarios (error bars 95% C.I.)

Experimental Stage 2: Paired Comparison – the effects of motion reference point and tilt rate on drivers' task perception and performance

By taking into account only the maximum perceptible scale-factor, Stage 1 simply considered the perception of motion through Bode gain: the relationship between the magnitude of the demanded acceleration and the achieved specific force. Stage 2 considered the second vital element in motion cueing, controllability of the simulator resulting from the implementation of its MDA and the consequential filtering of the input acceleration signal. This filtering leads to a phase difference between the demanded and achieved specific forces. Large phase errors result in a significant time delay between the expected and perceived specific forces, rendering the closed-loop driver control process difficult to manage [Rei1]. Hence rather than riding as observers to a pre-scripted series of control inputs, Stage 2 closed the driver control feedback loop as participants now took on the role of interactive simulator drivers .

Motion cueing in Stage 2 was achieved using the classical algorithm. To begin the process of its optimisation in driving simulation, the overall scale-factors used were based on the maximum perceptible gleaned from Stage 1. This ensured that precious actuator stroke was not unnecessarily utilised in order to produce needlessly high specific forces through overly-scaled motion.

Two independent experimental factors were manipulated in Stage 2: MRP location and the maximum tilt rate achieved during tilt-coordination. The two independent experimental factors each had two levels:

- ***MRP-Location***
  - low (MRP level with hexapod upper rotation datum) - MRP_{hi}
  - high (MRP level with driver's eye-point in the simulator, 1.1m above datum) - MRP_{lo}
- ***Maximum-Tilt-Rate***
  - low (0.05rad/s, 2.86°/s) - $Tilt_{hi}$
  - high (0.15rad/s, 8.59°/s) - $Tilt_{lo}$

The four resulting motion cueing conditions were assessed both subjectively through a paired comparison (c.f. [Gra2]) and objectively by an analysis of driver performance measures. Hence, two specifically designed driving scenarios had to be developed, requiring both longitudinal and lateral control of the vehicle, that were sufficiently manageable to allow predictable and repeatable demands on motion cueing whilst allowing a continuous determination of task accomplishment against well-understood vehicle handling criteria. Furthermore, the scenarios had to appear natural and familiar to the participant driver. For these reasons, scenarios analogous to a tracking task were designed that mimicked common driving situations.

Driving scenarios

Given that the highest of the two levels of MRP-Location was 1.1m above the motion platform datum, the maximum possible roll and pitch angles achievable by UoLDS's motion system were subsequently limited to just under ±12° (0.209rad). Hence, any driving manoeuvre requiring a corresponding maximum sustained specific force through tilt-coordination could not exceed approximately 0.2g. To allow for extra hexapod actuator excursion in the handling of rotational accelerations by the motion system during the manoeuvre, the driving scenario was further limited to a linear acceleration of 0.15g. Longitudinally, a scenario was developed that required this value in braking by a near step-input of brake activation and resulting deceleration of the simulator vehicle. Laterally, the scenario required a similar acceleration in cornering through a near step-input of steering angle.

Longitudinal driving task

The common longitudinal driving situation chosen was braking at a set of traffic-lights. Car following on the approach to the traffic-lights was exploited in order to sufficiently control the degree of braking required.

The participant was seated in the vehicle cab viewing the visual scene as normal, but with the display showing full white. Once both the participant were ready (denoted by depressing the accelerator pedal), the visual scene was faded-in to present a typical two-lane urban scene with the participant "driving" at the speed limit of 40mph (64kph). A speed controller maintained this forward speed regardless of the driver's accelerator input. Another vehicle, also travelling at 40mph was located in front at a distance headway of 17.8m (time headway of 1s). Both vehicles were heading towards a signalised intersection, the state of the traffic-lights always being visible to the simulator driver beyond the low-profile lead vehicle. After 7s at constant speed, the traffic-lights changed from green to amber; 3s later they turned to red. As this moment, the lead vehicle underwent a step deceleration of 1.5m/s^2 in response to the red light and its brakelights illuminated.

During their pre-study briefing, participants were informed that the lead vehicle would decelerate the moment the traffic-light changed to red and at this point to "brake as smoothly as possible, maintaining a constant distance to the car in front". Whilst the driving task was to keep the distance gap stable, in effect it also became matching the step change in deceleration of the lead vehicle, guaranteeing (as much as possible in an interactive simulation) that the specific force demand of the motion system was equivalent between scenarios. Both subjective preference and objective performance in the tracking task of maintaining distance headway were assessed.

Lateral driving task

Laterally, the controllable driving situation selected was the negotiation of a circular curve requiring a near step-input of steering angle, undeniably a natural and familiar driving task. The curve radius (737.4m) and entry speed (74.4mph) were such that a 1.5m/s^2 linear lateral acceleration would be developed during the handling task. Its tracking element was the stipulation for accurate maintenance of the centre of the driving lane.

Once motion system parameters had been selected and the participant had indicated their readiness by depressing the accelerator pedal, the visual scene was faded-in to present a typical three-lane motorway with the participant located in the centre of the left-most lane. In order to manage forward speed throughout the 12.7s straight approach to the upcoming left-hand curve and to guarantee that the required lateral acceleration would be achieved during its negotiation, a speed controller maintained the forward speed regardless of the driver's accelerator input. Participants had been briefed to steer the curve "as smoothly as possible, keeping as close as you can to the middle of the lane that you are in".

Motion system tuning

In order to achieve the two levels of Maximum-Tilt Rate ($Tilt_{hi}$ and $Tilt_{lo}$), two different parameter sets of the classical algorithm were drawn up. They were obtained by trial and error as a result of objective, off-line tuning through an analysis of the MATLAB/Simulink model of the classical algorithm. Tuning was an iterative process

involving two fundamental stages in both the frequency and time domains. Parameter sets were selected to obtain the flattest possible transfer function given the tilt-limiting constraints. No additional parameter sets were required for the two levels of MRP height (MRP_{hi} and MRP_{lo}) since the demands of the MDA were identical in both situations.

The two levels of Maximum-Tilt-Rate were achieved through varying the cut-off frequency of the second-order low-pass tilt-coordination filter rather than by any non-linear rate-limiting of the filter's output. This ensured a smooth tilt acceleration, free of any jerks caused by rate-limiting. Although only tilt rate was specifically manipulated in the experimental design, tilt acceleration also has perceptible threshold limits and was also considered in the development of sub-threshold tilt-coordination, especially important in the $Tilt_{lo}$ condition.

Participants

In an effort to maintain consistency in the ratings offered by the randomly-selected sample, it was the intention that those who took part in Stage 1 would also participate in Stage 2. However, only eighteen of the twenty drivers did so. Both withdrawals (P15, ♂, 44.7yrs and P20, ♀, 41.1yrs) were due to issues of participant availability and the limited data collection epoch available prevented any replacements. Payments of £10 were made for participation.

Procedure

Each driving situation was presented twice, forming a scenario pair, each trial with a different permutation of MRP-Location and Maximum-Tilt-Rate in order to allow the paired comparison to be made. Participants had been briefed that during each pair the motion system would behave differently. At this point of the trial they were asked "compared to real driving, was the simulation of motion more accurate in the first or second presentation of the scenario pair?" The question had been introduced during their pre-experiment briefing, when they were also told that the visual scene would reinforce the illusion, but that it was important to answer based on their perceived realism, rather than their success in the tracking task.

Stage 2 was scheduled for a single, one-hour visit to the simulator. Each visit was split into two sessions, limited to the experience of either longitudinal or lateral driving tasks. One half of the participant sample undertook braking (longitudinal task) first with the other half's initial session involving steering (lateral task).

After a practice session, scenario pairs were presented so that participants could make their paired comparisons of motion cueing based on the question "was the simulation of motion more accurate in the first or second presentation of the scenario pair?". With four cases, six pairs were necessary. The order of the motion condition was balanced for order and carry-over effects across participants in a balanced design [Rus1].

Results

Results are presented separately for the longitudinal and lateral driving tasks. For each, both the subjective ratings of motion cueing condition realism and particular driving task performance were assessed.

The subjective data were analysed through a Least Significance Difference of the overall rating scores for each motion cueing condition in order to assess the significance of the variation in those scores [Ken1]. In addition, the maximum likelihood estimation of the preference probabilities (Bradley & Terry model [Bra1]) was also undertaken, resulting in the Noether "merit" value [Noe1]. These models provides the ability to express the relationship between conditions on a linear scale between -1 (lowest possible preference probability) and +1 (highest possible preference probability).

The objective data, on the other hand, were analysed through a repeated-measures ANOVA for the driver metrics in question. During the paired comparison, each motion cueing condition was experienced on three separate occasions. The mean of these three was taken as the participant's overall performance for the metric under evaluation.

Longitudinal driving task

Subjective measures

For Maximum-Tilt-Rate the subjective data (merit value, Figure 3, left) indicated that a slow tilt was considered more realistic than a more rapid one. However, the LSD analysis (Figure 3, right) suggested that participants had no significant preference for, or maybe any awareness of, a shifting in MRP-Location.

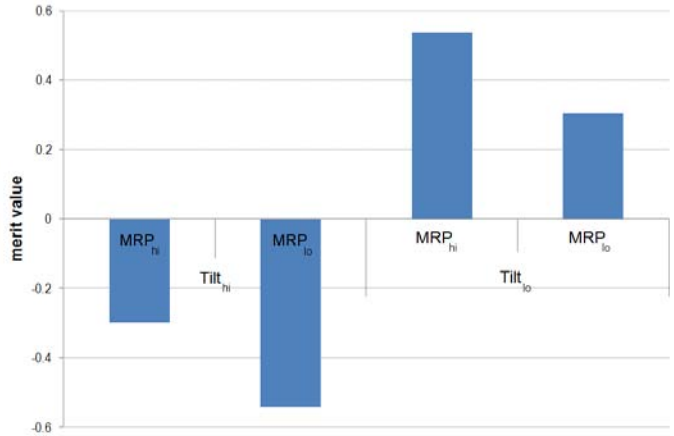

	$Tilt_{hi}$ MRP_{hi}	$Tilt_{hi}$ MRP_{lo}	$Tilt_{lo}$ MRP_{hi}	$Tilt_{lo}$ MRP_{lo}
$Tilt_{hi}$ MRP_{hi}		n.s.	sig.	n.s.
$Tilt_{hi}$ MRP_{lo}			sig.	sig.
$Tilt_{lo}$ MRP_{hi}				n.s.
$Tilt_{lo}$ MRP_{lo}				

Figure 3: merit value (right) and Least Significant Difference test of scores (significant or non-significant at p<0.05)

Objective measures

A repeated-measures ANOVA was carried out for task performance using standard deviation of longitudinal acceleration *sd_long_acc* (Figure 4) as the related dependent variable. A lower *sd_long_acc* was associated with better task performance. The error bars show the 95% confidence intervals of the means displayed. Both were normally distributed according to Kolmogorov-Smirnov tests.

There was a very strong main effect of Maximum-Tilt-Rate with significantly poorer task performance demonstrated when tilt rate was slow (*sd_long_acc* = 0.897m/s^2) rather than more rapid (*sd_long_acc* = 0.792m/s^2); $F_{(1,17)}$=17.0, *p*<.001, η^2=.50. There was also a reasonable main effect of MRP-Location with better performance exhibited when the MRP was in the higher (*sd_long_acc* = 0.802 m/s^2) rather than the lower position (*sd_long_acc* = 0.847 m/s^2); $F_{(1,17)}$=4.89, *p*=.041, η^2=.22. No interaction was evident; $F_{(1,17)}$=2.11.

In contrast to the subjective data, for Maximum-Tilt-Rate this performance measure (*sd_long_acc*) revealed convincingly that more accurate task performance was achieved in conditions of rapid tilt rather than one that developed more slowly. However, drivers also demonstrated no significantly smoother braking, in accordance with the task demands, when the MRP-Location was situated closer to their vestibular organs, rather than when it was positioned at the motion platform datum.

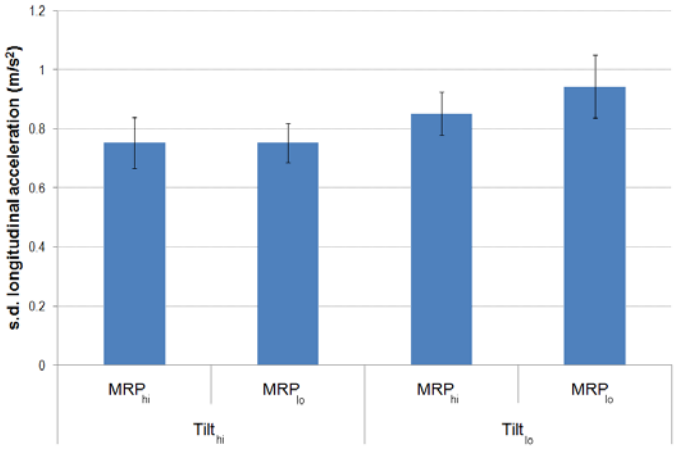

Figure 4: standard deviation of longitudinal linear acceleration (error bars 95% C.I.)

Lateral driving task

Subjective measures

Contrary to the longitudinal braking task, when participants were faced with curve negotiation, neither Maximum-Tilt-Rate nor MRP-Location appeared to have any influence over perceived motion cueing realism. The Least Significant Difference test of scores showed no significant difference between the motion-cueing conditions.

Objective measures

A repeated-measures ANOVA was carried out for the task performance the related dependent variables of standard deviation of lateral acceleration *sd_lat_acc* (Figure 5).In contrast to the longitudinal braking task, lateral task performance was hardly affected by either Maximum-Tilt-Rate or MRP-Location. With regard to standard deviation of lateral acceleration, there was a marginal (borderline but non-significant at 95%) effect of Maximum-Tilt-Rate with task performance degraded very slightly when tilt rate was slow (*sd_lat_acc* = 0.448m/s^2) rather than more rapid (*sd_lat_acc* = 0.430m/s^2); $F_{(1,17)}$=3.94, *p*=.064, η^2=.19. There was no effect of MRP-Location ($F_{(1,17)}$=0.480) and most definitely no interaction ($F_{(1,17)}$=0.002).

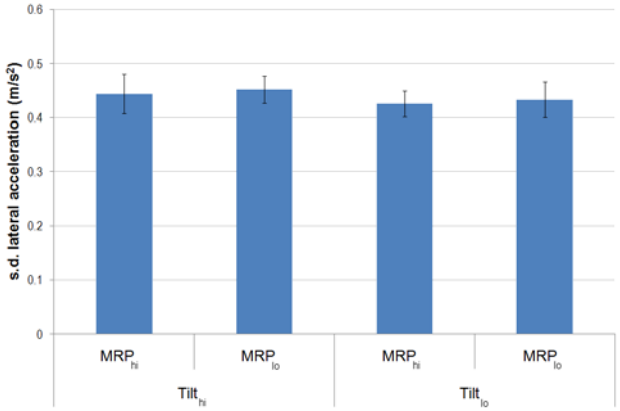

Figure 5: standard deviation of lateral linear acceleration (error bars 95% C.I.)

A fuller discussion of the significance of Stage 2 results with regard to the rest of the experimental design is made in the Discussion. But, based predominantly on the longitudinal performance data, a decision was made to fix MRP at the higher location of 1.1m above the platform datum level. The scene was now set for the most comprehensive evaluation of the three-staged experimental plan, Stage 3's three-factor optimisation of the perceptual trade-off of specific force and tilt rate errors.

Experimental Stage 3: Paired Comparison – the effects of overall scale factor, tilt rate and extended motion platform displacement on drivers' task perception and performance

With the maximum perceptible scale-factor and most suitable MRP location established, it was now possible to make a more thorough evaluation of the perceptual trade-off of specific force and tilt rate errors. Arguably, motion platform tilt rate, manipulated through the classical MDA's filtering of low frequency specific force input, has the greatest impact on this trade-off due to its significant effect on the speed with which tilt-coordination is developed. However, overall scale-factor also plays a significant role, since its scaling of the desired output reduces specific force error; effectively, less demand is easier to achieve.

In addition to scale-factor and tilt-coordination, the accuracy and longevity of the onset cue, handled by the classical algorithm high-frequency channel, also significantly affects specific force / tilt rate error. By sustaining the onset cue for a longer period, less specific force sag is perceptible. This can only be achieved by increasing the available displacement of the motion system in translation. Hence, the final piece in the classical MDA jigsaw is best found from an optimisation of all three of these factors. In combination they characterise the behaviour of the motion system and the inherent role that the classical algorithm plays in driving simulation. This motivation drove the fundamental aim of Stage 3: the appropriate combination of scale-factor, tilt rate and platform translational capacity. In all cases, the onset cue was always realised to some extent through hexapod translation; however, for platform translational capacity, the extra surge and sway provided by UoLDS's XY-table was either exploited or not. The resulting three independent experimental factors under manipulation each had two levels:

- ***XY***
  - on (XY-table in use)
  - off (XY-table not in use)
- ***Maximum-Tilt-Rate***
  - low (0.05rad/s, 2.86°/s)
  - high (0.15rad/s, 8.59°/s)
- ***Scale-Factor***
  - low (0.50)
  - high (0.87 / 0.90)

As in Stage 2, the motion cueing conditions were assessed subjectively through a paired comparison and objectively by an analysis of driver performance measures. The same longitudinal and lateral driving tasks were also employed. The MRP was located 1.1m above the platform datum level in line with the findings of Stage 2.

Motion system tuning

To achieve the required motion cueing conditions, eight different parameter sets of the classical algorithm were defined. These were tuned using the MATLAB/Simulink classical MDA model and the same idealised driver model as in Stage 2. Hence, each parameter set was optimised for best performance given the constraints of the independent variable manipulations. The symmetrical nature of the UoLDS motion system allowed identical parameters sets to be utilised for both longitudinal and lateral motion platform movement. The motion characteristics of the eight conditions are shown below:

Parameter set for $XY_{on}Tilt_{hi}SF_{hi}$

The Parameter set for $XY_{on}Tilt_{hi}SF_{hi}$ was typified by a low specific force error achieved through compromising tilt rate error. As a result, the Bode plot (opposite) shows a relatively flat transfer function as the output specific force is achieved quickly through a combination of rapid tilt and strong onset cueing, requiring a XY-table displacement of almost 3m in the process.

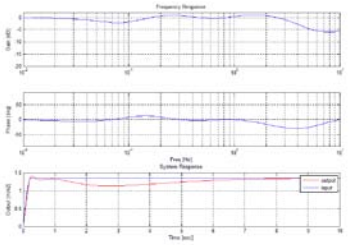

Parameter set for $XY_{on}Tilt_{hi}SF_{lo}$

$XY_{on}Tilt_{hi}SF_{lo}$ showed a more rapid conversion to the required steady-state conditions than when a higher scale factor was used. As a result of this reduced specific force error, its Bode plot is flatter.

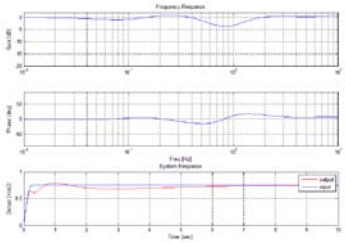

Parameter set for $XY_{on}Tilt_{lo}SF_{hi}$

The response of $XY_{on}Tilt_{lo}SF_{hi}$ demonstrated the typical sag associated with slowly developing tilt-coordination. Its Bode plot shows significant gain and phase errors around the 0.07Hz and 1Hz input frequencies and the underlying specific force takes quite some time to build up for the specific driving task at hand. These delays were mitigated as much as possible by the use of the maximum 5m available XY-table excursion.

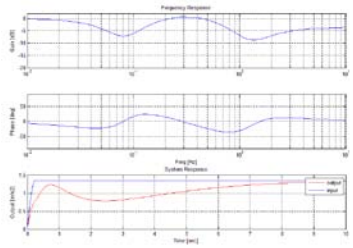

Parameter set for $XY_{on}Tilt_{lo}SF_{lo}$

In comparison to its highly scaled equivalent, $XY_{on}Tilt_{lo}SF_{lo}$ boasts a better frequency response due to the reduced specific force demanded. Apart from less phase lag, its response does not differ all that much from the corresponding high tilt rate condition $XY_{on}Tilt_{hi}SF_{lo}$ due to the impact of the XY-table.

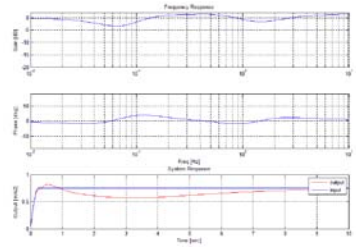

Parameter set for $XY_{off}Tilt_{hi}SF_{hi}$

The impact of no additional translational capacity afforded by the XY table is immediately apparent for $XY_{off}Tilt_{hi}SF_{hi}$. Even though hexapod translation has been maximised, the Bode plot shows a considerable attenuation and phase lag around the 0.5Hz region. This is characterised in the time history by a specific force that takes around 2s to reach the desired level, despite the high tilt rate, for the specific driving task.

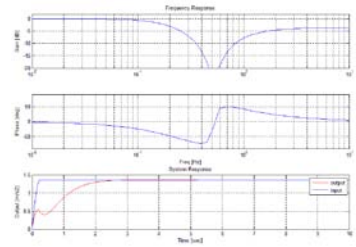

Parameter set for $XY_{off}Tilt_{hi}SF_{lo}$

For $XY_{off}Tilt_{hi}SF_{lo}$, lowering the scale factor does mitigate somewhat the poor frequency response associated with no XY-table movement, personified by a much flatter Bode plot. However, in terms of onset cueing, it does not differ at all from its highly scaled cousin $XY_{off}Tilt_{hi}SF_{hi}$.

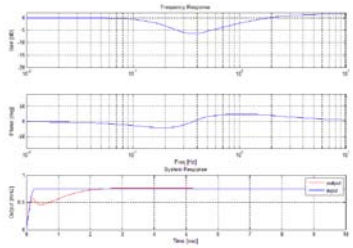

Parameter set for $XY_{off}Tilt_{lo}SF_{hi}$

$XY_{off}Tilt_{lo}SF_{hi}$ is epitomised by one of the least flat transfer function of all eight of the motion cueing conditions, suggesting attenuated and delayed motion cueing at best. Limited translation and slow tilt combine to result in a theoretically laboured development of specific force.

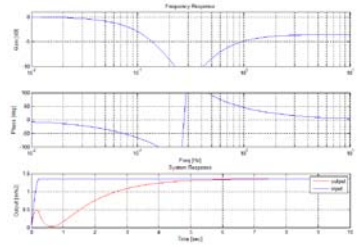

Parameter set for $XY_{off}Tilt_{lo}SF_{lo}$

In terms of its off-line assessment, the unfortunate frequency response of $XY_{off}Tilt_{lo}SF_{hi}$ is marginally enhanced by a reduced scale-factor. That said, there is still a significant sag in the perceived specific force, although the reduced demand does allow the output to reach the input somewhat more promptly.

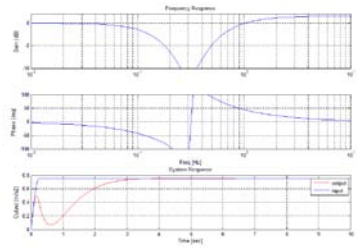

Stage 3 Hypothesis

According to the offline tuning, the flattest transfer functions, i.e. those involving low scale factors, rapid tilt and extended XY motion capabilities would affect the most appropriate cueing and hence the best available conditions for accurate task performance. However, the super-threshold nature of the associated tilt coordination would prove unpopular in terms of perceived accuracy of this cueing.

Participants

The same eighteen drivers who took part in Stage 2 also formed the population sample for Stage 3. Due to the increased duration of the study (see next section), payments of £20 were made for participation.

Procedure

After a practice session, the experimental paired scenarios began in one of four pre-defined sequences outlining the order of presentation of the 28 pairs of motion cueing conditions. A central, single sequence was exactly balanced for order and carry-over effects according to Russell's balanced paired comparison design [Rus1]. This was reversed for a second ordering. Finally, a third and fourth sequence were found by alternating the order of presentation of a condition within a specific scenario pair. For each participant, two of these four sequences were presented for each modality of the two driving tasks. The result was the quasi-counterbalancing of the motion cueing conditions witnessed during Stage 3. The large number of scenario pairs resulted in a one-hour experimental session. Hence, to alleviate participant fatigue and boredom, a short break was allowed at the half-way stage, after the presentation of scenario pair 14.

Results

Results are presented separately for the longitudinal and lateral driving tasks. As in Stage 2, the subjective data were analysed through a Least Significance Difference of the overall ratings and the objective data by repeated-measures ANOVA. The mean of all seven experiences of each motion cueing condition was taken as the participant's metric of task performance for each dependent variable under evaluation.

Longitudinal driving task

Subjective measures

Fitting a Bradley-Terry linear model to the subjective ratings revealed that the null hypothesis indicating an equality of objects could be rejected with a high degree of confidence (p=1.39x10^{-11}). An application of Maximum Likelihood Ratio theory demonstrated a satisfactory test of fit the model using (p=.37). The resulting assessment of the Noether merit value for each of the eight motion cueing conditions, on a linear scale between -1 and +1, is illustrated in Figure 6.

Overall, the subjective data indicated a strong preference, in terms of more realistic motion cues, for the low Maximum-Tilt-Rate than a more rapid development of tilt angle. However, this was the case only when the slow tilt was supplemented by extended motion platform translation, made available by the XY-table. In the other six motion conditions, there was a general inclination towards the lower of the two Scale-Factors, but this effect never reached statistical significance at the 95% confidence level.

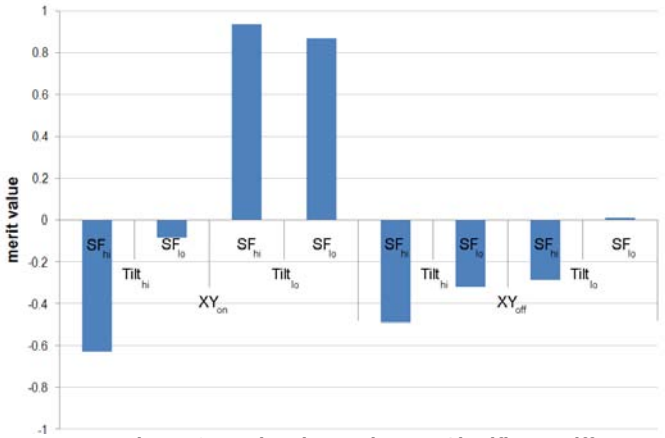

			XY_{on}				XY_{off}			
			$Tilt_{hi}$		$Tilt_{lo}$		$Tilt_{hi}$		$Tilt_{lo}$	
			SF_{hi}	SF_{lo}	SF_{hi}	SF_{lo}	SF_{hi}	SF_{lo}	SF_{hi}	SF_{lo}
XY_{on}	$Tilt_{hi}$	SF_{hi}		n.s.	sig.	sig.	n.s.	n.s.	n.s.	sig.
		SF_{lo}			sig.	sig.	n.s.	n.s.	n.s.	n.s.
	$Tilt_{lo}$	SF_{hi}				n.s.	sig.	sig.	sig.	sig.
		SF_{lo}					sig.	sig.	sig.	sig.
XY_{off}	$Tilt_{hi}$	SF_{hi}						n.s.	n.s.	n.s.
		SF_{lo}							n.s.	n.s.
	$Tilt_{lo}$	SF_{hi}								n.s.
		SF_{lo}								

Figure 6: merit value and Least Significant Difference test of scores (significant or non-significant at p<0.05)

Objective measures

A repeated-measures ANOVA was carried out for the task performance related dependent variable of standard deviation of longitudinal acceleration (Figure 7). The error bars show the 95% confidence intervals of the means displayed. Both were normally distributed according to Kolmogorov-Smirnov tests of normality.

Regarding driving task success as inversely proportional to the variability of longitudinal acceleration (*sd_long_acc*), there were very strong main effects for all three experimental factors. First, performance was superior when extended translational movement was available during the onset cue (0.758m/s^2), compared to when the XY-table was not active (0.876m/s^2); $F_{(1,17)}$=25.6, p<.001, η^2=.60. There was also less variation in braking when tilt rate was rapid (0.756m/s^2) rather than more slow (0.879m/s^2); $F_{(1,17)}$=47.2, p<.001, η^2=.74. Finally, there was also a considerable benefit of reducing the specific force demand, smoother braking being demonstrated when the motion was unscaled (0.791m/s^2) compared to scaled (0.843m/s^2); $F_{(1,17)}$=18.2, p<.001, η^2=.52.

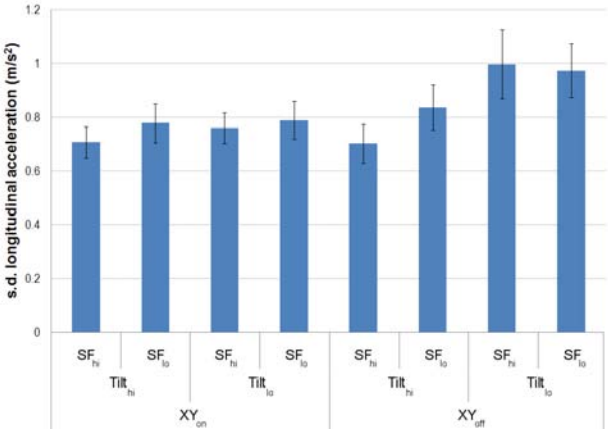

Figure 7: standard deviation of longitudinal linear acceleration (error bars 95% C.I.)

In addition to the main effects, there was also a significant interaction of Maximum-Tilt-Rate and Scale-Factor. When tilt-coordination was slow, task performance was similar with unscaled (0.878m/s^2) and scaled motion (0.881m/s^2). However, as tilt rate increased, braking performance was more inconsistent with a scale-factor of 0.5 (0.806m/s^2) rather than in conditions of no effective scaling (0.704m/s^2); $F_{(1,17)}$=5.86, p=.030, η^2=.25.

Lateral driving task

Subjective measures

A Bradley-Terry model of the subjective data revealed that the variations made to the parameters sets of the eight motion cueing conditions did impact significantly perceived realism; p=1.93x10^{-8}. The model fitted the observed data reliably (p=.85) and allowed an assessment of the Noether merit value of the four motion cueing conditions illustrated in Figure 8.

On the whole, for the lane keeping task, the consistent subjective data indicated a strong preference in terms of perceived realism for motion cues scaled by 50%, especially when supplemented by the extended motion platform translation capabilities afforded by the XY-table. However, for the handling manoeuvres required, Maximum-Tilt-Rate had no impact on participant ratings.

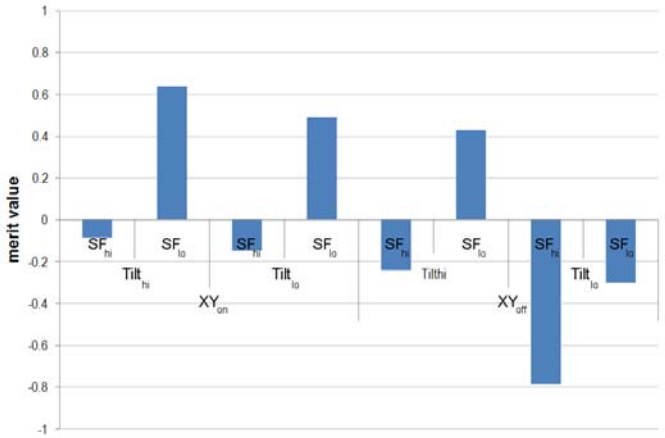

			XY_{on}				XY_{off}			
			$Tilt_{hi}$		$Tilt_{lo}$		$Tilt_{hi}$		$Tilt_{lo}$	
			SF_{hi}	SF_{lo}	SF_{hi}	SF_{lo}	SF_{hi}	SF_{lo}	SF_{hi}	SF_{lo}
XY_{on}	$Tilt_{hi}$	SF_{hi}		sig.	n.s.	sig.	n.s.	sig.	sig.	n.s.
		SF_{lo}	sig.		sig.	n.s.	sig.	n.s.	sig.	sig.
	$Tilt_{lo}$	SF_{hi}	n.s.	sig.			sig.	n.s.	sig.	n.s.
		SF_{lo}	sig.	n.s.			sig.	n.s.	sig.	sig.
XY_{off}	$Tilt_{hi}$	SF_{hi}	n.s.	sig.	sig.	n.s.		sig.	sig.	n.s.
		SF_{lo}	sig.	n.s.	sig.	n.s.	sig.		sig.	sig.
	$Tilt_{lo}$	SF_{hi}	n.s.	sig.	sig.	n.s.	sig.	sig.		n.s.
		SF_{lo}	sig.	n.s.	sig.	sig.	n.s.	sig.	n.s.	

Figure 8: merit value and Least Significant Difference test of scores (significant or non-significant at p<0.05)

Objective measures

A repeated-measures ANOVA was carried out for the dependent variables related to lateral task performance: standard deviation of lane position (*sd_lp*), normally distributed according to Kolmogorov-Smirnov tests. Figure 9 illustrates the strong main effect of XY observed on sd_lp.

Steering performance was significantly more accurate, demonstrated by a reduced variation in lane position when the XY-table was active (0.162m) compared to when it was inactive (0.183m); $F_{(1,17)}$=17.3, p<.001, η^2=.51. No main effects of either Maximum-Tilt-Rate ($F_{(1,17)}$=1.90) or Scale-Factor ($F_{(1,17)}$=3.79) were apparent.

One of the major findings of Stage 3 was the notable significant interaction of XY and Maximum-Tilt-Rate; $F_{(1,17)}$= 5.23, p=.036, η^2=.21. With the XY-table in operation, task performance differed little as tilt rate was reduced from high to low (from 0.164m to 0.160m). However, without any additional sway motion, a reduction in tilt rate resulted in a marked performance degradation (from 0.173m to 0.193m).

A similar interaction was also observed between XY and Scale-Factor. When XY-table sway was available, a reduction in scale-factor had little impact on participant's ability to execute the task (from 0.162m to 0.163m). Conversely, without such platform movement, lane tracking became more varied with unscaled motion as opposed to that scaled by 50% (from 0.190m to 0.176m).

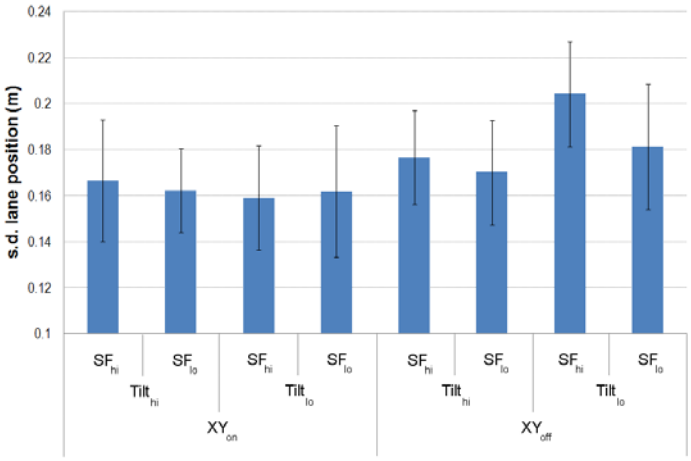

Figure 9: standard deviation of lane position (error bars 95% C.I.)

Discussion

Stage 1

Whilst influenced by [Gro1]'s and [Gra1]'s studies, the fundamental aim of Stage 1 was to ensure that, during the optimisations of the classical MDA in Stages 2 and 3, those motion cueing conditions incorporating a high scale-factor did not unnecessarily utilise precious actuator stroke through overly-scaled motion. The results were determined using a robust and well-established Just Noticeable Difference methodology.

The observed maximum perceptible scale-factors did not differ particularly in terms of the modality of the driving manoeuvres, longitudinal or lateral. However, there were slight, but statistically significant, differences detected between motion cues characterised by translation (0.9) and tilt (0.87). Nevertheless, the variation in maximum perceptible scale-factor of just 0.03 between the two degrees-of-freedom of platform movement is practically negligible. To all extent and purposes, the results indicated that any scale-factor of linear acceleration in any direction need never exceed 0.9.

Of the two studies, Stage 1 probably more closely resembled a study of [Ber1] than that of [Gro1]. Accordingly, the results were more closely aligned to the former's insinuation that unity scale-factors are most appropriate in providing a convincing perception of the magnitude of motion cues. However, Stage 1 differed from both in that participants were not required to rate the believability or realism of the motion cues, simply to discriminate between those that were scaled and those that were not. Hence, rather than emulating the previous studies, which concluded implementation strategies for MDA based merely on the perceived magnitude of motion cues, Stage 1 was able to inform Stages 2 and 3 to reach such conclusions based also on the inherent MDA phase lag and its subsequent impact on simulator controllability.

Stage 2

The significance of these results varied considerably depending on the modality of the driving task in question. In braking, whilst participants expressed no particular preference for a MRP location close to the head, such placement of the MRP did result in marginally better longitudinal task performance (lower sd_long_acc). During the same manoeuvres, they also consistently and strongly favoured the development of slow tilt rate over one that arose more rapidly. However, the fondness for a slow tilt rate was not borne out by the performance metrics, which indicated, conversely, that the driving task was achieved more accurately in rapid-tilt motion cueing conditions.

The lateral task did not show any such substantial and sizeable differences. Participants demonstrated no partiality towards any of the motion cueing conditions and only for a single performance metric, minimum time-to-line-crossing, was anything approaching a robust effect revealed. That result confirmed high Maximum-Tilt-Rate as the

most likely to produce more accurate steering performance, although its impact was far from substantial in terms of the amount of that improvement.

By and large, the findings of Stage 2 opposed those of [Fis1] and [Fis2] whose drivers favoured rapid tilt rates, also demonstrating a weak predilection towards a high MRP location. Whilst the dramatic nature of the emergency stop task required [Fis1] may have influenced participants' desire for a fast acting motion cue, the preferences expressed during the more mundane roundabout negotiation [Fis2] are harder to explain away.

Stage 3

A consistent theme in the results observed in both of Stage 3's driving tasks was the lack of consistency between the subjective perception of realism and the objective measures of task performance. Such an issue did not crop up during [Gra2]'s lane-change study, which reported that perceived realism correlated well with lateral task performance. The nature of this steering task was generally dictated by relatively high frequency steering inputs, demanding a similarly high frequency response of the motion cueing. The present study, on the other hand, utilised a lane keeping rather than a lane changing task, characterised by a dominant low frequency domain. Its results undeniably demonstrate that more significant differences exist between the perception and performance with motion cues under longitudinal tasks compared to lateral tasks. That Grant et al. (2009) did not employ a longitudinal task and the fact that the lateral task existed in an altogether different frequency range could easily explain the observed perception/performance correlation differences between the two studies.

Conclusions

Summary of main findings

The lack of perception/performance consistency reported here leads to a dilemma as how best to handle the specific force / tilt rate error trade-off when making use of the classical MDA in research driving simulation applications. When large motion platform translations are made possible by a XY-table, the motion cues most realistic to drivers stem from the reduction of tilt rate errors at the expense of specific force errors. The same is true, admittedly not as clear cut statistically, even when onset cues are handled less effectively without such additional translation capabilities of the motion system. However, the motion cues that are most beneficial in terms of the successful accomplishment of longitudinal and lateral driving tasks doubtlessly originate from the reduction of specific force errors at the expense of tilt rate errors.

With its three-stage experimental plan, this study has attempted to provide a robust, defendable and original investigation into a topic area that is sparsely populated in the driving simulation literature. Given the caveat that its conclusions can only be drawn for the specific longitudinal and lateral driving tasks examined, the following can be drawn from the various stages of the present investigation:

- Scale-factors over 0.9 for motion platform translation or tilt are unnecessary. Above this point, motion cues cannot be perceptibly differentiated from unscaled motion.
- Drivers are not able to perceive a relocation of Motion Reference Point to a position close to the head. Such placement does, however, result in marginally smoother braking, in line with the longitudinal task requirements employed in this study.
- Especially when complemented by extended motion platform translation, braking cues that result from sub-threshold tilt-coordination are rated as more realistic than those emanating from a rapid development of tilt angle.
- Conversely, in line with the longitudinal task requirements of this study, braking is performed more smoothly in conditions of rapid, above-threshold tilt-coordination.
- Braking is smoother with the improved onset cueing made possible by extended motion platform surge.
- Braking is smoother when longitudinal motion cues are effectively unscaled.
- Especially when complemented by extended motion platform sway, the perceived realism of steering cues is enhanced when motion cues are scaled by 50%. Realism is not influenced by the rate limiting of tilt-coordination.
- Cornering is smoother in conditions of rapid, above threshold tilt-coordination.
- Lane position is less varied during cornering with the improved onset cueing made possible by extended motion platform sway.

Implications for simulator design

Motion platforms exist in various guises. Specifications stretch from relatively cheap, small systems limited in their available displacement to those more costly, but affording the simulation engineer a much more expansive

representation of the dynamic range of typical driving. By comparing subjective assessments of realism and objective measures of performance, the main objective of this work was to investigate the most appropriate motion cueing to achieve both a strong perceived correlation between real and virtual conditions (perceptual validity) and behavioural correspondence (behavioural validity). Generally, drivers consider scaled motion cues developed at a low tilt rate most realistic. Conversely, unscaled cues presented at rapid tilt rates appear to foster more accurate driving task performance.

These results do suggest an apparent conflict. However, armed with the data summarised in the bulleted list above, design implications for research driving simulators can be drawn. In terms of fidelity and motion cueing, the most appropriate tuning depends on the specific focus of the driving simulator. The fundamental characteristics of the simulator should maximise its internal validity, a concept introduced at the start of this chapter. Internal validity is lost if driver behaviour is specifically affected by the limitations of the simulator (Kaptein, Theeuwes & van der Horst, 1996). Consequently, should driver behavioural research be the simulator's focus, it is logical to place the importance of behaviour and performance over that of perceived realism. Therefore, the first main theoretical contribution of this work is that optimal motion cueing (resolution of the specific force / tilt rate error trade-off) in a research driving simulator is achieved by minimising specific force error at the expense of tilt rate error.

However, before we jump to too hasty a main conclusion, it should be remembered that the interaction of motion platform translation capability and tilt-rate was significant. This interaction occurred repeatedly, observed in both the performance metrics used in the longitudinal task and two of the three lateral task measures. When the XY-table was operational, driving task performance varied little between sub-threshold and more rapid tilt-coordination. However, while the XY-table was inactive, both driving tasks were better achieved with a high platform tilt rate.

This interaction supports the following theoretical contribution. In a small motion system, without the benefit of the XY-table, the constraints of internal validity force the hand of the simulation engineer to minimise specific force error at the expense of tilt rate error. However, a more expansive motion platform, characterised by greater translational capacity, affords the luxury of achieving motion cues that not only bring about accurate driving task performance, but also attain maximum perceived realism. In such a system, the apparently conflicting goals of perceptual and behavioural validity can be aligned much more closely. Whether the benefits of such a system can actually outweigh is another debate.

References

[Ber1] Berger, D.R., Schulte-Pelkum, J. & Bülthoff, H.H. (2010). Simulating believable forward accelerations on a Stewart motion platform. ACM Transactions on Applied Perception, 7(1), pp. 5:1-5:27.

[Bra1] Bradley, R.A. & Terry, M.E. (1952). Rank analysis of incomplete block designs: I. The method of paired comparisons. Biometrika, 39(4), pp. 324-345.

[Con1] Conrad, B., Schmidt, S.F. & Douvillier, J. G. (1973). Washout circuit design for multi-degrees-of-freedom moving base simulators. Proceedings of the American Institute of Aeronautics and Astronautics Visual and Motion Simulation Conference, Palo Alto (CA), 10th September - 12th September 1973, paper number AIAA-1973-929.

[Dag1] Dagdelen, M., Reymond, G., Kemeny, A., Bordier, M. & Maïzi, N. (2009). Model-based predictive motion cueing strategy for driving simulators. Control Engineering Practice, 17(9), pp. 995-1003.

[Fis1] Fischer, M. & Werneke, J. (2008). The new time-invariant motion cueing algorithm for the DLR dynamic driving simulator. Proceedings of the Driving Simulation Conference (DSC Europe 2008), Monaco, 31st January - 1st February 2008.

[Fis2] Fischer, M., Lorenz, T., Wildfeuer, S. & Oeltze, K. (2008). The impact of different motion cueing aspects concerning the perceived and subjectively rated motion feedback during longitudinal and lateral vehicle control tasks. Proceedings of the Driving Simulation Conference (DSC Asia/Pacific 2008), Seoul, 10th – 12th September 2008.

[Gra1] Grant, P.R. & Lee, P.T.S (2007). Motion-visual phase error detection in a flight simulator. Journal of Aircraft, 44(3), pp. 927-935.

[Gra2] Grant, P.R., Blommer, M., Artz, B. & Greenberg, J. (2009). Analysing classes of motion drive algorithms based on paired comparison techniques. Vehicle System Dynamics, 47(9), pp. 1075-1093.

[Gro1] Groen, E.L., Valenti Clari, M.S. & Hosman, R.J.A.W (2001). Evaluation of perceived motion during a simulated takeoff run. Journal of Aircraft, 38(4), pp. 600-606.

[Hos1] Hosman, R.J.A.W. & van der Vaart, J.C. (1981). Effects of vestibular and visual-motion perception on task performance. Acta Psychologica, 48, pp. 271–281.

[Ken1] Kendall, M.G. & Babington-Smith, B. (1940). On the method of paired comparisons. Biometrika, 31(4), pp. 324-345.

[Lev1] Levitt, H. (1971). Transformed up-down methods in psychoacoustics. Journal of the Acoustical Society of America, 49(2), pp.467-477.

[Noe1] Noether, G.E. (1960). Remarks about paired comparisons. Psychometrika, 25(4), pp. 357-367.

[Nor1] Nordmark, S., Lidström, M. & Palmkvist, G. (1984). Moving base driving simulator with wide angle visual system. SAE Technical Paper Series 845100, Society of Automotive Engineers, Warrendale, PA, USA.

[Par1] Parrish, R.V., Dieudonne, J.E., Bowles, R.L. & Martin, D.J. (1975). Coordinated adaptive washout for motion simulators. Journal of Aircraft, 12(1), pp. 44-50.

[Rei1] Reid, L. D. & Nahon, M. A. (1985). Flight Simulation Motion-Base Drive Algorithms: Part 1 – Developing and Testing the Equations. University of Toronto Institute for Aerospace Studies Report 296, University of Toronto.

[Rei2] Reid, L. D. & Nahon, M. A. (1988). Response of airline pilots to variations in flight simulator motion algorithms," Journal of Aircraft, 25(7), pp. 639-646.

[Rus1] Russell, K.G. (1980). Balancing carry-over effects in round robin tournaments. Biometrika, 67(1), pp.127-131.

[Sch1] Schroeder, J.A. (1999). Helicopter flight simulation motion requirements. NASA Technical Report, NASA-TP-1999-208766.

[Sta1] Stanney, K. M., Mourant, R. R. & Kennedy, R. S. (1998). Human factors issues in virtual environments: a review of the literature. Presence, 7(4), pp. 327–351.

[Sch2] Schroeder, J.A., Chung, W.W.Y. & Hess, R.A. (2000). Evaluation of a motion fidelity criterion with visual scene changes. Journal of Aircraft, 37(4), pp. 580-587.

Tongji University Advanced Driving Behavior and Traffic Safety Research Simulator (TUDS simulator)

Hangfei Lin, Xuesong Wang, Zhizhou Wu,

Tongji University, School of Transportation Engineering

Maria Pinto, Viola Cavallo,

French Institute of Science and Technology for Transport, Development and Networks (Ifsttar)

Alexandre Troale, David Charondière, Christian Schost, Gilles Gallée

Oktal

Poser Session

In 2011, an 8 DoF driving simulator was delivered by Oktal (France) to the Tongji University (Shanghai, China) designed for research on driver behaviour and new road infrastructures. This simulator is one of the world's largests, and provides the driver with an highly immersive driving environment. To obtain the most realistic behaviour of the driver inside the simulator, human performance and subjective state (simulator sickness) were considered as main issues during the design and development of this simulator.

This driving simulator consists of a 6 meters wide dome housing a Megane Renault and a wide 250° display system for a complete immersion of the driver in an extremely realistic visual and sound environment. The dome stands on a 8 DoF (Degrees of Freedom) dynamic platform equipped with six electrical actuators and mounted on tracks of 20 meters by 5 to render perfect motion feedbacks (acceleration, braking, vibration, curves). The simulator is controlled and driven by the SCANeR™studio software that allows simulating vehicle and road environment, and creating vehicles and scenarios.

Most driving simulators are tools for Driver-in-the-loop experiments. Because the driver is part of the system when the driving simulator is used, the validation process was adapted to include the driver early in the development process.

Standard validation procedures were defined to ensure that all subsystems are operational (car cockpit, visual system, motion system …). After engineering validation tests, the interactions between the subsystems were tested like the effects of the motion system on the visual system stability, latency between the action on the commands of the car and the reaction of the motion and visual systems, reliability… These validation procedures are mostly standard for any integrated system.

For the first time, the validation process set by Oktal for Tongji University Simulator was also completed with advanced tests on the complete system taking into a count the driver in the loop. Accordingly, the test procedures included a complete experiment, with a protocol, casting, test and analysis phases. The protocol was conceived by the workgroup of the Tongji University, Oktal and IFFSTAR researchers. This test included forty drivers, to evaluate three main criteria for the future use of the simulator: simulator sickness, braking distance and realism of the displayed infrastructure elements.

This work opens the discussion on standard criteria and procedures that could be useful in the future to qualify a simulator based on driver-in-the-loop system instead of only technical specification of the sub-systems

Figure 1: Tongji University advanced driving simulator.

Renewal of the Renault Ultimate Simulator

Volkhard Schill [1], Thomas Schulz [2], Dr. Andras Kemeny [3], Jean-Christophe Collinet [4],Olivier Legrand [5], Renaud Deborne [6]

(1) VSimulation GmbH, Leydenallee 38, 12167 Berlin, Germany, v.schill@vsimulation.com
(2) IMTEC GmbH, Am Rosengarten 1, 14621 Schönwalde-Glien, Germany, thomas.schulz@imtec-inside.de
(3) Renault CTS, FR TCR AVA 013, 1 Ave. du Golf, 78288 Guyancourt, andras.kemeny@renault.com
(4) Renault CTS, FR TCR AVA 013, 1 Ave. du Golf, 78288 Guyancourt, jean-christophe.collinet@renault.com
(5) Renault CTS, FR TCR AVA 013, 1 Ave. du Golf, 78288 Guyancourt, olivier.legrand@renault.com
(6) Renault CTS, FR TCR AVA 013, 1 Ave. du Golf, 78288 Guyancourt, renaud.deborne@renault.com

The well-known Ultimate Driving Simulator has been refurbished. The initial design used an open cabin.
The new simulator uses a Renault Twingo cabin.

Fig. 1. Ultimate simulator initial design

Fig. 2. Ultimate simulator new design

The renewal has been performed by the three German based companies IMTEC, VSimulation and Hahlbrock.
The new cabin sits on a special designed base frame. The screen, build from fiber plastic, is mounted on that frame as well. Five projectors are mounted on top of a standard car rack with an innovative support frame. The alignment of the projectors is adjusted by an auto calibration system.
A new steering system with better performance is integrated in the cabin. The new interface is based on the existing interface from Renault.

The new system is up and running since December 2011. The installation took five weeks.
Some technical details:
The total weight of the newly installed parts base frame, screen, cabin and projection system is below 850kg. That allows the operation of the simulator with two people despite its small 1000kg payload.
The first Eigenfrequencies are at 8.7Hz.
Two projectors are mounted in portrait orientation; the other three are mounted in landscape orientation. The horizontal field of view is 200°, the vertical field of view varies from 25° to 46°.
Image quality has been improved drastically. That includes resolution and brightness, quality of the edge blending, mechanical stability of projectors and screen and the auto alignment feature.
The immersion of the simulation is much better. This is caused by the real cabin, a better steering system, a better sound system, a much higher coverage from outside noises and a better quality of the visual system.
The new system is in operation and gets approval from its users.

Performance optimization of a hexapod on a lateral rail with force feed forward compensation

Van der Borch, P.[1], Hoffmeyer, F.[2], Bert Thalen[3]
(1) Moog B.V. The Netherlands, E-mail: pvanderborch@moog.com,
(2) Daimler A.G. Germany, E-mail: friedrich.hoffmeyer@daimler.com
(3) Moog B.V. The Netherlands, E-mail: bthalen@moog.com

Abstract *– The 7-dof driving simulator at Daimler AG uses the lateral rail for all cues in Sway (T_y). This implies that no cues in T_y are generated by the hexapod. Still movements of the hexapod in the other 5 DoF generate disturbances in T_y. Why are there disturbances if the dome is not moving in T_y direction by the hexapod? This is due to the fact that a cue in one of the other directions does change the cog (center of gravity) location in y direction. If the mass is accelerating in T_y it causes a reaction force of the lateral rail. If the disturbance reduction of the control loop of the lateral rail is not good enough to withstand these inertia forces, the lateral rail will move and thus generate a false cue. Since, these inertia forces are very predictable (we know in advance what motion is demanded from the hexapod).they are suited for feed forward. From the demanded accelerations of the dome, an inertia force in T_y can be computed. This signal is used as feed forward to the demanded T_y accelerations. The effect of the feed forward compensation becomes very clear from measurements of the position error of the lateral rail.*

An extra motion system like a lateral rail with the matching software controls is a leap forward to the Stewart platform to overcome the limited workspace for a specific direction. The extended workspace is essential for evaluating vehicle dynamics in a driving simulator. The feed forward compensation of the inertia forces are a key element to get the optimal performance out of the complete motion system, leading to maximum accelerations and minimal false cues.

Key words: *driving simulator, vehicle dynamics, feed forward control, Moog, Daimler AG*

Introduction

Driving simulators

Stewart platforms, also known as hexapods, have been used to generate motion cues for driving simulators for many years now. Driving simulators have been used for various purposes like human machine interface (HMI) testing and design and more recently also for testing and designing driver assistant systems. In these later applications, where drivers' reaction to an active driving assistant system is tested, the realism of the motion cues dictates the quality of the test result.

The recent use of a driving simulator for vehicle dynamics development sets the demands of the motion system to the next level. For testing, evaluating and designing vehicle dynamics, the motion cues are key to the test and they require a state-of-the-art motion system.

The purpose of the driving simulator, or better to say the role of the motion cue, has a significant influence on the design of the driving simulator motion system. Based on a long experience providing high-performance flight simulation and leading-edge testing systems to the automotive and aerospace markets, the current performance of the Moog electric actuators makes it possible to build driving simulators that allow realistic vehicle dynamics testing to support the latest generation of test, research and assessment.

As a starting point for a motion base design, the Stewart platform is chosen as it has a very compact design to generate 6 DOF motion cues that offer many advantages over alternative solutions. When evaluating vehicle dynamics, one specific direction may need much more excursion than the other directions; the limited excursions of a Stewart platform are no longer sufficient to make the required sustained accelerations. This challenge is addressed by mounting the Stewart platform on a moving base, like an x-y table or a lateral rail. However, a moving base underneath the hexapod results into a challenging control problem. Movement of one mass is considered a disturbance for the movement of the other mass. It is essential to have an optimal disturbance reduction without losing performance, to make effective use of the extra stroke of a lateral rail or x-y table. If the

construction or control of additional degrees of freedom introduces disturbances or bumps in the simulator, the additional value is negative instead of positive.

The play and friction free lateral rail of the driving simulator at Daimler AG, together with the nature of the moving mass disturbances or inertia disturbances makes the system very suitable for feed forward compensation. This paper discusses the control problems and applied solutions by Moog implemented at this 7-dof driving simulator.

Driving simulator system description

The motion system of the Daimler driving simulator consists of a base frame that can move in lateral direction. On this frame a hexapod with a dome on top. The total moving mass in lateral direction is 23 tons. The dome with car and equipment has a mass of 7200kg. The hexapod has a stroke of 1.5m per actuator. The motion system is depicted in Fig. 1.

Fig. 1. The motion system of the Daimler driving simulator.

Problem description

The high level problem description is “One can feel unwanted bumps while driving”. If we translate this to a more technical problem definition, it becomes “While making the commanded accelerations, the motion system makes extra disturbance movements”. The disturbances can be quantified in either position error or measured acceleration. The base frame is standard equipped with an accelerometer. This accelerometer is used as feedback sensor in the control loop of the base frame. In more detail, the base frame is controlled by a cascaded control loop of current, acceleration, velocity and position, see Fig. 2.

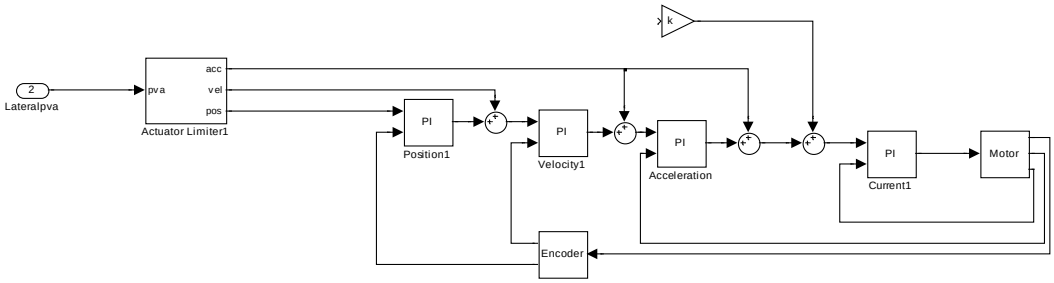

Fig. 2. Lateral rail Control loop without Force calculation.

The current loop has a high bandwidth. The acceleration loop has a relatively low gain, not to introduce any noise disturbance from the accelerometer into the system. The velocity and position loop have an even lower gain. Their purpose is just to remove the steady state offsets. The performance of the base frame with this control loop is very good. The current loop is able to make the demanded accelerations. The feedback is hardly used. This becomes different if the disturbance behaviour is investigated. Here it becomes clear that the relatively low control gains are

not strong enough to take out the disturbance effects. It is this disturbance reduction that can explain the main problem description. The base frame is not a rigid mass that is moving. The hexapod with dome is moving as well. The hexapod movements introduce disturbances to the base frame movement.

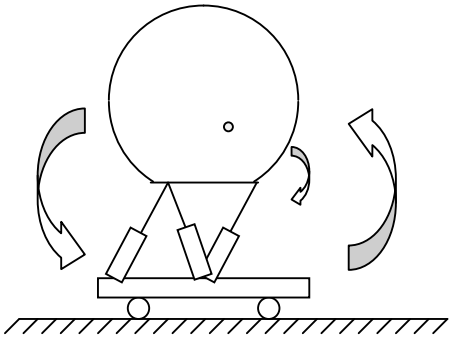

Fig. 3. Interaction between hexapod and base frame, between base frame and hexapod and between dome and hexapod actuators.

As said in the introduction, Daimler uses the lateral rail for all cues in T_y direction. The disturbance for the lateral rail is the T_y component of the 5 other DoF accelerations of the dome mass. Acceleration in Roll (R_x) has the largest contribution to this effect. Let us demonstrate how acceleration in R_x causes acceleration in T_y of the dome mass.

In Fig 4 the black dot represents the location of the Centre of Gravity (CoG). As the dome moves from -16 deg (blue) to +16 deg (black) the CoG has moved in y direction. This acceleration in T_y causes a reaction force of the lateral rail, which needs to be generated by the lateral rail control.

Instead of using feedback control, which is rather weak in this particular system we can use this acceleration in T_y as feed-forward for the lateral rail control. The advantage of using feed forward is that it is faster and thus gives a better disturbance rejection. The disadvantage is that it relies on a good estimation of the disturbance or that disturbances that are not modelled by the feed forward algorithm are not taken into account. So feed forward improves the disturbance rejection for the known disturbances, but not in general.

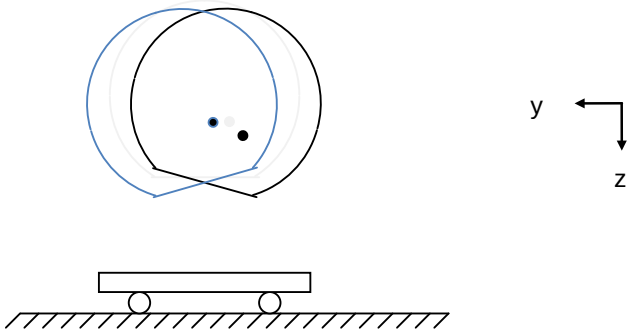

Fig 4. Moving CoG introduces lateral forces.

Force feed forward compensation

Lateral force computation

The positive effect of the feed forward compensation depends heavily on the quality of the force prediction. In the previous paragraph, the force prediction was briefly introduced. In this paragraph we will elaborate the force computation in more detail. Additionally the way how the computed forces are used in the control loop will be described.

Platform force calculation

The platform accelerations are known in the Rotation Reference Point (RRP). As the CoG is not located in the RRP, additional forces are required to follow the commanded trajectory. These forces are generated by the six hexapod actuators and their reaction forces are supported by the lateral rail. The force component in T_y is supported by the lateral motor.

To compute the forces in the RRP, the position vector between RRP and CoG is needed as well as the mass, I_{xx}, I_{yy} and I_{zz}. With some precise straight forward vector algebra the forces are known. This force is directly injected after the acceleration loop of the lateral rail control.

Implementation in control loops

In Fig. 2 the control loops without force feed forward are depicted. In Fig. 5, the calculation of the platform forces is added. Also in this picture it is made clear that the T_y component of the forces is used in the feed forward path of the lateral control.

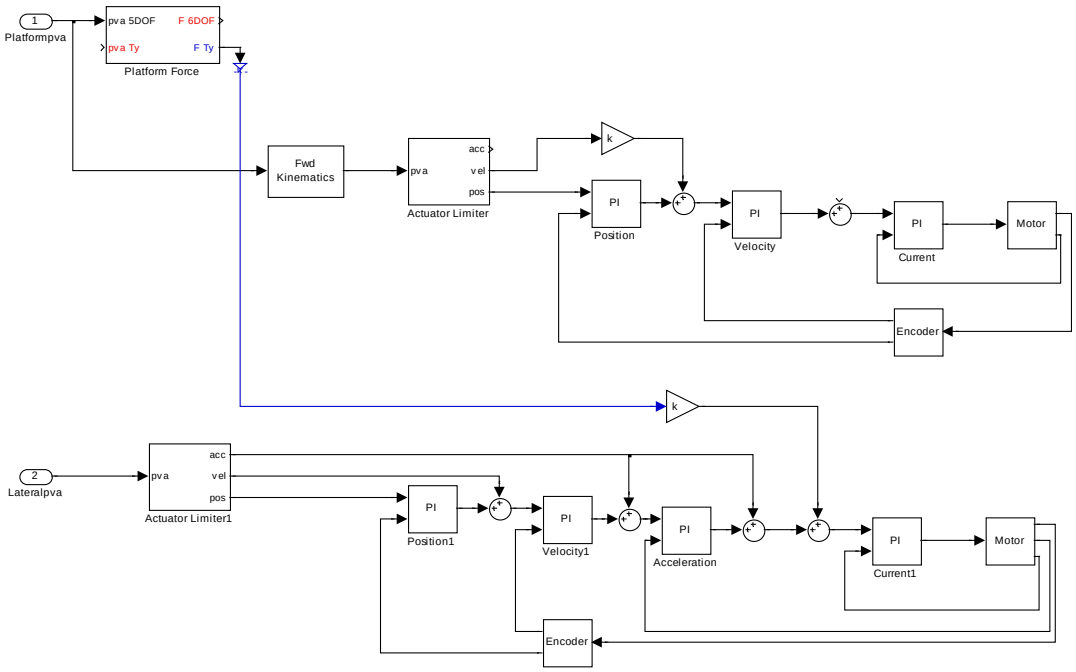

Fig. 5. Control loop with force feed forward to the lateral rail.

Disturbances from the base frame to the hexapod

Now that we realize that the moving dome disturbs the base frame, we can reason in the same way that the moving base frame disturbs the hexapod movement. Although the control strategy of the hexapod is different and its disturbance rejection by itself is much better, a feed forward injection of the known disturbances must have a positive effect. With the force computations needed for the lateral rail feed forward, we are already half way done with computing the actuator forces. In fact, if we are able to reduce the disturbances of the hexapod, we are improving the force prediction used in the lateral rail feed forward.

Actuator force calculation

The majority of the mass is obviously the dome and its content. However the six actuators do contribute to a significant extent. Let us zoom in to the actuator forces. The motion of the dome starts by a rotation of the motor axis. The motor axis and spindle are one part. Due to the rotational speeds, its inertia force cannot be neglected.

$$T_{act} = I_{act} * (a_{act} / (2\pi * \text{spindle ratio})) \qquad (1)$$

Further, the moving parts of the actuator have mass and thus contribute.

$$F_{act} = m_{act\_moving} * a_{act} \qquad (2)$$

Finally, the complete actuator rotates in 2 degree of freedom around the bottom joint.

Friction and Pneumatic support

Now that the ideal motion and forces are described, two more components are required to model the actuator forces as accurate as possible.

First, the actuators have pneumatic assistant system, lifting the wait, and so reducing the current.

$$F_{pneu} = m_{dome} * g \qquad (3)$$

Secondly, a friction force must be modelled. Modelling friction could be an article in itself. A simplified vicious model seems a good starting point.

$$F_{friction} = c * v_{act} \qquad (4)$$

Implementation in the control loops

In Fig. 6 the control loops with force feed forward to both the hexapod and the lateral rail are depicted.

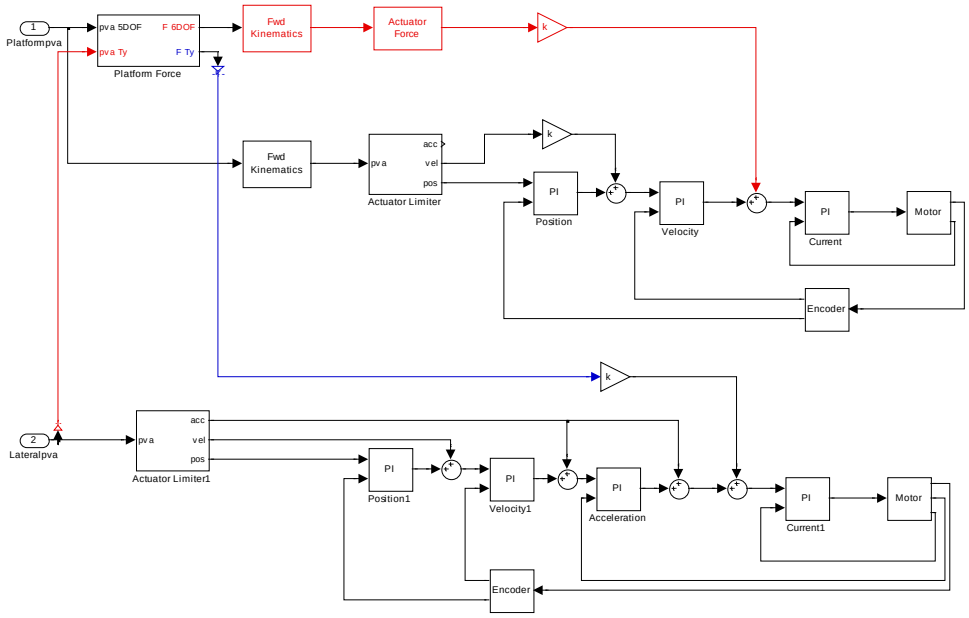

Fig. 6. Control loop with force feed forward to both lateral rail and hexapod.

Results

The effect of the feed forward compensation on the motion of the dome and on the lateral motion (T_y) can be illustrated by measurements. To simplify this proof, we apply a single frequency sinusoid to one of the other DoFs and we measure the position error of the lateral rail. In Fig. 7 the results are plotted. In T_x and T_z a 1m/s^2 sinusoid of 1Hz is applied. In R_x, R_y, R_z a 1rad/s^2 sinusoid of 1Hz is applied. The blue line is the position error with feed forward compensation; the green line is the position error without feed forward compensation.

From this figure it becomes clear that feed forward compensation does have a huge impact when the dome is moving in R_x and R_z. For the other directions, the effect is less which can be explained by a lower contribution in lateral disturbance.

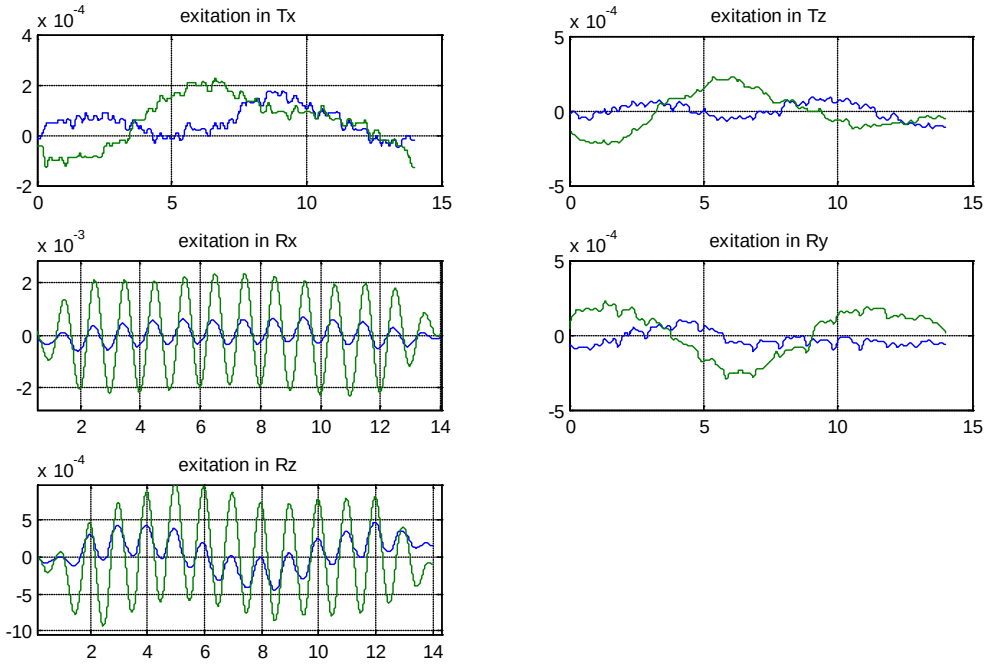

Fig. 7. Position error due to dome motion with (blue) and without (green) force feed forward.

Conclusion

For vehicle dynamics evaluation a next level driving simulators is required. Only a stiff and reactive motion base that has enough stroke in critical directions like T_y and R_z is able to support the development of virtual testing with a human in the loop.

For combined motion systems in which a hexapod is moving on a lateral rail or yaw table, it is crucial to cope with reaction forces that independent motion systems create.

With the Moog feed forward algorithms the reaction forces are under the threshold of human sensitivity.

References

The references are classified in alphabetical order. The reference uses the first 3 letters of the first authors of the referenced article, followed by an Arabic number. References are given under square brackets and are cited in the text as [Smi1].

[1] Drosdol, J. and Panik, F. (1985) "The Daimler-Benz Driving Simulator: A Tool for Vehicle Development", *SAE Technical Paper Series, no.850334*

[2] http://www.grid1.tv/videos/featured/the-dallara-simulator

[3] J. Colditz, L. Dragon, R. Faul, D. Meljnikov, V. Schill, T.Unselt, and E.Zeeb, (2007), "Use of Driving Simulators within Car Development;" *Conference Proc. DSC North America, Iowa, September 2007.*

[4] J.-H Song. W.-S Lee, (2008) "Evaluation of a Lane Departure Warning System on a Driving Simulator", *Conference Proc. DSC Asia Pacific, Seoul, September 2008.*

[5] Käding, W. and J. Breuer, (2006), "The use of driving simulators for the evaluation of driving assistance systems", *Conference Proc. DSC Europe 2006.*

[6] Käding, W. and F. Hoffmeyer, (1995), "The Advanced Daimler-Benz Driving Simulator, *SAE Technical Paper Series, no.950175.*

[7] Dupuis, M. and Strobl, M, and H.Grezlikowski, (2010), "OpenDrive 2010 and beyond-status and future of the de facto standard for the description of road networks", *Conference Proc. DSC Europe 2010.*

[8] P.J Feenstra, M. Wentink, Z.C. Roza and W. Bles (2007), Desdemona, an alternative moving base design for driving simulation," *Conference Proc. DSC North America 2007.*

[9] T. Brown, B. Dow, D.Marshall, S.Allen. (2007), "Validation of stopping and turning behaviour for novice drivers in the National Advanced Driving Simulator, ," *Conference Proc. DSC North America 2007.*

[10] T. Chapron, J-P. Colinot, (2007), "The new PSA Peugeot-Citroen Advanced Driving Simulator, Overall design and motion cue algorithm, ," *Conference Proc. DSC North America 2007.*

[11] W. Käding, E.Zeeb, (2010), "25 years driving simulator research for active safety", *Conference Proc. International Symposium on Advanced Vehicle Control (AVEC), Loughborough 2010 .*

How to build Europe's largest eight-axes motion simulator

Gerd Baumann[1], Thomas Riemer[1], Christoph Liedecke[2], Philip Rumbolz[2], Andreas Schmidt[2]

(1) FKFS, Stuttgart, Germany; E-mail: {gerd.baumann, thomas.riemer}@fkfs.de
(2) Universität Stuttgart; E-mail: {christoph.liedecke, philip.rumbolz, andreas.schmidt}@ivk.uni-stuttgart.de

Abstract *– This paper gives an overview of the new Stuttgart Driving Simulator for passenger cars which has been designed and realized in a joint effort of Stuttgart University and FKFS. The focus of the simulator is research upon driver's behaviour as well as design and testing of driver assistance systems.*

The simulator is based on a motion system with eight axes. In terms of motion space it is currently the largest motion simulator in Europe. As a special feature the simulator supports the integration and exchange of modified real passenger cars.

The paper describes the concept and the design of the Stuttgart Driving Simulator. An outlook on typical applications is given.

Key words: *motion simulator, eight axes, vehicle integration, driver assistance systems*

Introduction

Within the framework of the high-tech strategy and the IKT2020 research program of the German federal government, Stuttgart University started the interdisciplinary research project VALIDATE in July 2008 with the goal of reducing CO_2 emissions of road vehicles. The project was funded by the German Federal Ministry for Education and Research (BMBF) until December 2011. Further funding was granted by Ministry of Science, Research and Arts of Baden-Württemberg, in the context of a project named ElefAnt with the goal of optimizing electric vehicles and drivelines.

The funding enables the design and setup of a very sophisticated research platform for the design of electronic systems for energy reduction in a partial or complete virtual environment. Especially driver assistance and driver information systems, which indirectly lead to a reduction in energy consumption by supporting the driver in operation of the vehicle, are regarded [Pie1].

It is known that the individual driving style has an enormous impact on the vehicle's energy consumption [Rum1]. Therefore it was decided that a high-quality driving simulator should be part of the research platform. Such a simulator allows detailed investigation of the human driver's behaviour whereas unpredictable influences of traffic and weather can be suppressed.

Design of the Stuttgart Driving Simulator

Overview

Fig.1 shows the Stuttgart Driving Simulator. A new building with a dimension of 20 by 15 metres has been designed for the particular needs of the simulator.

The eight axes motion system consists of three parts:

- A gantry moves on three rails in the X direction and allows the simulation of longitudinal acceleration and braking.
- The gantry itself carries further rails. A sled moves on these rails in the Y direction and allows the simulation of lateral acceleration.
- The sled carries a hexapod system which allows translation and rotation with six degrees of freedom. It is mainly used to simulate pitch, roll and yaw motion as well as vertical movement. Furthermore, the hexapod supports the XY linear system in longitudinal and lateral acceleration simulation.
- The lightweight simulator dome is completely manufactured of carbon fibre and aluminium composite materials. The interior dome wall is used as a projection surface. Twelve projectors create a circumferential image.

Two doors in the dome allow persons to access the simulator vehicle from the driver's and co-driver's side. For this purpose the motion system moves the

dome to a parking position. Thereafter an access ramp, designed as a “flap bridge”, descends automatically and lets persons enter and leave the dome.

Fig. 1. Overall view and dome interior of the Stuttgart Driving Simulator

Scope of application

Both Stuttgart automotive research institutes IVK and FKFS have a long tradition of research on driver’s behaviour. Examples are the driver reaction under special aerodynamic conditions [Kra1] and the benefit of hybrid-electric propulsion for different driver types [Fri1].

IVK and FKFS have special experience in real-world test driving. This means that a sufficient number of drivers is recruited whose distribution of gender, age and yearly mileage reflect the population. These probands drive vehicles on selected routes in order to represent average driving in a particular region, e.g. Germany. By evaluation of measurements it is possible to identify potential improvements in vehicle technology with respect to fuel efficiency, safety or comfort [Rum2].

The results of such on-road studies are highly meaningful but cause substantial effort in terms of time and money. Furthermore it is neither possible to perform safety related driving manoeuvres with “normal” drivers nor doing this in real traffic. Furthermore, road testing does not provide reproducible traffic and weather conditions.

Hence, FKFS and IVK are tending to transfer road testing partially into simulation. The Stuttgart Driving Simulator has been mainly designed for the following scope of applications:

- Reduction of energy consumption by analysing and influencing the individual driving style and its impact on efficiency,
- design and investigation of driver’s reaction on new driver assistance systems and human-machine interfaces and
- research on future safety systems, mainly collision avoidance systems with a focus on the protection of pedestrians and children.

References

[Fri1] Fried, O.: Betriebsstrategie für einen Minimalhybrid-Antriebsstrang. Universität Stuttgart, Dissertation, 2003. Shaker-Verlag. ISBN 3-8322-2496-3.

[Pie1] Piegsa, A.; Rumbolz, P.; Schmidt, A.; Liedecke, C.; Baumann, G.; Reuss, H.-C.: VALIDATE – Basis for New Sophisticated Research Platform for Virtual Development of Vehicle Systems. 2011 SAE World Congress, Detroit, 2011.

[Rum1] Rumbolz, P.; Piegsa, A.; Reuss, H.-C.: Messung der Fahrzeug-internen Leistungsflüsse und der diese beeinflussenden Größen im „real- life“ Fahrbetrieb. VDI Tagung: Innovative Fahrzeugantriebe, Dresden, 2010.

[Rum2] Rumbolz, P.; Baumann, G.; Reuss, H.-C: Messung der fahrzeuginternen Leistungsflüsse im Realverkehr. ATZ 05/2011, S. 416-421.